

MARTIN MARIETTA ENERGY SYSTEMS LIBRARIES



3 4456 0323381 9

2
CENTRAL RESEARCH LIBRARY
DOCUMENT COLLECTION

ORNL-3830

UC-10 - Chemical Separations Processes
for Plutonium and Uranium
TID-4500 (45th ed.)

CHEMICAL TECHNOLOGY DIVISION
ANNUAL PROGRESS REPORT
FOR PERIOD ENDING MAY 31, 1965

CENTRAL RESEARCH LIBRARY
DOCUMENT COLLECTION

LIBRARY LOAN COPY

DO NOT TRANSFER TO ANOTHER PERSON

If you wish someone else to see this
document, send in name with document
and the library will arrange a loan.



OAK RIDGE NATIONAL LABORATORY

operated by

UNION CARBIDE CORPORATION

for the

U.S. ATOMIC ENERGY COMMISSION

Contract No. W-7405-eng-26

CHEMICAL TECHNOLOGY DIVISION
ANNUAL PROGRESS REPORT
for Period Ending May 31, 1965

D. E. Ferguson – Division Director
R. G. Wymer – Chemical Development
Section A Chief
R. E. Blanco – Chemical Development
Section B Chief
K. B. Brown – Chemical Development
Section C Chief
M. E. Whatley – Unit Operations Section Chief
H. E. Goeller – Process Design Section Chief
R. E. Brooksbank – Pilot Plant Section Chief

NOVEMBER 1965

OAK RIDGE NATIONAL LABORATORY
Oak Ridge, Tennessee
operated by
UNION CARBIDE CORPORATION
for the
U. S. ATOMIC ENERGY COMMISSION



3 4456 0323381 9

1.

2.

3.

4.

5.

Contents

SUMMARY	1
1. POWER REACTOR FUEL PROCESSING	30
1.1 Hydrolysis of Uranium and Thorium Carbides	31
1.2 Development of Processes for Graphite-Base Fuel.....	33
1.3 Studies on the Processing of Uranium-Plutonium Oxide Fuel	39
1.4 Studies on the Processing of Thorium-Uranium Fuel	43
1.5 Chloride Volatility Studies with Uranium and Plutonium.....	46
1.6 Development of Mechanical Processes.....	48
1.7 Development of Close-Coupled Processes.....	59
1.8 Conceptual Plant Studies	65
2. FLUORIDE VOLATILITY PROCESSING.....	69
2.1 Molten-Salt Processing of Uranium-Aluminum Alloy Fuel	70
2.2 Volatilization of PuF_6 from Molten Salts Containing High Concentrations of Uranium.....	75
2.3 Recovery of Plutonium and Uranium from Falling Molten-Salt Droplets and from Beds of Solid Particles by Fluorination	76
2.4 Fluidized-Bed Volatility Process Development for Stainless-Steel- and Zircaloy-Clad UO_2 Fuels.....	79
2.5 Design of a Fluidized-Bed Pilot Plant for Zirconium- and Stainless-Steel-Clad UO_2 Power-Reactor Fuels	81
2.6 Sorption of PuF_6 by Metal Fluorides.....	85
2.7 Sorption of UF_6 by NaF	87
2.8 Continuous In-Line Monitoring of Gas Streams in Fluoride Volatility Processing.....	88
2.9 Vapor-Liquid Equilibria of UF_6 - NbF_5 System	90
2.10 Phase Equilibria Studies Pertinent to Fluoride-Volatility Processing of Fuels or Mixtures Containing Chromium	91
2.11 Volatilization of UF_6 from Sol-Gel-Derived ThO_2 - UO_2	92
2.12 General Corrosion Studies.....	94
3. WASTE TREATMENT AND DISPOSAL.....	96
3.1 Conversion of High-Level Radioactive Wastes to Solids	96
3.2 Disposal of Intermediate-Level Radioactive Waste.....	114

3.3	Treatment of Low-Level Radioactive Wastes.....	119
3.4	Engineering, Economic, and Safety Evaluation.....	134
4.	TRANSURANIUM ELEMENT PROCESSING.....	140
4.1	Development of Chemical Processes.....	140
4.2	Development of Process Equipment.....	148
4.3	Design and Fabrication of Process Equipment	151
4.4	Construction of the Transuranium Processing Plant.....	152
5.	CURIUM PROCESSING	157
5.1	Process Development.....	157
5.2	Curium Recovery Facility: Equipment and Flowsheet Testing	160
5.3	Solvent Extraction Processing of ^{243}Am and ^{244}Cm	161
5.4	Ion Exchange Purification and Separation of ^{243}Am - ^{244}Cm	166
5.5	Processing of $^{241}\text{AmO}_2$ Targets	168
5.6	Development of Alternative Processes: Separation of Lanthanides and Actinides.....	172
6.	DEVELOPMENT OF THE THORIUM FUEL CYCLE	174
6.1	^{233}U Storage and Distribution Facility.....	174
6.2	Development of the Sol-Gel Process	174
6.3	Development of Methods for Producing Microspheres	177
6.4	Design of the Thorium-Uranium Recycle Facility	182
6.5	Development of Equipment for the Thorium-Uranium Recycle Facility	185
7.	SEPARATIONS CHEMISTRY RESEARCH	193
7.1	Extraction of Metal Chlorides by Amines.....	193
7.2	Extraction of Metal Nitrates by Amines	193
7.3	Reagents for Separating Polonium(IV) from Bismuth.....	195
7.4	New Extraction Reagents	197
7.5	Performance of Degraded Reagents and Diluents	197
7.6	Biochemical Separations	200
7.7	Extraction Properties of Lanthanide and Actinide Complexes	201
7.8	Recovery of Rubidium from Ores	203
7.9	Recovery of Beryllium from Ores	205
7.10	Recovery of Acid by Amine Extraction	207
7.11	Recovery of Thorium from Granitic Rocks	207
7.12	Separation of Biological Macromolecules	210
7.13	Extraction of Alkaline Earths by Di(2-ethylhexyl)phosphoric Acid	210
7.14	Intermolecular Bonding in Organic Mixtures.....	211
7.15	Synergism in the Extraction of Strontium by Di(2-ethylhexyl)phosphoric Acid	213
7.16	Synergism and Diluent Effects in the Extraction of Cesium by 4-sec-Butyl-2- α -methylbenzylphenol (BAMBP)	214

7.17	Kinetics of Extraction of Iron by Di(2-ethylhexyl)phosphoric Acid	217
7.18	Activity Coefficients of the Solvent Phases	218
8.	RECOVERY OF FISSION PRODUCTS BY SOLVENT EXTRACTION	222
8.1	Cesium	222
8.2	Isolation of Cerium and Promethium	224
8.3	Ruthenium	226
8.4	Treatment of Waste that Contains Dissolved Stainless Steel or Large Amounts of Aluminum Ion	226
8.5	Engineering Studies	226
9.	CHEMISTRY OF PROTACTINIUM.....	228
9.1	Extraction from Sulfuric Acid Solutions	228
9.2	Absorption Spectra in Sulfuric Acid Solutions	230
9.3	Recovery of Protactinium	231
10.	IRRADIATION EFFECTS ON HETEROGENEOUS SYSTEMS	233
10.1	Radiolysis of Water Adsorbed on Silica Gel.....	233
11.	HIGH-TEMPERATURE CHEMISTRY.....	236
11.1	Fabrication Status of the High-Temperature, High-Pressure Spectrophotometer System	236
11.2	Spectral Studies of Ionic Systems	237
11.3	Measurement of Liquid Densities at High Temperature and High Pressures.....	241
11.4	Computer Programs for Spectrophotometer Studies	242
12.	MECHANISMS OF SEPARATIONS PROCESSES	248
12.1	Activities of the Three Components in the System: Water–Nitric Acid–Uranyl Nitrate Hexahydrate at 25°C.....	248
12.2	Activities of Tributyl Phosphate in Mixtures Containing Tributyl Phosphate, Uranyl Nitrate, and Water	248
12.3	Computer Resolution of Spectrophotometric Data on Uranyl Nitrate–Nitric Acid–Water Systems	250
13.	CHEMICAL ENGINEERING RESEARCH	252
13.1	The Stacked-Clone Contactor	252
13.2	Effect of Ionizing Radiation on Coalescence in Liquid-Liquid Systems	253
13.3	In-Line Detection of Particles in Gas Streams by Scattered Light.....	256
13.4	Solvent Extraction Engineering Studies: Correlation of Pulsed-Column Flooding Data.....	259
14.	REACTOR EVALUATION STUDIES	261
14.1	Studies of the Cost of Shipping Reactor Fuels	261
14.2	Studies of the Cost of Processing Fuel	263
14.3	Studies of the Cost of Preparing Fuel by the Sol-Gel Process	266
14.4	Computer Code for Studies of Overall Power Costs	268

14.5	The TRUFIZ Computer Code	269
14.6	Manual of Shipping-Cask Design	269
14.7	Criticality Control in Fuel Cycle Plants	269
15.	CHEMICAL APPLICATIONS OF NUCLEAR EXPLOSIONS	271
15.1	Project Coach	271
15.2	Focusing Electrophoresis for Separation of Heavy Elements	272
15.3	Hypervelocity Jet-Sampler Development	272
15.4	Feasibility of Producing Chemicals with Nuclear Explosives	272
15.5	Stimulation of Natural Gas Wells by Nuclear Devices: Project Gasbuggy	273
15.6	Magnesium Ores	273
15.7	Copper Ores	274
16.	PREPARATION AND PROPERTIES OF ACTINIDE-ELEMENT OXIDES	275
16.1	Fundamental Studies of Thoria Sols and Gels	275
16.2	Surface and Sintering Properties of Sol-Gel Thoria	281
17.	ASSISTANCE PROGRAMS	285
17.1	Eurochemic Assistance Program	285
17.2	Projects for Improving ORNL Waste Systems	285
17.3	A Demonstration of the Disposal of Solid, High-Level Radioactive Waste in Salt	286
17.4	Disposal of Radioactive Waste by Hydrofracturing	287
17.5	Construction and Startup of the High Radiation Level Analytical Laboratory	288
17.6	High-Level Alpha Laboratory	289
17.7	Storage Facility for ^{233}U , Building 3019	289
17.8	Filter Tests in the Nuclear Safety Pilot Plant	290
17.9	Studies of Radiation Shields for Fission Sources	291
17.10	Irradiation and Decontamination Evaluation Tests on Selected Protective Coatings	296
18.	MOLTEN-SALT REACTOR PROCESSING	299
18.1	Continuous Fluorination of Molten Salt	300
18.2	Distillation of Molten Salt	301
18.3	Reconstitution of Fuel for a Molten-Salt Breeder Reactor	302
18.4	Chromium Fluoride Trapping	302
18.5	Alternative Processing Methods for a Molten-Salt Breeder Reactor	303
19.	WATER RESEARCH PROGRAM	306
	PUBLICATIONS, SPEECHES, AND SEMINARS	307
	ORGANIZATION CHART	317

Summary

1. POWER REACTOR FUEL PROCESSING

In the development of new nuclear power reactor concepts, fuels that can be used for long times and at very high temperatures are continuously being sought. This sometimes leads to the use of fuels for which the chemical reactions encountered in fuel processing are not well understood. The development of new recovery processes for such fuels is directed toward the demonstration of chemical methods and engineering practices for recovering and decontaminating the uranium, thorium, and plutonium. In the studies described here, two approaches are being followed: the development of both mechanical and chemical head-end methods designed to produce suitable aqueous feeds for solvent extraction and the development of non-aqueous processes such as chloride volatility, which may either precede or circumvent solvent extraction or fluoride volatility processes.

1.1 Hydrolysis of Uranium and Thorium Carbides

Fundamental studies of the hydrolysis of uranium and thorium carbides are continuing. High-purity samples of the uranium carbides UC, $U_4(C_2)_3$, and $UC_{1.85}$, when hydrolyzed in 4 to 16 M HNO_3 at $90^\circ C$, produced uranyl nitrate, soluble organic acids (mellitic and oxalic), and an off-gas consisting of NO_2 , NO, and CO_2 . The samples were passive to treatment in 0.001 to 0.5 M HNO_3 . Thorium carbide samples in the range of $ThC_{0.81}$ to $ThC_{2.14}$ were prepared; below ThC_1 the samples contained Th metal and ThC_1 . The dicarbide was found to have the composition $Th_{1.95}$ rather than $ThC_{2.00}$. When hydrolyzed in water between 25 and $99^\circ C$, ThC_1 produced hydrogen and methane, and $ThC_{1.95}$ produced C_2 to C_8 hydrocarbons and waxes. When samples of uranium and thorium carbides were prepared with tungsten carbide as an

impurity (up to 8 wt %), the amount of hydrocarbons produced in hydrolysis decreased, and the production of hydrogen and waxes increased. The impurities were present as WUC_2 and W_2C (in thorium).

1.2 Development of Processes for Graphite-Base Fuel

Work on graphite-base fuels last year was devoted to the development of burn-leach processes for pyrolytic-carbon-coated ThC_2 - UC_2 and ThO_2 - UO_2 fuel particles contained in graphite. Two alternatives were studied: (1) burning at $750^\circ C$ in fluidized beds followed by leaching in boiling nitric acid and (2) submerged combustion in oxygenated dilute nitric acid at $300^\circ C$ and 1500 to 2000 psi. The latter process is called the Pressurized Aqueous Combustion (PAC) process.

In the burn-leach process, uranium and thorium are recovered from graphite-matrix fuel by burning the graphite in a fluidized bed of alumina and dissolving the resultant uranium and thorium oxides in a strong acid leachant to provide feed for solvent extraction processing. Prototype HTGR fuel compacts were burned and leached in engineering-scale equipment, with 99.7% recovery of the uranium and thorium. The burning was done in bench scale in a 2-in.-diam fluidized bed of alumina at a rate of 20 g-moles of carbon per minute per square foot of cross section to produce a bed containing 28% of combined metal oxides. The bed was leached at 110 to $118^\circ C$ in a 1.5-in.-diam upflow column, with provision for recycling the leachant (13 M HNO_3 - 0.1 M F^- - 0.04 M Al^{3+}).

In parallel laboratory leaching tests on mixtures of alumina and combustion ash containing 6% U_3O_8 , 25% ThO_2 , and 69% Al_2O_3 , 99.5% of the uranium and thorium were recovered as 0.6 M $Th(NO_3)_4$ in 5 to 7 hr in boiling ≥ 4 M HNO_3 - 0.02

to 0.05 M HF—0.0 to 0.1 M $\text{Al}(\text{NO}_3)_3$. About 2% of the alumina dissolved. Since coated-particle ThO_2 - UO_2 microspheres settle to the bottom of a fluidized bed, leaching tests on undiluted microspheres were made; complete dissolution to 0.5 M $\text{Th}(\text{NO}_3)_4$ was achieved in 3 to 6 hr in boiling 13 M HNO_3 —0.05 M HF. Lower nitric acid concentrations were much less effective as leachants.

PAC process tests were made in both an autoclave and in a semicontinuous chemical reactor. In this process, the nitric acid is not consumed when an excess of oxygen is present. In 24-hr autoclave tests with HTGR fuel compacts containing mixed thorium-uranium carbide in 2 M HNO_3 , all the carbon was burned to CO_2 , and all the fuel dissolved when the O_2 -to-C and NO_3^- -to-(Th + U) ratios were ≥ 1 and ≥ 50 respectively. The high NO_3^- -to-(Th + U) ratio is required because aqueous uranium and thorium nitrates hydrolyze readily at high temperatures. The pyrolytic carbon coatings on fuel particles are not attacked until all matrix carbon is oxidized. The oxidation rate for unfueled moderator-grade graphite is much lower, 0.15 to 0.24 $\text{g}\cdot\text{g}^{-1}\cdot\text{hr}^{-1}$, than the rate for fueled graphite. In tests with carbon-coated 97% ThO_2 —3% UO_2 microspheres, complete dissolution was obtained in 24 hr in 2 M HNO_3 at 300°C when the NO_3^- -to-(Th + C) mole ratio was 100. Under similar conditions, only 49% of pure ThO_2 was dissolved in 24 hr.

During the first half of last year, development of a burn-leach and a burn-volatility process for graphite-base Rover fuel was completed.

1.3 Studies on the Processing of Uranium-Plutonium Oxide Fuel

In the laboratory, acid-leaching studies were made on stainless-steel-clad oxide fuel declad by a new process developed under the Fluoride Volatility Processing program (see Sect. 2). In this process, the fuel assemblies are contacted with 40% HF—60% O_2 at 600°C in a fluidized bed of alumina. The cladding is converted to “stainless steel” oxides and fluorides and the UO_2 - PuO_2 fuel to U_3O_8 - PuO_2 powder. A typical fluidized-bed decladding product contained 25% U_3O_8 , 13% stainless steel compounds, 5% fluorine, and 67% Al_2O_3 . When leached for 5 hr in boiling 1 to 15 M HNO_3 that was ≤ 1 M in $\text{Al}(\text{NO}_3)_3$, 99.6% of the uranium was dissolved to produce a leachate 0.2 M in uranium and 0.6 M in fluoride. About 80 to 90% of the

fluoride, 2% of the alumina, and 16 to 85% of the iron in the bed product was also leached; use of higher HNO_3 concentrations increased the solubility of iron. To reduce the amount of fluoride in the decladding product, the bed was pyrohydrolyzed with steam or with O_2 —3% H_2O at 200 to 600°C for 3 hr. About 85% of the fluorine was removed. The beds were then leached for 10 hr in boiling 10 M HNO_3 to produce 0.2 M HNO_3 —0.05 M HF solutions; sufficient alumina was also leached to complex the HF. Uranium recovery amounted to 99.7 to 99.9%, and the iron content was reduced to 6%.

As to the Sulfex decladding process, hot-cell tests with fast-reactor fuel samples (irradiated up to 99,000 Mwd per ton of uranium), containing 20% PuO_2 —80% UO_2 clad in stainless steel, showed that it cannot be applied satisfactorily to this type of fuel, since 1.5% of the uranium and plutonium in the fuel was dissolved by the boiling 6 M H_2SO_4 decladding reagent. Thus, the waste solution produced by the Sulfex process would have to be specially processed to recover this loss. In addition, over half of the ^{137}Cs appeared in the decladding waste solution; the presence of this long-lived gamma emitter would materially increase the cost of permanent disposal of decladding waste.

Parallel tests of the shear-leach process on identical fuel samples were very successful. The irradiated samples dissolved at practical rates in boiling 3.5 to 10 M HNO_3 without fluoride catalyst, which was not the case with tests on unirradiated UO_2 - PuO_2 samples. Leaching of the oxide core from both Sulfex-declad pellets and chopped fuel pins was accomplished in 3 hr with boiling 5 M HNO_3 . The small residue of refractory material remaining with the stainless steel hulls retained only 0.13% of the uranium and plutonium originally in the fuel sample.

Related dissolution tests with unirradiated high-density PuO_2 microspheres in boiling 14 M HNO_3 —0.5 M HF resulted in the very low dissolution rate of 7×10^{-3} $\text{mg min}^{-1} \text{cm}^{-2}$; only 8.5% of the PuO_2 dissolved in 37 hr.

1.4 Studies on the Processing of Thorium-Uranium Fuel

Sulfex decladding and shear-leach studies were made with both unirradiated and irradiated stainless-steel-clad ThO_2 —4% UO_2 prepared by the sol-gel process. Hot-cell tests on the dissolving of

irradiated samples [3000 to 98,000 Mwd per metric ton of (Th + U)] in boiling Thorex reagent [13 M HNO_3 -0.04 M HF-0.04 M $\text{Al}(\text{NO}_3)_3$] indicated that irradiation markedly increases the dissolution rate over that for unirradiated oxide. For example, more than 99.8% of the thorium and uranium was dissolved in 24 hr, as compared with 75 hr for nearly complete dissolution of unirradiated material. The macro amounts of fission products from these highly irradiated specimens were soluble in the product solutions, which were 1 M in $\text{Th}(\text{NO}_3)_4$, 10 M in HNO_3 , and 0.05 M in total fission products. Cyclic dissolving, which left a 6% heel of undissolved thoria-urania, produced a 1 M thorium product solution after 5 hr. The residues consisted of undissolved thoria-urania, cladding, corrosion products, and contaminants from the fuel rod, such as insulation and alumina. The thorium and uranium could be recovered from the residue by leaching with fresh Thorex reagent. In the Sulfex decladding tests, there was a 0.33% loss of thorium and uranium to the decladding solution.

Protactinium was successfully recovered by adsorption on unfired Vycor from thorium-uranium nitrate fuel solutions prepared from specimens irradiated to 75,000 Mwd/metric ton and cooled 26 days before processing. In three hot-cell experiments, the specimens were first dissolved in refluxing 13 M HNO_3 -0.05 M HF, and the protactinium was then preferentially adsorbed on columns of 60- to 80-mesh unfired Vycor glass. More than 99.4% of the protactinium was adsorbed, and more than 95% was eluted with 0.5 M oxalic acid. The protactinium was decontaminated of zirconium-niobium, total rare-earth beta emitters, and ruthenium by factors of 9, 6000, and 2800 respectively.

Evaluation of other inorganic adsorbents was continued. The distribution coefficients for protactinium were measured for silica gel and Bio-Rad ZP-1 and for 0.5- to 12-M HNO_3 solutions containing 4, 50, and 100 g of thorium per liter. The coefficients ranged from 1400 to 5800 for the silica gel and from 100 to 29,000 for Bio-Rad ZP-1. As much as 95% of the protactinium was unadsorbable by Bio-Rad ZP-1 in the more dilute nitric acid solutions.

1.5 Chloride Volatility Studies with Uranium and Plutonium Oxides

In laboratory studies at temperatures up to 400 to 600°C, the direct chlorination of unirradiated

UO_2 - PuO_2 pellets with 85% Cl_2 -15% CCl_4 was unsuccessful. Therefore, before chlorination, the pellets were oxidized at 500 to 800°C in oxygen to produce U_3O_8 - PuO_2 powder, but only pellets containing less than 20% PuO_2 were affected by this treatment. Pure U_3O_8 was easily converted to volatile uranium chlorides at 400 to 500°C. Pellets containing 99% U_3O_8 -1% PuO_2 were nearly unreactive at 300 to 350°C; at 400 to 500°C all the uranium and 50% of the plutonium were volatilized in 3 to 4 hr. Complete volatilization was achieved at 600°C, but sintering and melting (probably of UO_2Cl_2) were observed. About 3.3×10^5 and 100 moles of chlorine were required to transport 1 g of Pu at 427 and 727°C respectively.

1.6 Development of Mechanical Processes

Since second-generation power-reactor fuel assemblies cannot be sheared satisfactorily when intact, the rods must be removed before they are sheared. Pulling single rods is too slow, and pulling all rods at one time crumples the assembly sheath. Therefore, a device was designed and built for pulling single rows of rods. Loose arrays of 64 pulled rods were easily sheared in the 250-ton prototype shear. Shearing tests on 3-in.-diam Zircaloy-2-clad uranium-metal annular fuel rods were equally satisfactory. The shearing force was 82 tons; 30% of the area was sheared through before the rod was broken. A new feeding device, external to the shear, successfully replaced the internal stop on the shear, which was hard to repair with remote manipulators.

A mockup was used to demonstrate the remote handling and transfer of a filled sheared-fuel basket between the shear and dissolver. All operations went smoothly. Also, experiments and calculations showed that the fission product heating of stored sheared fuel will not be excessive and will not cause pressure surges in the dissolver when quenched.

Abrasive-disk sawing of Zircaloy-2 assembly end fittings in air was shown to present a definite fire hazard; sawing under water sprays was somewhat safer but produced fines in a size range ($\leq 400 \mu$) considered dangerous. However, a 7:1 automatic dilution by abrasive material is believed to lessen the risk.

Leaching of stainless-steel-clad UO_2 sheared fuel in boiling 7 M HNO_3 in a 90-liter batch thermo-siphon leacher was complete in 2 hr. Leaching of

$\text{ThO}_2\text{-UO}_2$ in 13 M HNO_3 -0.04 M F^- -0.1 M Al^{3+} was much slower. The leaching rate decreased with thorium loading and increased with temperature. The length of the sheared section had little effect on the rate.

A leached-hull monitor, using delayed-neutron activation analysis, was developed. It has a sensitivity of about 1 mg of ^{235}U , ^{239}Pu , or ^{233}U per kilogram of leached hulls. This corresponds to a loss of less than 0.01% of the fuel in a typical low-enriched uranium power-reactor assembly.

1.7 Development of Close-Coupled Processes

When uranium, thorium, and plutonium are recycled in nuclear reactors, short-lived isotopes are built up which decay rapidly through a series of high-energy gamma-emitting daughters. Since these isotopes cannot be separated easily from the major isotopes in which they are contaminants, the recovered fuels are very gamma active and must be reconstituted into replacement fuel assemblies by remote manipulation. Thus, high decontamination from fission products may not be necessary. A new program was begun this year to develop low-cost, low-decontamination processes capable of achieving factors of 10 to 100 from fission products. Emphasis has been placed primarily on seeking a simple process which will effect reductions in capital, operating, and analytical costs. Attempts are also being made to close-couple the head-end and separations steps with subsequent operations such as the sol-gel process.

Laboratory experiments with thorium-uranium nitrate fuel solutions in studies to substitute precipitation, ion exchange, or electro dialysis for solvent extraction were generally unsatisfactory, and in all cases decontamination factors (DF's) less than 10 were obtained. Precipitants evaluated included dibasic ammonium phosphate, oxalic acid, and 30% hydrogen peroxide. Ion exchangers tested included Dowex 1, Dowex 50W, JP-1, and silica gel. Although electro dialysis was also unsuccessful in decontaminating fuel solutions, it may be useful in separating fission products in aqueous wastes into useful fractions; for example, a mixture was separated into fractions containing Zr-Nb and Ru; Eu, Ce, and Sr; La; and Cs by appropriate pH control.

A simple, efficient differential solvent extraction contactor was developed and satisfactorily tested. A 0.2 M acid-deficient 1.5 M Th-0.1 M U fuel solu-

tion was contacted first with 3% TBP in *n*-dodecane to extract uranium and then with 30% TBP in *n*-dodecane to recover thorium. Uranium and thorium recoveries were 99.9 and 87%, respectively; uranium decontamination factors from Th, total rare earths (TRE), Zr-Nb, and Ru were 16, 2.6×10^4 , 300, and 500 respectively. Thorium decontamination factors from U, TRE, Zr, and Ru were 7×10^4 , 16, 6, and 4 respectively. One feature of the new unit is that it can be shut down and restarted very quickly. Tentative flowsheets for the recovery of U and Th either separately or together in a mixer-settler containing three extraction, one scrub, and three strip stages were evolved; di-*sec*-butyl phenylphosphonate (DSBPP) in diethyl benzene (DEB) was used. About 99% U recovery was obtained, with a thorium-decontamination factor of 6000. New flowsheets, calling for either solvent extraction (DSBPP in DEB) or ion exchange (Dowex 50), were developed to separate stored ^{233}U from the daughter isotopes of ^{232}U . Immediately after processing, the solvent extraction process resulted in a DF of 1000, and the ion exchange process resulted in a DF of 2. However, after two weeks, the activity of both products was the same. The reduction of Pu(IV) to Pu(III) in nitrate solution was satisfactorily accomplished with 4% H_2 -Ar in a platinized-alumina bed. This method avoids the use of ferrous sulfamate or uranous ion.

A new method was developed to remove nitrate from thorium-uranium nitrate solutions, a required step in the sol-gel process. The nitrate was extracted with either 0.2 M Primene JM-T in *n*-dodecane or 0.2 M 1-nonyldecylamine in *n*-dodecane. The nitrate-to-thorium mole ratio in the aqueous phase approached 0.2 as a limit. Sol-gel ThO_2 prepared from the amine-extraction product is now being evaluated. Amine extraction may be a possible alternative to presently used steam denitration.

1.8 Conceptual Plant Studies

Two conceptual plant studies were prepared during the past year. The first, for a small on-site plant associated with a 500- to 3000-Mw (electrical) boiling-water reactor station using slightly enriched fuel, was based on use of existing technology. The second, concerning a plant for processing HTGR fuel, provided a design for a burn-leach head-end process to be associated with a solvent extraction plant.

2. FLUORIDE VOLATILITY PROCESSING

The investigation of fluoride-volatility processes at ORNL is part of an intersite program to develop an alternative to aqueous methods for the recovery of values from spent nuclear reactor fuels. The program here is presently in transition between molten-salt and fluidized-bed methods.

Except for laboratory experiments on removal of plutonium and perhaps protactinium from molten salt, work on molten-salt methods is finished. The final study in the pilot plant was a demonstration of the recovery of uranium from fully irradiated, short-decayed aluminum-base fuel elements.

The AEC has announced a goal of having a fluoride-volatility technology for processing low-enrichment UO_2 fuel completely developed through "cold" engineering, "cold" semiworks, and "hot" pilot-plant programs by July 1, 1969. Our principal contribution to this effort will be the installation and operation of a fluidized-bed volatility pilot plant in Building 3019. First priority in pilot-plant experiments will be given to studies of the HCl process for removal of Zircaloy cladding as developed at Argonne National Laboratory. Design of the pilot plant has begun. Supporting laboratory- and bench-scale studies are also being conducted. Thus far, laboratory studies here have been mostly concerned with the use of $HF-O_2$ for removing stainless steel cladding from UO_2 fuel elements. The retention of plutonium by alumina was studied in a miniature test reactor only $\frac{1}{2}$ in. in diameter.

2.1 Molten-Salt Processing of Uranium-Aluminum Alloy Fuel

Development of a molten-salt fluoride-volatility process for aluminum-base fuels has been completed. Phase-diagram data for the system $KF-ZrF_4-AlF_3$ have been refined in the region of interest. The effect of NaF addition to waste salt was determined. Finally, a pilot-plant development program was essentially completed. This program culminated in the processing of fuel cooled only 25 days.

The molten-salt fluoride-volatility process consists in dissolution of fuel elements in a molten fluoride salt, fluorination to separate the uranium (as UF_6) from the salt and most of the fission products, and further purification and recovery of the UF_6 . The process proved satisfactory in

pilot-plant operations. Uranium losses ranged from 0.1 to 0.9%, and averaged about 0.6%. Decontamination from fission products was quite good. In one run, decontamination factors were generally in the 10^3 to 10^7 range; in all other runs, they ranged from 10^6 to 10^{10} . Chemical purity of the product UF_6 was lower than desirable; principal contaminants were fluorides of molybdenum, aluminum, and sodium. Dissolver corrosion during the program was about 5 mils, consistent with previous experience. The release of radiation emitters to the atmosphere and the radiation dosage to personnel were controlled satisfactorily, even though decay at the time of processing was less than would normally be expected.

2.2 Volatilization of PuF_6 from Molten Salts Containing High Concentrations of Uranium

The volatilization of plutonium is an essential part of a molten-salt volatility process for low-enrichment fuel. Although PuF_6 recoveries greater than 99% have been demonstrated in previous laboratory tests, 20 to 30 hr of fluorination was required. This presents a serious corrosion problem. A possibly useful method for shortening the time required for volatilization would be the maintenance of a high concentration of uranium in the melt by using a UF_6-F_2 mixture during fluorination. In one test, with a melt containing initially 25% uranium, 32% of the PuF_6 was evolved in 1 hr of fluorination, compared with about 15% in a previous test with no uranium present. These results, however, were not encouraging enough to warrant further study.

2.3 Recovery of Plutonium and Uranium from Falling Molten-Salt Droplets and from Beds of Solid Particles by Fluorination

Additional laboratory development work was conducted to test the feasibility of recovering fissile material from molten-fluoride mixtures by spraying the melt downward into fluorine gas at high temperatures. Such a method would reduce corrosion and achieve the large ratio of fluorine gas to molten salt that is necessary for rapidly recovering plutonium from power-reactor fuels. This type of molten-salt-gas contactor may also be useful in a continuous processing scheme.

In uranium fluorinations, volatilization of more than 99.9% of the contained uranium was achieved with molten-salt droplets 150 μ or less in diameter. Fluorinations were made in a tower 5 ft long, and the temperatures were between 550 and 650°C. Fluorinations of five salt blends have been completed. A correlation equation applicable to this type of uranium fluorination is presented.

As to plutonium fluorination, five experiments were made in which plutonium was volatilized from falling droplets of 50-50 mole % NaF-ZrF₄ containing initially 0.258 or 0.0026 wt % plutonium as PuF₃. The extent of the best removal was 87.6% for 75- μ drops at 640°C. These drops had a residence time of about 7.3 sec in the 52-in.-long fluorination section of the falling-drop column. The degree of plutonium removal was independent of the initial plutonium concentration. An equation based on diffusion control is presented for correlating the plutonium data.

Another possible method for recovering uranium from fluoride salt without excessive corrosion consists in fluorinating static beds of particles. In laboratory tests, about 99% of the uranium was removed from spheres, 60 to 150 μ in diameter, by fluorination for 2 to 3 hr at temperatures between 450 and 480°C (solidus temperature, 512°C). However, during fluorination, the salt sintered into a hard, porous mass. Thus, fluorination of solid particles does not compare favorably with the spray-fluorination scheme and will not be investigated further.

The work with uranium is now complete; after a few more experiments, the plutonium work will be terminated. A few similar experiments with protactinium will be made in the near future. We conclude that although plutonium is more difficult to volatilize from a falling drop than uranium, falling-drop fluorination is a chemically feasible method for recovering plutonium and uranium from molten fluorides.

2.4 Fluidized-Bed Volatility Process Development for Stainless Steels and Zircaloy-Clad UO₂ Fuels

Bench-scale laboratory studies have been carried out in support of development of fluidized-bed volatility processing from low-enrichment UO₂ fuel clad in Zircaloy-2 or stainless steel. These studies have been mainly of chemical and physical effects observed in the use of HF-O₂ as a declad-

ding agent for either Zircaloy or stainless steel, and of plutonium and uranium volatilization in the subsequent fluorination treatment. A small fluidized bed was developed to expedite some of the tests. This mini-test unit is 1/2 in. in diameter and uses only about 5 to 8 g of bed material.

Use of HF-O₂ mixtures for decladding stainless steel or Zircaloy-clad fuel results mainly in sintered oxides that convert only slowly to the corresponding fluorides. The oxides retain to a large extent the shape of the original metal. Treatment with fluorine rapidly converts the "stainless steel" oxides to the fluoride form, with accompanying complete physical degradation to a fine powder; for ZrO₂ this is not so. Extensive volatilization of chromium fluoride occurs while fluorinating stainless steel residue.

The presence of 10% or more of stainless steel residue in a fluidized bed of alumina hinders fluidization during the fluorination period. This is also true of UO₂ when it is first hydrofluorinated to UF₄ or UO₂F₂ in the HF-O₂ decladding treatment and then fluorinated in a second step. Presumably the presence of a high fluoride content in the alumina bed promotes sintering and caking.

Good plutonium-volatilization results were obtained with alumina beds spiked with PuO₂, although the temperature of fluorination is quite important. Recoveries of better than 99.5% were demonstrated in short-time tests at and below 500°C. At higher temperatures (up to 650°C), diffusion of lower plutonium fluorides (PuF₃ or PuF₄) into the alumina leads to greater plutonium retention in the bed, at least in short-cycle testing.

Further development studies will be of factors affecting plutonium and uranium retention in the decladding-fluorination reactor. A related study is also planned of the factors that cause the bed material to sinter or cake.

2.5 Design of a Fluidized-Bed Pilot Plant for Zirconium- and Stainless-Steel-Clad UO₂ Power-Reactor Fuels

A fluidized-bed fluoride-volatility pilot plant is being designed to study the processing of UO₂ power-reactor fuels at high levels of radioactivity. These studies will be made to obtain data needed to design a full-scale commercial plant.

First priority will be given to processing Zircaloy-clad UO₂ by reaction with HCl, followed by

a two-zone oxidation-fluorination step. The use of HF-O_2 is preferred for decladding and oxidizing stainless-steel-type fuels. If results of earlier developmental studies are favorable, the use of HF-O_2 will also be studied for processing zirconium-clad fuels. Although the method for separating UF_6 , PuF_6 and volatile fission products is not definite at present, thermal decomposition of PuF_6 to solid PuF_4 , followed by distillation of the UF_6 and volatile fission product fluorides, is presently favored. A possibility exists that BrF_5 vapor will be used instead of fluorine to volatilize only the uranium, thus effecting an early separation of the uranium from the plutonium. The plutonium would later be converted to PuF_6 by fluorine.

The facility is sized for a charge of about 40 kg of UO_2 and 200 g or more of plutonium, depending on nuclear-safety limitations. The primary reactor will be 8 in. in inner diameter.

Several design studies are under way, and design and layout for major head-end equipment items are progressing. Engineering of instrumentation has begun, as has development of a critical-path schedule.

Modifications to improve the containment features of the Building 3019 penthouse have been designed, and craft work is about to begin.

2.6 Sorption of PuF_6 by Metal Fluorides

A possible method for recovering PuF_6 in fluoride-volatility processing might consist in the use of solid sorption similar to the manner in which UF_6 is trapped on NaF . Accordingly, the sorbability of PuF_6 on a large number of inorganic fluorides and alumina was examined. As yet, no sorbent has been found from which desorption is feasible, at least up to 500°C . All the alkali and alkaline-earth fluorides, with the exception of MgF_2 , sorbed significant amounts of PuF_6 , indicating the existence of stoichiometric complexes. Fluorides of other elements showed that sorption was greater at higher temperatures.

The most highly developed sorbent, NaF , has been used at 325 to 400°C with a high degree of success in quantitatively sorbing PuF_6 from a stream of UF_6 and fluorine, but efforts to desorb the plutonium at temperatures up to 600°C in dynamic tests have been unsuccessful. A high

concentration of fluorine is required in the UF_6 - PuF_6 gas stream passing through an NaF bed at 325 to 400°C to prevent formation of an NaF-UF_5 complex.

2.7 Sorption of UF_6 by NaF

Sodium fluoride is used to separate UF_6 from other volatile fluorides by a process of selective sorption-desorption. Sorption data for $\text{UF}_6\cdot\text{NaF}$, $\text{WF}_6\cdot\text{NaF}$, and $\text{MoF}_6\cdot\text{NaF}$ that will be useful in defining separations-process conditions are reported. The capacity and durability of NaF pellets made at the Paducah Gaseous Diffusion Plant (for about $\$1/\text{lb}$) were compared with the values of these properties determined for the pellets purchased from Harshaw Chemical Company at $\$5/\text{lb}$. Performance of the two types was the same.

2.8 Continuous In-Line Monitoring of Gas Streams in Fluoride-Volatility Processing

For proper control of the various phases of the fluoride-volatility processes, continuous in-line monitoring devices must be developed for use with multicomponent corrosive gas streams. A spectroscopic method for UF_6 determination and a gas chromatographic method for hydrofluorinator off-gas monitoring are being developed.

The feasibility of using ultraviolet spectrometry to continuously monitor UF_6 concentrations in gas streams was studied preliminarily in the laboratory. The absorption coefficient of UF_6 at 3686 \AA was found to be $5.5 \text{ liters mole}^{-1} \text{ cm}^{-1}$ for the pressure range 10 to 100 mm Hg . An approximate value of $3610 \pm 1000 \text{ liters mole}^{-1} \text{ cm}^{-1}$ for the absorption coefficient was determined at 2140 \AA for a previously unreported absorption peak. More work is needed before this method can be utilized.

2.9 Vapor-Liquid Equilibria of $\text{UF}_6\text{-NbF}_5$ System

As a part of continuing studies on fluoride volatility methods of reprocessing nuclear fuels, the separation of UF_6 from volatile impurities by distillation is being considered. For this reason, the vapor-liquid equilibria of UF_6 and one such impurity, NbF_5 are being determined. The 150°C isothermal equilibrium curve was determined from total-pressure-liquid-composition measurements,

and an isobaric (6 atm) equilibrium curve is being determined by direct measurements of vapor and liquid compositions. The critical constants of NbF_5 are being determined.

2.10 Phase Equilibria Studies Pertinent to Fluoride-Volatility Processing of Fuels or Mixtures Containing Chromium

Studies of phase equilibria of systems containing CrF_3 were conducted in attempts to establish a suitable mixture of molten fluorides for use as a solvent in the processing of stainless-steel-clad or -base fuels. Attention was focused on the solubility of one constituent, chromium, and information was obtained specifically on the $3\text{LiF} \cdot \text{CrF}_3$ - $3\text{KF} \cdot \text{CrF}_3$ and $\text{NaF} \cdot \text{CrF}_3$ systems. The latter was of special interest because of the use of NaF as a sorbent for the volatile chromium fluorides formed in volatility processing, and further work on this aspect of the process will be continued. No additional work on the development of molten-salt solvents for "stainless steel" fluorides is planned because of the emphasis on the use of fluidized-bed reactors.

2.11 Volatilization of UF_6 from Sol-Gel-Derived $\text{ThO}_2\text{-UO}_2$

A possible method for recovering uranium from thorium-uranium sol-gel microspheres would consist in the direct fluorination of the uranium from the oxide at high temperature. A small-scale examination of this possibility initiated during the past year demonstrated that spheres 149 to 210 μ in diameter containing 3.9 wt % uranium cannot be successfully fluorinated at reasonable temperatures. Treatment for 3.5 hr at 650°C removed only 15% of the uranium.

2.12 General Corrosion Studies

The relatively high rate of corrosion of both the hydrofluorinator (dissolver) and the fluorinator is a serious deficiency of the molten-salt fluoride-volatility process. Work was continued on introducing an inert gas just below the surface of the molten fluoride to help reduce corrosion of the hydrofluorinator at the molten-salt-gas interface. A melt of 52-37-11 mole % NaF-LiF-ZrF_4 at 650°C

was used for all tests because of its exceptionally high degree of corrosivity. The results of experiments with coupons in the 4-in.-diam containers showed that conditions could be obtained for definitely reducing corrosion. Argon and helium were the most effective sparge gases. In the individual 2-in.-diam containers, however, only slight protection was obtained.

Because of the reorientation of the overall program toward fluidized-bed processes and the indifferent results of the experiments, corrosion studies as related to molten-salt processes were discontinued.

3. WASTE TREATMENT AND DISPOSAL

3.1 Conversion of High-Level Radioactive Wastes to Solids

Engineering Studies. — Development of methods for converting high-level radioactive liquid wastes to solids using simulated wastes was continued. The development of the pot calcination processes was successfully completed with tests in 16-in.-diam pots which confirmed the mathematical model for predicting filling rates as a function of pot diameter. Two successful Rising-Level Potglass tests were made using simulated Purex waste at processing rates equivalent to the rate of waste production from a plant processing 2 tons of uranium per day. These tests were made with an induction heating furnace. Based on present operating experience at ORNL with resistance and induction heating furnaces, resistance heating is recommended for use with pot systems.

An initial test of the continuous process in a 20-in.-diam horizontal continuous melter using a resistance furnace was successful from an operational viewpoint. However, the melter failed due to excessive corrosion after 250 hr of operation. Further development of this process has been terminated for the immediate future.

High-Level Radioactive Waste Disposal: Laboratory Studies. — A computer code was developed for retrieving and correlating the mass of data generated in the program for developing glassy melts for the fixation of high-level wastes. Initial readout was obtained on ORNL melt compositions. Compositions received from Hanford will also be included in the code. Melts were prepared which contained up to 32% total waste oxides, including

simulated fission products expected from fuel irradiated as high as 35,000 Mwd/metric ton. These materials melt at about 800°C and are sufficiently fluid at 850 or 900°C to permit their use in a continuous melting process. Melts containing Purex FTW-65 waste with simulated fission products from a fuel burnup of 10,000 Mwd/metric ton were successfully run in semiengineering-scale continuous melters. In these tests, phosphate volatility was generally <0.5%, sulfate volatility <5.0%, molybdenum volatility 1 to 2%, and iron and ruthenium volatilities 20 to 30%. Some anomalous results were observed.

Corronel 230, 50% Ni-50% Cr, Inconel, and Nichrome V show some possibility as substitutes for platinum as a material of construction for a continuous melter. Corrosion tests are still in the early stages. A thermal conductivity probe was developed for the measurement of levels of solution, calcine, and glass in the rising-level (RL-Potglass) process.

Pilot Plant Design. — Active liaison with Hanford personnel on the design and startup of the pot calcination phase of the Hanford Waste Solidification Engineering Prototypes has continued. The equipment is being tested to verify the design before installation in the Hanford Fuels Recycle Pilot Plant in August of 1965. Design studies conducted recently include pressure transients in the pot calciner off-gas line, thermocouple selection for the calciner and furnace, the composition of Nuclear Fuel Services wastes, a review of the furnace design, and participation in the scheduling of runs for the hot pilot plant experiments.

3.2 Disposal of Intermediate-Level Radioactive Waste

Nuclear installations generate large volumes of intermediate-level radioactive wastes, such as evaporator concentrates, second- and third-cycle solvent extraction raffinates, and slurries or solids (residues from low-level treatment processes). A process has been developed for incorporating these wastes in emulsified asphalt. Use of free-flowing emulsified asphalt permits mixing of wastes and asphalt at ambient temperature or above.

Asphalt products containing 20 to 80 wt % solids from waste have been prepared from simulated ORNL waste-evaporator bottoms. Leach rates for ^{137}Cs and sodium were $5 \times 10^{-4} \text{ g cm}^{-2} \text{ day}^{-1}$

after about six months. The leach rate for ^{106}Ru was $7 \times 10^{-6} \text{ g cm}^{-2} \text{ day}^{-1}$ after six months. The products showed sufficient radiation stability to a dose of 10^8 rads. Leach rates were not affected by this radiation dose.

Design of a pilot plant to incorporate 100 gal of ORNL waste-evaporator bottoms in emulsified asphalt per 8-hr shift has been completed and installation started.

3.3 Treatment of Low-Level Radioactive Wastes

Scavenging-Precipitation Foam-Separation Process. — Pilot Plant Studies. — The Scavenging-Precipitation Foam-Separation process for treating low-level radioactive waste water was studied on a pilot plant scale — 300 gal/hr for scavenging-precipitation and 120 gal/hr for foam separation. The process consists in (1) precipitating calcium, magnesium, and radiation emitters in a sludge-blanket clarification step that includes the use of Grundite clay for sorption of cesium and (2) achieving further decontamination in a countercurrent foam column. The foam-separation equipment includes a 2-ft-square by 8-ft-high countercurrent foam column, three 2-ft-square foam stripping columns in series for recovering surfactant from the decontaminated waste, an air-recirculation system to provide air for foam generation, a centrifuge foam breaker, and three orifice foam breakers.

It was more difficult to generate a stable foam in the pilot plant foam column than it was in the smaller columns (maximum diameter, 6 in.) used for laboratory and engineering studies. The foam section was baffled to prevent foam circulation by filling the countercurrent section with 1.5-in.-diam by 1.5-in.-long Pall rings, and the concentration of surfactant in the liquid pool at the bottom of the column was kept much higher than it had been in the smaller columns. Under these conditions the foam column alone provided strontium decontamination factors of up to 200, compared with factors of less than 20 found previously.

The strontium decontamination factors were proportional to the parameter V/LD (where V and L are gas and liquid flow rates, respectively, and D is an effective bubble diameter), as in the laboratory studies. The use of the parameter V/LD as a basis for process control appears valid for a large system even though the foam contains bubbles that vary widely in size.

A test of the entire process was made that lasted 93 hr at steady state. The overall decontamination factors were 1050, 8, 4.2, 1.3, 20, 2.2, and 50 for Sr, Cs, Ru, Co, Ce, Sb, and Zr-Nb respectively. The concentrations of these elements in the treated product, in terms of percentage of the maximum permissible concentration in water, were 2, 0.6, 0.3, 0.1, 0.2, 0.02, and 0.0001 respectively. Thus, the process is suitable for use at many nuclear installations where low-level radioactive wastes contain comparable amounts of radioactivity. The scavenging-precipitation equipment was operated at a feed rate of 5 gpm and the foam-separation system at 2 gpm. The ratio of the volume flow rate of the liquid feed to the volume flow rate of the condensed foam was 31. The capacity of the foam separation system is apparently limited by the low capacities of the air-supply equipment and the centrifugal foam breaker now in use.

Laboratory Studies. — The two-step process for decontaminating low-level radioactive waste water (LLW) was tested. This process consists in precipitating and eliminating most of the hardness (calcium and magnesium) and radioactivity in a suspended-bed sludge column and producing further decontamination in a foam column having an 80-cm-high countercurrent section. Overall decontamination factors for Sr, Co, Ru, and Ce were $>3.7 \times 10^3$, 2.3 to 4, 2 to 5, and 50 to 180 respectively. The cesium decontamination factor was 20 when 60 ppm of Grundite clay (baked at 600°C for 20 min) was added to the LLW during the precipitation step. The height equivalent to a theoretical stage for strontium removal in the foam column was about 3 cm. The ratio of surface to liquid flow rate is the crucial factor governing satisfactory strontium decontamination in the foam column. The metal-ion decontamination factor in the foam-separation step is proportional to the ion distribution coefficient and inversely proportional to the volume reduction and liquid throughput. In the search for biodegradable surfactants, two were found that exhibited very good removal of strontium from solutions. Fast and economical analytical methods for the determination of surfactants and radionuclides in LLW were developed and tested.

Water-Recycle Process. — A Water-Recycle Process is being developed for low-level radioactive waste (LLW) treatment. It is based on the demineralization of all water entering a nuclear

installation. Then, after passage through an atomic installation, the water would be decontaminated, demineralized, and recycled for reuse. Feasibility studies were made in the laboratory with neutral ORNL LLW. The system included: (1) clarification of LLW using zeta-potential-controlled additions of coagulant (alum) and coagulant aid (activated silica), (2) demineralization and decontamination of the supernatant by cation-anion ion exchange (Dowex 50W-Dowex 1), and (3) treatment with a column of activated carbon. Demineralization capacity (0.1% specific conductance breakthrough) is expected to be as high as 2500 volumes. Breakthrough of some radionuclides occurred either simultaneously with bulk ionic breakthrough or soon after, as indicated by specific-conductance measurements. Thus, continuous monitoring of specific conductance could be a convenient indicator of bed exhaustion. Overall decontamination factors (DF's) ranged from 10^2 to 10^4 for individual activities. For ^{90}Sr and ^{137}Cs , the DF's were comparable to or better than those obtained in the Scavenging-Precipitation Ion-Exchange process; for ^{106}Ru and ^{60}Co , the DF's were 10 to 1000 times higher. Thus, the proposed system appears very promising.

Selective Sorption of Phosphates on Activated Alumina. — To make the scavenging-precipitation ion exchange process economically attractive, phosphates, which interfere with the precipitation step, were removed by sorbing them on activated alumina. For example, results of experiments with tap water spiked with normal and dehydrated phosphates showed that when the water is passed downflow through Alcoa F-1 activated alumina, more than 99% of the normal phosphate can be removed from 3000 bed volumes (BV) when the phosphate concentration is 5 ppm. Dehydrated forms of phosphate were removed to a greater extent. The volume reduction factor (BV of product water per BV of regenerant waste) was 2000, a very favorable ratio of throughput to regenerant waste. Of the aluminas tested, the F-1 grade was best.

The simplicity and low cost of the process may make it attractive for removing phosphates from water streams that have been polluted with phosphate builders used in household detergents. Increased levels of phosphates interfere with standard water-treatment procedures and contribute to greater taste and odor problems in potable water.

3.4 Engineering, Economic, and Safety Evaluations

A detailed estimate of the costs of "perpetual" tank storage of wastes from processing power reactor fuels is being undertaken to establish a basis for comparison with costs for alternate waste management schemes. In this study the concept of double containment of radioactivity is applied throughout, and in all instances the design and operation of the facility emphasize safety over any potential savings in costs.

Storage of Purex and Thorex solvent extraction raffinates as both acid and alkaline solutions is considered, and storage of Zirflex and Sulfex de-cladding wastes in alkaline form is postulated. Tanks are enclosed in steel-lined concrete vaults for secondary containment and are similar to those at Savannah River. Decay heat is removed by circulating water through banks of coils submerged in the waste.

The estimated capital costs of tank farms for storing acid raffinate waste range from \$21 million to \$47 million, and farms for storing alkaline raffinate cost from \$27 million to \$50 million. In terms of the electricity originally produced from the fuel, the costs are 0.007 to 0.015 mill/kwhr and 0.009 to 0.016 mill/kwhr for acid- and alkaline-waste farms respectively. These costs are to be used in a computer code that calculates the total present-worth storage costs based on the optimal tank size for a given rate of interest on capital and return on investment.

4. TRANSURANIUM ELEMENT PROCESSING

The High Flux Isotope Reactor (HFIR) and the Transuranium Processing Plant (TRU) have been built at ORNL to produce large quantities of the heavy actinide elements as part of the USAEC Heavy Element Production Program. These materials will be used in basic research in laboratories throughout the country. The HFIR is scheduled to go critical by August and to power by December 1965, while the installation of equipment in the TRU should be completed and startup preparations under way by the same date. Special irradiations of the available ^{242}Pu , being done in a Savannah River production reactor this year, will produce a few milligrams of californium prior

to the operation of the HFIR. Up to a milligram will be recovered in the Curium Recovery Facility beginning in January 1966, and the remainder will be processed through the TRU a few months later. Design and development work on the target elements, to be remotely fabricated in the TRU, is under the direction of the Metals and Ceramics Division. The major phases of the project, including design and construction of the building, the development of the chemical separations processes, and the design, fabrication, and installation of the chemical process equipment are the responsibilities of the Chemical Technology Division and are reported here.

4.1 Development of Chemical Processes

During the past year the recovery and decontamination of americium and curium were demonstrated at full-scale radioactivity levels in the Curium Recovery Facility (CRF); in addition, americium and curium were further purified by LiCl anion exchange and separated by the carbonate precipitation method. This work, as well as laboratory support given to CRF processing, is reported in Chapter 5. Investigations were continued on developing and testing techniques for intra-actinide separations by ion exchange; additional ^{242}Pu was converted to dense oxide and incorporated into HFIR targets; and sol-gel methods for preparing actinide oxides suitable for HFIR targets were studied.

An adequate solvent extraction process to separate transcalifornium elements is not available, and chromatographic elution from cation resin with α -hydroxyisobutyrate solution has been the only reliable method for separating californium, einsteinium, and fermium from each other. Since scale-up of this process to 10- to 100-mg quantities may be complicated because of disturbance of the resin bed by radiolytic gases, additional separation methods would be desirable.

In an effort to develop a new separation system, the anion exchange behavior of the transcurium elements with ethylenediaminetetraacetic acid (EDTA) and other actinide complexing agents was investigated. It was demonstrated that EDTA anionic complexes of the heavy actinides, loaded on anion exchange resin, can be used in a separation scheme. Einsteinium-californium and fermium-einsteinium separation factors of 1.41 and 1.90

were achieved; in a laboratory demonstration of the process, an einsteinium product fraction was obtained which contained 99% of the einsteinium and no detectable californium or fermium.

The dissociation constants of lanthanide complexes with 1,2-diaminocyclohexanetetraacetic acid (DCTA) corresponded to cation exchange separation factors of 2.0 to 2.5 between adjacent heavy lanthanides and indicated that DCTA might be useful in obtaining transcurium element separations by cation exchange. The dissociation constants of the DCTA complexes with Am, Cm, Bk, Cf, Es, and Fm were therefore determined. However, it was found that unlike the heavy lanthanide elements, the Cf, Es, and Fm dissociation constants are not appreciably different in this system; cation exchange separation factors of only 1.23 for Es/Cf and 1.35 for Fm/Es could be obtained.

High Flux Isotope Reactor targets will be made from pressed pellets of aluminum powder and actinide oxide, and it is essential that the aluminum phase be continuous in order to ensure satisfactory heat transfer during irradiation. When very fine actinide oxide particles are mixed with -325 mesh aluminum powder and pressed into cermets, the oxide phase is continuous and the thermal conductivity of the pellet is low. But, with oxide particles ranging from 20 to 200 μ in diameter, the aluminum phase will be continuous, and conductivity will be satisfactory for irradiation in high neutron fluxes.

A process employing hydroxide precipitation for preparing dense, coarse particles of PuO_2 has been reported previously; during this past year the process was used to prepare 180 g of ^{242}Pu as PuO_2 for incorporation into 18 HFIR targets. These targets are being irradiated at the Savannah River Plant.

As part of the preparation of PuO_2 by hydroxide precipitation, the dried oxide must be ground and screened, about 25% of the resulting particles are less than 20 μ in greatest diameter and must be recycled. Preparation of PuO_2 by a sol-gel method would eliminate the dissolution and valence adjustment necessary for recycle, and the preparation of uniform microspheres from a plutonium sol would eliminate grinding and screening. For these reasons, efforts to prepare plutonium sols have continued, and sphere-forming techniques have been investigated. This work is still in progress; however, stable plutonium sols have been prepared in the laboratory, and plutonium sols have been

used to prepare uniform microspheres that densify when fired.

For similar reasons, a sol-gel method for preparing americium and curium oxide for incorporation into HFIR targets would be convenient, and laboratory efforts to prepare lanthanide sols as stand-ins for americium and curium have been initiated. Stable lanthanide sols capable of producing dense microspheres have been made, and the methods will be evaluated for the production of americium and curium sols.

4.2 Development of Process Equipment

Engineering studies of the process equipment are continuing in order to test equipment, make necessary modifications, and develop operating procedures. Remote mechanical handling tests of equipment racks and components in a full-scale mockup of the processing cell are nearly complete.

Flowsheet tests of the Tramex solvent extraction process for separating actinides from lanthanides were conducted in glass pulsed columns. Extraction of americium was consistently good; the loss was less than 0.1%, and the stage height was 6 to 10 in. Scrubbing of europium was efficient, confirming previous tests (decontamination factor greater than 2000). In the stripping column an unexpectedly high loss of americium caused by entrainment in the waste organic was noted. This loss was reduced to acceptable values by increasing the concentration of hydrochloric acid in the strip reagent from 1 to 4 M.

The first phase of the hydraulic testing of the full-scale metal columns was completed. After temporary modification of lines and flow elements, design flow rates were attained, and good control of feed rates and interfaces was possible.

4.3 Design and Fabrication of Process Equipment

The TRU facility will be equipped with two solvent extraction cycles; a head-end system, including a dissolver; feed-adjustment tank and centrifuge for feed clarification; ion exchange columns for cleanup and special separations; and miscellaneous equipment.

Design of the equipment is nearing completion, and shop fabrication of the components and connecting jumper piping is nearly 80% complete. The

only equipment not yet designed is that for separating the heavy actinides (californium, einsteinium, fermium) from each other and the equipment for preparing curium oxide for the recycle rods. This design of the equipment, just started, has been held up pending completion of flowsheet development.

4.4 Construction of the Transuranium Processing Plant

The Transuranium Processing Plant was completed in late May, twenty-three months after start of construction and six weeks beyond the scheduled completion date. No major problems arose. Installation of the process equipment is just under way and should be completed by late fall.

5. CURIUM PROCESSING

A joint program between the Isotopes Division and the Chemical Technology Division was established to produce curium heat sources for use in thermoelectric converters. The Chemical Technology Division is responsible for providing process technology, facilities, and operations to isolate gram amounts of curium. Nearly 17 g of ^{244}Cm was purified, separated from ^{243}Am , and transferred to the Isotopes Division for incorporation into an experimental heat source and for distribution to other AEC installations. Six irradiated targets of $^{241}\text{AmO}_2$ in an aluminum matrix were also processed to separate ^{242}Cm from the aluminum and fission products, but not from residual americium. To date, 3.56 g of purified ^{242}Cm has been delivered to the Isotopes Division, and another 14 g will be processed early next fiscal year.

5.1 Process Development

The chemical processes for isolating curium include dissolving the target in dilute hydrochloric acid; using the Clanex process to convert certain feed solutions from the nitrate form to the chloride and/or to remove aluminum; using the Tramex process to separate americium-curium from fission products; and precipitating Am^{5+} (as a double carbonate) to separate it from curium. Most of the laboratory development and testing of these processes was completed last year, and process

development during this report period was confined to problems associated with full-scale processing in the Curium Recovery Facility at high levels of radioactivity.

As to process improvements, the entrainment of product during stripping operations in the Tramex and Clanex processes was markedly reduced by increasing the mixer speed and the ratio of the strip and solvent volumes.

Other laboratory studies indicated that the solubility of the rare earths exceeds 44 g/liter in a feed solution 12 M in LiCl, 0.2 M in HCl, and 0.1 M in SnCl_2 . That concentration of rare earths is not expected to be reached in any of the feed solutions. Also, the radiolysis of feed solutions and the consequent oxidation of cerium to the tetravalent (extractable) state were studied. It was found that methanol does not consistently prevent radiolysis nor the oxidation of trivalent cerium, both of which must be avoided as much as possible. Other studies showed that ^{244}Cm - ^{243}Am solutions received from the Savannah River Plant can be processed, even when the sodium nitrate content is as high as 0.5 M.

5.2 Curium Recovery Facility: Equipment and Flowsheet Testing

Further changes were made in the process equipment to incorporate piping and vessels made of more suitable structural materials. Cold testing was completed, and hot operation began in November 1964. During five months of hot operation with radioactive feed material, the equipment performed quite well, with the exception of several failures of the mixer-settler drive train and several failures of the feed transfer pump.

Changes in the flowsheets were made to overcome problems arising from Zircaloy-2 corrosion products, interfacial solids, excessive solvent extraction losses, cerium oxidation and extraction, and the radiolytic effects of high power densities.

Final forms of the flowsheets were satisfactory for processing ^{244}Cm and were suitable for processing ^{242}Cm up to a limit of 6 w/liter (0.05 g/liter) in the chloride (Tramex) system. In the nitrate system (Clanex), power density was not limiting up to 16 w/liter. It is hoped that higher power densities can be achieved in the chloride system with more development, thus permitting a greater capacity for ^{242}Cm . Contrary to expectations,

adding methanol to the Tramex feed failed to inhibit radiolysis of the free acid and did not prevent gassing. This is believed to be due to the presence of impurities such as iron, nickel, and copper in the actual process solutions but not present in the laboratory experiments.

5.3 Solvent Extraction Processing of ^{243}Am and ^{244}Cm

In the initial processing campaign of the Curium Recovery Facility, 24 g of ^{244}Cm contaminated with about 100 times that amount of rare earths was processed; 19 g of product was recovered. About 19 g of ^{243}Am was also recovered. Decontamination factors of over 1000 for the rare earths were achieved in one cycle when SnCl_2 was used as a reductant for Ce(IV) formed by radiolysis; methanol was ineffective in inhibiting acid destruction and gassing in the feed solutions. The americium-curium mixture was transferred to cell 3 of the Curium Recovery Facility, where it was further purified and the ^{244}Cm was separated from the ^{243}Am .

5.4 Ion Exchange Purification and Separation of ^{243}Am , ^{244}Cm

During initial solvent extraction processing, americium-curium product was obtained which required additional purification. Glass ion exchange equipment was installed in cell 3 of the Curium Recovery Facility, and additional decontamination was obtained by LiCl anion exchange. In addition, ^{244}Cm was separated from ^{243}Am by precipitating americium as $\text{K}_3\text{AmO}_2(\text{CO}_3)_2$.

A total of 16.6 g of ^{244}Cm was purified by ion exchange, separated from ^{243}Am , and transferred to the Source Fabrication Facility of the Isotopes Division for incorporation into an experimental heat source and for distribution to other AEC laboratories. The ^{243}Am was converted to the oxide, most of which was also distributed to other AEC laboratories for use in research programs. An additional 1.9 g each of ^{244}Cm and ^{243}Am were purified and will be used for process development.

5.5 Processing of $^{241}\text{AmO}_2$ Targets

Six targets of irradiated AmO_2 containing a total of 6.75 g of ^{242}Cm were processed for recovery of

the curium and residual ^{241}Am . During processing, 1.31 g of ^{242}Cm decayed. Of the remaining 5.44 g, 3.56 g of high purity was sent to the Isotopes Division and 1.13 g, mostly recycle material, was saved for process-development studies. Radiolytic destruction of the SnCl_2 reductant was much too great at power levels above 6 w/liter. For example, at higher radiation levels the solutions could be processed without mechanical difficulties, but cerium could not be separated from the actinides.

5.6 Development of Alternative Processes: Separation of Lanthanides and Actinides

The Talspeak process separates trivalent actinides from lanthanides and many other elements by two cycles of extraction with di-(2-ethylhexyl)-phosphoric acid (HDEHP) from lactic acid solutions containing sodium diethylenetriaminepentaacetate (Na_5DTPA). Neodymium is the least extractable lanthanide and californium apparently the most extractable trivalent actinide, slightly more so than einsteinium and fermium. Laboratory tests of a flowsheet designed for processing feed solutions containing high concentrations of lanthanum were successful in separating americium from nearly all contaminants. Preliminary tests indicate excellent removal of contaminants in feed preparation by extraction with tributyl phosphate followed by stripping with lactic acid.

6. DEVELOPMENT OF THE THORIUM FUEL CYCLE

The Thorium Fuel Cycle work is part of the Thorium Utilization Program of ORNL. The overall objective is the development of the fuel-cycle technology required for economical power production in thorium-fueled reactors. Much of the work carried out in this program by the Chemical Technology Division has been in close cooperation with the Metals and Ceramics Division. Oxide fuels and the preparation of microspheres of those fuels are being emphasized, but some work on preparation of thorium-uranium carbides and other systems is being carried out to exploit the versatility of the sol-gel process.

6.1 ^{233}U Storage and Distribution Facility

During the past year, design of a ^{233}U storage and purification facility was completed and installation was begun. Storage wells for solids such as $^{233}\text{U}_3\text{O}_8$ in amounts up to about 100 kg of ^{233}U have been installed, and tanks and other equipment for liquid storage are being made and installed. With the purification facility (1 kg of ^{233}U per day) being fabricated and the existing solvent extraction system used for Thorex process demonstration, a versatile intermediate-scale facility for producing ^{233}U highly purified from all but isotopic impurities and attendant decay products is now available.

6.2 Development of the Sol-Gel Process

In the laboratory, sol-gel process studies were carried out on methods to control the porosity of thoria and thoria-urania materials and to prepare nitrides of thorium. Experiments were also carried out to prepare zirconia by sol-gel methods.

6.3 Development of Methods for Producing Microspheres

Continuous preparation of microspheres of thoria from a 3 M thoria sol was demonstrated on an engineering scale in a tapered-column system employing a two-fluid nozzle at a thoria feed rate of 230 g of ThO_2 per hour. Over 72% of the microspheres had diameters of $230 \pm 20 \mu$, and over 85% were in the range 200 ± 50 . This represents excellent size control. In addition to the results obtained with the two-fluid nozzle, encouraging results were obtained with a rotating disperser. This kind has the advantage over the two-fluid nozzle in that it permits a significantly higher production rate.

As part of the development of a process for making microspheres, equipment for a coated-particle development laboratory was designed and installed. This laboratory was built and will be operated as a cooperative undertaking with the Metals and Ceramics Division. It includes equipment for forming, drying, calcining, and carbon-coating oxide and, eventually, carbide microspheres. Equipment is sized to produce about 5 kg/day of microspheres. At present the coater does not have that capacity, but development work under way in the Metals and Ceramics Division is directed to-

ward increasing the capacity to that level. In this laboratory, equipment and methods will be developed for the production of coated microspheres of oxides and carbides by completely remote operations. These processes will be conducted in the Thorium-Uranium Recycle Facility.

6.4 The Thorium-Uranium Recycle Facility

A major effort has been directed toward designing and getting construction started on the Thorium-Uranium Recycle Facility (TURF). Construction is under way, and completion of the entire facility is scheduled for March 31, 1967. Completion of the construction contract is scheduled for December 1966. Equipment design, construction, and testing is proceeding concurrently with the facility construction. Equipment initially installed will provide a capability for producing up to about 50 kg/day of metal-clad thorium-uranium oxide fuels. Enough space has been provided to permit installation of a versatile, close-coupled head-end processing complex and to accommodate a complete line of equipment for making coated microspheres. Equipment fabrication and operation of this facility are shared with the Metals and Ceramics Division.

6.5 Development of Equipment for TURF

In the Chemical Technology Division, equipment development and testing, beyond that being carried out in connection with the Coated Particle Development Laboratory, has centered about a vertical tube calciner for oxide to be vibratorily packed into metal fuel tubes. The calciner meets capacity, product quality, and other requirements imposed on it, but there has been a tendency for the oxide to bridge near the top of the furnace. Present efforts are directed toward solving this problem.

Equipment to simulate the TURF cells has been installed, and tests in this cell mockup have started.

7. SEPARATIONS CHEMISTRY RESEARCH

New separations methods and reagents are being developed, principally for uses in radiochemical processing but also for other purposes extending from extractive metallurgy to biochemical

separations. The current emphasis is on solvent extraction technology, although other separation methods are receiving a growing share of attention. Reagents that were developed in the former raw-materials program at ORNL have continued to show extended utility. Additional reagents have also been discovered in more recent evaluation studies. The present program in separations chemistry can be divided into three interdependent types of research activity: (1) Descriptive Chemical Studies (Sects. 7.1 to 7.7) of the reactions of substances to be separated and of separations reagents, of the controlling variables in particular separations, and of new compounds that may be potential reagents. (2) Development (Sects. 7.8 to 7.12) of selected separations into specific complete processes, both where no workable process yet exists and where existing processes are less than satisfactory, carried where warranted to the point that large-scale performance can be predicted. (3) Fundamental Chemical Studies (Sects. 7.13 to 7.18) of the equilibria and reaction mechanisms involved in separation systems, both to increase knowledge and to help define potential applications.

7.1 Extraction of Metal Chlorides by Amines

As part of a program on surveying the extraction characteristics of many metals from various systems with representative amines data were obtained for the extraction of 31 different metal ions from HCl and LiCl-0.2 M HCl solutions over the range 0.5 to 10 M total chloride. Combined with previous work, this makes a total of 60 metal ions that have been studied in these systems. With few exceptions, the extraction power of the amine for the metal varied in the order: Aliquat 336 (quaternary amine) > Alamine 336 (tertiary amine) > Amberlite LA-1 (secondary amine) > Primene JM (primary amine).

7.2 Extraction of Metal Nitrates by Amines

In survey extractions of metal nitrates by tri-laurylamine nitrate (TLA), extraction coefficients of the group IB metal ions by 0.2 M TLA in toluene decreased in this order: gold >> silver >> copper, being about 50, 0.01, and 0.0005 from 3 M HNO₃ and 10, 0.2, and 0.0001 from 12 M HNO₃. Corresponding extraction coefficients for some other

group B metal ions were 0.5 to 1 for mercury, 0.002 to 0.005 for selenium, and less than 0.001 for antimony, with little dependence on nitric acid concentration. Continued study of nitrosyl-ruthenium extraction by TLA suggested identification of the extractable species at high aqueous nitric acid concentration as HRuNO(NO₃)₄·H₂O and RuNO(NO₃)₂·2H₂O. On dilution from 12 to 3 M HNO₃, they hydrolyze to nonextractable species with first-order rate constants of 0.10 to 0.15 min⁻¹ and 0.01 min⁻¹. They are extracted to form, probably,



and



The latter is then converted to the former with a rate constant of 0.075 min⁻¹.

7.3 Reagents for Separating Polonium(IV) from Bismuth

Several types of amines and neutral organophosphorus compounds showed a potential for separating ²¹⁰Po(IV) from bismuth by solvent extraction from hydrochloric acid solutions. For example, from 8 M HCl, nearly all of the reagents studied gave efficient polonium extractions; and in some cases, the polonium-bismuth separation factor was greater than 1000. The data suggest a number of potentially practicable process flow-sheets. The development of processes would be greatly facilitated if a nonradioactive stand-in could be found for polonium. Preliminary tests indicate that tellurium will be of limited usefulness for this purpose.

7.4 New Extraction Reagents

Fourteen new substituted phenols, many of which are structurally similar to the efficient cesium extractant 4-sec-butyl-2-(α -methylbenzyl)-phenol (BAMBP), were tested for their ability to extract cesium from dilute caustic solutions. Although some of the phenols under certain conditions extract cesium more strongly than BAMBP, none appears superior to BAMBP as a process extractant.

7.5 Performance of Degraded Reagents and Diluents

Studies were continued on the stabilities of alkylbenzenes, especially diethylbenzenes, and of the reagent di-(*sec*-butyl) phenylphosphonate. The principal products of the reactions between diethylbenzene and dilute nitric acid are ethylacetophenones and α -nitroethyl ethylbenzenes. Minor degradation products include ethylbenzoic acid. Very little nitration of the benzene ring was detected. The combined products are thermally stable to 160°C as determined by differential thermal analysis (DTA). A new variation of the DTA method was used to determine an approximate value for the heat of degradation of diethylbenzene (50 to 70 kcal/mole). Degradation of a TBP-diethylbenzene solution did not lower its flash point. Tests proved that degraded impurities, and not the major degradation products, account for much of the fission product extraction power of some degraded diethylbenzenes. Commercial alkylbenzenes made from α -olefins were not as stable as *n*-nonylbenzene and diethylbenzene. Undiluted di-(*sec*-butyl) phenylphosphonate was irradiated while being stirred with nitric acid, and the fission product extraction power of the irradiated material was less than that of tributyl phosphate in a comparable test. Nitration of both reagents occurred, but the products have not yet been identified. Less than 1 part of phenol per 250 parts of the phosphonate was detected, showing little tendency for phenol formation at the potentially active site ortho to the phosphorus bond.

7.6 Biochemical Separations

A new reverse-phase column (extraction) chromatography system has been devised which affords significant fractionation of the different transfer ribonucleic acids (t-RNA's) from *E. coli*. The column packing consists of a quaternary ammonium liquid extractant, dimethyldilaurylammonium chloride in isoamyl acetate, supported on hydrophobic diatomaceous earth. The mixed t-RNA's were dissolved in the mobile aqueous phase and were sequentially eluted from the column with increasing concentration of NaCl in the eluate. Magnesium ions had a pronounced effect on the chromatographic behavior of specific t-RNA's. In one

experiment, the position of 16 specific t-RNA's in the eluate fractions was established by radiochemical amino acid biochemical assay.

A sample of mixed t-RNA's was chromatographed, and the phenylalanine-accepting t-RNA fractions were pooled and rechromatographed. The bulk of the material eluted in a symmetrical ultraviolet-absorbing peak which coincided with the phenylalanine radioactivity peak, indicating clean separation. A purity of at least 74% was calculated after making a reasonable assumption for the molar extinction coefficient of phenylalanyl-t-RNA.

Experiments are under way to prepare larger quantities of the phenylalanine-accepting t-RNA for further biochemical and physicochemical investigations.

7.7 Extraction Properties of Lanthanide and Actinide Complexes

Di(2-ethylhexyl)phosphoric acid (HDEHP) extracts lanthanum from lactic acid solutions as a lactate complex with varying ratios of lactate to lanthanum, such that the maximum loading capacity of HDEHP is about 1.5 equivalents of lanthanum per mole of HDEHP.

7.8 Recovery of Rubidium from Ores

The phenol extraction (Phenex) process, originally developed for recovering cesium from reactor wastes and from ores, was applied to recovery of rubidium from alkaline-ore leach liquors. Rubidium is extracted with 4-*sec*-butyl-2-(α -methylbenzyl)-phenol (BAMBP) in hydrocarbon diluent and stripped with dilute acid to give a pure rubidium salt.

7.9 Recovery of Beryllium from Ores

Further studies of a primary-amine extraction process for recovering beryllium from sulfuric acid digests of low-grade beryllium ores continued to give favorable results. The development of a more economical stripping method, which uses dilute ammonium fluoride solutions, has been of particular interest.

7.10 Recovery of Acid by Amine Extraction

A tentative process for recovering and purifying phosphoric acid by tertiary amine extraction was tested with a sample of commercial, wet-process phosphoric acid. Phase-separation problems, obstacles to commercial applications, were encountered.

7.11 Recovery of Thorium from Granitic Rocks

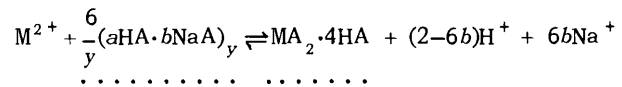
In a bench-scale demonstration of an improved flowsheet for treating granite, about 60% of the thorium and 65% of the uranium were recovered from a composite of three drill cores from the Conway formation. The thorium and uranium were dissolved by an acid-cure-percolation-wash treatment of the crushed rock and were recovered from solution by amine extraction. Processing costs for treating granite of this particular composition are estimated at about \$35 per pound of thorium-plus-uranium recovered.

7.12 Separation of Biological Macromolecules

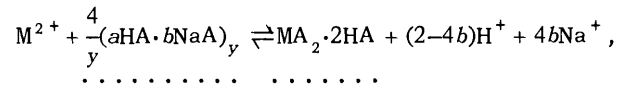
A versatile cold room for preparing large quantities of biologically important macromolecules was designed and is being built. The facilities consist of a room controlled at a temperature of about 4°C, refrigerated centrifuges, and a variety of auxiliary equipment. Initial activities will include the preparation of purified transfer ribonucleic acids (from *E. coli*), for which there is a great need in fundamental biochemical research programs.

7.13 Extraction of Alkaline Earths by Di(2-ethylhexyl)phosphoric Acid

Extraction equilibria of Be, Mg, Ca, and Ba from sodium nitrate solutions by benzene solutions of di(2-ethylhexyl)phosphoric acid (HA) were determined as functions of pH and HA concentration, in comparison with previously reported equilibria of strontium extraction. The order of extractability is: $\text{Be} \gg \text{Ca} > \text{Mg} \geq \text{Sr} > \text{Ba}$. The suggested extraction reactions (dotted underlines for organic-phase species) are



for calcium, strontium, and barium at $\Sigma A \geq 0.125 M$ and for magnesium at $\Sigma A > 0.25 M$; and



with probably some water also extracted, at lower HA concentrations for magnesium and calcium, for strontium and barium from dilute aqueous solution (0.5 M NaNO₃), and for beryllium under all conditions tested.

7.14 Intermolecular Bonding in Organic Mixtures

Qualitative and quantitative information about intermolecular association in the organic solutions of several solvent extraction systems was obtained through infrared spectra, nuclear magnetic resonance, diluent vapor-pressure depression, and dielectric constant. Association was found between tributyl phosphate (TBP) and several di(2-ethylhexyl)phosphates (SrA₂, SrA₂·4HA, NaA), and between 4-sec-butyl-2-(α -methylbenzyl)phenol and di(2-ethylhexyl)phosphoric acid, octanol-1, and acetophenone. Dielectric constants of TBP-water mixtures, measured at 2°C to obtain water contents significantly above the 1:1 mole ratio, showed a small but definite break at the 1:1 ratio, indicating that the controversial association species TBP·H₂O does actually exist, although probably very weakly bound.

7.15 Synergism in the Extraction of Strontium by Di(2-ethylhexyl)phosphoric Acid

Since previous work showed that NaA·3HA and SrA₂·4HA are principal organic-phase species in the extraction of strontium from sodium nitrate solutions by solutions of di(2-ethylhexyl)phosphoric acid (HA) alone, an obvious hypothesis to explain synergism from added tributyl phosphate (TBP) is that TBP replaces some or all of the molecular HA to form a more favorable strontium complex. This hypothesis was supported by (1) shift in the extraction maximum toward higher pH, and its relative decrease at high TBP concentration;

(2) shift of the power dependence of extraction coefficient on pH from the series of values expected for $\text{SrA}_2 \cdot 4\text{HA}$ to values expected for $\text{SrA}_2 \cdot 2\text{HA} \cdot x\text{TBP}$ and for $\text{SrA}_2 \cdot y\text{TBP}$; and (3) change of the power dependence of extraction coefficient on HA concentration from 3 (for $\text{SrA}_2 \cdot 4\text{HA}$) to 2 (consistent with $\text{SrA}_2 \cdot 2\text{HA} \cdot x\text{TBP}$). If the coordination number of the strontium ion does not change, so that TBP replaces HA 1:1, then x (above) should be 2 for the formation of $\text{SrA}_2 \cdot 2\text{HA} \cdot 2\text{TBP}$ in the synergistic extraction at low pH. Estimates of the power dependence of extraction coefficient on TBP concentration do not contradict this hypothesis, but they show nonlinear effects, indicating that some other variable not yet accounted for also varies with the TBP concentration.

7.16 Synergism and Diluent Effects in the Extraction of Cesium by 4-sec-Butyl-2-(α -methylbenzyl)phenol

Continued study of synergistic cesium extraction by 4-sec-butyl-2-(α -methylbenzyl)phenol (BAMBP) mixed with organic acids, by means of equilibrium distribution, infrared absorption, and nuclear magnetic resonance, indicates that the synergism is due to the availability of the proton from the much stronger acid for the cation exchange, while BAMBP molecules continue to provide most or all of the solvation that contributes to organic-phase solubility of the cesium. With a dialkylphosphoric acid and two carboxylic acids (HX), the principal extract species formed at low pH are probably $\text{CsHX}_2 \cdot 2\text{BAMBP}$, $\text{CsHX}_2 \cdot 2(\text{BAMBP})_2$, and $[\text{Cs} \cdot 2(\text{BAMBP})_2]^+ \text{HX}_2^-$. Comparison of diluents of different hydrogen-bonding capabilities showed that in chloroform (acceptor-type, not self-hydrogen-bonded), extraction was somewhat lower than in carbon tetrachloride (no hydrogen bonding). In octanol-1 (donor-type, self-hydrogen-bonded) and in acetophenone (donor-type, not self-hydrogen-bonded), extraction at BAMBP concentrations above 1 M were considerably lower because of stronger competition from BAMBP-diluent association; at lower BAMBP concentrations the dependence on BAMBP concentration changed from third to first power, showing that these donor-type diluent molecules can replace BAMBP molecules in solvating the cesium BAMBPate.

7.17 Kinetics of Extraction of Iron by Di(2-ethylhexyl)phosphoric Acid

Iron(III) is one of several metal ions that are very slow to reach equilibrium in extraction by di(2-ethylhexyl)phosphoric acid (HA). The extraction rate is first order with respect to aqueous iron concentration in acid perchlorate solutions. The rate constant k is directly proportional to the interfacial area but nearly independent of stirring rate. This and the relatively high activation energy (≈ 10 kcal/mole) indicate that the rate is controlled by a chemical reaction at the interface. The rate-controlling step (or the pathway) must change at an extractant concentration of about 0.4 M HA in *n*-octane, since several parameters change rather abruptly at about that concentration: at $[\text{HA}] \leq 0.2$ M, $k \propto [\text{HA}]^{0.3}$ and $[\text{H}^+]^{-1}$, activation energy ≈ 15 kcal/mole; at $[\text{HA}] \geq 0.5$ M, $k \propto [\text{HA}]^{1.5}$ and $[\text{H}^+]^{1.8}$, activation energy ≈ 10 kcal/mole. The rate constant decreases with increasing aqueous perchlorate concentration, consistent with an association quotient

$$Q = [\text{FeClO}_4^{2+}] / [\text{Fe}^{3+}][\text{ClO}_4^-] \approx 1.$$

7.18 Activity Coefficients of the Solvent Phases

Further evaluations of departures from ideality, expressed either as activity coefficients (γ) or as apparent average aggregation numbers (\bar{n}) of real or hypothetical polymeric species assumed to be ideal, were obtained by both direct measurement of diluent vapor-pressure lowering and isopiestic balancing. As previously found for tri-*n*-octylamine (TOA) and its bisulfate (TOAHS), \bar{n} for its normal sulfate (TOAS) was nearly independent of organic-phase water content up to 90% of saturation, increasing only from 0.85 at $a_w = 0$ to 1.10 at $a_w = 0.902$. The activity coefficient of TOAS in dry benzene decreased nearly linearly from 1 at infinite dilution to 0.769 at 0.355 *m*; TOAS thus departs less far from ideality than does the free base TOA ($\gamma = 0.628$ at 0.354 *m*).

To resolve a discrepancy between published values, the activity of tributyl phosphate (TBP) when saturated with water at 25°C was determined by means of an isopiestic series. At saturation ($a_w = 1$), mole fraction $X_{\text{TBP}} = 0.489$ and activity $a_{\text{TBP}} = 0.515$, with pure TBP as the standard

state. At lower water contents ($X_w = 0.36$), $a_{TBP} = X_{TBP} \pm 0.003$, and $a_w = (2.073 \pm 0.01)X_w$. Partial molal free energies of solution and excess partial molal free energies were calculated for both components.

In continuing improvement of the equipment and techniques for precisely measuring small vapor-pressure differences, the possibility of using an inverted cup floating in mercury was examined by derivation of its equation of motion and by trial of a preliminary model. A model for detailed testing has been designed that should have about 40 times the sensitivity of a simple mercury manometer.

8. RECOVERY OF FISSION PRODUCTS BY SOLVENT EXTRACTION

8.1 Cesium

In batch extraction tests, contaminant metals such as Ca, Ba, Mo, and Tc were not extracted from alkaline solutions by 4-*sec*-butyl-2-(α -methylbenzyl)phenol (BAMBP), further confirming the high selectivity of this extractant for cesium. BAMBP was degraded extensively upon contact with acid nitrite solutions, but the reaction was avoided by adding sulfamic acid to the system to destroy the nitrite. BABMP showed no reaction with alkaline nitrite solutions.

8.2 Isolation of Cerium and Promethium

Cerium oxidation with silver-catalyzed persulfate occurred at maximum rate with about 2 *M* HNO₃ in the aqueous phase. More than 98% of the cerium was oxidized and subsequently extracted with di(2-ethylhexyl)phosphoric acid in 20 to 30 min at 60°C, using 1.8 moles of persulfate per mole of cerium.

The separation of promethium from other rare earths was studied with a number of different types of extractants. Batch studies indicated that, in the previously developed flowsheet for separating rare earths by extraction with tributyl phosphate (TBP) from concentrated nitric acid, flows of scrub acid and solvent can be greatly reduced to make the process more attractive for large-scale use. In addition, promising results were obtained with di(2-ethylhexyl)phosphoric acid. Separation factors between adjacent rare earths of about 2.5 were obtained with this extractant at relatively

low (0.2 to 0.4 *M*) nitric acid concentrations. Separation factors with 2-ethylhexylphenylphosphonic acid were also about 2.5, but precipitation of the extractant-rare-earths complex occurred in some tests. Separations with a primary amine in a sulfate system were much less effective.

8.3 Ruthenium

A tentative process was outlined for recovering ruthenium from acid Purex waste by extracting with a tertiary amine and stripping with dilute caustic solution.

8.4 Treatment of Waste That Contains Dissolved Stainless Steel or Large Amounts of Aluminum Ion

The fission product recovery processes originally developed for treating Hanford Purex wastes are being studied for application to wastes of different compositions. In batch tests, strontium, rare earths, and cesium were recovered effectively from simulated "stainless steel" wastes complexed with tartrate and diethylenetriaminepentaacetate. Complexing with relatively large amounts of tartrate also allowed treatment of wastes that contain large amounts of aluminum nitrate (wastes from the TBP-25 process).

8.5 Engineering Studies

The basic engineering data for designing mixer-settlers for recovering cesium from Purex-type waste by solvent extraction with a substituted phenol, 4-*sec*-butyl-2-(α -methylbenzyl)phenol (BAMBP), were determined in a single-stage prototype. The flow capacity of the settler was nearly independent of mixing and at the normal flow ratios was 290 gal hr⁻¹ ft⁻² for extraction and 730 gal hr⁻¹ ft⁻² for stripping. Stage efficiencies greater than 90% were easily attained for both extraction and stripping at a power input of less than 10 hp per 1000 gal and a residence time of less than 2 min.

9. CHEMISTRY OF PROTACTINIUM

Solvent extraction studies of protactinium in sulfuric acid solutions were continued. Evidence has been obtained that in 2.5 *M* H₂SO₄ relatively

extractable polymeric species occur for protactinium concentrations between a few thousandths and a few hundredths of an mg per ml, but at higher concentrations less extractable species appear. These less extractable species are probably larger polymers in slow equilibrium with the extractable species.

Spectrophotometric studies in both sulfuric and hydrochloric acid solutions are being started, and preliminary data for concentrated sulfuric acid solutions of protactinium from three different sources have each given a different spectrum.

Recovery of the ^{231}Pa borrowed from England for use in preparing ^{232}U has been completed, and all the material has now been returned to England. The equipment used for processing the ^{232}U some three years ago was exhumed from the burial ground, and 1.65 g of protactinium was recovered from the dissolver vessel.

10. IRRADIATION EFFECTS ON HETEROGENEOUS SYSTEMS

The radiolysis of water adsorbed on silica gel was investigated in an attempt to determine whether or not energy transfer from the gel to the adsorbed water took place. $G(\text{H}_2)$ values as a function of water coverage were measured and found to be greater than the value for pure water, indicating either energy transfer or sensitization of the adsorbed water.

11. HIGH-TEMPERATURE CHEMISTRY

The major objectives of this program are to develop and to exploit various spectrophotometric techniques for studying the properties of aqueous solutions, primarily those of uranium and the trans-uranium, rare-earth, and transition-group elements. The principal effort is directed at construction of a high-temperature, high-pressure spectrophotometer and associated equipment that can be used to study spectra of these elements in solutions at temperatures up to the vicinity of the critical point of water. A special autoclave and a temperature-control-and-measuring system were built for measuring liquid densities at high temperatures and pressures by means of x-ray photography. Preliminary spectral studies of UO_2^{2+} and Pu^{4+} ions were made up to 95°C with existing spectrophotometers

equipped with a digitized punched-card output. The effects of nitrate complexation and hydrolysis on the spectra were also investigated. Computer codes for the IBM-7090 and CDC 1604-A computers were written for various types of manipulations of spectral data, for calculating reaction rates, for resolving complex spectra into individual adsorption bands, for spectral band model and profile studies, for spectral band overlap studies, and for the convolute smoothing of digitized spectral data.

11.1 High-Temperature, High-Pressure Spectrophotometer System

A high-temperature, high-pressure spectrophotometer and associated cells and other systems were specially designed for ORNL by the Applied Physics Corporation, but fabrication is not yet complete. The main spectrophotometer is scheduled for delivery by August. It is anticipated that installation of the locally constructed subsystems can be completed before the arrival of the main spectrophotometer. The design is such that, ultimately, solutions containing high levels of alpha emitters of interest in heavy-element chemistry can be studied. The spectrophotometer system will permit the study of the solution chemistry behavior and equilibria, reaction kinetics, and spectral properties of elements and complex species in solution up to the vicinity of the water critical point (372°C). Work has continued on the development of equipment and techniques for studying aqueous solutions at high temperatures and pressures. The prototype spectrophotometric absorption cell constructed as part of the subcontract development work has performed satisfactorily in tests at ORNL. Conditions included temperatures up to 365°C and pressures to 8000 psi, applied simultaneously.

11.2 Spectral Studies of Ionic Systems

Studies of the effects of ionic species (complexing ions) and temperature on the spectra of the uranyl ion in perchloric acid systems at fixed ionic strengths were continued. Experimental conditions of interest to us are: temperature, metal ion (uranyl) and ligand concentrations, acidity (hydrolytic complications), ionic strength, and isotope effects of the solvents (light and heavy water). Experiments have been carried out for the uranyl ion in per-

chloric acid and perchlorate systems in the acid-excess region, at the stoichiometric point, and in the region of hydrolysis over the temperature range of 25 to 95°C at several ionic strengths and at several uranyl ion concentrations. As the acidity is lowered through the stoichiometric point into the region where the uranyl ion becomes progressively more hydrolyzed, significant spectral changes are observed. Also, as the acidity is lowered, the effect of increased temperature in promoting hydrolysis becomes more pronounced.

Improved computer techniques developed for the mathematical resolution of complex overlapping spectra were applied to a study of the fundamental parameters of the absorption spectra of the UO_2^{2+} ion and related systems. Our results show that some prior inferences, from unresolved spectra, concerning the UO_2^{2+} band intensities (and half-band widths) are in error. We have, to our knowledge, for the first time resolved the absorption spectrum of the uranyl ion by nonlinear least-squares computational means over the 3300- to 5000-A region into 14 absorption bands. The effects on the spectra of UO_2^{2+} of the progressive complexation of UO_2^{2+} by NO_3^- were studied as a function of several experimental parameters. Even under conditions where hydrolysis effects are non-existent, changes of varying magnitudes are observed, for example, in all three parameters of each band with all experimental conditions invariant except temperature.

11.3 Measurement of Liquid Densities at High Temperatures and High Pressures

As an important adjunct to the program for the spectrophotometric study of solutions at high temperatures and high pressures, a method has been devised for measuring the densities of aqueous solutions at accurately measured temperatures and pressures up to the solution critical points. A high-temperature, high-pressure autoclave (dilatometer) and related facilities were designed and built to permit the accurate measurement of liquid densities under these conditions. The volume of a weighed solution of a known composition is determined in the dilatometer by taking an x-ray photograph to show the position of the vapor-liquid interface in a calibrated section of the dilatometer. This system has now been completely installed and has been operated. At 95°C the dilatometer

results on uranyl perchlorate solutions agreed with pycnometric results to within 0.4%. Up to about 300°C dilatometer results on water agree with steam-table values to within 0.5% or better, using a conventional thermocouple system. At higher temperatures the error increased because the temperature was not known accurately enough. Equipment installed recently permits the measurement of the temperature to within about 0.05°C.

11.4 Computer Programs for Spectrophotometric Studies

A generalized nonlinear least-squares computer program (MRØCØS) for the mathematical resolution of complex overlapping spectra has been completed. The program will resolve complex overlapping spectral bands and fine structure, and is now available for the IBM-7090 computer and automatic off-line plotting equipment. Using this code, the spectra of a number of uranyl ion systems have now been resolved.

A set of computer programs and subroutines were written for the CDC 1604-A computer to smooth spectral data. A least-squares convolution-smoothing technique is employed. Output from the very flexible set of programs can be in many forms, including binary coded decimal and binary tapes, tabulations, punched cards, or CALCOMP graphical plotting. All necessary combinations of experimental spectral data, cell-balance data, and conical-screen attenuator data can be handled and smoothed.

12. MECHANISMS OF SEPARATIONS PROCESSES

The thermodynamics of solvent extraction by tributyl phosphate (TBP)—hydrocarbon-diluent solutions are being studied by means of vapor pressure measurements and analytical partition data. Vapor pressures of water and nitric acid over the three-component system water—nitric acid—uranyl nitrate hexahydrate and corresponding pressures over the two-component systems water—nitric acid and water—uranyl nitrate hexahydrate were analyzed by integrating the Gibbs-Duhem equation. This integration was performed by using an empirical four-parameter function which is then used to calculate the activity coefficients of uranyl nitrate hexahydrate. These parameters describe

the variation of water and nitric acid activities with acid and uranyl nitrate hexahydrate concentrations with a standard deviation of about $\pm 10\%$.

The distribution of uranyl nitrate and water between TBP and aqueous uranyl nitrate solutions was used to calculate the activities of tributyl phosphate by means of the Gibbs-Duhem equation. Rational activities of TBP are tabulated for aqueous uranyl nitrate concentrations ranging from 0 to 2.0 *M*. These activities, together with literature data on the activities of water and uranyl nitrate hexahydrate, were used to calculate the thermodynamic equilibrium constant for the partition reaction. Partial molar volumes in the organic phase were calculated and used to calculate a free energy change of -7.47 kcal/mole for the partition reaction. Organic-phase densities are presented as an empirical equation, with the molar concentrations of water and uranyl nitrate as the independent variables.

A generalized computer program for the resolution of spectrophotometric data into a series of Gaussian distributions, with least-squares-adjusted parameters corresponding to band area, position, and half-width, is described. A second nonlinear program, useful for cases difficult or even impossible to converge by the modified Gauss-Newton method, is also mentioned. As a result of this work, preliminary information is presented on the variation in area of spectral bands for 0.1 *M* uranyl nitrate as a function of nitric acid concentration (0.01 to 7.9 *M*).

13. CHEMICAL ENGINEERING RESEARCH

13.1 The Stacked-Clone Contactor

A seven-stage stainless steel experimental stacked-clone contactor was used to determine operating performance with a variety of solvent systems including 100% TBP-1 *M* sodium nitrate, 18% TBP-3 *M* sodium nitrate, and hexone-water. The unit was run at flow ratios (A/O) as high as 50, with good capacities and stage efficiencies consistently over 60%. The Purex flowsheet was successfully demonstrated, as was the ability of the device to recover more than 99.9% of the uranium.

13.2 Effect of Ionizing Radiation on Coalescence in Liquid-Liquid Systems

The work on the effect of ionizing radiation on coalescence of drops on a plane interface was completed and a mechanism which explains the data was postulated. Data are presented on the effect of temperature, liquid properties, and drop diameter, as well as radiation type and intensity. Alpha and fission product irradiation alone are effective in enhancing coalescence, apparently by chemically disturbing the surface tension over a very small region during impact.

13.3 In-Line Detection of Particles in Gas Streams by Scattered Light

The detection of particles in a gas stream by scattered light depends on the intense illumination of a well-defined, very small volume. Recently, a helium-neon laser was tested to replace the other conventional light sources, and it increased the signal-to-noise ratio by a factor of 2 for particles in the micron range. Also, a technique was developed for electronically shaping the pulse from the photomultiplier detector so that the pulse can be satisfactorily analyzed by a multichannel pulse-height analyzer.

13.4 Solvent Extraction Engineering Studies: Correlation of Pulsed-Column Flooding Data

The literature and all available sources were exploited to accumulate data on flooding in pulsed columns, and 2300 data points representing 23 different chemical systems were accumulated and used to test over 200 proposed correlating equations by a multiple-regression analysis. Up to 13 variables were used, including column diameter, pulse-plate spacing, hole size, free area, pulse amplitude and frequency, solution densities and viscosities, and interfacial tension. Most correlations grouped the variables in dimensionless groups. When equations of the type originally proposed by Thornton and Pike were modified to include new coefficients generated by the regression analysis, they fitted the data well.

14. REACTOR EVALUATION STUDIES

This program is supported jointly by the Reactor Division and the Chemical Technology Division and includes studies on various proposed advanced-reactor and fuel-cycle systems to determine their feasibility and economics. The work in this Division during the past year included calculation of the costs of fuel shipping and processing and of preparing sol-gel oxide in connection with the advanced converter evaluation, ^{233}U value study, and other reactor evaluation programs. Also included were the development of computer codes for calculating shipping and processing costs and the overall cost of nuclear power, and for calculating individual and gross concentrations and radioactivities of thorium, uranium, transuranium elements, and fission products produced during reactor operation at constant flux or constant power. A manual on the design of casks for shipping spent fuel was published. Criticality problems and neutron-gamma shielding problems in fuel cycle plants were also studied.

15. CHEMICAL APPLICATIONS OF NUCLEAR EXPLOSIONS

Laboratory development of processes for recovering transplutonium elements from the proposed Project Coach detonation was completed. The tentative process flowsheet was tested on kilogram samples of radioactive debris from the Gnome detonation, which is presumed to be similar to that for Project Coach, and was satisfactory for obtaining a primary concentrate of the transplutonium elements. The process includes water leaching the debris to remove salt, which leaves a water-insoluble residue that contains the transplutonium elements; then, acid leaching the water-insoluble residue to put the transplutonium elements into solution; and, finally, concentrating the transplutonium elements by carrier precipitation with calcium oxalate. Focusing electrophoresis did not appear promising as a method for separating milligram quantities of transplutonium elements. In experiments in which lanthanides were used as stand-ins, separation bands were always overlapped.

Tests to demonstrate a jet-sampler method for removing a target irradiated about a meter from a detonating nuclear device were conducted with

chemical explosives at the Vincentown, New Jersey, test area under a purchase order to Frankford Arsenal. The tests showed that copper or iron targets were focused into hypervelocity jets and that the target material traversed the length of the test chamber at a velocity comparable to or faster than those at which the spherical shock front develops and moves out from a nuclear detonation.

The production of industrial chemicals by utilizing underground nuclear explosions does not appear economically attractive. Unless yields from the nuclear device are about a megaton, the cost of the heat energy or pressure generated by the device is much too high.

Laboratory tests were started to determine the rate of exchange of tritium and hydrogen in systems containing methane and water. This investigation is necessary to help evaluate the feasibility of stimulating gas production from wells by using nuclear explosives.

Studies were begun on problems that would arise from the presence of radiation emitters during the processing of ore bodies that have been fractured by a nuclear explosive. A feasibility study is being made on the recovery of magnesium oxide or magnesium from large deposits of olivine (about 48% MgO) that may be fractured by nuclear explosives.

Studies were begun on problems that might arise from the presence of radioactivity in the processing of copper ore bodies that have been fractured by nuclear explosives.

16. PREPARATION AND PROPERTIES OF ACTINIDE-ELEMENT OXIDES

The chemistry underlying the current sol-gel process for making dense nuclear-fuel oxides is the surface chemistry of colloidal thoria and of other colloidal oxides being prepared analogously. The purpose of the Actinide Oxides Program is to determine the properties that control the behavior of these oxides during their preparation.

The adsorption of nitric acid on crystalline thoria is limited to one nitrate ion per two surface sites, assuming equal exposure of the (100) and (111) faces. The free energy of adsorption is a function of the fraction of reacted surface sites, being about -5.7 kcal per mole of nitric acid at half of saturation. The enthalpy of adsorption,

determined from the temperature coefficient of the surface equilibrium, is estimated to be about -7.6 kcal/mole.

Hydrous amorphous thoria has been found to undergo spontaneous crystallization at room temperature when allowed sufficient time, about 24 months in the present study.

The viscosity of colloidal thoria in nitric acid solutions at pH 2 implies that the fundamental crystallites exist in the sol associated together in weak, reversible, highly unsymmetrical flocs. Viscometry of sols in pH 3.6 nitric acid also implies the existence of highly anisotropic flocs of crystallites which are only partially reversibly dissociated.

Weight-loss data for dehydrating gels of nitrate-stabilized thoria at temperatures below 600°C were correlated by equations from absolute-reaction-rate theory, which showed the enthalpy and entropy of activation of dehydration to be 10 kcal/mole and -45 eu respectively. The enthalpy and entropy of dehydration were 9.1 kcal/mole and $+22.2$ eu respectively.

Sintering of -400 -mesh compacts of thoria-gel particles at temperatures between 600 and 1100°C could not be correlated by any single-mechanism sintering model, probably because of the existence of an ultrafine (less than $1\ \mu$) size fraction, which superimposed interparticle shrinkage on intraparticle shrinkage. Compacts made from coarser gel particles, from which the ultrafine fraction had been removed, gave sintering results that correlated with the previously established surface-diffusion sintering model. At temperatures between 1000 and 1120°C , erratic growth, breakdown, and regrowth of the grain structure of sintering thoria gel were observed in the early stages of sintering. This process was observed repeatedly, but its cause is still obscure.

17. ASSISTANCE PROGRAMS

During the past year, several engineering efforts for others have been carried out by the Chemical Technology Division. These include a continuation of the Eurochemic Assistance Program; liaison on the construction and startup of the High Radiation Level Analytical Laboratory for the Analytical Chemistry Division; preparation of two preliminary design and cost estimates for a proposed Alpha

Laboratory Facility (also for the Analytical Chemistry Division); consultation to the Operations Division on the construction and startup of the two plant-waste-improvement projects; design and fabrication of equipment for the Health Physics Division experiments on waste disposal in salt and waste disposal by hydrofracturing; design and installation of a ^{233}U storage facility in Building 3019; design and installation of a test unit for evaluating absolute filters and charcoal beds in the Nuclear Safety Pilot Plant for the Reactor Division; calculations, using advanced shielding codes, of gamma and neutron shields for special point isotropic fission sources; and irradiation-contamination-decontamination tests on selected commercial protective coatings and plastics.

17.1 Eurochemic Assistance Program

The Laboratory continued to coordinate the exchange of technical information between Eurochemic and the AEC production sites and National Laboratories for the AEC Division of International Affairs. E. M. Shank completed his third year at Mol, Belgium, as U.S. Technical Advisor to Eurochemic during the construction and startup of the Eurochemic fuel-processing plant. Construction of the plant and its auxiliary facilities is now about 90% complete. Cold startup will begin in mid-1965, and hot startup is scheduled for the end of 1966.

17.2 Projects for Improving ORNL Waste Systems

The Chemical Technology Division continued to supply consultation to the General Engineering and Construction and the Operations Divisions during construction and startup of the two plant-waste-system improvement projects. The first of these, the Melton Valley waste collection and transfer system, was completed in February 1964 and is now in service. The second, the intermediate- and high-level-waste evaporator and high-level-waste storage tanks, will be completed and cold-tested by January 1966. This project was delayed because of the late delivery of the two 50,000-gal high-level-waste storage tanks. A preliminary design and cost estimate was prepared for venting and filtering the off-gases from the six concrete intermediate-level-waste tanks, W-5 to W-10, to the main plant stack.

17.3 A Demonstration of the Disposal of Solid, High-Level Radioactive Waste in Salt

Assistance was provided by the Division on the experiment concerning the disposal of solid waste in salt (Project Salt Vault). The experiment is being conducted by the Health Physics Division in a salt mine at Lyons, Kansas. The first tests will include the use of fully irradiated, 90-day-cooled Engineering Test Reactor fuel assemblies to simulate the heat and radiation from solid-waste containers. All equipment for transporting the fuel assemblies from Idaho to Kansas and handling them at the mine has been designed and built, and the first experiment is scheduled for September 1965.

17.4 Disposal of Radioactive Waste by Hydrofracturing

The engineering on the Health Physics Division experiments on the disposal of intermediate-level radioactive aqueous wastes by hydrofracturing is being coordinated by the Process Design Section of this Division. In this program, the aqueous wastes are mixed with cement and clay, and then they are pumped at high pressure into an approximately 1000-ft-deep hole in the ORNL test area in lower Melton Valley. When sufficient pressure is exerted, the rock strata are fractured at the bottom of the hole, and the waste is distributed in a thin slab around the hole, where it sets up as a concrete sheet.

Cores of the grout sheets of previous injections have been obtained and analyzed. The mixes seem satisfactory; radionuclide retention is quite good. The injection facility was modified, and another injection was made to test an improved mix and changes in equipment and procedure. Further coring will be done, and the facility will be modified for regular disposal of laboratory waste.

17.5 Construction and Startup of the High Radiation Level Analytical Laboratory

The Chemical Technology Division continued to supply the necessary technical liaison between the Laboratory, the AEC, the designers (Vitro Corporation), the construction contractor (Foster and Creighton Company), and cost-plus-fixed-fee

contractor (H. K. Ferguson Company) during construction of the High Radiation Level Analytical Laboratory for the Analytical Chemistry Division. Installation of equipment was completed late in 1964, and the facility is in use. Assistance included liaison on the completion of construction by H. K. Ferguson Company and ORNL field forces and the preparation of operating and maintenance procedures and manuals.

17.6 High-Level Alpha Laboratory

A preliminary design and cost study was made for a new Alpha Laboratory Facility for joint use by the Analytical Chemistry, Chemical Technology, and Metals and Ceramics Divisions. The laboratory would contain twenty-eight 16- by 32-ft alpha laboratories, four supporting "cold" laboratories, a 32- by 64-ft deep-bay area for large alpha experiments, and office and service facilities. The facility, which would be administered by the Analytical Chemistry Division, is estimated to cost about \$5,000,000. At the request of management, an alternative design was prepared in which half the proposed facility was added to the High Radiation Level Analytical Laboratory and the other half to the Thorium-Uranium Fuel Cycle Development Facility. This proposal was abandoned when it became apparent that such an alternative was considerably more expensive than the original proposal.

17.7 Storage Facility for ^{233}U , Building 3019

Oak Ridge National Laboratory now serves as a national storage and dispensing facility for reactor-produced ^{233}U fuel formed by neutron irradiation of thorium. Therefore, expanded storage capacity for ^{233}U nitrate solution was installed in the Building 3019 pipe tunnel, an additional bank of storage wells for dry solids ($^{233}\text{U}_3\text{O}_8$) was drilled into a cell dividing wall in the 3019 penthouse, and a small-scale solvent extraction facility (1 kg of uranium per day) was installed in the newly constructed alpha-contained laboratory located in the former solvent makeup room in the 3019 operating gallery. During the past year, about 20 kg of stored ^{233}U was separated from the radioactive daughters of ^{232}U for designated AEC uses. The ^{233}U inventory has been increased by addition of 40 kg containing 45 ppm of ^{232}U and 80 kg

containing 200 ppm of ^{232}U . Prior to the new acquisitions, nearly 50 kg of ^{233}U with a ^{232}U content of 38 ppm was on hand.

17.8 Filter Tests in the Nuclear Safety Pilot Plant

At the request of the Reactor Division, the Chemical Technology Division designed and installed an absolute-filter-charcoal-bed combination unit for testing in the Nuclear Safety Pilot Plant (NSPP). The system includes a Demister, absolute filter, and a charcoal bed all incorporated in a remotely removable canister, a sealed compressor for gas circulation, and three May-pack samplers. The system is designed for a flow of 20 cfm of steam and gas at 300°F and 50 psig pressure. The radioactive gases and particles for the NSPP tests will be generated by melting irradiated fuel elements with a plasma torch in a steam-air atmosphere.

17.9 Studies of Radiation Shields for Fission Sources

Advanced shielding codes for an IBM 7090 computer were used to calculate the radiation dose rates from fission sources through shields that are commonly used in cell walls, cell windows, and shipping casks. The dose rates were calculated for various concretes, water, CH_2 , and mixtures of H_2O or CH_2 with lead, iron, and boron for shield thicknesses up to 150 cm.

17.10 Irradiation and Decontamination Evaluation Tests on Selected Protective Coatings

Various commercial protective coatings and plastics were evaluated in irradiation-contamination-decontamination tests. Gamma radiation was used, and the irradiations were carried to the coating-failure level. Epoxy coatings were the most resistant, and vinyl coatings were the most easily decontaminated. The samples were irradiated both in air and in deionized water in a ^{60}Co source.

18. MOLTEN-SALT REACTOR PROCESSING

18.1 Continuous Fluorination of Molten Salt

The most attractive process for removing the uranium from Molten-Salt Breeder Reactor (MSBR) fuel involves continuous fluorination to produce volatile UF_6 . Although technology exists for batch fluorination, corrosion rates are high. A frozen-wall technique for protecting a tower in which fluorine may be bubbled countercurrent to the fuel salt is proposed. For a reference 1000-Mw (electrical) reactor, the fuel stream, cooled for 1.5 days, will have a specific heat generation rate of 3×10^4 Btu $\text{hr}^{-1} \text{ft}^{-3}$, which will give an adequate heat flux to support a frozen layer on a cooled wall. Experimental work has been started on a 1-in.-diam nickel continuous countercurrent fluorinator with a salt depth of 48 in., from which mass transfer data can be obtained.

18.2 Distillation of Molten Salt

The proposed Molten-Salt Breeder Reactor will use a fuel carrier salt of ^7LiF and BeF_2 . After the uranium has been removed by fluorination, this mixture can be partially separated from the fission product poisons, particularly the rare earths, by semicontinuous low-pressure distillation. At 1000°C the still will operate at a pressure of about 1 mm Hg, and since BeF_2 has a vapor pressure 100 times that of LiF , the still pot will contain little BeF_2 . A 1000-Mw (electrical) MSBR would require a processing rate of about 15ft^3 of salt per day. Preliminary experimental work has been directed toward the determination of the relative volatilities of the salt and contaminants. A cold-finger technique for sampling the vapor phase of an equilibrium still was employed. The trivalent rare earths had relative volatilities, with respect to LiF , ranging from 0.01 to 0.05. Cerium tetrafluoride showed a relative volatility of about 0.15; and CsF , RbF , SnF_2 , and ZrF_4 are more volatile than LiF and cannot be separated this way. The less volatile fission products are accumulated in the still bottoms and will be discharged on a time cycle that will probably be determined by the heat generation rate. Small prototype stills have been constructed to study the problems of heat transfer, condensation, and boiling.

18.3 Reconstitution of Fuel for a Molten-Salt Breeder Reactor

Since the carrier salt and UF_6 are purified separately, they must be recombined for return to the reactor. This is best accomplished continuously in a column in which the barren salt and UF_6 are introduced at the bottom, along with salt containing UF_4 , which is recycled from the top. The UF_6 first reacts with the UF_4 to form a nonvolatile intermediate fluoride, which is then reduced again to UF_4 in the upper part of the column with hydrogen. Three tests were made in a 4-in.-diam reaction vessel where the off-gas could be monitored to detect UF_6 that had not been absorbed. Complete absorption of the UF_6 had occurred, to the limit of detection. Better data on the rate of absorption and subsequent hydrogen reduction are necessary for optimal design.

18.4 Chromium Fluoride Trapping

Among the problems associated with the terminal recovery of the uranium from the fuel salt of the Molten-Salt Reactor Experiment (MSRE) is the separation of chromium fluoride from UF_6 . The chromium is introduced by corrosion. Packed beds of pelleted NaF at 400°C have been found to effectively trap the volatile CrF_5 . Eight tests were made with a sodium fluoride bed 1½ in. in diameter with an effective length of 6 ft. The bed accommodated gas rates (CrF_5 in fluorine) of 0.4 to 0.9 std liter/min. Over periods from 2 to 5 hr, 11 to 20 g of chromium fluoride was deposited. Different kinds of sodium fluoride pellets were tested, one of which is found to be quite satisfactory for use in processing the MSRE fuel.

18.5 Alternative Processing Methods for a Molten-Salt Breeder Reactor

A scheme that may be competitive to the distillation method for purifying the fuel salt is reduction of the fission product poisons to form metals that might be either assimilated into a molten metal phase or filtered from the salt. Since the free energies of formation of the rare-earth fluorides lie between those of LiF and BeF_2 , for reduction of rare-earths to take place it is necessary that stable intermetallic compounds be formed.

Experimental extractions were made with various molten-metal phases, including mixtures of metallic lithium, magnesium, aluminum, and tin. Little success was observed in assimilating rare earths into these metal phases. However, intermetallic compounds of the form $Be_{13}M$ were found that were highly insoluble in the salt phase or any metal phase tested. These compounds form granular solids which are easily removed by sedimentation or filtration. Studies to exploit this possibility for fuel-salt processing are continuing.

19. WATER RESEARCH PROGRAM

Oak Ridge National Laboratory is carrying out a program of basic research on the properties of water and its solutions under the auspices of the Office of Saline Water, Department of the Interior. This program has as its long-range goal the development of methods for the economical purification of water in such amounts and of such purity that it may be used for irrigation and for drinking. Work in the program is under the direction of K. A. Kraus and is interdivisional. It is reported in part in a series of reports issued annually by the Department of the Interior. The most recent report in the series is *Saline Water Conversion Report, 1964*. Because the work is reported formally in the above series, only this abstract of the work carried out by Chemical Technology Division personnel is presented in this report.

Studies carried out in the Chemical Technology Division have followed several lines. One has been measurements of thermodynamic properties of water-organic liquid mixtures, in the hope that such mixtures will exhibit the properties of, and so serve as models for, salt-excluding organic membranes. This hope has been reinforced by the finding that the distributive selectivity and the activity coefficients of inorganic salts in the mixtures are similar functions of their water contents over a wide range of organic structures, from esters to amides and organic salts. Correlations of activity coefficients and miscibility gaps with dielectric constants, salt types, and water thermodynamic activity have contributed to the information necessary to establish the utility of organic liquids as membrane models.

In another line of study, methods are being sought to alter the hydrodynamic conditions near

a solid surface to promote rates of mass transfer of a solute between the surface and the circulating fluid. (This study is under the direct supervision of D. G. Thomas, Reactor Division, ORNL.) This research is specifically intended to reduce the concentration polarization problems encountered in reverse osmosis and electro dialysis of brackish waters. The study is focused upon measurements of mass-transfer promotion from wires or cylinders supported above the mass-transfer surface near the edge of the hydrodynamic boundary layer. Using an air-naphthalene system, Thomas has found that such detached promoters may give average mass-transfer rates twice as high as those obtained without the promoters, and at certain points the rates may be three or four times as high. These studies are now being extended with an aqueous system with properties closer to those found in desalination processes. Initial results with this system indicate that the percentage increase in mass-transfer rates in the aqueous system will be at least as high as that observed in the gaseous system, although there are not enough data yet to predict what the optimum conditions will be or what degree of promotion ultimately can be obtained.

A third line of study is directed to metals and metal oxides and the relation of their surface properties to the adhesion of inorganic salts precipitated from aqueous solution onto them. This work has shown that the adhesion of salts precipitated from solutions containing orthophosphate is profoundly influenced by pH and orthophosphate concentration. Further, a fixed stoichiometry exists between the phosphate molecules which are sorbed on the metal oxide surfaces and the number of metal oxide sites on the surface. The stoichiometry was found to be determined by the shape of the phosphate molecule, the concentrations of the various dissolved phosphate species (e.g., PO_4^{3-} , HPO_4^{2-} , H_2PO_4^-), and the geometric array of the reactive sites on the surface of the solid. The kinetics of phosphate sorption on thorium, cerium(IV), and zirconium oxides was found to be described by a rate equation which contains both a linear depletion term and a term exponential in the extent of coverage. This is interpreted to mean that the activation energy for sorption of phosphate increases linearly with the quantity of phosphate sorbed.

1. Power Reactor Fuel Processing

Laboratory and engineering-scale development of processes for recovering fissionable and fertile material from spent power reactor fuels is continuing. Considerable emphasis was placed on basic chemical studies; however, major efforts were also continued on chemical applications, engineering development, and small-scale hot-cell testing of the more promising fuel-recovery processes.

Basic chemical studies on carbide fuels included nitric acid hydrolysis experiments with UC_2 , the preparation of pure ThC, ThC_2 , and ThC- ThC_2 mixtures and studies of their hydrolytic characteristics in water, and the effect of tungsten carbide impurity on the hydrolysis of both uranium and thorium carbides. Process development for thorium-uranium-graphite fuels included alumina fluidized-bed burning studies on pyrolytic-carbon-coated ThC_2 - UC_2 and ThO_2 - UO_2 fuel particles contained in graphite. Nitric acid leaching studies were conducted with the fuel ash. Wet-combustion-leaching studies in oxygen and dilute nitric acid at 250°C and 1500 to 2000 psi were also begun. Development of burn-volatility and burn-leach processes for graphite-based Rover fuel was completed.

Hot-cell comparison tests of the Sulfex and shear-leach processes were made with stainless-steel-clad UO_2 -20% PuO_2 and ThO_2 -4% UO_2 fuel samples irradiated to 99,000 Mwd per metric ton of fuel. Stainless-steel-clad oxide fuels were successfully declad with HF- O_2 at 600°C. Nitric acid leaching studies were made on the declad material both with and without a prior pyrohydrolysis step at 600°C (with steam or O_2 -3% H_2O) designed to remove residual fluorides formed during decladding and to reduce the solubility of iron during leaching.

The adsorption of ^{233}Pa on unfired Vycor and its subsequent elution with oxalic acid was successfully demonstrated with 26-day-cooled

ThO_2 - UO_2 fuel samples irradiated to 75,000 Mwd per metric ton of thorium. Alternative adsorption studies with silica gel and zirconium phosphate (Bio-Rad ZP-1) were also made. Unirradiated UO_2 -17% PuO_2 fuel pellets were successfully oxidized to U_3O_8 - PuO_2 powder in O_2 at 800°C; pellets containing more than 20% PuO_2 were unreactive. The resulting U_3O_8 - PuO_2 powders were then chlorinated at 500°C in 85% Cl_2 -15% CCl_4 ; volatilization of uranium and plutonium chlorides was only partially successful. Reduction of Pu(IV) to Pu(III) in nitrate solution with Ar-4% H_2 was satisfactorily demonstrated. The catalyst was platinized alumina.

Development of the shear-leach process with unirradiated fuel elements on a full engineering scale was continued. Work last year included: (1) removing fuel rods from second-generation fuel assemblies by remote row pulling; (2) shearing tests on loose bundles of fuel rods and on Zircaloy-2-clad uranium metal (annular fuel); (3) further safety evaluations on the mechanical head-end handling of zirconium fines; (4) evaluations of handling problems of, and fission product heat generation in, baskets of sheared fuels; and (5) further leaching tests on sheared UO_2 and ThO_2 - UO_2 fuels. Also, a monitor for determining the residual ^{235}U , ^{239}Pu , or ^{233}U content of leached metal hulls by delayed-neutron activation analysis was developed. The monitor is sensitive to a residue equal to less than 0.01% of the fissile material before leaching.

A new program for developing low-decontamination close-coupled processes for Th-U recycle fuels was begun. Results of scouting tests to evaluate the capability of electro dialysis, ion exchange, and precipitation processes were relatively unsuccessful; therefore, the main effort was devoted to the development of low-cost differential solvent extraction equipment and methods. Amine solvent extraction was evaluated

as an alternative to steam denitration of thorium nitrate for the preparation of thorium sols.

Conceptual plant studies were completed for (1) a small-capacity (1/10 to 1/6 ton/day) fuel processing plant using conventional head-end and solvent extraction technology and (2) an HTGR graphite-base fuel processing plant employing a burn-leach-solvent-extraction flowsheet.

1.1 HYDROLYSIS OF URANIUM AND THORIUM CARBIDES

Uranium, thorium, and plutonium carbides are starting to be used as reactor fuels, both as the pure compounds and as ingredients in fuel-graphite mixtures. For example, uranium monocarbide in NaK-bonded stainless steel tubes is being used as the second-core fuel for the Consumer's Public Power (Hallam, Nebraska) reactor, and pyrolytic-carbon-coated UC_2 - ThC_2 particles in a graphite matrix are being used as fuel in the High-Temperature Gas-Cooled reactor (HTGR, Peachbottom, Pennsylvania). The TARGET-type reactor will use undiluted carbon-coated ThC_2 - UC_2 particles packed in longitudinal holes in graphite fuel rods; plans are also under way to use carbon-coated ThO_2 - UO_2 microspheres as fuel. Development efforts on the processing of fuel carbides are discussed in this section; the work on process developments for graphite-base fuels is reviewed in Sect. 1.2.

Basic chemical studies on the preparation and hydrolysis of uranium, thorium, and other carbides were continued. This work included studies on (1) the hydrolysis of UC_2 in nitric acid;^{1,2,3} (2) the preparation and hydrolysis of ThC , ThC_2 , and ThC - ThC_2 mixtures in water;^{4,5} and (3) the effect of tungsten carbide impurity on the hydrolysis of uranium and thorium carbides.

¹L. M. Ferris and M. J. Bradley, *Off-Gases from the Reactions of Uranium Carbides with Nitric Acid at 90°C*, ORNL-3719 (December 1964).

²L. M. Ferris and M. J. Bradley, "Reactions of the Uranium Carbides with Nitric Acid," to be published in the *Journal of the American Chemical Society*.

³J. R. Flanary et al., *Hot-Cell Studies of Aqueous Dissolution Processes for Irradiated Carbide Reactor Fuels*, ORNL-3660 (September 1964).

⁴M. J. Bradley and L. M. Ferris, "Hydrolysis of Thorium Carbides Between 25 and 99°C," to be published in the *Journal of Inorganic and Nuclear Chemistry*.

⁵M. J. Bradley and L. M. Ferris, "The Effect of Tungsten on the Hydrolysis of Uranium Dicarbide," to be published in *Inorg. Chem.* 4 (May 1965).

Hydrolysis of Uranium Carbides in Nitric Acid^{1,2}

Dissolution of uranium carbides in 4 and 16 M HNO_3 at 90°C was investigated to determine the composition of the gases evolved. Other studies were conducted to determine the behavior of the carbides in 0.001 to 0.5 M HNO_3 solutions. Relatively high-purity uranium monocarbide (UC), sesquicarbide [$U_4(C_2)_3$], and dicarbide ($UC_{1.85}$) samples were used in all cases. Each carbide, when contacted at 90°C with 4 and 16 M HNO_3 , yielded uranyl nitrate, soluble organic acids, NO_2 , NO , CO_2 , and traces of N_2O . No hydrogen, CO , or gaseous hydrocarbons (the hydrolysis products with water alone) were produced. With 4 M HNO_3 , NO was the predominant nitrogen oxide, whereas NO_2 was the chief nitrogen oxide evolved in reactions with 16 M HNO_3 (Table 1.1). Between 50 and 80% of the carbide carbon was converted to CO_2 ; the remainder was converted to oxalic acid (0 to 11%), mellitic acid (2 to 9%), and unidentified highly substituted aromatic compounds.

The carbides were almost completely passive in boiling 0.001 to 0.5 M HNO_3 and in solutions of sodium, calcium, uranyl, aluminum, and thorium nitrates where the nitrate concentration was 0.05 M. This behavior has not yet been explained.

Preparation and Hydrolysis of Thorium Carbides^{4,5}

Thorium carbide specimens with total-C/Th atom ratios varying from 0.8 to 2.1 (4 to 10 wt % carbon) were prepared by arc-melting high-purity thorium metal and carbon. These specimens were examined by chemical, x-ray diffraction, and metallographic analyses, and their hydrolysis properties studied.^{4,6} The thorium monocarbide phase was found over a range of compositions from about $ThC_{0.94}$ (4.6% carbon) to at least $ThC_{0.81}$ (4.0% carbon) and probably lower. The maximum combined-C/Th atom ratio obtained by arc-melting with graphite electrodes was 1.95 (9.2% carbon) rather than the expected 2.00 (9.4% carbon). Specimens with compositions varying from $ThC_{0.99}$ to $ThC_{1.88}$ (4.9 to 8.9% carbon) were two-phase mixtures of the mono- and dicarbides. There was no evidence for any significant range of composition for the dicarbide.

⁶M. J. Bradley and T. M. Kegley, Jr., *Correlation of Composition with the Microstructures of Arc-Cast Thorium Carbides*, in preparation.

Table 1.1. Approximate Compositions of the Gases Evolved in Reactions of the Uranium Carbides with Nitric Acid at 90°C

Carbide	HNO ₃ Concentration (M)	Gas Composition (mole %)			
		NO	NO ₂	N ₂ O	CO ₂
UC	4	74	12	2	12
UC ^a	16	7	88	0	5
U ₄ (C ₂) ₃	4	74	8	4	14
U ₄ (C ₂) ₃	16	26	62	1	11
UC _{1.85}	4	68	11	3	18
UC _{1.85}	16	21	65	1	13

^aReaction time in this experiment was only 6 hr.

The thorium carbides reacted with water to produce thorium oxide and hydrocarbons.⁴ Thorium monocarbide produced mostly methane, and also two moles of hydrogen for each mole of thorium in excess of the 1:1 thorium-to-carbon atom ratio. Thorium dicarbide (ThC_{1.95}) produced C₂ to C₈ hydrocarbons, wax, and hydrogen. The preponderance of hydrocarbons with an even number of carbon atoms in the gas from the hydrolysis of the dicarbide is to be expected because of the presence of discrete C₂ units in the dicarbide crystal lattice.⁷ Carbon spacing in the thorium monocarbide lattice has not been studied, but the carbon is probably present as single C units as in uranium monocarbide,⁸ which also yields methane when hydrolyzed.⁹ Varying the reaction temperature between 25 and 99°C caused no change in the hydrolysis products from either the thorium mono- or dicarbides, although the reactions were considerably faster at the higher temperatures. The total volume of gas evolved decreased from 110 ml (STP)/g to 49 ml/g as the total-C/Th atom ratio increased from 0.81 to 1.95 (Fig. 1.1); there was no further change in volume as the total-C/Th atom ratio increased above 1.95. Specimens with compositions between ThC and ThC_{1.95} gave the products expected for ThC-ThC_{1.95} binaries, showing a regular decrease in the amount of meth-

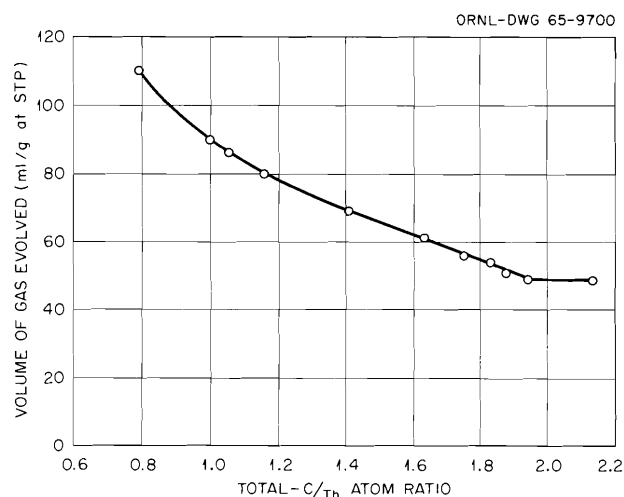


Fig. 1.1. Effect of C/Th Atom Ratio on the Volume of Gas Evolved in the Hydrolysis at 80°C of As-Cast Thorium Carbides.

ane and an increase in the amount of C₂ to C₈ hydrocarbons as the total-C/Th atom ratio increased (Fig. 1.2). Within experimental error, the specimen with the total-C/Th atom ratio of 2.14 (combined-C/Th ratio of 1.95) gave the same products as the specimen with the total-C/Th ratio of 1.95.

Effect of Tungsten Impurity on Hydrolysis of Uranium and Thorium Carbide

Tungsten, as an impurity in uranium and thorium dicarbides, had a pronounced effect on the hydroly-

⁷E. B. Hunt and R. E. Rundle, *J. Am. Chem. Soc.* 73, 4777 (1951).

⁸A. E. Austin, *Acta Cryst.* 12, 159 (1959).

⁹M. J. Bradley and L. M. Ferris, *Inorg. Chem.* 3, 189 (1964).

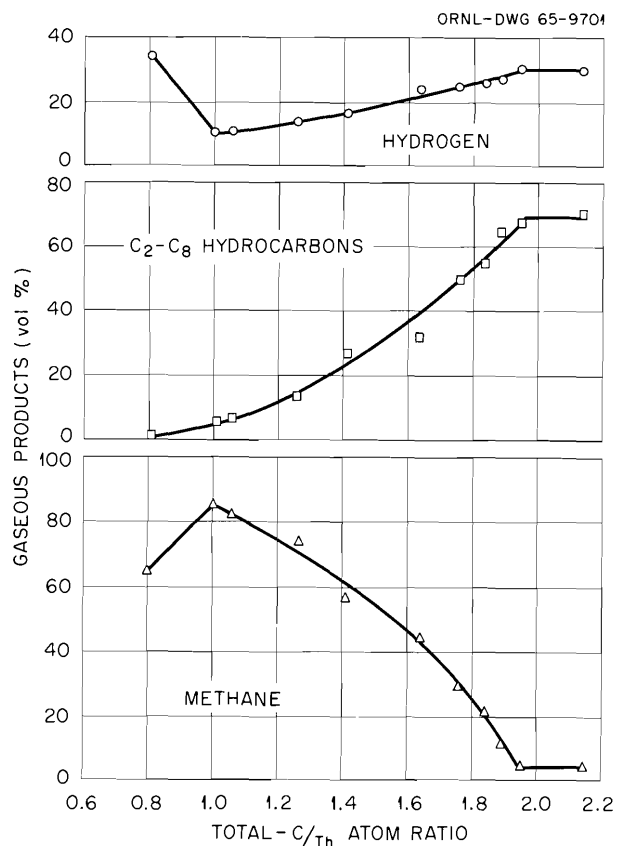


Fig. 1.2. Effect of C/Th Atom Ratio on the Gaseous Products from the Hydrolysis at 80°C of As-Cast Thorium Carbide.

ysis reaction, causing a marked decrease in the amount of gaseous C_2 to C_8 hydrocarbons and an increase in the amount of wax and free hydrogen (Table 1.2).^{4,5} This emphasizes the importance of preparing and using high-purity carbides for hydrolysis studies and indicates that some of the discrepancies in the literature on carbide chemistry may be caused by relatively small amounts of impurities in the specimens used by the investigators. The tungsten in the uranium dicarbide specimen was present primarily as WUC_2 , which was recovered as an insoluble residue after hydrolyzing the carbide and dissolving the resulting $UO_2 \cdot xH_2O$ in hydrochloric acid. About half the tungsten in the thorium dicarbide specimen was recovered as W_2C after hydrolysis; it is not known which chemical species of tungsten (W , W_2C , or WC) reacted.

1.2 DEVELOPMENT OF PROCESSES FOR GRAPHITE-BASE FUEL

Development of processes for recovering fuel materials from spent thorium-uranium-graphite fuels has included studies on the burning of pyrolytic-carbon-coated ThC_2-UC_2 and ThO_2-UO_2 fuel particles contained in graphite (TARGET reactors, or the Peachbottom reactor). Burning

Table 1.2. Effect of Tungsten Impurity on the Reaction of Uranium and Thorium Dicarbides with 80°C Water

	W/(U or Th) Atom Ratio for:			
	Thorium Dicarbide		Uranium Dicarbide	
	0.00005	0.09	0.00003	0.10
Volume of gas evolved,				
ml (STP) per gram of carbide	48	67	39	51
Gas composition, vol. %				
Hydrogen	30	74	33	75
Methane	3	3	17	7
C_2 to C_8 hydrocarbons	67	23	50	18
Carbon distribution, % of carbon reacting				
Methane	1	1	4	3
C_2 to C_8 gaseous hydrocarbons	51	30	33	20
Wax	12	52	20	52
Unaccounted for	35	17	43	25

was done in a fluidized bed of alumina; the resulting mixtures of alumina and fuel oxides were satisfactorily leached in HNO_3 , catalyzed with HF , to recover the fuel. A pressurized aqueous combustion (PAC) process is also being evaluated. Here, the fuel is contacted with dilute nitric acid and oxygen to produce CO_2 and a fuel nitrate solution. This is done at a pressure of 1500 to 2000 psi, at temperatures up to 300°C . Development of both aqueous and volatility processes for Rover fuels was completed. Both processes employ a common fuel-combustion head-end operation.

Burn-Leach Process

The work on the burn-leach process for Rover fuels¹⁰ has been modified and extended to apply the process to pyrolytic-carbon-coated $\text{ThC}_2\text{-UC}_2$ and $\text{ThO}_2\text{-UO}_2$ fuels. This effort has included engineering-scale tests of fluidized-bed burning (alumina beds) and leaching of crushed HTGR (Peachbottom) fuel compacts¹¹ and laboratory-scale leaching tests on both HTGR-fuel burner ash and $\text{ThO}_2\text{-UO}_2$ microspheres. The mixed oxide (or carbide) fuel particles are 150 to 500 μ in diameter, and the pyrolytic carbon coatings are about 100 μ thick.

Burning can be done in fluidized beds of aluminum oxide or similar inert material as the heat transfer agent. The fluidized bed is preferred

because it provides uniformly controlled combustion and because it is easily adapted to continuous operation. The $\text{ThC}_2\text{-UC}_2$ fuels burn to a $\text{ThO}_2\text{-U}_3\text{O}_8$ ash, which is finely divided and becomes dispersed uniformly through the Al_2O_3 fluidizing medium. The $\text{ThO}_2\text{-UO}_2$ sol-gel microspheres do not break up during burning and collect at the bottom of the fluidized bed because of their high density. Thus, for the latter fuel, very little of the Al_2O_3 follows the $\text{ThO}_2\text{-UO}_2$ into the leaching step.

The conditions used in a typical burning run in a 2-in.-diam fluidized-bed burner are given in Table 1.3. The product bed was green-gray and consisted of slightly discolored Al_2O_3 and finely divided $\text{ThO}_2\text{-U}_3\text{O}_8$ powder; the alumina did not powder. No sintering or clinker formation occurred, and the bed material was free flowing. The sieve analysis of the product is given in Table 1.4. The dry bulk density of the bed, 28% of which consisted of fuel oxides, was 2.25 g/cm^3 .

Except for a short time during startup, the off-gas, as shown by the LIRA infrared absorption analyzers, consisted of more than 95% CO_2 and less than 3% CO . Utilization of O_2 was almost complete. Temperature control was very easy, and no cooling was needed during most of the run. After all the fuel had been charged, burnout of the carbon took about 3 hr. During the first hour, the CO_2 concentration was higher than 90%; during the second hour, it fell slowly to about 60%, and the CO content rose slightly. In the last hour, there was a rather abrupt decrease in both CO_2 and CO content; zero reading on the LIRA's was reached in about 45 min.

After the bed was cooled, it was transferred to a 1.5-in.-diam glass fluidized-bed leacher and

¹⁰Rover Fuel Reprocessing Development, June 1, 1963, to July 1, 1964, ORNL-CF-64-12-5 (confidential).

¹¹Unit Operations Quarterly Report for April-June, 1965 (ORNL-TM report, to be published).

Table 1.3. Fluidized-Bed Burning Run Conditions for HTGR Fuel

Fuel	Crushed ($\frac{1}{8}$ -in.-diam) HTGR "A" fuel compacts, each containing 52 g of Th, 10 g of U, and 285 g of C; total charge 2.7 kg; 200 g charged initially; 100 g charged every 15 min thereafter
Alumina	Equal weights of 60- and 90-mesh Norton RR grade; 0.6 liter, 1.21 kg, 12 in. settled height
Temperature	750 to 775°C
O_2 flow rate	12 liters/min (STP); 1.15 ft/sec at 750°C
Product	$\text{Al}_2\text{O}_3\text{-ThO}_2\text{-U}_3\text{O}_8$; 0.7 liter, 1.664 kg

Table 1.4. Sieve Analysis of Product from Fluidized-Bed Burner

Sieve Mesh Size	Weight Percent
-30 + 50	21.2
-50 + 60	12.7
-60 + 100	30.2
-100 + 140	16.4
-140 + 170	3.6
-170 + 200	2.5
-200	13.5

leached with boiling, circulating Thorex dis-solvent (13 M HNO₃-0.04 M HF-0.1 M Al³⁺). After 1 hr, the ThO₂-U₃O₈ was 90% dissolved; after 7 hr, dissolution was 99.7% complete. The leached bed was finally washed with water. The combined leach-wash solution was 0.26 M in Th. The maximum possible concentration of thorium in the blended stream would be about 0.35 M for bed material of this loading (28 wt %), the limitation being the solids-disengagement volume required at the overflow. The useful range of fluidization velocity was 0.58 to 0.92 cm/sec. At less than 60% bed expansion, corresponding to a solution velocity of 0.58 cm/sec, the bed was not fully fluidized by the Thorex solution.

The leaching equipment included a 1½-in.-diam glass column in which the bed material was supported on a perforated Teflon disk covered with 6/16-mesh Al₂O₃. The overflow solution from the top of the column was continuously airlifted to a standpipe that provided head for returning the solution through a stainless steel heater and rotameter. A hot oil jacket on the 1½-in. glass section permitted close temperature control of the bed. Disengagement of solids in the 3-in.-diam enlarged upper section of the column was satisfactory as long as the solution was not permitted to boil actively. Total entrainment of solids in the column overflow amounted to less than 1% of the weight of leached solids, and caused no operational difficulties.

Laboratory-scale studies have also shown that excellent uranium and thorium recoveries can be achieved by leaching the product bed with various boiling, fluoride-catalyzed nitric acid solutions. The burner product bed consisted of 6% U₃O₈, 25% ThO₂, and 69% Al₂O₃. In 5- to 7-hr leaches

with boiling reagent, more than 99.5% of both the uranium and thorium were recovered when the nitric acid concentration in the leachant was 4 M or higher and the hydrofluoric acid concentration was 0.02 to 0.05 M (Table 1.5). The presence of up to 0.1 M Al(NO₃)₃ in the leachant had no adverse effect on the recoveries. Each product solution was about 0.6 M in thorium, and less than 2% of the alumina had been dissolved in each case. Uranium and thorium recoveries were not acceptable when the bed material was leached with either 13 M HNO₃ alone or with 2 M HNO₃-0.05 M HF (Table 1.5), indicating the need for the fluoride catalyst and relatively high nitric acid concentration in the leachant. Leaching at temperatures below the boiling point will be investigated in future studies.

Another type of graphite-base fuel being considered consists of carbon-coated ThO₂-UO₂ microspheres dispersed in a graphite matrix. Although no extensive experimentation with this type of fuel has yet been done, the oxide particles are not expected to be affected during combustion of the graphite matrix and should settle to the bottom of the burner because of their high density.¹² All the ThO₂-UO₂ microspheres could then be withdrawn from the burner with very little dilution by alumina. Thus, the leaching step would essentially involve dissolution of undiluted ThO₂-UO₂ microspheres.

In recent tests, nearly theoretically dense sol-gel ThO₂ microspheres, 300 to 600 μ in diameter, were dissolved in 3 to 6 hr in boiling 13 M HNO₃-0.05 M HF (Table 1.6); the product solutions were about 0.5 M in thorium. Similar results were obtained even when the microspheres were dissolved in the presence of a large excess of Norton RR alumina. In contrast to the finely divided oxide product from burning of fuel that contains Th-U dicarbide particles, Th-U dioxide microspheres probably cannot be dissolved in a short time in solutions of low nitric acid concentration (Table 1.6). In 6-hr experiments, the amounts dissolved increased with increasing nitric acid concentration, other conditions being the same.

¹²E. L. Nicholson, L. M. Ferris, and J. T. Roberts, *Burn-Leach Processes for Graphite-Base Reactor Fuels Containing Carbon-Coated Carbide or Oxide Particles*, paper presented at the EURATOM symposium on "Fuel Cycles of High-Temperature Gas-Cooled Reactors," Brussels, Belgium, June 10-11, 1965, ORNL-TM-1096 (Apr. 2, 1965).

Table 1.5. Results of Laboratory-Scale Leaching of Fluidized-Bed Material with Boiling HNO_3 -HF- $\text{Al}(\text{NO}_3)_3$ Solutions

Bed material: 6% U_3O_8 , 25% ThO_2 , 69% Norton RR alumina
Leaching time: 5 to 7 hr; final solutions were about 0.6 M in Th

Leachant Composition (M)			Amounts Leached (%)		
HNO_3	HF	$\text{Al}(\text{NO}_3)_3$	U	Th	Al
2	0.05	0	83.6	83.0	0.2
4	0.05	0	99.9	99.9	1.9
4	0.05	0.1	99.7	99.5	
13	0.0	0	27.7	14.8	
13	0.01	0	61.1	57.6	
13	0.02	0	99.9	99.6	
13	0.05	0	99.9	99.9	1.9
13	0.05	0.1	99.9	99.9	

Table 1.6. Dissolution of Sol-Gel ThO_2 Microspheres in Boiling Fluoride-Catalyzed Nitric Acid

Reaction time: 6 hr

Microsphere Diameter (μ)	Reagent Composition (M)		Amount Dissolved (%)
	HNO_3	HF	
250-300	2	0.05	20
420-600	2	0.05	33
250-300	4	0.05	57
420-600	4	0.05	73
250-300	13	0.05	100
420-600	13	0.05	100

Pressurized Aqueous Combustion of Graphite Fuels

Combustion of the carbon matrix and subsequent dissolution of the uranium and thorium from graphite-base fuels in a pressurized vessel containing nitric acid and oxygen is being studied as a low-temperature alternative to the burn-leach process. Such a process appeared potentially attractive based on results reported for the Zimmerman process for sewage or waste disposal^{13,14}

or for the oxidation of coal.¹⁵ Tests have been made at temperatures up to 300°C both in a batch autoclave and in a system in which gases were continuously admitted and removed. Most of the

¹³F. J. Zimmerman, *Chem. Eng.* **65**, 117 (1958).

¹⁴G. H. Teletzke, "Wet Air Oxidation," presented at 56th Annual Meeting, AIChE, Houston, Tex., Dec. 1-5, 1963.

¹⁵T. R. Savich and H. C. Howard, *Ind. Eng. Chem.* **44**, 1409 (1952).

Table 1.7. Effects of O_2/C and $NO_3/(Th + U)$ Mole Ratios on the Combustion-Dissolution of HTGR Fuel in Pressurized Nitric Acid Solutions

Temperature: 300°C
Fuel composition: 12% Th, 6% U, 82% C

Experiment No.	Reaction Time (hr)	Mole Ratios		Amounts Burned or Dissolved (%)		
		O_2/C	$NO_3/(Th + U)$	C	Th	U
1	24	0.58	63	89.3	6.0	8.0
2	24	0.71	63	91.4	8.0	19.0
3	24	1.1	57	99.6	99.9	99.7
4	24	1.6	61	100.0	100.0	100.0
5	24	1.7	11	99.9	38.0	33.0
6	24	2.0	12	100.0	50.0	53.0
7	24	1.8	32	99.6	60.0	96.0
8	6.3	2.1	57	86.8	17.0	12.0
9	6.0	1.9	113	95.0	36.0	45.0
10	24	0.0	53	44.0	0.0	2.0

effort was devoted to the nitric acid oxidation-dissolution of unfueled graphite and simulated HTGR fuel (carbon-coated Th-U dicarbide particles dispersed in a graphite matrix); however, some work also was done with other aqueous solutions and with ThO_2-UO_2 microspheres.

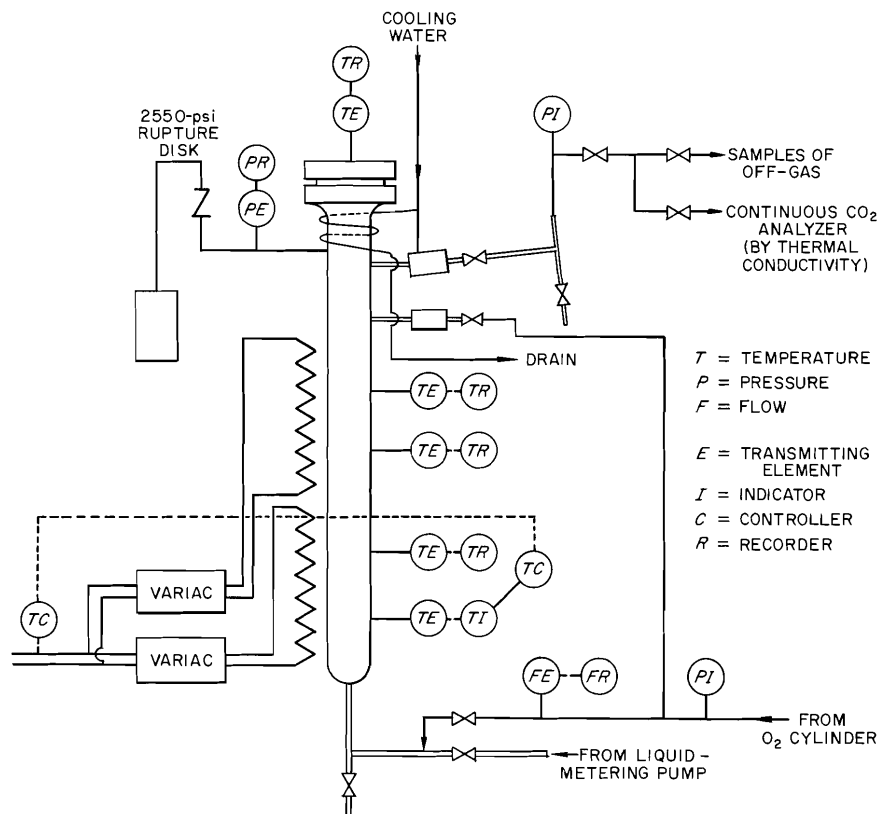
In the batch autoclave tests, the effects of the O_2/C and $NO_3/(Th + U)$ mole ratios on the oxidation and dissolution of HTGR fuel samples (12% Th, 6% U, 82% C) were investigated. The coated fuel particles in the sample were about 500 μ in diameter (400- μ -diam dicarbide kernels with 50- μ -thick pyrolytic carbon coatings); about 90% of the total carbon was present as the graphite matrix. In 24-hr reactions in nitric acid solutions at 300°C, complete combustion of the carbon and solubilization of the uranium and thorium were achieved only when the O_2/C and $NO_3/(Th + U)$ mole ratios were greater than about 1 and 54, respectively (Table 1.7). The pressure of the system at 300°C was 1500 to 2000 psi. Combustion of the carbon apparently occurred according to the overall reaction: $C + O_2 \rightarrow CO_2$. Further confirmation of the stoichiometry was obtained from gas analyses, which showed mainly CO_2 and excess oxygen, and from analyses of the solutions, which verified that little or no nitric acid was converted to nitrogen oxides when sufficient oxygen was present. The need for maintaining a

high $NO_3/(Th + U)$ ratio was not surprising, considering that thorium and uranium contained in nitrate solutions hydrolyze at high temperatures. Previous studies of the hydrolysis of thorium nitrate solutions¹⁶ showed that a minimum NO_3/Th mole ratio of about 25 was required to keep thorium in solution at 300°C in 2 M HNO_3 .

In those experiments where only about 90% of the total carbon was oxidized (Table 1.7, experiments 1, 2, and 8), the residue appeared, under the microscope, to consist solely of unattacked carbon-coated particles. The same behavior was noted in 6-hr reactions with 2 and 4 M HNO_3 . Most of the matrix was oxidized, but the particles remained almost intact (Table 1.7, experiments 8 and 9).

Additional studies of the oxidation of unfueled graphite were made in a reactor designed for the continuous addition and removal of gases or solution (Fig. 1.3). However, since the volume of gas in the reactor was minimized to avoid long time lags, most of the tests were made with batch charges of solution and continuous flows of gases only. The graphite, contained in a basket made with screen, was loaded at room temperature through the flanged joint, nitric acid was added

¹⁶HRP Quart. Progr. Rept. July 31, 1960, ORNL-3004 (October 1960).



MATERIAL: 347 STAINLESS STEEL
 PIPE SCHEDULE: $\frac{1}{2}$ -in. SCHED.-160 REACTOR BODY, 2000 psi-RING-JOINT FLANGES,
 $\frac{1}{4}$ - AND $\frac{1}{8}$ -in. SCHED.-80 CONNECTIONS TO REACTOR, OTHER TUBING AND FITTINGS
 RATED AT > 2000 psi AT ROOM TEMPERATURE

Fig. 1.3. Schematic Arrangement of the Pressurized Aqueous Combustion Reactor System for Processing Graphite Fuels at 300°C and 2000 psi.

with the solid or by a high-pressure metering pump, and oxygen or gas mixtures were metered into the reactor from gas cylinders. The gas, which bubbled up through the solution, provided the necessary agitation. The removal of gas at room temperature was controlled manually by a needle valve. The CO_2 content of the effluent gas was monitored continuously by a thermal-conductivity analyzer and was also determined by analyses of gas samples. Twenty-one runs were made with $\frac{1}{4}$ - and $\frac{1}{2}$ -in. cubes or $\frac{1}{2}$ -in.-square sticks of moderator-grade graphite. The results were analyzed in terms of reaction rates: grams of graphite oxidized to CO_2 per hour per gram of graphite present.

In these tests, the oxidation rates increased with increasing nitric acid concentration, temper-

ature, and surface area of the graphite. The rates for 2 M HNO_3 were about twice those for 1 M HNO_3 , and the rates at 300°C were about 1.5 times those at 275°C . As the surface area of the graphite was increased, the reaction rate increased, but not proportionally. In two tests, the reaction rates were proportional to the external surface area to the 0.4 and the 0.7 power. The degree of agitation also seemed to have a pronounced effect. It was not possible to vary the agitation in this system without varying one or more of the other variables; however, several different effects could be explained if agitation is important. For the $\frac{1}{4}$ - by $\frac{1}{4}$ -in. graphite cubes, the reaction rate constants (hr^{-1}), assuming the reaction to be first order, were practically constant, regardless of the number of cubes present or of whether the cubes were dis-

tributed over a larger volume by mixing them with stainless steel Raschig rings. The rate constants calculated for moderator-grade graphite are:

Temperature (°C)	Rate Constant (hr ⁻¹)		
	1 M HNO ₃	2 M HNO ₃	4 M HNO ₃
275	0.06	0.10–0.15	0.19–0.25
300	0.08–0.12	0.15–0.24	

Very high rates of graphite oxidation were obtained in a run with an HTGR fuel specimen. The high gas flow rate, the increased agitation, the friability of the specimen, and the presence of the uranium and thorium dicarbides in the compact may have all contributed to the higher rate. The consumption of nitric acid was greatly decreased by starting the oxygen flow when the reactor temperature reached 180 to 200°C and continuing the flow until the reactor had cooled to below 240°. In previous runs, where the flow of oxygen was controlled to achieve operation at constant temperature, the effluent nitric acid concentrations were often less than 25% of the charge concentrations. This was probably due to a deficiency of oxygen during heatup and cooldown without oxygen flow.

Reagents other than nitric acid were briefly tested in the autoclave with HTGR fuel compacts at 300°C. Water, NaOH solutions, 2 M NaNO₃, and H₂SO₄-KMnO₄ were tried, but none was as effective as dilute nitric acid.

Preliminary autoclave experiments were also conducted on the dissolving of sol-gel ThO₂-UO₂ microspheres in pressurized nitric acid solutions. Complete dissolution of high-density, 300- μ -diam 97% ThO₂-3% UO_{2.4} microspheres was achieved in 24 hr in 2 M HNO₃ at 300°C when the NO₃/(Th + U) mole ratio was about 100. Pure ThO₂ microspheres (260 to 300 μ in diameter) were much less reactive. In 24-hr reactions with 2 M HNO₃ at 300°C, the amounts dissolved were 17, 20, 35, and 49% when the NO₃/Th mole ratios were 10, 30, 50, and 100 respectively.

Development of Processes for Rover Fuel

Development of a burn-leach and a burn-volatility process for graphite-base Rover fuel on a labora-

tory scale¹⁷ and on an engineering scale¹⁸ has been completed. A conceptual plant study¹⁹ based on the development work has also been completed.

Because this work is classified, it cannot be reviewed here. Unlike last year, when a supplement to the annual report covering the Rover work was issued,²⁰ no supplement will be issued this year since the more recent work is fully covered in the topical reports noted above.

1.3 STUDIES ON THE PROCESSING OF URANIUM-PLUTONIUM OXIDE FUEL

Basic chemical and hot-cell studies on the processing of pressurized-water-reactor UO₂ and fast-reactor UO₂-PuO₂ fuels were continued. A new decladding process for stainless steel fuels, in which the cladding is destroyed with HF-O₂ at 600°C, was developed, and leaching of the treated fuel in nitric acid was demonstrated with unirradiated fuel samples. Since the resulting fuel solutions contained excessive amounts of fluorides, a preleaching pyrohydrolysis step was developed. It eliminated 85% of the fluoride as volatile HF. Also, dissolution experiments with nearly theoretically dense PuO₂ microspheres demonstrated that they dissolve very slowly in HNO₃-HF; hot-cell tests will be run to determine whether irradiated material dissolves faster.

Sulfex process hot-cell tests on stainless-steel-clad UO₂-20% PuO₂ fuel samples irradiated to 99,000 Mwd per metric ton of U + Pu at cladding temperatures up to 700°C resulted in high (1.5%) uranium and plutonium losses and high (60%) release of ¹³⁷Cs to the decladding solution. Parallel tests with the shear-leach process showed it to be the superior processing method for this type of fuel.

¹⁷L. M. Ferris, *A Burn-Leach Process for Recovery of Uranium from Rover Fuel: Terminal Report of Laboratory Development*, ORNL-3763 (March 1965).

¹⁸R. W. Horton, summary of engineering-scale development on processes for reprocessing of Rover fuels will be issued as a topical report (confidential).

¹⁹E. L. Nicholson, private communication.

²⁰*Rover Fuel Reprocessing Development, June 1, 1963, to July 1, 1964*, ORNL-CF-64-12-5 (confidential).

Leaching of UO_2 from Stainless-Steel-Clad Fuel Disintegrated by $HF-O_2$

Studies of the leaching of mixtures of alumina, U_3O_8 , and "stainless steel" oxides, resulting from the decladding of stainless-steel-clad reactor fuel with $HF-O_2$, were begun. The leachant was a solution of HNO_3 and $Al(NO_3)_3$ in various proportions. In this new process, the cladding on stainless-steel-clad UO_2 fuels can be disintegrated and oxidized by reaction with $HF-O_2$ mixtures (see also Sect. 2.4, fluoride volatility processes). Reaction at 600 to 650°C, preferably in a fluidized bed of inert alumina, results (1) in the disintegration and conversion of the stainless steel cladding to oxides and (2) in the oxidation of the UO_2 to U_3O_8 powder. The product always contains some fluorine, present as UO_2F_2 and "stainless steel" fluorides.

The bed material used in most of the experiments was produced by contacting simulated Yankee fuel (UO_2 pellets clad in type 348 stainless steel tubes) with 40% $HF-60\% O_2$ at 600°C in a fluidized bed of Norton RR alumina. (We are indebted to J. J. Reilly and C. B. Bartlett of Brookhaven National Laboratory for supplying this material.) It was composed of 25% U_3O_8 , 13% stainless steel oxides, 5% fluorine (as

fluoride), and 69% Al_2O_3 . Uranium recoveries better than 99.6% were obtained by leaching for 5 hr with boiling 1 to 15 M HNO_3 (Table 1.8). To enhance the leaching of fluorides from the bed and to partially complex the fluoride, $Al(NO_3)_3$ was added to the leachant; but in concentrations up to 1 M , it had no effect on the recoveries.

The fluoride must be complexed to inhibit corrosion of stainless steel process vessels. If the bed product used in these studies can be considered typical, the fluoride concentration in the product solution will be about three times the uranium concentration; in these experiments, the product solutions were about 0.2 M in uranium and 0.6 M in fluoride.

Generally, 80 to 90% of the fluoride was leached from the bed irrespective of the leachant used (Table 1.8). The amount of iron dissolved increased from about 16 to 85% as the nitric acid concentration increased from 1 to 15 M (Table 1.8). If the alumina fluidizing medium is not to be reused, leaching with dilute acid would probably be desirable to avoid large amounts of iron in the raffinate from subsequent solvent extraction. The leaching of nickel and chromium has not yet been studied. In all cases, less than 2% of the alumina was dissolved.

Table 1.8. Leaching of a Product Bed Resulting from the Disintegration of Stainless-Steel-Clad UO_2 by $HF-O_2$

Composition of bed: 25% U_3O_8 , 13% "stainless steel" oxides, 69% Al_2O_3 , 5% F

Samples were leached 5 hr with boiling leachant; final solutions were 0.2 M in U

Experiment No.	Leachant Composition (M)		Amounts Dissolved (%)			
	HNO_3	$Al(NO_3)_3$	U	Fe	Al	F
1	1	0	99.9	16	0.9	84
2	2	0	99.9	24	1.5	84
3	2	0.5	99.7	24		84
4	2	1.0	99.8	19		89
5	4	0	99.7	27	1.2	84
6	4	0.5	99.7	31		90
7	4	1.0	99.6	16		88
8	10	0	99.9	60	1.5	99
9	10	0	99.9	68	1.8	86
10	10	0.25	99.9	50		80
11	10	0.5	99.7	55		79
12	15	0	99.8	85	1.0	

Pyrohydrolysis of the clad fuel prior to leaching with nitric acid considerably reduced the fluoride content of the bed. In 3-hr reactions with steam, the fluorine content of the bed was reduced from about 5 to 0.07% as the steam temperature was increased from 200 to 600°C (Table 1.9). A sample of bed contacted with steam for 3 hr at 600°C was leached for 5 hr with boiling 10 M HNO₃. The uranium recovery was greater than 99.9%. The product solution was 0.2 M in uranium and only 0.06 M in fluoride. About 86% of the fluorine had been removed by pyrohydrolysis. Also, only about 40% of the iron was leached, showing that pyrohydrolysis decreases the reactivity of iron somewhat (compare this value with the data in column 5 of Table 1.8).

Comparable results were obtained by heating a bed sample for 5 hr at 600°C in a stream of 97% O₂-3% H₂O (produced by bubbling oxygen through water at 25°C) and leaching the residual solids for 5 hr with boiling 10 M HNO₃. The uranium recovery was 99.7%, and the product solution was 0.2 M in uranium and 0.05 M in fluoride. About 82% of the fluorine had been removed by pyrohydrolysis. During leaching, sufficient alumina (2%) was dissolved to make the product solution 0.05 M in aluminum. (Adequate complexing of the fluoride is achieved with an Al/F mole ratio of 1.) In a similar experiment, the residue was leached with 2 M HNO₃ after pyrohydrolysis. The uranium recovery was 99.8%; about 85% of the fluoride was removed, and, significantly, only 6% of the iron had dissolved. The results of these preliminary experiments suggest that removal of most of the fluorine from

the bed prior to leaching with dilute acid would not only minimize corrosion in the leacher and other process vessels but also would allow nearly quantitative uranium recovery without dissolving much of the stainless steel oxides.

Sulfex-Process Tests with Irradiated 20% PuO₂-80% UO₂ Fuel

Prototype fast-reactor, stainless-steel-clad fuel samples, containing either swaged or pelleted 20% PuO₂-80% UO₂, were made and then irradiated at cladding temperatures up to 700°C to burnups ranging from 5000 to 99,000 Mwd/metric ton. This phase of the work was done by the General Electric Company at Vallecitos Atomic Laboratory. These specimens were subsequently used in hot-cell studies at ORNL²¹ to determine the feasibility of processing this fuel by the Sulfex process, in which the cladding is dissolved in H₂SO₄ followed by dissolution of the PuO₂-UO₂ core in HNO₃ or HNO₃-HF. Similar tests to evaluate the shear-leach process for these fuels are reviewed in Sect. 1.3.3.

In hot-cell tests of the adaptability of the Sulfex process to this type of fuel, the stainless steel cladding was removed from the fuel specimens by refluxing in boiling 6 M H₂SO₄ for 4 hr at 105°C; the stainless steel was not passivated. Losses of uranium and plutonium to the decladding solution were excessively high in all runs and averaged 1.55%. Nearly 60% of the fission product cesium from each sample also appeared in the decladding solution, something not previously encountered in Sulfex process tests.

The presence of so much cesium in the cladding solution is attributed to the high temperature of the fuel samples during irradiation. The cladding temperatures were 700°C, and the fuel center-line temperatures were considerably higher, about 2000°C. At this temperature, much of the ¹³⁷Xe that forms in the PuO₂-UO₂ can easily migrate to the voids in the fuel, where it decays to ¹³⁷Cs (ref. 22) and is ultimately dissolved during chem-

Table 1.9. Fluorine Removal by Pyrohydrolysis from a Product Bed from the HF-O₂ Disintegration of Stainless-Steel-Clad UO₂ Fuel

Reagent, steam; reaction time, 3 hr

Temperature (°C)	Fluorine Content of Residual Solids (%)
Original sample	5.3
200	5.6
400	3.4
600	0.07

²¹J. H. Goode, *Hot-Cell Dissolution of Highly-Irradiated 20% PuO₂-80% UO₂ Fast Reactor Fuel Specimens*, ORNL-3754 (in preparation).

²²B. F. Rider and C. P. Ruiz, "Determination of Atom Percent Fission in Uranium Fuel," *Progr. Nucl. Energy, Ser. IX* 3(1-3), pp. 25-60, Pergamon, New York, 1962.

ical decladding. This phenomenon has not been observed with other fuel samples since they have been irradiated in water-cooled reactors, where temperatures are much lower.

Sulfex processing of this type of fuel does not appear economically attractive because the excessive loss of plutonium and uranium to the decladding solution will force the use of additional processing steps to recover the fissionable material. In addition, the presence of over half of the long-lived ^{137}Cs in the decladding solution would introduce additional problems in the management of intermediate-radioactivity-level waste because the cooling capacity of waste storage tanks for this stream was based mainly on the presence of ^{60}Co . The additional decay heat due to cesium would require either greater dilution of the decladding waste and larger waste tanks or use of expensive water-cooled tanks.

Shear-Leach Process Tests with Irradiated 20% PuO_2 -80% UO_2 Fuel

Companion hot-cell dissolution studies with 20% PuO_2 -80% UO_2 fast-reactor fuel samples irradiated from 9000 to 99,000 Mwd/metric ton at cladding temperatures up to 700°C indicate that the shear-leach process may be successfully applied to this fuel.²³ Dissolution rates for both swaged and pelleted oxides were determined by leaching sheared stainless-steel-clad specimens and by dissolving Sulfex declad specimens (see Sect. 1.3.1) in strong nitric acid (3.5 to 10 M). Fluoride catalyst was not required in most instances.

Both swaged and pelleted oxides were dissolved completely in less than 5 hr at all nitric acid concentrations greater than 3 M (Fig. 1.4). The dissolution rates were independent of the density of the oxide before irradiation (maximum, 96%), irradiation level, and original concentration of

the dissolvent. The lower rate for sheared fuel (Fig. 1.4) is due to the much smaller area of oxide exposed to the dissolvent.

Leaching of the sample irradiated to 99,000 Mwd/metric ton with 5 M HNO_3 for 3 hr produced a solution 0.52 M in $\text{UO}_2(\text{NO}_3)_2$ and 0.12 M in $\text{Pu}(\text{NO}_3)_4$; it contained 3.60 mg of fission products per milliliter. Although the bulk of the fission products was dissolved in the leaching acid, an insoluble residue of uranium, plutonium, and fission-product molybdenum and zirconium oxides, equivalent to 2.2% of the fuel oxide, remained after leaching. Only 0.13% of the uranium and plutonium originally present in the fuel sample was found in the residue. These results suggest, however, that some form of feed clarification is required prior to solvent extraction of this type of fuel.

In previous studies²⁴⁻²⁹ on the dissolving of unirradiated, high-density UO_2 , PuO_2 , and UO_2 - PuO_2 , it was found that mixed oxides, containing as much as 35% PuO_2 , could be dissolved in nitric acid without the aid of fluoride catalyst only when the PuO_2 was in solid solution in the UO_2 . Recent studies with unirradiated, high-density PuO_2 microspheres of nearly 100% theoretical density indicate this material to be extremely difficult to dissolve. In tests with refluxing 14 M HNO_3 -0.05 M HF, the dissolution rate was only $0.007 \text{ mg min}^{-1} \text{ cm}^{-2}$; only 8.5% of the PuO_2 dissolved in 37 hr. Hot-cell tests with irradiated samples will be made to determine whether irradiation results in increased rates.

²⁴R. E. Blanco and C. D. Watson, "Head-End Processes for Solid Fuels," chap. 3, *Reactor Handbook*, vol. II, *Fuel Reprocessing*, Interscience, New York, 1961.

²⁵L. G. Russell, "Plutonium Ceramics as Nuclear Fuels," chap. 3-2, *Progr. Nucl. Energy, Ser. IV* 4, Pergamon, New York, 1961.

²⁶F. L. Culler and R. E. Blanco, "Feed Preparation for Aqueous Processes," P/1930, *Proc. U.N. Intern. Conf. Peaceful Uses At. Energy, 2nd, Geneva, 1958* 17, 259 ff. (1958).

²⁷W. M. Coshin, *Fast Oxide Breeder - Fuel Irradiation Experiments*, KAPL-1784 (August 1957).

²⁸A. L. Uriarte and R. H. Rainey, *Dissolution of High-Density UO_2 , PuO_2 , and UO_2 - PuO_2 Pellets in Inorganic Acids*, ORNL-3695 (April 1965).

²⁹J. M. Gerhart, GE-VAL, personal communication.

²³J. H. Goode, *Hot-Cell Dissolution of Highly-Irradiated 20% PuO_2 -80% UO_2 Fast Reactor Fuel Specimens*, ORNL-3754 (in preparation).

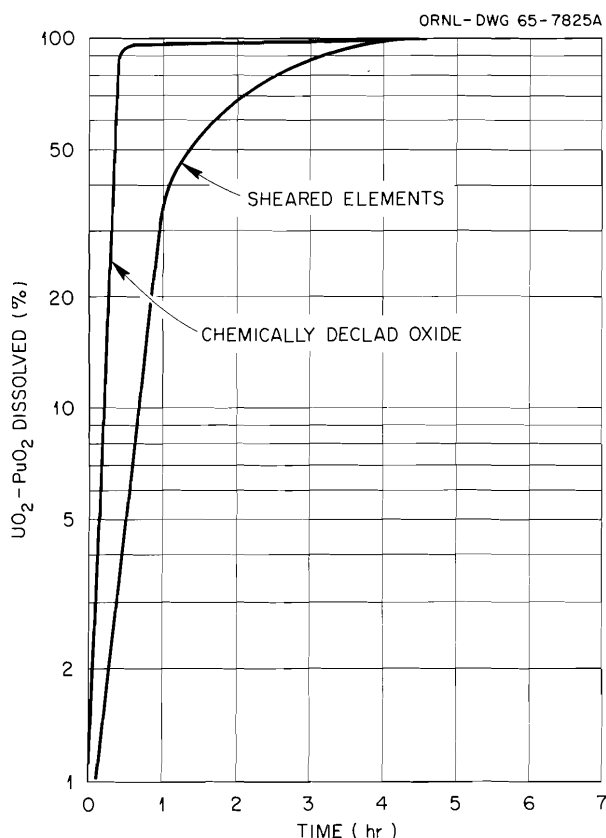


Fig. 1.4. Effect of Head-End Treatment on Dissolution of Irradiated 80% UO_2 -20% PuO_2 in Boiling 3.5 to 10 M HNO_3 .

1.4 STUDIES ON THE PROCESSING OF THORIUM-URANIUM FUEL

The Sulfex and shear-leach processes were compared in tests with ThO_2 -4% UO_2 fuel samples that had been irradiated in a water-cooled reactor to burnups of 3000 to 98,000 Mwd per metric ton of Th + U. Three types of samples were used; sol-gel, pelleted, and arc-fused. The shear-leach process, even though fuel dissolution rates were somewhat lower, was superior since the Sulfex process resulted in a thorium-uranium loss of 0.3% to the decladding solution. In all tests, irradiated sol-gel ThO_2 - UO_2 dissolved much faster than unirradiated sol-gel oxides.

The adsorption of ^{233}Pa from Th-U-Pa nitrate fuel solutions on unfired Vycor was demonstrated in hot-cell tests with 26-day-cooled ThO_2 - UO_2 fuel samples irradiated to 75,000 Mwd per metric

ton of Th + U. Both the adsorption and subsequent elution with oxalic acid were successful, and more than 95% of the dissolved ^{233}Pa was recovered. Silica gel and zirconium phosphate were also tested as adsorbents.

Dissolution Studies on Stainless-Steel-Clad ThO_2 - UO_2

Hot-cell head-end studies were made to further compare and evaluate the adaptabilities of the Sulfex and shear-leach processes to the processing of highly irradiated stainless-steel-clad ThO_2 -4% UO_2 fuels.^{30,31} These tests were made with sol-gel-prepared, pelleted, and arc-fused ThO_2 - UO_2 fuel samples irradiated in water-cooled reactors up to 98,000 Mwd per metric ton of Th + U. Data were also obtained on the nature of undissolved refractory residues and on the solubilities and rates of dissolution of the macro amounts of fission products present in the highly irradiated samples.³² Much of this work was done in cooperation with General Electric scientists at Vallecitos Atomic Laboratory.³³⁻³⁶

In the Sulfex tests, sectioned fuel samples were declad in boiling 6 M H_2SO_4 . The uranium and thorium loss to the decladding solution averaged 0.33%, which is about 10 times as great as losses obtained in previous tests with prototype Consolidated Edison pelleted-fuel samples irradiated to 20,000 Mwd per metric ton of Th + U. The sol-gel irradiation samples used in the current

³⁰L. M. Ferris and J. W. Ullmann, *Dissolution of Sol-Gel-Derived and Arc-Fused ThO_2 - UO_2 Fuel Particles in HNO_3 -HF Solutions: Laboratory Studies*, ORNL-TM-867 (May 19, 1964).

³¹M. E. Whatley et al., *Unit Operations Section Monthly Progress Report for March 1964*, ORNL-TM-887 (September 1964).

³²J. H. Goode and J. R. Flanary, *Dissolution of Irradiated, Stainless-Steel-Clad ThO_2 - UO_2 in Fluoride-Catalyzed Nitric Acid Solutions: Hot-Cell Studies on Pelletized, Arc-Fused, and Sol-Gel-Derived Oxides*, ORNL-3725 (January 1965).

³³R. W. Darmitzel, *Post-Irradiation Examination of ORNL Fuel Cycle Capsules*, GEAP-4397 (September 1963).

³⁴D. T. Ikeuye et al., *ORNL-RML Services Program Progress Report for January 1964*, GEAP-4472 (1964).

³⁵D. T. Ikeuye et al., *ORNL-RML Services Program Progress Report for February 1964*, GEAP-4500 (1964).

³⁶D. T. Ikeuye et al., *ORNL-RML Services Program Progress Report for July 1964*, GEAP-4549 (1964).

tests were originally made from $\text{ThO}_2\text{-UO}_2$ that was 60% -10 +16 mesh, 15% -16 +200 mesh, and 25% -200 mesh. After irradiation and decladding, the $\text{ThO}_2\text{-UO}_2$ size distribution averaged 96.7% +10 mesh, 2.1% -10 +20 mesh, and 1.2% -20 mesh, which indicates that considerable sintering and agglomeration of the fuel oxide occurred during irradiation.

The dissolution rates of the irradiated $\text{ThO}_2\text{-UO}_2$ fuels, whether sol-gel derived, pelleted, or arc-fused, were all nearly the same in boiling 13 M HNO_3 -0.04 M HF, with or without 0.04 M $\text{Al}(\text{NO}_3)_3$. The Sulfex-declad specimens dissolved faster than the sheared samples, but only because larger oxide areas were available for reaction. For example, Sulfex-declad sol-gel samples irradiated to 17,000 Mwd/ton were 97% dissolved in 7 hr and 99.8% dissolved in 24 hr. Previous tests with identical unirradiated material resulted in 73% dissolution in 7 hr and complete dissolution in 75 hr³⁰ (Fig. 1.5). In all cases, the dissolver solution (1 M $\text{Th}(\text{NO}_3)_4$ -10 M HNO_3) was a satisfactory solvent extraction feed. Solutions obtained from irradiated fuel were 0.05 M in fission products.

Because of the very long total-dissolution times found in earlier tests with unirradiated fuel, a cyclic dissolution procedure was developed.^{30,31} With this method, steady-state conditions for unirradiated fuel were achieved in two cycles of 20 hr each, after which a 13% heel (13% of the total Th + U added in two charges) remained. The dissolver solution was 0.8 M in thorium. With

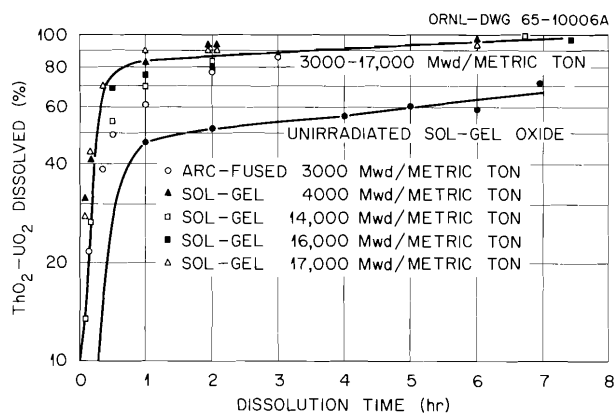


Fig. 1.5. Effect of Irradiation on Dissolution of Sol-Gel-Prepared $\text{ThO}_2\text{-UO}_2$ in 13 M HNO_3 -0.04 M KF -0.1 M $\text{Al}(\text{NO}_3)_3$.

sol-gel fuel irradiated to 17,000 Mwd per ton of Th + U, steady state was reached after four 5-hr cycles. The total heel was 6%, and the thorium concentration in the solution was 1 M. The final heel was completely dissolved in two 5-hr heel-cleanout cycles with Thorex dissolver.

Most of the fission products in the irradiated fuel samples were soluble in the dissolver solutions; however, small amounts of Sb, Mo, Ru, and Zr-Nb were found in the residues. These residues, which comprised about 0.75% by weight of the initial $\text{ThO}_2\text{-UO}_2$, contained 0.06% of the original $\text{ThO}_2\text{-UO}_2$, stainless steel cladding fragments, corrosion products, and alumina and silica (Fiberfrax insulation). To improve solvent extraction, the residues should be removed from the feed solution.

Studies on the Adsorption of Protactinium

The presence of 27.4-day ^{233}Pa accounts for a large fraction of the beta and gamma radioactivity associated with short-decayed thorium-uranium reactor fuels. To reduce the radioactivity to acceptable levels for solvent extraction and to ensure a more complete recovery of the ^{233}U , such fuels are usually allowed to decay 150 to 180 days before processing. To avoid this long decay period, an adsorption process for the separation of protactinium from thorium and uranium on unfired Vycor has been developed.³⁷ Significantly, the recovered protactinium would also be a source of isotopically pure ^{233}U .

During the past year, hot-cell experiments were made to determine the effects of macro amounts of fission products and high levels of radioactivity on the process. Additional studies were made to determine the protactinium distribution coefficients between thorium-nitric acid solutions and silica gel or zirconium phosphate (Bio-Rad ZP-1).

Adsorption of Protactinium on Unfired Vycor. - Hot-cell experiments showed that protactinium can be recovered from short-decayed thorium-uranium fuel solutions by adsorption on unfired Vycor glass.³⁸ Thorium-uranium fuel specimens

³⁷Chem. Technol. Div. Ann. Progr. Rept. May 31, 1964, ORNL-3627, pp. 13-16.

³⁸J. G. Moore et al., Adsorption of Protactinium on Unfired Vycor: Initial Hot-Cell Experiments, ORNL-3773 (April 1965).

irradiated to 75,000 Mwd/metric ton in an average neutron flux of 2×10^{14} and allowed to decay 26 days were dissolved in refluxing 13 M HNO₃-0.05 M HF. More than 99% of the fuel dissolved, leaving a residue containing less than 0.1% of the uranium and up to 20% of the protactinium. In process application, the protactinium losses could be minimized by cyclic dissolution. In each of three experiments, more than 99.4% of the dissolved protactinium was adsorbed by passing the dissolver solution through a bed of 60- to 80-mesh unfired Vycor, 0.9 cm in diameter and 17 cm long. The flow rate in the first experiment was 0.3 ml/min but was increased to 1 ml/min for the second and third runs. The feed to the third experiment was made 0.1 M in Al(NO₃)₃ to complex the fluoride in the feed.

The high degree of radioactivity of the feed had little effect on the adsorption process. In the third run, the feed contained Th, 69 mg/ml; U, 1.80 mg/ml; and ²³³Pa, 0.032 mg/ml. It was 10.1 M in HNO₃, 0.05 M in HF, and 0.1 M in Al(NO₃)₃, and each ml contained gamma emitters equivalent to 1.7×10^{11} counts/min. Based on analyses of the effluent, 99.6% of the protactinium

had been adsorbed, corresponding to about 0.5 mg of ²³³Pa per gram of unfired Vycor. About 0.1% of the ²³³Pa was lost when the column was washed with 6 column volumes of 10 M HNO₃-0.1 M Al(NO₃)₃. Elution with 8 column volumes of 0.5 M oxalic acid removed 97.7% of the adsorbed protactinium. About 90% of the original ²³³Pa was recovered at a concentration 5.5 times that in the feed. The protactinium had been separated from zirconium-niobium, total rare-earth beta, and ruthenium by decontamination factors of 9, 6030, and 2870 respectively. The protactinium concentration profile of the effluent and eluate (Fig. 1.6) was similar to that previously reported for ²³¹Pa solutions.³⁹

Although there were several inconsistencies noted in the protactinium analyses, the results of the hot-cell experiments showed the feasibility of recovering protactinium from short-decayed, highly irradiated thorium-uranium fuel by adsorbing it on unfired Vycor. Additional hot-cell experiments are planned for specimens irradiated to

³⁹Chem. Technol. Div. Ann. Progr. Rept. May 31, 1963, ORNL-3452, pp. 13-14.

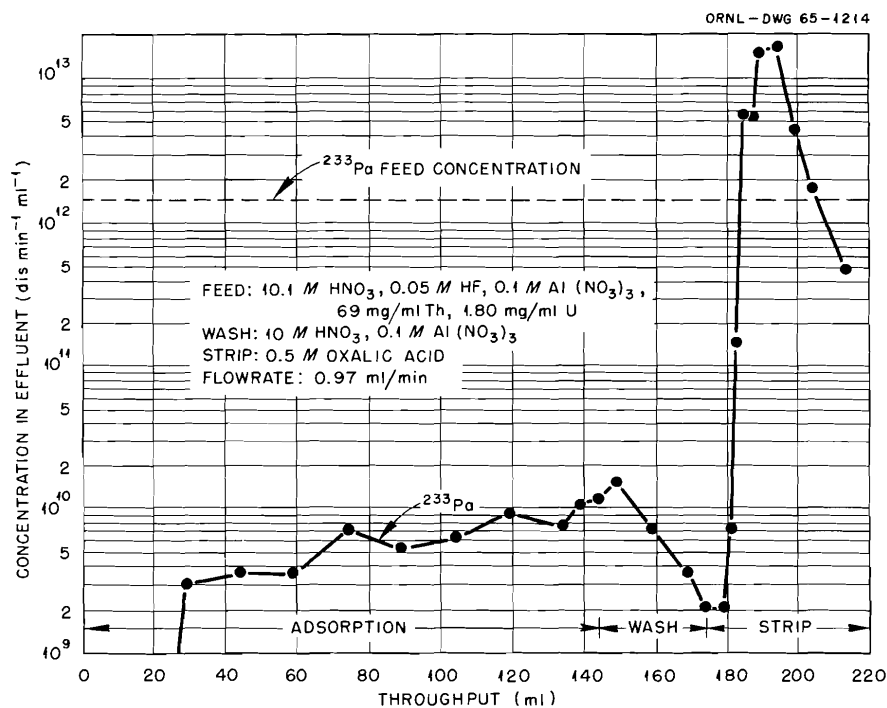


Fig. 1.6. Concentration of ²³³Pa in Column Effluents During Adsorption on Unfired Vycor, Washing, and Desorption.

5000 Mwd per metric ton of Th + U to determine the upper capacity limit of unfired Vycor for protactinium adsorption, the maximum concentration factor obtainable with oxalate elution, and the effect of aluminum on the solubility of protactinium during the dissolution of thorium-uranium fuels in 13 M HNO₃-0.05 M HF.

Adsorption of Protactinium on Other Inorganic Exchangers. - As in earlier investigations,⁴⁰ the results of adsorption experiments with silica gel and Bio-Rad ZP-1 (a zirconium phosphate exchanger) continue to show a good potential for separating protactinium from irradiated thorium,

The adsorption properties of silica gel and Bio-Rad ZP-1 were compared by contacting them with 0.5 to 12 M HNO₃ solutions containing 4.50 and 100 g of Th per liter and ²³³Pa equivalent to 1 to 5 × 10⁵ counts min⁻¹ ml⁻¹. Except for slight minima at 3 to 5 M HNO₃, the distribution coefficients obtained with silica gel increased as the nitric acid concentration increased or as the thorium concentration decreased. The coefficients ranged from 2100 to 5800 for solutions containing 4 g of Th per liter; from about 1900 to 4000 for a Th concentration of 50 g/liter; and from 1450 to 2380 for a Th concentration of 100 g/liter. The amount of unadsorbable protactinium ranged from 0.6 to 1.9% and was independent of the nitric acid or thorium concentration. With Bio-Rad ZP-1, the coefficients ranged from 100 to 29,000 for thorium solutions (4 g/liter) in which the molarity of the HNO₃ ranged from 0.5 to 12 M. Although 45% of the protactinium was unadsorbable from 0.5 M HNO₃, less than 0.4% was unadsorbable from solutions that were ≥ 3 M in HNO₃. With solutions containing 50 and 100 g of Th per liter and 0.5 to 12 M in HNO₃, the coefficients ranged from 400 to 19,000 and 200 to 8000 respectively. At both thorium concentrations, more than 95% of the protactinium was unadsorbable from solutions 1 M in HNO₃. With 3 M HNO₃, 3% was unadsorbable when the Th concentration was 50 g/liter, and 15% when the concentration was 100 g/liter. Nearly all the protactinium was adsorbable at higher nitric acid concentrations.

To complete the comparison, approximate distribution coefficients obtained for unfired Vycor are: 600 to 5000 for a solution containing 5 g of

Th per liter; 500 to 4200 for a concentration of 50 g/liter; and 400 to 3400 for a concentration of 100 g/liter. Although the distribution coefficients are higher for Bio-Rad ZP-1 than for unfired Vycor, preliminary experiments showed that ZP-1 is attacked by 0.5 M oxalic acid; therefore, other agents must be found for eluting the protactinium from this material.

1.5 CHLORIDE VOLATILITY STUDIES WITH URANIUM AND PLUTONIUM

Chlorination is being studied as a volatility method for recovering uranium and plutonium from UO₂-PuO₂ fuels. Quantitative recovery of the uranium and plutonium and decontamination from fission products by a factor of at least 50 to 100 is required so that the product chlorides can be reconverted to oxide fuel, possibly by a sol-gel method. Direct chlorination with 85% Cl₂-15% CCl₄ of UO₂-PuO₂ fuel pellets containing up to 35% PuO₂ was studied briefly. In all cases, the rate of reaction was too low to be of practical use in the temperature range of interest, 400 to 600°C.

Prior work with UO₂ fuel⁴¹ showed that rapid chlorination could be achieved after converting UO₂ pellets to U₃O₈ powder with oxygen at 500 to 800°C. Oxidation not only results in the conversion of the uranium to a higher valence state but also yields a product of high specific surface area. Similar oxidation experiments showed that UO₂-PuO₂ fuel pellets generally could be converted to U₃O₈-PuO₂ powder when the PuO₂ content of the pellet was 17% or less (Table 1.10). However, pellets containing 20% or more PuO₂ were generally unaffected by oxygen, even after long reaction periods at temperatures up to 800°C. A more critical evaluation of the oxidation behavior of UO₂-PuO₂ pellets cannot be made since, in general, the pellets used had not been carefully characterized. However, these preliminary data do indicate that an oxidation-chlorination process for fuel containing more than 20% PuO₂ may not be feasible.

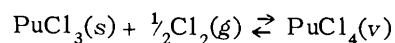
Chlorination, with several reagents, of the U₃O₈-PuO₂ powders resulting from the reaction

⁴⁰Chem. Technol. Div. Ann. Progr. Rept. May 31, 1964, ORNL-3627, p. 16.

⁴¹Chem. Technol. Div. Ann. Progr. Rept. May 31, 1964, ORNL-3627, pp. 17-19.

of $\text{UO}_2\text{-PuO}_2$ pellets with oxygen was studied in an effort to find the best chlorinating agent. Of the reagents tested, which included chlorine, $\text{CCl}_4\text{-N}_2$ mixtures, phosgene, and CO-CCl_4 mixtures, a mixture of 85% Cl_2 -15% CCl_4 (produced by bubbling chlorine through liquid CCl_4 at 25°C) gave the best results. Pure U_3O_8 was readily converted to volatile uranium chlorides at 400 to 500°C (Table 1.11). With a 1% PuO_2 -99% U_3O_8 powder, the rates of chlorination were too low to be practical at 300 to 350°C. At 400 to 500°C, nearly complete volatilization of the uranium was achieved in 3- to 4-hr reactions, but only up to 50% of the plutonium volatilized. Complete volatilization from the hot zone of the reaction vessel of both uranium and plutonium

chlorides was achieved at 600°C with an excess of chlorine. Calculations⁴² based on equilibrium data for the reaction⁴³



showed that about 3.3×10^5 and 100 moles of chlorine are required to transport 1 g-atom of PuCl_4 at 427 and 727°C respectively. Thus,

⁴²T. A. Gens, *Thermodynamic Calculations Relating to Chloride Volatility Processing of Nuclear Fuels. II. The Capacity of Chlorine for Transporting Plutonium Tetrachloride Vapor During Reaction of $\text{U}_3\text{O}_8\text{-PuO}_2$ with Carbon Tetrachloride*, ORNL-3693 (October 1964).

⁴³R. Benz, *J. Inorg. Nucl. Chem.* **24**, 1191 (1962).

Table 1.10. Reactivity of $\text{UO}_2\text{-PuO}_2$ Pellets in Oxygen at High Temperatures

Experiment No.	PuO_2 Content of Pellet (%)	Oxidation Temperature (°C)	Reaction Time (hr)	Oxidation of UO_2 to U_3O_8
1	0	400	0.5	Yes
2	0	600	3.0	Yes
3	1	600	1.0	Yes
4	1	600	3.0	Yes
5	5	600	1.0	Yes
6	17	600	3.0	Yes
7	17.8	600	1.0	Yes
8	20	600	19.0	No
9	20	800	20.0	No
10	20 ^a	600	3.0	Yes
11	35	800	18.0	No

^aThis pellet was fired to only 1300°C during manufacture; the others were fired at 1600°C.

Table 1.11. Reaction of $\text{U}_3\text{O}_8\text{-PuO}_2$ Powders with 85% Cl_2 -15% CCl_4 at Various Temperatures

Experiment No.	PuO_2 Content of Mixture (%)	Temperature (°C)	Reaction Time (hr)	Amount Volatilized (%)		Moles of Cl_2 used per Gram-Atom of Pu Volatilized
				U	Pu	
1	0	400	5.5	100		
2	0	500	3.5	100		
3	1	300	5.0	14	5	3×10^6
4	1	350	2.75	35	2	6×10^5
5	1	400	4.0	99	23	8×10^4
6	1	500	3.0	93	49	1×10^4
7	1	600	3.0	59	29	3×10^5
8	1	600	6.0	100	100	7×10^4

failure to achieve complete volatilization of plutonium chloride at the lower temperatures may have been due to a deficiency of chlorine.

The optimum temperature for the chlorination of U_3O_8 - PuO_2 powders has not yet been determined but will probably be less than $500^\circ C$, where large amounts of chlorine are required to transport plutonium chloride. During chlorination at $500^\circ C$, definite evidence for sintering and some indication of melting were obtained. At $600^\circ C$, formation of a liquid phase (possibly UO_2Cl_2 or a similar compound) was always noted during the chlorination of powders containing up to 17% PuO_2 .

1.6 DEVELOPMENT OF MECHANICAL PROCESSES

Development of the shear-leach process with unirradiated fuel assemblies on a full engineering scale was continued. In this process for fuels clad with stainless steel or Zircaloy-2, the multirod assemblies are sheared in a 250-ton shear, either with or without disassembly, and the sheared fuel is leached in nitric acid to produce solvent extraction feed. Significant developments discussed in this section are summarized in the next paragraph.

Because second-generation power-reactor fuels may not always be satisfactorily sheared intact in the 250-ton shear, a useful prototype fuel-rod row puller was built. Shearing tests on bundles of loose rods and on an annular Zircaloy-2-clad uranium-metal fuel rod were satisfactory. Studies on the remote handling and fission product heat generation in baskets of sheared fuel showed that no serious problems exist there. Head-end studies on the safety aspects of zirconium fines indicate that a fire or explosion hazard may exist in the removal of assembly end boxes by sawing with abrasive disks. Leaching tests on metal-clad ThO_2 - UO_2 were concluded. A delayed-neutron activation analysis monitor for determining the residual fuel content of leached hulls showed that losses in the range of 0.01% can be consistently detected.

A pictorial flowsheet of the shear-leach process as applied to second-generation fuels where fuel disassembly is required is shown in Fig. 1.7. An optimized layout of equipment for the same fuel type is shown in Fig. 1.8. This conceptual layout is based largely on the results of the developments

carried out over the past several years on the process.

Fuel Disassembly Tests

Since some second-generation power-reactor fuels cannot be sheared satisfactorily without first being disassembled, mechanical equipment (Fig. 1.9) consisting of a hydraulic cylinder, gripper head, bumper, cradle, ejector, and elevating jacks was built to demonstrate multitube withdrawal from the "egg crate" of the Consolidated Edison core B fuel assembly. After the inert end adapters are removed from a fuel assembly by sawing with an abrasive disk, the remaining "egg crate," containing the fuel rods, is placed in the cradle, which in turn is placed on the rollers on the rod puller platform and clamped into position. The fuel assembly is then forced against the ejector plate by the bumper and hydraulic cylinder which pushes one row of 13 or 14 fuel tubes about 3 in. through a slot in the bumper into the jaws of the gripper head. The tubes are finally clamped with the gripper head and pulled from the parent assembly by a hydraulic cylinder. The procedure is repeated until the assembly is emptied of tubes. After each row of tubes is withdrawn, the assembly is raised with elevating screws to properly align the next row with the ejector plate and the slot in the bumper. The loose tubes are then loaded into an open-top envelope for shearing.

In tests with this equipment, a force of 332 to 420 lb was required to eject a row of 14 UO_2 -filled tubes from the assembly into the gripper head, and a force of 238 to 315 lb was then required to withdraw them. It is expected that the force required to displace fuel tubes may be slightly higher after the assembly has been irradiated; roughened surfaces will develop because of the formation of oxides.

Shearing Tests

Shearing tests with the 250-ton prototype fuel shear were made this year on both Zircaloy-2-clad UO_2 multitube fuel assemblies and on coextruded Zircaloy-2-clad uranium metal.

A stacked 8×8 array of unsecured Zircaloy-2-clad UO_2 fuel tubes (0.4395 in. in outer diameter, with a 0.32-mil wall) was sheared into 1-in.

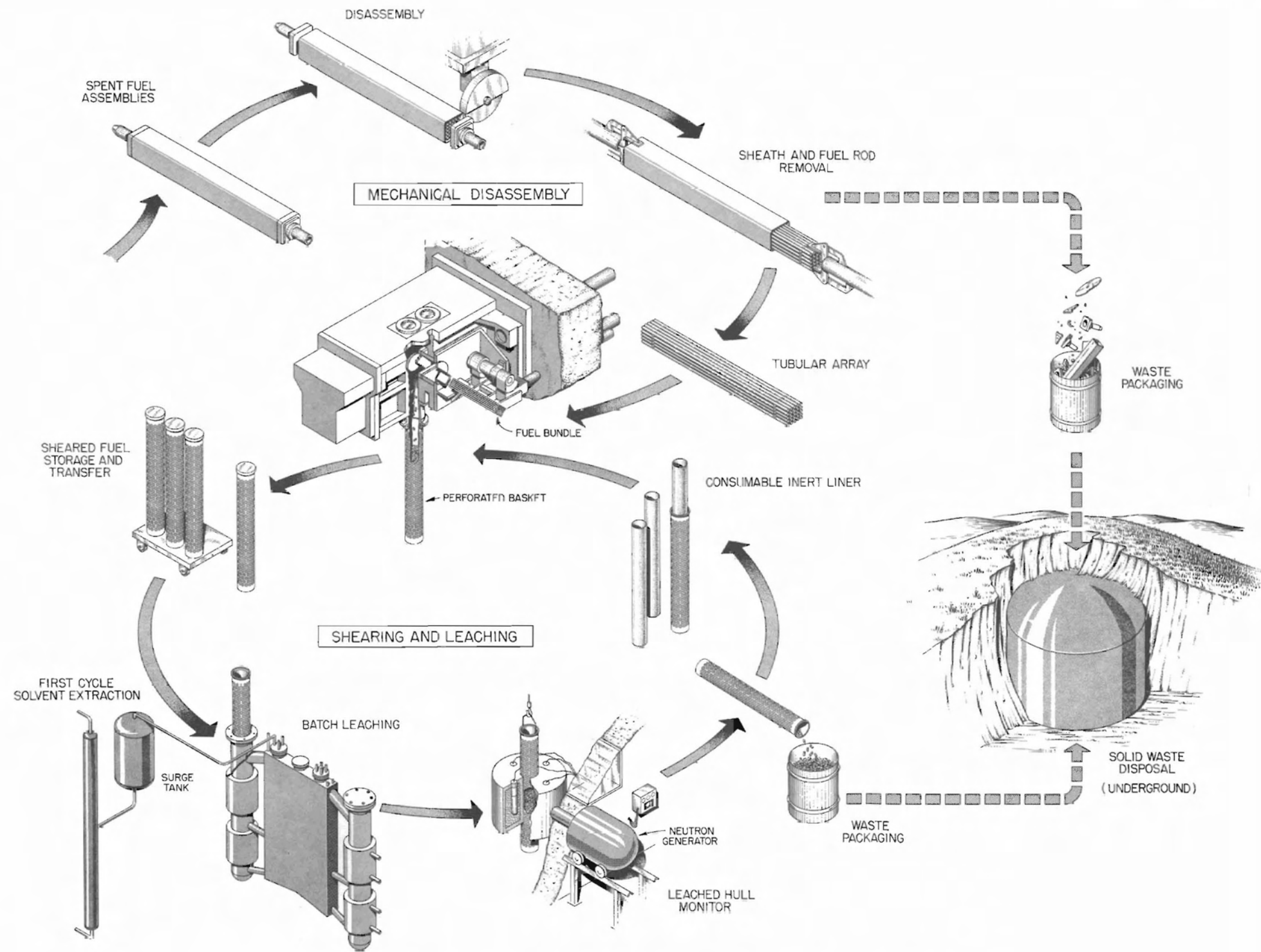


Fig. 1.7. Flowsheet for Shear-Leach Process for Second-Generation Power-Reactor Fuels.

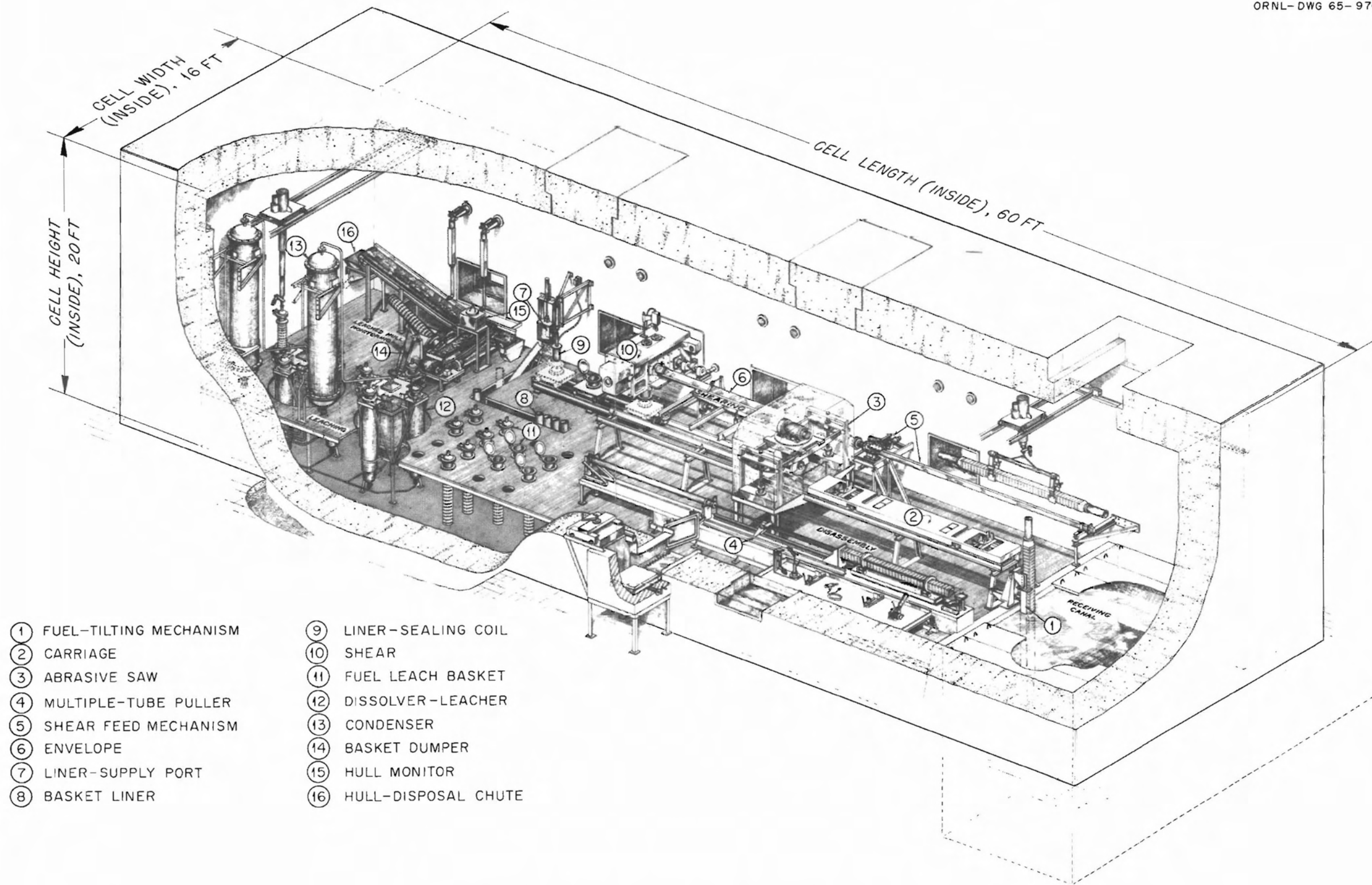


Fig. 1.8. Optimized Layout of Equipment for the Shear-Leach Process.

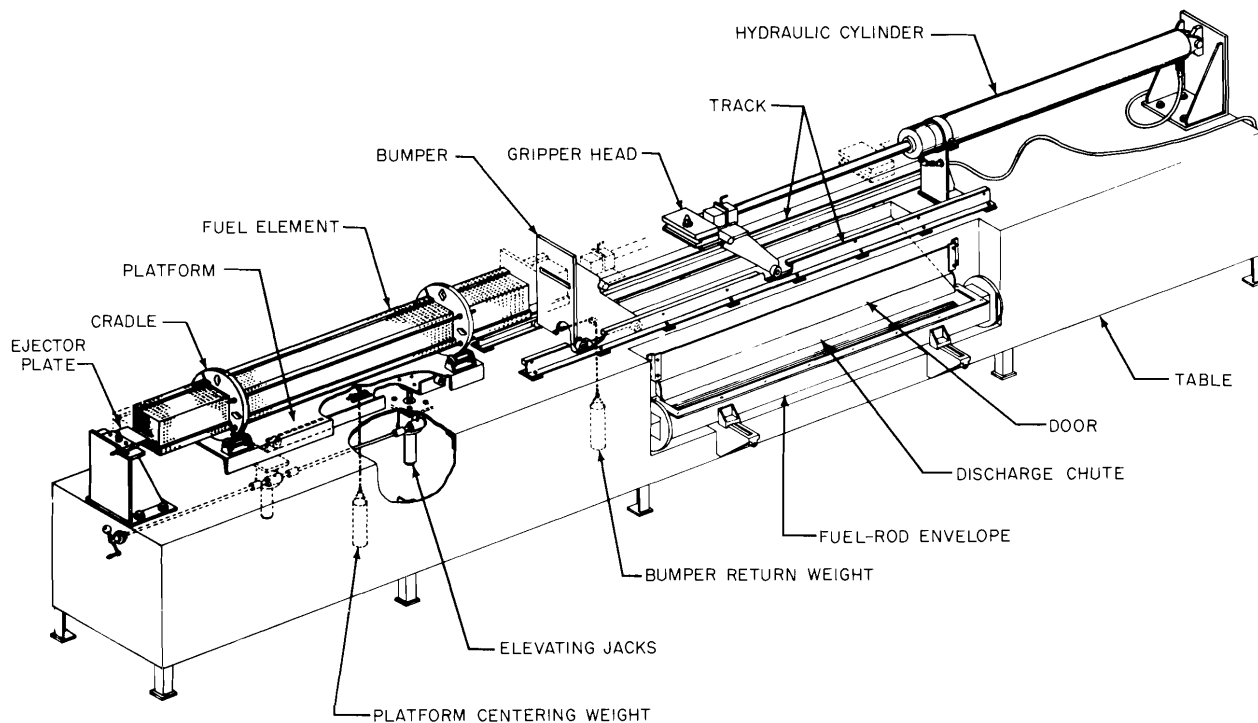


Fig. 1.9. Equipment for Withdrawing Rows of Fuel Rods from Second-Generation Power-Reactor Fuel Assemblies.

lengths. It was observed that there was less end closure of the brittle zirconium than with the more ductile stainless steel, which results in the dislodgement of considerably more fuel. Some sparking, about one to three sparks per cut, was observed. The shearing force required was from 50 to 60 tons. From these tests, it appears that zirconium-clad fuels will be easier to shear than stainless-steel-clad fuels.

Fuel assemblies consisting of 3-in.-diam coextruded Zircaloy-2-clad uranium metal were successfully sheared into $\frac{1}{2}$ -, 1-, $1\frac{1}{2}$ -, and 2-in. lengths. One fuel assembly was sheared at a time; the fuel was "gagged" or clamped during shearing, using semicircular inserts in the fixed blade holder and gags. There was no discernible difference in the power required or appearance of the sheared sections when using a straight or tapered semicircular moving blade. The shearing force varied from 45 to 82 tons and was independent of length sheared. About 30% of the cross section of the fuel was sheared, and the remainder was broken. There was only a small amount of wiping of the Zircaloy-2 cladding over the face

of the exposed uranium. Some sparking occurred during shearing, but there appeared to be no real hazard involved in shearing this type of fuel.

Shear Evaluation Tests

A rack-and-pinion feeding mechanism was installed and tested on the 250-ton prototype shear, replacing the hydraulic system. Replacement was made so that the length to be sheared from a fuel assembly could be controlled by the external feed mechanism itself rather than by an internal stop inside the shear, which experience had shown to be difficult to repair. The new mechanical device operated satisfactorily in shearing tests with various types of fuel-assembly prototypes.

Inspection of the shear after 10,100 cuts revealed an appreciable increase in the galling of the gibs (type 420 stainless steel) as compared with the galling after 7600 cuts. It is estimated that the shear has been stroked an additional 10,000 times for various reasons, resulting in a total of nearly

20,000 strokes. Some of the galling is attributed to misalignment in the shear; this has been corrected. For the most part, the shear was operated dry, but a lubricant, such as a molybdenum disulfide suspension in water, is desirable. The gibs were cleaned by grinding. Measurements indicated a hardness of 53 Rockwell C for the Stoody-I liners and 47 for the gibs. The liners were only moderately galled.

Remote-Handling Tests with Fuel Leaching Baskets

In the batch shear-leach process, a solid consumable liner of 10-mil carbon steel is inserted in the perforated basket to confine the sheared fuel during shearing, storage, and transport. To avoid losing fuel, there must be a dust-tight seal between the liner and perforated basket. A mockup cell was built and successfully operated to demonstrate the feasibility of using a Magneforming machine capable of producing up to 4500 ft-lb of energy to expand the liner into the groove. To attain maximum efficiency with the Magneformer, a highly conductive material was taped to the inside of the liner in the area to be expanded. Aluminum tape with an adhesive backing was the most satisfactory. The cell-mockup operation also demonstrated the use of a hinged Tube-Turn closure as a means of sealing the top of the basket during transport; a Grayloc connector provided a satisfactory seal between the basket and leacher. In concluding these tests, a short color movie was made to illustrate the simplicity and feasibility of these remote manipulator operations.

Heat Transfer Tests with Fuel Leaching Baskets

Leaching baskets filled with sheared, highly irradiated, spent reactor fuel will, because of heat generated by the fission products, reach some steady-state temperature in storage while awaiting transfer into the leaching equipment. Estimates were made of the amount of sensible heat in a typical basket of stainless-steel-clad UO_2 fuel and of the possible consequences of a sudden release of this heat from several such baskets of fuel in contact with nitric acid in a large leaching vessel.

The thermal conductivity k ($\text{Btu hr}^{-1} \text{ft}^{-1} \text{ } ^\circ\text{F}^{-1}$) for sheared stainless-steel-clad UO_2 is being determined experimentally to aid in the evaluation. The measured heat transfer coefficient for dislodged UO_2 fines in an air atmosphere, consisting of a mean particle size of 120μ and 38% voids, increased linearly from $0.256 \text{ Btu hr}^{-1} \text{ft}^{-2} \text{ } ^\circ\text{F}^{-1}$ at 200°F to 0.448 at 1600°F .

In initial calculations, a k of 0.2 and 0.4 was selected, and a typical second-generation UO_2 fuel, having a specific power of 23.5 w/g and a burnup of 20,000 Mwd/ton, was chosen. The cooling time was assumed to be 180 days. It was further assumed that a nominal 8-in.-diam leaching basket would be filled to a depth of 6 ft with 1-in. lengths of sheared fuel. The filled baskets would be stored in an open array approximately as shown in Fig. 1.8 (item 11). Heat transfer from the sealed baskets to the cell atmosphere, at an ambient temperature of about 120°F , would occur by both radiation and natural convection.

It was also assumed that during the initial 15-min contact in the acid, the carbon-steel liner and all dislodged UO_2 fines are dissolved, and that all sensible heat is transferred from the sheared fuel. In a leacher sized to dissolve 1 metric ton of uranium, a maximum of about 55,000 kcal of heat would be released from a total of six baskets during this time. Assuming good mixing of the leachant, as little as 300 gal could absorb this amount of energy in being heated from 90°F to about 190°F . The mass of stainless steel in leachers of this size represents an additional heat sink of about 30,000 kcal between initial and final temperatures of 120 and 190°F respectively. Therefore, the amount of acid it would be possible to flash during this initial period would probably not cause any significant pressure rise. The results of this preliminary calculation are summarized in Table 1.12.

A more exact calculation will be made pending completion of k measurements and evaluation of the induced activity.

Safety Studies on Finely Divided Zirconium

To evaluate the safety of sawing and shearing zirconium, fuel tubes filled with UO_2 were sawed and sheared; the fines are being metallurgically examined.

Table 1.12. Estimated Heat Release from a Basket of Fully Irradiated Sheared, Stainless-Steel-Clad UO₂ During Initial 15-min Immersion in 6 M HNO₃ at 72°F

Heat Source	Weight (kg)	Heat Release (kcal/kg)	Heat Release (kcal)	
			k = 0.2	k = 0.4
UO ₂ -stainless steel fuel quenching	261 ^a		-4510 ^b	-3550 ^b
Decay heat	261	-1.46	-380	-380
Mild steel dissolution ^c	2.22	-997	-2210 ^d	-2210 ^d
UO ₂ fines dissolution ^c	70.2	-31.1	-2180 ^e	-2180 ^e
Total heat release			-9280	-8320

^aWeight of 1-in. sheared lengths of UO₂-SS contained in a basket liner 7.75 in. in inner diameter and 6 ft high. Uranium weight is about 175 kg.

^bBasket temperature profile is for a volume heat source; C_p for 75% UO₂-25% stainless steel = 0.072 Btu lb⁻¹ deg⁻¹. Center-line temperature of fuel in basket, 790°F; basket liner temperature, 435°C; basket surface temperature, 355°F; ambient temperature, 120°F.

^cThe iron and UO₂ would not normally dissolve at 120°F, placing the overall calculation on the conservative side.

^dMild steel liner is 0.010 in. thick; dissolution reaction: Fe + 6HNO₃ → Fe(NO₃)₃ + 3H₂O + 3NO₂.

^eReaction: UO₂ + 4HNO₃ → UO₂(NO₃)₂ + 2H₂O + 2NO₂.

Zircaloy-2 rods ($\frac{3}{8}$ in. in outer diameter) were cut with an abrasive disk saw with and without coolant water, with a medium-hard abrasive blade (Manhattan No. 225) rotating at about 10,450 surface feet per minute. The rods were fed through the saw at 3 in./min. Dry cutting of the zirconium presents a definite fire hazard, as evidenced by the brilliant stream of sparks and dense smoke produced. Therefore, wet cutting is recommended, especially where the abrasive sawing will be done in the presence of uranium metal or other materials, whether pyrophoric or combustible. Of the particles collected from the dry abrasive sawing, 79 and 31 wt % of them were less than 400 and 44 μ in size respectively. The volume ratio of abrasive blade consumed to zirconium particles produced was 7.3 to 1.

Sawing with a wet abrasive disk (three water spray nozzles directed on the saw blade) decreased the spark stream to an occasional spark. The amount of zirconium fines from wet sawing is twice that produced in dry cutting because of the burning during the dry cutting. With wet cutting, the weight of Zircaloy-2 particles smaller than 400 μ (the size range where special handling is recommended in hot cells) was 94.5% of the total produced; 39% of them were smaller than 44 μ (Table 1.13).

Table 1.13. Particle-Size Distribution of Zircaloy-2 Fines Produced by Wet Sawing of $\frac{3}{8}$ -in.-diam Tubes

Particle Size (μ)	Percentage of Fines (wt %)
< 2000	99.04
< 840	97.7
< 420	95.3
< 250	90.0
< 149	77.5
< 88	62.4
< 74	55.7
< 44	38.7

Tests by the Bureau of Mines⁴⁴ have established that dry zirconium powder (90% ≤ 6 μ) can ignite explosively and spontaneously when dispersed in air at room temperature or when heated in air to 190°C. Since 39% of the Zircaloy-2 fines from wet sawing are smaller than 44 μ, it is assumed that a considerable amount is in the 6-μ range and

⁴⁴Zirconium Fire and Explosion Hazard Evaluation, TID-5365 (Aug. 7, 1956).

should be kept under water until discarded. Once the Zircaloy-2 powders are wet, they should be kept wet because powders containing 16% or less moisture are considered particularly hazardous. Special procedures must be followed in handling the fine powder even when stored under water because the powder settles into a compact mass that can exclude much of the water. Fires have started⁴⁵ when such packed powders were disturbed. Since the Zircaloy-2 particles are highly diluted with the abrasive particles (volume ratio, 1 to 6.6; weight ratio, 1 to 2.9), it is probable that this dilution provides a built-in safety factor in preventing spontaneous or static-spark reactions.

The literature on the relationship between fineness of the powder (and other factors) and fires or explosions shows the following: The dry powder is ignitable at room temperature by static electricity.⁴⁵ Powders containing 16% or less moisture may explode spontaneously in a vacuum.⁴⁴ The surface area of powders in square meters per gram is within 10% of the reciprocal of the average particle size in microns. When the area per gram approaches 0.1 m², careful handling is necessary.⁴⁶ Violent explosions, which have resulted in fatal injuries, have all involved particles smaller than 62 μ (230 mesh).⁴⁷ Scrap finer than 20 mesh (800 μ) and coarser than 120 mesh (125 μ) should be collected under water and mixed half and half with sand or grinding-wheel grit.⁴⁷ Powders that have a water content of 3 to 16% and that have been stored for a fairly long time are the most hazardous.⁴⁸ Crystal-bar Zircaloy-2 irradiated to 540 Mwd showed no appreciable amount of hydrogen pickup. The microhardness of Zircaloy-2 irradiated to 15.2×10^{19} nvt increased from 135 to 173 DPH as measured at a 50-kg load.⁴⁹

⁴⁵National Safety Council Data Sheet No. 382, rev., 1957.

⁴⁶W. R. DeHollander, *An Evaluation of the Zirconium Hazard*, HW-44989 (Aug. 15, 1956).

⁴⁷W. W. Allison, *Zirconium, Zircaloy, and Hafnium Safe Practice Guide for Shipping, Storing, Handling, Processing, and Scrap Disposal*, WAPD-TM-17 (Rev.) (December 1960).

⁴⁸F. B. Holt and S. G. Wilson, *A Code of Practice for the Handling of Zirconium and Its Alloys*, No. IGR-TD/S-578, United Kingdom AEC (July 1957).

⁴⁹M. L. Bleiberg and L. S. Castleman, *Effects of Neutron Bombardment upon the Properties of Zirconium and of a Zirconium-Tin Alloy*, WAPD-78 (Mar. 17, 1953).

Engineering-Scale Leaching Studies

Batch leaching tests with sheared, unirradiated stainless-steel-clad UO₂ and UO₂-ThO₂ fuels were continued in an engineering-scale 90-liter Pyrex and stainless steel leacher (Fig. 1.10) in which the leaching section is 9 in. in inner diameter and 10 ft tall. Heat is supplied by a steam jacket with an inside surface area of 6.6 ft². In the leacher, boiling induces a counterclockwise circulation through a side arm arranged to impinge dissolvent on the bottom of the leacher; this produces the same general effect as would be attained with an air-sparge draft tube. Fuel charges in a slotted fuel basket varied from 18 to 36 kg.

The consumable carbon-steel liner dissolved in about 2 min. As the liner dissolved, 14 to 38% of the core was discharged from the basket and settled to the bottom of the leacher.

The overall heat transfer coefficient, based on the inside area of the jacket, is fairly constant for both water and a solution containing 250 g of Th per liter at steam pressure of 20 to 60 psig. For water, the coefficient varied from 164 to 180 Btu hr⁻¹ ft⁻² °F⁻¹, and for the thorium solution, from 200 to 210.

In one test, in which UO₂ was leached from 1-in.-long sheared sections of stainless steel cladding with boiling 7 M HNO₃, total dissolution was attained in 2 hr. Because UO₂ dissolves rapidly, variables affecting the rates were studied more satisfactorily with slower-dissolving ThO₂-UO₂, using boiling (120°C) 12.7 M HNO₃-0.04 M F⁻-0.1 M Al³⁺ as the solvent. Typical UO₂-ThO₂ leaching data are presented in Fig. 1.11, which shows the effect of dissolution time on terminal thorium loading, boilup rate as represented by steam pressure, and a comparison of 1/2- and 1-in. sheared lengths. The duration of all tests was sufficient to ensure that 99.9% of the uranium and thorium would dissolve. With the exception of one run, all fuel was sheared to 1-in. lengths.

Leaching times for 1/2- and 1-in. sheared lengths were nearly equal (18 hr and 19 hr). Leaching times for equivalent thorium loadings in the solutions were roughly doubled by reducing the steam pressure from 60 to 20 psi. At the same steam pressure, the time required to achieve a given thorium loading was approximately linear between 0.5 and 0.7 M Th but increased rapidly at higher loadings. Dissolution data obtained with a per-

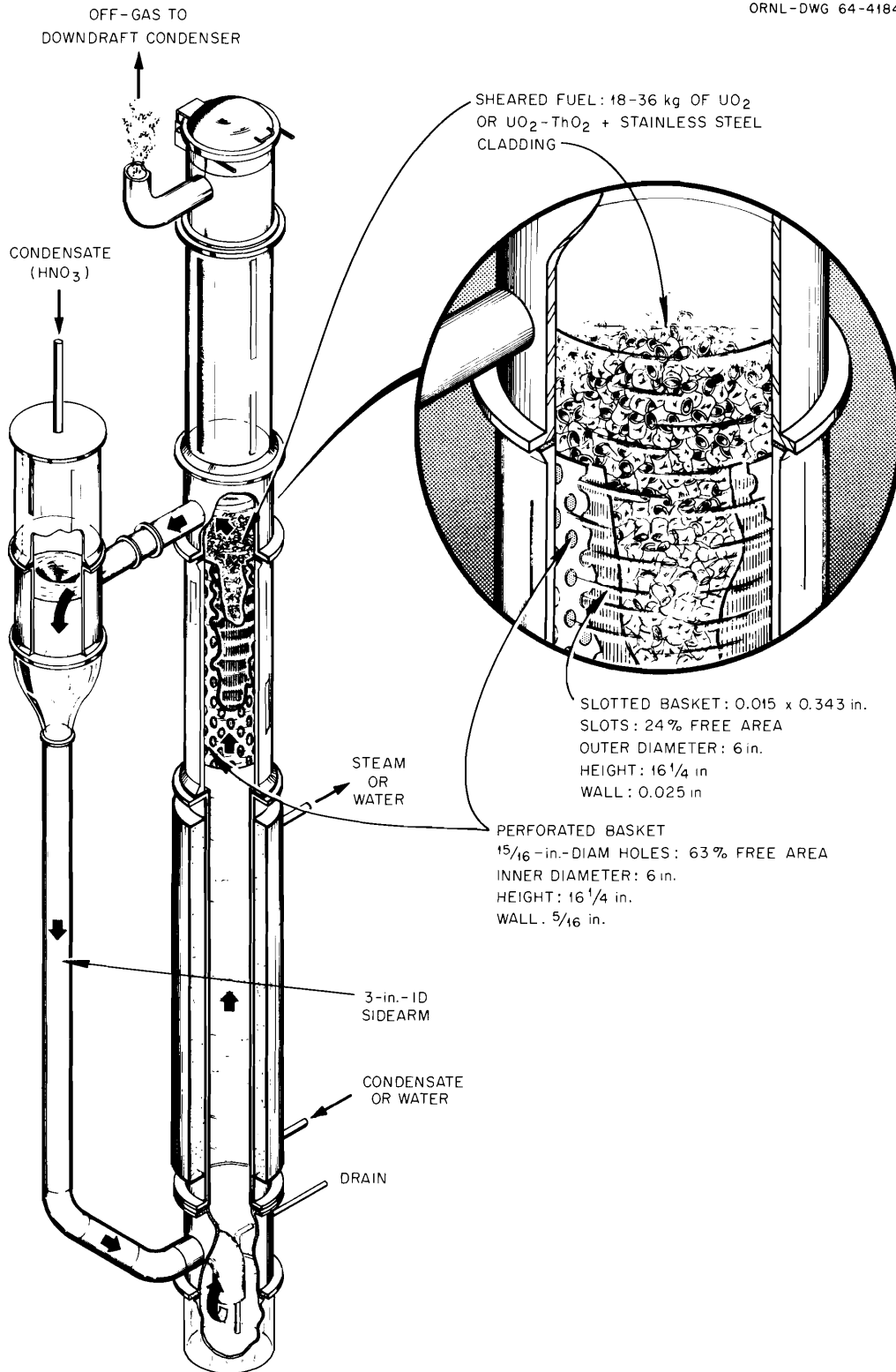


Fig. 1.10. Engineering-Scale 90-liter Batch Leacher for Dissolving Oxide Fuel from Sheared Cladding.

forated basket containing $\frac{1}{8}$ -in. holes on $\frac{1}{2}$ -in. centers (4.2% free area) were nearly the same as the data for the slotted basket shown in Fig. 1.10. This type of basket discharges the same amount of fines as the slotted basket does during the dissolution of the liner.

In producing a dissolver product approximately 1 M in Th or U when using a dissolvable 10-mil-thick carbon-steel basket liner, the resultant solution is nearly 0.1 M in Fe (about 11 g of iron per kilogram of core).

Monitoring of Leached Hulls⁵⁰

To be assured that the leaching of uranium, plutonium, or thorium from stainless steel or Zircaloy-2 cladding in the shear-leach process is complete, it would be very advantageous for a fuel processor to use a reliable monitor for

⁵⁰W. J. Ross, J. W. Landry, and J. E. Strain, "Monitoring of Leached Fuel Elements with a Neutron Generator," *Nucleonics* (August 1965).

testing the leached hulls. Several methods for such monitoring were evaluated, and a prototype was developed and tested. It can detect about 1 mg of ^{235}U , ^{239}Pu , or ^{233}U per kilogram of leached hulls. This corresponds to a fuel loss of less than 0.01% for typical low-enriched uranium power-reactor fuels. The proposed monitor is based on delayed-neutron activation analysis and is applicable to either stainless steel or Zircaloy-2 hulls.

The prototype monitor, capable of testing 20 (150 cm³ or 200 g) leached hulls at a time, was successfully demonstrated. A larger unit, capable of monitoring a 7-in.-diam fuel basket in successive 4-in. vertical increments (2.5 liters or 2.7 kg of hulls) is now being made. An illustration of the smaller test unit is shown in Fig. 1.12, and of the larger unit in Fig. 1.13.

In the test mockup, separate chambers made of paraffin blocks were used for irradiating and counting. The chambers were separated to prevent the boron in the BF_3 neutron detection tubes from being depleted by the neutron flux in the irradiation chamber. Operation consisted in placing 20 hulls

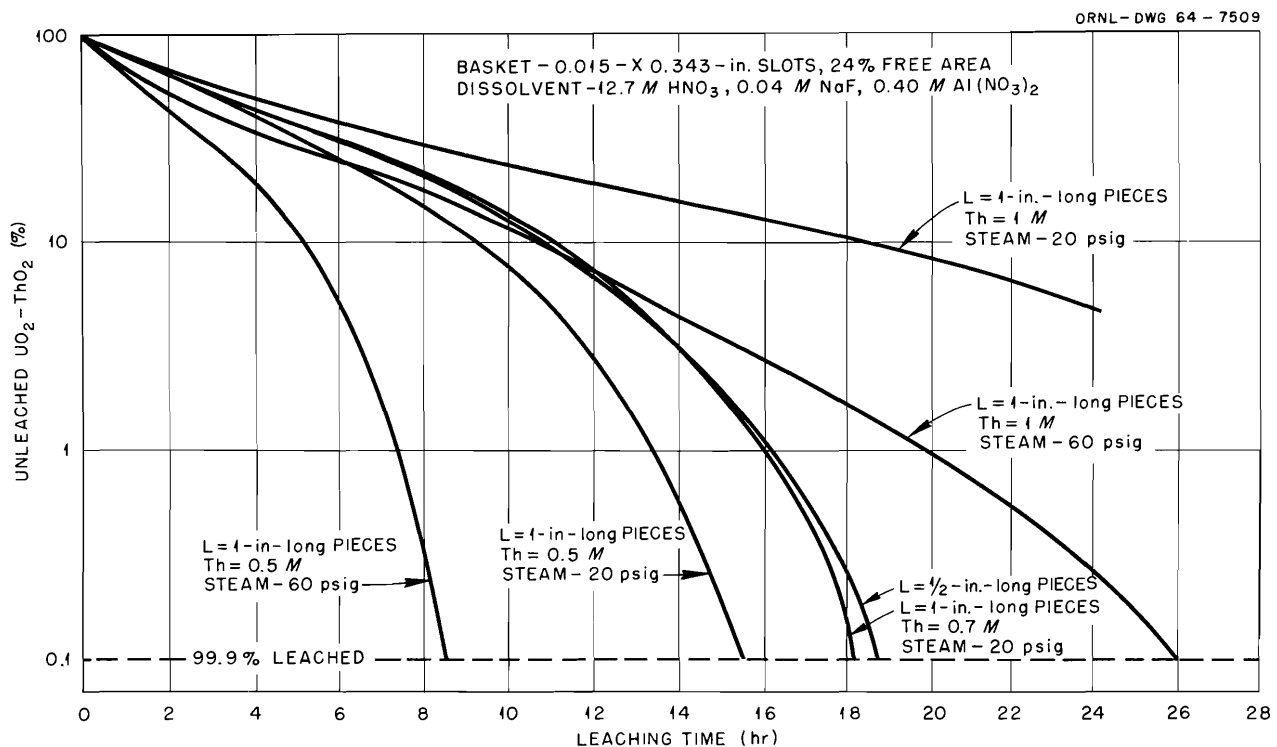


Fig. 1.11. Effect of Thorium Loading, Dissolution Temperature, and Length of Sheared Fuel in the Batch Leaching of Unirradiated $\text{UO}_2\text{-ThO}_2$ from Sheared Stainless-Steel-Clad Power-Reactor Fuel Elements.

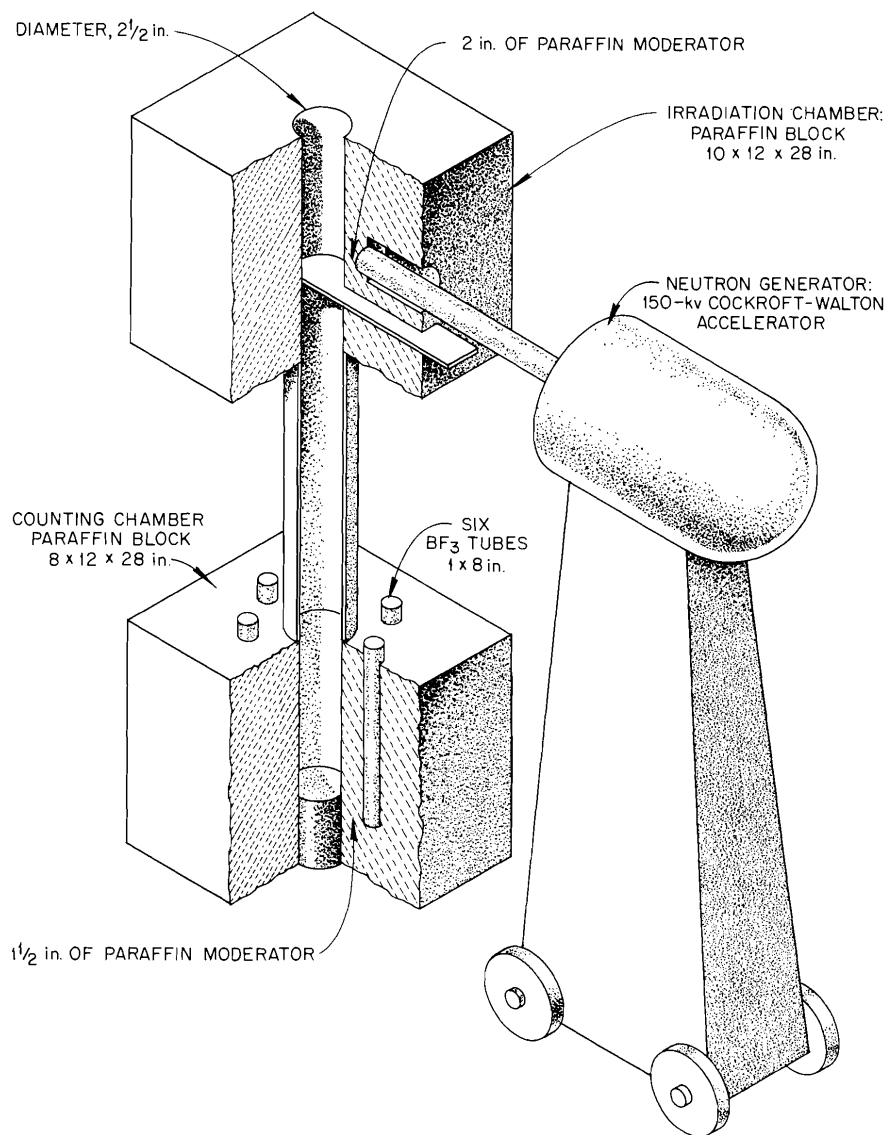


Fig. 1.12. Mockup Monitor for Testing Leached Fuel Cladding for Residual Fuel.

in the irradiation chamber (in the position marked "1" in Fig. 1.12) and irradiating them with thermal neutrons for about 20 sec. Within the following 2 sec, the floor of the chamber (the slide) was opened, and the activated hulls were dropped into the counting chamber (position "2" in Fig. 1.12), where the delayed neutrons from the activated hulls were counted for the next 30 sec. The average thermal-neutron flux during irradiation was 1.89×10^6 , and the average fast flux (14-Mev neutrons) was 1.67×10^8 . The efficiency of the

BF_3 counting system was only a few tenths of a percent because the BF_3 tubes were unmatched. Batches of 20 hulls containing weighed amounts of ^{235}U gave the results indicated in Table 1.14.

It was found that a 7-in.-diam basket of leached hulls must be monitored in vertical increments not exceeding 4 in. This specification was arrived at in the following way: The thermal-neutron flux in the irradiation chamber (6 cm in diameter and 8 cm long) was mapped by manganese detectors. The counts obtained from ^{235}U in a hull

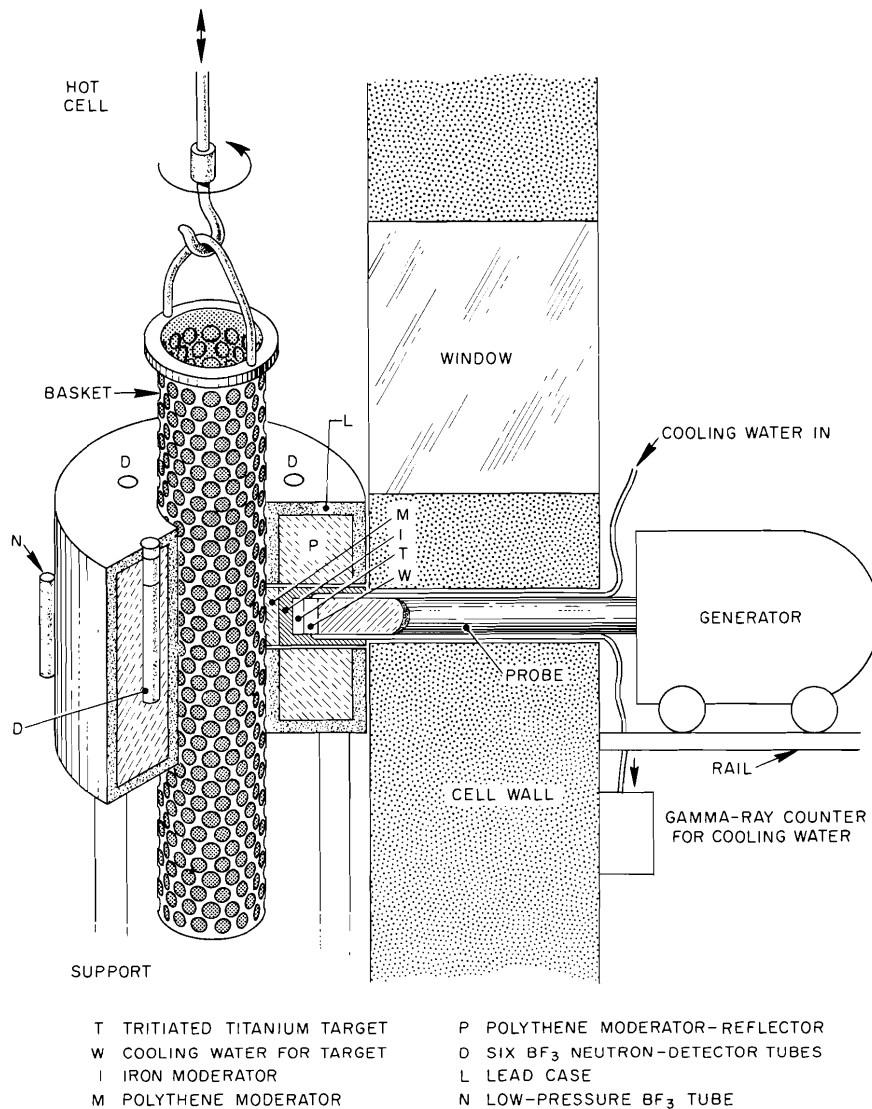


Fig. 1.13. Prototype Plant Monitor for Testing Leached Fuel Cladding for Residual Fuel.

can be determined within a variation of $\pm 15\%$ when the chamber is filled with hulls and when the position of the hull that contains the ^{235}U is varied throughout the volume of the chamber. Axial variation was $\pm 15\%$, and radial variation $\pm 5\%$. The sensitivity of the instrument decreased as the hull was moved along the axis away from the center of the chamber.

It is expected that the larger monitor (Fig. 1.13) will retain the 1- to 5-mg ^{235}U sensitivity obtained in the mockup test and that it will operate on about a 10-sec cycle. Table 1.15 shows the bases for these conclusions.

Other methods which were evaluated but which were less sensitive or completely inadequate included: (1) monitoring the residual 2.18-Mev gamma rays from $^{144}\text{Ce-Pr}$ either by gamma spectrometry or by detecting the neutrons generated by the $^9\text{Be}(\gamma, n)^8\text{Be}$ reaction; (2) monitoring the low-energy gamma and x-ray emission from ^{235}U and ^{239}Pu ; (3) comparing the gamma-ray emissions from $^{134,137}\text{Cs}$ and ^{60}Co ; and (4) comparing the absorptions of two gamma-ray energies, that from a ^{137}Cs source with that from a ^{241}Am source.

The instrument may also have general use as a waste monitor. For example, besides monitoring

Table 1.14. Neutron-Counting Results Obtained in Prototype Leached-Hull Monitor

Number and Type of Hulls Counted	Counts per Minute ^a
20 empty hulls; this is the background	6
19 hulls empty and 1 with 1 mg of ²³⁵ U	16
19 hulls empty and 1 with 5 mg of ²³⁵ U	47
18 hulls empty, 1 hull with 1 mg of ²³⁵ U, and 1 hull with 5 mg of ²³⁵ U	49
19 hulls empty and 1 with 100 mg of ²³⁵ U	650

^aBackground has not been subtracted.

Table 1.15. Comparison of Operating Characteristics of 150-cm³ Prototype Monitor and Proposed Plant Model

	150-cm ³ Prototype	Proposed Plant Model
14-Mev neutron flux	1.67×10^8	10^{11}
Thermal-neutron flux	1.89×10^6	1.3×10^{10}
Neutron flux utilization efficiency, %	1.13	13
BF ₃ counting delay, sec	2	0
BF ₃ counting efficiency, %	0.42	4-5

leached hulls, it may be useful for finding fuel shards in fluoride volatility processing waste and for determining fuel losses in liquid wastes from solvent extraction operations.

1.7 DEVELOPMENT OF CLOSE-COUPLED PROCESSES

The presence of 74-year ²³²U in recycled ²³³U, 1.9-year ²²⁸Th in recycled ²³²Th, and 13-year ²⁴¹Pu in recycled ²³⁹Pu makes the high-decontamination processing of recycle reactor fuels unnecessary because of the high gamma radiation background of the daughters of these short-lived isotopes in the recovered fuel. That is to say, since the recovered material must be handled by remote manipulation in any case, the decontamination from fission products need not be great — just enough to prevent their accumulation during multiple fuel cycles. Therefore, a program was

started this year to develop low-cost recovery methods, adaptable to remote operation, which will provide decontamination factors of 10 to 100 from fission products.

The processing cycle for recycle reactor fuel will probably consist in removing the cladding and/or moderating material by a physical head-end process (e.g., shear-leach, shear-burn, etc.); separating the neutron poisons from the fuels by a chemical method; reconstituting the fuel, probably by the sol-gel route (Sect. 6); and remotely refabricating the fuel assemblies. The product solution from the decontamination step must also meet the restrictions imposed by the subsequent sol-gel process regarding the type and amount of impurities present.

Work done this year to find a substitute for solvent extraction included research on methods such as electrodialysis, precipitation, and ion exchange, which might provide cheaper ways of obtaining low-decontamination recovery of the

fuel. So far, the outlook for these methods has not been promising. Therefore, a reexamination of solvent extraction chemistry and equipment was begun in an attempt to achieve cost savings through the use of simplified equipment and operating methods capable of obtaining lower decontamination factors. One result of these studies, which could reduce the subsequent waste-management costs, has been the satisfactory reduction of Pu(IV) to Pu(III) in nitrate solutions with Ar-4% H₂ in a column of platinized alumina. Another result has been the development of satisfactory solvent extraction and ion exchange flowsheets for removing ²²⁸Th and its daughters from ²³³U.

In the sol-gel process, ThO₂ sols, about 0.2 M in nitrate, are currently prepared by steam denitration of Th(NO₃)₄ solution. An alternative process, in which the sol is prepared by amine extraction of nitrate from Th-U nitrate solutions, was developed. Sol-gel materials produced by this new method are now being evaluated.

Studies of Decontamination by Precipitation, Ion Exchange, and Electrodialysis

Scouting experiments on the use of precipitation, ion exchange, and electrodialysis of acid deficient solutions as alternatives to solvent extraction to effect low decontamination of reactor fuels from fission products were generally unsuccessful.

Precipitation. - Thorium-uranium precipitation studies were made by using dibasic ammonium phosphate, oxalic acid, and 30% hydrogen peroxide as precipitants. Dibasic ammonium phosphate produced the most quantitative precipitation; however, most of the fission products were carried with the thorium-uranium precipitate. For example, more than 99.6% of the thorium and uranium and 98.8% of the fission product gamma activity were precipitated by adding 0.32 to 2 moles of dibasic ammonium phosphate per mole of thorium to a solution that was about 0.5 M in Th, 0.026 M in U, and 0.37 M in NO₃⁻ and which contained 1.6 × 10⁶ counts min⁻¹ ml⁻¹ of gross gamma activity. With solutions in which the nitrate-to-thorium ratio was varied from 4:1 to 0.4:1, the amount of thorium and uranium precipitated was independent of the nitrate concentration. However, the volume of the precipitate increased as the nitrate concentration increased, ranging from about 15% of the

original solution volume at 0.4 mole of NO₃⁻ per mole of Th to 60% at 4 moles of NO₃⁻ per mole of Th.

Ion Exchange. - Preliminary ion exchange studies were also made to determine if the fission products could be adsorbed from acid-deficient thorium-uranium solutions. When a solution that was 0.49 M in Th, 0.025 M in U, and 0.15 M in NO₃⁻ and which contained 2.1 × 10⁶ counts min⁻¹ ml⁻¹ of gross gamma was passed through columns containing various adsorbents, less than 20% of the activity was adsorbed on Dowex 50W and ZP-1. None of the fission products were adsorbed on silica gel or Dowex 1.

Electrodialysis. - Thorium-uranium nitrate solutions and mixed-fission-product solutions were electrodialyzed in an attempt to remove and separate fission products. Electrolytic processes have an advantage over others because they do not require the addition of reagents that may give difficulty in subsequent operations. In electrodialysis, ion exchange membranes are used to separate the compartments of the electrolytic cell and thereby increase the efficiency of ion separation.

During a 6-hr electrodialysis of solutions that were about 0.5 M in Th, 0.02 M in U, and 0.3 M in NO₃⁻ and which contained 2 × 10⁶ counts min⁻¹ ml⁻¹ of gross gamma, 50 to 55% of the thorium and uranium and 10% of the gamma activity precipitated on the cathodic membrane. When the cell was maintained at 2.5 v, the initial current was 198 ma; but during the 6-hr experiment, the current dropped to 22 ma. About 35% of the gamma activity, mostly ¹³⁴⁻¹³⁷Cs, transferred to the cationic compartment, and less than 0.1% transferred to the anionic.

Attempts to separate fission product elements from a thoria sol by electrodialysis were also unsuccessful, due both to limited migration of the fission products and to the instability of the sol in the electrolytic field. Only 5 to 10% of the fission products migrated to the cathodic compartment and none to the anodic after 5 hr at a potential of about 25 v. The positively charged ThO₂ sol migrated to the cationic membrane, where it precipitated. Very limited success in preventing the precipitation was achieved by dilution and stirring. Addition of sodium ethylenediaminetetraacetate (EDTA) or sodium citrate increased the removal of fission products to better than 30% but decreased the stability of the sol.

The EDTA complexes of the long-lived fission product elements have been separated – in the absence of thorium – in an electro dialysis cell by varying the pH of the solution.⁵¹ The pH's at which 90% of the Zr-Nb, Ru, Eu, Ce, Sr, and La transferred as anions were <0.5, 1.4, 1.8, 2.2, 2.4, and 3.6 respectively. Cesium remained cationic at pH values as high as 11. Separation into groups containing Zr-Nb and Ru; Eu, Ce, and Sr; La; and Cs were obtained by controlling the pH during electro dialysis. This migration of fission products may have application in isotope production or in waste disposal but does not seem practical in fuel processing.

Solvent Extraction Studies

Since largely negative results were obtained in scouting tests to evaluate precipitation, ion exchange, and electro dialysis as possible alternatives to solvent extraction as low-decontamination processes, emphasis has been increased this year on the development of simple and versatile solvent extraction equipment and flowsheets designed to decrease operating and analytical costs. Cost analyses showed that no substantial capital saving can be made by decreasing the cost of the solvent extraction contactor but that savings can be made by decreasing the complexity of the operation, thereby decreasing the number of analytical samples required and by having one operations crew perform various tasks in sequence rather than concurrently (see Sect. 1.8.1).

Work in this area has included the development of an efficient and reliable single-stage differential contactor and the development of flowsheets for use in decreased-stage mixer-settlers. New solvent extraction and ion exchange flowsheets were also developed for the cleanup of stored ²³³U, and a new method for reducing Pu(IV) to Pu(III) with Ar-4% H₂ was demonstrated.

Development of Differential Contactor. – Present solvent extraction processes for recovering and decontaminating fissionable and fertile materials from fission products use complex contactors that require closely supervised operation and many chemical analyses. Therefore, cheaper and simpler, but less efficient, contactors are being

investigated for this application. One device being evaluated is a differential extractor, which is a simple one-stage mixer-settler unit in which a static aqueous phase is maintained in the equipment while the organic phase is slowly passed through the unit. The two phases are stirred together vigorously in the mixer section and continuously circulated to the settler, where they disengage. The organic phase overflows continuously from the equipment, and the aqueous phase is circulated back to the mixer. A back-extraction unit may be operated similarly or may be modified to operate with the organic as the static phase. Due to the nature of the contactor, concentration of the product ion in the organic phase is at near saturation during a large portion of the recovery cycle, thereby increasing decontamination from impurities. The simplicity of this type of contactor results in satisfactory operation with a minimum of care and makes it adaptable to intermittent operation, such as one shift per day. The simplicity of the operation also minimizes analytical requirements.

In a typical test with a prototype unit, a 0.2 M acid-deficient solution 1.5 M in Th and 0.1 M in U was contacted first with 6 volumes of 3% TBP in *n*-dodecane and then with 7 volumes of 30% TBP in *n*-dodecane. More than 99.9% of the uranium and 87% of the thorium were extracted. The uranium product was decontaminated from thorium, rare-earth elements, zirconium, and ruthenium by factors of 16, $\geq 2.6 \times 10^4$, 300, and ≥ 500 respectively. The thorium-product decontamination factors from uranium, rare-earth elements, zirconium, and ruthenium were 7×10^4 , 16, 6, and 4 respectively. Better separation from rare earths is expected with more radioactive feeds.

The equipment was operated easily, and operation was nearly automatic. Also, the unit could be stopped and restarted easily. For example, several experiments were shut down overnight by turning off the solvent flow, allowing the solvent in the system to collect in the disengaging section, which required about 15 min, removing the accumulated solvent from the tube, and turning off the mixer. The next morning the system was restarted by simply turning on the mixer and the solvent pump. Because of the high saturation of thorium in the solvent during the first portion of the thorium cycle, two organic phases were present, but the equipment continued to operate satisfactorily.

⁵¹A. Facchini and R. H. Rainey, *The Separation of Long-Lived Fission Product Elements by Using Ethylenediaminetetraacetate in an Electro dialysis Cell*, ORNL-TM-1035 (1965).

In both the uranium and the thorium cycles, the solvent was nearly saturated during extraction of the first 75% of the material. Then, after a short transition period, the concentration in both the solvent and the aqueous phases decreased exponentially (Fig. 1.14). Operating variables may therefore be controlled with a minimum of analyses.

Countercurrent Recovery Processes. - In addition to the differential extraction studies discussed above, tentative flowsheets were outlined for recovering uranium alone, and for the simultaneous recovery of uranium and thorium in a countercurrent (mixer-settler) system with three extraction, one scrub, and three stripping stages. The process for recovering uranium alone was successfully demonstrated in a batch countercurrent test with an 8 M H⁺ dissolver solution that contained 6.9 g of U and 216 g of Th per liter. About 99% of the uranium was recovered with 0.25 M di-sec-butyl phenylphosphonate (DSBPP)

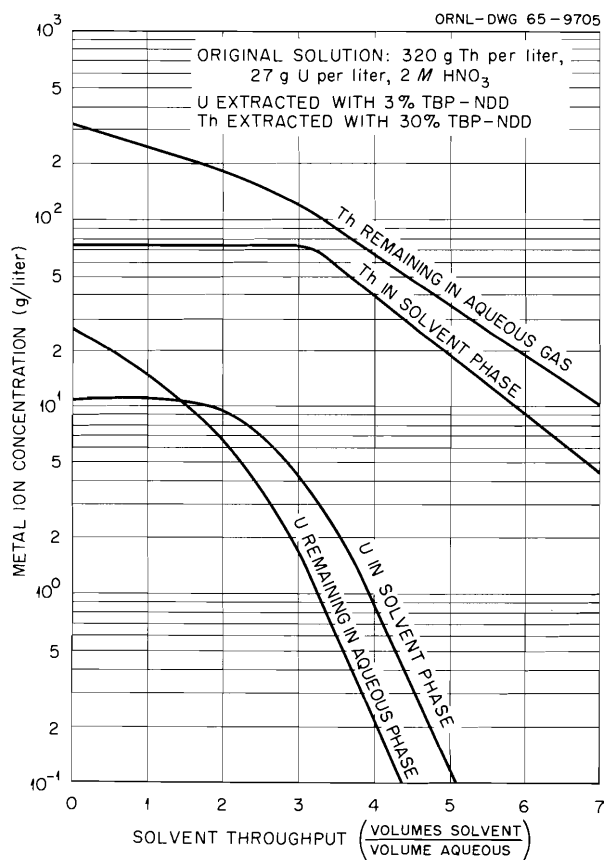


Fig. 1.14. Concentration of Uranium and Thorium During Extraction in a Differential Contactor.

in diethylbenzene (DEB) (Fig. 1.15). The extraction product was stripped with water; most of the third-stage strip solution was recycled to the scrub and extraction section. The product solution contained about 32 g of U and 0.16 g of Th per liter; the decontamination factor for uranium from thorium was about 6000. Decontamination factors from fission products were not determined in this test; however, subsequent tests, in which the stage samples were spiked with fission products and reequilibrated, indicated that decontamination factors from rare earths, zirconium-niobium, and ruthenium of >1000, >100, and >100, respectively, could be expected.

The number of stages and their arrangement were essentially the same for corecovery of uranium and thorium, but the solvent was 1 M TBP in diethylbenzene. The thorium product solution was withdrawn from the first stripping stage and the uranium product from the third.

Development of Process for Purifying ²³³U. - Since ORNL is a national depository for ²³³U, large quantities (several hundred kilograms) will soon be stored in new storage facilities being installed in Building 3019 (see Sect. 17.7). After its initial separation from the thorium in which it was produced, or after its decontamination following use as a reactor fuel, the stored ²³³U rapidly becomes radioactive again as a result of the buildup of the daughters of the ²³²U contaminant. The 2.6-Mev gamma from ²⁰⁸Tl is the controlling activity for shielding requirements, but other daughters also emit considerable gamma activity. Consequently, before the ²³³U is shipped to users, it is advisable to remove the ²³²U daughters immediately before shipping.

Although adequate cleanup of ²³³U can be accomplished in the existing Thorex solvent extraction pilot plant in Building 3019, the procedure is awkward and expensive since a large amount of thorium must be added as a neutron poison; the equipment is not geometrically safe. The added thorium also serves as a salting agent in the extraction of the ²³³U with 3% di-sec-butyl phenylphosphonate in diethylbenzene (DSBPP in DEB). For decontamination of large withdrawals, use of the pilot plant is probably warranted on a temporary basis; but for small shipments, new flowsheets, using either solvent extraction or ion exchange, were developed, and a new solvent extraction system using small, geometrically safe equipment was provided for this service.

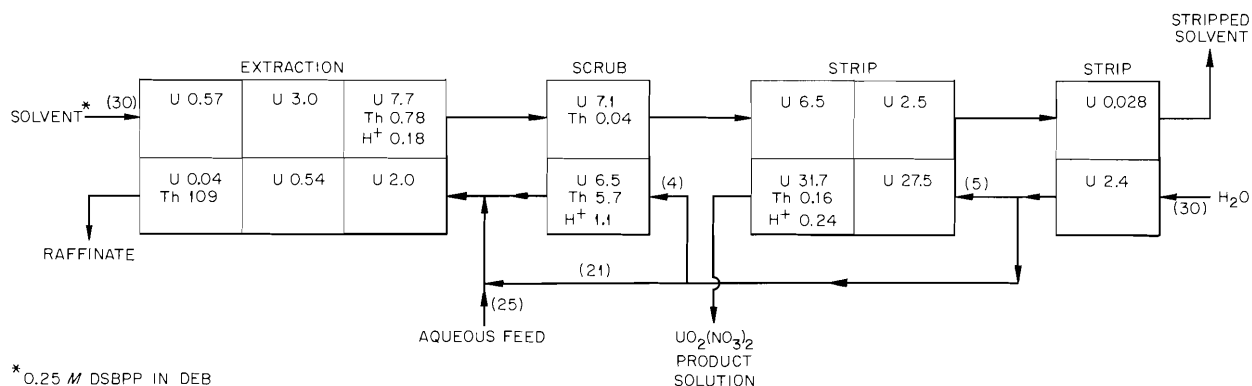


Fig. 1.15. Flowsheet for Selectively Recovering Uranium from U-Th Fuel Solution with DSBPP in DEB in a Reduced-Stage Mixer-Settler. Aqueous feed: prepared by dissolving unirradiated $\text{UO}_2\text{-ThO}_2$ fuel in 13 M HNO_3 -0.04 M HF; 8 M in H^+ , and contained, in grams per liter, 6.9 U, 216 Th, 6.7 Fe, 1.0 Al, and 0.37 Cr. Numbers in the blocks show the steady-state molar concentration of H^+ and the uranium and thorium concentrations, in grams per liter, of stage samples from batch countercurrent test. Numbers in parentheses show the relative volume flows.

Laboratory experiments with the new processes showed that the ^{233}U may be decontaminated from the daughters of ^{232}U either by extracting with 30% tributyl phosphate in *n*-dodecane (TBP in NDD) or by adsorbing the ^{228}Th (the immediate daughter of ^{232}U) on Dowex 50W ion exchange resin. However, solvent extraction is preferred because of better decontamination. The solvent extraction flowsheet feed stream compositions and rates are as follows:

Feed: 0.43 M $\text{UO}_2(\text{NO}_3)_2$, 0.3 M $\text{Al}(\text{NO}_3)_3$;
1 vol

Scrub: 0.2 M $\text{Al}(\text{NO}_3)_3$, 0.1 M $\text{Al}(\text{OH})(\text{NO}_3)_2$;
0.1 vol

Solvent: 30 vol % TBP, 70% NDD; 1.2 vol

About 4.5 hr after extraction, the reduction of ^{208}Tl activity was nearly a factor of 600 but decreased to about 100 after 44 hr and to 10 after 19 days (Fig. 1.16).

The ion exchange experiments consisted in passing solutions of various uranium concentrations through a column containing Dowex 50W resin, 50 to 100 mesh. The first day after treatment, the decontamination factor from ^{208}Tl was only about 2, but it increased to about 10 after 12 days (Fig. 1.16). Decontamination from ^{208}Tl and the resin throughput capacity both decreased as the concentration of uranium was increased.

When the solution contained 28 g of U per liter, the maximum decontamination factor was about 12, and the capacity was greater than 4.6 g of U per milliliter of resin. When the solution contained 123 g of U per liter, the maximum factor was about

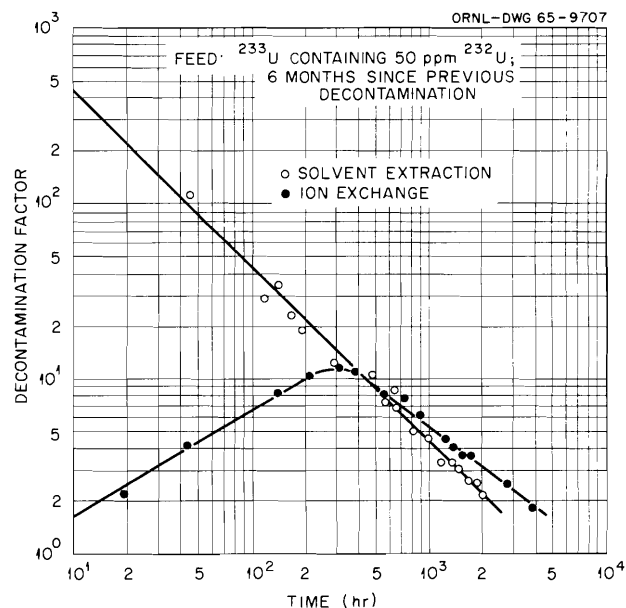


Fig. 1.16. Comparison of Decontamination of ^{233}U from the Daughters of ^{232}U by Solvent Extraction or Ion Exchange.

10 (Fig. 1.17), and the capacity was about 3.6 g of U per milliliter of resin.

These data (Fig. 1.16) indicate that even though solvent extraction provides a greatly superior initial decontamination factor (nearly 1000, compared with 2 for ion exchange), the radioactivity of the ^{233}U product for all times beyond two weeks after cleanup is the same for both methods.

Reduction of Plutonium by Hydrogen. — To achieve satisfactory separation of uranium and plutonium in the partitioning cycle of the Purex solvent extraction process, the plutonium is reduced from Pu(IV) to Pu(III). In present operations, ferrous sulfamate or uranous nitrate is normally used as the reductant. Use of the former introduces iron and sulfate into the intermediate-level waste system, which should be avoided, if possible, for good waste management. If uranous nitrate is used, its ^{235}U content must match that of the uranium in the fuel; this can lead to increased cost. In experiments done this year, an Ar-4% H_2 mixture was found to be a satisfactory plutonium reductant without the disadvantages of either of the ones presently used.

In laboratory experiments, 30% TBP (0.1 N in HNO_3) containing 95 g of U and 1 g of Pu(IV) per liter, an aqueous solution 0.5 N in HNO_3 , and Ar-4% H_2 were passed cocurrently through a column packed with alumina pellets containing 0.5% platinum. Holdup time of the solutions in

the column was about 10 min. More than 99% of the plutonium was reduced and transferred to the aqueous phase. When 100% hydrogen was used, some of the uranium was reduced, but there was no noticeable reduction of uranium with the diluted hydrogen. The Ar-4% H_2 mixture is also safe since it is below the explosive limit of hydrogen. In plant operation, the organic-aqueous mixture from this plutonium reduction step would be fed into a partitioning column, where the separation of the uranium and plutonium would be completed.

Denitration of Thorium Nitrate by Amine Extraction

The extraction of nitrate from thorium nitrate and from thorium-uranium nitrate solutions with amines is being investigated in the laboratory as an alternative to the currently used steam-denitration process for the preparation of Th (and Th-U) oxide sols for use in the sol-gel process.

In single-batch extraction experiments, an aqueous solution, about 0.4 M in Th, 0.02 M in U, 1.8 M in NO_3^- , and 0.1 N in H^+ and containing gamma emitters equivalent to 2×10^6 counts $\text{min}^{-1} \text{ml}^{-1}$ (gross gamma) was contacted with 0.2 M Primene JM-T in n -dodecane for 2 hr at 90°C . When the initial mole ratio of amine to aqueous nitrate was varied from 0.25 to 1.9, the nitrate became less extractable as the solution

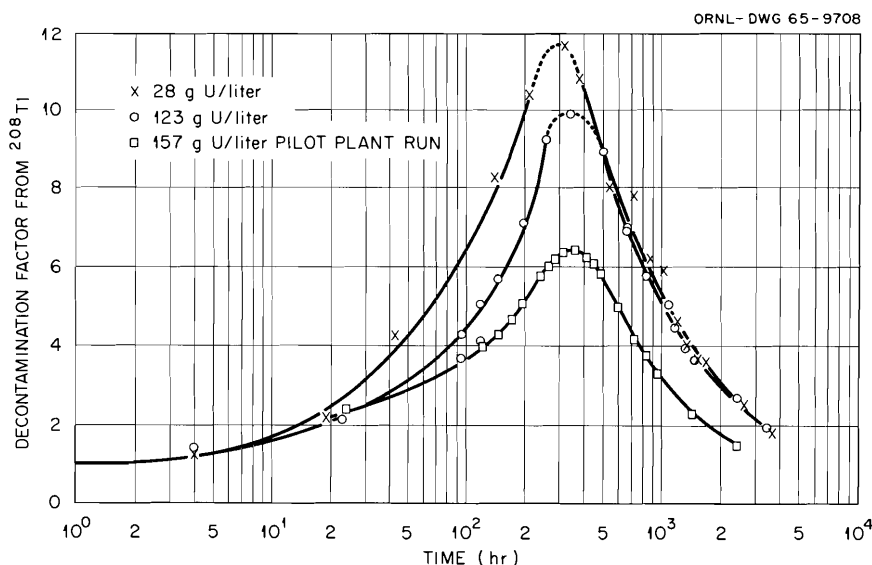


Fig. 1.17. Effect of Feed Concentration on Separation of ^{233}U from ^{208}Tl by Ion Exchange.

became more acid deficient. In these tests, the aqueous nitrate-to-thorium mole ratio approached a value of 0.2 asymptotically. Less than 0.5% of the thorium, uranium, and gamma activity was extracted with the nitrate. Increasing the contact time from 2 to 6 hr, or using multiple contacts rather than a single contact, did not reduce the final nitrate-to-thorium ratio below 0.2. Extractions at room temperature led to emulsions. A 1-nonyldecylamine solution also satisfactorily extracted nitrate from thorium-uranium nitrate solutions.

The thorium sols prepared by amine extraction were dried and fired at 1150°C. Although both amines yielded a product solution with nearly the same thorium-to-nitrate ratio, the solutions prepared by extracting the nitrate with 1-nonyldecylamine contained only about $\frac{1}{20}$ as much carbon as those prepared with Primene JM-T. Contacting 10 vol of 0.2 M 1-nonyldecylamine in *n*-dodecane with 1 vol of 0.4 M Th(NO₃)₄ for 2 hr at 90°C produced a sol 0.4 M in Th, 0.16 M in NO₃⁻, and 0.01 M in C at a pH of 5.13. When fired at 1150° for 4 hr in air, it produced a dull-gray glassy oxide with a density (measured by mercury penetration) of 9.81, a porosity of 2.00%, and a surface area of 0.004 m²/g. The same sol when fired in Ar-4% H₂ produced a white oxide with corresponding values of 9.72, 2.66%, and 0.017 m²/g.

The acid-deficient thorium-uranium nitrate solutions prepared in these experiments were also used in some of the fission product decontamination tests, where precipitation, ion exchange, and electro dialysis were tried (Sect. 1.7.1).

1.8 CONCEPTUAL PLANT STUDIES

The preparation of conceptual plant studies and cost estimates for present and new processes was continued this year. Three studies were made. The first, a conceptual plant for a burn-leach and a burn-volatility process for Rover fuel, is reported elsewhere¹⁹ for classification reasons. The second included the designing and costing of a conventional small on-site processing plant ($\frac{1}{10}$ to $\frac{1}{6}$ ton of U per day) for a boiling-water reactor station of the Oyster Creek type (proposed by Jersey Central) with an output of about 3000 Mw (electrical). The third study was for a burn-leach head-end facility, to be associ-

ated with an existing solvent extraction plant, for HTGR fuel (ThC₂-UC₂-graphite).

Studies on the Design of Small Plants

A design and cost study of a small on-site plant for processing reactor fuel is nearing completion. The plant is designed to be operated in conjunction with a 500- to 3000-Mw (electrical) boiling-water reactor station operating on slightly enriched fuel. A number of design and cost studies already exist for chemical processing plants for the variety of fuels from power-reactor complexes expected during the next decade. However, in almost all these studies, central plants of large capacity were assumed.

There has been recurring interest in the capital and operating cost of a small plant at a single power station of modest size, from 500 to 3000 Mw (electrical). In the immediate future, plants of only relatively small processing capacity will be needed. Furthermore, the diversity of fuel-element designs and the widely scattered distribution of power reactors, in operation or proposed, may favor the small, single-purpose processing plant, operated in close conjunction with the power station, as opposed to large, central, multipurpose plants. If the chemical plant is small enough, many of its auxiliaries can be those of the reactor station whose fuel it will process. Stack facilities, waste treatment, maintenance shops, and administrative facilities such as offices and lunchrooms can be shared by the reactor and chemical plant with savings to both.

This small-plant design study reflects operating and maintenance procedures and standards consistent with power-reactor installations. It provides reasonably accurate cost data for fuel processing in a plant operating on the site of a power station, which, for the purpose of this study, was assumed to be the Oyster Creek nuclear power station proposed by the Jersey Central Power and Light Company. The zirconium-sheathed, slightly enriched fuel element of this reactor is similar to those used in previous cost studies, making comparison with those results reasonably valid.

A fairly conservative Purex-type flowsheet was assumed for the 23,000-Mwd/ton, 120-day-cooled fuel. Equipment design was based on the rack concept throughout, to facilitate both maintenance

and installation. It was assumed that most heavy maintenance would be purchased by contract, as would most of the analytical services, to avoid the high cost of elaborate shops, analytical facilities, and the corresponding staff personnel. Capital-cost estimates were based on detailed conceptual equipment design and flowsheets, but the capital costs of buildings were estimated on the basis of factors derived from Commission experience. The estimates of operating costs do not include in-process inventory charges or credit allowance for the plutonium product. The capital and operating costs are summarized in Table 1.16.

A power station consisting of two 500-Mw (electrical) reactors of the Oyster Creek type will discharge fuel at a rate of about 51,000 kg of uranium per year. Based on the above estimated operating costs, the fuel-processing unit cost is \$51 per kg of U. Similarly, assuming a burnup of 23,000 Mwd/ton and a thermal efficiency of 30%, the fuel-processing-cost contribution to the cost of power would be 0.29 mill/kwhr.

This cost study will be completed by estimating the capital and operating costs of a supplemental addition to the small plant for converting plutonium and uranium nitrates to oxides, and fabrication of complete fuel assemblies for recycle to the reactor.

While it is recognized that considerable uncertainty exists in cost estimates that are not based on detailed design and development, con-

servative estimates were used throughout this study, and a reasonably accurate detailed engineering design estimate might well result in a somewhat lower figure. But the probable disparity does not justify the expense of a detailed design and engineering cost estimate.

Design Studies on Processing of HTGR Fuel

A preliminary plant design and capital- and operating-cost estimate was made for a head-end facility for processing spent HTGR fuel elements ($\text{ThC}_2\text{-UC}_2\text{-graphite}$; see also Sect. 1.2). The plant would provide for the following services:

1. receiving and storing the spent fuel elements,
2. crushing them,
3. burning the graphite in a fluidized bed,
4. leaching the burner ash,
5. adjusting the leachant to acid-deficient conditions suitable for solvent extraction,
6. storing the adjusted leachant, and
7. storing the raffinate from the solvent extraction plant.

This head-end facility was assumed to be located at a conventional fuel processing plant, such as the one built by Nuclear Fuel Services, Inc. (NFS). At this plant, the uranium and thorium would be recovered separately by solvent extraction, the

Table 1.16. Capital and Operating Costs for Small On-Site Processing Plant Using Established Technology

Capital Cost	
Building structure	\$2,257,000
Equipment and installation	2,964,000
Plant total	\$5,221,000
Contingency (25%)	1,305,000
Startup and training (1 year's direct operating costs)	930,000
Total capital investment	\$7,456,000
Annual Operating Cost ^a	
Operating cost — direct	\$ 930,000
Capital investment — annual charge	1,680,000
Total annual operating cost	\$2,610,000

^aExclusive of fuel in-process inventory charges and exclusive of plutonium credit.

thorium returned to the head-end facility for decay storage, and the fission product waste concentrated for disposal.

The study was made for a fuel that contains sol-gel oxide microspheres coated with pyrolytic carbon, which was assumed to be the favored HTGR fuel of the future. The fuel element was assumed to be a 4.5-in.-diam, 20-ft-long graphite "log" from which the fueled particles are not easily separable; thus, provisions are made for crushing and burning the entire element. Each element contains 107 kg of carbon and about 10.9 kg of thorium plus uranium, before irradiation. After an assumed burnup of 50,000 to 80,000 Mwd/metric ton in about six years of irradiation and six months' decay for fission product heat reduction and protactinium decay, the element contains about 10 kg of thorium plus uranium, the balance having been converted to fission products.

The nominal processing capacity is 40 elements a day for 225 days a year. Two parallel lines of equipment were provided for crushing, fluidized-

bed burning, leaching, and feed adjustment. At the nominal throughput rate, such a facility could handle the fuel from reactors having a combined installed capacity of 10,000 Mw (electrical). The cells for unloading and storing fuel were designed for remote operation and limited remote maintenance; the chemical process cells were designed for direct maintenance. Analytical, administrative, chemical supply, waste disposal, and plant utility services were assumed to be provided by the associated solvent extraction plant (not costed), with appropriate enlargements where necessary.

The estimated capital cost of the head-end facility is \$9,040,000 (Table 1.17). This includes \$1,260,000 for the second processing line, an expenditure that could be postponed until required if the plant were started on a fraction of its design load. The standby operating cost, that is, the minimum cost of labor, utilities, and overhead for maintaining the plant when fuel is not being processed, is estimated to be \$115,000 a year. Additional labor and overhead costs when fuel

Table 1.17. Capital-Cost Estimate for HTGR Head-End Facility

Item	Cost ^a
Building and services	\$ 550,000
Building equipment	130,000
Cell structure	1,295,000
Cell services	565,000
Cell equipment	247,000
Process equipment	1,098,000
Process piping	906,000
Process and radiation instrumentation	350,000
Outside equipment	346,000
Site improvements	50,000
Utilities	85,000
	Subtotal
	\$5,622,000
Engineering and inspection (20%)	\$1,124,000
	Subtotal
	\$6,746,000
Contingency (25%)	\$1,687,000
	Subtotal
	\$8,433,000
Interest during construction, startup costs, and working capital	\$ 607,000
	Total
	\$9,040,000

^aInstalled cost, including contractor's overhead and profit.

is being processed are estimated at \$350 a day. The cost of oxygen and alumina is estimated at \$846 a day for one burner line, or \$1020 for two lines. The lower unit cost for two lines is the result of lower oxygen costs at the high usage rates. The costs of nitric acid, other chemicals,

waste disposal, etc., were not estimated separately since they were considered to be a part of the normal solvent extraction costs. The costs of these items should be nearly the same as those for standard metal-clad oxide fuel on an equivalent throughput basis.

2. Fluoride Volatility Processing

The investigation of fluoride-volatility processes at ORNL is part of an intersite program to develop an alternative to aqueous methods for the recovery of values from spent nuclear reactor fuels. Fluoride-volatility methods effectively separate uranium (and plutonium, when present) from fission products by formation of the highly volatile UF_6 and PuF_6 . Studies here have ranged from laboratory-scale to pilot-plant demonstrations with irradiated fuel elements.

The development of fluoride-volatility methods at ORNL is presently in transition between the use of molten-salt and fluidized-bed methods. Previously, emphasis was on (1) processing molten-salt reactor fuels or metallic fuels that had been dissolved in molten salt, and (2) on the use of solid sorbents for removing volatile fission product fluorides from the UF_6 produced by the reaction of fluorine with the UF_4 in the melt. Specifically, processes were developed for recovering highly enriched uranium from the molten salt used in the Aircraft Reactor Experiment, from zirconium-clad alloys of zirconium and uranium, and, most recently, from aluminum-clad alloys of aluminum and uranium. Work on molten-salt methods was terminated with the successful demonstration in the Volatility Pilot Plant of the recovery of uranium from aluminum-base fuel elements. One exception is a few more studies of the removal of plutonium (and probably protactinium) from droplets of molten salt falling through a fluorine atmosphere.

Work on the newly emphasized fluidized-bed methods begun during this reporting period was prompted by the announced AEC goal of having a fluoride-volatility technology for low-enrichment fuel reprocessing completely developed through "cold" engineering, "cold" semiworks, and "hot" pilot-plant programs by July 1, 1969. Our principal contribution will be the installation and operation of a pilot plant in several of the shielded cells of

Building 3019. Laboratory- and bench-scale studies in support of the program will also be conducted. First priority will be given to the process using anhydrous gaseous HCl for removing Zircaloy cladding. The use of $HF-O_2$ for removing stainless steel and Zircaloy claddings will be studied in that order if smaller-scale tests now in progress show that the methods based on the use of $HF-O_2$ are feasible. The development work for the fluoride volatility fluidized-bed method has been performed mostly at Argonne National Laboratory (particularly the work with HCl), with lesser amounts at Brookhaven, ORNL, and the Oak Ridge Gaseous Diffusion Plant.

The possible advantages of fluoride-volatility processes over aqueous methods are as follows: (1) Chopping of the fuel rods from power reactors will probably not be necessary. (2) Radiation damage to reagents will not be a problem when processing short-decayed fuel. (3) Problems of nuclear safety are less severe. (4) Fewer processing steps are required. (5) Highly radioactive waste from fluoride-volatility processing is dry and highly concentrated.

Fluidized-bed methods for processing low-enrichment UO_2 power-reactor fuels appear more promising than molten-salt methods because of the excessive corrosion of the reaction vessel expected while plutonium is being fluorinated from a bath of molten salt. Use of a spray tower or frozen-wall reactor would lessen this corrosion, but the state of development of both these methods is considerably less advanced than the fluidized-bed approach.

Sections 2.1, 2.2, 2.3, and 2.12 are concerned with molten-salt methods; sections 2.4, 2.5, and 2.11 are specific to fluidized-bed work, and the other sections deal with problems related to fluoride-volatility methods in general.

2.1 MOLTEN-SALT PROCESSING OF URANIUM-ALUMINUM ALLOY FUEL

Aluminum-base fuels are a major portion of the anticipated processing load from reactors fueled with enriched uranium. Since the anticipated volume of zirconium-base fuels is too small to justify a plant for processing these fuels alone, the molten-salt fluoride-volatility process previously developed for zirconium-base fuels¹ was adapted to the processing of uranium-aluminum alloy fuel. Laboratory development and engineering studies of the molten-salt fluoride-volatility process for aluminum-base fuels have been reported.^{2,3} This section describes additional laboratory development and pilot-plant processing of fuel that had cooled for only a short time.

Development work directed toward adaptation of the molten-salt fluoride-volatility process to aluminum-base fuels has been completed. Liquidus temperatures for the system $\text{KF-ZrF}_4\text{-AlF}_3$ have been more precisely defined in the composition ranges in which melting difficulties had been encountered. Composition and temperature limitations were determined for discharging NaF into waste salt.

Pilot-plant tests included the processing of "dummy" aluminum elements and of irradiated fuel that had been cooled for as short a time as four weeks. The pilot plant is being decontaminated in preparation for corrosion evaluation and dismantling.

Investigation of Phase Equilibria⁴

In pilot-plant experiments, solidification and precipitation were encountered with salt mixes that presumably should have been molten. To lessen this difficulty, more precise liquidus values were obtained for $\text{KF-ZrF}_4\text{-AlF}_3$ melts with compositional ratios of pilot-plant interest.

At one stage of the molten-salt fluoride-volatility process, waste NaF pellets from the movable-bed

¹Chem. Technol. Div. Ann. Progr. Rept. May 31, 1964, ORNL-3627, p. 29.

²Ibid., p. 40.

³M. R. Bennett *et al.*, "Fused-Salt Fluoride-Volatility Process for Recovering Uranium from Spent Aluminum-Based Fuel Elements," *Ind. Eng. Chem., Process Design Develop.* (in press).

⁴Work performed by B. J. Sturm and R. E. Thoma, Reactor Chemistry Division.

absorber are disposed of by discharge into the molten fluorides from which the uranium has been volatilized. The effect on liquidus temperatures of NaF addition to molten $\text{KF-ZrF}_4\text{-AlF}_3$ was determined to ascertain how much NaF could be disposed of in this way.

The System $\text{KF-ZrF}_4\text{-AlF}_3$: Refinement of Phase-Equilibrium Diagram. – Liquidus temperatures in a portion of the $\text{KF-ZrF}_4\text{-AlF}_3$ system were redetermined. Very pure materials are required for such measurements, partly because the visual determination of the liquidus point of the melt depends on the appearance of a precipitate, and partly because some impurities markedly change the liquidus temperature. For example, near $\text{KF} \cdot \text{ZrF}_4$, oxides in concentrations up to 0.25 mole % increase the liquidus temperature about 5°C for every 0.01% oxygen (as oxide). The pure materials required for measurements of liquidus temperatures were obtained by subliming ZrF_4 and AlF_3 and by distilling KF from a melt with 2.3 mole % UF_4 .⁵

A phase diagram of the system $\text{KF-ZrF}_4\text{-AlF}_3$ had been published previously.⁶ Because of difficulties in keeping salt molten in the pilot plant, additional data were obtained to more precisely define the 550 and 600°C isotherms (Fig. 2.1).

⁵R. E. Thoma, B. J. Sturm, and E. H. Guinn, *Molten-Salt Solvents for Fluoride-Volatility Processing of Aluminum-Matrix Nuclear Fuel Elements*, ORNL-3594 (August 1964).

⁶Chem. Technol. Div. Ann. Progr. Rept. May 31, 1964, ORNL-3627, p. 40.

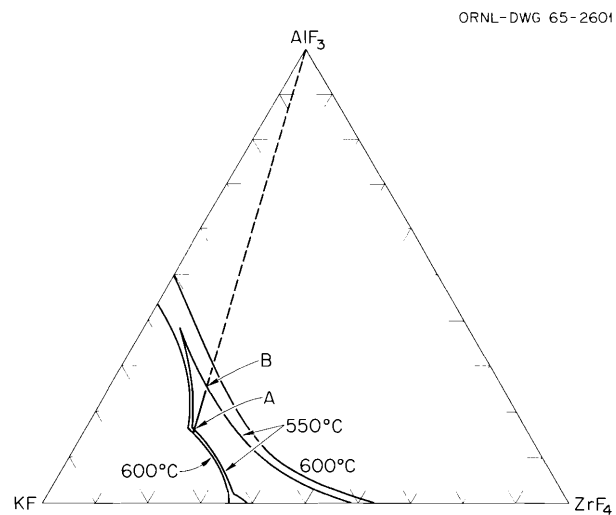


Fig. 2.1. Portion of $\text{KF-ZrF}_4\text{-AlF}_3$ Phase Diagram. Compositions in mole %.

Even though the shift from earlier data was slight from the standpoint of composition, changes in liquidus temperatures were significant. The precise location of point A was important because with increasing KF concentration the liquidus temperature rises very steeply to the K_3ZrF_7 - K_3AlF_6 join. Because of the resemblance of structures of cubic K_3AlF_6 [isostructural with $(NH_4)_3AlF_6$] and K_3ZrF_7 [isostructural with $(NH_4)_3ZrF_7$],⁷ considerable solid solution exists along this join.

Based on earlier data, we had thought that the desirable procedure was to operate along the line AB. In light of the new data, which show a sharper temperature rise near A and less room for aluminum addition between A and B, starting with about 64-36 mole % KF-ZrF₄ is obviously preferable.

Effects of NaF on KF-ZrF₄-AlF₃ Melts. — Sodium fluoride was added to KF-ZrF₄-AlF₃ melts to determine its effect on liquidus temperatures. While this study served as part of the search for a lower-melting solvent, capable of dissolving more AlF₃, its principal purpose was to determine the effect of adding a part of the NaF in the movable-bed absorber to the fluorinator. The compositions chosen for the study, 52.0-31.0-17.0 and 51.2-23.3-25.5 mole % KF-ZrF₄-AlF₃, were approximately those obtained at the end of the volatility process by, respectively, a single-step dissolution of aluminum in 62.5-37.5 mole % KF-ZrF₄ solvent and a two-step dissolution with additional KF provided for the second step. The melts were found to dissolve substantial amounts of NaF at 600°C, the process temperature (Fig. 2.2). The liquidus temperatures were lowered to about 500°C at NaF concentrations of 10 and 13 mole % for the respective solvents. They were raised to 600°C at 17 and 20 mole % respectively.

Pilot-Plant Processing of Short-Cooled Uranium-Aluminum Alloy Fuel

Process development in the pilot plant was the final phase of the ORNL program to adapt the molten-salt fluoride-volatility process to aluminum-base fuels. Both the process and equipment were essentially those used in the earlier zirconium program. Pilot-plant studies were carried out with

⁷R. W. G. Wyckoff, *Crystal Structures*, vol. II, chap. IX, p. 31, Interscience, New York, 1951.

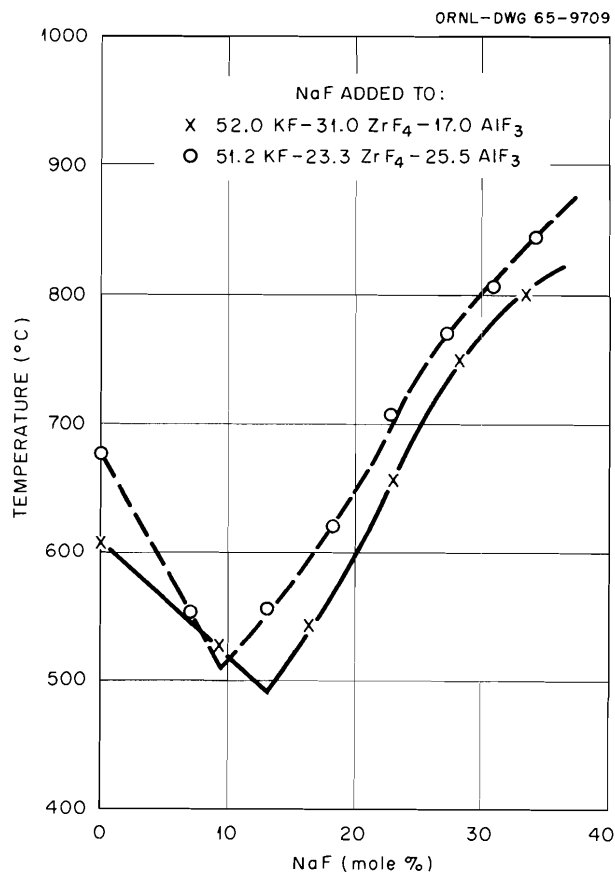


Fig. 2.2. Liquidus Temperatures at Various NaF Concentrations in KF-ZrF₄-AlF₃, Showing the Effect of NaF Discharge into Volatility Pilot Plant Waste Salt.

nonirradiated simulated fuel and with highly burned fuel elements. The program culminated in the successful processing of highly enriched fuel, 26% burned, after only 25 days cooling. (The amount burned is the percentage of ²³⁵U fissioned.)

Description of Process for Uranium-Aluminum Alloy Fuel as Studied in the Pilot Plant. — The process used in the pilot plant for recovering uranium from aluminum-base fuels was essentially the same as that used earlier for zirconium-base fuels. Since that process was described last year,⁸ this report will only briefly outline most of the process; changes will be described in detail.

The flowsheet showing equipment and flow patterns that were used for processing uranium-aluminum alloy fuel elements is shown in Fig. 2.3.

⁸Chem. Technol. Div. Ann. Progr. Rept. May 31, 1964, ORNL-3627, p. 30.

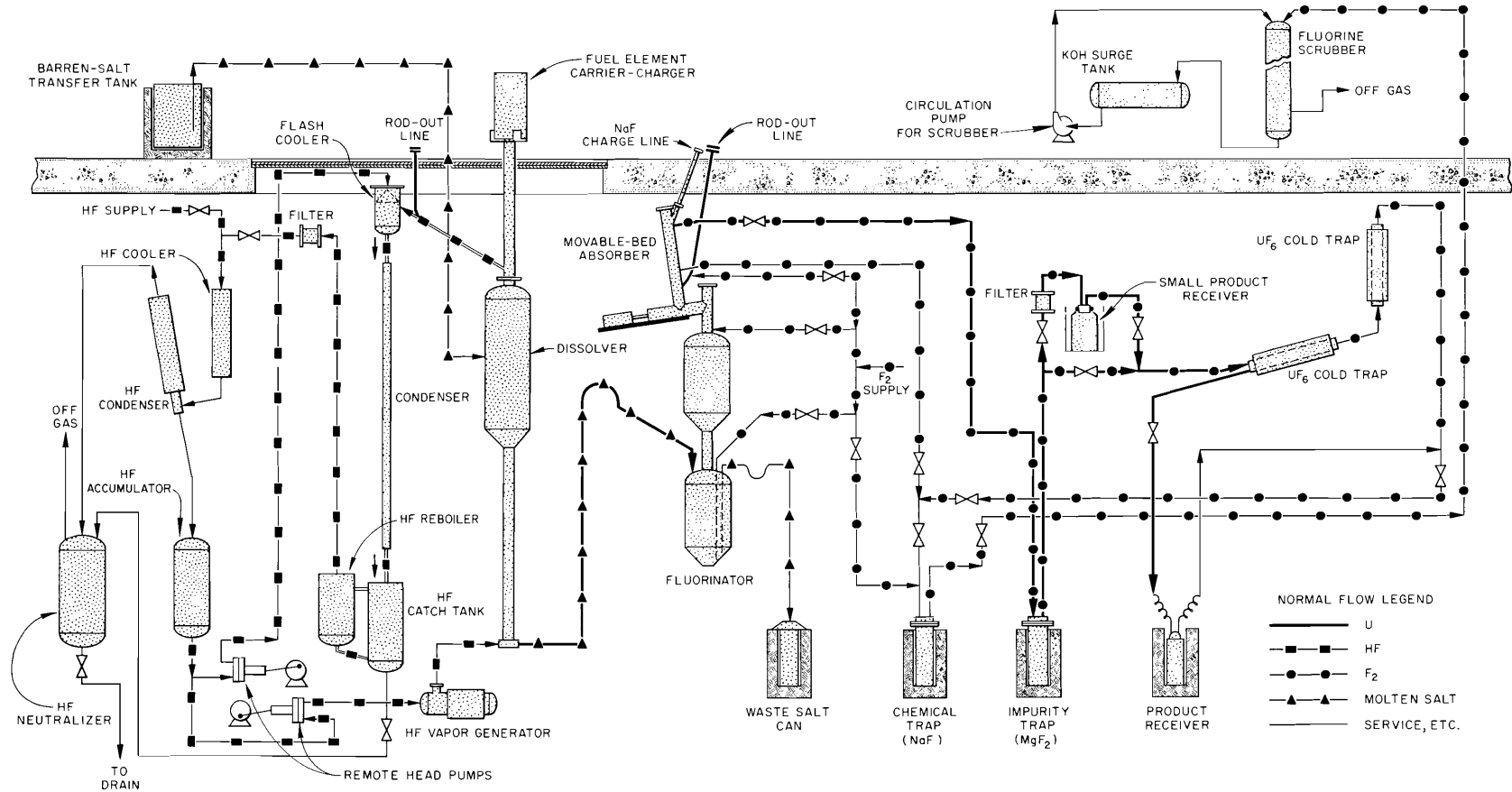


Fig. 2.3. Process Flow Diagram of Volatility Pilot Plant.

This flowsheet encompasses the dissolution of fuel elements in a molten fluoride salt, fluorination to separate the uranium (as UF_6) from the salt and from most of the fission products, and further purification and recovery of the UF_6 . These steps are described below in the same order.

Fuel and Salt Charging. – Fuel elements, such as ORR assemblies, were lowered into the dissolver and then covered with a molten fluoride salt at about 600°C . [The composition of the salt, either KF-ZrF_4 or $\text{KF-ZrF}_4\text{-AlF}_3$, may be any point within the 600°C isotherm (Fig. 2.1) provided that it permits the desired aluminum dissolution without causing the liquidus temperature to exceed 550°C .] One convenient salt mixture was 64-36 mole % KF-ZrF_4 , made by melting commercial K_2ZrF_6 and ZrF_4 . When this mixture was added as a liquid to the heel remaining from the preceding run, the resulting salt had a low enough liquidus temperature to operate a "safe distance" above the liquidus temperature and below the melting point of aluminum (about 655°C).

Fuel Dissolution. – The metallic fuel plates were dissolved by sparging anhydrous HF through the melt at about 600°C (575°C in two runs, to 620°C in run) converting the metal to AlF_3 and UF_4 . Sparging rates have ranged from 20 to 130 g/min, but were generally about 100 g/min. Times required for complete dissolution ranged from 11 to 29 hr. After dissolution was complete, the salt was transferred to the fluorinator for uranium removal.

Uranium Fluorination. – Salt was held in the fluorinator at 30 to 50°C above its highest measured transition temperature; the temperature of the last five fluorinations was 550°C . Fluorine contact for about $1\frac{1}{2}$ hr converted the UF_4 to UF_6 . The volatile UF_6 entered the movable-bed absorber, leaving most of the fission products in the salt.

Product Purification and Recovery. – The UF_6 leaving the fluorinator was further purified in a sorption-desorption cycle. This resulted in the discharge of some contaminants to the off-gas system, retention of some on MgF_2 pellets, and return of the remaining ones to the waste salt. Most of this purification was done in the movable-bed absorber, which was filled with NaF pellets. The pellets in the first section, at 400°C , retained some of the fission and corrosion products but allowed the UF_6 to pass through. In the next section, held at 150°C , the NaF sorbed the UF_6

but allowed some of the remaining contaminants to flow out into the off-gas system.

One of the contaminants discharged to the off-gas system was TeF_6 , so a tellurium trap was installed in the off-gas line downstream from the fluorine scrubber. The trap consisted of nickel mesh heated to 400°C , a gas cooler, and an activated-charcoal bed near ambient temperatures (less than 50°C). Although appreciable amounts of tellurium were trapped, a significant fraction was carried through to the off-gas stack. Some of the tellurium was released after evolution from the fluorinator had ceased; thus, the trap extended the release time of tellurium to the atmosphere.

After fluorination and sorption were completed, the entire movable-bed absorber was heated to 400°C . The UF_6 was desorbed, passed through a bed of MgF_2 pellets for removal of technetium and neptunium, and condensed as a solid in cold traps.

Results of Pilot-Plant Runs. – The aluminum processing program in the pilot plant included ten dissolution runs, ten uranium fluorinations, and eight desorptions. The dissolution runs, in chronological order, were: two dummy dissolutions (aluminum only), three dummy dissolutions spiked with UF_4 , four runs with irradiated fuel, and a dummy run for cleanout. Fluorinations and desorptions started with the first spiked run; but in the second and third hot runs, the salt was fluorinated in two batches. Since the runs with non-irradiated material served primarily to establish system operability, data are presented below only for the four hot runs.

Fuels Processed. – Two fuel elements from the Low-Intensity Test Reactor were processed in the first hot run, RA-1; the burnup amounted to 24%, and the elements had cooled for about $1\frac{1}{2}$ years. There were two Oak Ridge Reactor (ORR) elements in each of the next two runs; RA-2 fuel was 31% burned and had cooled for six months, and RA-3 fuel was 28% burned and had cooled for 80 days. Only one ORR element was processed in RA-4; this element was 28% burned and was processed after only 25 days of cooling.

Uranium Losses. – After the six fluorinations, the uranium remaining in the salt ranged from less than 0.1 to 8.7 ppm. These losses, added to other losses, resulted in nonrecoverable uranium losses for the four runs of 0.1, 0.8, 0.9, and 0.5% of the uranium charged in the individual runs.

Table 2.1. Over-All Decontamination Factors in Volatility Pilot Plant Aluminum Program^a

Run. No.	Decay Time (days)	Nonvolatile Isotopes					Volatile Isotopes						
		Sr ^b	⁹¹ Y	¹³⁷ Cs	¹⁴⁰ Ba	¹⁴⁴ Ce	⁹⁵ Zr	⁹⁵ Nb	⁹⁹ Mo	Ru ^c	Sb ^d	Te ^e	¹³¹ I
RA-1	~570	6 × 10 ⁹		>4 × 10 ⁹			>2 × 10 ⁸	>9 × 10 ⁸		1 × 10 ⁶	8 × 10 ⁶		
RA-2	175	5 × 10 ⁸		2 × 10 ⁹		>4 × 10 ¹⁰	>3 × 10 ⁹	>2 × 10 ⁹		6 × 10 ⁶	>1 × 10 ⁷		
RA-3	80	>4 × 10 ⁹	4 × 10 ⁹	>1 × 10 ⁸	>2 × 10 ⁸	>6 × 10 ⁹	>4 × 10 ⁹	>7 × 10 ⁹		2 × 10 ⁸	1 × 10 ⁶	7 × 10 ⁷	>2 × 10 ⁶
RA-4	25	5 × 10 ⁶	1 × 10 ⁷	2 × 10 ⁵	>9 × 10 ⁷	1 × 10 ⁷	5 × 10 ⁷	1 × 10 ⁷	36	>6 × 10 ⁶	1 × 10 ³	6 × 10 ⁵	4 × 10 ⁶

^aDecontamination factor is defined as the ratio of quantity of nuclide in fuel per gram of uranium to quantity in product per gram of uranium.

^b⁸⁹Sr and ⁹⁰Sr.

^c¹⁰³Ru and ¹⁰⁶Ru.

^d¹²⁵Sb and ¹²⁷Sb.

^e^{127m}Te, ^{129m}Te, and ¹³²Te.

Decontamination Factors. — Fission product decontamination factors (DF's) are shown in Table 2.1. The DF's are satisfactory with the exception of those for antimony and 67-hr ⁹⁹Mo in RA-4. Generally speaking, the DF's listed for the first three runs are about one order of magnitude lower than those achieved in the zirconium program. We believe that this is due, at least in part, to fluorinating at 550°C rather than at 500. The reduced DF's in RA-4 may be due to one or more of the following factors: First, if the sintered-metal filter just upstream of the product cylinder had failed, NaF fines could have carried fission products into the UF₆ cylinder. Second, in RA-4, the additional HF sparge at the end of dissolution was shortened, and a higher percentage of the fission products may have reached the fluorinator. Finally, and this factor seems most significant, discharge of NaF from the movable-bed absorber may have been insufficient. In the aluminum program, 3.8 kg of NaF (about 11% of the bed) was discharged each run, compared with about 6.5 kg in the zirconium program. Insufficient bed discharge would result in an upward migration and eventual breakthrough of some fission products.

Cationic Contaminants. — Cationic contamination of the UF₆ product was higher than desirable. Analyses from individual runs (and even from multiple samples from the product of a single run) were too inconsistent for valid interpretation. After the products from all hot runs were combined for shipment, the composite product was sampled,

and the analytical results appeared quite reasonable. Most of the cationic contaminants, including Cr, Cu, Fe, Ni, and Zr, were present to the extent of less than 50 parts of cation per million parts of uranium. Boron content was 75 ppm, and potassium was about 500. Three others were present in macro quantities; approximate values were: Mo, 0.1%; Al, 0.3%; and Na, 1%. Molybdenum content of the product was dependent on conditions of operation of the movable-bed absorber. Either the temperature during absorption should have been increased slightly or the bed should have been held at 150°C for a longer time before desorption was started. The high sodium content led us to suspect that the sintered-metal filter had failed, allowing NaF fines to be carried through. The high aluminum content has not yet been explained.

Release of Radiation Emitters to the Atmosphere. — Some radioactivity was released through the stack to the atmosphere during the hot runs. Rare gases were released during dissolution but constituted only a fraction of the maximum permissible concentration (MPC) at ground level. The only other detectable releases occurred at the time of fluorination. In RA-4, the total ¹⁰⁶Ru release was less than 3 mc, and the total ¹³¹I was less than 10 mc. The total tellurium release was about 20 curies; of this, 6 curies was 78-hr ¹³²Te, which decays to 2.3-hr ¹³²I and to stable xenon. Again, the ground-level radioactivity during the release was only a fraction of the MPC.

Personnel Exposure to Radiation. — Radiation exposure was watched closely to determine the

effectiveness of personnel-exposure control during the processing of short-cooled fuel. Even during the "hottest" run, exposures were reasonable and, with one exception, were within the maximum limits for routine radiation exposure. This exception arose from the need for immediate handling of the product cylinder, principally for sampling. Radioactivity from the RA-4 product cylinder was high (about 50 r/hr at contact), due primarily to 67-hr ^{99}Mo and 6.75-day ^{237}U . As a result, the operator handling the product cylinder at the time of the run received an accumulated dose of 150 millirads during the week of the run. No other operator received 100 for the week.

Corrosion. — Corrosion data from laboratory- and engineering-scale studies have been reported.³ Measurements of corrosion in the pilot plant have been started. First preliminary results [136 thickness readings (ultrasonic meter)] indicate that dissolver corrosion during the aluminum program averaged 5 mils; if corrosion during decontamination is ignored, this is equivalent to about $\frac{1}{2}$ mil per dissolution. A few readings as high as 30 mils are believed to indicate total depth of pits.

2.2 VOLATILIZATION OF PuF_6 FROM MOLTEN SALTS CONTAINING HIGH CONCENTRATIONS OF URANIUM

One of the key operations in the fluoride-volatilization process is the recovery of plutonium as the hexafluoride. However, PuF_6 is not easily volatilized from the molten fluoride by direct fluorination. One method for achieving this may consist

in the use of a high uranium concentration in the melt to act as a fluorine carrier, an approach studied during this reporting period.

Previous work showed that more than 99% of the PuF_6 could be volatilized from molten fluoride salts in 20 to 30 hr. The use of salts having a high initial concentration of uranium (as UF_4) was studied as a way of increasing the rate of evolution of PuF_6 . At an initial uranium concentration in the melt of about 25%, the percentage of PuF_6 volatilized in 1 hr increased to about 32%, compared with about 15% volatilized in an hour in an earlier test with no uranium present. These results were not good enough to warrant further work.

Volatilization Rate and Equilibrium Constant Generally Increased as Initial UF_6 Content was Raised

Apparatus and Operation. — The tests were made in nickel reactors, each 8 in. high by 1 in. in outer diameter, containing 50 g of LiF-NaF-ZrF_4 (31-24-45 mole %) and about 1 g of plutonium added as PuF_3 . In a series of five 1-hr fluorination tests, the uranium concentration in each test was adjusted by adding UF_4 to the extent of about 5, 10, 15, 20, and 25 wt %. All tests were made at 600°C , with a fluorine flow rate of 100 ml/min (STP). Results of the tests (Table 2.2) show a significant increase in the PuF_6 volatilization rate and corresponding equilibrium constant K (K is the ratio of moles of plutonium in the gas phase divided by the moles of plutonium in the salt phase).

Table 2.2. Effect of Uranium Concentration on Rate of Volatilization of PuF_6 from Molten LiF-NaF-ZrF_4 (31-24-45 Mole %) at 600°C

Test No.	Uranium in Salt (wt %)		Plutonium in Salt (ppm)		PuF_6 Volatilized (%)	Half-Time (hr)	Equilibrium Constant, K
	Initial	Final	Initial	Final			
1	4.74	0.0004	1140	972	14.8	4.4	0.32
2	9.19	0.0015	1060	854	19.1	3.3	0.43
3	14.8	0.130	805	607	23.3	2.6	0.69
4	19.4	0.125	627	576	8.2	8.1	0.20
5	24.5	0.25	805	553	31.6	1.8	0.94

The cause for the erratic results in test 4 is unknown, but it does not appear to signify any change in the general trend of the data. The effective half-time of 4.4 hr at about 5 wt % initial uranium is comparable with values obtained in tests where the uranium concentration varied between zero and 0.5 wt %. At about 25 wt % uranium (Table 2.2), this value was reduced to less than half.

2.3 RECOVERY OF PLUTONIUM AND URANIUM FROM FALLING MOLTEN-SALT DROPLETS AND FROM BEDS OF SOLID PARTICLES BY FLUORINATION

A laboratory investigation of the fluorination of UF_4 and PuF_3 from falling droplets of molten fluoride was made to determine the feasibility of a falling-drop tower.

With this method, the rate of corrosion of the contactor should be less than that for a fluorinator operated batchwise with the salt phase continuous.

The possible recovery of uranium from fluoride salt by fluorination of solid salt particles was also investigated in the laboratory. Compared with bubbling fluorine through molten fluoride, this method also would be much less corrosive to the container.

Data on uranium volatilization from falling droplets of molten salt have been extended from the work reported previously⁹ to include five salt

blends. Results clearly indicate that this approach to recovering the uranium can lead to much faster removal than that provided by bubbling fluorine through a pool of the molten fluorides.

With respect to the volatilization of plutonium by fluorinating falling droplets of fluoride melts, five laboratory experiments were made. The results led to the conclusion that a spray-fluorination process for plutonium recovery is chemically feasible. Most of the plutonium work is now complete and will be discontinued after a few more experiments with the low-plutonium-content salt. A few similar experiments with protactinium will be performed in the near future.

To study the possibility of volatilizing fissile material by fluorinating beds of powdered fluorides, five laboratory-scale fluorinations were made. Although this approach results in much less corrosion, the salt sinters at the operating temperature. For this and other reasons the method had little to recommend it, and the work was terminated.

Volatilization of Uranium from Falling Droplets

The tests to study the volatilization of uranium from falling droplets of molten salt used the equipment described last year.¹ In this equipment, the fluorination zone was 3 in. in diameter and a maximum of 56 in. high. These additional tests extended the previous information to cover the salt compositions given in Table 2.3.

A correlation equation that fits the data for all five salts, with appropriate changes in constants,

⁹Chem. Technol. Div. Ann. Progr. Rept. May 31, 1964, ORNL-3627, pp. 61-64.

Table 2.3. Correlation Equation Constants for Five Salt Blends

Salt Composition (mole %)				Weight Fraction Uranium	Initial Liquidus Temperature (°C)	Log <i>k</i>	<i>α</i>
NaF	LiF	ZrF ₄	UF ₄				
31.7	31.7	31.7	5	0.132	455	15.78	1.45
48.75		48.75	2.5	0.0542	510	21.58	2.84
48.0		48.0	4	0.0843	515	21.58	2.84
45.5		45.5	9	0.1733	550	28.79	4.35
37.4		56.1	6.5	0.119	630	40.25	7.16

× 10⁴

has been developed. The equation follows, and the values of the constants are also listed in Table 2.3:

$$\frac{1}{C_u} - \frac{1}{C_{o,u}} = \frac{kt}{D^2} e^{-\alpha/T},$$

where

D = droplet diameter, μ ,

T = fluorination temperature, $^{\circ}\text{K}$,

t = fluorination time, sec,

$C_{o,u}$ = original uranium concentration, wt fraction,

C_u = final uranium concentration, wt fraction,

α, k = empirical constants.

All data indicate that a spray-fluorination process for recovering uranium from molten fluoride salt can remove more than 99% of the uranium when

the droplets are 200 μ or less in diameter. The temperature must be about 600 $^{\circ}\text{C}$ and the fluorination column 5 to 6 ft long.

Volatilization of Plutonium from Falling Droplets

The plutonium falling-drop fluorination tests were identical to the uranium tests except that glove boxes enclosed the top and bottom of the fluorination column and the fluorination section was only 52 in. long and 3 in. in diameter. Table 2.4 summarizes the results of five falling-drop fluorinations of salts 50-50 mole % in NaF and ZrF_4 , containing either 2.58 or 0.026 mg of plutonium, as PuF_3 , per gram of salt. Note that plutonium removals are much less dependent on fluorination temperature and drop diameter than are uranium removals. Also, the fraction of the plutonium removed is independent of the initial plutonium concentration.

Table 2.4. Results of Fluorination of Plutonium from Falling Droplets of Molten Salt

Initial salt: 50-50 mole % NaF- ZrF_4 + PuF_3

Average Run Temperature ($^{\circ}\text{C}$)	Size Range (μ)	Plutonium Concentration (mg/g)		Plutonium Removal (%)	Fluorination Time (sec)
		Initial	Final		
506	63-88	2.58	1.232	52.2	7.3
	88-105		1.45	43.8	4.5
	105-125		1.58	38.7	3.2
	125-149		1.09	57.8	2.2
	149-177		1.34	48.2	1.6
543	53-63	2.58	0.79	69.5	12.4
	63-88		1.19	53.8	7.3
	88-105		1.56	39.3	4.5
	105-125		2.04	21.0	3.2
609	53-63	2.58	0.45	82.7	12.4
	63-88		0.50	80.4	7.3
	105-125		0.93	64.0	3.2
	125-149		1.06	58.8	2.2
640	53-63	2.58	0.33	87.4	12.4
	63-88		0.32	87.6	7.3
	88-105		0.39	85.0	4.5
	105-125		0.48	81.3	3.2
624	63-88	0.026	0.0156	40.0	7.3
	88-105		0.0055	79.0	4.5
	105-125		0.0088	66.0	3.2

The plutonium-volatilization data were successfully correlated by use of an equation developed by Skelland and Wellek¹⁰ for spray extraction:

$$\frac{dC}{dt} = -k_d \frac{A}{V} C,$$

where k_d is calculated from the Sherwood number, and

C = average plutonium concentration in the droplet, mg/g, or any convenient units,

A = droplet surface area, cm^2 ,

V = droplet volume, cm^3 , and

t = fluorination time, sec.

The diffusion coefficients used in the Sherwood number were estimated by the Stokes-Einstein equation.¹¹ All other required data are from Cohen *et al.*¹²

A typical plot of the experimental data vs the equation-predicted line is shown in Fig. 2.4. From this plot we can calculate the length of column required to volatilize more than 99% of the plutonium from a drop 97 μ in diameter. At 650°C, a column 20 ft long is required. Although this is a much longer column than would be required for similar uranium volatilization, it still is a practical length for a production-scale plant.

¹⁰A. H. P. Skelland and R. M. Wellek, *A.I.Ch.E. J.* **10**, 491 (1964).

¹¹R. B. Bird, W. E. Stewart, and E. N. Lightfoot, *Transport Phenomena*, p. 514, Wiley, New York, 1960.

¹²S. I. Cohen, W. D. Powers, and N. D. Greene, *A Physical Property Summary for ANP Fluoride Mixtures*, ORNL-2150 (Aug. 23, 1956).

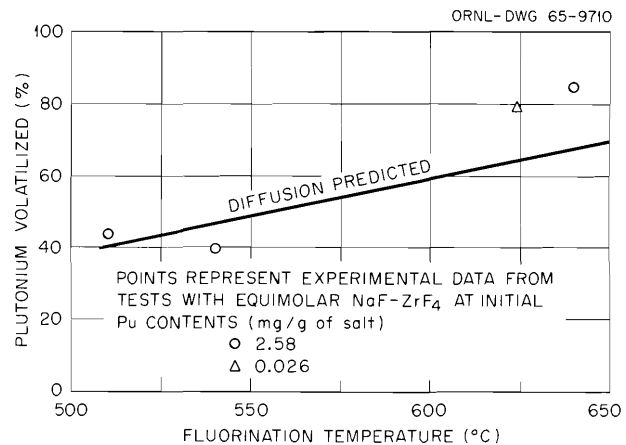


Fig. 2.4. Volatilization of Plutonium from 97- μ Drops of Molten NaF-ZrF_4 Falling Through a 52-in.-High Fluorination Column.

Volatilization of Uranium from Static Beds of Solid Particles

The particles for use in the solid-salt fluorinations were first formed by feeding pulverized, sieved salt through a helium-filled tower heated above the liquidus temperature of the salt. The molten droplets were then frozen, collected, and resieved for use in tests of the idea that uranium could be volatilized from beds of solid particles. The fluorinations were conducted in $\frac{1}{4}$ -in.-OD nickel U-tubes.

The results of the five fluorinations are given in Table 2.5 and indicate that very good uranium removals are possible in 2 to 5 hr. Unfortunately, each time that good uranium removal was attained, the powder sintered into a hard, porous mass.

Table 2.5. Results of Static-Bed Fluorinations

Initial salt: 8.4 wt % uranium, as UF_4 , in 50-50 mole % NaF-ZrF_4

Fluorination Temperature (°C)	Size Range of Particle (μ)	Time (hr)	Uranium Removed (%)	Condition of Salt After Run
400	105-125	2.0	Nil	Free flowing
452	53-63	2.0	98.5	Sintered
473	63-88	3.0	98.2	Sintered
474	125-149	2.0	99.1	Sintered
480	63-88	5.0	99.3	Sintered

2.4 FLUIDIZED-BED VOLATILITY PROCESS DEVELOPMENT FOR STAINLESS-STEEL- AND ZIRCALOY-CLAD UO_2 FUELS

This study is intended to complement chemical-process development work being done at Argonne and Brookhaven National Laboratories on a fluidized-bed method of recovering uranium and plutonium from zircaloy- or stainless-steel-clad, low-enrichment UO_2 power-reactor fuels. Work at Argonne is primarily on the HCl process for zirconium-base fuels, while Brookhaven personnel are concentrating on studying operational problems related to the HF- O_2 process at an engineering scale. While the intersite goal is the development of the overall technology for the volatility processing of low-enrichment fuels, ORNL's principal contribution will be a pilot-plant-scale demonstration of the process with highly irradiated fuels. These laboratory studies are specifically in support of the latter effort.

Bench-scale laboratory studies of the proposed fluidized-bed volatility process have been directed mainly toward observing the important chemical effects and making small-scale process runs with both uranium and plutonium present, in addition to cladding materials. Most of the preliminary work has been carried out in a $\frac{1}{2}$ -in.-diam fluidized-bed unit whose size is especially convenient for the plutonium tests. Work on the HF- O_2 decladding method for stainless steel has been emphasized to date. Future work will extend to use of HF- O_2 in Zircaloy runs and to use of HCl as a Zircaloy decladding method. Also to be studied are factors affecting plutonium and uranium retention and bed sintering or caking in the decladding-fluorination reactor.

Description of Fluidized-Bed Volatility Processes

In fluidized-bed volatility processes the decladding, oxidation, and pulverization are conducted in a fluidized bed of alumina. The bed acts mainly as a medium for removing the heat derived from the various chemical reactions.

Zircaloy-clad fuel will be treated with gaseous HCl at about 400°C to convert the cladding to volatile $ZrCl_4$, or the cladding will be oxidized to ZrO_2 by reaction with gaseous HF- O_2 at 600°C. In the HCl case, the $ZrCl_4$ will be converted to ZrO_2 by reaction with steam in a separate fluidized bed of alumina or sand.

Stainless-steel-clad fuel will be treated with HF- O_2 at about 600°C to convert the cladding to the oxides of stainless steel.

Pulverization of the UO_2 fuel previously declad with HCl can be accomplished by reaction with oxygen to form U_3O_8 and PuO_2 , or HF- O_2 can be used to form UF_4 , PuF_4 , and UO_2F_2 . When HF- O_2 is used for removing either zirconium or stainless steel cladding, pulverization is done by continued treatment with HF- O_2 to again form UF_4 , PuF_4 , and UO_2F_2 .

The oxides or fluorides of uranium and plutonium are then converted to the volatile hexafluorides by reaction with fluorine in the same fluidized bed of alumina. The UF_6 and PuF_6 are subsequently collected in a cold trap. Methods for separating and purifying the two products are still tentative. The ANL reference flowsheet, dated January 1, 1965, calls for decomposing PuF_6 to PuF_4 at 350°C in the absence of fluorine, followed by distillation of the UF_6 . Beds of NaF and MgF_2 would be used for further purification.

The use of BrF_5 is also being considered as a way of separating the plutonium from the uranium early in the process. Gaseous BrF_5 would react with uranium compounds to form UF_6 without reacting with the plutonium. The latter would be removed by treatment with fluorine. Details of this process are being explored at ANL.

Mini-Test Fluidized-Bed Unit

A small-scale, disposable fluidized-bed (mini-test) unit consists simply of a specially machined 30° cone bottom welded to $\frac{1}{2}$ -in.-OD nickel tubing (Fig. 2.5). No disengaging section has been found necessary with this unit if linear velocities of 0.75 ft/sec or less are employed. The normal alumina bed loading is about 5 g. A principal advantage in its use is that the entire bed can be taken as a sample, thus avoiding the sampling uncertainties present in handling larger quantities.

Oxidation of Zircaloy-2 by HF- O_2 Mixtures

Boat tests with Zircaloy-2 specimens (wafers 0.56 in. in diameter and 0.125 in. thick) gave oxidation rates of 32 to 41 mils/hr at 600°C with 40% HF- O_2 . At 650°C the rate decreased to 18 mils/hr. At 600°C with 67% HF- O_2 , the rate was

PHOTO 69560

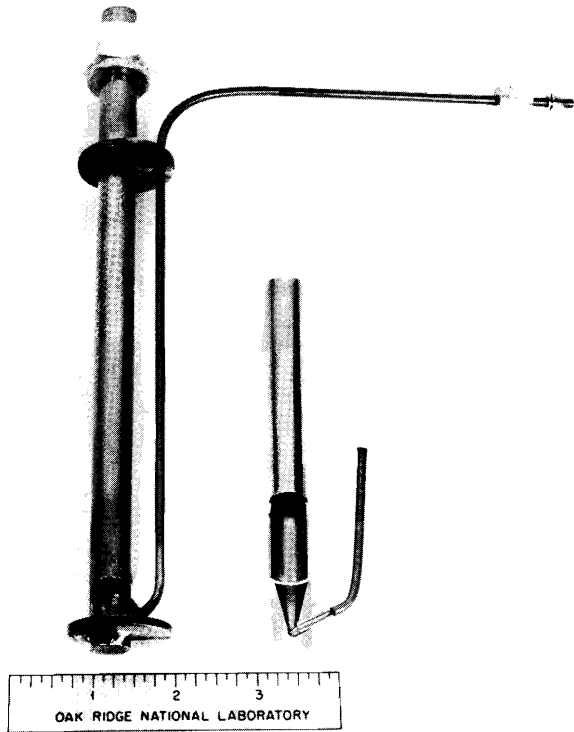


Fig. 2.5. Miniature Fluidized-Bed Reactor.

33 mils/hr. X-ray-diffraction tests on the product showed the presence of both ZrO_2 and $ZrOF_2$, with wet-chemical analyses indicating a predominance of the latter. The product oxide or oxyfluoride seemed to have considerable strength, indicating that little breakup would occur in fluidized-bed operation.

Form of "Stainless Steel" Oxides Resulting from $HF-O_2$ Decladding Step

Analyses have indicated that the fluoride content of type 304L stainless steel oxide material, resulting from $HF-O_2$ treatment at 550 to 650°C, varies from 1 to 5%, dependent on the process time. The conversion from oxide to fluoride is relatively slow due to unfavorable thermodynamics rather than to kinetics. The opposite is true when these oxides are contacted with fluorine at 600°C. Here, rapid conversion and physical degradation occur along with volatilization of a large fraction of the chromium (60 to 80%). Comparative fluorination

tests indicated a much greater degree of degradation of the stainless steel oxides than of the ZrO_2 .

Uranium Volatilization Tests in Mini-Test Unit

Preliminary results with the mini-test fluidized-bed unit indicate that some loss of fluidization occurs at UO_2 concentrations in the alumina bed (Norton RR, 90 to 120 grade) of only 10%. This effect is promoted by having present an equal weight of stainless steel oxides formed by the $HF-O_2$ decladding process. The effect is most prevalent when 100% fluorine is introduced at temperatures above 500°C; the effect can be minimized by using a mixture of fluorine and nitrogen (about 1% fluorine) for 15 to 30 min at the beginning of a run in order to condition or convert part of the oxide to the fluoride form.

Plutonium Volatilization in Mini-Test Unit

Tests similar to the uranium runs were carried out with PuO_2 additions to alumina in the mini-test fluidized-bed unit (Fig. 2.5). A series of four 1-hr fluorination tests were made using 5 g of alumina (Norton RR, 120 mesh) and a fluidization gas velocity of 0.5 fps. Starting with about 125 mg of PuO_2 in the bed (about 2% plutonium), the retentions at temperatures of 450, 500, 550, and 600°C were, respectively, 0.4, 0.36, 4.5, and 48% of the initial amount. Corresponding material balances were 103, 101, 117, and 134%. A subsequent rerun of the 600°C test, in which cross-contamination was indicated, gave a retention value of 18.8%. The noticeable increase in plutonium retention on the bed with increasing temperature indicates appreciable diffusion of plutonium into the alumina particles at temperatures of about 550°C and above. Two additional tests at 550°C, in which the effect of time on plutonium retention was studied, indicated that retention at that temperature reaches a relatively constant value and that removal of the plutonium is not limited by the amount of fluorine gas employed. The losses incurred in tests of 30-min and 2-hr duration were, respectively, 4.88 and 4.15%. Modifications of certain conditions, such as increasing the particle size of the alumina from 120 to 90 mesh and preconditioning the 120-mesh alumina with fluorine at 500°C for 30 min prior to PuF_6 volatilization, caused no significant changes

in plutonium retention compared with results of previous tests. In the first case, with 90-mesh alumina at 500°C for 1 hr, 0.40% of the plutonium was retained. In the second, where preconditioning was employed, the retention was 0.56 wt %.

Further tests of this type are planned to examine the many variables of interest in the proposed fluidized-bed volatility pilot plant. These will include the effect of uranium, cladding materials, and fission products on the completeness of uranium and plutonium volatilization. Process variables, such as grade of alumina, bed recycle, temperature, and flow conditions, will also be examined.

2.5 DESIGN OF A FLUIDIZED-BED PILOT PLANT FOR ZIRCONIUM- AND STAINLESS-STEEL-CLAD UO_2 POWER-REACTOR FUELS

A fluidized-bed fluoride-volatility pilot plant (FBVPP) is being designed for installation in Building 3019. The processing of both Zircaloy- and stainless-steel-clad UO_2 power-reactor fuels will be studied in the facility at irradiation levels up to about 15,000 Mwd/ton.

The primary goal of such studies will be to obtain data needed in the design of a full-scale commercial plant. Some of the specific benefits to be derived include the following: a determination of the behavior of actual fission products in the process, particularly during the purification of plutonium; acquisition of experience in operating and maintaining a fluidized-bed processing plant under conditions of intense radioactivity; and demonstration of the safety of the fluidized-bed fluoride-volatility method.

Design studies are under way, and a preliminary flowsheet (combination process and engineering) has been prepared (Fig. 2.6). Design of the major equipment items required in the decladding and pulverization-fluorination phases has started. This phase of the plant should be installed during calendar year 1966.

Process Description

The Zircaloy cladding will be removed by reaction with either HCl or HF- O_2 ; the latter reagent is preferred for removing stainless steel cladding. The $ZrCl_4$ formed in the Zr-HCl reaction will be

converted to ZrO_2 by reaction with steam in a separate fluidized bed of alumina or sand. Following pulverization of the UO_2 pellets by reaction with oxygen (HF- O_2 in the case of stainless steel), the uranium and plutonium compounds will be converted to their hexafluorides by reaction with fluorine. The method for separating UF_6 , PuF_6 , and volatile fission products is not definite at present, but thermal decomposition of PuF_6 to solid PuF_4 , followed by distillation of the UF_6 and volatile fission product fluorides, is presently favored. A possibility exists that BrF_5 vapor will be used instead of fluorine to volatilize the uranium first. The plutonium would then be converted to PuF_6 by fluorine. (See Sect. 2.4 for more details of the process.)

The facility is sized to process a charge of about 40 kg of UO_2 and 200 g or more of plutonium, depending on nuclear-safety limitations. The primary reactor will be 8 in. in inner diameter and about 12 ft high and will accommodate a fuel element 60 in. high with a 5.4-in. square cross section.

Process Engineering

Design studies are under way on fuel procurement and handling, on safety measures for handling plutonium compounds, on the solution of accountability problems expected in the facility, and on methods for calculating the fission product and transuranium-element content of the fuel to be processed. The stoichiometry of the process has been coded in FORTRAN for calculation by a digital computer. A study is under way at BMI to assemble and evaluate data available for predicting corrosion of major process equipment planned for the pilot plant.

In addition to the preparation of the preliminary flowsheet previously mentioned, equipment design and layout studies are under way for the primary reactor (Fig. 2.7), its off-gas filter (Fig. 2.8), and the pyrohydrolyzer. This work is being done at the Oak Ridge Gaseous Diffusion Plant by their Engineering Development Department and Plant Engineering Division. Fuel-charging equipment is being designed and incorporated into the equipment layout, and an instrumentation flowsheet and instrument requirements are being developed. The project will be scheduled by the critical-path method; development of the network diagram is under way.

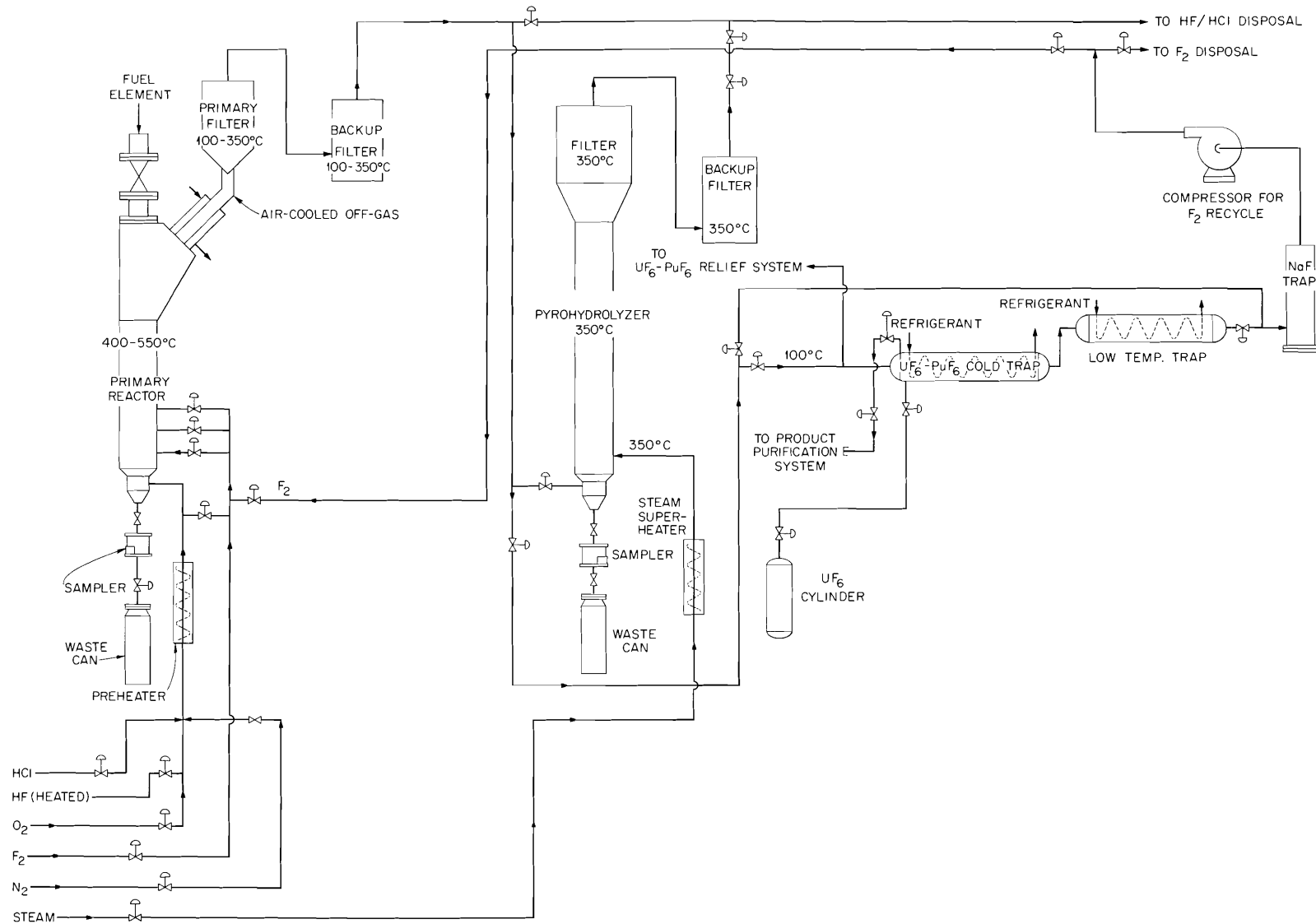


Fig. 2.6. Process Flow Diagram of Fluidized-Bed Volatility Pilot Plant.

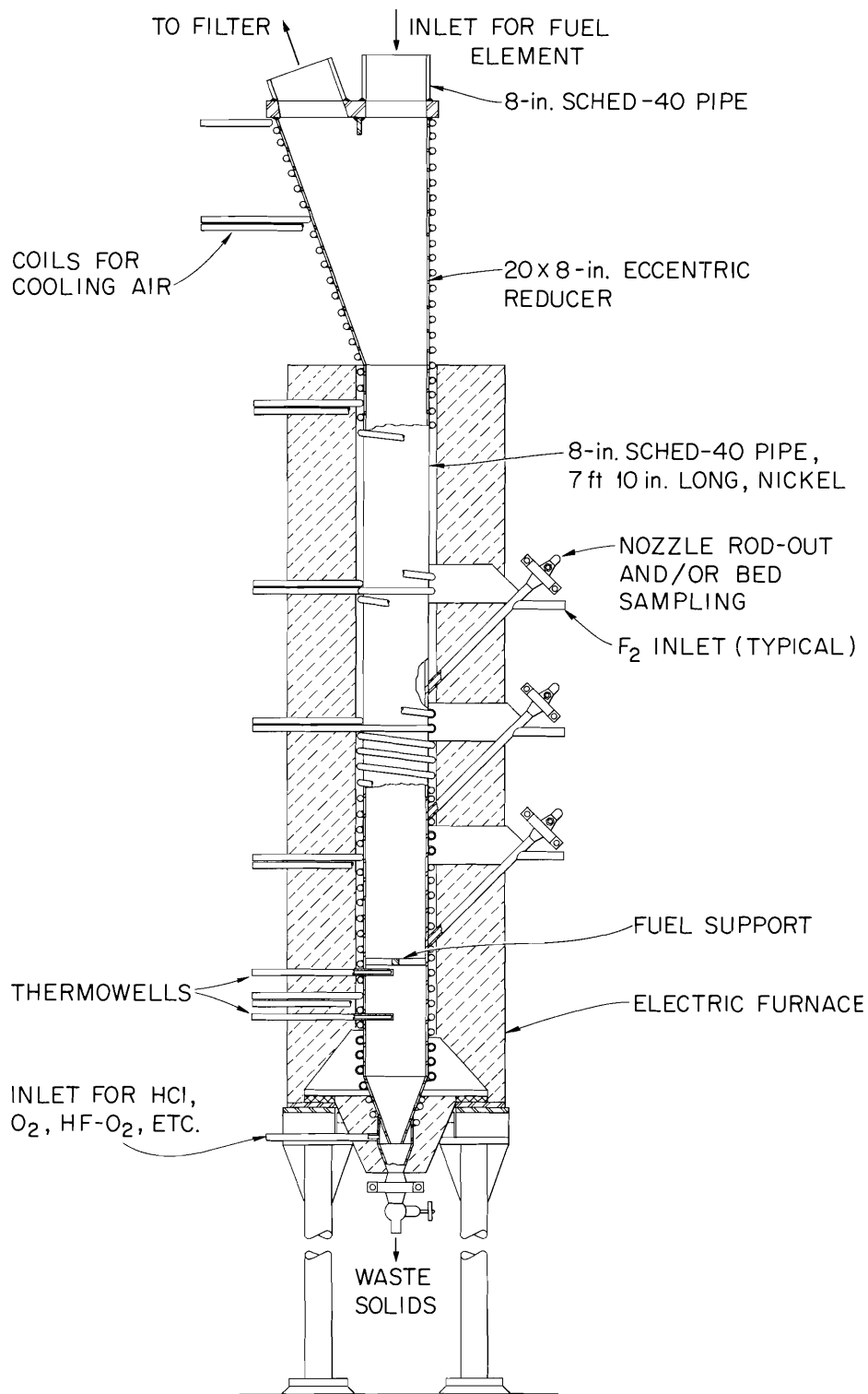


Fig. 2.7. Primary Reactor Proposed for FBVPP.

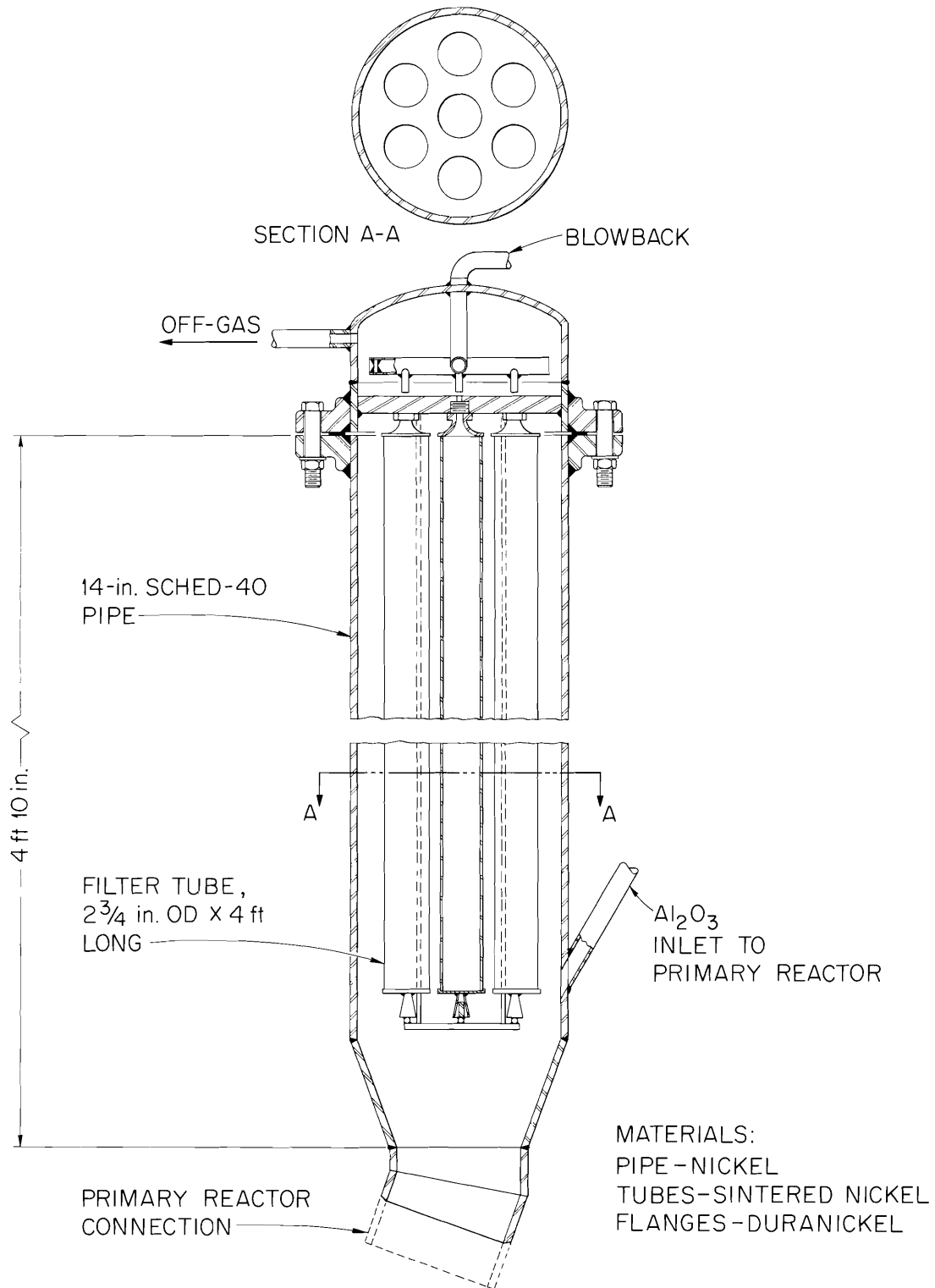


Fig. 2.8. Main Filter for Off-Gas as Proposed from Primary Reactor and Pyrohydrolyzer (FBVPP).

Building Preparation

Modifications to improve the containment features of the Building 3019 penthouse have been designed, and craft work is about to begin. Air locks at entrances are being added, and cracks will be sealed to help increase the difference between atmospheric pressure and that inside the penthouse.

2.6 SORPTION OF PuF_6 BY METAL FLUORIDES

The possibility exists that a sorption-desorption method can be developed for PuF_6 similar to the method whereby UF_6 is sorbed by and desorbed from NaF . A program aimed at evaluating the sorption and desorption of PuF_6 with various materials in both static and dynamic tests is being carried out.

Examination in static tests of 31 different inorganic fluorides and alumina showed that appreciable PuF_6 sorption occurs only with the alkali and alkaline-earth elements at temperatures up to 360°C . This agrees generally with results of dynamic tests reported previously.¹³ Attempts at desorption at temperatures up to 500°C in the static tests were unsuccessful. Sodium fluoride at 350°C was shown in dynamic tests to be highly effective in separating PuF_6 from UF_6 when sufficient excess fluorine was present to prevent the formation of UF_5 . However, desorption of the plutonium from the NaF does not appear feasible.

The sorption results are not favorable to the development of a process specifically aimed at purifying PuF_6 . While sorption of PuF_6 by NaF (and possibly other group I and II elements) is feasible, recovery would require aqueous leaching or dissolution. Thus, a sorption process could perhaps best be employed as a means of decontaminating UF_6 from traces of plutonium.

Exploratory Sorption Program

The first part of the exploratory sorption program, which is completed, consisted in semiquantitatively examining in static tests the PuF_6 sorption characteristics of 31 substances in the temperature

range 100 to 360°C , and the desorption characteristics at temperatures up to 500°C . The second part of the program, now under way, consists in further quantitative testing of the more promising sorbents over a broader temperature range under dynamic flow conditions.

Static Sorption and Desorption Tests. — The equipment for the semiquantitative static tests consisted of a 3-in.-diam, 15-in.-high reactor connected to a vacuum pump and a source of fluorine and nitrogen. The reactor was heated at the bottom and top. In each test, up to 21 sorbents (2 mg each) were placed in 1-cm^2 dishes arranged and supported 10 in. from the bottom of the reactor. The reactor was then sealed, flushed with nitrogen, and filled with fluorine. The bottom of the reactor was heated to 600°C for 30 min to convert the PuF_3 to the volatile PuF_6 ; during this time the sorbents reached a temperature of 360°C . The temperature at the test array was then reduced by cooling (circulating water through coils about the reactor) to 125°C in about 30 min, at which temperature the samples remained for 15 min. The excess PuF_6 was removed by vacuum and flushing with nitrogen. For these sorption studies, the samples were removed at this point, and the plutonium content of each was determined by gamma counting. Calibration with alpha counting was obtained on a sufficient number of samples to establish the reliability of the simpler gamma-counting method. Metal analysis was used in some cases (KF , RbF , CsF , and BeF_2) to accurately ascertain the amount of salt involved.

For the desorption studies, the same equipment and test materials were used, except that at the end of the sorption step the temperature of the test array was raised to at least 500°C over a period of about 1 hr, during which, at 100°C intervals, the gas was evacuated down to a pressure of about 1 mm Hg and then replaced with a fresh atmosphere of fluorine. Cooling and sample analysis were the same as before.

The sorbents were selected on the basis of availability, cost, and previous sorption data.¹³ Each sorbent was tested at least twice for sorption and desorption; when the data appeared inconsistent, additional samples were tested. For none of the test materials did desorption appear to have occurred; therefore, only sorption data appear in Table 2.6. These data show that significant complex formation occurs with all the alkali-metal

¹³Chem. Technol. Div. Ann. Progr. Rept. May 31, 1964, ORNL-3627, pp. 59-60.

Table 2.6. Sorption of PuF_6 on 31 Metal Fluorides and Alumina
Ratio of weights, Pu/metal fluoride or alumina

Metal Fluorides ^a													
Li	0.8	Be	1	Al	0.02	Sn	0.005	Cr	0.01	Mn	0.01	Fe	0.001
Na	1.4	Mg	0.03	In	0.01	Pb	0.005					Co	0.001
K	2.2	Ca	0.3	Tl	0.002							Ni	0.005
Rb	0.6	Sr	0.5										
Cs	0.6	Ba	0.4	Sc	0.01	Zr	0.01						
				Y	0.05	Hf	0.015						
Cu	0.005	Zn	0.005			Th	0.001						
Ag	0.002	Cd	0.002	La	0.02								
				Ce	0.02								
Alumina													
0.01													

^aCategorized roughly according to periodic groups.

fluorides and all the alkaline-earth fluorides except MgF_2 . For a few of the poorer sorbents, cadmium, copper, and nickel, the plutonium content appeared to increase after the "sorption step," and reruns verified the data. These results are interpreted to mean that at the higher temperatures those sorbents more readily react with PuF_6 . (The PuF_6 adsorbed during the desorption test was derived from the fluorination of previously deposited PuF_4 or PuF_3 in the upper part of the reactor and from desorption from other samples.)

Dynamic Sorption and Desorption Tests. — In dynamic tests, the sorption capacity of NaF (porous type, made from $\text{NaF} \cdot \text{HF}$) relative to CaF_2 was demonstrated. Passing 135 mg of PuF_6 in a large excess of fluorine through a 4-g CaF_2 bed (12 to 20 mesh) at 100°C resulted in sorption of only 39%. The concentration of the trapped plutonium in the four separate 1-g sections of this bed was quite uniform, confirming that the trapping efficiency was low. In a similar test with CaF_2 but at a higher temperature (400°C), 67% was sorbed and there was almost twice as much plutonium trapped in the first section as in the last section of the

bed. By comparison, 99.91% of the PuF_6 was sorbed by NaF at 400°C, with nearly all of it in the first section.

A desorption test was run with 148 mg of PuF_6 sorbed on a 2-g bed of NaF. Passage of fluorine (150 ml/min) through this bed at 600°C for 2 hr gave only a 0.32% desorption, as measured by trapping on a second NaF bed at 350°C. This irreversibility was confirmed in a special set of dynamic sorption runs where 10 mg of PuF_6 was passed through a 2-g NaF bed. At 100, 200, 300, 400, 500, and 600°C the respective amounts of plutonium not trapped were 1.4, 0.21, 0.20, 0.07, 0.05, and 0.04%. The trapping effectiveness of NaF under the conditions of this test appeared approximately constant in the 400 to 600°C range.

The separation of PuF_6 from UF_6 was studied in several tests in which they were passed together with excess fluorine through 2-g beds of NaF (12 to 20 mesh) held at 350°C. In three tests, starting with 0.5 g of 20% PuF_6 - UF_6 , the respective sorptions for PuF_6 on the first bed were 99.7, 99.9, and 99.72%. The corresponding losses of uranium by cosorption were 0.24, 0.34, and 0.21%.

In all the high-temperature tests with NaF, a blue-green coloration was observed after PuF_6 had been sorbed, possibly indicating autodecomposition of the PuF_6 to PuF_4 . The difficulty of desorbing plutonium is possibly related to stabilization of the tetravalent state in a PuF_4 -NaF complex. The mechanism of PuF_6 sorption probably involves formation of a PuF_6 -NaF stoichiometric complex, followed by reduction to PuF_4 and the liberation of fluorine.

2.7 SORPTION OF UF_6 BY NaF

In the fluoride-volatility process, fixed beds of NaF pellets are used for sorbing UF_6 from a gas stream that may also contain fluorides of corrosion products, fission products, or both. Data on the rate of removal of UF_6 from gas streams by fixed beds of NaF and data on changes in pellet characteristics after repeated sorption-desorption are necessary for design of sorber systems. Also, knowledge of the sorption and desorption characteristics of possible contaminants in the gas stream is necessary for selecting optimum conditions for operating the fixed beds of NaF to obtain the desired purity consistent with reasonable uranium losses. At present, the pelleted NaF used in the process is purchased from the Harshaw Chemical Company for about \$5/lb. Since the starting material, powdered NaF, is available for about 15¢/lb, a study of pellet production from NaF powder was carried out on a subcontract basis with the Paducah Gaseous Diffusion Plant to determine whether or not the cheaper material was satisfactory for process use.

Experimental determination of UF_6 capacity and stability against degradation of the Paducah pellets has been completed. We concluded that the Paducah material will perform as well as the Harshaw material for the present application. The most important factor in making a choice between the two types will be relative cost; initial estimates indicate a cost of less than \$1/lb for the Paducah material, contrasted to \$5/lb for the other.

The gasometer used for characterizing the NaF pellets was also used to prepare and measure the dissociation pressure of the compounds $\text{UF}_6 \cdot \text{NaF}$, $\text{WF}_6 \cdot \text{NaF}$, and $\text{MoF}_6 \cdot \text{NaF}$.

Evaluation of Pellets Made at Paducah Gaseous Diffusion Plant

Pellets prepared at Paducah during the early stages of the study had satisfactory sorption characteristics, but lacked the structural stability necessary for repeated use in fixed-bed sorbers. Preliminary tests of sorption characteristics and structural stability were made with the gasometric system described previously.¹⁴ With this system, the quantity of UF_6 sorbed by pellets exposed to pure UF_6 at a pressure of about 100 mm Hg and a prescribed temperature was easily measured. The pellets were exposed to three cycles of sorption-desorption, and the intercycle changes in sorption characteristics were measured. Degradation of pellet structure was observed at the end of the test.

Later, pellets were prepared by agglomeration of an NaF-powder-water mixture followed by drying at 250 to 350°C and sintering at 650 to 700°C. Preliminary tests of these newer Paducah pellets indicated good sorption characteristics and structural stability. In view of these results, more extensive tests were made, as described below.

Two series of tests were conducted to determine the effectiveness of the bed for UF_6 removal and its capacity for UF_6 . In these tests, a quantity of the NaF was placed in a 2-in.-diam sorption vessel between 5-in.-long entrance and exit sections that had been filled with $\frac{1}{8}$ -in.-diam Monel shot. A flow of 0.0043 g-mole/sec of gas having a UF_6 concentration of 1.69 mole % was passed through the vessel. The vessel was kept at a temperature of 100°C, and the concentration of UF_6 in the off-gas was measured. The absorbed UF_6 was then desorbed at 400°C with an F_2 flow of 0.5 standard liter/min. Three sorption-desorption runs were made in each series. The time variation of the UF_6 concentration in the effluent during the second series of runs, where an NaF bed depth of 14.5 cm was used, is shown in Fig. 2.9. The effectiveness of the bed for UF_6 removal was slightly greater during the second and third runs than during the first. Little difference in sorption behavior was observed between the last two runs; this indicates that little degradation of the NaF

¹⁴S. Katz, *Apparatus for the Gasometric Study of Solid-Gas Reactions: Sodium Fluoride with Hydrogen Fluoride and Uranium Hexafluoride*, ORNL-3497 (Oct. 15, 1963).

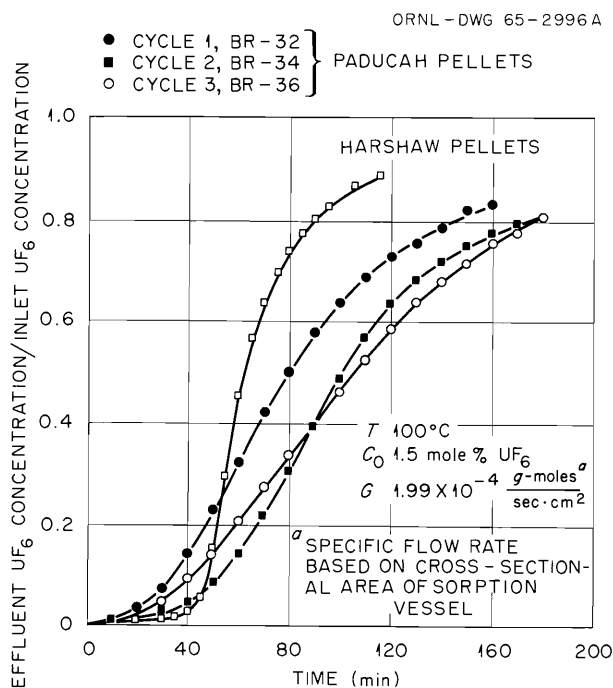


Fig. 2.9. Effect of Cyclic Sorption-Desorption on Bed Capacity for Paducah NaF Pellets and a Comparison with First-Cycle Capacity of Harshaw NaF Pellets. Second series of tests.

was occurring. The effluent curve for a bed of pelleted NaF of the Harshaw type having the same weight as the bed of Paducah material is also shown for comparison. The initial UF_6 concentration in the effluent from this bed is lower than that from the Paducah material; however, the final UF_6 capacity is slightly greater. The differences between bed capacities and initial rates of UF_6 removal are considered negligible for the present application.

After three cycles (BR-32, -34, -36, Fig. 2.9) the two beds of NaF were examined visually for pellet degradation. Almost no powdered NaF was observed, and the pellets did not appear to have lost structural stability. Overall, the Paducah pellets were satisfactory.

Preparation of Complexes of UF_6 , WF_6 , or MoF_6 with NaF and Measurement of Dissociation Pressures

Supplementing the previously reported^{15,16} preparation of $\text{UF}_6 \cdot 2\text{NaF}$, $\text{WF}_6 \cdot 2\text{NaF}$, and

$\text{MoF}_6 \cdot 2\text{NaF}$, the compounds $\text{UF}_6 \cdot \text{NaF}$, $\text{WF}_6 \cdot \text{NaF}$, and $\text{MoF}_6 \cdot \text{NaF}$ were prepared in the gasometer. These new complexes were made by first preparing $\text{UF}_6 \cdot 2\text{NaF}$, $\text{WF}_6 \cdot 2\text{NaF}$, and $\text{MoF}_6 \cdot 2\text{NaF}$ by reaction of the metal hexafluoride with thin layers of dispersed NaF at the respective temperatures of 150, 165, and 185°C. (The sodium fluoride had previously been dispersed by decomposition of $\text{NaF} \cdot 4\text{HF}$ or $\text{UF}_6 \cdot 2\text{NaF}$.) The $\text{MF}_6 \cdot 2\text{NaF}$ complex was then treated with the appropriate metal hexafluoride at 75°C to form the $\text{MF}_6 \cdot \text{NaF}$ complex. The equations for the dissociation pressures of the new complexes are:

$$\log P_{\text{mm}} = 11.06 - (3.48 \times 10^3)/T \text{ for } \text{UF}_6 \text{ over } \text{UF}_6 \cdot \text{NaF},$$

$$\log P_{\text{mm}} = 7.44 - (2.13 \times 10^3)/T \text{ for } \text{WF}_6 \text{ over } \text{WF}_6 \cdot \text{NaF},$$

$$\log P_{\text{mm}} = 7.29 - (1.83 \times 10^3)/T \text{ for } \text{MoF}_6 \text{ over } \text{MoF}_6 \cdot \text{NaF},$$

where P_{mm} is pressure in mm of mercury, and T is temperature in °K.

2.8 CONTINUOUS IN-LINE MONITORING OF GAS STREAMS IN FLUORIDE VOLATILITY PROCESSING

Continuous analysis of volatile fluorides in gas streams is of considerable importance in the operation of the fluoride-volatility processes. Proper control of the various phases of these processes and the evaluation of the equipment require that the concentration of one or more of these fluorides be the primary controllable variable.

Severe demands are made on the analytical instruments used in fluoride-volatility processing. The instrument must measure concentrations in multicomponent mixtures of chemically similar species, it must withstand the corrosive action of fluorides, and it must accept remote calibration

¹⁵Chem. Technol. Div. Ann. Progr. Rept. May 31, 1964, ORNL-3627, p. 52.

¹⁶S. Katz, "Use of High-Surface-Area Sodium Fluoride to Prepare $\text{MF}_6 \cdot 2\text{NaF}$ Complexes with Uranium, Tungsten, and Molybdenum Hexafluorides," *Inorg. Chem.* 3, 1958 (1964).

and repair when used for measuring radioactive materials. The signal from the instrument should be a simple function of concentration, and it should not reflect effects of any corrosive action by the gases.

The instruments previously used have not all met the requirements listed above. We are presently developing an ultraviolet spectroscopic method for monitoring UF_6 , and a column-chromatographic method for monitoring HF. Both methods fulfill most of the requirements for fluoride-volatility instrumentation. Although other volatile fluorides have been successfully analyzed in-line by gas chromatography, HF presents a special problem. In laboratory analyses it reportedly gives poor peaks and reacts with the column material. However, we feel that these effects will be minimized by repeated automatic sampling, since each sample will effectively pretreat the column for the next sample.

Preliminary studies have been made to determine the requirements for an ultraviolet spectroscopic method for continuously monitoring UF_6 concentrations in gas streams. In this study, static samples of UF_6 were analyzed to confirm and expand basic data about the UF_6 spectrum and to examine the necessary techniques for uv analysis. Two peaks that might be useful in monitoring applications were investigated; more work is needed before either can be utilized.

A fluidized-bed reactor for the HF-catalyzed destructive oxidation of stainless steel cladding material is being built, and it requires instruments to monitor oxygen, hydrogen fluoride, water vapor, and possibly CrO_2F_2 in the off-gas stream. We installed a dual-column chromatograph (Barber-Colman, series 5000) for this purpose. The instrument is particularly useful for this program because it can indicate the presence of unexpected species in the off-gas and also give quantitative analyses.

Measurement of Absorptivity of UF_6 in Ultraviolet Region

The UF_6 spectrum was measured with a Cary spectrophotometer (model 14M). The spectroscopic cell used in this study was made entirely of nickel; the windows were sapphire, $\frac{7}{8}$ in. in diameter and $\frac{1}{16}$ in. thick; and the O-ring seal was made of Teflon.

A schematic of the transfer system is shown in Fig. 2.10. All lines are made of $\frac{1}{4}$ - or $\frac{3}{8}$ -in. copper tubing. Connections are made with Monel Swagelok fittings. The NaF trap is made of nickel and holds about 1 kg of NaF. The Sanborn pneumatic differential-pressure indicator and the Robertshaw-Fulton Bourdon-tube gage are made of Monel. Valve 3, attached to the cell by a short length of nickel tubing, is a Hoke M-482 Monel valve. All others are Hoke 413 Monel valves.

Before using the cell we completely removed any traces of moisture by flushing with ClF_3 , and then conditioned the cell with UF_6 at 15 psig and $75^\circ C$ for 16 hr. The transfer system was evacuated with valves 2, 3, 4, and 7 open (Fig. 2.10), flushed with UF_6 , and then reevacuated. A sample of gas was then admitted to the cell, its pressure being indicated on the gages. We assumed the gas in the cell to be at room temperature.

The Beer-Lambert law of absorption defines the "molar absorptivity" of a substance by the following equation:

$$\log \left(\frac{I_0}{I} \right) = \alpha C_i z, \quad (1)$$

where

I = light intensity,

I_0 = initial intensity,

C_i = concentration of species i , moles/liter,

z = path length, cm, and

α = molar absorptivity (a function of wavelength), liters mole⁻¹ cm⁻¹.

Three sets of samples of pure UF_6 were analyzed for a quantitative measure of its absorptivity at 3686 Å. The values of molar absorptivity were calculated by Eq. (1) from readings of $\log (I_0/I)$ given by the spectrophotometer, the known concentration of UF_6 , and the known path length of the cell. The value of the molar absorptivity at 3686 Å was calculated to be 5.5 liters mole⁻¹ cm⁻¹. This value was independent of pressure in the range 10 to 100 mm Hg. We found a previously unreported peak for UF_6 at 2140 Å and determined an approximate value for the molar absorptivity — about 3610 ± 1000 liters mole⁻¹ cm⁻¹.

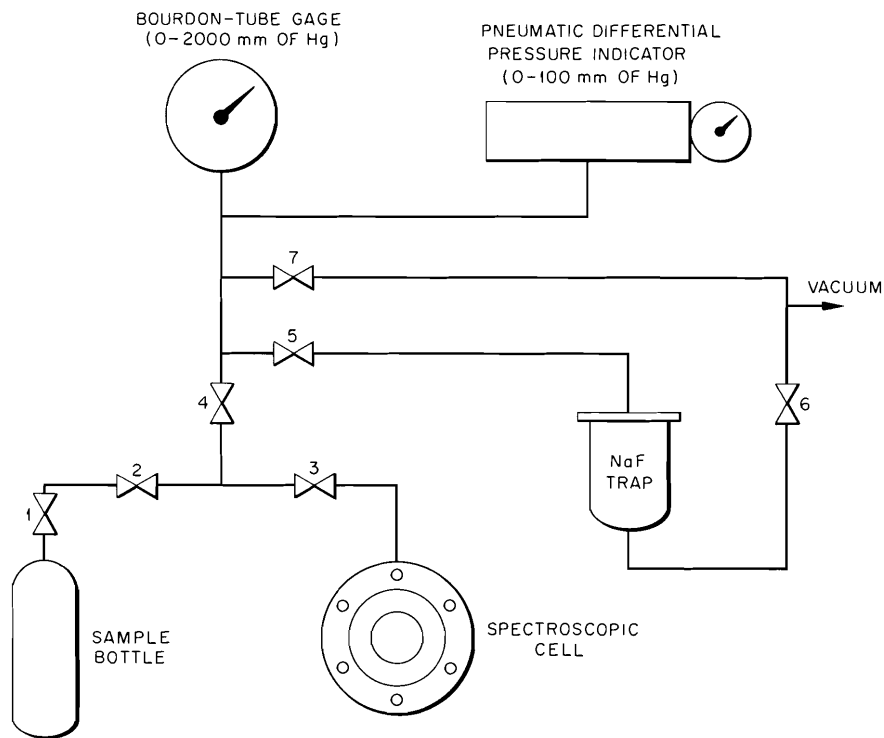


Fig. 2.10. System for Transferring Gas Sample into Spectroscopic Cell.

2.9 VAPOR-LIQUID EQUILIBRIA OF $\text{UF}_6\text{-NbF}_5$ SYSTEM

During the recovery of uranium from spent nuclear fuels by a fluoride-volatility process, the UF_6 is contaminated by other volatile metal fluorides. Distillation is being considered as a method for separating the UF_6 from those impurities; but, to design the distillation system, more must be known about the vapor-liquid equilibria of the impurities and the UF_6 . One such fluoride impurity is NbF_5 . In high-burnup fuels, it would be produced in significant quantities as a fission product, and it would also present a problem when the fuel element contained niobium initially. Hence, an investigation is under way to determine the vapor-liquid equilibria of $\text{UF}_6\text{-NbF}_5$ in the pressure region 0 to 12 atm at 80 to 250°C.

The isothermal determination of total vapor pressure for the entire composition range is complete, and experimental data points on vapor composition vs liquid composition at constant pressure have been determined at a few scattered points in the composition range. Preliminary

determination of critical constants has been made. The experimental work still to be done includes the remainder of the isobaric data and confirmation of the critical constants. Design, fabrication, and operation of equipment suitable for precise work with these materials in the temperature and pressure region shown have been very difficult and time consuming.

Experimental Work

Two equilibrium stills were constructed and operated. The first was of an isothermal design that was used to determine the total-pressure-vs-liquid-composition relationship at 150°C (Fig. 2.11). The data were fitted with the Scatchard-Hamer equations:¹⁷

$$\log \gamma_1 = A + 2z_1[(V_1 B/V_2) - A]z_2^2,$$

$$\log \gamma_2 = B + 2z_2[(V_2 A/V_1) - B]z_1^2,$$

¹⁷G. Scatchard and W. J. Hamer, *J. Am. Chem. Soc.* **57**, 1805-9 (1935).

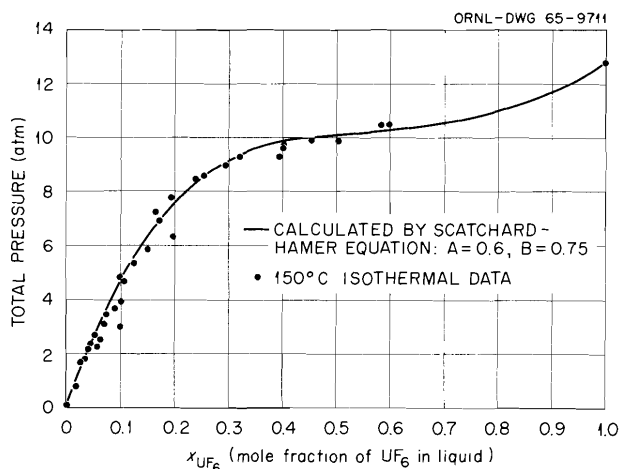


Fig. 2.11. Comparison of Isothermal Data for UF_6 - NbF_5 System with Scatchard-Hamer Equation Using Dalton's Law Assumption.

where

γ_i = activity coefficient of i ,

$z_1 = x_1 / [x_1 + (V_2/V_1)x_2]$,

$z_2 = x_2 / [x_2 + (V_1/V_2)x_1]$,

V_i = molar volume of i ,

x_i = mole fraction of i ,

A, B = constants, which were varied to produce fit of data, and assuming that

$$P = \gamma_1 x_1 P_1^0 + \gamma_2 x_2 P_2^0,$$

where P is total pressure and P_i^0 is vapor pressure of i at 150°C . With uranium hexafluoride as component 1, the values of A and B that gave the best fit were: $A = 0.6$; $B = 0.75$. This relationship was used to calculate (assuming that Dalton's law held) the 150°C isotherm shown in Fig. 2.12. As soon as the critical constants of NbF_5 can be determined, the x - y diagram will be recalculated by use of the Lewis and Randall fugacity rule, which provides better accuracy for vapor mixtures at pressure above 1 atm. The second equilibrium still is of an isobaric design and is now being used to determine both the x - y diagram and the boiling-point curve at 6 atm.

The critical constants of NbF_5 are being obtained in an apparatus that measures the constant-volume pressure-temperature relationship up to 650°C and 2000 psi. Preliminary data indicate the

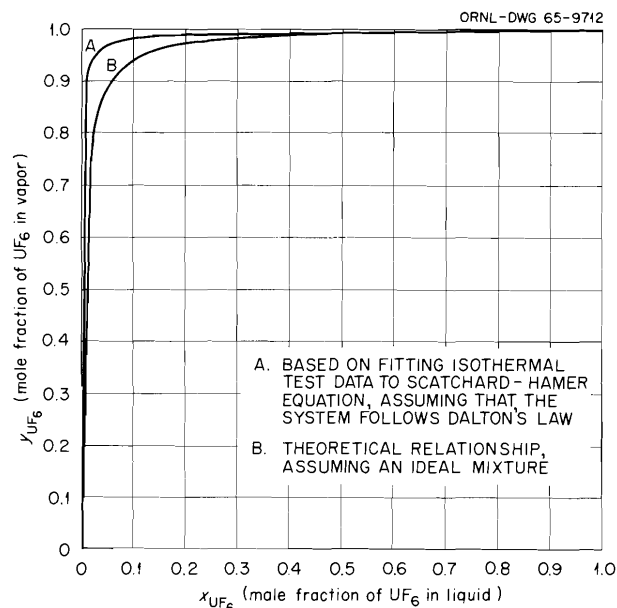


Fig. 2.12. Vapor-Liquid Equilibria of UF_6 - NbF_5 System at 150°C .

critical temperature to be between 480 and 520°C and the critical pressure to be between 40 and 50 atm.

In support of the above experiments, an apparatus for preparing and purifying about 100 g of NbF_5 per day was built. The NbF_5 is prepared by contacting niobium metal shavings with fluorine at 400°C . The resulting product is purified by distillation in an 18-in.-high packed column and collected overhead.

2.10 PHASE EQUILIBRIA STUDIES PERTINENT TO FLUORIDE-VOLATILITY PROCESSING OF FUELS OR MIXTURES CONTAINING CHROMIUM¹⁸

As part of an attempt to develop a fluoride-volatility process for stainless-steel-clad or -base reactor fuels, phase equilibria studies were continued in search of a molten fluoride mixture capable of dissolving the fluorides of the constituents of stainless steel. Also, a brief study of the phase and chemical equilibria in the system NaF -

¹⁸Work performed by B. J. Sturm and R. E. Thoma, Reactor Chemistry Division.

CrF_3 was made. Data from the latter study might also be useful in relation to a possible solvent system for "stainless steel" fluoride, but, probably more importantly, they may be pertinent to defining the capacity of a NaF sorption trap for volatile chromium fluorides produced in the fluorination of chromium-bearing melts.

Work on the development of a fluidized-bed process for fuels that contain or are clad in stainless steel is described in Sect. 2.4, and other studies of the chromium fluoride problem are described in Sect. 18, "Chemical Processing for the Molten-Salt Reactor Experiment."

As reported last year, molten KF-ZrF_4 was an acceptable solvent for stainless steel fluoride, but the reaction between stainless steel and HF was quite slow. During the current report period, the phase diagram of the LiF-FeF_2 system was determined, and the effect of CrF_3 was examined across the composition section $3\text{LiF}\cdot\text{CrF}_3-3\text{KF}\cdot\text{CrF}_3$. Although the results were encouraging, work on solvents for stainless steel fluoride will be deemphasized in favor of studies more directly applicable to a fluidized-bed fluoride-volatility process.

Some study of phase equilibria in the system NaF-CrF_3 was made as a possible guide to determining the limit of the melting or sintering temperature imposed when using NaF beds for sorbing the volatile chromium fluorides. Further work on chromium fluorides will be restricted to studies connected with the development of a fluidized-bed process.

Solvents for Use with Fuels That Have a Stainless Steel Matrix

Development of a molten-salt solvent for processing stainless steel fuels would most probably be based on use of one or more of the alkali-metal fluorides to act as melting-temperature depressants. The phase diagram of the LiF-FeF_2 system (Fig. 2.13) was determined by direct visual observation and thermal analysis of molten mixtures. The diagram is characterized by a eutectic mixture containing 38.5 mole % FeF_2 at 620°C . In the LiF-NiF_2 system, FeF_2 and NiF_2 were found to be nearly equal in their effects on the liquidus.

To depress the melting point further, KF would be particularly effective, as noted in the KF-LiF

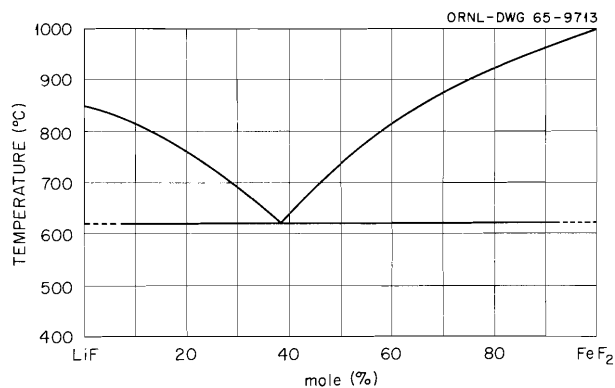


Fig. 2.13. The System LiF-FeF_2 .

phase diagram.¹⁹ The use of KF-LiF mixtures is suggested, therefore, as a solvent convertible into multicomponent, low-melting-point $\text{KF-LiF-NiF}_2\text{-FeF}_2\text{-CrF}_2\text{-CrF}_3$ solutions. The solubility of CrF_3 in the KF-LiF eutectic is expected to be low at processing temperatures of about 600°C because of the high liquidus temperatures that prevail across the composition section $3\text{LiF}\cdot\text{CrF}_3-3\text{KF}\cdot\text{CrF}_3$ (Fig. 2.14). Chromium is a minor constituent of the alloy, however, and its solubility is expected to be adequate.

Separation of Chromium Fluoride from UF_6 Adsorbed by NaF

Preliminary examinations were made of phase and chemical equilibria in the system NaF-CrF_3 because of its relation to possible solvent systems (now deemphasized) as well as to the separation of UF_6 from NaF sorber beds. A phase diagram of the system NaF-CrF_3 , constructed from visual and thermal analysis experiments, is shown in Fig. 2.15.

2.11 VOLATILIZATION OF UF_6 FROM SOL-GEL-DERIVED $\text{ThO}_2\text{-UO}_2$

The possibility of recovering uranium from sol-gel-derived thorium-uranium by direct fluorination at high temperature was investigated in the laboratory during the past year. This work was aimed at

¹⁹R. E. Thoma (ed.), *Phase Diagrams of Nuclear Reactor Materials*, p. 15, ORNL-2548 (Nov. 6, 1959).

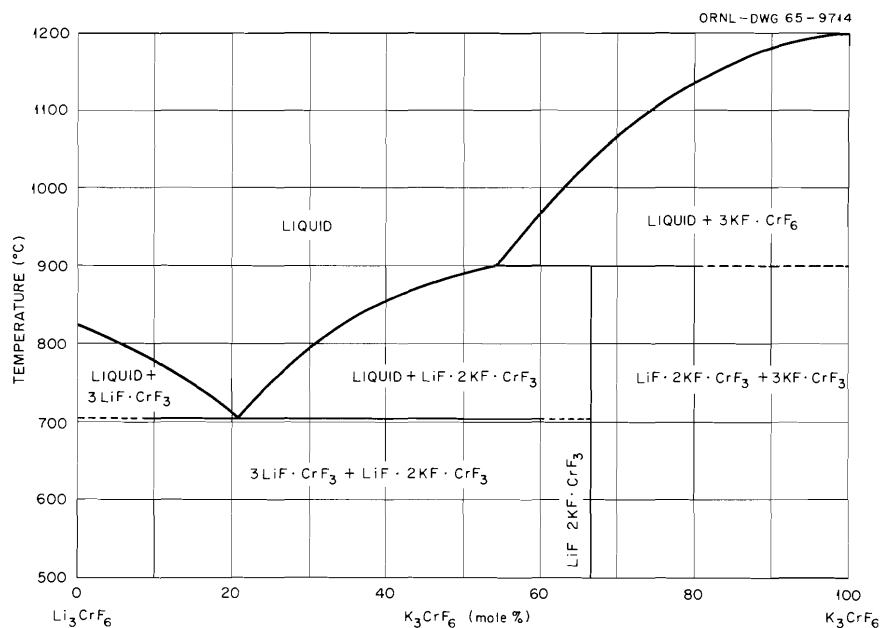


Fig. 2.14. Section of the System KF-LiF-CrF₃: The Quasi-Binary System 3LiF·CrF₃-3KF·CrF₃.

developing a nonaqueous process for recovering fissile material from spent fuel elements.

Three fluorinations were conducted with thorium-urania (3.9 wt % uranium) sol-gel microspheres.

Their diameters ranged from 149 to 210 μ , and the fluorination temperatures were between 480 and 660°C.

The tests showed that fluorination of uranium from thorium-urania containing small amounts of urania will be very difficult unless the particles are less than 10 μ in diameter. Also, better success would be expected if the uranium content were higher. Sintering may not be a serious problem since it was nearly absent in one successful fluorination.

Future work will include fluorination of smaller microspheres and urania-thoria of different ratios.

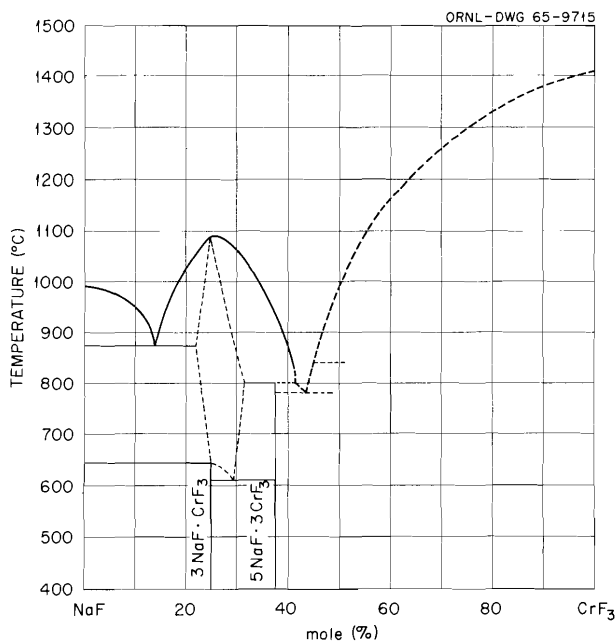


Fig. 2.15. The System NaF-CrF₃.

Uranium Not Readily Removed by Fluorinating ThO₂-UO₂ Microspheres

Fluorinations were performed on 3- to 4-g samples in $\frac{1}{4}$ -in.-OD nickel U-tubes. After fluorination, the samples were analyzed for thorium, uranium, nickel, and fluoride.

The results of the three runs performed to date are summarized in Table 2.7. Fluorination of the microspheres proceeds quite slowly due to their very low porosity and the large amount of thorium,

Table 2.7. Results of Sol-Gel Microsphere Fluorinations

Initial thoria-urania composition: 3.9 wt % uranium

Fluorination Temperature (°C)	Microsphere Size Range (μ)	Time (hr)	Uranium Removed (%)	Fluorine Penetration (μ)	Condition After Run
480	149-177	3.5	Little	~0	Same as initial
647	149-177	3.5	15	4	Sintered
657	177-210	1.0	7	2.5	Slightly sintered

both of which impede the diffusion of fluorine into the microspheres. For example, calculations, based on the amount of uranium removed, showed that the depth of penetration was only about 4 μ in the 3.5-hr run, and about 2.5 μ in the 1-hr run.

2.12 GENERAL CORROSION STUDIES

The relatively high rate of corrosion of both the hydrofluorination and fluorination vessels is a serious fault of the molten-salt fluoride-volatility process. Studies related to the molten-salt process for aluminum-base fuels have been made at laboratory and engineering scales here, and at a laboratory scale at Battelle Memorial Institute (BMI). Results are mentioned in Sect. 2.1 of this report. This section (2.12) is concerned with the concluding experiments of a series made at BMI to determine the effectiveness of introducing an inert gas just below the surface of the salt melt in minimizing corrosion during hydrofluorination.

As a part of process development, early studies (mostly on a laboratory scale at BMI) were aimed at determining the corrosiveness of different salt melts to various metals. Much effort has also been devoted to the determination of corrosion during engineering- or pilot-plant-scale²⁰ tests of the process.

During the last two years, two possible ways of minimizing corrosion during hydrofluorination were studied: electrochemical protection and intro-

duction of an inert gas just below the surface of the melt. Results of the electrochemical studies and the first five of the inert-gas studies were summarized last year,²¹ and the electrochemical studies were reported.^{22,23} This period, the inert-gas studies were finished and a letter report issued.²⁴

Experiments with coupons and inert gases in 4-in.-diam Hastelloy B containers showed that conditions could be obtained to definitely reduce corrosion. In individual 2-in.-diam containers made of INOR-8, however, only slight protection was obtained. Argon and helium were more effective than nitrogen, hydrogen, or a mixture of hydrogen and argon. A melt of 52-37-11 mole % NaF-LiF-ZrF₄ was used at 650°C for all tests because of its exceptionally high corrosivity.

Results of the study showed that introduction of an inert gas below the surface of the salt melt may have useful possibilities for reducing rates of attack by HF and molten fluorides on reaction vessels. The optimum procedures for its use, however, have not been established thus far. Apparently an engineering type of study would be necessary to determine the effect of vessel design,

²¹Chem. Technol. Div. Ann. Progr. Rept. May 31, 1964, ORNL-3627, p. 70.

²²P. D. Miller, L. K. Matson, and E. F. Stephan, *Cathodic Protection of the Hydrofluorinator*, BMI-X-312 (Sept. 25, 1964).

²³L. K. Matson et al., *Cathodic Protection in Fused Fluoride Salts at 1200°F*, presented at National Association of Corrosion Engineers Conference, Mar. 15-19, 1965.

²⁴P. D. Miller, L. K. Matson, and E. F. Stephan, *Corrosion Protection of the Hydrofluorinator by an Inert Gas Sparge*, BMI-X-329 (Feb. 5, 1965).

²⁰E. L. Youngblood et al., *Corrosion of the Volatility Pilot Plant INOR-8 Hydrofluorinator and Nickel 201 Fluorinator During Forty Fuel-Processing Runs with Zirconium-Uranium Alloy*, ORNL-3623 (March 1965).

gas flow pattern, and gas flow rate on rates of attack. Because of the reorientation of the overall program toward fluidized-bed processes and the indifferent results of the experiments, corrosion studies as related to molten-salt processes were discontinued.

Details of equipment, test procedures, and results have been reported in ref. 24, available upon request to the Director, Chemical Technology Division, ORNL.

3. Waste Treatment and Disposal

The waste treatment and disposal development program was designed to develop a comprehensive waste management system for nuclear wastes, including their final disposal, and to estimate the cost of this operation. The effective economic management of radioactive effluents is a prerequisite to the natural growth of a nuclear power industry. The proposed system is shown in Fig. 3.1. High-level radioactive wastes (HLW), which contain nearly all the fission products, are converted to solids. Intermediate-level radioactive wastes (ILW), characterized by their generally high salt content, are incorporated in asphalt; any contained water is simultaneously volatilized. Low-level radioactive wastes (LLW) are treated to remove the radioactivity, and the decontaminated water is discharged to the environment. The recovered solids are combined with the ILW. Both the HLW and ILW solid products can be shipped to an ultimate disposal site.

3.1 CONVERSION OF HIGH-LEVEL RADIOACTIVE WASTES TO SOLIDS

Three solidification processes have been developed in the ORNL program using nonradioactive simulated waste: the pot calcination process (Potcal), the rising-level process (RL-Potglass), and the continuous potglass process (Con-Potglass).¹⁻³ The Potcal and RL-Potglass processes will be tested with radioactive waste in a pilot plant at Hanford. ("Glass" includes true glasses and rocklike crystalline products.) The primary concept of the pot processes is that an evaporator and a solidification unit should be used together

¹F. L. Culler, Jr., et al., *Chem. Technol. Div. Ann. Progr. Rept. May 31, 1964*, ORNL-3627.

²M. E. Whatley et al., *Unit Operations Sect. Monthly Progr. Rept. May 1964*, ORNL-TM-937.

³*Waste Treatment and Disposal Semiann. Progr. Rept. July-December 1964*, ORNL-TM-1081 (in press).

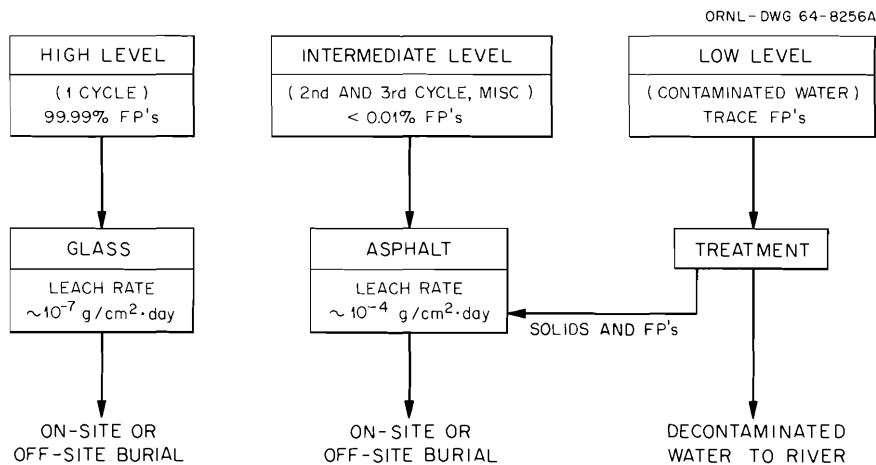


Fig. 3.1. ORNL Waste Management Program.

in a loop. Advantages of this system have been described previously and a flowsheet given,¹ illustrating the interchangeability of the three pot processes in a fixed loop system.

The development of the Potcal process has been successfully completed (total of 80 experiments). In the final test with FTW-65-X3 (27 gal of waste per ton of uranium) Purex waste, the process was successfully demonstrated using an 8-in.-diam pot and a 15-in. susceptor as a heater in an induction furnace. Previous tests with 16-in.-diam pots confirmed the mathematical model for predicting filling rate as a function of diameter and showed the impracticability of using the pot wall as the susceptor. In this case the pot walls failed in two tests due to inability to maintain uniform heating. Based on tests at ORNL with both heating systems, resistance heating is the preferred method.

Development of the RL-Potglass process is continuing in both laboratory and engineering-scale studies. Principal objectives are to (1) develop "neutral" glass-ceramic phosphate or silicate formulations for Purex wastes (with or without sulfate) which have low melting points and low corrosivities and (2) to more precisely define operating conditions in full-scale equipment, including control of dusting and monitoring of phase levels in the pot. Further development of the Con-Potglass process has been terminated for the immediate future.

Engineering Studies

The engineering development program was principally concerned with testing induction heating for the calcining and glass-forming systems concurrently with continued development of the RL-Potglass and Con-Potglass processes. The furnace consisted of a 15-in.-diam susceptor contained in 16-in.-diam coils. Three Potcal tests were made which completed the development of this process. Two successful RL tests were made using FTW-65-X3 simulated Purex waste (≈ 27 gal per ton of uranium processed) and induction heating. Further tests are required to define operating conditions more closely, using both sulfate-bearing and nonsulfate types of Purex waste as well as aluminum wastes. A single Con-Potglass run was satisfactory on an operating basis, but the corrosion rate was too high in stainless steel equipment.

Based on tests performed at ORNL, either induction or resistance heating can be used for the Potcal and Potglass processes. Resistance heating appears to offer fewer operating problems and is recommended for the pot systems.

Pot Calcination Process. — In the Potcal process, the concentrated aqueous waste is fed to the calcination pot continuously, and the aqueous level in the pot is controlled by a proportional thermocouple probe. Solids build up on the walls radially until the pot is filled. The aqueous feed is then stopped, and the solids are heated to 900°C to calcine them. The Potcal process has been successfully demonstrated previously with simulated Purex, TBP-25, and Darex wastes in 88-in.-high pots having 6- and 8-in. diameters, using resistance heating.¹⁻³

Two Potcal tests were made with a 16-in.-diam pot as the susceptor in the 150-kw furnace³ (Tables 3.1 and 3.2). These two tests resulted in pot failures from local overheating of the calciner because of the difficulties in controlling the induction flux and heat transfer in the nonuniformly insulated inductive susceptor. After the failure of the two 16-in.-diam pots, when used as direct susceptors, a 15-in. susceptor was installed in the induction furnace to act as a heat radiator. Eight-inch pots were used with this susceptor. One successful calcination test and two rising-level tests (see below) were made with the 15-in. susceptor and 8-in.-diam pots. The average feed rate in the Potcal test was 8.8 liters/hr. The bulk density of the solids obtained from induction heating of the calciners was 1.10 to 1.42 g/cm³ for the calcined solids. These are comparable to the bulk densities of solids obtained with the resistance-heated calciner.

One important result from the 16-in.-diam tests was the confirmation of the mathematical model for solids deposition. Figure 3.2 shows good agreement between the predicted solids filling rate and the filling rate obtained for test R-84, a 16-in. calcination test. The average filling rates were 24 and 14 liters/hr in the two tests. The filling rate in the second test was low because the lower coils of the induction furnace failed midway through the test.

Rising-Level Potglass Process. — In the RL-Potglass process the concentrated aqueous feed, containing glass-forming additives, is fed directly into the pot, the liquid is vaporized, and the solid residue is melted to a glassy solid. The

additives can be added directly to the evaporator or continuously to the feed line entering the pot. With proper glass formulation the operating temperature should be 900°C or lower. As the level rises, three phases are present: liquid glass at the bottom, a small solid interface, and a small aqueous supernatant pool. The overhead vapors are condensed and returned to the evaporator, thus preserving the advantages of the loop concept.

Two rising-level, essentially duplicate, tests were made in 8-in.-diam by 9-in.-high type 304L stainless steel pots (Tables 3.1 and 3.2). The purpose of these tests was to determine the amount of solids entrained into the off-gas, to determine the magnitude of pressure surging in the off-gas line, to determine the approximate maximum production rate, and to examine the quality of glass made by using lithium and phosphate as the major glass additive components. The feed composition in Table 3.2 shows the calcium nitrate and glass-forming additives added to the

simulated waste as well as the final composition. The glass-forming additives were added directly to the waste, whereas the calcium nitrate was added through a separate addition line at a controlled volume ratio. The amount of off-gas dusting and the pressure surges were small during both tests. The feed rate for these tests varied from 8 to 10 liters/hr, equivalent to the waste from processing 2 tons of uranium per day. The dense glass formed in these tests appeared to be satisfactory (Fig. 3.3).

Continuous Glass Process. — The initial test of the 20-in. horizontal continuous melter (type 304L stainless steel) was successful from an operational viewpoint, even though the melter failed due to corrosion. The melter was operated with feed for a total of 80 hr and was held at temperature (900 or 700°C) for 250 hr. During this time the average feed rate with FTW-65-X3 (27 gal per ton of uranium) was 26 liters/hr, with maximum feed rates up to 50 liters/hr (26 liters/hr

Table 3.1. Pot Tests Using 18-in. Induction Furnace and FTW-65-X3 Simulated Purex Waste

Test No.	Process	Average Feed Rate (liters/hr)	Product Specifications			Calcination or Melt Time (hr)	Nitrate in Solids (ppm)
			Bulk Density (g/cm ³)	gal per ton of uranium ^a	Vol Liquid Waste / Vol Solid Waste		
R-83	Potca1-16	24	1.3	2.56	10.6	<i>b</i>	
R-84	Potca1-16	14.6		2.60	10.4	<i>b</i>	30,000
R-85	Potca1 8-in. pot susceptor	8.8 ^c	1.42	2.64	10.2	8 ^d	10,000
R-86, -87	RL-Potglass 8-in. susceptor ^e	8.8	2.13 ^e	3.1	11.3	7 ^d	10
R-88	RL-Potglass 8-in. susceptor ^f	9.9	2.3 ^f	3.33	10.5	12 ^d	200

^aEquivalent to tons of uranium originally processed.

^bPot wall failed; prematurely terminated.

^cLow because of excess foaming.

^dTime to reach 900°C after liquid feed terminated.

^eViscosity was 27.5 poises at 850°C in laboratory tests.

^fViscosity was 15.1 poises at 900°C in laboratory tests.

is equivalent to the waste from processing 6.1 tons of uranium per day). The FTW-65-X3 glass (Table 3.2) melts at 750°C and has an acceptable fluidity at 850 to 875°C for use in the continuous melter (viscosity is 27.5 poises at 850°C and 15.1 poises at 900°C). The run was terminated when the vessel failed at the interface level. Of the corrosion specimens tested in this experiment, Corronel 230 and types 446 and 310 stainless

Table 3.2. Composition of Synthetic Purex Waste and the Glass Formed from It

Simulated FTW-65-X3 waste, 27 gal per ton of uranium

Component	Concentration
Original Waste	
HNO ₃	1.5 M
Fe(NO ₃) ₃	0.3 M
Ni(NO ₃) ₂	0.03 M
Al(NO ₃) ₃	0.15 M
Cr(NO ₃) ₃	0.06 M
Na ₂ SO ₄	0.45 M
Addition to Prevent Volatilization of Sulfate (in Potcal Process)	
Ca(NO ₃) ₂	0.20 g-mole per liter of feed
Additions to Form Glass (in RL-Potglass Process)	
H ₃ PO ₄	1.5 g-moles per liter of feed
LiOH	1.5 g-moles per liter of feed
Al(NO ₃) ₃	0.5 g-mole per liter of feed
Composition of Glass	
NO ₃ ⁻	0.02 wt %
Fe ³⁺	5.28 wt %
Al ³⁺	8.37 wt %
Na ⁺	7.65 wt %
SO ₄ ²⁻	21.2 wt %
PO ₄ ³⁻	45.3 wt %
Li ⁺	3.6 wt %
Ca ²⁺	7.2 wt %

steel appeared to be promising materials of construction for the horizontal melter. A new melter was fabricated of type 310 stainless steel because of its commercial availability. The purpose of this first continuous test was to gather design operating data, to test the new FTW-65-X3 glass mix for compatibility, and to obtain corrosion data on a number of metal specimens.

The 20-in. continuous melter system consists of the melter located in a 90-kw Global furnace, the feeding equipment, the off-gas handling equipment (which consists of a condenser and a gas-scrubbing column), and a condensate dilution tank (Fig. 3.4). This system is very similar to the 8-in. melter reported previously. The melter (Fig. 3.5) is 20 in. in diameter, 40 in. long, and has four water-cooled equally spaced feed lines. The operating melt level is 3 in. deep. A baffle in the rear of the melter, which has a 1½-in. clearance, keeps the floating calcine from flowing into the discharge pipe. Figure 3.5 shows the melter, without insulation, positioned in the Global furnace. The 90-kw Global

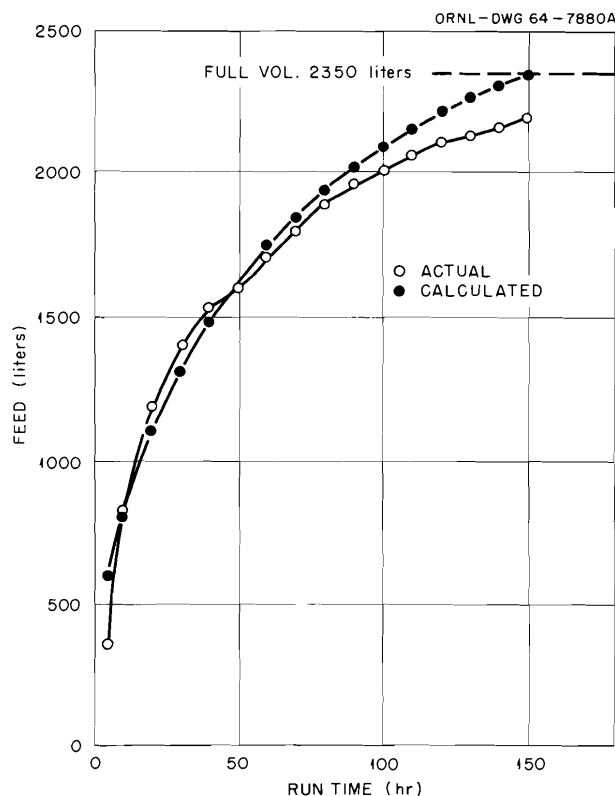


Fig. 3.2. Actual and Calculated Volumes of Feed vs Time for Potcal Test R-84. Calculated volumes were obtained by use of the radial-deposition model.

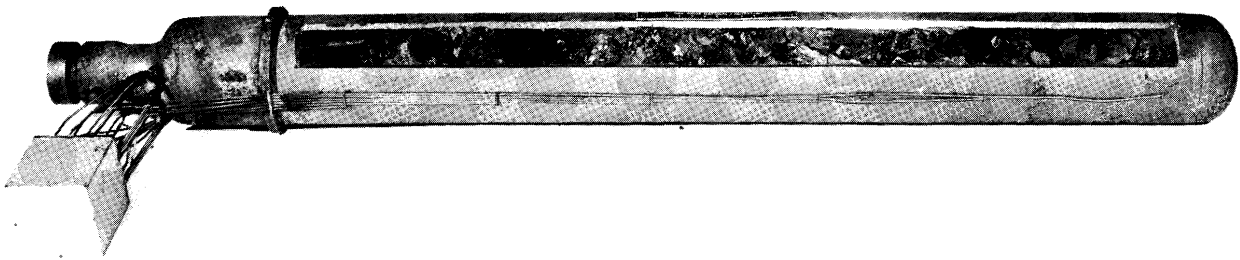


Fig. 3.3. Simulated Purex Glass.

ORNL-DWG 64-4659A

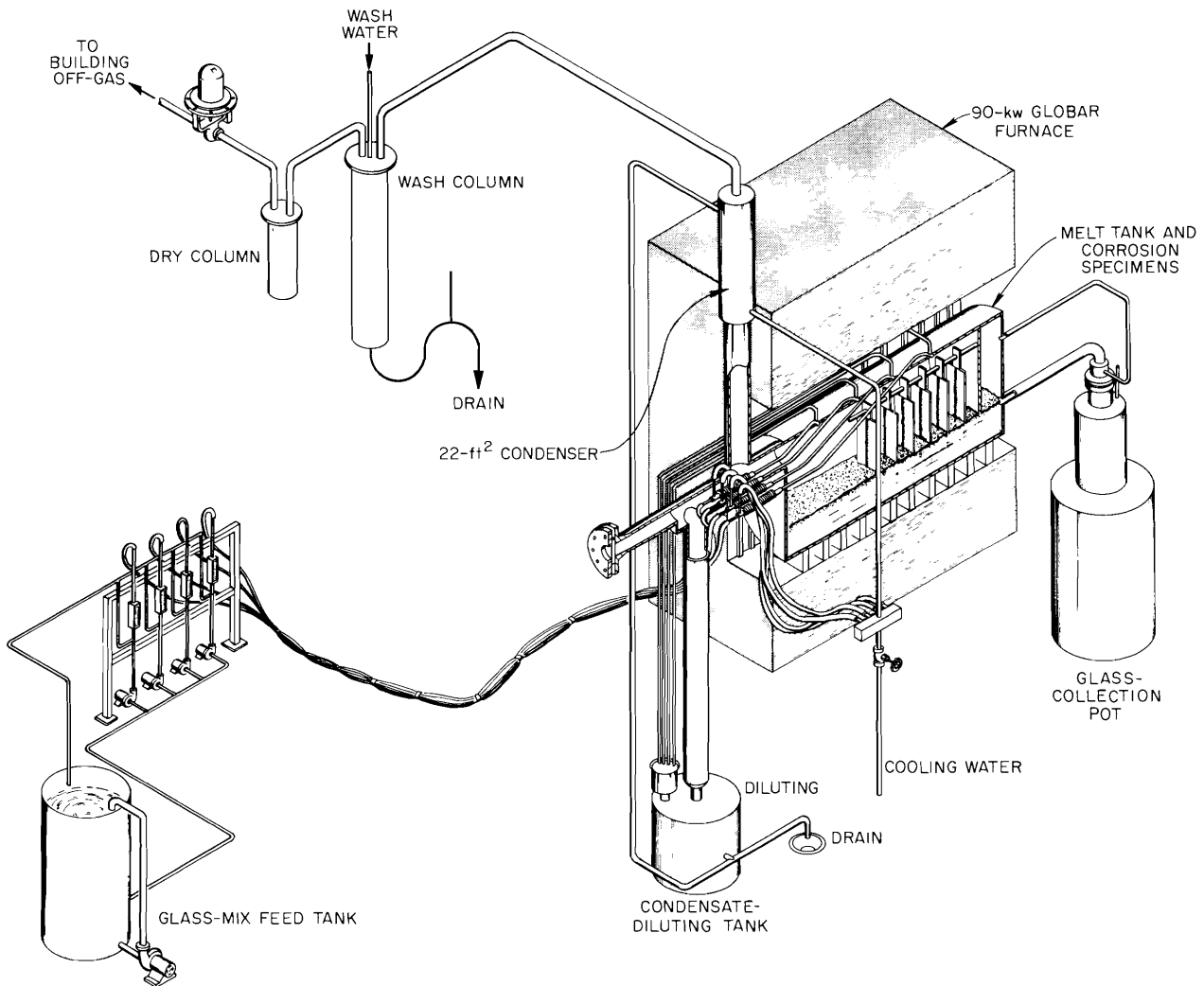


Fig. 3.4. Process Flowsheet of 2-in.-diam Continuous Melter.

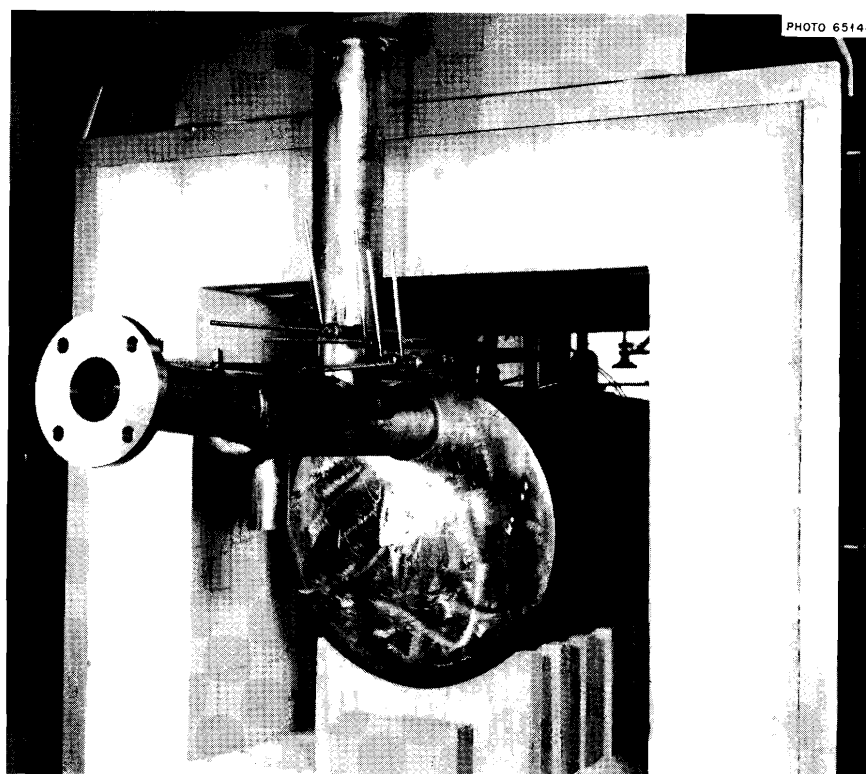


Fig. 3.5. 20-in. Continuous Melter.

furnace has three zones. The hot vapors pass into the updraft condenser. The condensables pass down the off-gas pipe, flushing off the solids, into the condensate receiver (Fig. 3.6). The feed system consists of a hold tank, which has a recirculation pump to keep solids in the suspended feed. A separate pump is used to feed the four water-cooled feed lines. The feed is monitored with rotameters and controlled manually, using ball valves. Needle and globe valves were tested for throttling but were unsuccessful because solids accumulated in the valves.

Evaluation of Induction and Resistance Heating.

— Either induction or resistance heating can be used for the Potcal and Potglass processes. Resistance heating appears to offer fewer operating problems and is recommended for the pot systems. Further evaluation is required in heating units containing all of the refinements required for radioactive operations to make a final choice.

The following observations are made:

1. An induction furnace can be dangerous because of the large amount of electrical power
2. Operations with the present induction equipment have been unpredictable. Cross coupling

that can be concentrated rapidly in a small area of a susceptor, which can cause an extremely high heat flux and temperature. The more probable causes of uncontrolled high temperatures are the failures of sensing devices such as thermocouples or power relays. If a malfunction does occur, positive feedback to the induction coil from the overheated susceptor does not occur if the insulation is adequate to prevent excessive heat loss under normal operation. In contrast, the resistance furnace can be safer because the heating coil is hotter than the heated vessel. Most commonly used resistance coils have a failure temperature of about 1250°C or lower, which is lower than the melting temperature of the metals usually used for heated-vessel construction. The failure of a resistance coil in preference to the heated vessel, in case of malfunction of the control system, is a desirable characteristic.

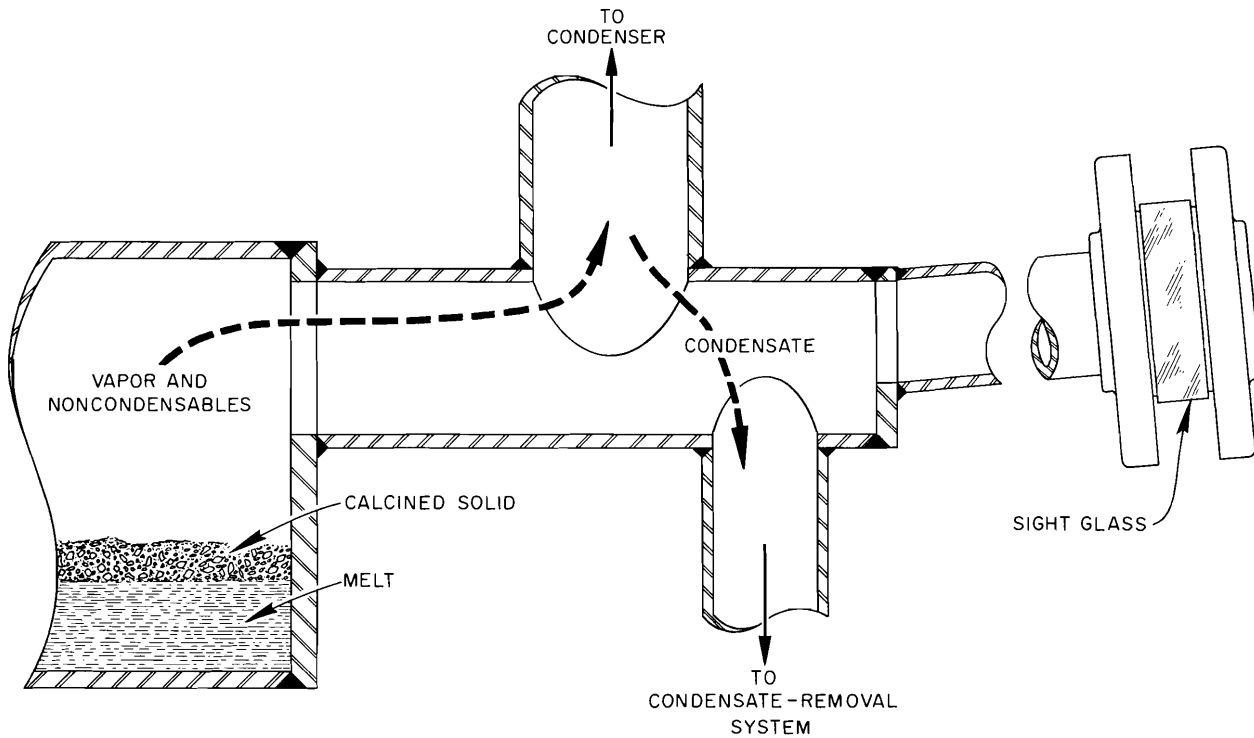


Fig. 3.6. Detail of Vapor Condensate Equipment for Continuous Waste Melter.

between adjacent coil zones has prevented the maximum use of heating capacity in a given zone when required; up to 10 to 15% of the energy could be transferred to, and cause excessive heating in, an adjacent zone.

3. The heat loss for the induction system was 49 to 86% vs 10 to 29% for the resistance furnace.
4. The high-frequency current from the induction unit interfered with other nearby electronic equipment.
5. The heating units used in the ORNL tests did not include all of the refinements such as forced air or water cooling tubes required for use with highly radioactive wastes. Hence, final evaluation of such items as cost, in-cell space requirements, weight, and cooling characteristics and temperature control must await comparative tests with radioactive wastes in specially designed resistance and induction units.

High-Level Radioactive Waste Disposal: Laboratory Studies

Laboratory studies included the development of suitable glasses ("glass" in this report includes both true glasses and rocklike crystalline solids) for the incorporation of a variety of waste types derived from the Purex solvent extraction process (Table 3.3); the development of a computer code for retrieval and correlation of data generated in the melt developmental program at ORNL and at other sites; the accurate measurement of melt viscosity and its correlation with the operational characteristics required of the melt in the RL-Potglass and Con-Potglass processes; the operation of a small-scale continuous melter to study volatilities of various elements and the corrosion of materials of construction for a continuous melter; and the development of a thermal conductivity probe for measuring the levels of aqueous solution, solid calcine, and molten glass in a melter.

Table 3.3. Composition (g-moles per liter of waste) of Simulated Purex Waste Solutions Without Fission Products

Constituent	FTW-65 Waste			
	Unconcentrated, Representing 82 gal per ton of Uranium	FTW-65-X3 ^a	Nonsulfate	
			Low Iron	High Iron ^b
H ⁺	0.5	1.5	3.0	6.76
Na ⁺	0.30	0.9	0.6	0.20
Al ³⁺	0.05	0.15	0.2	
Fe ³⁺	0.10	0.30	0.05	1.35
Cr ³⁺	0.02	0.06	0.006	0.005
Ni ²⁺	0.01	0.03	0.006	0.002
Hg ²⁺	0.0035	0.0105		
SO ₄ ²⁻	0.15	0.45		
PO ₄ ³⁻	0.005	0.015	0.02	
SiO ₃ ²⁻	0.01	0.03		
F ⁻	0.0005	0.0015		
NO ₃ ^{-c}	~1.0	~3.1	~4.3	~11.03

^aThe FTW-65-X3 represents the highest concentration of this waste type that can be conveniently simulated by direct makeup from laboratory reagents without heating the solution.

^bJ. M. Holmes, *Acid 1st Cycle Waste*, ORNL-TM-1013 (Dec. 7, 1964). The composition as listed is too concentrated to be a stable solution.

^cEnough NO₃⁻ to balance in each waste.

Glass Formulation. — Objectives of the glass-formulation development program are to:

1. produce a glass that is not corrosive toward conventional materials of construction;
2. hold fission products and sulfate in the solid product and eliminate side streams;
3. achieve a large volume reduction and a high concentration of waste oxides in the glass;
4. produce a solid product that is stable under storage conditions, mechanically strong, insoluble, and a good heat conductor;

5. develop universal matrix glasses that can be used with a wide variety of waste compositions;
6. operate safely and economically.

Past work has been concentrated primarily on phosphate glasses because (1) phosphates are more readily handled in acid solution than are silicates, (2) low-melting glasses are more readily prepared from phosphates than from silicates, (3) phosphate appears to be more compatible with sulfate retention in the glass than is silicate, and (4) phosphate is compatible with the use of phosphite as a reductant for ruthenium.

A computer code was developed for retrieving and correlating the data from the development of melts for fixation and ultimate storage of highly radioactive wastes. Initial readout was obtained on 397 ORNL melt compositions, and a search for meaningful correlations has begun. The code can accommodate all data currently generated with respect to compositions, properties, and conditions of preparation of such solids. Provision is made for future entry of additional data in the code. The code is also designed to provide a convenient method for exchanging data between groups working on the problem at different sites. A series of compositions of the high-phosphate (Brookhaven) type were received from Hanford for coding. Specific details of the computer program are given in a topical report now in preparation.

Melt-development studies are continuing, with emphasis on decreasing melting temperatures, melt viscosities, and corrosivities. For this study, the upper limit on operating temperature of a melter has been chosen as 900°C, since the rate of reaction of steam with stainless steel increases rapidly with increasing temperature, beginning at about 910°C.⁴ Most of the melt development has been done with high-sulfate Purex waste, primarily the FTW-65-X3 type, but some work was with non-sulfate Purex wastes containing very low to high concentrations of iron (Table 3.3).

A melt previously found to be suitable for the rising-level method of fixation (melt 1, Table 3.4) was found to be too viscous at 900°C for use in a continuous melter. The addition of simulated fission products equivalent to fuel burnups of 10,000 and 35,000 Mwd/metric ton increased both the melting temperature and the viscosity of the melt. Dilution of the melt with fluxing agents, primarily sodium, lithium, phosphate, and aluminum, together with the omission of calcium, reduced both the melting temperatures and the viscosities of the melts to acceptable ranges for continuous operation, even in the presence of the simulated fission products (melts 2 and 3, Table 3.4 and Fig. 3.7). Preliminary viscosity measurements have been made with a modified falling-sphere apparatus⁵ (Fig. 3.8). More data are necessary for definition of the viscosity ranges required for use in the RL-Potglass and Con-Potglass processes.

⁴H. H. Uhlig, *Corrosion Handbook*, p. 514, Wiley, New York, 1955.

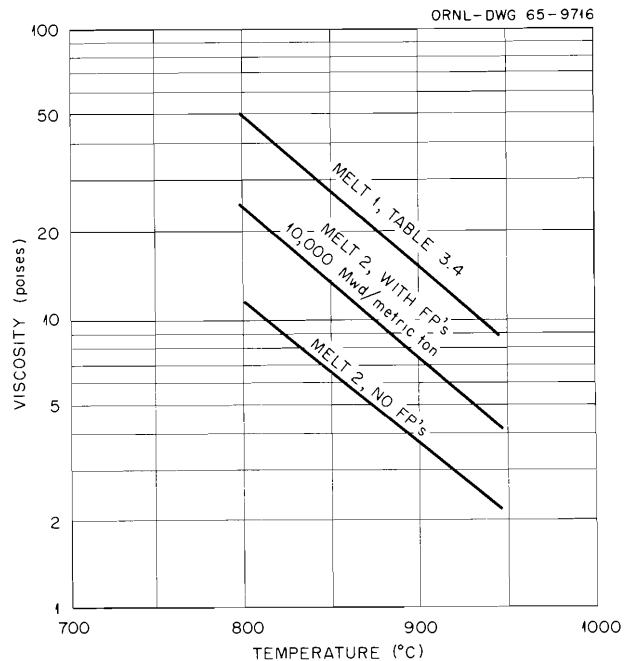


Fig. 3.7. Viscosity of Phosphate Melts Incorporating Purex FTW-65 Waste.

Calculation of the amounts of fission products resulting from fuel burnups of 10,000 and 35,000 Mwd/metric ton, using the data compilation of Blomeke and Todd,⁶ resulted in appreciable changes in both distribution and total amounts of fission products from the actual composition used (Table 3.5). The revised compositions will be used in future ORNL work.

Satisfactory melts were readily developed for fixation of nonsulfate low-iron Purex waste with 10,000 Mwd/metric ton equivalent fission products (melts 5 and 6, Table 3.4). Scoping studies on the development of melts for the fixation of non-sulfate high Purex waste are designed to lower the melting temperatures and the viscosities, and to increase the volume reductions obtained using as reference the melts developed for the stainless

⁵F. L. Culler, Jr., et al., *Semiann. Progr. Rept, Chemical Technology Division, June 1 to Nov. 30, 1964*, ORNL-TM-1081; see also L. Shartsis and S. Spinner, "Viscosity and Density of Molten Optical Glasses," *J. Res. Natl. Bur. Std.* **46**, 176 (1951).

⁶J. O. Blomeke and M. F. Todd, *Uranium-235 Fission-Product Production as a Function of Thermal Neutron Flux, Irradiation Time and Decay Time*, ORNL-2127, Part II, vols. 1, 3, *Summations of Individual Chains, Elements and the Rare Gas and Rare Earth Groups* (1957).

Table 3.4. Compositions of Mixes for Producing Purex Glasses
With and Without Simulated Fission Products

Additives (g-moles per liter of waste)	FTW-65-X3				Nonsulfate	
	1 ^a	2 ^a	3 ^b	4 ^b	5 ^a	6 ^a
H ₃ PO ₄	1.5	3.6	11.2	11.2	2.0	2.0
LiOH	1.5	2.4	7.5	7.5		
NaOH		2.7	8.45	8.45		
Ca(NO ₃) ₂	0.2					
Al(NO ₃) ₃	0.5	0.75	2.35			
Pb(NO ₃) ₂					0.2	0.3
Wt % waste oxides (theoretical)						
No FP's	39.6	20				
10,000 Mwd/metric ton FP's ^a	52	30			24	22
35,000 Mwd/metric ton FP's ^b			30.1	32.2		
Approx. mp (°C)						
No FP's	800	700				
10,000 Mwd/metric ton FP's	1000	800			800	800
35,000 Mwd/metric ton FP's			800	800		
Sulfate Loss ^c (wt %)						
No FP's	19.6	10.2				
10,000 Mwd/metric ton		10.6				
35,000 Mwd/metric ton						

^aUsing Hanford-BNL simulated fission product composition (Table 3.5).

^bUsing ORNL simulated fission product composition (Table 3.5).

^cFrom thermogravimetric tests, assuming total weight loss to be sulfate. Semiengineering-scale fixation tests normally give a much lower value.

steel (Darex) waste.⁷ Results are still in a preliminary stage.

Volatility and Corrosion Tests in a Continuous Melter. — A series of continuous fixation experiments (Con-Potglass process) were run on Purex FTW-65-X3 waste using as the continuous melter a fixation pot modified by the addition of a bottom outlet with an overflow weir. Later models also

incorporated a storage chamber in which the product could be retained in molten form until the end of the day's operation (Fig. 3.9). The melting chamber itself was 4 in. in diameter and 24 in. long. Fixation rates obtained in this melter were as high as 7 liters of feed (waste plus additives) per hour; about 4 liters/hr appeared to be a more realistic figure for steady-state operation. A rate of about 1 liter/hr was used in most of these experiments, since it was difficult to start up, reach steady state, and operate for an appreciable length of time during a normal 8-hr working day. Consequently, the experiments were operated on

⁷W. E. Clark and H. W. Godbee, *Laboratory Development of Processes for Fixation of High-Level Radioactive Wastes in Glassy Solids: Wastes Containing (1) Aluminum Nitrate and (2) the Nitrates of the Constituents of Stainless Steel*, ORNL-3612 (July 1964).

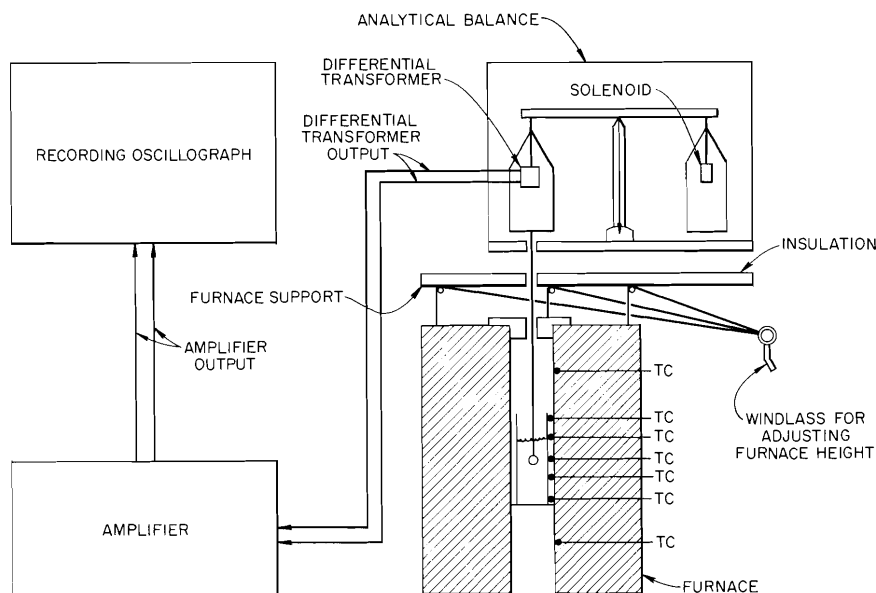


Fig. 3.8. Restrained-Sphere Apparatus for Determining the Melt Viscosity.

an intermittent rather than a long-term continuous basis.

The objectives of these experiments were to investigate the volatility of various constituents and the corrosion of the melter during the continuous melting process as well as to define practical operating problems such as the required ranges of melt viscosity, the possibility of operational difficulty from solids building up in the melter, and the deposition of solids in the off-gas line.

A continuous melting process requires a more fluid (less viscous) melt than the rising-level (RL-Potglass) process. Continuous operations for about four days and intermittent operation for total periods of about 38 hr without opening the melter resulted in no buildup of solids in the melter using melt 2, Table 3.4 (Purex FTW-65-X3 waste). The results of the studies of volatility and entrainment (Table 3.6) showed that iron and ruthenium had the highest volatilities, since 20 to 30% of the total amounts of these elements either reported to the condensate or collected as solids in the off-gas line. The volatility results for iron are doubtlessly too high because severe corrosion occurred in the stainless steel off-gas line and condenser coils. High iron volatility is, however, consistent with the results of earlier

experiments done under rising-level conditions.⁸ Sulfate volatility was erratic, ranging from 0.67 to 14.8%. This variation was probably caused by upsets in operating conditions, though these were not obvious at the time, possibly because of the brevity (<8 hr) of each operating period. Consistently, 1 to 2% of the molybdenum volatilized. Minimum values of entrainment determined from the total amounts of lithium, aluminum, and/or phosphate reporting to the condenser, off-gas lines, and scrubbers were rather consistently 0.2 to 0.5% of the total solids present. It is expected that these solids would be retained in a loop system. Operation of the melter in conjunction with a close-coupled evaporator⁹ should hold the amount of volatile and entrained solid from the loop to

⁸W. E. Clark, H. W. Godbee, and C. L. Fitzgerald, *Laboratory Development of Processes for Fixation of High Level Radioactive Waste in Glassy Solids. 3. Wastes from the Purex Solvent Extraction Process*, ORNL-3640 (in press).

⁹C. W. Hancher, J. C. Suddath, and M. E. Whatley, *Engineering Studies on Pot Calcination for Ultimate Disposal of Nuclear Waste: Formaldehyde-Treated Purex Waste for 1965 (FTW-65)*, ORNL-TM-715 (Jan. 6, 1965); see also C. W. Hancher and J. C. Suddath, *Pot Calcination of Simulated Radioactive Wastes with Continuous Evaporation*, ORNL-TM-117 (Dec. 26, 1961); R. E. Blanco and F. L. Parker, *Waste Treatment and Disposal Progr. Rept. for February to April 1963*, ORNL-TM-603 (Dec. 16, 1963).

less than 0.1% of the solids present, especially if a small amount of reductant is added to the evaporator to lower the ruthenium volatility. The off-gas line may require periodic flushing in any case.

Table 3.5. Simulated Fission Product Concentrations
g-moles per liter of waste for 333 liters of waste per ton of uranium (80 gal per ton of uranium)

Element	10,000 Mwd/Metric Ton Equivalent		35,000 Mwd/Metric Ton
	Hanford- BNL ^a	ORNL ^b	Equivalent, ORNL ^c
Zr	0.021	0.045	0.1675
Mo + Tc	0.025 ^d	0.044 ^d	0.1643 ^d
(Mo)		(0.035)	(0.1321)
(Tc)		(0.009)	(0.0322)
Y + lanthanides	0.045	0.081 ^e	0.2966 ^e
(Ce)		(0.022)	(0.0741)
(Others)		(0.059)	(0.2225)
Rb + Cs	0.014	0.025	0.0982
(Rb)	(0.007)	(0.006)	(0.0209)
(Cs)	(0.007)	(0.019)	(0.0773)
Sr + Ba	0.011	0.022	0.0832
(Sr)	(0.0055)	(0.014)	(0.0503)
(Ba)	(0.0055)	(0.008)	(0.0329)
Ru, Rh, Pd	0.028 ^f	0.016 ^f	0.0841 ^f
IO ₃		0.0017	0.0068
Total g-moles	0.144	0.2347	0.8871

^aPersonal communication from G. Rey, HAPO, to BNL Waste Disposal Group, Mar. 10, 1964. Fission product distributions are for the Plutonium Recycle Test Reactor (PRTR).

^bCalculated according to J. O. Blomeke and M. F. Todd, *Uranium-235 Fission-Product Production as a Function of Thermal Neutron Flux, Irradiation Time and Decay Time*, ORNL-2127, part II, vols. 1 and 3, "Summations of Individual Chains, Elements, and the ¹³Rare Gas and Rare-Earth Groups," assuming 3×10^{13} nvt (thermal), decay time of 10^7 sec, irradiation time of 3×10^7 sec, $N_{25}^0 = 5.1 \times 10^{25}$ (2% ²³⁵U).

^cCalculated from ORNL-2127, part II, vols. 1 and 3 (see *b* above), assuming 10^{13} nvt (thermal), decay time of 10^7 sec, irradiation time of 10^8 sec, $N_{25}^0 = 1.72 \times 10^{26}$ (6% ²³⁵U).

^dAll added as MoO₃.

^eAdded as "didymium nitrate" plus cerous nitrate.

^fAll added as RuCl₃.

The unavoidable presence of ruthenium in a stainless steel off-gas line will doubtless accelerate corrosion if the line is kept at a temperature low enough to allow condensation of nitric acid. Corrosion of "dry" stainless steel (i.e., at ~150°C) is negligible in this off-gas, and the corrosion of titanium in the "wet" off-gas and condensate is also quite low.¹⁰

Platinum, Corronel 230, 50% Ni-50% Cr, Hastelloys C and F, Inconel, Ni-onel, Nichrome V, BMI-HAPO 20, and stainless steel types 304L, 310, 446, and Carpenter No. 20SCb were exposed in the melter in the form of long strips, rods, or wires which extended from the vapor space in the top of the melter, through the solution and calcine layers, and into the melt. Penetration rates were determined by micrometer measurements at numerous positions along the length of the specimens before and after exposures.

All materials tested except platinum showed appreciable rates of attack, the maximum generally occurring at or near the position of the melt interface. The high-nickel alloys, Corronel 230, Nichrome V, Inconel, and 50% Ni-50% Cr were the most resistant of the conventional alloys tested. The maximum penetrations of these alloys, based on exposure times at operating temperature, varied from 0.176 mil/hr for Corronel 230 at 900°C to 0.945 mil/hr for Inconel at 950°C (Table 3.7).

Level Detection During Formation of Melt. — A modified "thermal conductivity probe"¹¹ was used to determine the type of material (glass, calcined solid, liquid, or gas and vapor) filling various zones or regions in a pot during melt formation. This device can make use of the thermocouples already in the pot, so that little or no additional paraphernalia will be required inside the pot. It has the additional advantage that the thermocouples do not lose their utility as temperature sensors. The probe consists basically of a heat sink, which could be the wires of a thermocouple itself, and a temperature-sensing device

¹⁰W. E. Clark, P. D. Neumann, L. Rice, and D. N. Hess, *Laboratory Development of Processes for Fixation of High-Level Radioactive Wastes in Glass. 4. Corrosion Studies on Candidate Materials of Construction*, ORNL-3816 (in preparation); see also R. E. Blanco and F. L. Parker, *Waste Treatment and Disposal Quart. Progr. Rept. August-October 1962*, ORNL-TM-482, pp. 18-19.

¹¹H. S. Carslaw and J. C. Jaeger, *Conduction of Heat in Solids*, 2nd ed., p. 345, Oxford University Press, London, 1959.

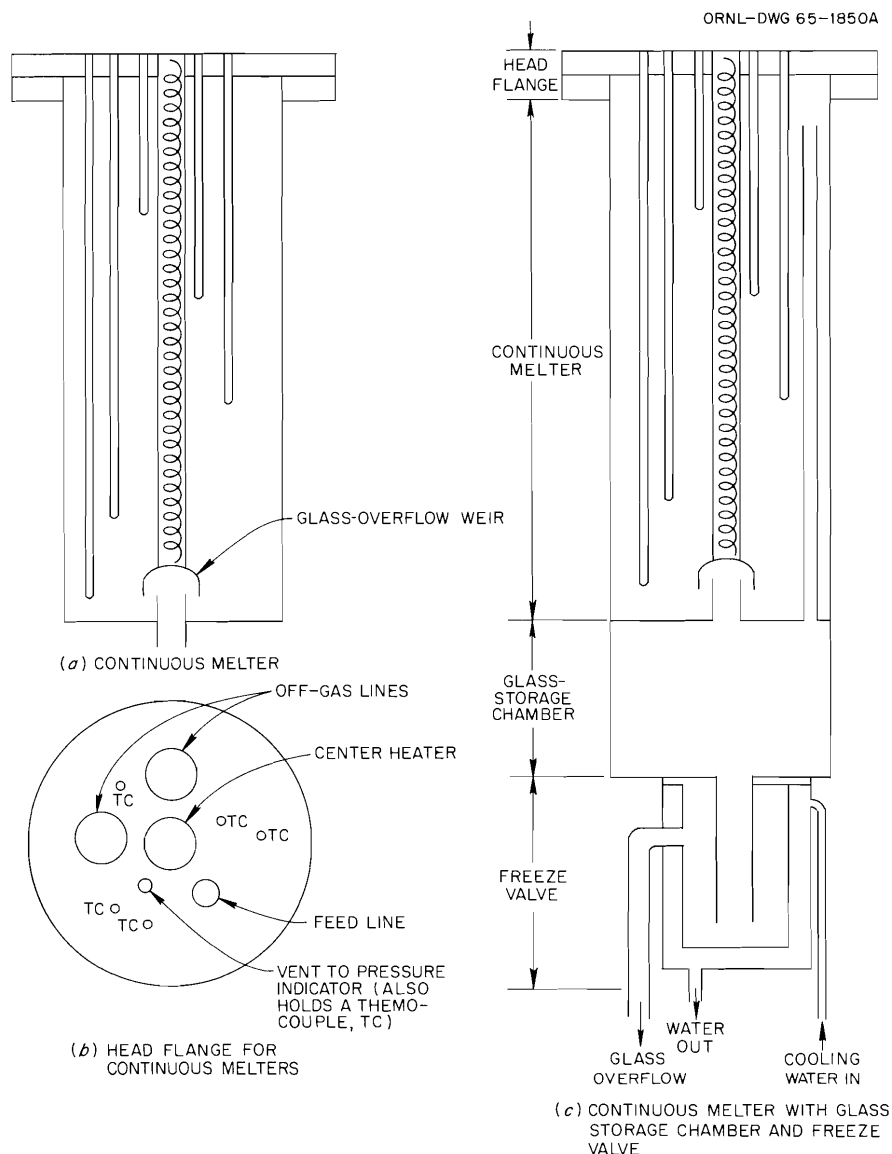


Fig. 3.9. Continuous Melters Used in Semiengineering-Scale Fixation Experiments.

such as a thermocouple. The probe is heated (or cooled), and the response of the temperature sensor is recorded. This response is a measure of the effective thermal conductivity of the medium surrounding the probe.

Experiments were carried out with a probe 1 in. in diameter and 22 in. long, concentrically located in a pot 4 in. in diameter and 24 in. long. The probe was heated by a Nichrome-wound heater that extended the full length of the probe. Chromel-Alumel thermocouples were attached to the 1-in. tube at different radial and longitudinal

positions. The materials tested at various temperatures in the pot were air, a magnesia powder (to simulate calcined material), and a phosphate glass. The heater dissipated about 20 w/lin in.

Representative results with one of the thermocouples at 850°C when surrounded by each of the above different materials are shown in Fig. 3.10. These results show that such a probe has promise as a device to permit discrimination between regions filled with glass, calcine, or gases. A heater capable of dissipating more power per unit of length than the one used in these studies will

Table 3.6. Volatility and Entrainment of Various Elements During Fixation of Purex FTW-65 Waste in a Continuous Melting Process^a

	Experiment No.									
	Melter Discharge Open ^b				Melter Discharge Closed ^c					
	1	2	3	4	5			6		
Simulated fission products present (10,000 Mwd/metric ton equiv) ^d	Yes	Yes	No	No	700					
Approximate softening temp., °C	700	700	600	600	700	700				
Maximum operating temp., °C		875 ^e	850	850	950	900				
Melt viscosity at operating temp., poises		10	6.5	6.5	~4.1	7.4				
Volatility and entrainment (wt % of total present)	Volatility (condensate plus scrub solution)				Volatility (cond. + scrub)	Entrainment (off-gas lines)	Total	Volatility (cond. + scrub)	Entrainment (off-gas lines)	Total
SO ₄ ²⁻	1.4	14.8	1.1	0.73	1.16	1.0	2.16	7.19	1.69	8.88
PO ₄ ³⁻	0.5	0.35	0.23	0.24	2.1		2.10	0.24		0.24
Fe ³⁺	3.7		2.5	1.9	18.41	12.91	31.32	15.8	10.6	26.4
Ru					<i>f</i>	<i>f</i>	21.73 ^f	16.6	3.92	20.52
Mo					0.76	0.45	1.21	1.29	0.52	1.81
Al ^g					0.24		0.24			
Li ^g								0.36	0.05	0.41

^aMelt additives (g-moles per liter of waste): 3.6 H₃PO₄, 2.7 NaOH, 2.4 LiOH · H₂O, 0.75 Al(NO₃)₃ · 9 H₂O.

^bFigure 3.9a.

^cFigure 3.9b.

^dBNL-Hanford composition (see Table 3.5).

^eThere was a short temperature excursion to 925°C.

^fThe bulk of the ruthenium in both condenser and off-gas lines was recovered as solids. These were collected for analysis.

^gAnalyzed for as indicators of entrainment.

shorten the time required to distinguish between substances. The time required in these studies to make these distinctions was about 1.5 min (Fig. 3.10). A remaining problem in the use of such a probe is the effect of films or layers that will build up on the probe during the filling of a pot with melt.

Pilot Plant Design

Active liaison with Hanford personnel on the design and startup of the pot calcination and rising-level Potglass equipment for the Hanford Waste Solidification Engineering Prototypes Pilot Plant continues. This equipment is presently

Table 3.7. Corrosion During Fixation of Purex FTW-65 Waste in a Continuous Melting Process^a

Candidate Material	Scoping Tests: $T = 875\text{--}900^\circ\text{C}$; Time - Variable	Maximum Corrosion Rate (mils/hr)		Remarks
		Test 1: 950°C , $35\frac{1}{4}$ hr	Test 2: 900°C , $36\frac{1}{4}$ hr	
Platinum	No attack; no weight change	0	0	No attack in any test
Corrone1 230			0.176	No marked local attack; maximum attack at melt interface
Incone1	Slight attack	0.943	0.508	Nearly all attack near melt interface
50% Ni-50% Cr		0.356	0.566	Nearly all attack near melt interface
Nichrome V		0.288		Visible local corrosion in and just above melt
BMI-HAPO 20	Severely attacked at melt interface	1.78		Excessive corrosion at melt interface
Type 446 SS			0.867	Considerable attack over entire specimen; maximum attack at melt interface
Ni-o-nel	Slight attack	Excessive		Completely destroyed in melt
Hastelloy F	Attack varied from slight to excessive			Eliminated in scoping tests
Hastelloy B	Very severe pitting attack			Consistently poor in all phases
Hastelloy C	Excessive local attack			Eliminated in scoping tests
Carpenter No. 20SCb	Heavy pitting attack			Eliminated in scoping tests
Type 310 SS	Heavy attack in vapor			Consistently poor in vapor
Type 304L SS	Attack in melt and at melt interface			Insufficiently resistant for construction of a continu- ous melter

^aMelt 357 in computer readout. Additives (g-moles per liter of waste): $3.6 \text{ H}_3\text{PO}_4$, 2.7 NaOH , $2.4 \text{ LiOH} \cdot \text{H}_2\text{O}$, $0.75 \text{ Al}(\text{NO}_3)_3 \cdot 9 \text{ H}_2\text{O}$.

undergoing design-verification tests. It will be installed in the Hanford Fuels Recycle Pilot Plant in August of 1965.

An analog computer study was made of the transient response to surges in vapor rate generated while feeding liquid waste to a pot calciner operating at temperatures up to 900°C. The system currently installed for the design verification tests at Hanford is shown in Fig. 3.11. Vapors from the pot calciner flow through a 2-in. vapor line to the condenser, where the steam and nitric acid are condensed. Noncondensable vapors flow to the evaporator through a 2-in. line which may contain a jet. This jet would be used to increase vapor circulation rates if required. The condensate flows by gravity from the condenser to the evaporator. A water seal pot is installed in the vent line from the pot calciner to serve as an emergency relief valve in case the normal vapor line plugs. The maximum allowable height of liquid in the water seal before it vents is 24 in. The seal vent is also connected to the evaporator, which serves as a common plenum for both the condenser and seal pot vents.

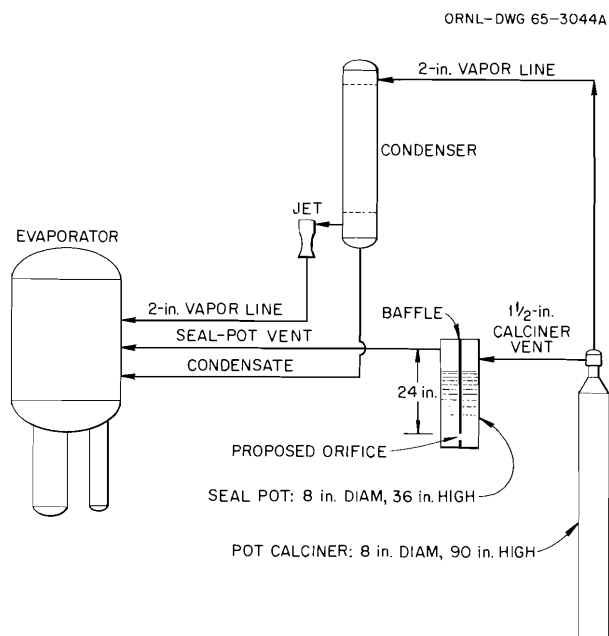


Fig. 3.11. Pot-Calciner Vapor and Vent System.

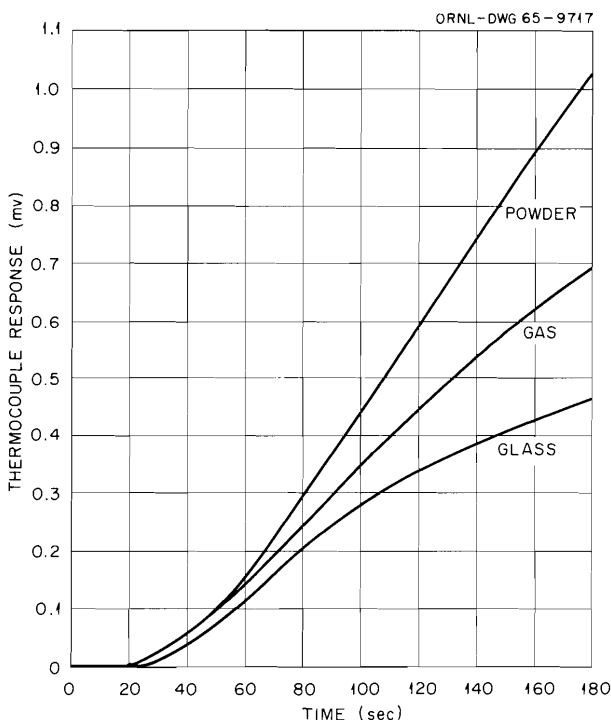


Fig. 3.10. The Response of a Chromel-Alumel Thermocouple at 850°C as a Function of the Surrounding Medium when Heated at a Uniform Rate.

The system was simulated on a PACE TR-10 analog computer, using the following basic assumptions:

1. The pressure in the evaporator would be constant and at a slight vacuum.
2. The normal vapor rate would be about 148 cfm, which approximates the maximum boilup rate from a 12-in.-diam pot calciner during the initial feeding period. The vapor-line pressure differential at this rate would be about 6 in. H₂O without installation of the jet downstream of the condenser, and 10.2 in. H₂O with the jet installed.
3. The prime cause of pressure fluctuations in the system is the surges of vapor at instantaneous rates considerably above the normal rate. These surges are probably due to fluctuations in the calciner feed rate, liquid level, and wall temperature. Vapor surges were simulated as step functions in the normal vapor rate for the purposes of this study.
4. The level in the seal pot could be simulated by treating the system as a manometer with a fluctuating pressure on the pot calciner side and a constant pressure on the evaporator side.

Results of a typical run are shown in Fig. 3.12, where the vapor rate, pot and evaporator pressure, and manometer differential height are plotted vs time. This run shows that for a 30% increase in vapor rate at a 2-sec frequency, the pot pressure increased to -20 in. H_2O from -27 in. H_2O , and the manometer differential height reached 23 in. H_2O ; so the seal was within 1 in. of venting. Results of all the computer runs are summarized in Fig. 3.13, which shows the maximum seal differential height as a function of the vapor rate increase and the step-function frequency. The latter is expressed in terms of ϕ , defined as the absolute value of the difference between an odd integer, $n = 1, 3, 5, \dots$, and the ratio of the step-function period to the natural period of the seal pot. As the period of the step function approached an odd multiple of the seal-pot natural period ($\phi \rightarrow 0$), the adverse effect of vapor rate increase was intensified. Curves B and C in Fig. 3.13 indicate that the seal was less likely to vent when the restriction caused by the $1\frac{1}{2}$ -in. jet was removed. Considerable improvement was obtained by inserting an orifice with an area of 4.54 in.² in the seal pot at the bottom of the baffle. This tended to dampen the manometer fluctuations, as shown in curve C, and also removed the effect of

vapor-surge frequency on the seal differential height. The data indicate that the system could take surges 70% above the normal rate without venting the seal. The area of the seal restriction (4.54 in.²) is about 35% greater than the area of the inlet pipe to the seal, so no severe restriction would be added to the flow of vapor through the seal-pot vent system.

As a result of this study, a recommendation was made that the jet in the condenser vent line be removed and that the area under the seal baffle be reduced to 4.54 in.² in order to dampen out the effects of the vapor fluctuations on the seal-pot level.

A study of thermocouple materials for the pot calciner and its furnace was made to determine the most economical and reliable materials for the Hanford pilot plant. Two classes of thermocouple service were specified. For the furnace liner and susceptor, the thermocouples must be stable for at least 100 hr at $1100^\circ C$ and for 1000 hr at $1000^\circ C$. These couples will be used for many tests and therefore could be constructed of more costly materials such as platinum. For the pot calciner the thermocouples must be stable for at least 100 hr at $900^\circ C$ and for very long times at temperatures below $700^\circ C$.

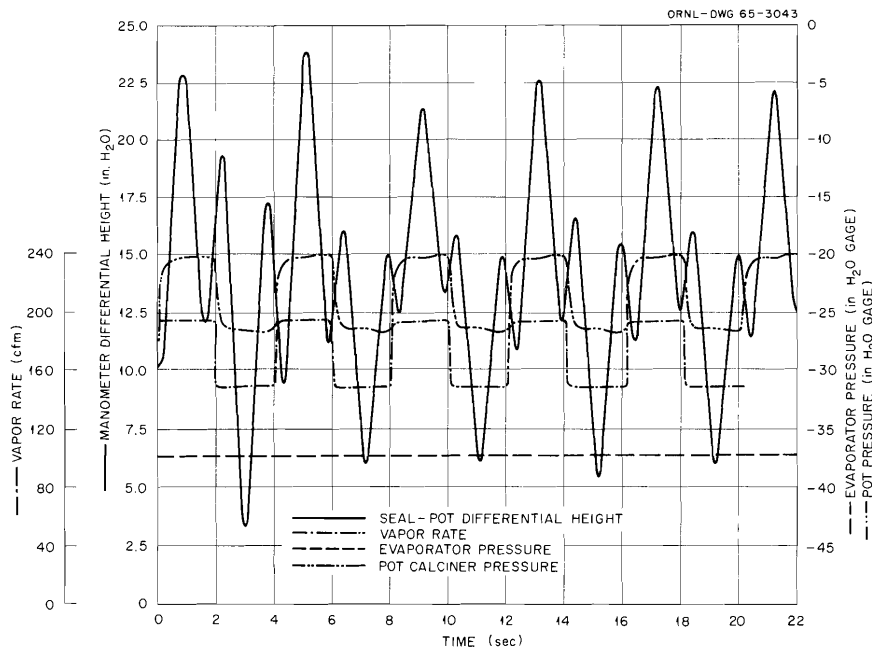


Fig. 3.12. Typical Computer Plot of Pot-Calciner Pressure-Transient Study.

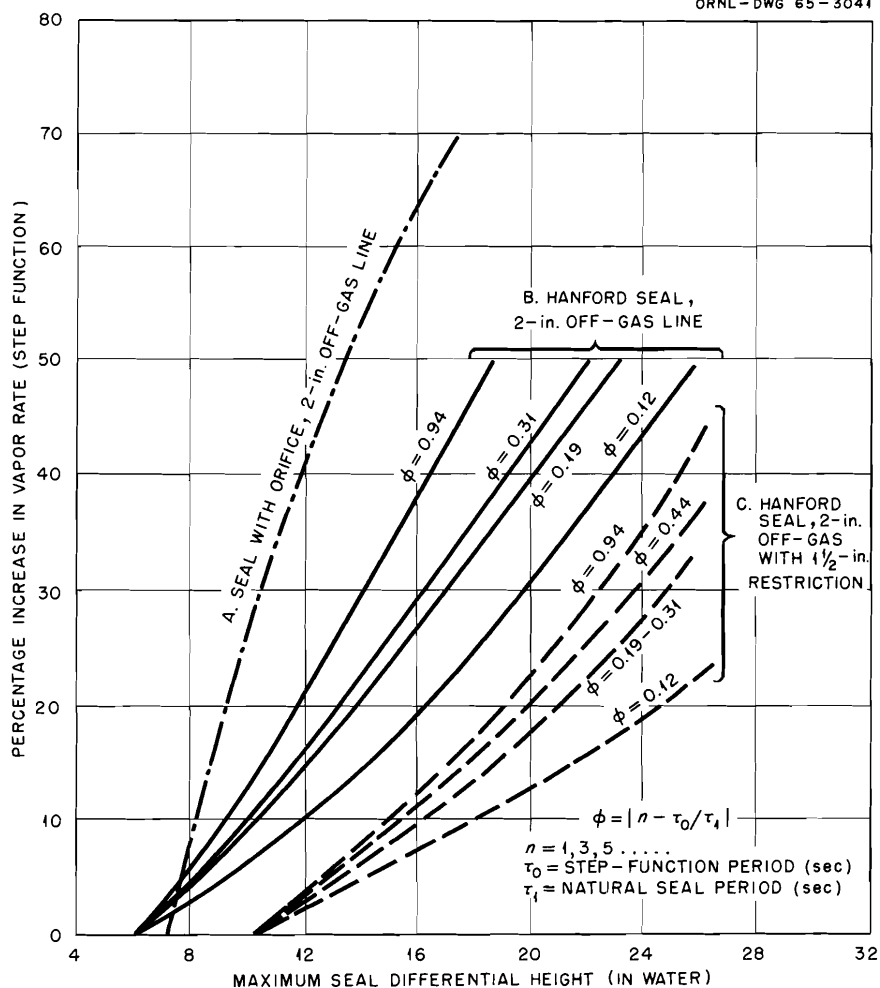


Fig. 3.13. Pot-Calciner Pressure-Transient Study: Effect of Step Function on Water-Seal Differential Height.

Thermocouples recommended were as follows:

1. Furnace liner and susceptor - Pt vs Pt-10% Rh thermocouple wires sheathed in Inconel or Hastelloy X, with MgO insulation.
2. Pot calciner - Chromel-Alumel thermocouple wires sheathed in type 310 stainless steel. Since these thermocouples will probably be used only once during a calcination, they must be as inexpensive as possible, consistent with the service specifications.

Further recommendations included the use of 20 gage as the minimum wire diameter, ungrounded wires to obtain longer life, and investigation of the new Chromel-P wire, which contains a small quantity of niobium and a special type of Alumel

which is essentially a nickel-silicon binary alloy. Improved high-temperature oxidation resistance is claimed for these newer materials.

A survey^{12,13} of the composition and quantity of wastes to be generated at the Nuclear Fuels Services Reprocessing Plant, near Buffalo, New York, was made to enable testing of this waste type in the hot pilot plant. Since fuels reprocessed in this plant will have very high burnups (up to 20,000 Mwd per metric ton of uranium), the wastes

¹²J. M. Holmes, *Survey of Nuclear Fuel Services, Inc., Waste Compositions*, ORNL-TM-1013.

¹³R. E. Blanco and F. L. Parker, *Waste Treatment and Disposal Semiann. Progr. Rept. July-Dec. 1964*, ORNL-TM-1081.

will contain high concentrations of stable and active fission products and will generate high internal heat fluxes in the calcine or glassy solids. Compositions were obtained for two types of Purex, Thorex, and TBP-25 wastes.

Formulation of a detailed schedule for pot calcination and rising-level glass tests in the hot pilot plant was completed recently with Hanford personnel. During the initial operating phase, three pot calcination tests will be run on Purex wastes having approximately 1000 to 2000, 5000, and up to 6000 Btu hr⁻¹ ft⁻³ of internal heat-generation rates. Two rising-level tests will be made: one on Purex waste containing tracer levels of radioactivity, and the other with up to 6000 Btu hr⁻¹ ft⁻³ of internal heat-generation rate. Both sulfate and nonsulfate Purex wastes will be tested in this initial phase. Tests on other wastes such as TBP-25, Thorex, and Darex will be considered during the second operating phase, which is scheduled tentatively for calendar year 1967.

3.2 DISPOSAL OF INTERMEDIATE-LEVEL RADIOACTIVE WASTE

Nuclear installations generate large volumes of intermediate-level radioactive wastes (ILW), such as evaporator concentrates, second- and third-cycle solvent extraction raffinates, and slurries or solids (residues from low-level treatment processes). These wastes are characterized by their modest levels of radioactivity, so that heating and radiation dose levels do not present serious problems, and by their high salt or solids contents, which prevent their efficient treatment by conventional ion exchange, precipitation, or foam-separation methods. The ORNL intermediate-level waste treatment program includes development of processes to remove the water from these wastes and to incorporate the dried solids in a cheap, inert, insoluble material before burial or contained storage. Incorporation of these wastes in asphalt or other plastic and elastic substances appears to be simple, inexpensive, and relatively insensitive to the type of material being incorporated, and, within limits, independent of local geologic and hydrologic conditions. Asphalt has good adhesive and coating properties and is insoluble in water, but its sensitivity toward radiation limits the activity level of included material.

At Mol, Belgium,¹⁴ a batch process has been developed for incorporating the wastes in asphalt.

The wastes — incinerator ashes, concentrated aqueous solutions, or filtered sludges with variable water content — are gradually introduced into hot asphalt (about 240°C) with violent stirring. Most of the work at Mol has been with sludges. At Marcoule, France,¹⁵ a continuous process has been developed for incorporating sludges in asphalt. The sludges to which emulsifying agents have already been added are mixed with hot asphalt (about 125°C). The major portion (80 to 90%) of the water in the sludges is exuded and thus separated from the coated wastes. The residual water in the asphalt mixture is boiled off and the mixture heated to about 130°C. Since most soluble activity would be in the exuded water, the process is applicable only to wastes in which the radiation emitters are tied up in the sludge solids. At ORNL, a process (Fig. 3.14) has been

¹⁴P. Dejonghe, N. Van de Voorde, J. Pyck, and A. Stynen, *Insolubilization of Radioactive Concentrates by Asphalt Coating*, final report No. 2, 1st part, concerning proposal 167, April 1, 1961, to March 31, 1963, EURAEC-695.

¹⁵J. Rodier, G. Lefillatre, and J. Scheidhauer, *Bitumen Coating of the Radioactive Sludges from the Effluent Treatment Plant at the Marcoule Center*, Review of the progress reports 1, 2, 3, and 4, CEA report 2331, 1963 (ORNL-tr-202).

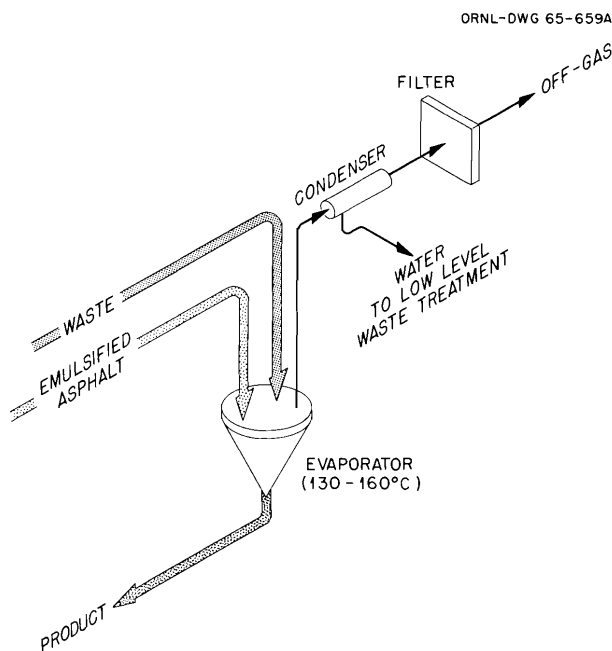


Fig. 3.14. Flow Diagram of Process to Incorporate ILW in Emulsified Asphalt.

developed for incorporating wastes in emulsified asphalt. Attractive features of the process include:

1. use of emulsified asphalt, which flows readily at room temperature;
2. evaporation at low temperatures so that entrainment of activity from the evaporator and thermal degradation of the asphalt are minimized;
3. agitation at modest rates (100 to 500 rpm, which provides adequate mixing and keeps the heated surfaces of the evaporator clean;
4. operation in batch or continuous manner;
5. incorporation of soluble and insoluble activity with equal effectiveness.

Asphalt products containing 20 to 80 wt % solids from waste have been prepared. The waste used in these studies was simulated ORNL waste-evaporator bottoms (Table 3.8), and the asphalt was an emulsified asphalt used in the surface treatment of roads. (This asphalt emulsion is defined in Federal Specifications SS-A-674b as type RS-2: a rapid-setting high-viscosity emulsified asphalt. The material used contained about 63 wt % base asphalt, 35 wt % water, and 2 wt % emulsifying agent.) Products containing 20 to

60 wt % solids from waste flowed freely from the evaporator at 130°C. The product containing 80 wt % solids from waste was removed with difficulty at 195°C.

Since the product containing 60 wt % solids from waste (Fig. 3.15) represented a good com-

Table 3.8. Composition of Simulated ORNL Intermediate-Level Radioactive Waste Solution Incorporated in Emulsified Asphalt

Density of solution at 25°C = 1.335 g/ml

Component	Molarity
Na ⁺	6.61
NH ₄ ⁺	0.19
Al ³⁺	0.22
SO ₄ ²⁻	0.35
Cl ⁻	0.056
OH ⁻	2.06
NO ₃ ⁻	4.64

PHOTO 67974R

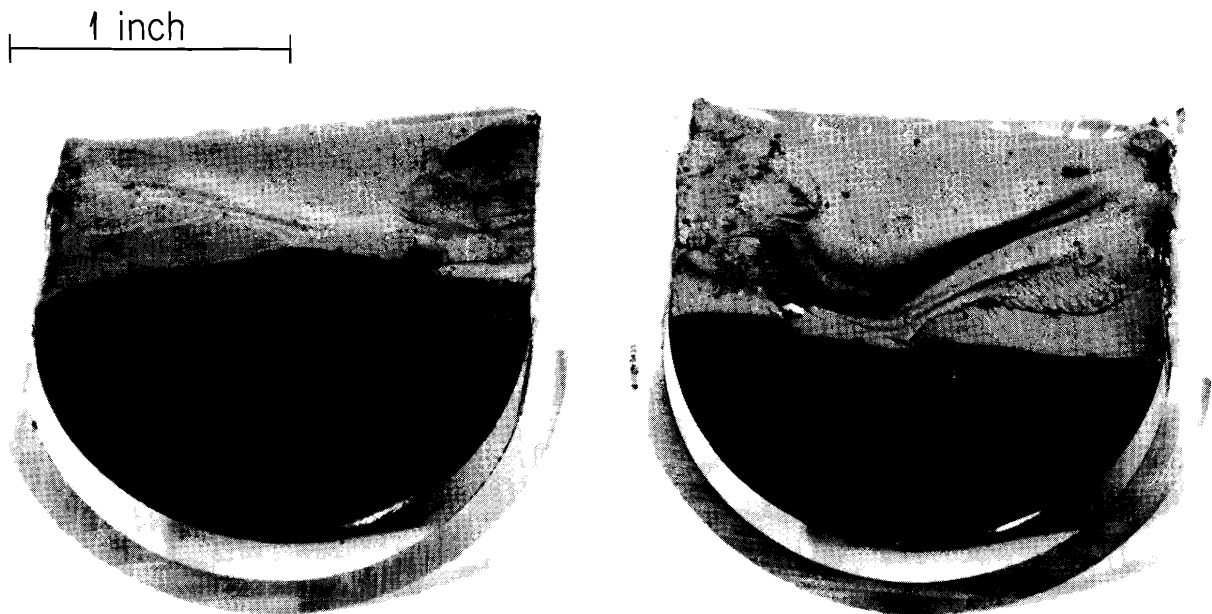


Fig. 3.15. Solids-Asphalt Product Incorporating 60 wt % Solids from Simulated ORNL ILW Solution. Nominal composition of product (wt %): 47.8 NaNO₃, 9.1 NaOH, 4.6 Al₂(SO₄)₃, 0.4 NaCl, 0.3 Na₂SO₄, and 37.8 asphalt. Density = 1.5 g/cm³. Volume reduction (volumes of waste per volume of product) = 2.

promise of properties – volume reduction, viscosity, ductility, etc. – it was studied in most detail. The process consisted in (1) adding the waste directly to emulsified asphalt with modest stirring – about 100 rpm, (2) boiling off the water, (3) raising the temperature of the product to the desired final temperature – usually 165°C, and (4) draining the product into an appropriate container. Although the process described above is a batch operation, it has been carried out with slight variation in procedure as a continuous operation.

Probably the best measure of how well the waste particles have been coated with asphalt is how resistant the product is to leaching by water. Thus, asphalt products containing 20 to 60 wt % solids from simulated ORNL waste-evaporator bottoms have been leached with water for periods of up to nine months. As expected, these leach tests indicate surface contamination of the samples, which decreases rapidly during the first several weeks (Figs. 3.16 and 3.17). The term

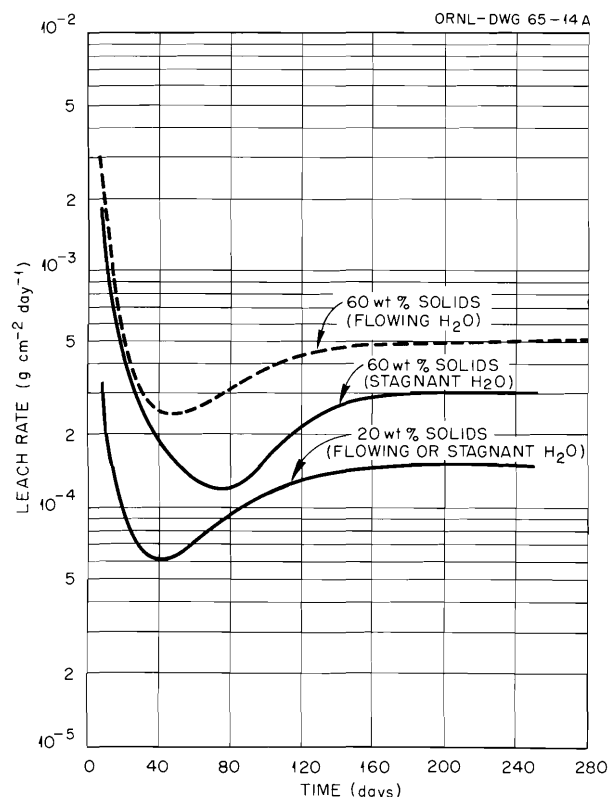


Fig. 3.16. Leach Rates of ¹³⁷Cs and Sodium from Products Incorporating ORNL ILW Solution.

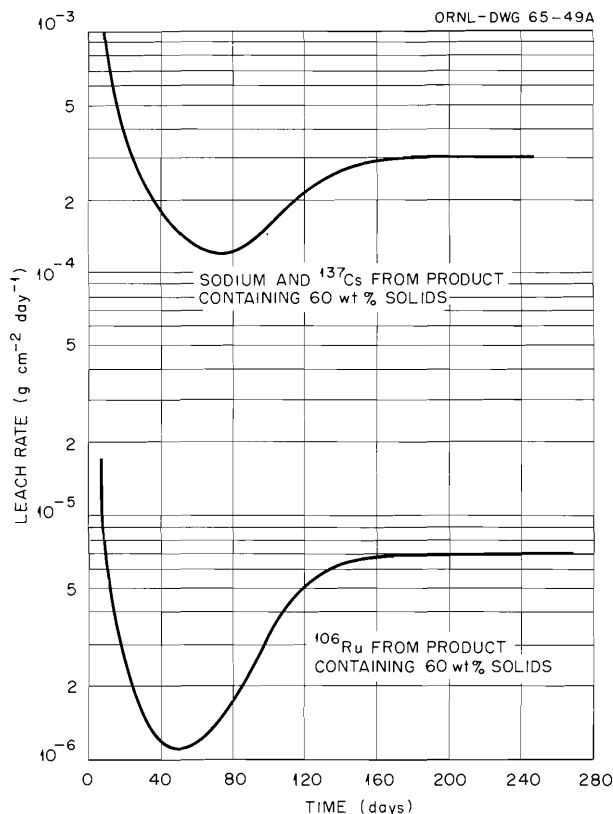


Fig. 3.17. Leach Rates of ¹³⁷Cs, Sodium, and ¹⁰⁶Ru from Asphalt Product Containing 60 wt % Solids from ORNL ILW Solution.

“leach rate” rather than “dissolution rate” is used, since the asphalt matrix does not dissolve. Leach rates were calculated by using the expression

$$\frac{\text{activity leached/cm}^2/\text{day}}{\text{activity/g of product}} = \text{g cm}^{-2} \text{ day}^{-1} .$$

Tests were made with stagnant (static test) and flowing (dynamic test) distilled water at 25°C. The water was sampled and completely replaced with fresh water at the end of each week.

The asphalt product containing 60 wt % solids from waste (Fig. 3.15 and Table 3.8) reaches an apparent steady-state leach rate for ¹³⁷Cs and sodium of $3 \times 10^{-4} \text{ g cm}^{-2} \text{ day}^{-1}$ in static tests, and about $5 \times 10^{-4} \text{ g cm}^{-2} \text{ day}^{-1}$ in dynamic tests after about six months (Fig. 3.16). The difference between leach rates determined by gamma counting of ¹³⁷Cs and flame-photometric determination of sodium in the same leachate was negligible. The product containing 20 wt % solids

(Fig. 3.16) reaches an apparent steady-state leach rate for ^{137}Cs and sodium about half that of the product with 60% solids - $1.5 \times 10^{-4} \text{ g cm}^{-2} \text{ day}^{-1}$. Unlike the results with the product containing 60% solids, the results with the product containing 20% solids are not influenced by whether the water is flowing or stagnant. These results suggest that there is a resistance to diffusion due to concentration in the leachate in the first case (60%) that is not apparent in the second (20%). The asphalt product containing 60 wt % solids from waste reaches an apparent steady-state leach rate for ^{106}Ru of $7 \times 10^{-6} \text{ g cm}^{-2} \text{ day}^{-1}$ (Fig. 3.17). The fact that the above leach rates for ^{137}Cs and sodium are 50 to 100 times higher than leach rates reported in Belgium¹⁴ and France¹⁵ implies that leach rate is a function of whether the incorporated activity is soluble or insoluble.

To evaluate the resistance of the asphalt product to irradiation, samples of the product containing 60 wt % solids from waste were irradiated by means of a ^{60}Co source to absorbed doses ranging from 10^6 to 10^8 rads. A dose of 10^6 rads had negligible effect on the asphalt sample (Fig. 3.18).

A dose of 10^7 rads caused it to swell very slightly (Fig. 3.19), while a dose of 10^8 rads caused the material to increase about 36% in volume (Fig. 3.20). Leach tests on a sample irradiated to a dose of 10^8 rads indicated that the irradiation has no effect on the leach rate.

Design of a pilot plant to incorporate 100 gal of ORNL waste-evaporator bottoms in emulsified asphalt per 8-hr shift by the above batch process has been completed and installation has started. Studies have been started to determine the long-term effect of incorporated radioactive elements on the physical (in particular, leach rate) and chemical (in particular, radiolytic gases formed) properties by incorporating low and high concentrations of radionuclides in asphalt samples.

Factors being investigated include the effect of stirring rate, temperature, and time at temperature on the final product; of radiation dose level on leach rate; of different base asphalts and emulsifying agents on the quality of the final product; and of solubility on the leach rate of a given compound, namely, $\text{Sr}(\text{NO}_3)_2$ vs SrCO_3 . A hazards survey and evaluation program has also been started.

PHOTO 69225

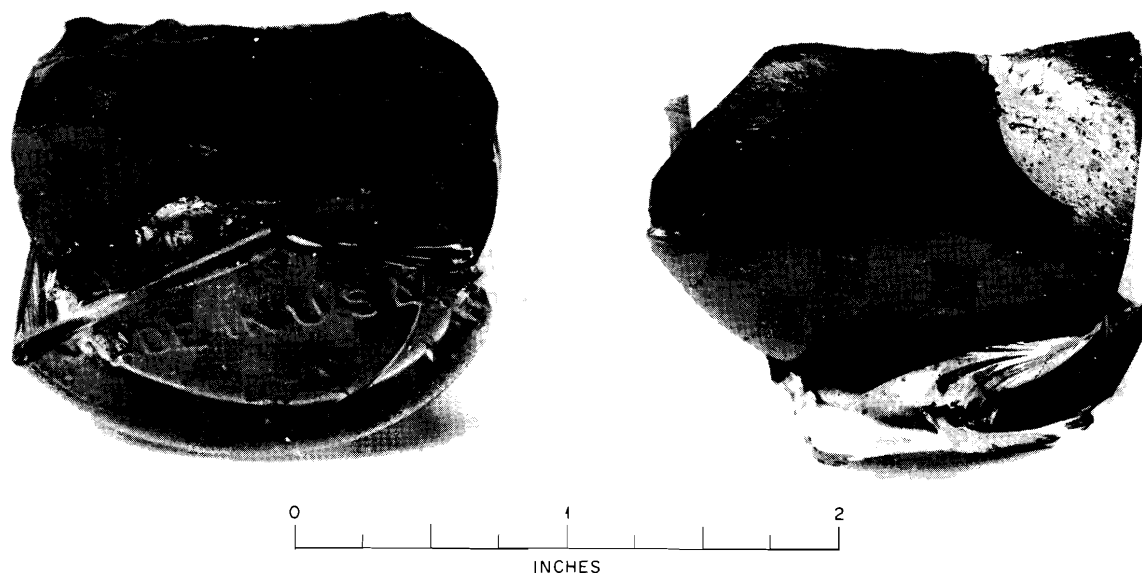


Fig. 3.18. Asphalt Product Containing 60 wt % Solids from ORNL ILW Solution After Irradiation to 10^6 Rads.

PHOTO 69224

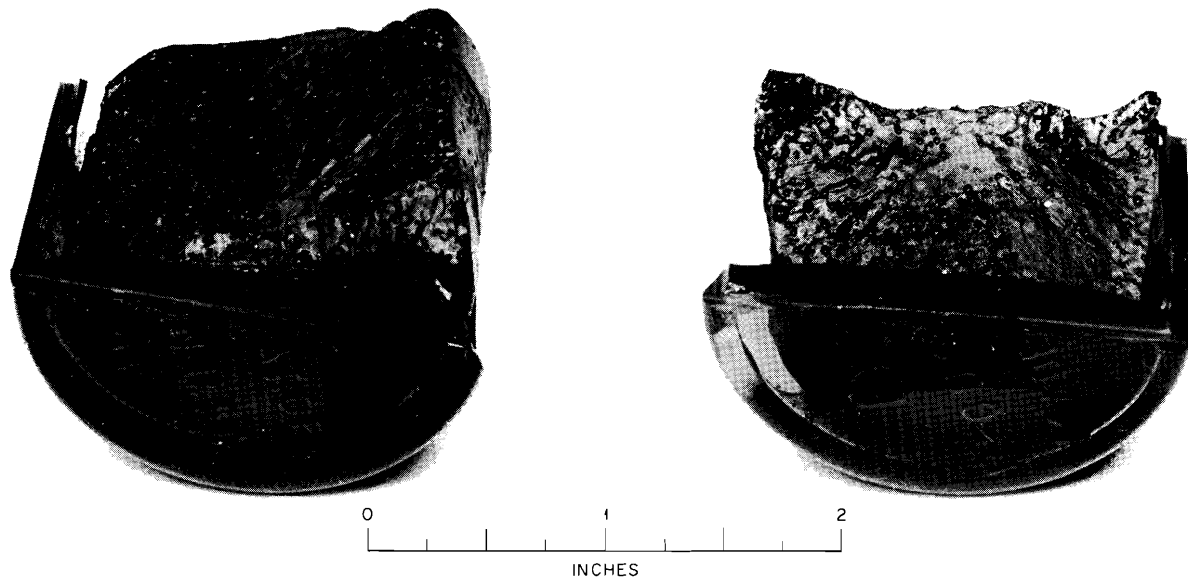


Fig. 3.19. Asphalt Product Containing 60 wt % Solids from ORNL ILW Solution After Irradiation to 10^7 Rads.

PHOTO 68256

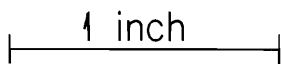


Fig. 3.20. Asphalt Product Containing 60 wt % Solids from ORNL ILW Solution After Irradiation to 10^8 Rads.

3.3 TREATMENT OF LOW-LEVEL RADIOACTIVE WASTES

Low-level radioactive wastes (LLW) consist of waters with low solids and radioactivity contents. They are customarily treated to remove radionuclides and then discharged to streams. The objective of the ORNL program is to develop, evaluate, and determine the cost of alternative processes for decontaminating LLW to less than the maximum permissible levels permitted for water,¹⁶ MPC_w, for occupational exposure (168 hr/week). The retained solids and radionuclides can be combined with high-level radioactive wastes for ultimate disposal, or they can be incorporated in asphalt or concrete and buried in restricted areas.

Two processes are being studied for treating LLW: the scavenging-precipitation foam-separation process and the water-recycle ion exchange process. The latter differs from the previously developed scavenging-precipitation ion exchange process¹⁷ in that it is designed to operate at neutral conditions. Since very pure demineralized water is produced in this process, recycle and reuse of this water appear to be more economical than to discharge it and continually demineralize fresh river water. The steps in this process are flocculation-precipitation to remove colloids, demineralization by ion exchange, and sorption of ruthenium and cobalt on activated charcoal. Initial tests on a laboratory scale have shown satisfactory results, demonstrating decontamination factors greater than 1000. Semiengineering-scale tests are scheduled for late in 1965.

Foam separation has the desirable characteristic that separation efficiency is almost independent of concentration at very low concentrations. When a metal ion is complexed with a surfactant in an aqueous solution and the system is foamed by bubbling air through it, the metal ion is removed from the solution on the surface of the foam bubbles. The feasibility of applying foam separation to the specific problem of treatment of LLW was investigated in the laboratory,¹⁸ and the development of equipment for a large-scale separation plant was

pursued.¹⁹ Subsequently, a foam-separation pilot plant for treating ORNL LLW was designed, installed,¹⁷ and operated.²⁰ No further development of the foam process for treating LLW is planned. Decontamination of LLW in the scavenging-precipitation foam-separation pilot plant²⁰ was accomplished in two steps: (1) precipitation of calcium, magnesium, and radionuclides in a scavenging-precipitation step that included the use of Grundite clay for sorption of cesium and (2) removal of strontium and other radionuclides by complexing with a foaming agent, dodecylbenzene sulfonate, and then removing the complex by foaming in a countercurrent foam-separation column.

The scavenging-precipitation system could be used alone, where decontamination factors for strontium and cesium of about 10 were required, or in combination with a foam system to achieve a strontium decontamination factor of 1000. Cesium is not removed in the foam system.

Scavenging-Precipitation Foam-Separation Process

Pilot Plant Studies. — The process flowsheets for the scavenging-precipitation and foam-separation systems are shown in Fig. 3.21a and b. The scavenging-precipitation system was run continuously under fixed operating conditions throughout the test program.

Low-level waste from the ORNL equalization basin²¹ was fed at 5 gpm to a flash mixer to which Grundite clay was added continuously. Caustic, sodium carbonate, and copperas were added in a second flash mixer to make the waste 0.005 M in NaOH, 0.005 M in Na₂CO₃, and 10 ppm in iron. The solution (pH 11.2) flowed to a flocculator

¹⁶Maximum Permissible Body Burdens and Maximum Permissible Concentrations of Radionuclides in Air and in Water for Occupational Exposure, U.S. Department of Commerce, NBS Handbook 69 (June 5, 1959).

¹⁷F. L. Culler, Jr., et al., *Chem. Technol. Div. Ann. Progr. Rept. May 31, 1964, ORNL-3627.*

¹⁸W. Davis, Jr., A. H. Kibbey, and E. Schonfeld, *Laboratory Demonstration of the Two-Step Process for Decontaminating Low-Radioactivity-Level Process Waste Water by Scavenging-Precipitation Foam Separation*, ORNL-3811 (in preparation).

¹⁹P. A. Haas, *Engineering Development of a Foam Column for Countercurrent Surface-Liquid Extraction of Surface-Active Solutes*, ORNL-3527 (to be published).

²⁰L. J. King, A. Shimozato, and J. M. Holmes, *Pilot Plant Demonstration of the Removal of Activity from Low-Level Process Wastes by a Scavenging-Precipitation Foam Separation Process*, ORNL-3803 (in preparation).

²¹K. E. Cowser, R. J. Morton, and E. J. Witkowski, "The Treatment of Large-Volume Low Level Waste by the Lime-Soda Softening Process," *Proc. U.N. Intern. Conf. Peaceful Uses At. Energy, 2nd, Geneva, 1958, P/2354, vol. 18, p. 161.*

Table 3.9. Summary of Pilot Plant Tests for the Foam System^a

Countercurrent foam column: 2 ft square by 8 ft high
 Recovery system: three 2-ft-square by 44-in.-high columns

	Tap Water Tests	Low-Level Waste Tests			
		Open Column ^b	Pall-Ring-Filled Column ^b	Pall-Ring-Filled Column Plus Recovery System	
				Preliminary Tests	93-hr Test
Liquid feed rate, gpm ^c	2	1-2	1-2	1-4	2
Air rate to foam column, scfm ^c	2-6	4-6	3-6	1-8	8
Air rate to each recovery stage, scfm ^c	4-6			1-3	1
DBS in feed, ppm ^c	25-220	55-400	100-470	47-490	120
DBS in bottom of column, ppm	10-130	10-290	35-350	61-413	128
DBS in condensed foam, ppm	1200-3850	1100-3600	1900-2900	1100-5600	1940
DBS in effluent, ppm	1-7			10-115	62
Volume reduction, feed/condensed foam	35-142	17-46	14-70	10-400	31
V/LD , cm ⁻¹		120-270	135-290	60-220	138
Strontium decontamination factor ^d		2-200 ^a	10-200 ^a	1-150 ^a	105 ^a

^aDoes not include decontamination factor for precipitation system (see Table 3.10).

^bFoam column without recovery system.

^cThese items are set conditions; others are measured results

^dIncludes both foam column and recovery columns.

where the hardness constituents (calcium and magnesium), the iron, and some of the radioactive ions precipitated as the carbonate and hydroxides to form a floc which scavenged radiocolloids and other colloidal impurities from the solution. The softened water was separated from the solids in a slowly agitated suspended-bed clarifier. The solids were discharged as a slurry to the drain but could be collected by filtration in an actual waste-treatment plant for disposal. When the foam-separation equipment was being operated, the desired amount of clarifier effluent was pumped through a deep-bed anthracite filter for final polishing and then to the foam column. Otherwise, the clarified effluent was discarded. Except for the additional flash mixer for adding Grundite clay, the equipment for the precipitation system was the same as that used for the scavenging-precipitation ion exchange process,²² a 5-gal Alsop flash mixer, a 4-ft-diam by 3-ft-high agitated flocculator, a 4-ft-

diam by 6-ft-high agitated sludge blanket clarifier, and 2-ft-diam by 33-in.-high Permutit vertical filters.^{17,22,23}

The foam system (Fig. 3.21b) was designed¹⁷ to have a capacity of at least 2 gpm of LLW, with a possibility that the capacity might be as high as 5 gpm. Unlike the precipitation system, the operating conditions for the foam system were varied during the test program (Table 3.9). A solution of

²²R. E. Brooksbank, et al., *Low-Radioactivity-Level Waste Treatment. Part II. Pilot Plant Demonstration of the Removal of Activity from Low-Level Process Waste by a Scavenging-Precipitation Ion-Exchange Process*, ORNL-3349 (May 20, 1963).

²³R. E. Brooksbank, L. J. King, and J. T. Roberts, "Pilot Plant Demonstration of the Removal of Radioactivity from Low-Level Process Waste Water by a Scavenging-Precipitation Ion-Exchange Process," presented at the Symposium on Radionuclide Exchange on Soils, Minerals, and Resins, American Chemical Society, Philadelphia, Pa., April 10, 1964.

sodium dodecylbenzene sulfonate (5000 ppm DBS) was added in the feed line to achieve the desired concentrations in the feed. The feed was introduced at the top of the 2-ft-square foam column through a distributor consisting of six $\frac{3}{8}$ -in.-IPS pipes with six 0.078-in.-diam orifices drilled along each pipe. A small deflector plate below each orifice prevented impingement of a liquid jet on the foam. The feed solution drained down the column countercurrent to about 8 ft of foam that was generated by bubbling air through nine 3-in.-diam spinnerettes (each having 3949 holes 60 μ in diameter) immersed in a 24-in.-deep pool of water at the bottom of the column. The foam moved up the column into a vertical foam-drying section and then into a 2-ft-square by 5-ft-long horizontal foam-drying section. Liquid drained from the foam and was collected and returned to the foam column through a liquid distributor located under the feed distributor. The drained foam passed on to a centrifugal foam breaker, where it was condensed.

When the surfactant recovery system was being used, liquid from the bottom of the foam column was pumped continuously to the surfactant recovery system where DBS was stripped both to conserve DBS and to reduce the DBS concentration in the treated waste. This system consists of three 2-ft-square by 44-in.-high foam-stripping columns. The water from the top column flowed by gravity through the stages in series and was then discarded. DBS was stripped as foam by bubbling air to each column through 9-in.-diam Micro Metallic stainless steel spargers immersed in a 24-in.-deep liquid pool. The average mean pore-size opening in the spargers is 10 μ (grade G). The foam from each column was condensed while passing through an orifice, and the condensate collected in a single 6-in.-diam glass column header. The recovery columns were maintained at atmospheric pressure and the glass column at $\frac{1}{2}$ atm.

Scavenging Precipitation. — The scavenging-precipitation portion of the plant was operated continuously for 91- and 45-day periods at a feed rate of 5 gpm of LLW. Grundite clay was added only during the final 93-hr test at a rate of 0.77 lb of clay per 1000 gal.

The total hardness of the LLW averaged 109 ppm as equivalent CaCO_3 . The total hardness of the clarifier effluent averaged 2 ppm and varied from 1 to 4. This is significantly lower than the hardness in the product from the precipitation step (6 to 10 ppm) in the scavenging-precipitation ion

exchange process,¹⁷ where the waste is made 0.01 *M* in NaOH and no Na_2CO_3 is used. The decontamination factor for strontium averaged 12, while that for cesium was 1 without Grundite clay and about 9 with it. The averages of the turbidities of the LLW and the filtered clarifier effluent were 4.3 and 2.3 ppm, respectively, as equivalent SiO_2 .

Foam Separation. — Initial tests were conducted at design conditions with tap water. The foam appeared to be stable, and the recovery system satisfactorily reduced the DBS concentration from 40 ppm in the feed to less than 5 ppm in the effluent (Table 3.9). However, later tests (see below) showed that actually up to 200 ppm of DBS was required in the feed to achieve stable foam conditions and satisfactory decontamination values, and the recovery system was not designed to handle this increased load. It was concluded that if properly matched equipment is used, the DBS concentration can be reduced to satisfactorily low values in effluent to be discharged.

The first tests of the foam system with LLW were largely unsuccessful because of turbulence and instabilities. Varying the operating condition, such as reducing the feed rate from 2 to 1 gpm, increasing the DBS concentration, or disconnecting the recovery system did not establish steady-state conditions. Strontium decontamination factors varied from 2 to 200 (Table 3.9).

The column was filled with Pall-ring packing (1.5 \times 1.5 in.) to act as baffles and to prevent channeling and circular turbulence. Further tests, made in the foam column alone under a variety of operating conditions, showed that steady-state conditions were achieved at a feed rate of 1 gpm, 200 ppm of DBS in the feed, and 4 cfm of air; the decontamination factor for strontium was 120 to 200. A similar test using the recovery column, with 1 cfm of air in each recovery stage, also showed steady-state operation with an average strontium decontamination factor of 105 (Table 3.9).

A final demonstration test was made where steady-state operation was maintained for 93 hr (Tables 3.9 and 3.10). Both the liquid feed rate and the air rate were doubled to 2 gpm and 8 cfm, respectively, to increase the processing rate while maintaining a constant extraction factor. The DBS concentration was decreased to 120 ppm. The strontium decontamination factors across the foam and precipitation system were 100 and 10, respectively, giving an overall value of about 1000.

Table 3.10. Decontamination Factors During the 93-hr Pilot Plant Test of the Scavenging-Precipitation Foam-Separation Process

	Foam Column	Recovery System	Foam System	Scavenging-Precipitation	Overall
Average Sr β	35	3	105	10	1050
(range)	(19-59)	(2-4)	(56-193)	(8.5-10.8)	(500-1500)
Average Cs γ	0.9	0.9	1.0	8.8	7.6
(range)	(0.5-2)	(0.8-1.3)	(0.5-1.8)	(5.13)	(4-11)
Co					1.3
Sb					2.2
Ru					4.2
Zr-Nb					> 50
Ce					> 20

Cesium, antimony, and ruthenium were removed only in the precipitation step, and zirconium-niobium only in the foam step, while strontium, cobalt, and cerium were removed in both. The data for Sb, Ru, Co, Zr-Nb, and Ce were widely scattered, since they were present in very low concentrations. The concentrations of Sr, Cs, Ru, Co, Ce, Sb, and Zr-Nb in the treated effluent were 2, 0.6, 0.3, 0.1, 0.2, 0.02, and 0.0001% of the maximum permissible concentration for water¹⁶ respectively. Thus, this process is suitable for use at many nuclear installations where low-level radioactive wastes contain comparable amounts of radioactivity. Higher decontamination factors could probably be attained in equipment designed to operate at higher V/LD ratios (see below). However, this could not be demonstrated in the present equipment because of limitation in the air supply and the capacity of the centrifuge.

Parameter V/LD . - The foam-column parameter V/LD (where V and L are the gas and liquid rates in the same units, and D is the effective bubble diameter) is related to the extraction factor and has been shown to be useful as a basis for process control in laboratory tests.¹⁸ Figure 3.22 shows the relationship between the strontium decontamination factor across the countercurrent foam column and the parameter V/LD for all of the pilot plant tests. These data are in good agreement with the

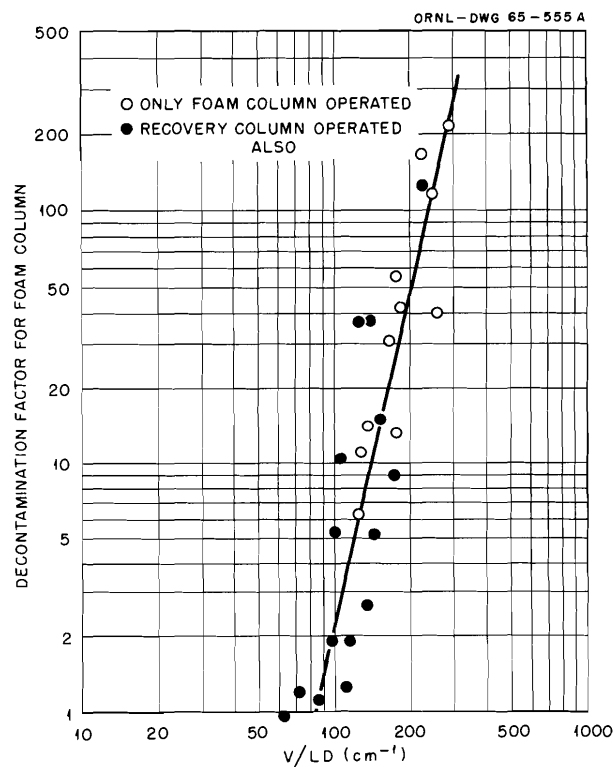


Fig. 3.22. Relationship Between the Decontamination Factor for Strontium Across the 2-ft-square \times 8-ft-high Countercurrent Foam-Separation Column and the Operating Parameter V/LD for All Pilot Plant Tests.

laboratory results. However, the utility of this parameter as a basis for process control is limited by a lack of knowledge concerning the relationship between effective bubble diameter and other process variables. Flow rates, solution temperature, gas distributor parameters, and concentrations of the surfactant and other constituents all affect the effective bubble diameter. Figure 3.23 shows the relationship that existed in the pilot plant between air flow rates and effective bubble diameter. The line indicates only the general tendency for bubbles to get larger at higher gas flow rates.

Laboratory Studies. — The two-step scavenging-precipitation foam-separation process^{24,25} for decontaminating ORNL low-level radioactive process waste water was successfully demonstrated on a laboratory scale with the foam-recycle option omitted. First, most of the hardness, initially 110 ppm as CaCO_3 , and most of the radiation emitters are precipitated in a suspended-bed clarifier (76 mm in inner diameter and 25 cm high) by making the water 0.005 M each in NaOH and Na_2CO_3 in the presence of 6 to 20 ppm of ferric ion coagulant. Residual soluble hardness at this point is less than 5 ppm, which is low enough to permit efficient strontium removal in the subsequent foam-separation step. Next, the almost clear supernatant is pumped to a countercurrent foam column (37 mm in inner diameter and 80 cm high, exclusive of 10-cm-ID \times 10-cm-high foam-drainage section; the foam phase in the countercurrent section was about 50 cm in height) where dodecylbenzene sulfonate surfactant is added simultaneously to the top and bottom of the column in a ratio of about 5:1 to a concentration of roughly 90 ppm. Most of the remaining radioactivity is removed in the foam generated by bubbling air through the solution. Overall decontamination factors (DF's) obtained for strontium, cobalt, ruthenium, and cerium were $>3.7 \times 10^3$, 2.3 to 4, 2 to 5, and 50 to 180 respectively. The process is also excellent for removing cesium, provided that about 60 ppm of baked (600°C for 20 min) Grundite clay is added to the water during the hardness-precipitation step. (Cesium is not removed in the

foam step.) In this way a cesium DF of 20 was achieved (Table 3.11). The height equivalent to a theoretical stage for strontium removal in the foam column was about 3 cm.

The crucial factor governing satisfactory strontium removal appears to be the regulation of gas and liquid flow rates (i.e., V and L respectively) and the average bubble diameter \bar{D} , such that the ratio $V/L\bar{D}$ will exceed 150. The $V/L\bar{D}$ for the above-mentioned demonstration runs was in the range 200 to 270, with an average bubble diameter of 0.06 to 0.08 cm. The liquid throughput was 40 to 42 gal ft⁻² hr⁻¹. The effect of the $V/L\bar{D}$ parameter on the strontium DF is shown in Fig. 3.24. These data represent flowsheet runs wherein total phosphorus concentration in the water varied from <0.1 to ~ 15 ppm, as orthophosphate, and include actual waste water as well as synthetic tap water solutions. No distinction could be made between the strontium decontamination factor data obtained with columns that were 53 and 80 cm in length. The large amount of data involved in these calculations was programmed for processing by the CDC 1604 computer.

The high-speed digital computer was also used for calculating the volume reduction factor (VR), another process variable that has direct bearing on process cost. The strontium DF, which is a function of foam density and linear velocity of the

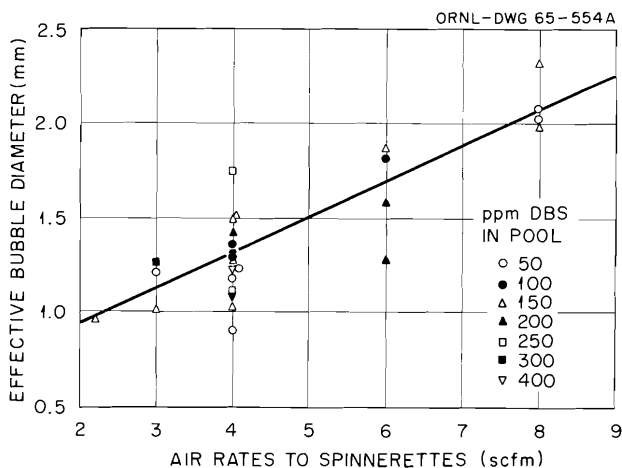


Fig. 3.23. Relationship Between the Effective Diameter of Bubbles in the 2-ft-square Countercurrent Foam-Separation Column and the Flow Rate of Air Through Nine 3-in.-diam Spinnerettes for all Pilot Plant Tests. Concentration of the surfactant DBS is included as a parameter.

²⁴Chem. Technol. Div. Ann. Progr. Rept. May 31, 1963, ORNL-3452, p. 86.

²⁵W. Davis, Jr., A. H. Kibbey, and E. Schonfeld, *Laboratory Demonstration of the Two-Step Process for Decontaminating Low-Radioactivity-Level Process Waste Water by Scavenging-Precipitation and Foam Separation*, ORNL-3811 (in preparation).

Table 3.11. Decontamination of Spiked ORNL LLW by the Foam Process

Feed: 0.005 M each NaOH and Na₂CO₃; ~60 ppm Grundite clay (~0.5 lb/10³ gal) added in one run only;

PO₄³⁻, <0.7 ppm in absence of Grundite and 2.4 ppm with Grundite present

Flows: Surfactant feed ≅ 90 to 100 ppm in foam column, added in a split stream with the ratio top/bottom = 5 to 5.5/1

Throughputs: Sludge column = 12 to 13 gal ft⁻² hr⁻¹

Foam column = 40 to 42 gal ft⁻² hr⁻¹

Bubble diameter = 0.06 to 0.08 cm

V/LD̄: With no Grundite, 273 cm⁻¹; with Grundite, 202 cm⁻¹

Component	Decontamination Factors											
	Sludge Column				Foam Column				Overall			
	With Grundite		No Grundite		With Grundite		No Grundite		With Grundite		No Grundite	
	Filtered ^a	Unfiltered ^a	Filtered	Unfiltered	Filtered ^b	Unfiltered	Filtered ^b	Unfiltered	Filtered	Unfiltered	Filtered	Unfiltered
Total												
hardness	32	6	40	<8	~1.1	~9	~1	>9	41	53	30	43
Ca	29	5	34	<8	~1.3	~9	~1	>10	39	49	27	>40
⁸⁵ Sr	20	16	70.5	42	338	212	12	13	7935	3725	630	705
¹³⁷ Cs	25	21	1.6	1.3	~1	1	1	1	21	20	1.3	1.3
⁶⁰ Co	2.5	2.9	4.5	4.1	1.3	1.1	1.1	1.0	2.4	2.3	3.5	4
¹⁰⁶ Ru	1.7	1.8	1.3	1.5	3.5	3.8	1.4	1.3	4	6	1.8	2.0
¹⁴⁴ Ce	44	24	>775	75	6.4	4.4	~2.2	1.3	280	118	>49	118.6
⁹⁵ Zr-Nb	(These activities were too low to measure)											

^aFiltered effluents are expected to give higher DF's than unfiltered effluents, owing to removal of precipitated solids; discrepancies are attributable to the standard deviations of the analytical and sampling techniques.

^bThese DF's are for soluble Ca²⁺ and total hardness ions only (no solids removal); this value is the ratio of filtered sludge effluent to filtered foam effluent analyses.

ORNL-DWG 65-9719

- COLUMN HEIGHT, 80 cm; TAP WATER, FOAM CONDENSATE RECYCLED (UNLESS INDICATED)
- COLUMN HEIGHT, 50 cm; TAP WATER; NO FOAM CONDENSATE RECYCLE
- SAME AS ABOVE EXCEPT LLW USED INSTEAD OF TAP WATER FEED
- NR NO RECYCLE OF FOAM CONDENSATE
- G GRUNDITE CLAY USED (0.5 lb/1000 gal)
- P HIGH PO_4^{3-} CONCENTRATE (5 TO 15 ppm); IN ALL OTHER CASES, 0 TO 5 ppm

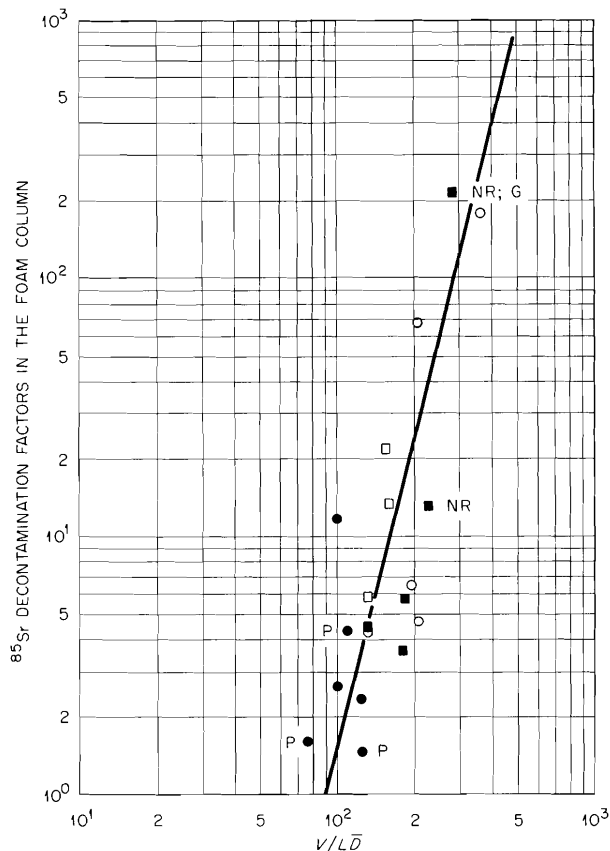


Fig. 3.24. Strontium Decontamination Factor as a Function of V/LD .

foam, varies inversely as both the VR and the foam column throughput rate, but is directly proportional to the strontium distribution coefficient (Γ/x) . Calcomp computer plots of VR vs strontium DF for various liquid throughput rates are given in Fig. 3.25 for an assumed strontium distribution coefficient of $3.4 \times 10^{-3} \text{ cm}^{-1}$.

A limited support program for the foam-separation pilot plant was also carried out. The need for a cheap, rapid method for determining the concentration of dodecylbenzene sulfonate (DBS) led to testing a methylene-blue colorimetric analytical method which uses a single chloroform extraction

of the dye-DBS complex. The few-parts-per-million concentration is read directly from the standard color wheel of a Hellige comparator. Maximum accuracy (within 10%) for the method was attained in the neighborhood of 1 ppm. The greatest error (about 50%) occurred at the still lower concentration range of 0.1 to 0.2 ppm. The method was adequate for DBS concentrations up to 2 ppm and was used for process control in the ORNL foam-separation pilot plant.

A continued search for better surfactants indicated that the purportedly more biodegradable surfactants Nacconol 40 FX (National Aniline Division, Allied Chemical Corporation) and Alipal LO 436 (General Aniline and Film Corporation) exhibit desirable physical and chemical properties under foam-separation process conditions, and are as good as the currently used DBS in effecting strontium decontamination, for example, values of $(\Gamma/x)_{\text{Sr}^{2+}}$ of the order of $1.5 \times 10^{-2} \text{ cm}$ at a surfactant concentration of 0.5 times the critical micelle concentration and at a pH of 4.

Determination of Nuclides in Solutions Containing Low Levels of Radioactivity. — One of the most difficult and expensive analyses associated with radioactive waste disposal is the determination of the amount of each of four to ten radioactive nuclides when present at the very low radioactivity levels of 10^2 to $10^5 \mu\mu\text{c/liter}$. The determination of nuclide concentrations by least-squares resolution of the gamma-ray spectra with a high-speed computer was tested and was found to provide a rapid, simple, and reasonably accurate method for these analyses at a cost of 5 to 25 times less than that for conventional methods.²⁶ The savings increase with the number of samples. The tests were made with solutions of ^{60}Co , ^{85}Sr , ^{141}Ce , and ^{144}Ce added as tracers to water containing ^{90}Sr , $^{95}\text{Zr-Nb}$, ^{106}Ru , ^{134}Cs , and ^{137}Cs . The lowest concentration of radioactivity was about one-tenth of the lowest value previously determined by this technique, that is, down to 10 counts/min. Evaporation by factors up to 20 was also evaluated for improving accuracies of analyses.

²⁶E. Schonfeld, A. H. Kibbey, and W. Davis, Jr., *Determination of Nuclide Concentrations in Solutions Containing Low Levels of Radioactivity by Least-Squares Resolutions of the Gamma-Ray Spectra*, ORNL-3744 (January 1965).

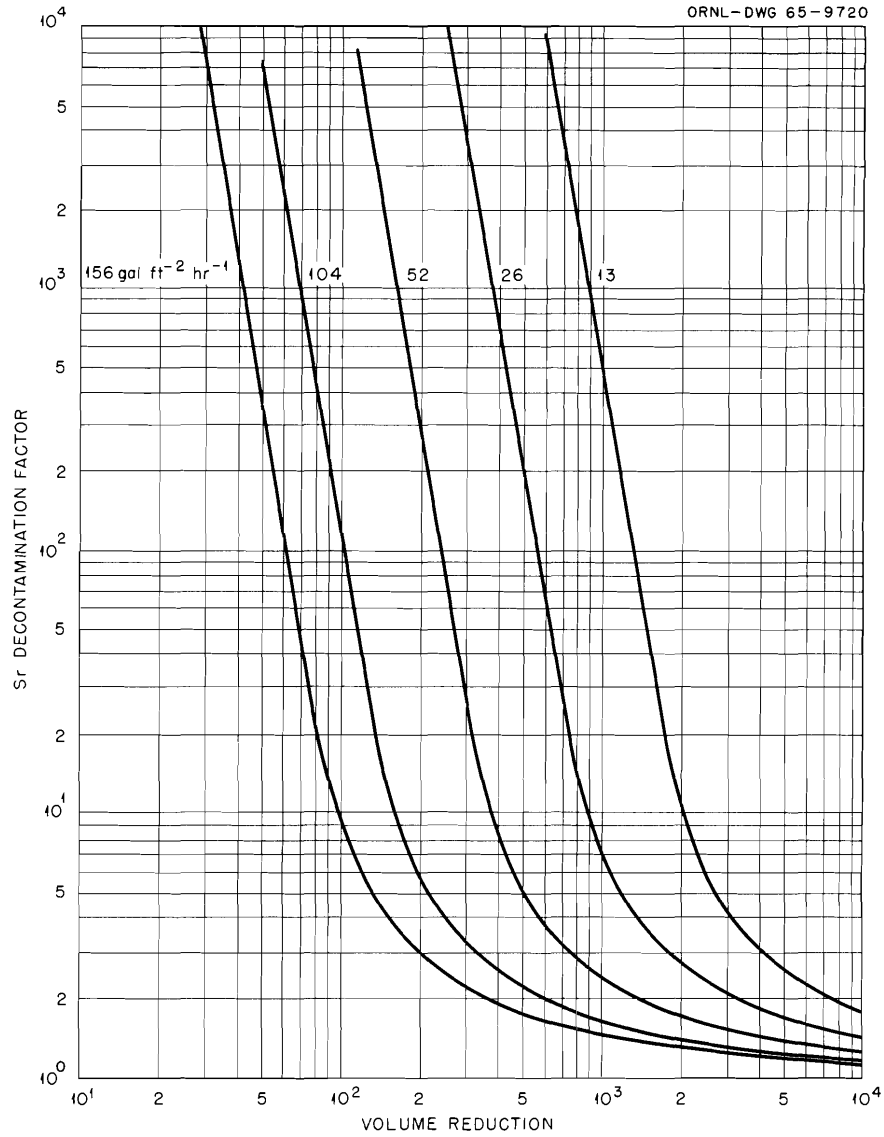


Fig. 3.25. Strontium Decontamination Factor as a Function of Volume Reduction.

For comparison, the solutions were also analyzed by standard radiochemical methods. Agreement between the two methods was excellent for ⁶⁰Co and ⁸⁵Sr for concentrations down to about 500 μμc/liter (scatter of ±5 to ±20%, Fig. 3.26). Agreement between the two methods was good for ¹³⁷Cs at activities down to 3000 to 4000 μμc/liter. More dilute solutions were successfully analyzed only if they were first concentrated by evaporation. The method is not recommended for determination of ¹⁰⁶Ru at activities below 1000 to 2000 μμc/liter, unless this nuclide constitutes a major fraction

of the total activity and if ⁸⁵Sr is a minor component.

Water-Recycle Process

The objective in developing a water-recycle process is to provide a water-treatment system to treat low-level radioactive waste with a low salt content and to return deionized, well-decontaminated water to the system, thus providing a closed circuit. Fresh water would be demineralized before introduction into the circuit (Fig. 3.27).

Status and Progress. — So far, the prospects look very promising. The process, still in the laboratory stage of development, has provided decontamination factors (DF's) ranging from 100 to 10,000 using low-level radioactive waste water (LLW) (in the hundreds for ^{144}Ce , ^{131}I , ^{106}Ru , ^{125}Sb , and $^{95}\text{Zr-Nb}$; in the thousands for ^{137}Cs and ^{90}Sr ; and in the ten-thousand range for ^{60}Co

and total rare earths). The DF's for ^{106}Ru and ^{60}Co were 10 to 1000 times as high as previous values obtained in the ORNL development program.

Next, the process will be tested in a micro pilot plant with water that simulates recycled process water; that is, it will represent water that has been demineralized and then contaminated through plant use. The results will be used to predict LLW processing costs in full-scale plants. In the past, micro pilot plant results have been largely confirmed in large-scale pilot plant tests.

Experimental Work and Results. — In its present state, the process consists in zeta-potential-controlled (ZP) batch clarification, cation-anion exchange, and sorption by granular activated carbon (Fig. 3.28). Detailed studies are being made of coagulants and coagulant aids that will produce optimum clarification for a continuous operation.

The best clarification (jar tests) was obtained when the water was made 20 to 30 ppm in $\text{Al}_2(\text{SO}_4)_3$ and 0.5 ppm in SiO_2 , in that order (Fig. 3.29). Here, the average ZP of the suspended solids in the waste changed from its original -14 to $+2.5$ mv. There were only 20 particles per cm^2 of membrane filter area per ml of clarified waste, contrasted to 300 for the raw waste.

Demineralization capacity (0.1% of ionic breakthrough as measured by specific conductance) with mixed-bed ion exchange (Dowex 50W—

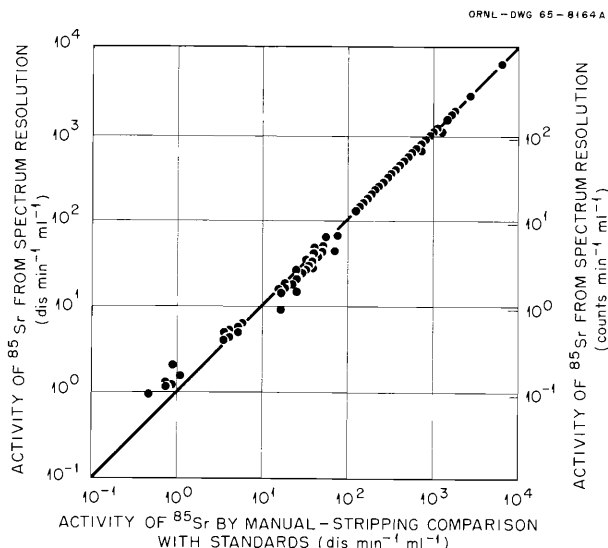


Fig. 3.26. Comparison of Two Methods for Estimating the ^{85}Sr Content of a Solution.

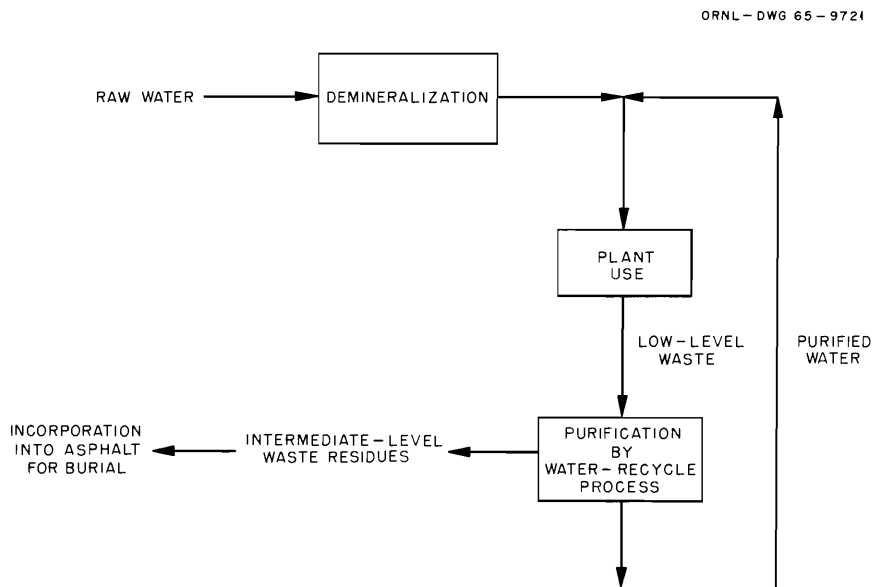


Fig. 3.27. Water-Recycle Flowsheet.

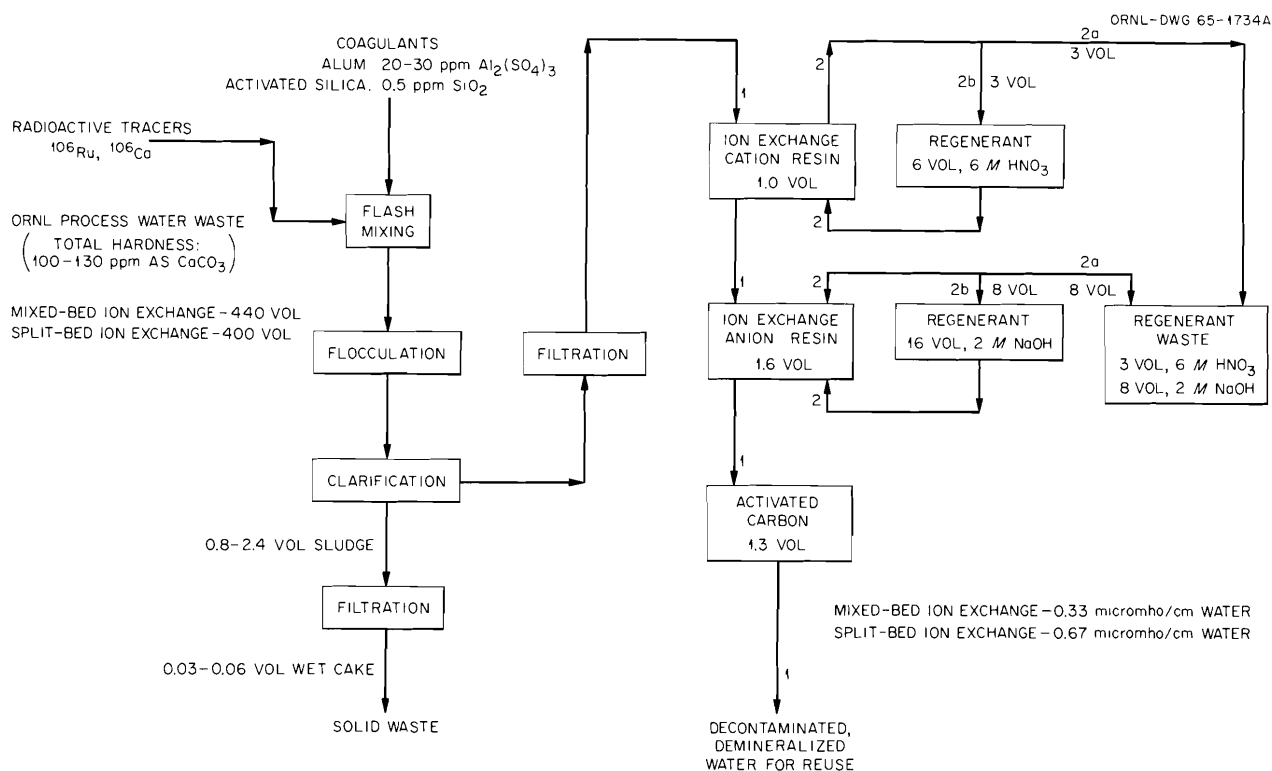


Fig. 3.28. Simulated Water-Recycle Flowsheet - Laboratory Development Using ORNL Low-Level Waste.

Dowex 1) was about 470 bed volumes of clarified LLW (total hardness: 100 to 130 ppm as CaCO_3) per bed volume (BV) of cation resin; with ORNL tap water, 560 BV's. Thus, in the case of ORNL waste, the salt content of the water was increased by about 20% during plant use, producing a corresponding 20% decrease in demineralization capacity. Hence, an increase in demineralization capacity to 2500 BV's would be predicted when treating low-level waste that contained only the salts added through plant use (Fig. 3.27). As expected, the use of separate cation and anion exchange columns yielded a capacity equal to about 90% of that for a mixed-bed column and resulted in a lower-quality (but still satisfactory) product water (0.67 micromho/cm, compared with 0.33 for the mixed-bed exchanger). Economically, separate beds may be desirable because regeneration is easier.

The overall DF's achieved with the present system ranged from 10^2 to 10^4 (Table 3.12). A large part of the DF's were obtained by clarification and ion exchange only. Significantly more

^{60}Co was removed when a column of activated carbon formed a part of the system. As expected, ion exchange alone removed most of the ^{137}Cs and ^{90}Sr . Specific conductance can be used as a simple indicator of bed exhaustion because ionic breakthrough precedes breakthrough of the radioelements (Fig. 3.30).

With separate beds, the cation column was regenerated with 6 BV's of 6 M HNO_3 , leaving only 0.1% of the radioelements on the resin. Regeneration of the anion column was not so efficient: 10 BV's of 2 M NaOH left 1% behind. Other regenerants may be needed.

To adapt the process to continuous operation, a study is being made of coagulant aids for improving the settling properties of the light alum floc. The change in the mutually repelling forces related to the ZP of the suspensoids appears to be an important criterion, since the neutralization of these forces is essential to achieving optimum coagulation and clarification.²⁷ The effects of

²⁷T. M. Riddick, *Tappi*, 47, 171 (1964).

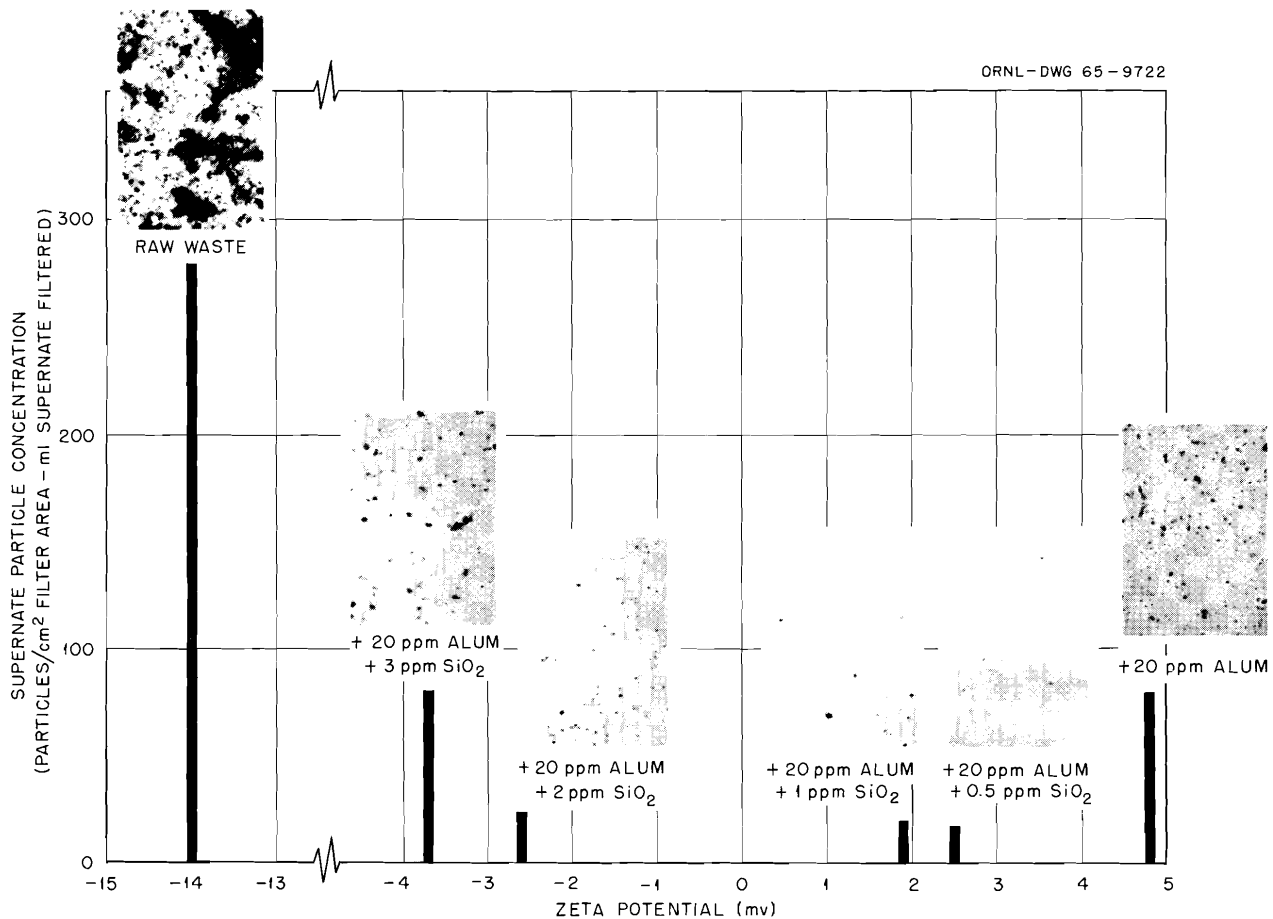


Fig. 3.29. Solids Filtered Out of Treated Waste Supernatant onto a Membrane Filter at a Zeta Potential of +2.5 mv. Jar-test conditions: 30 min of flocculation followed by 30 min of settling.

some coagulant aids on the ZP are summarized below:

1. Alum neutralizes the normally negative ZP of LLW (usually ranging from -12 to -18 mv). Sufficient alum (and other coagulant aids) should be added to bring the ZP to zero, with a tolerance of ± 5 mv.²⁷
2. Grundite clay gives bulk to the light alum floc and slightly decreases the amount of alum subsequently needed to attain zero ZP. The ZP of Grundite clay in tap water was about -10.8 mv, which is less negative than the average ZP of the suspensoids in LLW. Also, Grundite clay sorbs cesium selectively.²⁸

3. Activated silica, which can be added to toughen the fragile alum floc, increases the amount of alum needed to attain zero ZP. The ZP of activated silica in tap water is about -15 mv, which is about the same as that for the suspensoids in LLW.
4. An organic polyelectrolyte such as Primafloc C-3 (Rohm and Haas Company, Philadelphia, Pa.), which can be added during the flocculation step to assist in agglomerating the floc, produces greater changes in ZP upon small additions to the waste than those produced by inorganic coagulants such as alum. Only 0.5 ppm of Primafloc C-3 shifted the ZP from about -6 to +3 mv.

²⁸Chem. Technol. Div. Ann. Progr. Rept. May 31, 1964, ORNL-3627, p. 95.

Table 3.12. Decontamination Factors Obtained in the Water-Recycle Process Using ORNL Process Waste
Overall DF's of 10^2 to 10^4

	Individual Isotopes								Total Rare Earths	Gross Gamma	Gross Beta	Bulk Ions (Specific Conductance)
	^{144}Ce	^{60}Co	^{137}Cs	^{131}I	^{106}Ru	^{125}Sb	^{90}Sr	^{95}Zr - ^{95}Nb				
	Raw waste analysis, dis min^{-1} ml^{-1} or counts min^{-1} ml^{-1}											
Process 1 ^a	11.3	136	12.2	^b	25.4	0.8	29.1	1.2	15.1	77	52	330 ^c
Process 2 ^d	10.1	70.9	23.6	126.2	44.2	3.5	52.0	0.4	32.0	52	85	290 ^c
	Overall decontamination factors											
Process 1 ^a	150	6500	370	^b	200	20 ^e	1500	45 ^e	1500	390	870	1000
Process 2 ^d	340	12,000	2600	430	200	300	6300	160 ^e	11,000	130	1200	500

^aAlum-silica clarification, mixed-bed ion exchange, coconut-shell activated carbon. DF Values for 0.1% specific-conductance breakthrough.

^bNot determined.

^cThe dimensions of specific conductance are micromhos/cm.

^dAlum-silica clarification, separate-bed ion exchange, bituminous coal activated carbon. DF Values for 0.2% specific-conductance breakthrough.

^eThese are minimum values, since the radioactivity in the waste water was reduced to the analytical limits of detection (background).

Selective Sorption of Phosphates on Activated Alumina

The economical operation of the Scavenging-Precipitation Ion Exchange process depends on keeping the concentration of phosphates in the feed water below about 1 ppm.^{29,30} Sorption of these phosphates on a column of activated alumina as a first step in the process ensures complete precipitation of the hardness ions in the scavenging step.²⁹ Recent work, reported below, shows that Alcoa F-1 activated alumina is the cheapest and most useful sorbent.³¹

²⁹*Ibid.*, p. 93-95.

³⁰R. R. Holcomb, *Low-Radioactive-Level Waste Treatment. Part 1. Laboratory Development of a Scavenging-Precipitation Ion-Exchange Process for Decontamination of Process Water Waste*, ORNL-3322 (June 25, 1963); R. E. Brooksbank *et al.*, *Low-Radioactive-Level Waste Treatment. Part 2. Pilot Plant Demonstration of the Removal of Activity from Low-Level Process Wastes by a Scavenging-Precipitation Ion-Exchange Process*, ORNL-3349 (May 13, 1963).

³¹W. C. Yee, *The Selective Removal of Mixed Phosphates from Water Streams by Activated Alumina*, ORNL-TM-1135 (in press).

This study can lead to a broader application: the removal of phosphate from water at city water-treatment plants. For example, household cleaning formulations soon will no longer contain practically indestructible detergents, but many will still contain the phosphate builders. These builders promote increased biological activity that in turn results in unpleasant taste and odor.³² Also, phosphates complicate water clarification and softening.³³⁻³⁵

Experimental Work and Results. - The preferred process calls for downflow of the feed water through a column of the activated alumina. How-

³²F. W. Gilcreas, "Synthetic Detergents and Water Quality," *Water Works and Waste Engineering* **2**, 66 (1965).

³³R. S. Smith, J. M. Cohen, and G. Walton, "Effects of Synthetic Detergents on Water Coagulation," *J. AWWA* **48**, 55 (1956).

³⁴J. J. Morgen and R. S. Engelbrecht, "Effects of Phosphates on Coagulation and Sedimentation of Turbid Waters," *J. AWWA* **52**, 1303 (1960).

³⁵J. F. Malina, Jr., and S. Tiyaporn, "Effects of Synthetic Detergents on Lime-Soda Ash Treatment," *J. AWWA* **56**, 727 (1964).

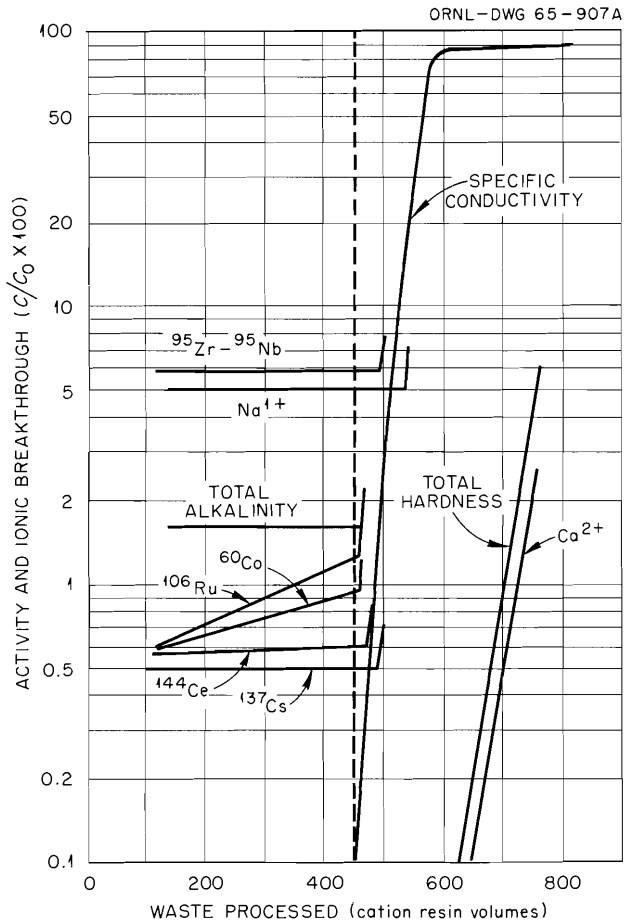


Fig. 3.30. Breakthrough of Bulk Ions and Radionuclides. Specific-conductance measurements signal imminent breakthrough of radionuclides because bulk ions break through first.

ever, if column plugging from suspended solids becomes a problem, then the less-efficient method of upflow through a fluidized bed can be used. The column can be regenerated with NaOH and HNO₃ solutions, in that order.

In downflow operation with tap-water solutions containing 5 ppm of phosphates (expressed as PO₄³⁻), more than 99% of NaH₂PO₄ was removed from 3000 bed volumes (BV) by Alcoa F-1 alumina (surface area, 250 m²/g), while the same percentage of Na₄P₂O₇, Na₅P₃O₁₀, and (NaPO₃)_{8.4} was removed from 4000 to 5000 BV's (Fig. 3.31).

Upflow operation in a fluidized bed was less efficient. In upflow operation with actual process water that contained an average of 1 ppm of mixed phosphates and suspended solids, only

80% of the phosphates was removed initially (Fig. 3.32). Apparently, saturation capacity had not been reached after almost 40,000 BV's of water had passed through the column. Although complete breakthrough was evident at 33,000 BV's, phosphate sorption resumed. It is possible that the composition of the process water had changed to a higher proportion of those forms of phosphate for which the bed has a higher capacity than for the ortho form (Table 3.13).

In a similar upflow test but with Alcoa H-51 alumina (surface area, 400 m²/g), the maximum breakthrough was 75% at 33,000 BV's, and 100% breakthrough was not reached (Fig. 3.32).

The column is regenerated by first passing 1 M NaOH through it to elute the phosphates, rinsing with water, passing 1 M HNO₃ through to restore the alumina to the acid form, and finally rinsing with water.³¹ The regenerating solutions and washes result in a volume equal to 12 BV's (Fig. 3.33). This leads to a favorable volume reduction factor (BV of product water per BV of regenerant waste) of about 2000. This value is based on a 1-ppm concentration of phosphates in the feed. A volume reduction factor of 20 is con-

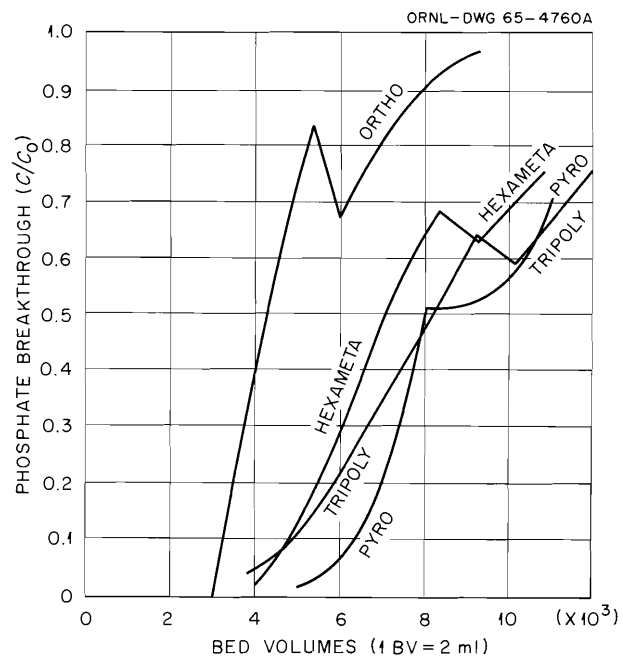


Fig. 3.31. Phosphate Sorption on Alcoa F-1 Activated Alumina. The alumina has a lower capacity for ortho-phosphate than for its dehydrated forms.

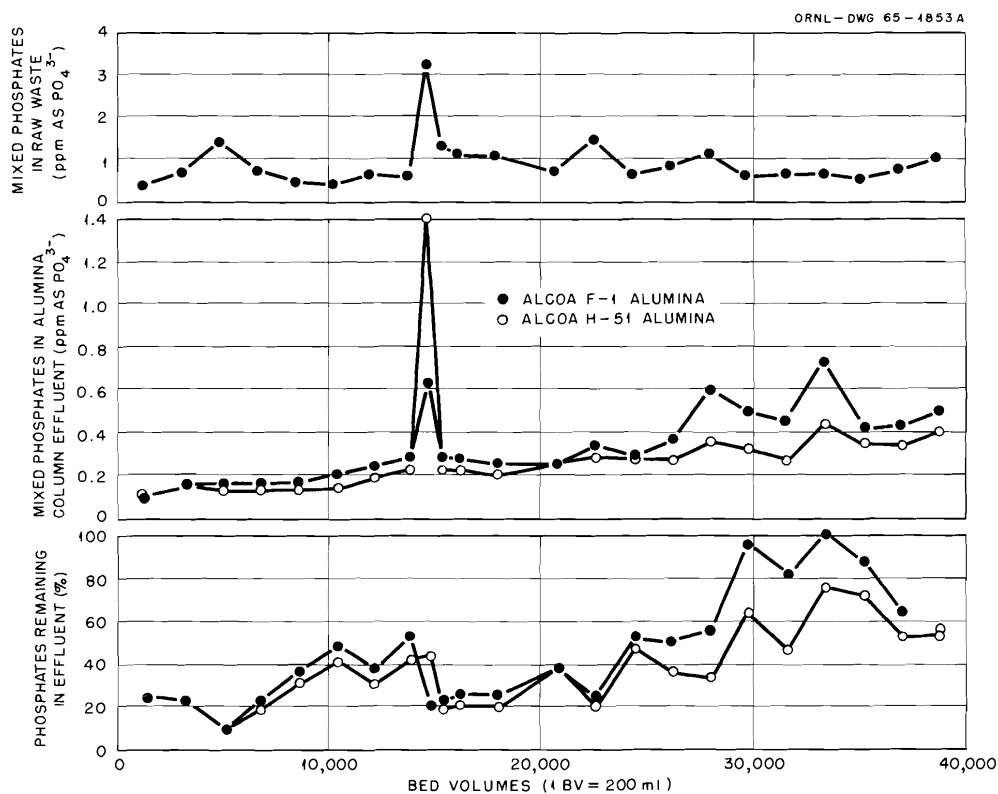


Fig. 3.32. Alumina Sorption of Mixed Phosphates Contained in Raw Low-Level Radioactive Waste Water by Upflow Through a Fluidized Bed.

Table 3.13. Comparison of the Capacities of the Individual Phosphates on Alcoa F-1 Activated Alumina with the Amount of Mixed Phosphates Sorbed from Low-Level Waste (LLW) by Upflow Through a Fluidized Bed of F-1 Material

Form of Phosphate	Feed Solution Concentration (ppm as PO_4^{3-})	Mode of Operation	Maximum Volume of Feed Solution Used Equivalent Volume		Phosphate Capacity ($\frac{\text{mg as } \text{PO}_4}{\text{g F-1 Alumina}}$)
			Actual Volume (BV's)	If Only 1 ppm of Phosphate (BV's)	
Ortho, NaH_2PO_4	5	Packed bed, downflow 2 min residence time	9,500	47,500	9
Pyro, $\text{Na}_4\text{P}_2\text{O}_7$	5	Same	11,000	55,000	> 30
Tripoly, $\text{Na}_5\text{P}_3\text{O}_{10}$	5	Same	12,000	60,000	> 30
Hexameta, $(\text{NaPO}_3)_{8.4(\text{av})}$	5	Same	11,000	55,000	> 25
Mixed phosphates in LLW	1(av)	Fluidized bed, upflow 2 min residence time	40,000	40,000	20

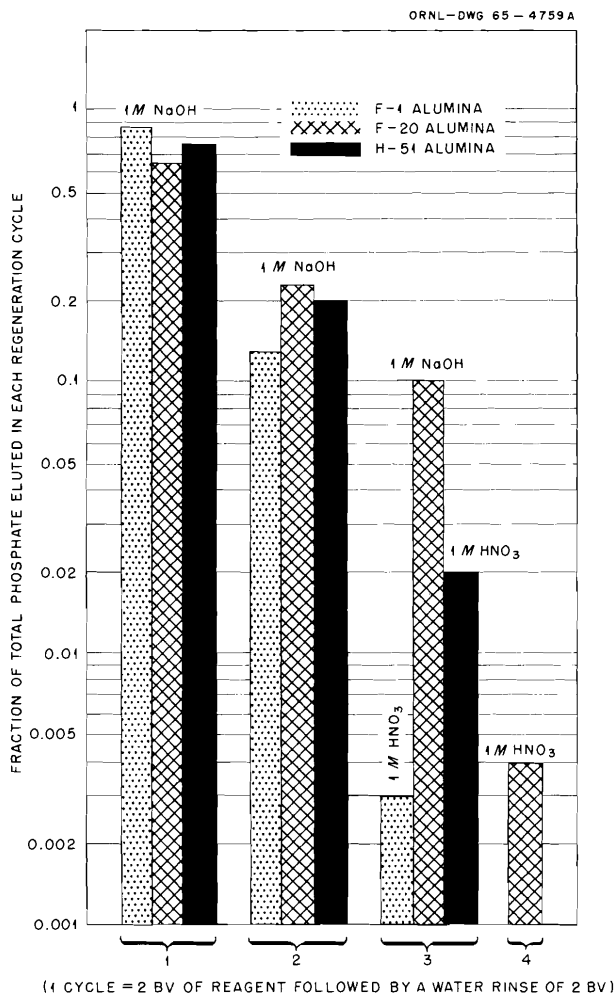


Fig. 3.33. Regeneration of Three Grades of Activated Alumina. Two cycles of 1 M NaOH and one of 1 M HNO₃ were sufficient to regenerate the F-1 and the H-51 alumina.

sidered the minimum, according to water-treatment workers.³⁶

A summary of the costs, surface areas, etc., of the aluminas tested is given in Table 3.14.

3.4 ENGINEERING, ECONOMIC, AND SAFETY EVALUATION

Although it is believed that the most responsible method of managing very radioactive liquid wastes

³⁶Personal communication from D. G. Stephan, Advanced Water Treatment Program, Robert A. Taft Sanitary Engineering Center, Cincinnati, Ohio.

Table 3.14. Alumina Evaluation for Sorption of Mixed Phosphates from Raw Low-Level Radioactive Waste

Conditions: Upflow through a fluidized bed

	Grade of Alumina ^a		
	Alcoa F-1	Alcoa ^b F-20	Alcoa H-51
Cost, ¢/lb	12	100	40
Surface area, m ² /g	250	250	400
Sorption capacity for mixed phosphates, mg as PO ₄ ³⁻ per g of alumina	19	17	>27
Mixed phosphates eluted, during regeneration, mg as PO ₄ ³⁻ per g of alumina	17	10	28
Regeneration-regenerant waste, bed volumes	12	16	12
Amount of alumina dissolved during regeneration, % of original alumina	8	5	35

^aProducts of the Aluminum Company of America, Pittsburgh, Pa.

^bPreviously studied (see ref 31).

from the processing of power reactor fuels will consist in converting them to solids and disposing of them permanently in salt mines, a possible alternative is long-term storage as liquids in tanks. As estimates of total fuel-cycle costs for advanced reactor concepts decline from previous highs of several mills/kwhr (electrical) to less than 1 mill/kwhr (electrical), the cost of about 0.03 mill/kwhr (electrical) allocated to waste management becomes increasingly significant. For these reasons, as well as for the purpose of establishing a basis for comparison of the costs of alternate waste management schemes, a detailed estimate of the costs of "perpetual" tank storage of wastes is being undertaken.

The basis of the study, the conceptual design of the tank farm, and the capital costs that have been developed are summarized below. Detailed cost data are being assembled for use in a computer code that calculates total storage costs as a function of tank size for a given filling rate,

life expectancy of the tank, interest on capital, and return on investment.

Basis of Study

As a basis for this study, a fuel processing plant having a nominal capacity of six tons of fuel per day is assumed, handling the fuel from an installed capacity of 22,400 electrical megawatts (70,000 thermal megawatts). The plant processes 1500 tons/year of uranium converter fuels irradiated to 10,000 Mwd/ton and 270 tons/year of thorium converter fuel irradiated to 20,000 Mwd/ton. Of the uranium converter fuels, 918 tons/year are clad with 0.025-in.-thick Zircaloy, and 582 tons/year are clad with 0.015-in.-thick stainless steel.

In processing these fuels 120 days after discharge from the reactors, wastes of two general categories are produced, each requiring essentially permanent containment (Table 3.15). Cladding wastes, consisting of Zirflex (from Zircaloy dissolution) and Sulfex (from stainless steel dissolution) wastes, are so corrosive to ordinary structural

materials that they are neutralized for storage. It is assumed that 0.1% of the gross fission products and 50% of the ^{137}Cs appear in these wastes, together with induced $^{95}\text{Zr-Nb}$ and ^{60}Co activity. They are stored separately in million-gallon tanks, the largest possible without requiring mechanical means for removing the decay heat. Purex and Thorex high-radioactivity solvent extraction raffinate wastes are combined and stored in tanks equipped with submerged cooling coils. Storage of the raffinates under both acid and alkaline conditions is considered.

It is assumed that the wastes are produced continuously and are accumulated in a tank farm during 20 years of plant operation. At the end of this accumulation period, the tank farm containing 4,080,000 gal of highly radioactive acid waste, or 24,480,000 gal of highly radioactive alkaline waste, and 65,800,000 gal of alkaline cladding wastes, is maintained for "perpetual" containment. During the 20 years of waste accumulation, the total fission product heat generation rate in the tank farm rises to 1.03×10^8 Btu/hr. Assuming no further accumulation after that time, the rate

Table 3.15. Characteristics of Wastes

	Cladding Wastes		Raffinates	
	Zirflex	Sulfex	Purex	Thorex
Volume, gal per kg of fuel				
Acid	1.7	1.34	100	200
Neutralized	1.8	2.0	600	1200
Production rate, gal/year				
Acid	2×10^6	7.8×10^5	150,000	54,000
Neutralized	2.15×10^6	1.14×10^6	900,000	324,000
Radioactivity after 120 days of decay, curies/gal				
Acid	38	28	37,000	37,000
Neutralized	36	19	6,200	6,200
Heat generation rate after 120 days of decay, Btu hr ⁻¹ gal ⁻¹				
Acid	0.42	0.3	433	433
Neutralized	0.4	0.2	72	72

drops by a factor of 4 over the next ten years, and decreases to insignificant levels over the next two to three centuries.

Description of Facility

After the desired adjustments of volume and acidity or alkalinity have been made in the fuel processing plant, the wastes are transferred through concrete-encased stainless steel pipes to a tank farm for long-term storage. In the design and operation of this tank farm, considerations of safety took precedence over any potential savings in cost. Figure 3.34 is a conceptual layout of a "completed" tank farm, containing a 20-year accumulation of waste. The farm is divided into two areas, one containing tanks of high-level radioactive waste and their associated cooling and ventilation facilities, and the other containing tanks of cladding wastes. In this farm the high-level radioactive wastes are stored as acid solutions in million-gallon tanks grouped around three sides of an operations building containing many of the major equipment items of the cooling and ventilation systems. A cooling tower and pumps, an emergency water storage tank, a water surge tank, and a stack and fans are also located in this

waste area. The cladding waste are stored in alkaline form in tanks of about 1.1-million-gallon capacity. Cooling is not provided for these wastes; each tank is ventilated individually through a filter at the surface. In addition to filled tanks, an empty tank in each area is always maintained on standby to receive the contents of any tank which may have failed.

The tanks are similar in design to those in use at the Savannah River Plant. They are cylinders having a diameter-to-height ratio of 3, are made of 1/2- to 1-in.-thick steel plate, and are housed in steel-lined concrete vaults with walls 3 to 3½ ft thick, buried under about 10 ft of earth. Stainless steel is used to contain acid wastes; carbon steel is used for alkaline wastes. The tanks are constructed in accordance with the ASME code for unfired pressure vessels, and all welds are completely radiographed. As to the mild steel tanks, the welds are stress-relieved by heating at 1000°F for 1 hr.

Heated air is circulated through the annular space between the tank and vault for dehumidification. The occurrence and severity of leaks are determined by monitoring for both liquid and airborne radioactivity in the annulus. The tanks have steel-lined interval columns for support, and, for storing highly radioactive waste, they

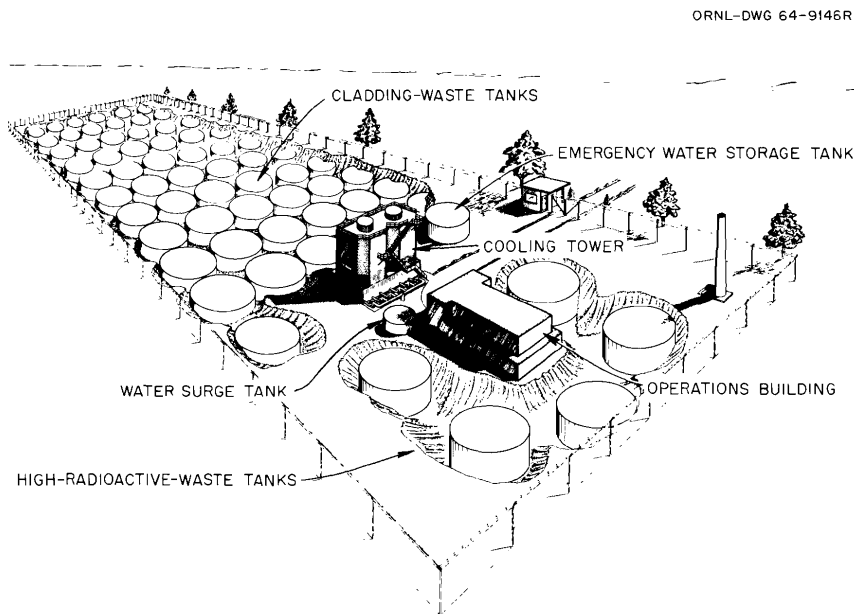


Fig. 3.34. Layout of Tank Farm for Storing Waste.

are equipped with cooling coils which serve as the primary means for removal of radioactive decay heat. A water-cooled condenser located in the operations building serves as the secondary means for heat removal, and steam produced from self-boiling wastes during emergencies is vented to this condenser through a 4-ft-diam off-gas header in the top of the tank. Air, which during normal operation is swept through the vapor space in the tanks at a rate of about 600 cfm to remove radiolytic hydrogen, is likewise vented through the off-gas header to fibrous glass filters and a 50-ft-high stack. Instruments are provided to measure and record the temperature, density, and liquid level of the tank contents, the concentration of hydrogen in the vapor space above the liquid, the pressure inside the tank, and to detect the presence of liquid and radionuclides in the annulus. The tanks are also provided with access holes for introducing sluicing jets and pumps for removing the wastes when this becomes desirable.

Since heat losses by conduction to the surroundings from tanks with these design features are relatively insignificant (7 to 8 Btu hr⁻¹ ft⁻² tank surface),³⁷ facilities for removal of the heat must be provided over the period of time (from 70 to 200 years) required for the heat generation rate in a tank to decrease to about 10⁵ Btu/hr. In all cases, several tank lifetimes are probably represented. In this study a cooling system was designed for the first 20 years of tank farm operation, and, when the wastes are transferred to new tanks from old or defective ones, smaller cooling systems designed to handle the heat loads at those times will be provided.

The tank contents are maintained at 140°F by circulation of water through vertical and horizontal coils submerged in the waste. To keep the pressure drop inside the coils at an acceptable level as well as to provide versatility of operation, the coils in each tank are arranged in banks of 1420-ft lengths of 3-in. sched-40 pipe. Each bank is connected to the water supply and discharge headers through valves that allow it to be placed in service or removed, as required.

The water from the coils is passed through external heat exchangers where the heat is transferred

to a secondary water cooling circuit, and then recycled through a 250,000-gal surge tank (500,000 gal for an alkaline tank farm) to the tank coils. Thirteen heat exchangers and one spare are provided, each with a rated heat duty of 9×10^6 Btu/hr. They are of the shell and tube type, with external dimensions about 5 ft in diameter and 18 ft long, and with 2000 ft² of heat-exchange area. Thirteen centrifugal pumps are provided for water circulation in this circuit, each with a rating of 600 gpm at 150 ft of water head.

The concentration of ionic impurities in the water of the tank coil circuit is maintained at about 1 ppm by passing a 100-gpm sidestream through a double-bed demineralizer system.

Heat is removed from the secondary circuit by passing the water through an induced-draft cooling tower before circulating it to the heat exchangers. The cooling tower is rated at 1.0×10^8 Btu/hr at a wet-bulb temperature of 75°F. Cooling water is circulated at a maximum rate of 20,000 gpm by five pumps (plus one spare), each capable of delivering 4000 gpm at 113 ft of water head.

In the event of a shutdown of the primary cooling system, the wastes in storage would self-heat to their boiling point over a period of ten or more hours. When the water boils, the heat is removed by condensation of the vapor in a water-cooled surface condenser located in the operations building. This condenser is sized to handle the maximum heat load of the tank farm, 1.0×10^8 Btu/hr, has dimensions 6 ft by 30 ft, and has a heat transfer area of 3000 ft². Cooling water for the condenser is supplied at a rate of 9000 gpm from the cooling water circuit and a 2-million-gallon emergency water storage tank, if necessary. The condensate is collected in a 50,000-gal tank adjacent to the condenser, and is pumped back to the storage tanks to maintain the proper waste volumes and concentrations. A 1500-kw Diesel-powered electrical power plant is also provided on-site for emergency use.

As to the acid-waste tank farms, all equipment and piping in the tank coil cooling circuit and in the emergency condenser circuit are made of type 304L stainless steel. All equipment and piping in the cooling tower circuit are made of carbon steel. In the alkaline-waste tank farms, both the cooling coil and cooling tower circuits are made of carbon steel; however, the emergency condenser circuit is made of stainless steel.

³⁷J. I. Stevens, "Treatment, Processing and Future Disposal of Radioactive Wastes at the Idaho Chemical Processing Plant," pp. 483-508 in *Disposal of Radioactive Wastes*, vol. 1, IAEA, Vienna (1960).

Table 3.16. Summary of Capital Costs^a for Storage of Power Reactor Wastes

	Number of Tanks	Size of Tanks (gal)	Costs (thousands of dollars)								Unit Costs		
			Outside Facilities	Outside Services	Operations Building	Process Equipment and Piping	Tanks	Subtotal	Engineering	Contingency	Total	\$ /gal of Net Storage Capacity ^b	mills/kwhr (electrical) ^c
High-level waste storage													
Acid waste storage	3	2×10^6	1400	460	1041	1444	12,000	16,345	2212	2784	21,341	5.34	0.0068
	4	1.6×10^6	1400	653	1041	1551	13,734	18,379	2276	3098	23,753	4.95	0.0076
	5	10^6	1400	735	1041	1616	13,486	18,278	2148	3064	23,490	5.87	0.0075
	8	6×10^5	1400	788	1041	1945	17,430	22,604	2389	3749	28,742	6.84	0.0092
	21	2×10^5	1400	2707	1041	2687	29,251	37,086	3473	6087	46,643	11.66	0.0149
Alkaline waste storage	6	4.8×10^6	1400	527	1041	1132	17,426	21,526	2358	3583	27,467	1.15	0.0088
	9	3.2×10^6	1400	677	1041	1059	19,244	23,421	2359	3867	29,647	1.16	0.0095
	13	2×10^6	1400	921	1041	1183	19,752	24,297	2338	3995	30,630	1.28	0.0098
	21	1.2×10^6	1400	1425	1041	1411	22,401	27,678	2552	4535	34,765	1.45	0.0111
	31	8×10^5	1400	2092	1041	1622	24,949	31,104	2814	5088	39,006	1.63	0.0124
	61	4×10^5	1400	2473	1041	2053	33,337	40,304	3477	6567	50,348	2.10	0.0161
Cladding waste storage	61	1.1×10^6		969			42,952	43,921	2363	6943	53,227	0.81	0.0170

^aNumbers represent initial costs only. They do not include replacement costs.

^bNet storage capacities are total capacities less the capacity of one "spare tank."

^cBased on assumed generation of 3.14×10^{12} kwhr of electricity over 20 years.

Capital Costs

Capital costs of tank farms with tanks varying in size from 200,000 to 2,000,000 gal for acid raffinate waste, and from 400,000 to 4,800,000 gal for alkaline raffinate waste, are summarized in Table 3.16. For cladding wastes the costs were estimated for the single case of storage in alkaline form in 1.1-million-gallon tanks. In every case a spare tank was included. These costs consist only of the initial costs and contain no provision for replacement. The total costs for tank farms to store highly radioactive acid wastes range from about \$21 million to \$47 million, and for alkaline raffinate waste from about \$27 million

to \$50 million. The corresponding cost per gallon of storage capacity varied from about \$5 to \$12 for acid waste and from about \$1 to \$2 for alkaline waste. The range in units of mills per kwhr of electricity produced, based on 20 years of generation, was 0.007 to 0.015 and 0.009 to 0.016 respectively. The capital cost for cladding wastes was \$53 million, corresponding to 81¢/gal and 0.017 mill/kwhr.

A detailed breakdown of these costs is being incorporated in a computer code where they will be used with allowances for operation, maintenance, amortization, and tank replacement to calculate total present-worth costs for "perpetual" storage.

4. Transuranium Element Processing

The Transuranium Processing Plant (TRU) and the High Flux Isotope Reactor (HFIR) are being built at ORNL to provide gram quantities of many of the transuranium elements and milligram quantities of some of the transcalifornium isotopes. These radioisotopes will be used in research work by laboratories throughout the country.

It may be useful to briefly summarize the entire program. Long-term irradiation of two 10-kg batches of ^{239}Pu in a Savannah River Laboratory (SRL) production reactor has produced about 1000 g of ^{242}Pu and 300 g each of ^{243}Am and ^{244}Cm . Following purification, these materials are to be further irradiated, after which the transcurium elements will be recovered as products and the residual plutonium and curium isotopes returned for additional irradiation. The original plans were for all the additional irradiation to be done in the HFIR, but within the past year the AEC decided to accelerate production by continuing the irradiation of a portion of the feed material in an SRL production reactor prior to operation of the HFIR. Over a six-month period which started in February 1965, this reactor will be operated at a thermal-neutron flux exceeding 2×10^{15} , utilizing a special fuel loading to achieve this very high flux. About 525 g of ^{242}Pu is being irradiated in three target forms: (1) six prototype HFIR targets containing 10 g each; (2) 18 actual HFIR target rods, also containing 10 g; and (3) the remainder in special slugs made at SRL. The remaining ^{242}Pu has been retained for the initial targets for the HFIR. From the SRL irradiation program, nearly 10 mg of californium will be produced, and the first milligram is scheduled to be recovered in the Curium Recovery Facility, starting in December 1965. The remainder will be processed in the TRU following startup early in 1966.

Chemical processes are being developed and tested at high activity levels, and equipment is

being designed to make target rods, dissolve and recover transuranium elements from the irradiated targets, and then prepare and ship the recovered products to customers. This report summarizes the development of the flowsheets and equipment required for these operations and progress in construction of the TRU. Development of the procedures for making the targets is under the direction of the Metals and Ceramics Division and is not reported here. Corrosion studies being done in the Reactor Chemistry Division are also reported elsewhere.

As to the Curium Recovery Facility (CRF), it has been completed and is being used to test transuranium process chemistry at full-scale activity levels, to recover multigram amounts of ^{243}Am and ^{244}Cm for incorporation into HFIR targets, and to purify gram amounts of ^{242}Cm and ^{244}Cm for use in thermoelectric converters (see Chap. 5). This facility was installed in cells 3 and 4 of the High Level Chemical Development Facility, Building 4507. The cell 4 complex is used for solvent extraction processing, and the cell 3 complex is used to obtain additional decontamination of ^{243}Am - ^{244}Cm by LiCl anion exchange and to separate ^{243}Am from ^{244}Cm by carbonate precipitation.

4.1 DEVELOPMENT OF CHEMICAL PROCESSES

Development of the chemical processes has continued for both the preparation of oxides for HFIR target feed material and the heavy-element separations. About 300 g of ^{243}Am and 300 g of ^{244}Cm , along with the associated rare-earth fission products, were recovered from the raffinate of the plutonium recovery step at Savannah River Laboratory and transferred as a nitrate solution to the CRF at ORNL. This material is presently

being processed for americium-curium recovery. In this processing, americium, curium, and rare earths are concentrated and converted to a chloride solution by the Clanex process, and the actinides are then isolated from lanthanides and other fission products by the Tramex process. The purified ^{242}Pu , ^{243}Am , and ^{244}Cm will be converted to dense oxide in the particle size range of 20 to 200 μ , made into targets by the Metals and Ceramics Division, and irradiated in the HFIR for 12 to 18 months. Plutonium targets are made in an unshielded glove-box line, while americium and curium targets can be produced only after the remote equipment is operable in the TRU.

The main-line HFIR-target processing method consists in dissolving the target in hydrochloric acid; separating the actinides from fission products and aluminum by the Tramex process; separating the transcurium elements from americium and curium by phosphonate extraction from dilute hydrochloric acid; separating berkelium from californium, einsteinium, and fermium by dialkyl phosphate extraction of Bk(IV) from concentrated nitric acid; and isolating californium, einsteinium, and fermium by chromatographic elution from a cation exchange resin.

Status and Progress

During the past year Clanex and Tramex processing was demonstrated at full-scale radioactivity levels in the CRF. This work, as well as laboratory support given to CRF processing, is reported in the Curium Processing section (Chap. 5). The developing and testing of techniques for intra-actinide separations by ion exchange were continued; additional ^{242}Pu was converted to dense oxide and incorporated into HFIR targets; and sol-gel methods for the preparation of actinide oxides suitable for HFIR targets were studied. More laboratory development work is planned for the berkelium recovery process as soon as sufficient amounts become available.

Since an adequate solvent extraction process for separating transcalifornium elements is not at hand, the search for new and improved ion exchange separation methods continues. We demonstrated that ethylenediaminetetraacetic acid (EDTA) complexes of the heavy actinides, loaded on anion exchange resin, can be used in a separation method, but it is still necessary to

evaluate the effects of temperature, resin particle size, and flow rate in order to completely optimize this process.

Dissociation constants of the 1,2-diaminocyclohexanetetraacetic acid (DCTA) complexes with the actinide elements were determined because previously measured dissociation constants of such lanthanide complexes had shown that the lanthanides could be separated effectively in this system. However, we found that the californium, einsteinium, and fermium dissociation constants are not appreciably different and that separation cannot be achieved.

A process employing hydroxide precipitation for preparing dense, coarse particles of PuO_2 was used to prepare 180 g of ^{242}Pu as PuO_2 for incorporation into 18 HFIR targets. These targets are being irradiated at SRL in a special fuel loading designed to maximize the flux.

Laboratory efforts to prepare dense PuO_2 , Am_2O_3 , and Cm_2O_3 by sol-gel methods are continuing; stable plutonium sols have been prepared, and these sols have been used to prepare uniform microspheres that densify when fired. Stable lanthanide sols capable of producing microspheres have now been made, and the methods will be evaluated for the production of americium and curium sols.

Actinide Separations by Ion Exchange

In an effort to find new methods for separating transcalifornium elements, the anion exchange behavior of the transcurium elements with EDTA and other actinide complexing agents was investigated, and the dissociation constants of the DCTA complexes with Am, Cm, Bk, Cf, Es, and Fm were determined.

Anion Exchange Separations of the Transplutonium Elements. — The anion exchange behavior of the transplutonium elements with EDTA and other polyamino polycarboxylic acids was investigated in an effort to develop a new separation system for these elements.

It was demonstrated that EDTA complexes of the heavy actinides may be loaded on anion exchange resins; Es/Cf and Fm/Es separation factors of 1.41 and 1.90 were achieved. These separations compare favorably with those obtained by α -hydroxyisobutyrate elution from cation resin. The transplutonium elements form an EDTA

complex of the form MeY^- , with one acetate group free to attach itself to a strong-base functional group of the anion exchange resin. The separations obtained are independent of the dissociation constants of the elements and appear to depend strongly on the size of the chelate. For this reason, differences in resin pore size and cross linkage are important. The best separations were obtained with 8 to 10% cross-linked resins. Good separations were also obtained with Amberlite IRA-900, which is described as a macroreticular resin.¹

Elution peaks for fermium, einsteinium, and californium obtained in the EDTA system are shown in Fig. 4.1, where the conditions are also shown. The Es/Cf separation factor of 1.41 is comparable to that obtained in the α -hydroxyisobutyrate elutions, but because of tighter elution bands, somewhat better separations were obtained in this system. At the conditions listed in Fig. 4.1, an einsteinium product fraction was obtained which contained 99% of the einsteinium and no detectable californium. This compares with an einsteinium product cut that contained 96% of the

einsteinium and 4% of the californium in a similar run with the α -hydroxyisobutyrate system. It is necessary to further evaluate the effects of temperature, resin particle size, and flow rate in order to completely optimize this process; column scale-up must be proved also.

Anion exchange separations based on other actinide complexing agents were evaluated. The ligands investigated include 1,2-diaminocyclohexanetetraacetic acid (DCTA), diethylenetriaminepentaacetic acid (DTPA), α -hydroxyisobutyrate, and nitrilotriacetic acid (NTA). Actinide complexes of DCTA and DTPA did not load on anion exchange resin. Actinide complexes of α -hydroxyisobutyrate and NTA on anion exchange resin gave no indications that adequate separations could be obtained.

Dissociation Constants of the Transplutonium Chelates of 1,2-Diaminocyclohexanetetraacetic Acid. — The dissociation constants of the DCTA complexes with Am, Cm, Bk, Cf, Es, and Fm were determined by ion exchange techniques. This investigation was made because the dissociation constants of lanthanide complexes with DCTA varied markedly from element to element, corresponding to cation exchange separation factors of 2.0 to 2.5 between adjacent heavy lanthanides. This indicated that DCTA might be useful in separating the transcalifornium elements from each other by cation exchange.

Dissociation constants of actinide and lanthanide complexes with DCTA are shown in Fig. 4.2. These values were calculated from distribution-coefficient data. Equilibrium distribution coefficients were determined for the transplutonium elements between ammonium-form Dowex 50-X8 cation resin (200 to 270 mesh) and 1.0 M NH_4ClO_4 solutions, both with and without DTPA. A weighed quantity of the resin was tumbled for 4 hr at 25°C with a solution containing radioactive tracer. Normally, equilibrium was achieved within less than half an hour. As this plot shows, the values for Am, Cm, Bk, and Cf closely parallel the lanthanide values, and separation factors between adjacent actinides in this series are about 2 to 2.5. Unfortunately, this is not true for the heavier actinides, and separation factors are only 1.2 for Es/Cf and 1.35 for Fm/Es. This separation does not compare favorably with that for the α -hydroxyisobutyric acid system, which provides a Cf/Es separation factor of 1.42.

¹Robert Kunin, "Amber-Hi-Lites," Rohm & Haas Co., November 1963.

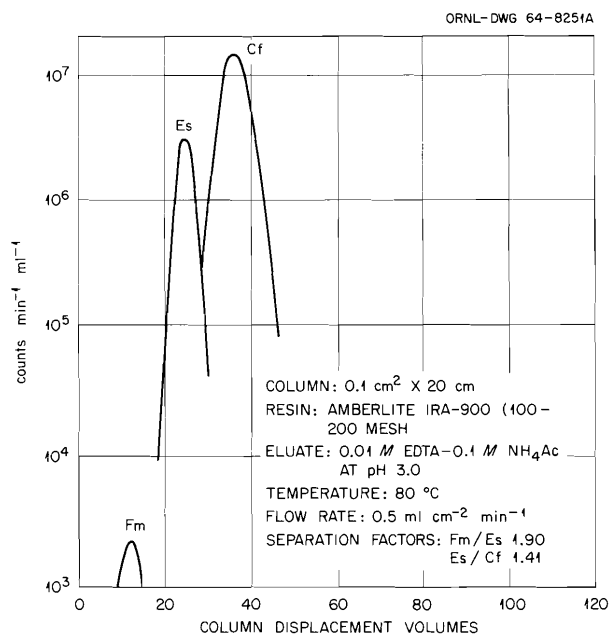


Fig. 4.1. Anion Exchange Separation of EDTA Complexes of Cf-Es-Fm.

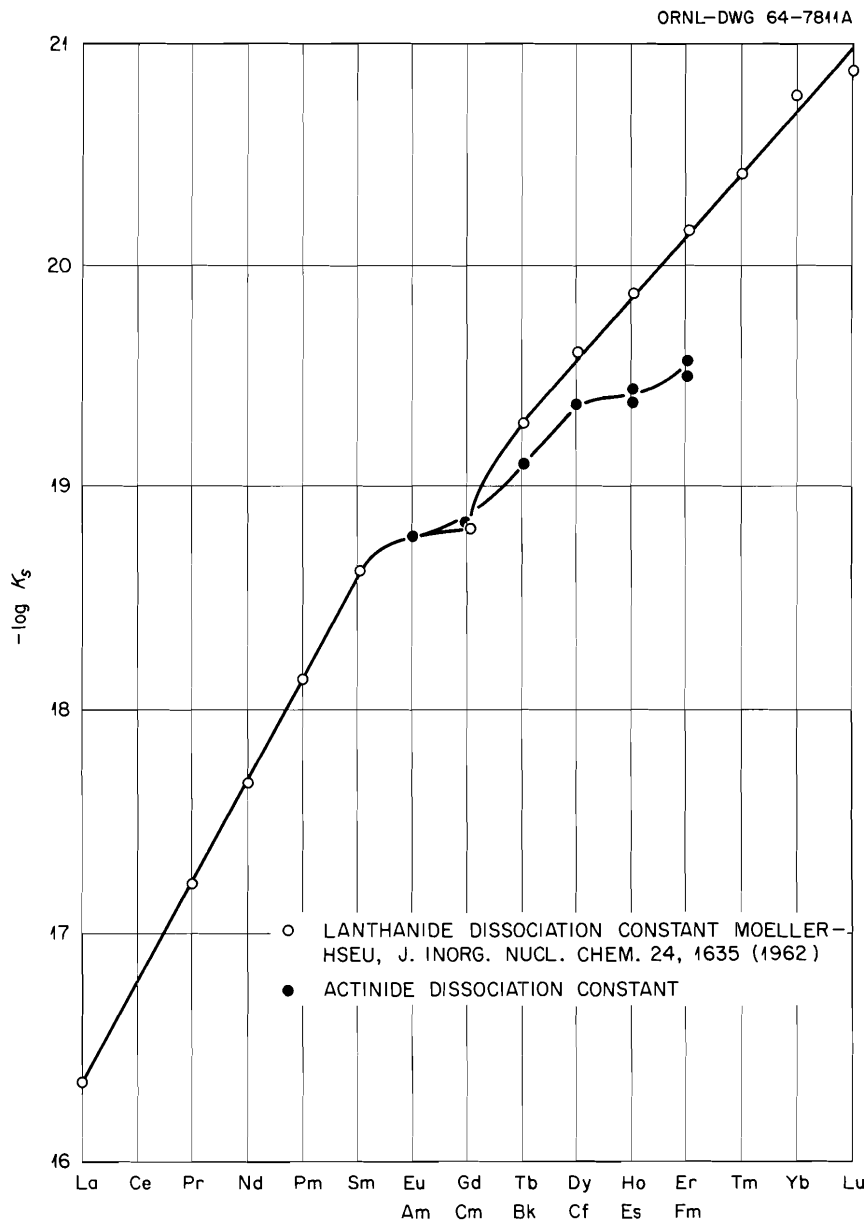


Fig. 4.2. Actinide-Lanthanide Dissociation Constants with 1,2-Diaminocyclohexanetraacetic Acid.

Preparation of Oxides for HFIR Targets. — High Flux Isotope Reactor targets will be made from pressed pellets of aluminum powder and actinide oxide, and it is essential that the aluminum phase be continuous in order to ensure satisfactory heat transfer during irradiation. When very fine actinide oxide particles are mixed with -325-mesh aluminum powder and pressed into cermets, the

oxide phase is continuous and the thermal conductivity of the pellet is low. But, with oxide particles ranging from 20 to 200 μ in diameter, the aluminum phase will be continuous, and conductivity will be satisfactory for irradiation in high neutron fluxes.

A process employing hydroxide precipitation for preparing dense, coarse particles of PuO_2 has

been reported previously;² during this past year the process was used to prepare 180 g of ^{242}Pu as PuO_2 for incorporation into 18 HFIR targets. These targets are being irradiated at Savannah River in a special fuel loading designed to maximize the flux.

When PuO_2 powder is made by the hydroxide precipitation process, grinding and screening are necessary; about 25% of the oxide is less than $20\ \mu$ in greatest diameter and must be recycled. On the other hand, preparation of PuO_2 by a sol-gel method would eliminate the dissolution and valence adjustment necessary for recycle, and the preparation of microspheres of uniform size from a plutonium sol would eliminate grinding and screening. For these reasons, efforts to prepare plutonium sols have continued, and sphere-forming techniques have been investigated. This work is still in progress. So far, stable plutonium sols have been prepared in the laboratory, and plutonium sols have been used to prepare uniformly sized microspheres, which calcine to dense PuO_2 spheres.

For similar reasons a sol-gel method for preparing americium and curium oxide for incorporation into HFIR targets would be convenient, and laboratory efforts to prepare lanthanide sols as stand-ins for americium and curium have been initiated. Stable lanthanide sols, capable of producing microspheres, have now been made, and the methods will be evaluated for the production of americium and curium sols.

PuO_2 Preparation. — The hydroxide precipitation method was used to prepare 246 g of PuO_2 which contained about 217 g of ^{242}Pu . The oxide was prepared in three batches and was ground to the desired particle-size range with a mortar and pestle. The following average sizes were obtained: $-70 +100$ mesh, 25%; $-100 +200$ mesh, 35%; $-200 +325$ mesh, 15%; and -325 mesh, about 25%. The -325 -mesh fines, which are not suitable for HFIR targets, were recycled.

About 203 g of this oxide, which contained 180 g of ^{242}Pu , was incorporated into 18 HFIR targets, now being irradiated in a Savannah River reactor. A special fuel loading, designed to maximize the flux, is used. These rods may be further irradiated in the HFIR prior to initial processing.

Plutonium Sol Preparations. — During continued investigation of plutonium sol procedures, it was established that plutonium sols can be prepared by digesting freshly precipitated $\text{Pu}(\text{OH})_4$ in sufficient HNO_3 to provide an NO_3^-/Pu mole ratio of about 1. To produce dense oxide from such sols, it is then necessary to reduce the nitrate concentration. This is done by drying the sol, heating the dried gel to remove nitrate, and resuspending the dried gel in water. Nitrate removed by this method depends on both time and temperature, and excessive denitration results in a nondispersible product. Plutonium sols have been prepared by this method with NO_3^-/Pu mole ratios in the range of 0.08 to 0.13.³ However, stable sols capable of producing dense oxide have been produced with ratios as high as 0.3.

Spectrography showed that the plutonium sol particles produced by digestion of the hydroxide with dilute HNO_3 are polymers. It is suspected that the size of the ultimate sol particle is determined by the degree of polymerization and can therefore be altered and possibly controlled by variations in each step of the procedure. Continued efforts are necessary to determine the micelle size produced by changes in procedure and to correlate micelle size and nitrate concentration with density and strength of calcined oxide.

Initial attempts to produce microspheres from a plutonium sol were successful. These spheres were produced from a plutonium sol concentrated to about 100 g of plutonium per liter. The spheres were formed by introducing sol from a syringe into slowly agitating drying liquid — 10% 2-octanol—90% 2-methyl-1-pentanol. The particle sizes obtained after calcination at 1150°C varied from 5 to $40\ \mu$. To produce microspheres of more uniform size, sphere-forming equipment which features a tapered column³ was installed in a glove box. This equipment was used to produce both PuO_2 - ThO_2 microspheres (made from mixed plutonium-thorium sols) and pure PuO_2 spheres. Plutonium dioxide—thorium dioxide spheres have been produced which contain 2, 10, 20, 30, and 50 wt % PuO_2 . The size after calcination at 1150°C was $200 \pm 20\ \mu$ in all cases, and toluene density determinations indicate that the densities were 97 to 99% of theoretical. Microphotographs

²Chem. Technol. Div. Ann. Progr. Rept. May 31, 1963, ORNL-3452, pp. 114–15.

³Chem. Technol. Div. Ann. Progr. Rept. May 31, 1964, ORNL-3627, pp. 169–76.

of $\text{PuO}_2\text{-ThO}_2$ spheres before and after calcining are shown in Figs. 4.3 and 4.4. These spheres contained 50 wt % PuO_2 .

Plutonium dioxide microspheres were successfully made from four separate sol preparations, which indicates good reproducibility. However, the drying medium used to produce the spheres was not satisfactory. The drying rate appeared to be excessive, and hollow, broken spheres were produced. Satisfactory results were obtained, however, with the following drying mixture: 59.6 vol % 2-ethyl-1-hexanol, 40 vol % 2-octanol, and 0.4 vol % "Amino O." Microphotographs of PuO_2 spheres before and after calcination at 1150°C are shown in Figs. 4.5 and 4.6. Diameters of the calcined spheres varied from 110 to $150\ \mu$,

and densities better than 95% of theoretical were indicated by toluene density determinations.

Microsphere Preparations from Lanthanide Oxide Sols. — During initial attempts to produce lanthanide sols, various methods were investigated with $\text{La}(\text{NO}_3)_3$, $\text{Gd}(\text{NO}_3)_3$, and $\text{Nd}(\text{NO}_3)_3$. While several methods produced partial lanthanum sols which dried to glassy solids, a completely satisfactory method was not found.

In early tests, electrolysis of gadolinium from a nitrate solution through a cation membrane into a cathode compartment containing water provided the most favorable-appearing sol which formed in the cathode compartment. It was concentrated by evaporation and used to prepare microspheres, which retained their shape after calcining at

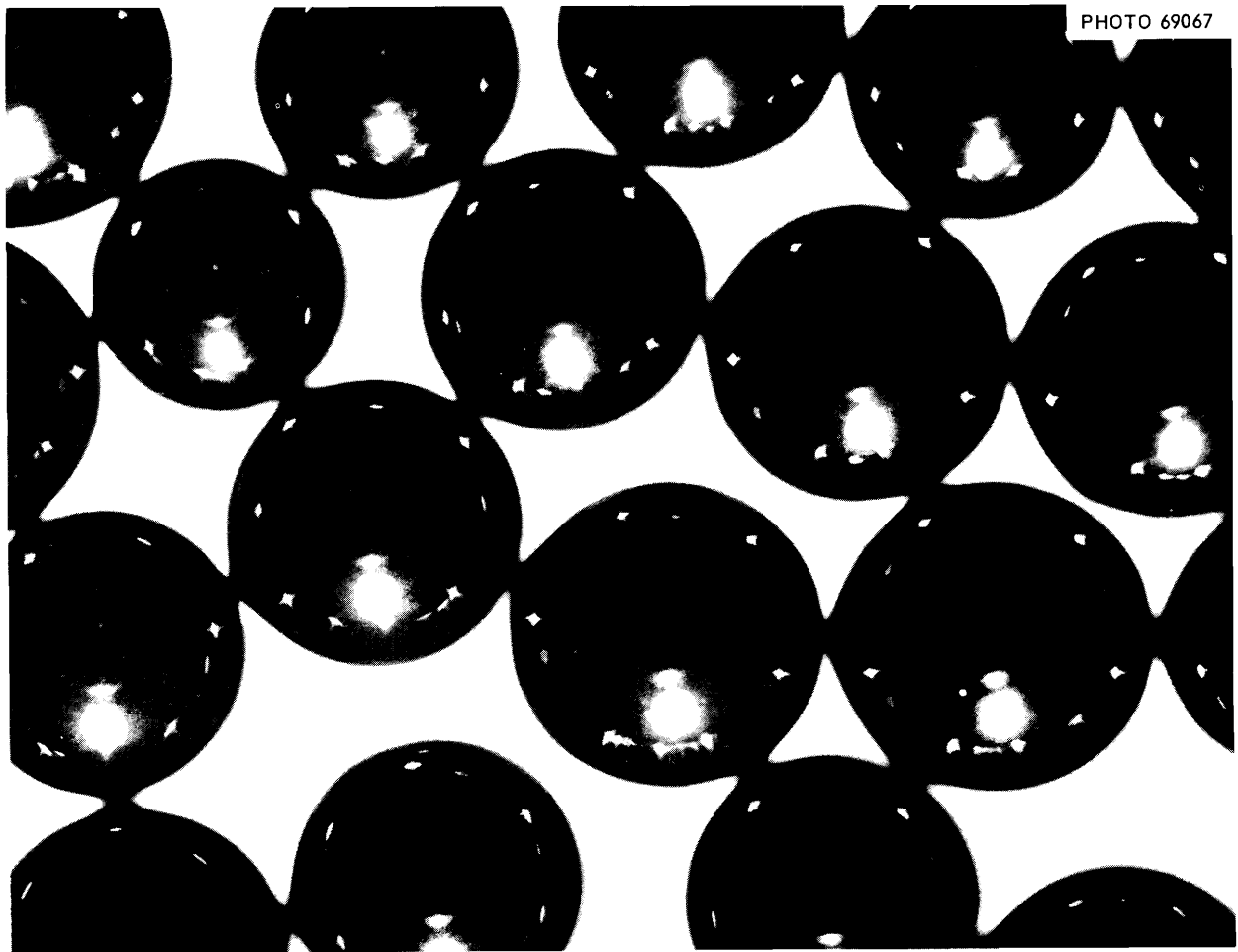


Fig. 4.3. $\text{PuO}_2\text{-ThO}_2$ Microspheres, Uncalcined. Diameter, 210 to $250\ \mu$.

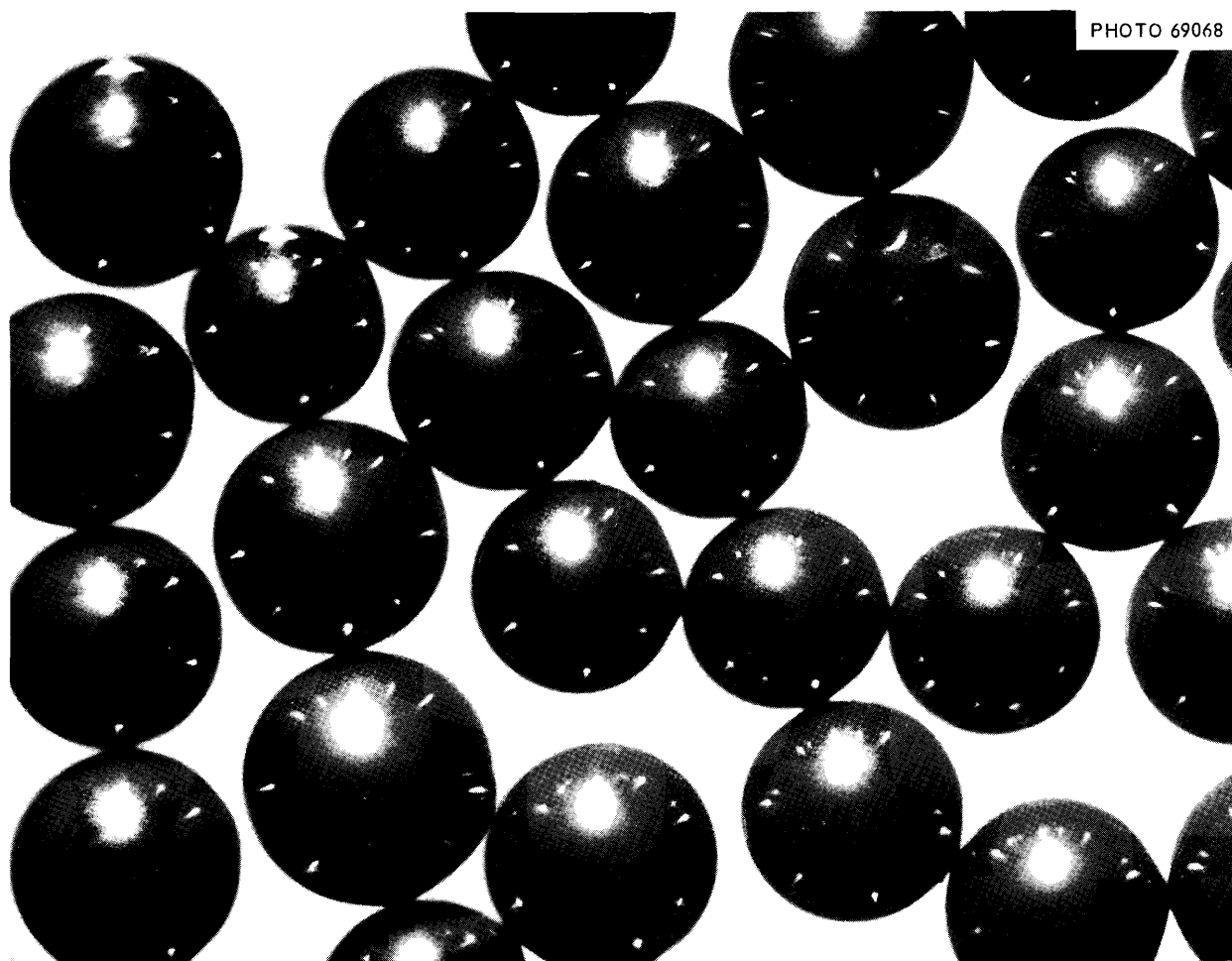


Fig. 4.4. $\text{PuO}_2\text{-ThO}_2$ Microspheres, Calcined at 1150°C . Diameter, 180 to $210\ \mu$.

1000°C . However, they were fragile, and microscopy showed excessive surface imperfections. During these preparations, freshly precipitated hydroxide exhibited a strong tendency to peptize, an indication of sol-forming characteristics, but in a short time this tendency decreased.

In recent tests, similar behavior was observed with lanthanum hydroxides. Freshly precipitated hydroxides are amorphous, but upon aging they rapidly aggregate and are not conducive to sol formation. Accordingly, techniques were developed which minimized the difficulties and permitted making stable lanthanide sols amenable to microsphere production.

Thus, it has been possible to produce sols from praseodymium, neodymium, and gadolinium hydrox-

ides with nitrate-to-metal mole ratios of 0.03 to 0.04. In all cases, these sols have yielded microspheres that calcine to very glassy-appearing oxide spheres at 1000°C .

Photomicrographs of the praseodymium oxide spheres before and after calcination are shown in Figs. 4.7 and 4.8. They were formed by introducing a 2 M sol from a syringe into a beaker of slowly agitating drying liquid (20% 2-octanol-80% 2-ethyl-1-hexanol). Toluene densities were 99.5% of theoretical density for two different batches of spheres that had been calcined at 1000°C for 16 hr.

This work will be continued, and attempts will be made to correlate process variables with desirable product characteristics. In addition,

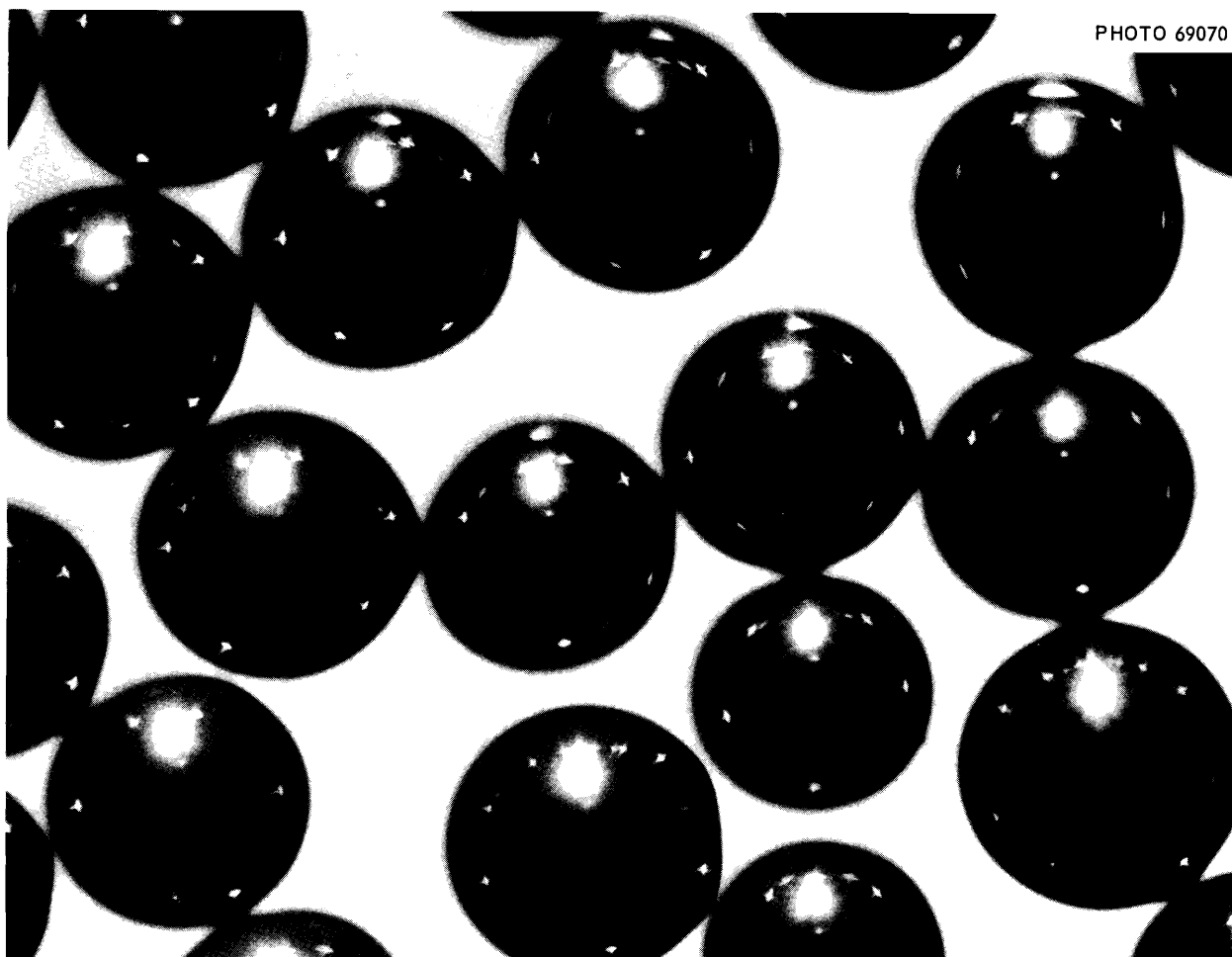


PHOTO 69070

Fig. 4.5. PuO_2 Microspheres, Uncalcined. Diameter, 180 to 220 μ .

equipment is being assembled so that these methods can be evaluated for the preparation of americium and curium sols.

Investigation of Sphere-Forming Techniques from Rare-Earth Nitrates. — In search of an alternative to the sol-gel approach, scouting tests were made to investigate the preparation of dense oxide spheres directly from nitrate solutions. Investigations were made both with $\text{La}(\text{NO}_3)_3$ and a mixture of rare-earth nitrates. The successful application of such a procedure could be useful in preparing americium, curium, and rare-earth product in solid form for safer shipping, and might also serve to prepare americium and curium oxides suitable for incorporation into HFIR targets.

According to one approach, concentrated nitrate solution is introduced as small droplets into a

column containing high-molecular-weight drying alcohols and a bottom layer of concentrated NH_4OH . Successful particle formation requires sufficient dehydration to form a "set" sphere while the droplet falls through the drying alcohol and the conversion of the nitrate to the hydroxide in the NH_4OH phase. Although it was possible in several instances to produce particles that retained their shape after calcination at 1000°C , the fired particles were irregular in shape and did not appear to be sufficiently hard and dense. In most of the preparations investigated, spheres were readily obtained in the column, but they frequently cracked or disintegrated while air drying at room temperature.

In general, the principal difficulty appeared to be the formation of crystalline-appearing particles

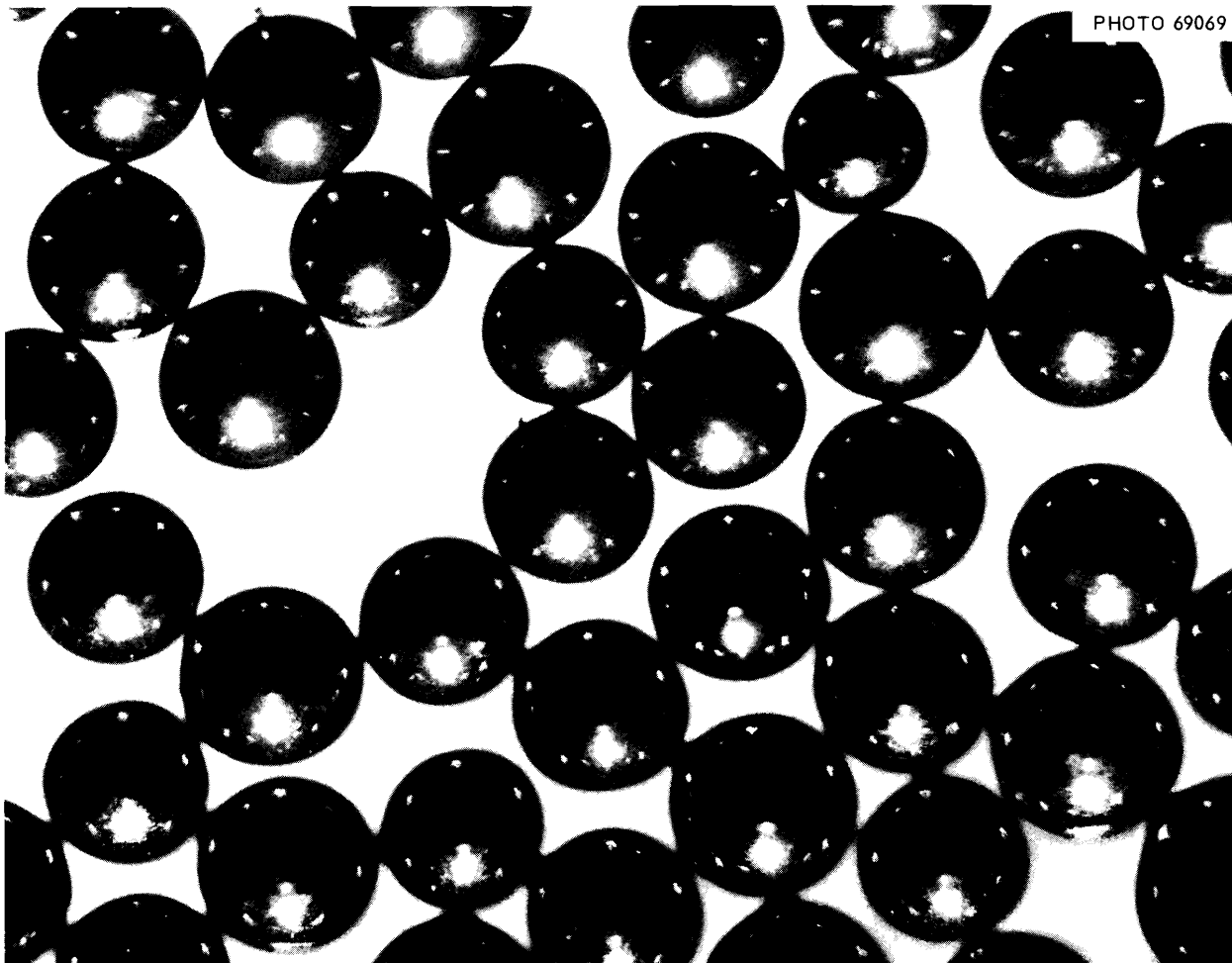


Fig. 4.6. PuO_2 Microspheres, Calcined at 1150°C . Diameter, 110 to $150\ \mu$.

rather than amorphous ones, the kind that harden and densify when calcined to the oxide at relatively low firing temperatures. Although all possible variables were not investigated, the method did not appear to be sufficiently promising to warrant further investigation.

4.2 DEVELOPMENT OF PROCESS EQUIPMENT

Engineering studies are being conducted to develop equipment and operating procedures for the Transuranium Processing Plant. Equipment racks and other components have been tested in a full-scale mockup to determine installation and removal techniques and to solve maintenance problems. The solvent extraction equipment

rack is being tested to determine hydraulic performance through one complete cycle of solvent extraction at design flow rates. Mass transfer data for the various flowsheets are measured in a prototype set of columns located in an alpha laboratory to permit use of transuranium elements.

Status and Progress

Testing of cell components, equipment installation and maintenance concepts, and various mechanical equipment in the full-scale cell mockup was continued in the past year and is now nearly complete. Tests of the solvent extraction flowsheet and equipment, in progress for the past two years, will continue. Satisfactory stage

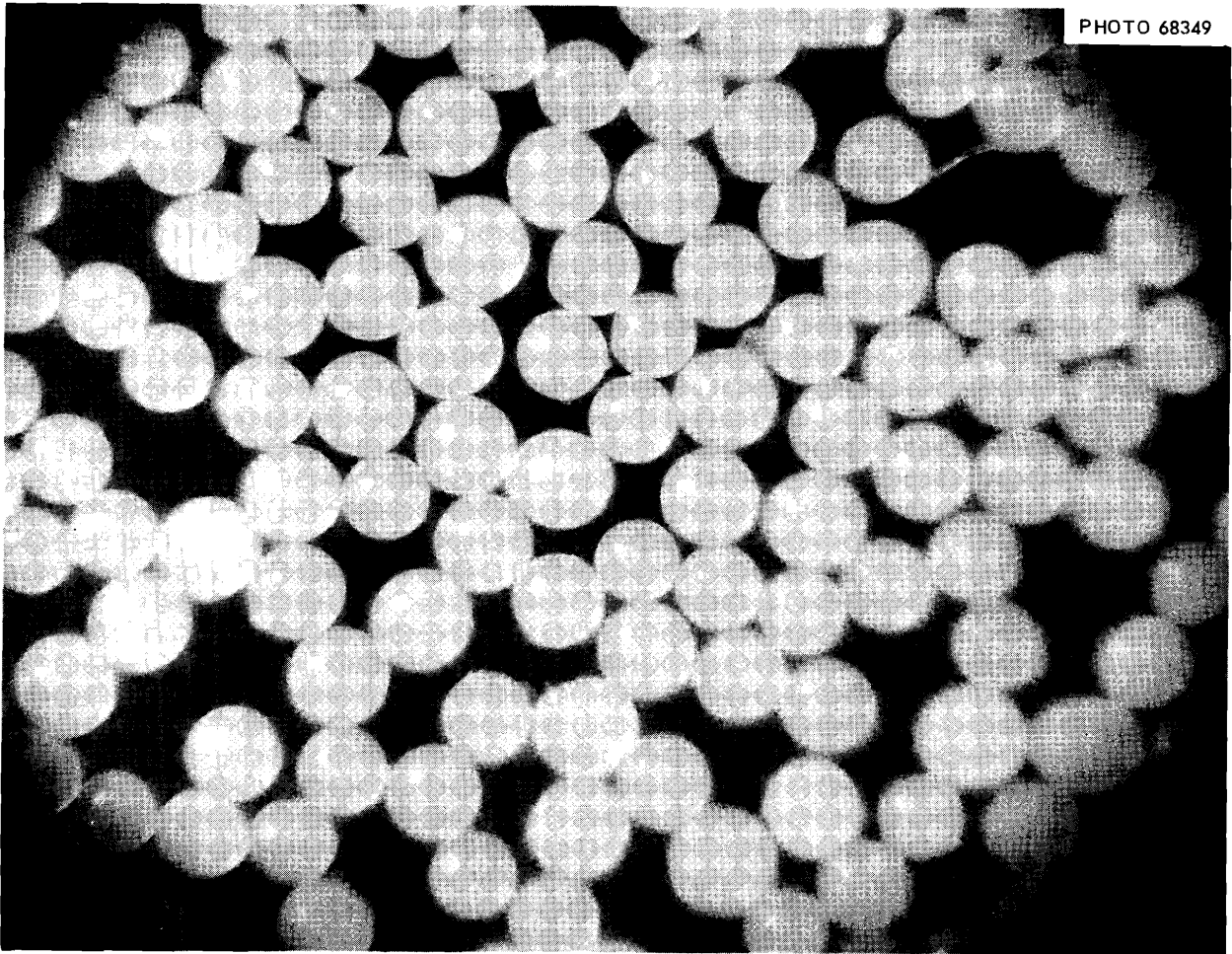


Fig. 4.7. Praseodymium Oxide Microspheres, Uncalcined.

heights, throughputs, and scrubbing efficiency were demonstrated in glass prototype columns for the Tramex flowsheet. High product losses to the waste organic stream were observed to be related to a very small amount of entrained aqueous phase. The hydraulic performance of the all-Zircaloy-2 solvent extraction equipment rack to be installed in the TRU was tested and found to be satisfactory after some minor piping changes.

Mockup Tests

Testing in the full-scale mockup of the processing cell is almost complete. Actual equipment full-scale prototypes were installed and

tested to ascertain that the required remote manipulation and maintenance could be done.

The test work on the equipment-transfer case and maintenance procedures for replacing an alpha seal window was completed.

A finished version of the TRU sampler station was installed in the mockup and tested. Only minor modifications were necessary to give satisfactory operation.

A revised version of the manipulator booting seal was tested and proved acceptable without changes. Two sliding O-rings provide the seal.

The cubicle cooling system, including the filter system, was installed and checked for ease of filter removal and for heat-removal characteristics.

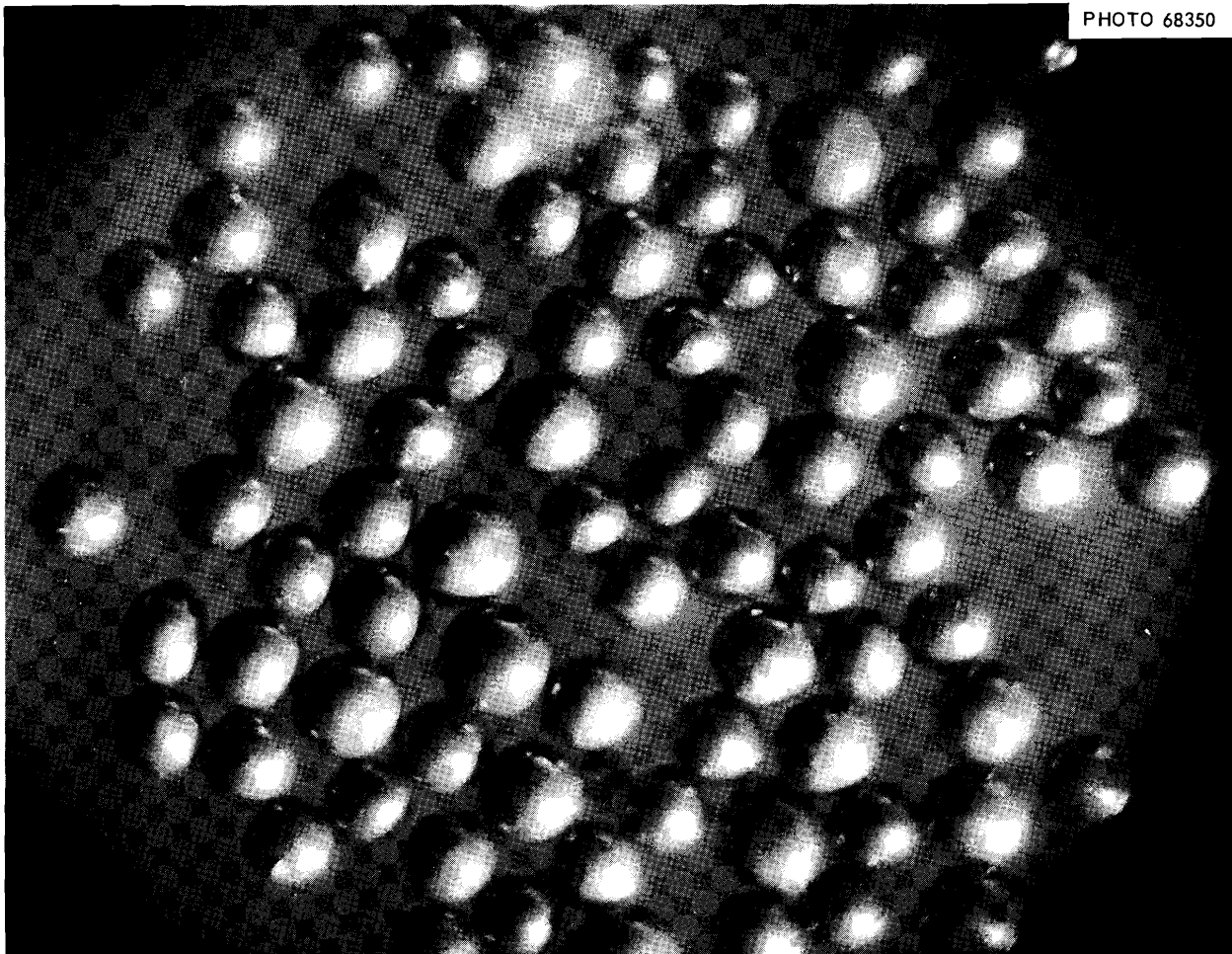


Fig. 4.8. Praseodymium Oxide Microspheres, Colcined at 1000°C.

Only minor changes were needed to give proper service.

Development of Pulsed Columns

The Traxex flowsheet for separating actinide and lanthanide elements was tested in glass pulsed columns ($\frac{3}{4}$ in. in diameter and 4 ft high) at throughputs equivalent to the design flow rate of the TRU columns, which are $1\frac{1}{2}$ in. in diameter and 5 ft high. The efficiency of the columns was determined by using ^{241}Am as a representative transuranium element and ^{152}Eu as a typical rare earth. Extraction of americium was consistently good; the loss was less than 0.1%. The stage height ranged from 6 to 10 in. for flow ratios

(aqueous/organic) of 1:1 to 2:3 and pulse frequencies of 40 to 50 cpm. Scrub stage heights agreed with previous tests — decontamination of the americium with respect to europium was greater than 2000, and the stage height for the scrub column was less than 18 in.

Stripping tests revealed an unexpected difficulty. Although only one theoretical stage is required, in initial tests 25% of the americium was lost to the waste solvent. The americium was in a small volume of entrained aqueous phase (0.4 vol %). By filtering or allowing the aqueous phase to settle over a long period of time, we established that less than 0.1% of the americium was in the solvent. The entrainment was caused by a spontaneous emulsification of the 1 M HCl strip reagent into the solvent. This is easily

observed by placing a drop of loaded solvent on the surface of 1 M HCl. Violent interfacial activity occurs immediately. Numerous batch mixing and phase separation tests were conducted in an effort to find a way of preventing the entrainment. The most successful methods were by stripping with higher concentrations of HCl or LiCl. Pulsed-column tests using 4 M HCl instead of 1 M HCl as the stripping agent demonstrated satisfactory stripping. The aqueous entrainment was reduced to less than 0.1 vol %, and the americium loss was only 0.1 to 1.3%.

The first phase of the hydraulic testing of the full-scale TRU pulsed columns was completed. Temporary modifications of the aqueous seal legs, solvent overflow lines, pulse restrictors, and solvent-pump elements permitted operation at design flow rates for both the Tramex and Pharex flowsheets. The feed metering system was calibrated, and the flow response to pressure setting was linear over the required range. At the design flow rate of 1 liter/hr, the standard deviation of flow at constant pressure was 6.9%. Good automatic control of the flows through the cascade of three columns was demonstrated. Pulse pumping of the solvent into the columns was shown to be reliable. Early failure of the diaphragms in the pulsers and pumps was caused in several cases by metal chips which had not been removed by the cleaning techniques used previously. The problem was eliminated by using ultrasonic cleaning of the parts before assembly.

4.3 DESIGN AND FABRICATION OF PROCESS EQUIPMENT

Equipment is being designed and built to process HFIR targets using both solvent extraction and ion exchange techniques. In this equipment the actinide elements will be separated from fission products produced in the irradiations and then separated as individual products. The equipment is mounted on racks to be located in four of the nine cubicles. Process tanks and much of the piping system are to be mounted in the tank-pit portion of the cell, behind and below the cubicles. All equipment, much of which is made of Hastelloy C, Zircaloy-2, and tantalum, is assembled with mechanical disconnects and is designed to be replaced by remote or semiremote techniques.

Status and Progress

Design of the equipment is 95% complete. That remaining is predominantly associated with special separations not presently defined accurately by precise chemical flowsheets. Fabrication of the process equipment, now 80% complete, is scheduled to be finished by September. Almost all purchased components are on hand, and all remaining fabrication jobs have been scheduled in the ORNL shops.

Equipment Design

Design was completed and drawings were issued for fabrication of the process piping for all seven process cells and for the majority of the equipment components. Design of the equipment for separating californium, einsteinium, and fermium is in progress. The precipitation equipment rack for the preparation of oxide for HFIR targets is still delayed, awaiting further flowsheet development. During the past year an all-Zircaloy-2 centrifuge, with operating speeds up to 6000 rpm, was added to the process, for feed clarification and other operations. Design and development of this equipment are in progress in the ORGDP Technical Division. The design of all service and makeup equipment and instrumentation outside the cell bank was completed.

Three equipment-installation packages, including drawings and specifications, were prepared to define the job of installing about 80% of the process equipment by a contractor. The remaining 20% will be installed by ORNL.

Equipment Fabrication

In the past year the fabrication of process equipment, just under way at the beginning of the year, progressed to approximately 80% completion. Most of the equipment components to be installed by a cost-plus-fixed-fee contractor have been completed. This equipment includes the nine cubicle service plugs, of which the one pictured in Fig. 4.9 is typical. In this and subsequent pictures (Figs. 4.10 and 4.11), the concept of prefabrication of piping and components in shop jigs for ease in installation may be rather clearly envisioned. Other components, to be installed by the contractor, which have been

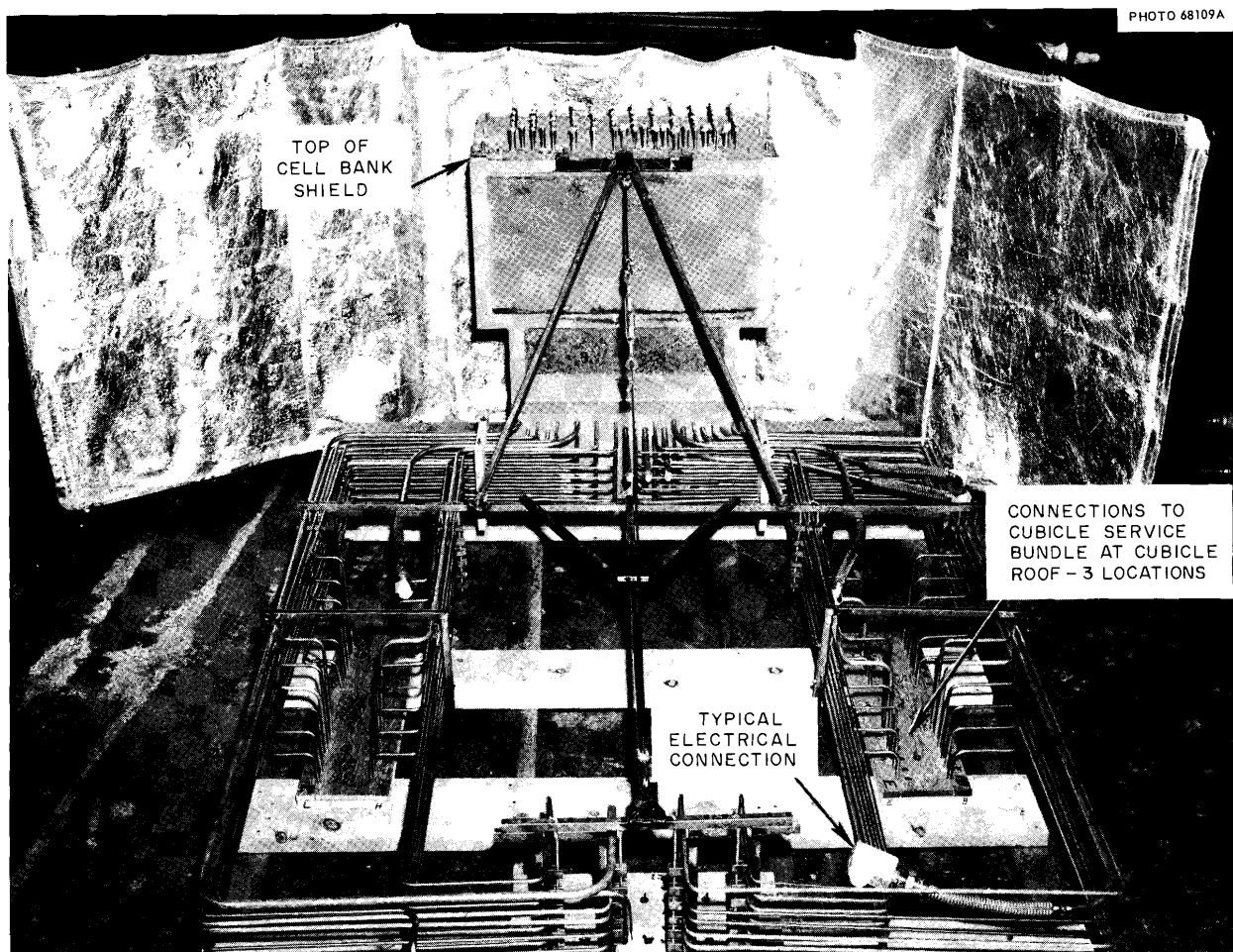


Fig. 4.9. Cubicle 5 Service Plug. The concrete plug, shown here in the shop assembly jig, contains 72 service tubes and 5 electrical conduits. The entire assembly is lowered into place above the cubicle, after which connections are made, remotely if required.

completed, include tank-pit service plugs, cubicle service lines, the interpit piping plugs, the waste and off-gas headers, and tank and equipment supports.

The equipment to be installed by ORNL includes the process tanks, equipment racks, and the connecting jumper piping. Seven of the ten equipment racks have been completed. The process tanks are being purchased, but ORNL craftsmen will install the piping nozzles. Some of the tank shells have been received from the vendors, and assembly of the piping is in progress.

The cubicle and pit process jumper piping is presently being fabricated in shop assembly

fixtures, as shown in Figs. 4.10 and 4.11. Disconnect positions in the cell bank are accurately located in the assembly fixture, and then all piping in a given pit or cubicle is assembled in the fixture. This procedure simplified both the design and fabrication of individual jumpers and guarantees the proper fit of piping in the cell bank. The fabrication of all process equipment is scheduled for completion by September.

4.4 CONSTRUCTION OF THE TRANSURANIUM PROCESSING PLANT

A new processing building, designated the Transuranium Processing Plant (TRU), containing

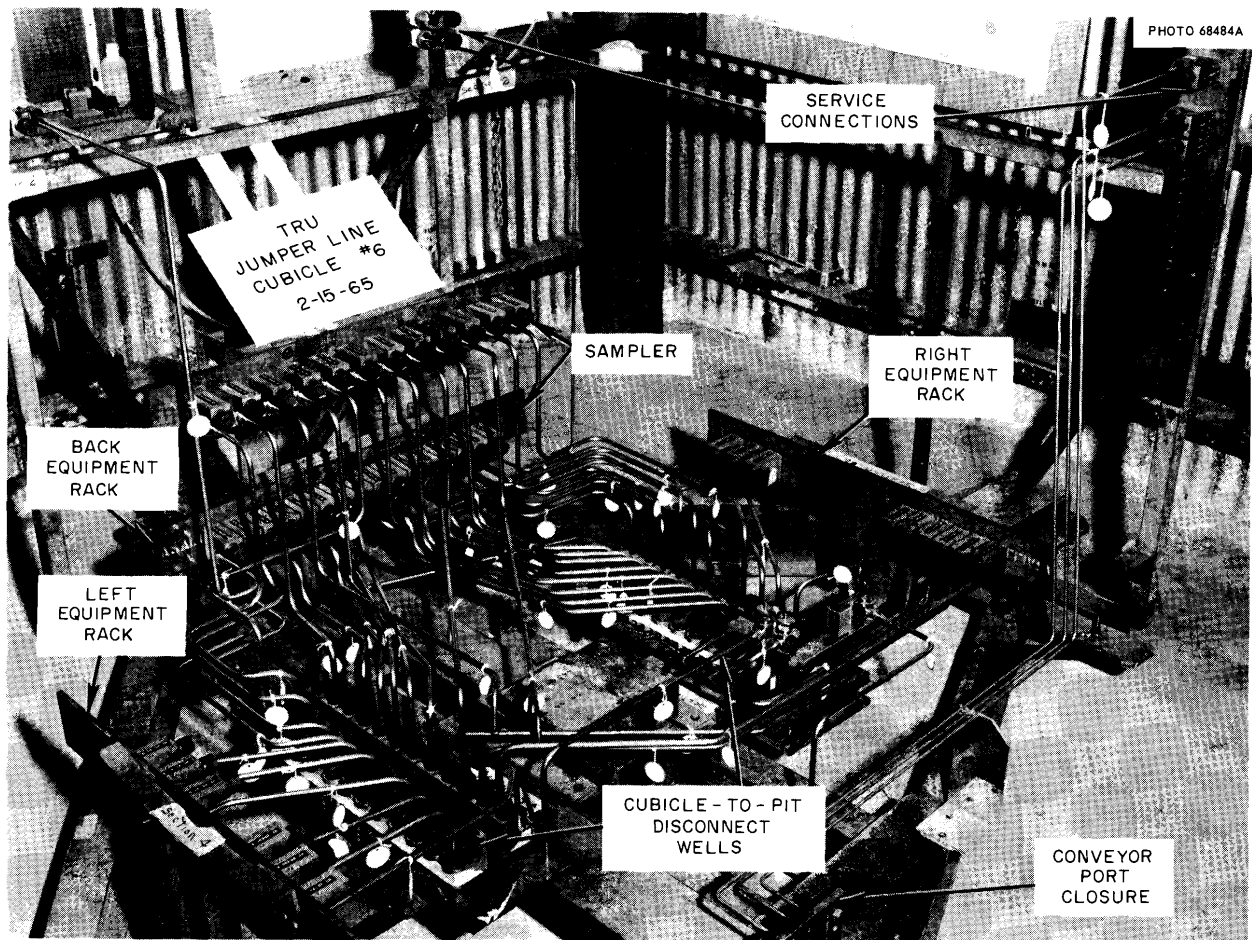


Fig. 4.10. Process Jumper Piping, Cubicle 6. About 50 lines are required to connect the equipment racks and the disconnect wells in the floor of the cubicles. Disconnect clamps in the jig are accurately located to $\pm \frac{1}{32}$ in., corresponding to actual in-cell positions.

nine shielded cells, eight laboratories, and related service areas, was designed and built to provide facilities for recovering the actinide elements from irradiated HFIR targets. Design of the building was started in 1961, and it is scheduled to be in operation early in 1966. The details of the design have been reported in previous annual reports.

Status and Progress

Construction of the TRU was completed by the lump-sum contractor in late May 1965, only a few weeks behind the original schedule. Installation to the process equipment is just under way. About 80% of this equipment will be installed under a

cost-plus-fixed-fee contract with the H. K. Ferguson Company, and the remainder will be installed by ORNL. Scheduled completion of this phase of the project is late fall.

Building Construction

The construction of the Transuranium Processing Plant was completed by the lump-sum contractor, Blount Brothers Construction Company of Montgomery, Alabama, in late May, about 23 months after the start of construction and 25 months after the contract was let by the Atomic Energy Commission. The lump-sum-contract construction consisted of the basic building, including the shielded cell bank; building services;

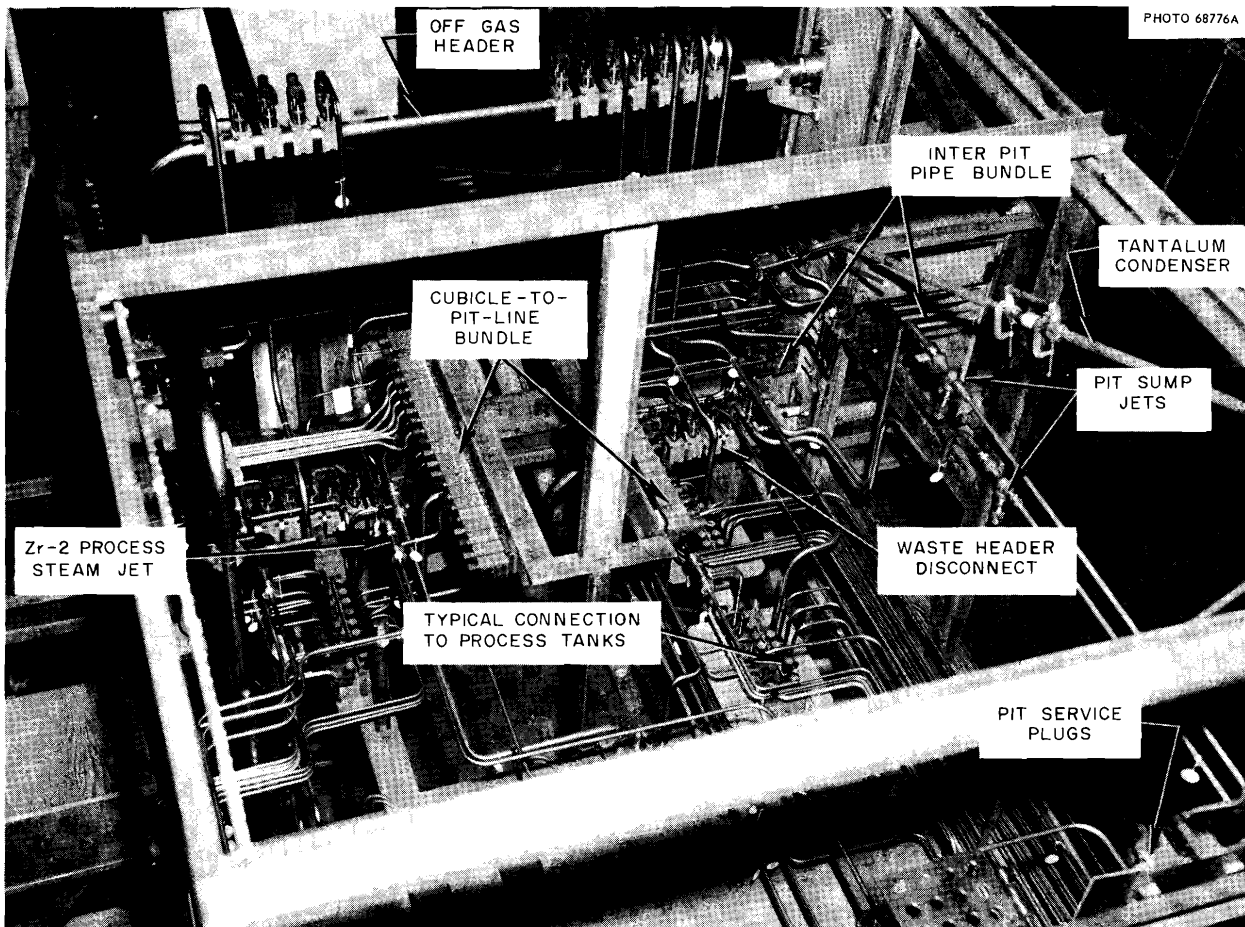


Fig. 4.11. Process Jumper Piping, Cell Pit 7. The headers and inter-pit plugs are actual cell equipment. Other equipment (tanks, service plugs, cubicle-to-pit line bundles) is simulated.

complete fire protection systems; complete building, cell, laboratory glove box, and process-equipment ventilation and control systems; waste accumulation and waste disposal piping systems; furnished laboratories and storage and equipment rooms; a 50-ton bridge crane in the limited access area; shielded plugs for operating cells and other radioactive environments; and liners for future installation of bulk shielding windows and the intercell transfer conveyor.

No major construction problems were encountered, although a scheduling problem was introduced when sandblasting and application of protective coatings were done simultaneously with other activities in the building, particularly welding. The problem could have been greatly minimized if the coatings on the cell bank roof plugs had been applied outside the building.

The glass-fiber-reinforced epoxy resin coatings, which are applied to all concrete surfaces inside the cell bank, have provided what appears to be a smooth and reliable wall liner at a reasonable cost, when compared with stainless steel or Hastelloy liners. The effects of time and radioactive exposure will provide the final test.

Installation of Process Equipment

About 80% of the remaining equipment installation in the TRU will be done by the H. K. Ferguson Company under a cost-plus-fixed-fee (CPFF) contract with the Atomic Energy Commission. The scope of that work will include the installing and testing of the waste-accumulation and disposal system and the off-gas scrubber;

installation of supports for process equipment located in the cell tank pits; installation of cell cubicle auxiliaries, including lighting, ventilation, and cooling and service piping; fabrication and installation of chemical makeup equipment piping; and installation of interconnecting piping between the makeup area and the cells.

The remainder of the process-equipment installation requires special procedures; which will be developed by ORNL for initial installation and future replacement of equipment in the cell cubicles and cell tank pits. This equipment will be installed by ORNL at the conclusion of the CPFF contract.

Design and Fabrication of Mechanical Equipment

Several items of mechanical equipment have been purchased by or made at ORNL and are

available for installation in the Transuranium Processing Plant. These include the self-propelled dolly for moving heavy equipment between the limited access area and the loading dock outside the building; the intercell conveyor and its control system for transferring supplies and small equipment between cell cubicles and between the cell cubicles and the exterior of the cell bank; the bulk-shielding viewing windows and their handling equipment; master-slave manipulators; and cell-cubicle lighting and cooling equipment.

Contracts are in force for the fabrication of the doors and door frames for the tops of the cubicles, the intercell conveyor port closure assemblies, and the postirradiation carrier for transferring irradiated targets from the HFIR to the TRU plant. This equipment is scheduled for delivery to the plant for installation by the CPFF contractor and ORNL.

ORNL-DWG 65-9723

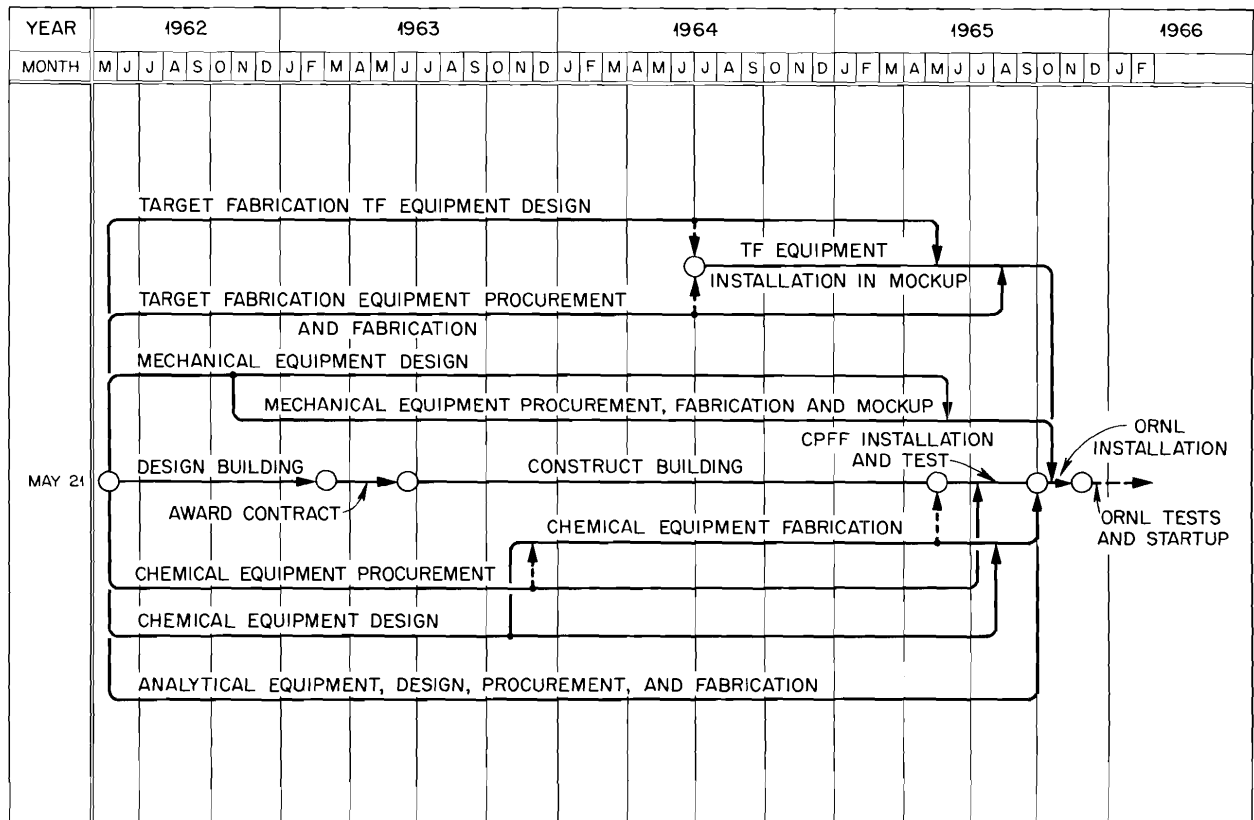


Fig. 4.12. Transuranium Processing Plant Summary Schedule, April 15, 1965.

Several items of mechanical equipment are being designed and/or fabricated so as to be available at startup and are not required for the installation contract. These include a sample solution carrier, a glove box for decontaminating process equipment, a carrier charging system for removing contaminated materials from the transfer area and cell bank, a waste disposal station for handling solid waste from the process, and an equipment transfer case and shield for removing contaminated equipment from the cell cubicles. Design studies have been started for a filter carrier for disposing of contaminated filters from the ventilation systems of both the TRU and TURF facilities. A study has also been initiated for the installation of periscopes into the TRU cell cubicles.

Critical Path Schedule

The critical path schedule for the Transuranium Processing Plant underwent a major updating in January 1965 to reflect changes in the course of project work and policy. Two major updatings and several minor ones have been made since the original schedule was formulated.

A summary of the new schedule is shown in Fig. 4.12. Target fabrication design was very nearly complete in May 1965. Fabrication and procurement of the remaining equipment in this

group should be complete in August 1965. The installation of functional target fabrication equipment in the three-cubicle mockup located in Building 4508 started in July 1964 and, according to the latest schedule, is expected to be finished by November 1965.

All chemical processing equipment being made or bought by ORNL for subsequent installation by ORNL will be available by September 1, 1965. All ORNL work is still on a schedule compatible with the original project schedule. There were no major unresolved procurement problems, nor were any foreseen.

For the most part, original manpower estimates used on the critical path schedule for the TRU project were insufficient. This was especially true for conceptual and early design items, where substantial increases were required to define many of the interconnecting and transfer operations prior to final design. Estimates on major design components were also inadequate, and many small related activities were overlooked or underestimated. Manpower estimates for all design jobs increased nearly 56%. To offset this increase, it was necessary to increase the design work force from 23 to 34.

Increases in shop estimates were less significant. Where they occurred, they resulted because certain fabrication techniques had to be developed for highly specialized items.

5. Curium Processing

A joint program between the Isotopes Division and the Chemical Technology Division has been established to produce curium heat sources for use in thermoelectric converters. The Chemical Technology Division is responsible for providing processing technology, facilities, and operations to isolate gram amounts of curium. Product curium in nitric acid solution is delivered to the Isotopes Division for fabrication of the thermoelectric heat sources. A number of process methods, facilities, and source materials are used for both the Curium Program and the closely related Transuranium Element Program (Chap. 4).

The Curium Recovery Facility (CRF) was originally planned for testing transuranium element processes at high radioactivity levels, but modifications have been made to increase capacity and to improve reliability so it can also be used to isolate multigram quantities of curium free of fission products. Nearly 17 g of ^{244}Cm was purified, separated from ^{243}Am , and transferred to the Isotopes Division for incorporation into an experimental heat source and for distribution to other AEC installations. This curium was isolated from a nitric acid concentrate, containing about 100 g of ^{243}Am , 100 g of ^{244}Cm , and 10 kg of rare-earth fission products and lanthanum, which Savannah River Laboratory prepared as feed material for the Transuranium Element Program. Six irradiated targets of $^{241}\text{AmO}_2$ in aluminum matrix were also processed to separate ^{242}Cm from aluminum and fission products but not from residual americium, since it does not interfere with subsequent use of the curium. To date, 3.56 g of purified ^{242}Cm has been transferred to the Isotopes Division, and an additional 14 g of ^{242}Cm will be processed early next fiscal year.

The Chemical Technology Division's part of the Curium Program includes laboratory-scale development of the chemical processes, searching for

alternative process methods that can be used in existing processing facilities, and design, construction, and operation of the CRF to test the processes and to isolate multigram amounts of ^{242}Cm and ^{244}Cm . Chemical processes, equipment, and feed solutions used in this program are closely related to those for the Transuranium Element Program (Chap. 4).

5.1 PROCESS DEVELOPMENT

The chemical processes for curium isolation include dissolving the target in dilute HCl; Clanex processing to convert nitrates to chlorides and/or to remove aluminum; Tramex processing to separate americium-curium from fission products; and carbonate precipitation of Am^{5+} to separate americium from curium. Complete process details are discussed in later sections.

Most of the laboratory-scale development and testing of these processes were completed last year and have been previously reported.^{1,2} Process development during this report period was confined to problems associated with full-scale processing in the CRF at high activity levels.

Status and Progress

Product entrainment, which had been excessively high, was reduced to reasonable proportions. In other studies, the solubility of rare earths in Tramex feed was determined. Also, it was determined that methanol is not a dependable preventive of the radiolysis of the chloride solutions

¹F. L. Culler *et al.*, *Chem. Technol. Div. Ann. Progr. Rept. May 31, 1963*, ORNL-3452, pp. 134-43.

²F. L. Culler *et al.*, *Chem. Technol. Div. Ann. Progr. Rept. May 31, 1964*, ORNL-3627, pp. 136-47.

used in the Tramex process. Thus, the sequels – loss of acid and oxidation of the cerium to the tetravalent state – cannot be consistently avoided through the use of methanol. This subject will receive further attention. In another study, it was shown that the time required for solvent extraction will be unaffected even when the sodium nitrate concentration in the americium-curium solutions received from the Savannah River Plant is as high as 0.5 *M*.

Laboratory Investigation of Product Entrainment During Clanex Stripping Operations

During initial high-activity-level operations in the Curium Recovery Facility (CRF), 1 to 2 vol % of the aqueous stripping solution, containing 30 to 50% of the americium-curium, was entrained by the waste solvent during both Clanex and Tramex stripping operations. Laboratory attempts were made to duplicate this and to find methods for preventing such excessive entrainment of product. Batch stripping experiments were used. Partially loaded solvent was prepared by contacting 0.6 *M* Alamine 336·HCl in diethylbenzene with simulated Clanex feed traced with ¹⁵²⁻⁵⁴Eu. Stripping was done by contacting the solvent with 0.3 vol of 1 *M* HCl with an interface mixer operating at 1725 rpm.

In general, when efficient mixing and long settling times were used, there was little product entrainment. For example, with two successive contacts when 2-min mixing times and 5-min settling times were used, aqueous entrainment in the

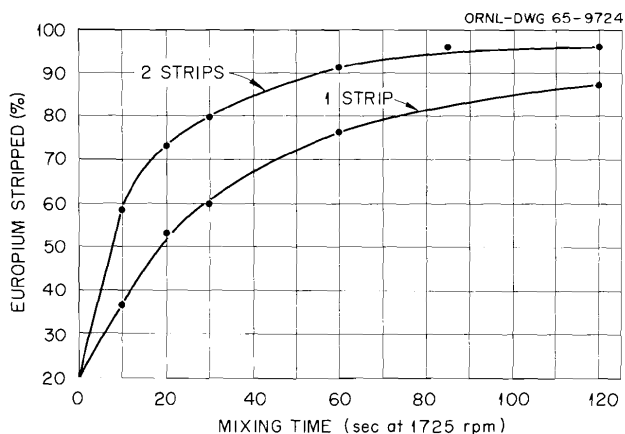


Fig. 5.1. Europium Stripping into 1 *M* HCl from 0.6 *M* Alamine 336·HCl-DEB as a Function of Mixing Times.

organic phase was about 3 to 4 vol %, while europium entrainment was less than 1%. Excessive entrainment of product was observed, however, when the mixing time was decreased from 120 to 10 sec (Fig. 5.1). The necessity for efficient mixing indicated by these data was corroborated by cell 4 operating experience, where product entrainment was reduced from 30–50% to 1–5% in both Clanex and Tramex runs by increasing mixer speeds and strip-to-solvent volume ratios. This did not affect the entrainment of the aqueous phase (1 to 2 vol %) in the organic.

Solubility of Rare Earths in Concentrated LiCl Solution

To reduce solids formation (through hydrolytic precipitation) in cell 4 processing at the CRF, it appeared desirable to increase the acid concentration in adjusted Tramex feed. Since increased acid requires increased salting strength to keep the distribution coefficients of the actinides sufficiently high, the solubility of rare earths in concentrated LiCl solution was investigated over the range of interest. Maximum rare-earth solubilities were not determined; however, the following simulated feeds were completely stable at room temperature:

Constituent	Concentration in Feed 1	Concentration in Feed 2
LiCl	12 <i>M</i>	13 <i>M</i>
HCl	0.2 <i>M</i>	0.3 <i>M</i>
SnCl ₂	0.1 <i>M</i>	0.1 <i>M</i>
Rare earths	44 g/liter	20 g/liter

A feed-adjustment procedure for solutions containing a high concentration of rare earths was also demonstrated in the laboratory. Here, the simulated feed was 6 *M* in LiCl, 0.2 *M* in HCl, and 20 ppm in zirconium. The rare-earth concentration was 20 g/liter. The solution was concentrated by evaporation until the LiCl and rare-earth concentrations were 12 *M* and 40 g/liter respectively. The boiling point was 136°C. This solution was allowed to cool to 100°C and was then diluted with an equal volume of solution 12 *M* in LiCl, 0.2 *M* in SnCl₂, and 0.4 *M* in HCl to produce an adjusted feed that was 12 *M* in LiCl, 0.2 *M* in HCl, 0.1 *M* in SnCl₂, and 20 ppm

in zirconium. It contained 20 g of rare earths per liter. The adjusted feed was clear, and there was no indication of precipitation or instability during preparation.

Cerium Oxidation and Acid Loss by Radiolysis in Tramex Feed Solution

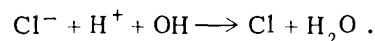
Laboratory-scale experiments are being conducted to study cerium oxidation and radiolytically induced acid loss from high-activity-level Tramex feed. Cerium oxidation results from the radiolytic production of chlorine oxidants and appears to be related to radiolytic acid loss. The rate of depletion of acid and the rate of production of chlorine were determined for Tramex feed solutions both with and without methanol present. Methanol and other reductants are being evaluated as means for preventing cerium oxidation and controlling acid loss. The solutions used in this study were samples of Tramex feed containing ^{242}Cm and corrosion-product impurities in 10 to 12 M LiCl.

In tests to date, methanol has been effective in preventing acid loss in some instances and much less so in others. For example, in one laboratory test with a sample of feed from the CRF, 2½ vol % methanol effectively stabilized free acid for over two weeks. The acid concentration remained nearly constant at 0.05 M during the first 2400 whr/liter of alpha exposure. In a second experiment, feed 0.3 M in HCl became acid deficient after an exposure of 900 whr/liter. This compares with complete acid loss after 700 whr/liter for feed that did not contain methanol. When the concentration of free acid in this experiment had decreased to 0.1 M, the rate of depletion of acid was equal to 0.58 meq/whr, which corresponds to a $G(-\text{H})$ of 1.58. In all cases, a decrease in the rate of depletion of acid was observed with increasing exposure to alpha radiation.

Methanol did inhibit the production of chlorine oxidants in Tramex feed. With 5 vol % methanol present, the concentration of oxidants (calculated as chlorine) appeared to remain nearly constant at less than 0.1 meq/liter; however, when methanol was not present, the concentration of oxidants increased with increasing exposure at the beginning of the experiment, reached a maximum at a dose of 120 whr/liter, and decreased thereafter at a rate of 0.025 meq/whr. The concentration of oxidants was equal to 21 meq/liter at the maximum.

The initial rate of production was approximately equal to 0.6 meq/whr.

The fact that the initial rate of production of oxidants (0.6 meq/whr) is nearly equal to the rate of depletion of acid (0.58 meq/whr) tends to support the hypothesis that initially the acid depletion is predominantly controlled by the reaction:



However, as indicated by the maximum on the chlorine-production curve, two or more competitive reactions are taking place.

Ethanol was also studied. While in the two experiments performed it effectively protected the free acid at concentrations as high as 0.3 M at alpha exposures of greater than 2000 whr/liter, a black insoluble organic layer formed after an exposure of 500 whr/liter.

With respect to preventing the oxidation of cerium, hydroxylamine hydrochloride was added to the scrubbing solutions and showed promise as a reductant. For example, Tramex feed 0.1 M in HCl was contacted with 0.6 M Alamine 336-HCl in diethylbenzene in a batch extraction experiment. The cerium extraction coefficient (E_a^o) was 1.94. The solvent phase was then scrubbed with an 11 M LiCl solution 0.1 M in $\text{NH}_2\text{OH}\cdot\text{HCl}$. An E_a^o for cerium of 0.13 was obtained after 30 sec of contact time, decreasing to an E_a^o of 0.01 after 1 min of contact time. This study is still in progress, and efforts to control acid loss and prevent curium oxidation will be continued.

Solubility of Sodium Nitrate in Clanex Feed

Since the latest shipment of ^{244}Cm - ^{243}Am from Savannah River was about 0.5 M in NaNO_3 , the solubility of NaNO_3 in simulated Clanex feed and its behavior during feed preparation were investigated. The results indicate that it should be possible to handle sodium concentrations as high as 0.5 M in the Savannah River concentrate without increasing the time required for solvent extraction.

It was determined that NaNO_3 solubility is greater than 1.5 M in synthetic feeds 7 M in NO_3^- from $\text{LiNO}_3 + \text{Al}(\text{NO}_3)_3$, and 0.2 M in HNO_3 . This is for feeds that contain 20 g of rare earths per liter and in which the aluminum concentration may vary from 0.33 to 1.33 M.

In a feed-adjustment demonstration, synthetic feed that contained 7 g of rare earths per liter and which was 6 M in HNO_3 and 0.5 M in NaNO_3 was concentrated by evaporation until the NaNO_3 concentration was nearly 5 M (bp = 118°C). The solution was cooled to 105°C, and the 3.5 moles of HNO_3 that remained in the feed were neutralized with dibasic aluminum nitrate. An appropriate amount of LiNO_3 solution was added, the feed volume was again adjusted by evaporation, and 0.2 M HNO_3 was added to the adjusted feed. Final solution concentrations were: NaNO_3 , 1.5 M; LiNO_3 , 1 M; $\text{Al}(\text{NO}_3)_3$, 2 M; HNO_3 , 0.2 M; and rare earths, 21 g/liter.

5.2 CURIUM RECOVERY FACILITY: EQUIPMENT AND FLOWSHEET TESTING

The Curium Recovery Facility in Building 4507 was designed and built to recover gram quantities of americium and curium from irradiated target materials and also from aqueous concentrates received from off-site. The recovered actinides will be used for research and for use in fabricating prototype thermoelectric generators. Provision was made for target dissolution, feed adjustment, solvent extraction, and product conversion to the appropriate chemical system as required. Additional equipment was provided for further purification by ion exchange and for separation of the americium from the curium.

Structural materials were chosen for their corrosion resistance to the nitrate-chloride system featured in the process. The designed system capacity was based on processing 2 g of ^{242}Cm per day. A specific objective of the program included early recovery of nearly 20 g of ^{244}Cm , 4 g of ^{242}Cm , and 20 g of ^{243}Am ; other objectives included testing of the flowsheets developed for separating and recovering these elements from irradiated feed materials.

Status and Progress

Improved equipment has replaced several items found deficient during cold testing. These changes include new Zircaloy-2 mixer-settlers to replace the Homolite ones, tantalum coils to replace Hastelloy C cooling coils in the condensate catch tank, condensers and a scrubber made of tantalum or Zircaloy-2 to replace the glass ones, and more-

rugged manipulators to replace the originals. All polyethylene lines were replaced with stainless steel or Zircaloy-2 tubing, except for the few that could be replaced remotely.

The Zircaloy-2 dissolver system installed in cell 3 was tested with nonradioactive targets and proved satisfactory. As an adjunct to the facility in cell 4, removable boxes housing laboratory-scale equipment for final-product purification and special separations were installed in cell 3. The facility was approved for operation with radioactive materials in November 1964 and has operated for five months, producing 19 g of ^{244}Cm and 4.6 g of ^{242}Cm . Soon a second ^{242}Cm run will be made. The facility will then be placed in routine operation, producing separated ^{244}Cm and ^{243}Am . Up to a milligram of ^{252}Cf will be recovered in early 1966.

Modifications to Equipment

The layout and arrangement of the equipment has been described previously.^{3,4}

The modifications to and replacement of equipment were concerned mainly with durability and materials of construction. The polyethylene tubing failed at sharp bends and in the welds, particularly in areas subject to thermal cycling, and was replaced with stainless steel, Hastelloy C, or Zircaloy-2 tubing. The glass scrubber and condensers were subject to frequent breakage in the glass-to-metal seal-transition pieces and were replaced with equipment made of tantalum or Zircaloy-2.

Experience with the sampler showed that more reliable operation could be obtained by replacing the bottle holder and elevating mechanism with a V-shaped guide behind the needle blocks. This allowed a direct impaling of the sample bottle while it was held by the manipulator.

The corrosion of the original Homolite mixer-settlers was faster than anticipated, especially in 8 M HCl. They were also subject to thermal-stress cracking. When this was discovered, design and construction of the replacement Zircaloy-2 mixer-settlers were accelerated. These new

³F. L. Culler *et al.*, *Chem. Technol. Div. Ann. Progr. Rept. May 31, 1963*, ORNL-3452, pp. 138-43.

⁴F. L. Culler *et al.*, *Chem. Technol. Div. Ann. Progr. Rept. May 31, 1964*, ORNL-3627, pp. 145-47.

mixer-settlers incorporate a pressure-reference reservoir for interface-level control and stream preheaters in the metal block. The glass phase separators were replaced with Zircaloy-2 separators integrally attached to the aqueous-phase outlet. Several other minor design improvements were also made to reduce the chances for air locking.

Many of the critical TRU disconnect clamps were replaced with clamps of the final design. The clamp swing arm is cam actuated by the bolt. In the older design, the swing arm rode a stud free of the nut. Slight corrosion made it difficult to break the swing arm free of the clamp body and move it out of the way of ferrules.

Unit equipment boxes housing laboratory-scale glass equipment for specific operations were made outside the cell and lowered into cell 3 after hot operations were started. Services to these boxes are supplied by temporary jumpers.

Performance of Equipment

Mixer-Settlers. — The mixer-settlers performed well during about five months of operation with radioactive materials. However, one of the mixer drives failed three times. A setscrew in the coupling at the drive-motor box came loose twice; this defect was corrected by replacing the screw with a pin. Also, a Woodruff key sheared in the universal joint on the extraction-bank drive shaft. Consequently, both the scrub and extraction bank were driven from the scrub-bank drive. This drive failed later when a pin came out of one of the universal joints and allowed the shaft to fall out. Then the drive gears were reversed to drive both banks from the extraction-bank shaft. In-cell repairs of the sheared key were made remotely — a spring-steel clip was attached across two universal joints.

Feed-Transfer Pump. — This pump, one of two TRU design installed in the cell, has failed to give satisfactory service. The failures consisted of diaphragm rupture, stuck check valves (fouling with a gummy substance), and recurring leaks at one of the gasketed joints. The dense, viscous feed solution is difficult to pump under any circumstances, and may contain solids as well. The present installation includes a filter in the pump suction line; but the high pressure drop across this filter, coupled with the many valved connections in the suction manifold, which fre-

quently leaked, contributed to the generally unsatisfactory performance of this pump.

Process Equipment. — Tantalum and tantalum-lined equipment has proved satisfactory in service. One of the glass-lined vessels, however, appears to have developed a hole in the lining.

Manipulators. — The rugged-duty extended-reach manipulators were superior to those of lighter construction originally installed, but they require much preventive maintenance to help avoid complete failures, which result in unscheduled halting of in-cell operations. The rapid deterioration of the remote "finger pads" in the cell rendered in-cell handling of tools hazardous. The pads as received were originally glued improperly and fell off after a few days service. Properly glued pads, however, deteriorated rapidly in service, presumably due to hard usage and attack by solvents, and were useless after about a week.

Flowsheet Testing

Chemical problems were introduced by the interaction of corrosion products from the new Zircaloy-2 equipment with the slightly acid solutions used in the original Tramex process. Accordingly, the flowsheet was modified to prevent these corrosion products from passing from Clanex product to Tramex feed. In addition, the process was modified to reduce the concentration of the stripping acid to 1 M because corrosion of the Zircaloy-2 mixer-settlers was unacceptably high when the 8 M HCl strip solution was used. With 1 M HCl, it was possible to back-extract zirconium from the final product with a wash of 0.5 M di-(2-ethylhexyl)phosphoric acid in Amsco. These changes, however, were not entirely successful in operation with radioactive feed materials. A fuller discussion of this and of the use of SnCl₂ as a reductant⁵ to control cerium oxidation and extraction in the Tramex process is given in Sects. 5.3 and 5.5 below.

5.3 SOLVENT EXTRACTION PROCESSING OF ²⁴³Am AND ²⁴⁴Cm

Feed for the process came from the long-term irradiation of 10 kg of ²³⁹Pu at the Savannah

⁵I. D. Eubanks, Savannah River Laboratories, private communication.

River Laboratory (SRL) as a part of the Transuranium Element Program. This material was processed there for separating and recovering the ^{242}Pu . The ^{243}Am - ^{244}Cm that remained was concentrated by a precipitation as double sulfates. A nitric acid concentrate that contained all the rare-earth-element fission products as well as these actinides was then shipped to ORNL.

Status and Progress

So far, a portion of this SRL concentrate, containing 24 g of ^{244}Cm , has been processed to recover about 19 g of ^{244}Cm as purified product meeting specifications; about 19 g of ^{243}Am , recovered along with the ^{244}Cm , was separated and purified. Early runs in this program were developmental, with the objective of testing and modifying the process to optimize it for operations at the even higher radiation levels to follow in processing ^{242}Cm . Off-specification product and miscellaneous process solutions generated during nonequilibrium operation, as well as a spill recovered from the floor of the cell, were successfully recycled for ^{244}Cm recovery. After the campaign, the cell was cleaned and prepared for recovering gram amounts of ^{242}Cm from irradiated $^{241}\text{AmO}_2$ targets, as discussed in Sect. 5.5.

Description of Process

Feed for the solvent extraction system was prepared from the SRL concentrate by evaporating to remove excess water and HNO_3 , neutralizing the remaining HNO_3 with acid-deficient aluminum nitrate, and then adjusting with LiNO_3 to 7.0 M total nitrate and 0.08 M HNO_3 . The actinides and lanthanides in nitrate form were converted to chlorides by processing according to the Clanex flowsheet (Fig. 5.2). In this process, americium, curium, and the rare earths were extracted into 0.6 M Adogen-HCl (tertiary amine hydrochloride) in a diluent of diethylbenzene (DEB). The extract was scrubbed with 7 M LiNO_3 -0.2 M LiCl -0.03 M HCl and then stripped into 1 M HCl. The stripped product was successively scrubbed with 1.0 M Adogen-HCl in DEB and 0.5 M di-(2-ethylhexyl)-phosphoric acid (HDEHP) in Amsco diluent.

Separation of the ^{243}Am - ^{244}Cm from rare earths and other fission products was done according to

the Tramex flowsheet (Fig. 5.3). The feed was prepared by evaporating excess HCl from the Clanex product and making the solution 11 M in LiCl , 0.08 M in HCl, and 0.1 M in SnCl_2 . In early runs, before we adopted SnCl_2 as a reducing agent in the feed,⁵ little decontamination from ^{144}Ce was obtained.

Americium and curium were first extracted into 0.6 M Adogen-HCl in DEB, and the extract was scrubbed with 11 M LiCl -0.03 M HCl and then stripped into 1 M HCl. The strip product was successively scrubbed with 0.6 M Adogen- HNO_2 in DEB and 0.5 M HDEHP in Amsco. The product solution was continuously evaporated to a small volume. Further purification of the ^{243}Am - ^{244}Cm product was accomplished by ion exchange, as described more fully in Sect. 5.4, and the two actinides were separated by precipitating Am(V) as the double potassium americium carbonate, while the curium remained in solution. The separated curium product was then converted to the nitrate form, and, after filtering (30- μ pores), transferred in solution to the Isotopes Division for reduction to the oxide and encapsulation.

Solvent Extraction Performance

After two trial runs, solvent extraction losses of ^{244}Cm averaging 1% of the feed were demonstrated in the Clanex runs (Table 5.1). In the better of the Tramex runs these totaled 0.4%.

Losses during extraction were successfully reduced by increasing the solvent-to-feed ratio to 3/1. Stripping losses were minimized by operating the stripping bank at near flooding conditions. A small amount of entrainment persisted and was recovered for recycle as a settled aqueous phase.

Almost no separation from fission products was obtained in the Clanex process (Table 5.2) except for ruthenium (decontamination factor, 400). In the Tramex cycle, a gross-gamma decontamination factor of 500 was demonstrated; decontamination factors for ^{106}Ru , ^{154}Eu , and ^{144}Ce were 60, 2000, and 3000 respectively.

Interfacial Solids. — One of the most serious problems encountered in the solvent extraction processing has been the formation of interfacial solids, primarily in the extraction contactor. The solids are believed to result from the hydrolysis of Zircaloy-2 corrosion products, but may also be due to silica or hydrolyzable ions. To help

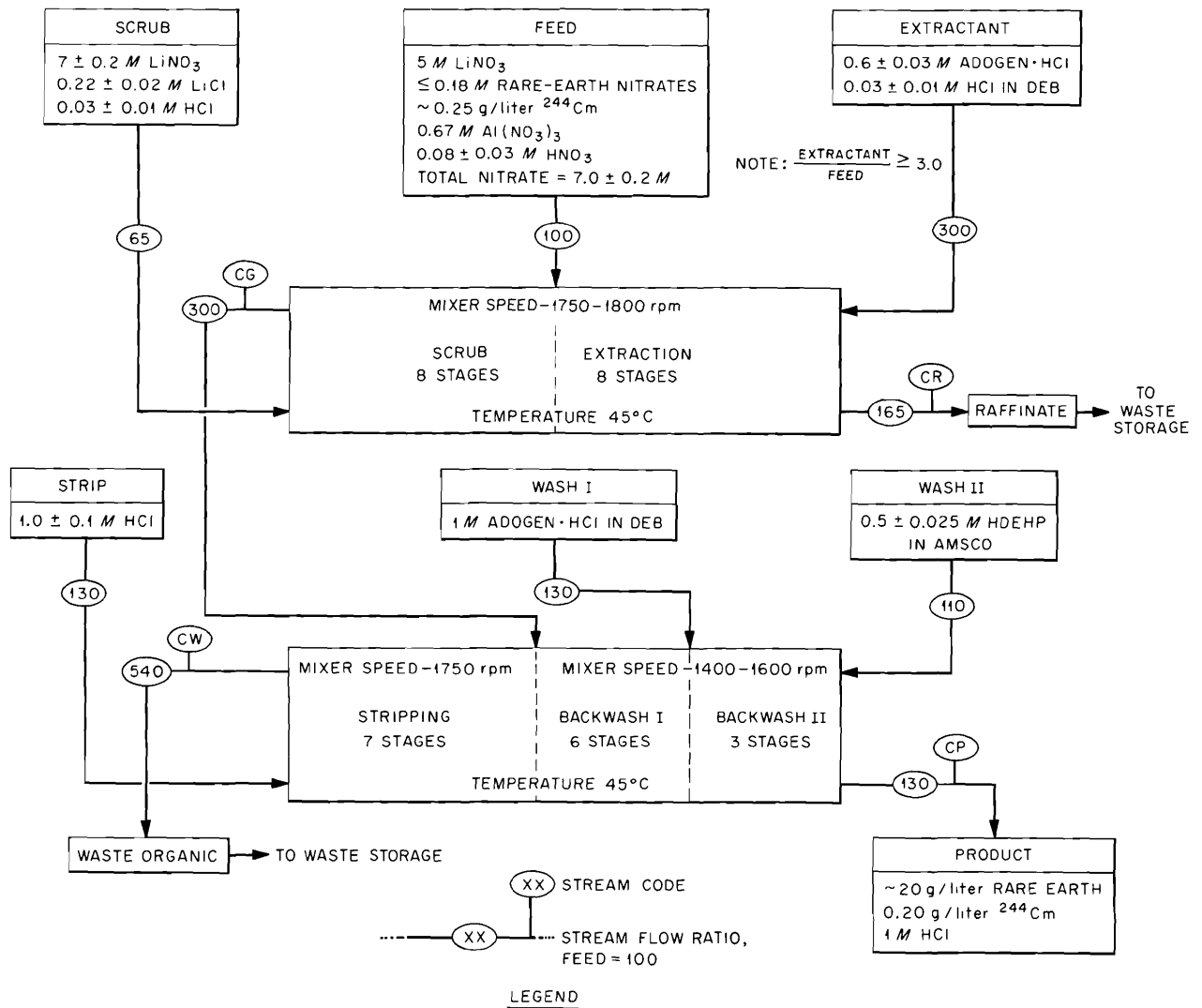


Fig. 5.2. Curium Recovery Flowsheet: Clanex-B.

eliminate this problem, the free acid in the extractant was increased to $0.15 M$ during the last Clanex run. This decreased the rate of solids formation but did not eliminate it completely. A further attempt was made in TR-3 by increasing the free acid in the extractant and in the feed both to $0.2 M$. To compensate for the depression of the curium distribution coefficient by all this acid, the LiCl concentration of the aqueous phase was increased to a nominal $12 M$. The mechanical operation of the mixer-settlers was excellent under these conditions, and the amount of solids formed was greatly reduced. Unfortunately, raffinate

losses exceeded 1%, and it was necessary to decrease the acidity of the extractant to get acceptable raffinate losses.

Separation of Cerium. — Cerium has been the fission product most difficult to remove in the Tramex process. Increasing the scrub/feed flow ratio was not effective in improving the separation from cerium, but incorporating SnCl_2 in the feed as a reductant to hold the cerium in the inextractable trivalent state was successful. However, SnCl_2 has two disadvantages: it is extractable in both valences and is also oxidized by the radiolysis products of the feed solution, which

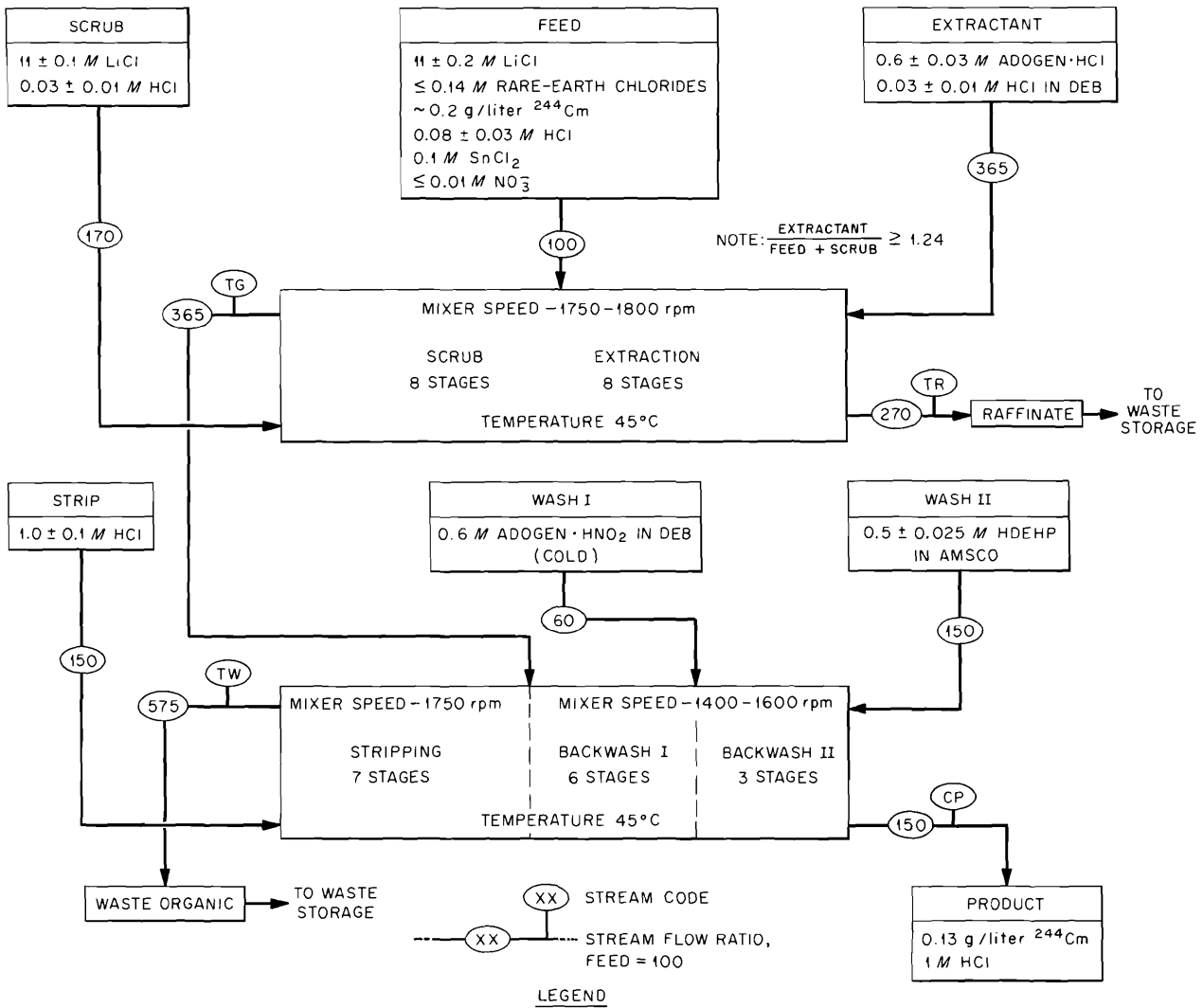


Fig. 5.3. Curium Recovery Flowsheet: Tramex-B.

Table 5.1. Solvent Extraction Losses of ²⁴⁴Cm

	Losses (% of feed)			
	CL-2	CL-3	TR-2	TR-3
Extraction	0.8	0.5	4.2	0.2
Stripping	0.3	0.4	0.2	0.2

Table 5.2. Decontamination Factors: ²⁴⁴Cm Program

	Gross Gamma	¹⁰⁶ Ru	¹⁵⁴ Eu	¹⁴⁴ Ce
CL-2	3		1	1
CL-3	1	400	1	1
TR-2 ^a	15		10	5
TR-2 ^b	200		150	200
TR-3	500	60	2000	3000

^aFirst part of run: no reductant. Process upset also reduced decontamination factors.

^bLatter part of run: SnCl₂ reductant added to feed.

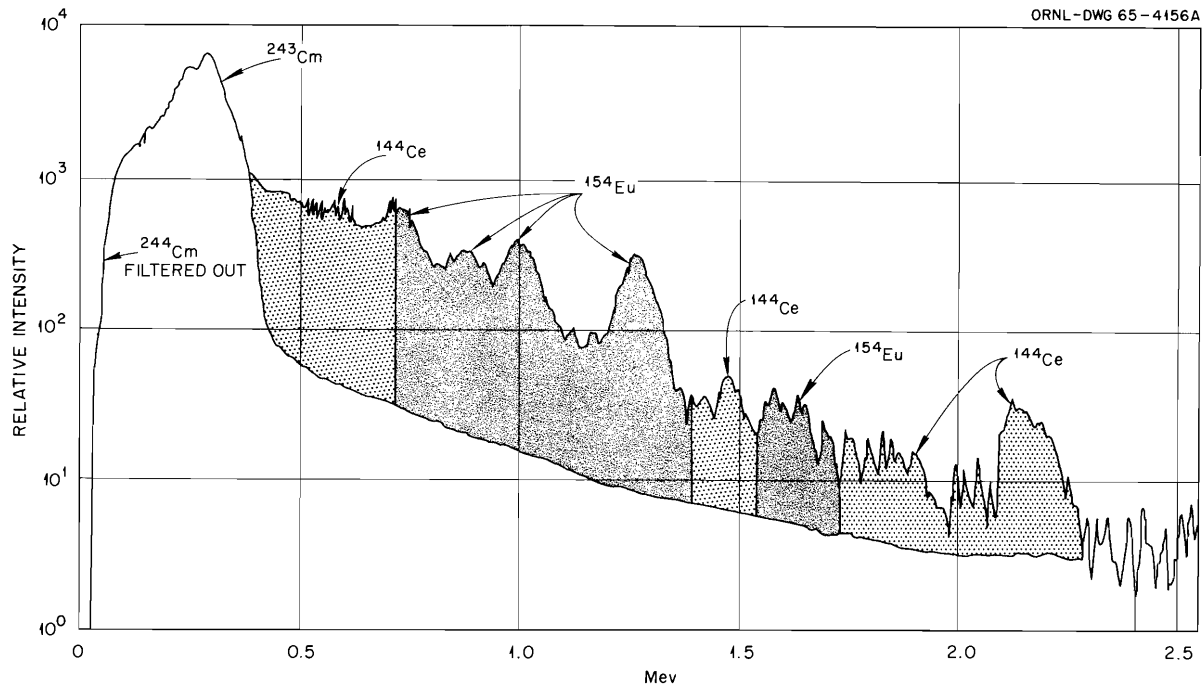


Fig. 5.4. Gamma-Ray Spectrum of ^{244}Cm Product.

Table 5.3. ^{244}Cm Product: Solution Purity

Constituent	Specification	TR-2(A)	TR-2(B)	TR-3
^{244}Cm , g/liter		0.951	0.994	3.74
Ni, g/liter	<1.0	0.2	0.24	0.8
Bi, Pb, Ca, Si (total), g per gram of Cm	<0.05	0.02	0.02	0.02
Other cations (total), g/liter	<1.0	0.10	0.06	0.69
Alkali metals (total), g/liter	<10.0	19.2	7.0	13.1

form at a rate proportional to the power density of the solution.

Radiolytic Effects. — In contrast to results reported in earlier flowsheet development studies,⁶ the presence of 2 vol % methanol in the Tramex feed failed to inhibit destruction of the free acid by radiolysis, or gassing during operations with radioactive feed solutions. However, it satisfactorily inhibited gassing and acid destruction in

product solutions recovered from these feed materials. Methanol may be catalytically destroyed by some contaminant in the feed that is not present in the product solution.

Purity of Product

In the ^{244}Cm product from the last Tramex run, TR-3, the principal gamma emitters were ^{243}Cm , ^{239}Np (daughter of ^{243}Am), ^{154}Eu , and ^{144}Pr (daughter of ^{144}Ce). The latter two had been

⁶F. L. Culler *et al.*, *Chem. Technol. Div. Ann. Progr. Rept. May 31, 1964*, ORNL-3627, p. 118.

removed to the point where they were no longer the principal gamma emitters in the product. A gamma-ray spectrum of the product is shown in Fig. 5.4, as taken through a 1-in.-thick cadmium filter to remove the high-intensity, but very-low-energy, gamma rays from ^{244}Cm and ^{144}Ce .

The chemical purity of the product was satisfactory; the major contaminants were lithium, which enters the product by entrainment of the scrub solution in the pregnant organic, and nickel, which follows curium quantitatively through the Tramex process. Table 5.3 shows the contaminants in three different batches of product. Although this material was transferred as a hydrochloric acid solution to cell 3 for further processing, had it been converted to the nitrate form and transferred into the product shipping container with a reasonable volume of flush solution, it would have met the Isotope Division's specifications for ionic contaminants, as shown in Table 5.3.

5.4 ION EXCHANGE PURIFICATION AND SEPARATION OF ^{243}Am - ^{244}Cm

During initial solvent extraction processing, americium-curium product was obtained which required additional purification. Glass ion exchange equipment was therefore installed in cell 3 of the Curium Recovery Facility, and additional decontamination was obtained by LiCl anion exchange. In addition, ^{244}Cm was separated from ^{243}Am by the carbonate-precipitation method.

Status and Progress

A total of 16.6 g of ^{244}Cm was purified by LiCl anion exchange, separated from ^{243}Am , and transferred to the Source Fabrication Facility of the Isotopes Division for incorporation into an experimental heat source and for distribution to other AEC laboratories.

The americium content in the curium product was 0.8%, and radioactive contaminants were reduced to a degree equivalent to less than 20% of the curium gamma activity. The separated ^{243}Am (17.3 g) was transferred to Building 3508 for further purification and conversion to the oxide. This purified americium oxide was then distributed to several other AEC laboratories for use in research programs. An additional 1.9 g each of ^{244}Cm and of ^{243}Am were purified and will also be used for process development.

Ion Exchange Purification

The americium and curium were purified in a number of ion exchange runs performed in a glass column 2 in. in diameter and 14 in. high, packed with 400 ml of Dowex 1-X8 resin (100 to 200 mesh). Flow rates of $0.5 \text{ ml min}^{-1} \text{ cm}^{-2}$ were used, and the column was kept at 65°C .

Americium, curium, and rare earths were loaded on the resin from 12 M LiCl-0.1 M HCl-2 vol % CH_3OH . Contaminant rare earths were eluted with 5 column displacement volumes of 10 M LiCl-0.1 M HCl-0.1 M $\text{NH}_2\text{OH}\cdot\text{HCl}$ -5 vol % CH_3OH , and ^{243}Am - ^{244}Cm product was then eluted with 2 displacement volumes of 8 M HCl.

The americium and curium as received from cell 4 were contained in about 4 liters of 6 M HCl. Column feed was prepared by concentrating this solution by evaporation to a volume of 250 ml. One liter of 12 M LiCl was added, and evaporation was continued until the LiCl concentration was 12 M (137°C). Concentrated HCl was added to make the feed 0.1 M in free acid. The feed was cooled to 50°C , and 2 vol % methanol was added to prevent acid loss due to radiolysis.

Hydroxylamine hydrochloride was required during the rare-earth elution to prevent oxidation of cerium to Ce^{4+} , which does not elute in 10 M LiCl. The last two column volumes during rare-earth elution were collected separately to detect curium breakthrough; typically the last column volume contained about 2% of the curium and was sometimes slightly contaminated with rare earths.

Of the ionic contaminants present in the feed, Ni, Fe, Cr, Co, and Cu loaded on the column. Nickel and copper were eluted with the rare earths, and iron remained on the column during curium elution. This behavior resulted in separation from all impurities except chromium and cobalt. However, when impurities were present in sufficient concentration, satisfactory rare-earth separations could not be obtained. It was found that 1 g of nickel would completely load the resin and drastically inhibit curium loading. When large amounts of impurities were present, they were partially removed before the column feed was prepared. Precipitation of americium-curium with excess NH_4OH resulted in their separation from Ni, Co, and Cu, which form soluble amine complexes.

During this processing, there was no indication of resin degradation, although the curium band on the column routinely provided a radioactivity level

equivalent to about 400 to 600 w/liter. Three consecutive runs with the same resin were possible before the pressure drop across the column increased. Two percent methanol by volume effectively stabilized the acid concentration of the feed and greatly inhibited the formation of radiolytic gas.

Separation of ^{243}Am from ^{244}Cm

Americium-243 was separated from ^{244}Cm by oxidizing the Am^{3+} to Am^{5+} with NaOCl or $\text{K}_2\text{S}_2\text{O}_8$ in the presence of 3 M K_2CO_3 . The oxidized americium precipitated as $\text{K}_3\text{AmO}_2(\text{CO}_3)_2$ and was recovered by filtration. The curium in the filtrate was precipitated as the hydroxide. The $\text{K}_3\text{AmO}_2(\text{CO}_3)_2$ and the $\text{Cm}(\text{OH})_3$ were then dissolved in nitric acid and stored separately.

Purified column product was first precipitated with NaOH to remove excess acid, lithium, and chromium. This hydroxide was a dense crystalline-appearing material which filtered readily. Following filtration, the hydroxide was dissolved in a minimum of 6 M HCl and added slowly to a rapidly agitating 3 M K_2CO_3 solution. The solution was digested at 80°C until americium and curium were completely dissolved as carbonate complexes. A 200% excess of either NaOCl or $\text{K}_2\text{S}_2\text{O}_8$ was added, and the mixture was digested for 2 hr at 80°C . Both oxidants effectively oxidized the Am^{3+} to Am^{5+} , and the pentavalent americium precipitated as $\text{K}_3\text{AmO}_2(\text{CO}_3)_2$ during the digestion step. However, when NaOCl was used, a small amount of americium was apparently oxidized to Am^{6+} , which does not precipitate. About 99.5% of the americium was removed by precipitation, leaving only 0.5% in solution, and about 1% of the curium was carried by the precipitate.

The $\text{K}_3\text{AmO}_2(\text{CO}_3)_2$ was a dense light-tan precipitate and filtered readily. The filter cake was washed with 3 M K_2CO_3 and then dissolved in 2 M HNO_3 . The curium content of this material was reduced from 1.0 to 0.02% by a second oxidation-precipitation cycle, and final conversion to AmO_2 was obtained by oxalate precipitation from the nitrate solution followed by calcination at 800°C .

Pentavalent ^{243}Am proved to be surprisingly stable in nitric acid solution. Spectrographic examination of 1 M HNO_3 solutions indicated a half-life of 18 days for Am^{5+} at 25°C . This sta-

bility seriously inhibited oxalate precipitation of the americium. Only about a third of the americium precipitated after the oxalic acid was added to the $\text{AmO}_2\text{NO}_3\text{-HNO}_3$ solution, and the precipitate was lemon-yellow, in contrast to the reddish-tan of Am^{3+} oxalate. The americium remaining in solution was completely stable for days and was finally reduced and precipitated by adding $\text{NH}_2\text{OH}\cdot\text{HCl}$ and then heating.

Most of the 17.3 g of ^{243}Am which was separated from curium was converted to oxide. Emission spectrography indicated that it was more than 99.9% pure.

Curium-244, which remained in the K_2CO_3 filtrate, was recovered by precipitation with NaOH . The precipitated hydroxide was filtered and dissolved in 2 M HNO_3 . The high pH provided by NaOH was necessary for this precipitation. Ammonium hydroxide was not effective even when concentrations as high as 4 M were used. Equipment difficulties encountered during the filtration of one batch of $\text{Cm}(\text{OH})_3$ were primarily responsible for the potassium and sodium present in the final curium product (Table 5.4). A glass frit plugged during filtration, and it was necessary to dissolve the curium hydroxide in nitric acid before all the K_2CO_3 solution had been removed.

Several interesting effects were noted during this processing: Purified ^{244}Cm was stored in 2 M HNO_3 at an activity level of about 50 w/liter for as long as six weeks in a glass container. During this time, about 100 cm^3 of silica accumulated due to alpha attack of the glass. The silica was granular and very easy to remove by filtration. Nitric acid solutions of ^{244}Cm did not evolve noticeable amounts of radiolytic gas; however, gas evolution in HCl solution was severe. Methanol, which does not appear to be useful in suppressing radiolytic gas formation when ionic impurities are present, was quite effective in reducing gas formation in HCl solutions of pure ^{244}Cm .

Purity of Product

Before processing, the Savannah River feed concentrate had a gross-gamma-to-gross-alpha ratio of 4.3×10^{-2} . Two cycles of solvent extraction processing produced product having gamma-alpha ratios varying from 3.1×10^{-3} to 8.9×10^{-5} , and this ratio was further reduced to 1.5×10^{-5} by ion exchange purification. The only sources of

Table 5.4. Summary of Contaminants in Cell 4 Products and in Curium Product After Final Purification

	Source Solutions from Cell 4 Processing					Final ^{244}Cm Product
	TR-1	TR-2A	TR-2B	TR-3	TR-3R	
Curium and ionic contaminant content, g ^{244}Cm	1.16	4.03	2.71	9.51	1.56	16.62
K						48.9
Li	6.4	86	19	38		1.9
Na				3.6		13.2
Al		0.05	0.06	0.02		<0.10
Ca	0.02	0.10	0.02	~1	0.06	~0.10
Co		0.2	0.06			
Cr		0.03	0.03	0.1	0.3	
Cu		0.05	0.1	0.1	0.6	
Fe		0.05	0.06	0.6	0.3	0.09
Mg		0.01		0.01		
Mo		0.02	0.03	0.06	0.3	
Mn		0.02	0.03			
Ni	1.3	~1	1.2	2.6	2.0	<0.10
Zr				1.3	0.1	~0.10
Rare earths	2.3	29.1	1.6	1.9	0.5	
Gross γ /gross α	8.9×10^{-4}	3.1×10^{-3}	2.5×10^{-4}	8.9×10^{-5}	1.3×10^{-4}	1.5×10^{-5}

gamma rays detectable in the final product were ^{243}Am and ^{244}Cm . The ^{243}Am content in the ^{244}Cm product was 0.8%. Detectable ionic impurities before and after processing are shown in Table 5.4. The alkali-metal impurities were introduced during americium-curium separation; and since these ions will be removed during subsequent curium fabrication procedures, no effort was made to remove them at this stage.

5.5 PROCESSING OF $^{241}\text{AmO}_2$ TARGETS

Gram quantities of ^{242}Cm are being prepared for heat sources. The large quantity of aluminum in the irradiated ^{241}Am targets and the high specific activity of the ^{242}Cm forced some changes in the flowsheets that had been tested with ^{244}Cm .

Status and Progress

Six irradiated $^{241}\text{AmO}_2$ targets, containing initially 21.4 g of ^{241}Am , were processed for

recovery of the ^{242}Cm . The residual ^{241}Am was not separated from the curium. At the time of dissolution, the targets contained 6.75 g of ^{242}Cm , which decayed to 5.44 g during the processing period. Of this amount, 3.56 g was transferred to the Isotopes Division, and 1.13 g was transferred to cell 3 of Building 4507 for development work.

At the end of this campaign, the facility was placed in standby, and preparations were made to receive another shipment of ^{243}Am - ^{244}Cm from the Savannah River Plant. Early in the new fiscal year, a second ^{242}Cm campaign will process about 14 g of ^{242}Cm .

Description of Process

Six irradiated $^{241}\text{AmO}_2$ targets were dissolved in HCl and processed for ^{241}Am - ^{242}Cm recovery. The targets each consisted originally of about 3.6 g of ^{241}Am as the oxide, incorporated in an aluminum-powder matrix. After irradiation, each contained about 1.1 g of ^{242}Cm and 1.0 g of ^{241}Am . After the targets had been dissolved in

dilute HCl, the solution was converted to the nitrate form and processed through a Clanex cycle to remove the aluminum. The Clanex product was then processed successively through two Tramex cycles. The final americium-curium product was converted to the nitrate and transferred to the Isotopes Division for conversion to the oxide and encapsulation. The solvent extraction flowsheet conditions were modified to adapt and optimize them for processing ^{242}Cm solutions at power densities of 6 to 16 w/liter.

Dissolution of Target. — Three targets were dissolved at a time. They consisted of 1.124-in.-OD by 5-in.-long aluminum cans containing the aluminum- AmO_2 compact. Each rod contained about 200 g of aluminum, and the aluminum basket used for lowering each target into the dissolver added an additional 22 to 24 g per target. The dissolution rate was controlled by metering 8 M HCl into the dissolver, which was held at 80°C. There was initially enough water present to cover the three targets. After all the acid was added, digestion at the reflux temperature was continued for 2 hr. The evolved hydrogen was continuously diluted to below the explosive limit by purging the dissolver and solution with air throughout the dissolution period. As the targets dissolved, the off-gas was continuously monitored for alpha-particle contamination and radioiodine. Although a moderate rise in both was observed, the amount of iodine detected in the off-gas and the absence of iodine in the solutions indicated that the off-gas scrubber was operating at an efficiency better than 99%.

Feed Adjustment. — Because of the high aluminum content of the targets, adjustment of the dissolver solution to produce a stable Tramex feed was impossible without excessively diluting the dissolver solution. Instead, the solution was converted to the nitrate form and processed through a Clanex cycle, which has a much greater capacity for aluminum.

Clanex. — After the targets were dissolved, the 8 M HCl solution was evaporated to about half its volume and added in small increments to 15.8 M HNO_3 , held at 85°C. After each portion had been added, the HCl was boiled off. Following this, incremental additions of HNO_3 were made and then boiled off until the chloride content of the residual solution was less than 100 ppm. The excess acid remaining was neutralized with dibasic aluminum nitrate (Diban), after which the

total nitrate concentration was brought to 7.0 M with LiNO_3 .

Tramex. — The actinides and lanthanides in the chloride Clanex product were concentrated by evaporation, and LiCl was added to bring the salt strength to 11 M. The free HCl was adjusted to 0.2 to 0.4 M, and the SnCl_2 concentration to 0.1 M. Because of the high power density of the target feed solution (about 18 w/liter), acid destruction was rapid; consequently, the acid concentration in the remaining feed was adjusted periodically. Similarly, the SnCl_2 concentration was also adjusted periodically. The actinide products from the first two Tramex runs were combined and converted to Tramex feed, but in the final run the power density of the solvent extraction feed was limited to about 6 w/liter. The feed stock was heated to the boiling point, 137°C, just prior to use (to remove Cl_2), and a portion was transferred to the feed head tank, where it was diluted with two volumes of a 10.8 M LiCl–0.15 M SnCl_2 –0.4 M HCl solution. The size of the batch was limited to give a maximum exposure of the reductant to ionizing radiation of 600 whr per equivalent of SnCl_2 in the time required to process that portion of the feed.

Solvent Extraction

The Clanex flowsheet (Fig. 5.2) was modified to obtain improved ^{95}Zr – ^{95}Nb separation in processing the target feed solutions. This consisted in (1) eliminating LiCl and HCl from the scrub solution and (2) substituting 0.6 M Adogen- HNO_3 for Adogen-HCl in the extractant. Increasing the HDEHP concentration to 0.8 M and using diethylbenzene (DEB) as diluent in wash II were done as a matter of operating convenience. The only change in the Tramex flowsheet (Fig. 5.3) was to increase the concentration of HDEHP in the DEB to 0.8 M for wash II.

Process Losses. — Solvent extraction losses are shown in Table 5.5. Extraction losses in the Clanex cycle averaged less than 0.01% of the feed; in the Tramex cycle they averaged 1.2%. Stripping losses averaged 0.35% in the Clanex cycle and 0.77% in the Tramex; in either case, the stripping losses were more a function of the settling time of the organic waste than of contactor conditions. The settled aqueous phase was withdrawn from the spent organic waste and held for later recycle to the process.

Decontamination Factors. — The decontamination factors obtained are summarized in Table 5.6. Although decontamination from ^{103}Ru , ^{95}Zr - ^{95}Nb , and ^{140}La was adequate, that from ^{144}Ce was low despite the addition of reductant to the feed. This is attributed to the rapid consumption and destruction of the reductant by direct radiolysis and by radiolysis products of the solution.

Niobium Contamination. — The reduction in ^{95}Zr - ^{95}Nb decontamination observed in the second series of Clanex-Tramex runs (CL-TR-5) is attributed to their plating out on the equipment and subsequent redissolving later in the runs. Although they were almost undetectable in the product in the first Tramex run and throughout about 90% of the second, their sudden appearance at the end of the run resulted in the lower values reported.

In the final run, separate measurements were made of the ^{95}Zr and ^{95}Nb activities. These

measurements supported the belief that the final product was contaminated during a process upset that caused ^{95}Nb to be carried into the product by some finely divided solids. During the first three-fourths of the run there was no indication of ^{95}Nb in the product.

Volatilization of Ruthenium. — The low ^{103}Ru decontamination factor obtained by solvent extraction in run TR-6 was mainly due to the fact that most of the ruthenium had already been removed by another mechanism. It came about this way: The feed-adjustment procedure in this run included periodic acidification and evaporation of the remaining feed concentrate to a solution that boiled at 137°C . The highly oxidizing radiolysis products that formed as a result of these successive adjustments oxidized the ruthenium to a volatile species, which was then collected in the condensate.

Table 5.5. ^{242}Cm Solvent Extraction Losses

	Loss (%)				
	CL-4	CL-5	TR-4	TR-5	TR-6
Extraction	<0.01	<0.01	1.1	1.6	0.77
Stripping	0.32	0.38	0.06	1.1	0.37

Quality of Product

Results of Chemical Analysis. — The aqueous ^{242}Cm product (chloride solution) was reduced to a small volume by evaporation and then converted to the nitrate system by successive additions of 8 M HNO_3 , evaporating to the original volume after each addition. This was continued until the chloride content was less than 100 ppm. When

Table 5.6. Decontamination Factors: ^{242}Cm Program

	Gross Gamma	^{103}Ru	^{95}Zr - ^{95}Nb	^{140}La	^{144}Ce
CL-4	10	10	100		
TR-4	20	40	3.6×10^3	>100	~1
Across both cycles	200	400	4.6×10^5	>100	~1
CL-5	10	10	400		
TR-5	15	30	200 ^a	>100	~1
Across both cycles	150	300	9.0×10^3	>100	~1
TR-6 ^b	15	~1 ^c	$>3 \times 10^3$ - ~700 ^d		80

^aClanex product contaminated with Zr-Nb during Tramex feed adjustment, which was conducted in the dissolver vessel.

^bTramex products from TR-4 and -5 combined and processed through a second Tramex cycle.

^cAn ^{103}Ru decontamination factor of ~10 was obtained in the feed adjustment step prior to solvent extraction.

^dIn TR-6, Zr and Nb activities were measured separately.

this point was reached, evaporation was continued to a small residual volume to reduce the HNO_3 content as much as possible. After filtration and adjustment to the desired volume with the water rinses used for clearing the transfer lines, the composition of the final product solution was that shown in Table 5.7, which includes, for comparison, the product specifications, all of which were met.

Residual Fission Products. — The gamma-ray spectrum of the final ^{242}Cm product (Fig. 5.5) shows that small amounts of ^{103}Ru , ^{144}Ce , and ^{95}Nb remained. As in the case of ^{244}Cm , the most prominent photopeaks were due to ^{243}Cm , while the very-low-energy peaks from ^{242}Cm and ^{141}Ce were filtered out. Curium-242, unlike ^{244}Cm , has measurable photopeaks in the vicinity of 0.6 and 0.9 Mev. The fission product gamma activities are of importance only as they compare with these photopeaks and with the long "smear" of photons at higher energies due to the spontaneous fissioning of ^{242}Cm . When averaged over an appropriate region of the spectrum, the fission product gammas had the intensity shown in Table 5.8, expressed as percentages of the curium gamma

Table 5.7. ^{242}Cm Product Solution Purity

Constituent	Specification	Product
^{242}Cm , g/liter	0.25 ^a	0.23
HNO_3 , M	1–4	2.5
Cl^- , g/liter	<0.1	<0.04
Ni, g/liter	<1	0.28
Bi, Pb, Ca, Si (total), g per gram of Cm	<0.05	~0.07 ^b
Alkali metals (total), g/liter	<10	4.0
Other cations (total), g/liter	<1	0.12
Suspended solids, g per gram of Cm	<0.01 ^c	

^aLimits energy level to ≈ 30 w/liter.

^bOnly calcium and lead were reported, these at the limit of detection. It is believed that the lead was a contaminant in the sample.

^cTo be filtered through a $30\text{-}\mu$ -pore filter at time of transfer.

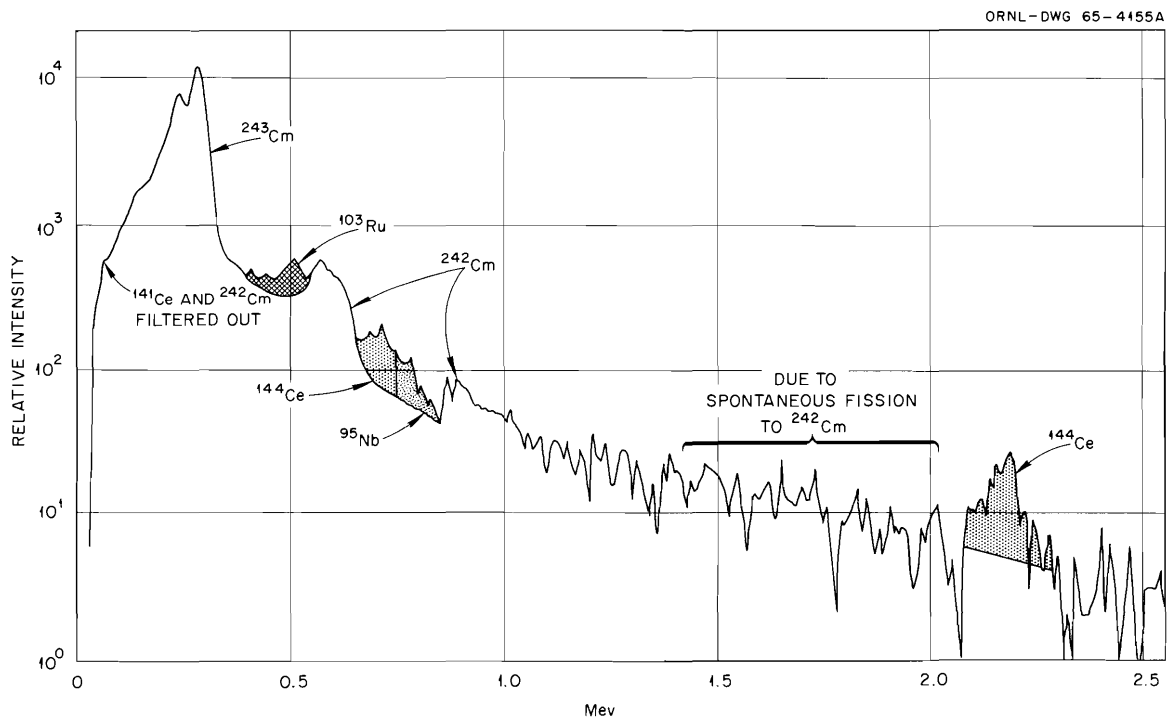


Fig. 5.5. Gamma-Ray Spectrum of ^{242}Cm Product.

Table 5.8. Fission Product Activity in ^{242}Cm Product

Energy Range (Mev)	Principal Fission Products	Percent of Curium Gamma Radioactivity
0.4–0.61	^{103}Ru	22
0.61–0.75	^{144}Ce	34
0.75–0.90	^{95}Nb	37
2.0–2.5	^{144}Ce	70

activity in the corresponding region of the spectrum. This degree of purity was entirely satisfactory for this initial campaign.

5.6 DEVELOPMENT OF ALTERNATIVE PROCESSES: SEPARATION OF LANTHANIDES AND ACTINIDES

Talspeak Process

Laboratory studies have continued to further develop and improve the Talspeak⁷ process for separating trivalent actinides from lanthanides by preferential extraction of the lanthanides with di-(2-ethylhexyl)phosphoric acid (HDEHP) from lactic acid solutions containing sodium diethylenetriaminepentaacetate (Na_5DTPA). This process appears to be quite promising, especially for isolating americium-curium, because of the large separation factors between lanthanides and americium-curium and because the solutions can be handled in existing extraction facilities constructed of stainless steel. Large-scale tests at high activity levels have not yet been made because the Curium Recovery Facility, which uses the Tramex process, had been designed and was being built when the Talspeak process was discovered.

Studies of the process during the last year included determination of einsteinium and fermium distribution coefficients, investigation of the behavior of ionic contaminants, demonstration of the process in laboratory countercurrent extraction runs, and investigation of a tributyl phosphate extraction method to prepare Talspeak feed.

⁷An acronym for "trivalent actinide-lanthanide separation by phosphorus reagent extraction from aqueous complexes."

Group Separation

Information on the relative extractabilities of the actinides and lanthanides has been extended to include einsteinium and fermium (Fig. 5.6). Since these two elements are slightly less extractable than californium, actinide-lanthanide group separation is determined by the separation factor between neodymium, the least extractable lanthanide, and californium, the most extractable transplutonium element. Extraction with HDEHP gives slightly better group separation than extraction with 2-ethylhexylphenylphosphoric acid [$\text{HEH}(\phi)\text{P}$].

Demonstration of Process

Process conditions were modified for group separation with feeds containing high concentrations of lanthanum, which is added as a carrier when americium, curium, and rare earths are recovered from dilute solutions by precipitation of mixed double salts with sodium sulfate. The experimental flowsheet shown in Fig. 5.7 was tested by a series of continuous countercurrent runs in mixer-settlers with feeds containing 20 g of lanthanum per liter spiked separately with tracer americium, lanthanum, and samarium, and with small groups of other elements at the 1-g/liter level. High yields of americium and high decontamination from lanthanum and samarium were obtained, as predicted from previous data. Decontamination was high from Cr, Co, Cu, Cd, Fe, Pb, Mn, Mo, and Ni, lower from Al and Sr, and poor from Ba and Zn. Silver and zirconium precipitated from aqueous process solutions containing DTPA.

Preparation of Talspeak Feed

Extraction of lanthanides and trivalent actinides into 1 M tributyl phosphate in diisopropylbenzene diluent from 2.0 M $\text{Al}(\text{NO}_3)_3$ followed by stripping with 1 M lactic acid can be used to prepare feed for the Talspeak process. This method eliminates the need for adding large amounts of lanthanum carrier, as is done in the sulfate precipitation method. Distribution coefficients were measured in batch equilibrations to determine the behavior of americium, lanthanides, and possible ionic contaminants. Americium and lanthanide extrac-

tion coefficients were greater than 10.0, and stripping coefficients were greater than 10,000. Good decontamination should be obtained for the following elements since extraction factors were

low (<0.0001 to 0.11): Al, Ba, Cr, Co, Pb, Mn, Mo, Ni, Ag, Zn, Cu, Fe, Na, and Sr. Zirconium precipitated on contact of the extractant with the aluminum nitrate solution.

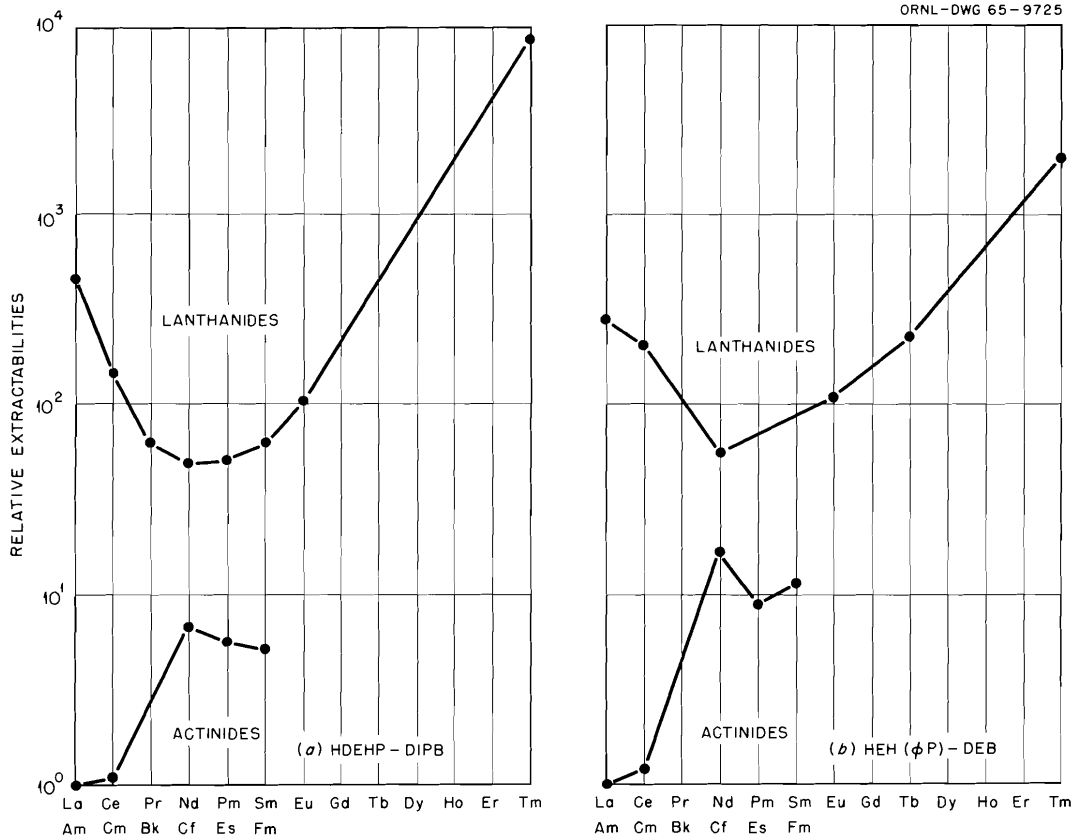


Fig. 5.6. Relative Lanthanide-Actinide Extractabilities by HDEHP and HEH(φP) from Lactic Acid-DTPA Solutions.

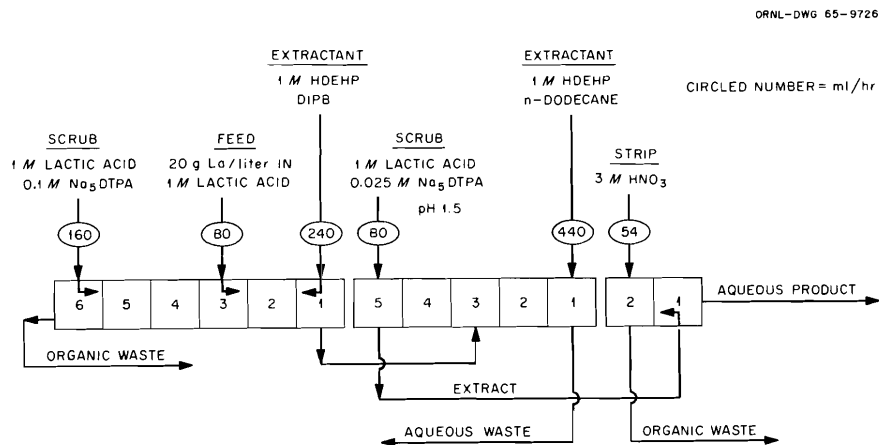


Fig. 5.7. Talspeak Flowsheet for Purifying Americium.

6. Development of the Thorium Fuel Cycle

6.1 ^{233}U STORAGE AND DISTRIBUTION FACILITY

Oak Ridge National Laboratory serves as a storage and dispensing center for reactor-produced ^{233}U nuclear fuel. Expanded and improved storage, purification, and handling facilities were added in Building 3019 to better discharge this responsibility. Five cylindrical storage tanks with a nominal capacity of 250 gal each are available to store ^{233}U nitrate solutions (Fig. 6.1). The tanks are 3 ft in diameter and 5 ft long.

Separate tanks permit the storage of ^{233}U solution according to the level of ^{232}U contaminant present, thereby allowing the material with a low ^{232}U content to be kept separate. Four hundred kilograms of ^{233}U may be stored at a criticality-approved concentration of 180 g of ^{233}U per liter with 70%-full tanks; presently, however, the concentration is kept to a more convenient 100 g/liter.

The tanks are made of type 304L stainless steel and depend on fixed nuclear poison present in the form of borosilicate-glass Raschig rings, which fill each tank and the emergency catch pan under the tanks. The boron content and isotopic ratio of the glass are carefully specified; it must contain 11.8 to 12.8% B_2O_3 , with the ^{10}B -to- ^{11}B ratio equal to 0.25. The rings are $1\frac{1}{2}$ in. in diameter, $1\frac{3}{4}$ in. long, and 0.219 in. thick. Thirty-one percent of the volume is occupied by the randomly packed rings.

The storage tanks are unit shielded by 4 in. of lead and are in an area that has $3\frac{1}{2}$ -ft-thick concrete walls. Future expansion is possible in space adequate for an additional three and possibly four tanks identical to those presently installed.

A 1-kg/day single-cycle, two-column solvent extraction facility was installed in an alpha-contained laboratory located in the gallery of Building 3019. This system augments the existing Thorex solvent extraction system, which can process 6

kg/day of ^{233}U . The small-scale columns are of type 304L stainless steel with a glass end, filled with 16-gage perforated pulse plates on $\frac{1}{4}$ -in. spacing. A rising-film evaporator capable of concentrating final product to 200 g/liter is included. The first-cycle aqueous feed and aqueous raffinate tanks are unit shielded with 4 in. of lead. It may also be necessary to lightly shield the extraction column.

Dry-solid storage space capacity was increased to about 100 kg of ^{233}U as an oxide encapsulated in welded aluminum cans 2.77 in. in outer diameter and 6.5 in. long. Eight additional storage wells (5 in. in outer diameter and 12 ft long, lined with 4-in. IPS pipe) were drilled from the penthouse in Building 3019 into the wall between cells 4 and 5. A similar set of nine holes 8 ft 3 in. long was already available.

6.2 DEVELOPMENT OF THE SOL-GEL PROCESS

The inherent simplicity of the sol-gel process for preparing ceramic reactor fuels provides an incentive for increasing its versatility. It appears that ceramic fuel bodies suitable both for vibratory compaction into metal tubes and for inclusion in various metal and ceramic matrices can be produced readily by the sol-gel process. Process development during the past year included studies of methods to control the porosity of the sol-gel particles, to prepare zirconia by sol-gel techniques, and to prepare thorium nitride.

Attempts to Control the Porosity of Sol-Gel Particles

A small percentage of voidage in sol-gel fuel particles may be desirable as traps for fission

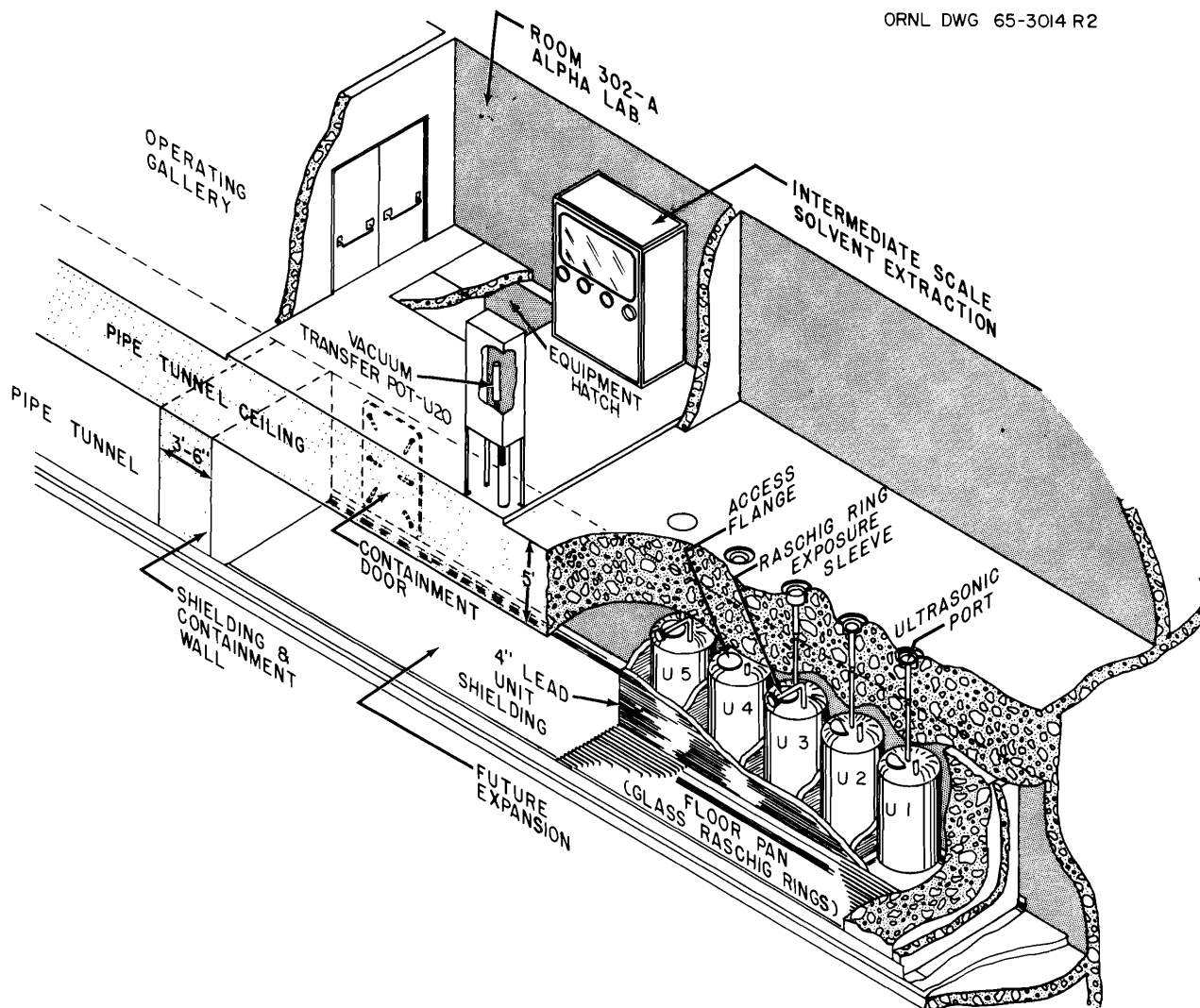


Fig. 6.1. ^{233}U Storage and Purification Facility.

product and other gases. It may also be useful as "sinks" for relief of strains generated by thermal and irradiation-induced stresses and for pressures on the element generated by accumulation of gas. Of equal importance is the fact that included porosity may speed up dissolution rates of the fuel by providing greater surface area.

Two methods have been investigated for producing porosity in sol-gel oxides. In one, a carbonaceous material (e.g., lampblack) was blended in the sol prior to gel formation. On drying and firing, the carbon was oxidized to CO or CO₂ and generated holes whose size and number is a function of the type and amount of carbonaceous material added. In the other method, incomplete firing was used,

thereby leaving porosity which had not been sintered out.

In the method where carbon was added to the ThO₂ sol, fragments fired in Ar-4% H₂ were produced having porosities proportional to the amounts of carbon added. Although the thorium oxide product was discolored (gray to black) instead of the normal white, the carbon content was less than 50 ppm. Some properties of the uranium-thorium oxide so prepared are summarized in Table 6.1. The open porosities (right column) suggest the extent to which acid may be able to contact oxide surface during dissolution. The rate of dissolution is expected to be related to the open porosity and to the surface area. A carbon-to-thorium atom

Table 6.1. Properties of Uranium-Thorium Oxide Containing Controlled Porosity

Carbon-to-Thorium Atom Ratio ^a	Uranium Content (wt %)	Density (g/cm ³)				Open Porosity ^d	
		By Mercury Porosimetry		By helium Pycnometry	(vol %)	(av)	
		Bulk ^b	Particle ^c				
0.0835	2.74	9.16	9.53	9.92	3.95		
0.0835	2.69	9.56	10.02		4.60	3.89	
0.0835	2.88	9.22	9.52	9.57	3.12		
0.0417	2.75	9.75	9.86		1.15	1.43	
0.0417	2.71	9.59	9.76	9.77	1.71		
0.0208	2.81	9.67	9.83	9.85	1.61	1.09	
0.0208	2.68	9.59	9.64	9.71	0.56		

^aCarbon added to the sol in preparation; the carbon content of the product was less than 100 ppm in all cases.

^bOnly gross voids and spaces between particles filled with mercury at 1 atm.

^cPores (diameter = 0.022 μ) within particles filled with mercury at 545 atm.

^dSpace within solid filled by mercury at 545 atm; calculated from the difference between bulk and particle densities.

ratio of 0.0417 would probably be preferred within the group listed in the table because it would be likely to pack to a density of 86% of theoretical and yet dissolve 5 to 15 times as fast as oxide without porosity built in.

In the method where no impurity such as lampblack was added to the preparation, the basic sol-gel procedure for preparing dense ThO₂ particles was followed up to the final firing step, and final firing temperature was the variable studied. Three preparations were fired in air at 1150, 1000, and 900°C respectively. The properties of the products obtained are shown in Table 6.2.

In these preparations, the bulk density (by immersion in mercury) and particle densities (by mercury intrusion) did not appear to be very reliable criteria for the accessibility of the oxide to the dissolvent. A water-absorption test was applied to samples ground to -100 mesh. The amount of water required to immobilize or "set" a sample of powder was determined by titration, and the results are given below.

Preparation Firing Temperature (°C)	Water Absorbed (g of H ₂ O per gram of ThO ₂)
1150	0.055
1000	0.064
900	0.097

Samples fired at 1000°C may be the choice within this group, since high liquid absorption and high mercury porosity are obtained while still maintaining a reasonably high density. The water-absorption results correlated well with water- and toluene-immersion densities. Dissolution of the sample fired at 900°C was complete after less than 0.5 hr in boiling 13 M HNO₃-0.04 M HF-0.04 M Al(NO₃)₃. The other two samples were only about 75% dissolved after 5 hr under the same dissolution conditions.

Zirconia Sols

Various methods for preparing zirconia sols are being studied. For example, reduction of the nitrate with formic acid or precipitation of the hydrous oxide and redispersion in zirconyl nitrate solution produced stable sols. Nitrate-to-ZrO₂ mole ratios of unity or greater were required to form the sols by either method. Precipitation of the hydrous oxide and reprecipitation with water or dilute nitric acid failed to make a stable sol. Likewise, steam hydrolysis was not very successful. Dehydration of the oxide appears to be irreversible at the temperatures necessary for denitration by steam (higher than 100°C).

As to the stable zirconia sols prepared by reducing the nitrate with formic acid, the final nitrate-to-ZrO₂ mole ratio was about 1 in both cases. Subsequently, the sols were formed to gel microspheres

Table 6.2. Effect of Firing Temperature on Properties of ThO₂

Firing Temp. (°C)	Density by:			Mercury Displacement	Porosity		Surface Area (m ² /g, Kr)
	H ₂ O	Toluene	Helium		(vol %)	(cm ³ /g)	
1150	9.86	9.903	9.97	9.83	0.1	0.001	0.019
1000	9.78	9.78	10.23 ^a	10.1	3.8	0.038	0.007
900	9.38	9.66	9.48	8.5	0.56	0.006	7.1 (Ne)

^aProbably erroneous.

in 2-ethyl-1-hexanol and then fired to oxide spheres having a density of 4.9 g/cm³. The theoretical density of zirconia is 5.6 g/cm³. In some of the preparations, the microspheres cracked on the "great circle" when fired.

Zirconia sols prepared by formate reduction of the nitrate ion were unexpectedly flocculated by small additions of thoria sol. When small amounts of zirconia sol are added to ThO₂ sol, an initial flocculation is reversed on digestion and agitation. The pH of the zirconia sol is lower than expected from the conductivity measurement. These findings are indirect indicators that these zirconia sols are negatively charged.

In the precipitation method for preparing sols, ammonia was added to 1 M zirconyl nitrate solution to a pH of 2.1, at which point hydrous oxide solid began to appear. The mixture was digested at 100°C for 20 hr and then the precipitation was completed by dropwise addition of ammonia. The mixture was filtered on a Büchner funnel, and the cake was washed six times with water. It was then treated with additional zirconyl nitrate solution to peptize it to a sol. Small additions (nitrate-to-ZrO₂ mole ratio of approximately 0.1) produced highly viscous, opaque sols. Larger additions caused settling to a gel. Still further addition (nitrate-to-ZrO₂ ratio of approximately 1) produced a fluid, transparent sol.

As prepared, the sols of various nitrate levels were all viscous and opaque. Specific conductances at 25°C increased linearly with nitrate level. After being digested at 70 to 80°C for 16 hr, the samples at high nitrate level (nitrate-to-ZrO₂ mole ratios of approximately 1) were transparent and fluid, with conductances at a plateau of about 4 × 10⁻² mho/cm. The sols low in nitrate (mole ratio less than 0.3) were stable, viscous,

and opaque, with a conductance of approximately 5 × 10⁻³ mho/cm. A sample with a mole ratio of about 0.3 was a transparent, soft gel.

In sols where nitrate-to-ZrO₂ ratios were less than 1, formate could be substituted for nitrate on an equivalent basis with no apparent change in the stability of the sol.

Thorium Nitride

Thorium nitride microspheres were successfully prepared in 10-g lots by firing thoria-carbon spheres in nitrogen at 1800 to 1850°C for 1 to 1.5 hr. Conversion of ThO₂ to nitrides was complete in this temperature range. When the temperature exceeded 1850°C, the spheres sintered to each other. X-ray diffraction analysis showed the presence of ThN, Th₂N₃, and thorium carbonitride. Carbon-to-thorium atomic ratios of 2 and 3.5 have been investigated. Much work remains to be done to define conditions leading to a pure nitride product.

6.3 DEVELOPMENT OF METHODS FOR PRODUCING MICROSPHERES

Process Development

Development of methods for preparing microspheres suitable for incorporation in various types of matrices was a major part of the development effort during the past year. The type of microsphere produced by sol-gel techniques is ideally suited for coating with carbon and other materials, and the coated products show promise of being excellent fuels and blankets for use in high-temperature gas-cooled reactors.

The preparation of thoria microspheres was demonstrated in a tapered-column system, operating continuously at the rate of 230 g of oxide per hour, starting with a 3 M sol. The microspheres are prepared by dispersing sol at room temperature in an immiscible organic liquid which has some solubility of water. The sol droplets must be suspended in the organic phase until enough water is extracted from the aqueous sol to cause gelation. After drying, the gel spheres are calcined at 1150°C to achieve densification prior to coating with pyrolytic carbon.

A schematic flow diagram of the equipment being used to produce gel spheres in the size range of 100 to 1000 μ is shown in Fig. 6.2. The organic

liquid, 2-ethy-1-hexanol, is pumped by a centrifugal pump through a Cuno Micro-Klean filter and then metered into three flow paths. Two of the streams enter the bottom of the column system and flow upward through a tapered glass column. One of these streams enters the column tangentially, creating a swirl in the lower half of the column; the second is introduced perpendicularly to the column wall. The third organic stream is used as a drive fluid in a two-fluid nozzle. The aqueous sol is metered by a syringe pump to the two-fluid nozzle and dispersed into droplets. These droplets fall through the upflowing organic until they reach their fluidizing velocity. As water is extracted from the aqueous droplets, the sol sets to a rigid

ORNL-DWG 65-9727

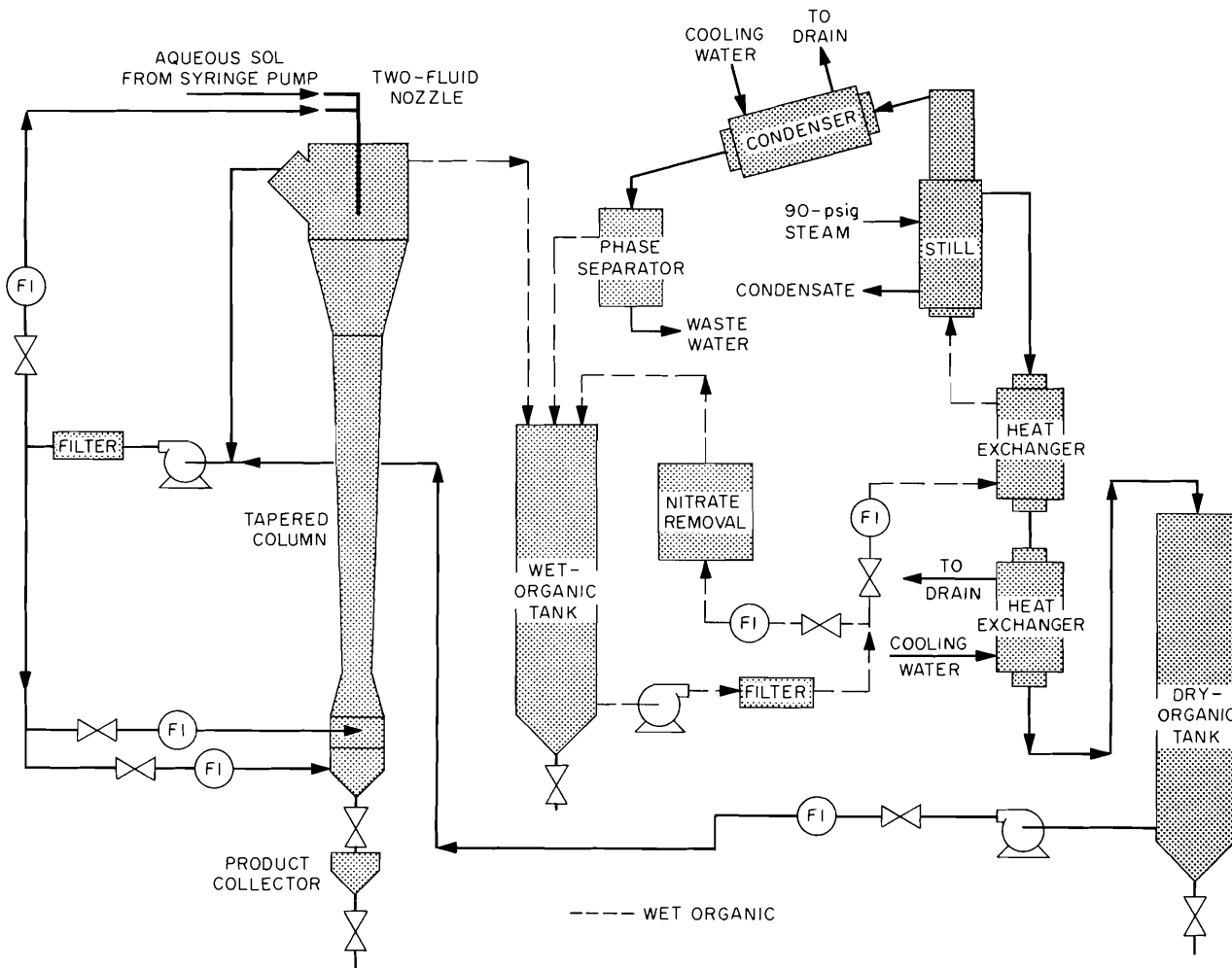


Fig. 6.2. Column for Forming Gel Microspheres and System for Recovering Solvent.

gel. The denser gelled particles require a higher fluidizing velocity.

This column system has been operated continuously at a sol flow rate of 5 ml/min by adjusting the organic fluidizing flow to allow the gelled spheres to fall through the minimum column cross-sectional area. To operate continuously, dry 2-ethyl-1-hexanol is metered to the suction side of the column pump at a flow rate of about 1 liter/min. The wet alcohol overflows from the column into a holdup tank, from which it is metered through a preheater and into a steam-heated still operating at about 150°C. The dried alcohol (containing about 0.5 wt % water) from the still is cooled to room temperature and flows by gravity to a second holdup tank. The vapors from the still are condensed and separated into two phases, a water-saturated alcohol phase and an alcohol-saturated water phase. The water-saturated alcohol phase is returned to the holdup tank.

In the course of forming sol droplets from these nitrate-stabilized sols, nitric acid is extracted into the alcohol phase. In some instances it is felt that the nitrate ion may cause undesirable oxidation of the fuel microspheres. In an attempt to remove the nitrate ion from the alcohol, it was recycled from the wet-organic tank to a 3-in.-diam column

containing 1.5 lb of Dowex 1-X8 ion exchange resin (hydroxide form). However, thoria microspheres produced with this system do not densify at the normal sol-gel calcination temperature of 1150°C. An aqueous scrubbing column is being investigated as a possible alternative method for removing nitrate.

In early stages of the work, sol droplets of controlled diameters were formed in the tapered-column system by discharging the sol through a small orifice. To avoid the undesirably small orifice sizes required for free-fall drop formation, a two-fluid nozzle was developed and is being used to form the droplets (see Fig. 6.3). The sol is introduced in the center of a flowing organic stream which acts as the drive fluid. The continuous sol is accelerated to the velocity of the drive fluid and then breaks up to give sol droplets with diameters 2.0 to 2.5 times the minimum diameter of the sol stream. A nozzle length of 10 in. has been used to ensure droplet formation before discharge into the tapered column.

The variables governing droplet formation by the two-fluid nozzle are related by the following equation:

$$D = k \sqrt{\frac{4f}{\pi V_{\max}}} \quad (1)$$

ORNL-DWG 65-9728

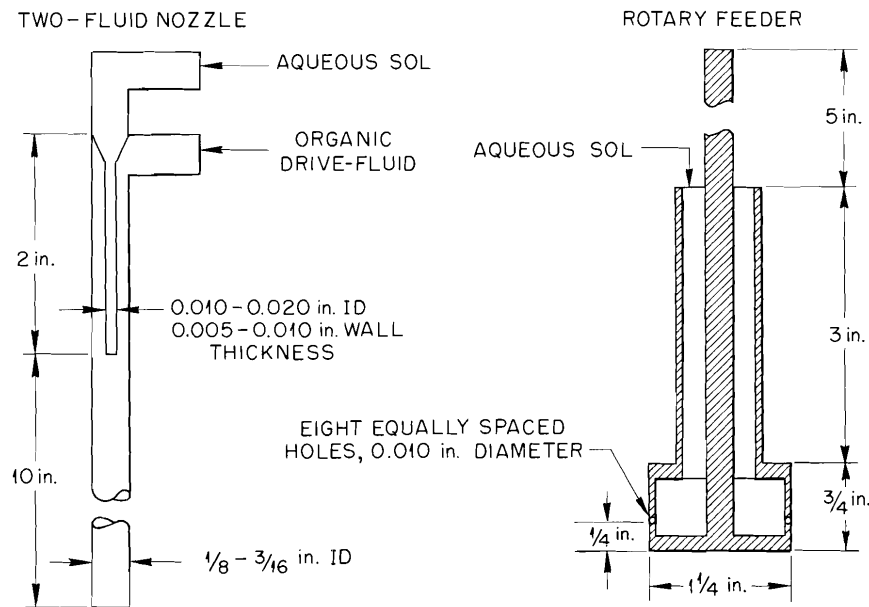


Fig. 6.3. Devices Used in Forming Sol Droplets.

where

D = sol droplet diameter, cm,

f = sol flow rate, cm^3/min ,

V_{max} = maximum drive-fluid velocity, cm/min ,

k = constant for a particular system, generally 2.0 to 2.5.

Theoretically, the diameter of the droplet should be independent of the diameter of the sol entry tube. To form uniformly size droplets with a two-fluid nozzle, the flow of the drive fluid must be laminar, and therefore the sol should be injected in such a manner as to minimize disturbances. A 10-in. nozzle has been used to ensure good droplet formation before discharge into the tapered column. Using two nozzles simultaneously, a 3.1 *M* thoria gel was fed through each two-fluid nozzle at a rate of $2.5 \text{ cm}^3/\text{min}$ for 4 hr. With a value of 2.4 for the constant k in Eq. (1), the flow rate of the drive fluid was set to produce spheres with a diameter of 230μ after calcination. About 950 g of thoria spheres were formed, with the following size distribution after calcination to 1150°C : 3.9 wt %, $>250 \mu$; 72.3 wt %, 210 to 250μ ; 13.5 wt %, 150 to 210μ ; and 10.3 wt %, $<150 \mu$.

Sol droplets in the desired size range have also been obtained with several types of rotary sol dispersers similar to the one shown in Fig. 6.3. A typical rotary disperser has eight holes, 10 mils in diameter, equally spaced at one elevation around a $1\frac{1}{4}$ -in.-diam cylinder. Initially, the disperser was run in air so that the droplet size could be controlled by the hole size and the centrifugal force on the forming droplet. This procedure was unsatisfactory because the sol drops were shattered into smaller droplets on entering the organic liquid. But encouraging results were obtained by running the disperser just under the surface of the organic liquid. This allows the shear forces in the organic liquid to have a significant part in controlling the size of the sol droplets; however, this effect may be minimized by altering the shape of the rotary disperser. Preliminary investigations indicate that the plugging of holes is not a problem and that the droplet size is relatively independent of sol feed rate, which has been varied from 5 to $15 \text{ cm}^3/\text{min}$. The major advantage of a rotary feeder, compared with a two-fluid nozzle, is its adaptability to scale up or to increased sol flow rates. Also, the sol flow to the rotary feeder is permitted to be less uniform than that for the two-fluid nozzle,

which requires continuous, nonpulsating, accurately metered flows of both sol and organic. With the rotary feeder shown in Fig. 6.3, about 195 g of thoria spheres were formed with the following size distribution after calcination to 1150°C : 6.2 wt %, $>300 \mu$; 30.0 wt %, 250 to 300μ ; 52.2 wt %, 210 to 250μ ; 7.7 wt %, 150 to 210μ ; and 3.9 wt %, $<150 \mu$. For this run, the sol feed rate was $5 \text{ cm}^3/\text{min}$ and the rotation speed was 460 rpm.

To prevent the sol droplets from coalescing and sticking to the walls of the glass column, a surfactant is dissolved in the organic phase. A surfactant concentration of 0.1 to 0.5 vol % in the alcohol seems to be sufficient. The following three surfactants are representative of the types that worked satisfactorily for certain sols and for droplets of a certain size: Ethomeen S-15 (Armour), Amine O (Geigy), and Span 80 (Atlas). Ethomeen S-15 was successful in forming thoria spheres in all sizes, whereas Span 80 can only be used for thoria sols whose droplets are in the size range of 200μ or smaller. Larger drops distort into non-spherical shapes when Span 80 is used, probably because it gives an appreciably lower interfacial tension. Thoria spheres in all sizes were satisfactorily formed with Amine O and Span 80 in combination, and for certain sols this system seems to be superior. A surfactant is necessary to make the process work; however, the type of surfactant required is not highly predictable for a new sol and a particular particle size range.

Glass columns of several shapes were studied, and the most successful system found so far is the tapered column. The present tapered column has a minimum diameter of 2 in., which expands to 3 in. over a column length of 40 in. The other types were variations of a straight column with a tapered central rod to form an annulus for organic flow. All the earlier column systems had the same defect: instability of flow. The alcohol was introduced perpendicularly at the bottom of the system, and a rather long converging section of column was believed necessary to develop a vertical velocity profile. With the vertical flow of alcohol, the particles and sol droplets were in continuous motion up and down the column. This system also produced a flow instability which allowed both sol drops and gelled spheres to fall out of the fluidized bed. Apparently, with a slight increase in the number of particles on one side of the column, the pressure-drop-flow-rate balance in the upflowing alcohol caused a further shift in

the bed of particles – a shift that could be corrected only by particles dropping out of the column. This flow instability was eliminated by introducing the alcohol stream tangentially at the bottom of the column and creating a swirl, as described earlier. Also, the rotational flow helped flatten the vertical velocity profile by adding to the vertical component next to the wall and reducing the upward flow near the center.

The continuous recycle of alcohol was demonstrated during numerous runs in which the water removed by the still represented 85% of the water in the original sol. During a recent run, the column and distillation systems were operated three shifts a day for 95 hr. The total volume of alcohol was 38 liters of 2-ethyl-1-hexanol with Amine O and Span 80 as the surfactants. About 27 liters of 3 M thoria sol was dispersed into the tapered column during the run, and 21.5 liters of water was removed from the distillation system. The density of the thoria spheres after calcination to 1150°C was almost the theoretically attainable for samples taken at various times throughout the run. As the run progressed, the alcohol darkened slightly; also, particle clustering began to occur. The tendency toward clustering was eliminated by addition of 0.1 vol % increments of Span 80. The apparent degradation or loss of surfactant with time and the presence of nitrate ion in the organic

phase may present problems if the alcohol is to be recycled for a long time.

Examples of the different sizes of thoria spheres that have been formed in 2-ethyl-1-hexanol and calcined at 1150°C are shown in Fig. 6.4. The first sample (left) was formed in a beaker at a stirrer speed of 1200 rpm. All the particles are less than 40 μ in diameter, and a high percentage of the spheroids have diameters less than 10 μ . The next three samples shown in Fig. 6.4 were formed in the tapered column; compared with the first sample, these three are photographically reduced in size by a factor of 8. The average diameters of these three samples are 250, 500, and 750 μ .

By combining the product from several runs in the tapered-column system, 19,400 g of thoria microspheres were prepared for evaluation tests, pyrolytic-carbon-coating studies, and other uses. After calcining at 1150°C and screening, the combined size distribution of these thoria samples was:

Weight (g)	Size Range (μ)
990	150–210
12,850	210–250
3,400	250–297
1,130	297–420
1,030	420–500

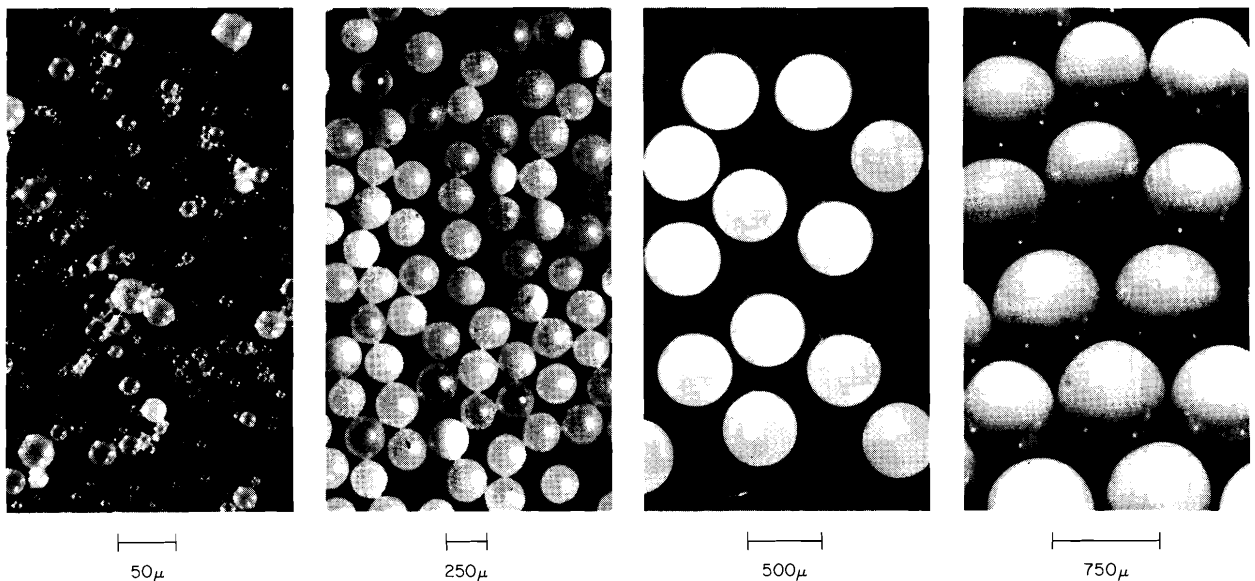


Fig. 6.4. Thoria Spheres Calcined at 1150°C.

About 65% of these oxide microspheres were prepared during the previously mentioned 95-hr continuous run.

Future work will be directed toward obtaining uniform sol dispersion at higher sol flow rates, increasing the size of the tapered column, and studying the effects of continuous recycle on the organic gel-forming medium.

Coated Particle Development Laboratory

A laboratory for developing remote operating procedures and methods amenable to scaleup of the sol-gel microsphere process and the coating of the microspheres with pyrolytic carbon in batches of up to 5 kg has been constructed in Building 4508. An objective of these studies is to define equipment and process requirements for use in the Thorium-Uranium Recycle Facility (TURF). This laboratory has been named the Coated Particle Development Laboratory (CPDL).

Three enclosures have been fabricated for sol-gel microsphere studies in the CPDL: a $4 \times 4 \times 11.5$ ft enclosure for making sol-gel microspheres, including solvent recovery by distillation; a $5\frac{1}{3} \times 4 \times 4$ ft enclosure with a $2\frac{1}{2} \times 4 \times 3$ ft well for drying microspheres; and a $4 \times 4 \times 4$ ft enclosure for calcining microspheres at 1150°C in Ar-4% hydrogen.

Hydrosols of fuel and blanket materials such as ThO_2 and $\text{ThO}_2\text{-UO}_2$ initially will be prepared elsewhere and transferred to the CPDL. Droplet formation will be done with either two-fluid nozzles or a rotary feeder. The two-fluid nozzles will each produce about 1.5 kg of oxide per day; the rotary feeder's capacity should be in excess of 10 kg/day and will exceed that of the distillation equipment and dryer.

The microsphere-forming column to be used in CPDL has a 9-in.-diam top section with peripheral overflow. The diameter of the top section tapers down to $4\frac{1}{2}$ in. in $2\frac{1}{2}$ ft of length. The top section supports the long, gradually tapered glass section located below. The tapered glass section is $5\frac{1}{4}$ ft long and reduces from $4\frac{1}{2}$ to 3 in. in $4\frac{1}{2}$ ft of length and then increases to $4\frac{1}{2}$ in. again in 9 in. of length. Glass was used for this portion of the column so that the hydrodynamic flow patterns can be observed.

Located below the main body of the forming column are two pots. The first is the vortex gen-

erator, where the correct hydrodynamic flow pattern is produced, and the second is the product collection pot.

The gelled microspheres will be transferred into the drying vessel by jetting from the product collection pot. This type of transfer is being studied because jet transfer of gelled microspheres will be desirable when the process is later performed remotely. The drying vessel has a porous bottom, which retains the microspheres and permits the 2-ethyl-1-hexanol to drain from them. This dryer design is preliminary and was chosen as the simplest for permitting drying studies that will define parameters for design of a larger unit. After draining is complete, the vessel is heated with a steam coil (150 to 160°C), and argon which has been preheated in a coil located concentrically within the steam coil is introduced as a carrier gas for evolved volatile materials. Three such drying vessels have been made.

After the drying step has been completed, the dried microspheres can be transported to the calcining furnace in the drying vessel under an argon blanket.

In general, the dried microspheres will be calcined in a box furnace to 1150°C before coating with graphite.

All equipment has been procured or fabricated, and installation is about 90% complete.

6.4 DESIGN OF THE THORIUM-URANIUM RECYCLE FACILITY

Building Design

Detailed design of the Thorium-Uranium Recycle Facility (TURF) was begun in April 1964 and completed in January 1965. There were few changes in design concept from that developed in title I, the principal change being lowering of the floors in the two large central processing cells to provide uniform headroom of 24 ft throughout these cells. The fixed-price-contract package, containing 331 drawings and 72 specification sections, was formally advertised for bid on January 28, 1965, and bids were opened on March 25. The low bid of \$3,240,000 by Blount Bros. Corporation was higher than the engineers' estimate of \$3,050,700. The contract was awarded on May 6, 1965; completion is scheduled for December 1966 for the fixed-price portion of the job. Overall completion is scheduled for March 31, 1967.

Status of ORNL Procurement for Fixed-Price Contractor

Those items that presented unusual problems in design or procurement and also those requiring lead times that would delay the construction project were deleted from the fixed-price contract and included in the ORNL procurement list. These include the in-cell crane and manipulator system; the three steel shielding doors; underground stainless steel ductwork; highest-quality stainless steel pipe, valves, fittings, and eductors; viewing windows and window forms; special penetrations through the cell walls; various untested items for the cell fire-protection system; and miscellaneous other items. So far, this effort has proceeded very smoothly, and it appears that all items can be delivered to the fixed-price contractor by the scheduled date.

Design of Mechanical Equipment Components

A mockup has been constructed to determine the suitability of design concepts for facility and process equipment. The mockup is full scale – 10 ft long and full cell width. It provides all services that will be available within the cells. Many of the items described below are included as part of this mockup.

Viewing Windows and Alpha Seals. – The requirements for viewing windows are somewhat different for TURF than for other facilities constructed recently. Because TURF is designed for possible use as an inert-gas cell bank, it is necessary that defective windows and alpha-seal glasses be replaceable with a minimum of contamination of the cell atmosphere with air, which in turn requires that the glass be replaceable from the radioactive side entirely by remote means. An alpha seal similar to that used in the Transuranium Plant windows was found acceptable. The test window and the handling devices used in the mockup tests are shown in Fig. 6.5.

The shielding for the bulk of the TURF cells consists of normal concrete, making it probable that zinc bromide windows can be used. Because of difficulties encountered with scaling of the copper-lined zinc bromide windows used in the High Radiation Level Analytical Laboratory, some tests have been started to determine the relationship of this phenomenon to the method for cleaning

copper, the presence of oxygen in the tank atmosphere, and composition of the weld.

Out-of-Cell Filters. – A filter bank is being installed for the TURF cell ventilation and hot off-gas. The bank is quite similar to that used in the Transuranium Plant. However, modifications were made in the design of that system to relax the construction tolerances required for proper fit of the large filter boxes. The essence of the design change is that a stainless steel bellows is used in the air line at each end of the box to provide for a large tolerance in box dimensions (Fig. 6.6). Another change in design permits testing of each of the two sets of filters in each filter box after they are installed.

Early in the facility design, an alternative method of filter changing was considered, and its development was vigorously pursued until it became apparent that the development effort could not be completed in time for inclusion in TURF design. This alternative method is called the “incessant filter” and is in use at Argonne National Laboratory and the High Radiation Level Examination Laboratory at ORNL, but only as single units.

TURF – Cell Service Sleeves and Plugs

Bent Service Penetration. – An essentially full-scale mockup of the two types of bent service sleeves was constructed in which plug development and testing could take place. Two complete plug assemblies were built for testing. One is a hydraulic-pneumatic-type plug having four $\frac{1}{2}$ -in. sched 40 pipelines running to a removable plug which connects to an expendable plug at a gasketed disconnect. The expendable plug has four flexible hoses terminating at the cell face in one portion of a remotely operable disconnect. The second plug assembly is an electrical plug that features a $1\frac{1}{4}$ -in. conduit with pin-type connectors for line connections (Fig. 6.7). These two mockup plugs have gone through operational changeout procedures and are satisfactory. Also, a technique of operation was established through the changeouts. Additional work will be required to develop several variations of these two types.

Stepped Service Penetrations. – One 4×6 in. service sleeve and four 6×8 in. service sleeves were built and installed in the mockup in which plug development and testing could take place. One complete plug assembly was made for each sleeve size. Both plugs contain electrical lines. The

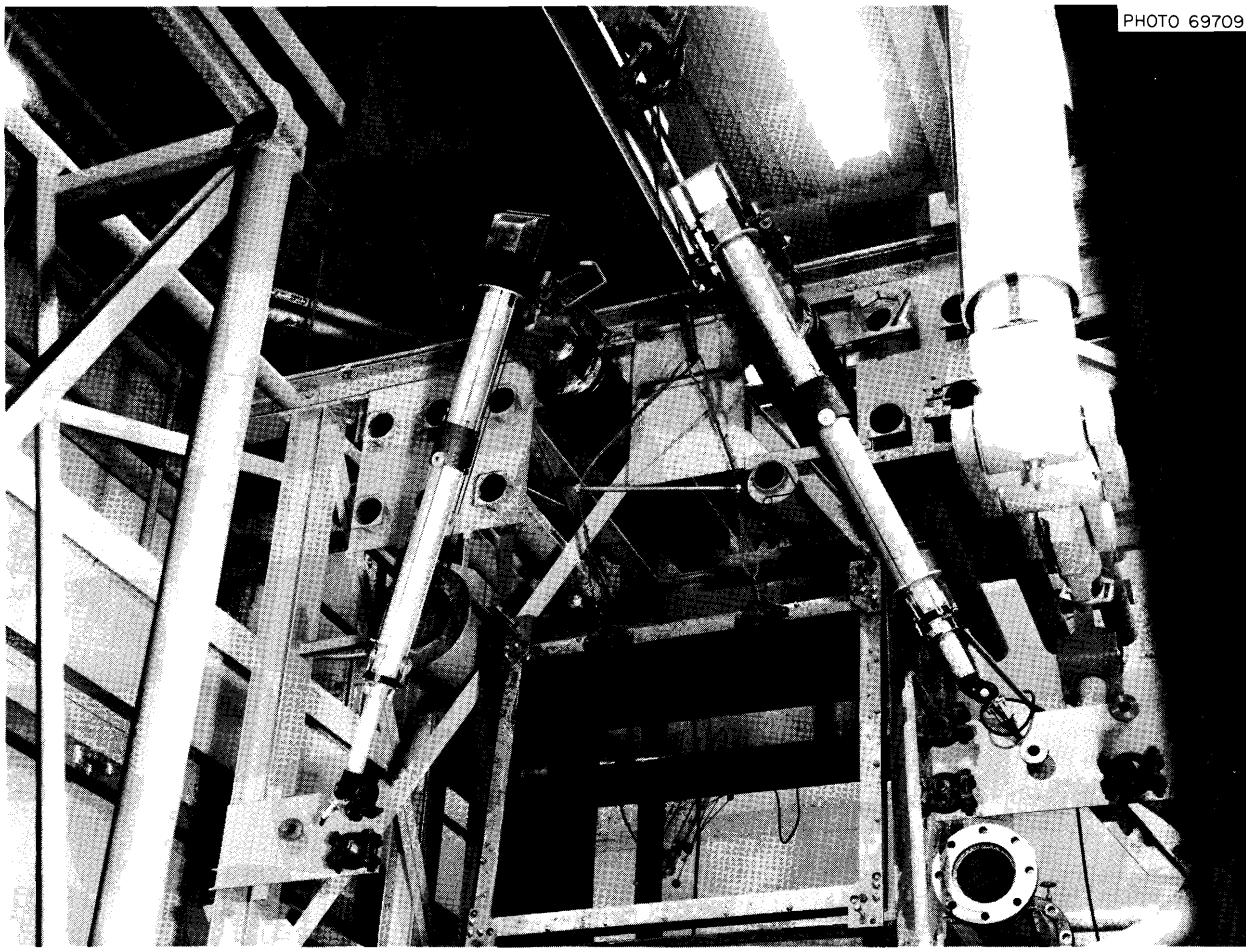


PHOTO 69709

Fig. 6.5. TURF Test Viewing Window and Mockup of Handling Device.

4 × 6 plug supplies power to the mockup cell lighting system. The stepped service plugs were tested through simulated operational changeout conditions and are satisfactory.

A remote connector has been developed which holds, locates, and aligns the electrical pin-type connectors for remote plugging and unplugging. Also, the necessary handling tools and fixtures for installation and removal of the plugs were designed and developed during the mockup program.

Cell Lighting Equipment. — The cell F lighting fixture is a two-piece plug, in which a 400-W mercury vapor lamp is mounted. A test fixture proved satisfactory in simulated operational changeout testing.

A lighting fixture for mounting the 1500-W quartz iodine lamps to be installed in cells B, C, D, E,

and G was designed and fabricated by Ceil Heat Company of Knoxville, Tennessee. Two of these fixtures were tested and proved very satisfactory. Their cost is about one-third that of standard commercial fixtures.

Cell Fire-Protection System. — A unique innovation in the design of a carbon dioxide fire-fighting system is being used to obviate difficulties encountered with conventional carbon dioxide systems as a result of the cooling produced by evaporation of carbon dioxide. In our adaptation, very-low-temperature carbon dioxide is excluded from the cells by allowing the liquid carbon dioxide to evaporate in the storage vessels and by subsequently heating the gas and regulating its pressure prior to discharge into the cells through orifices (Fig. 6.8). Factory Mutual's Engineering Division has been

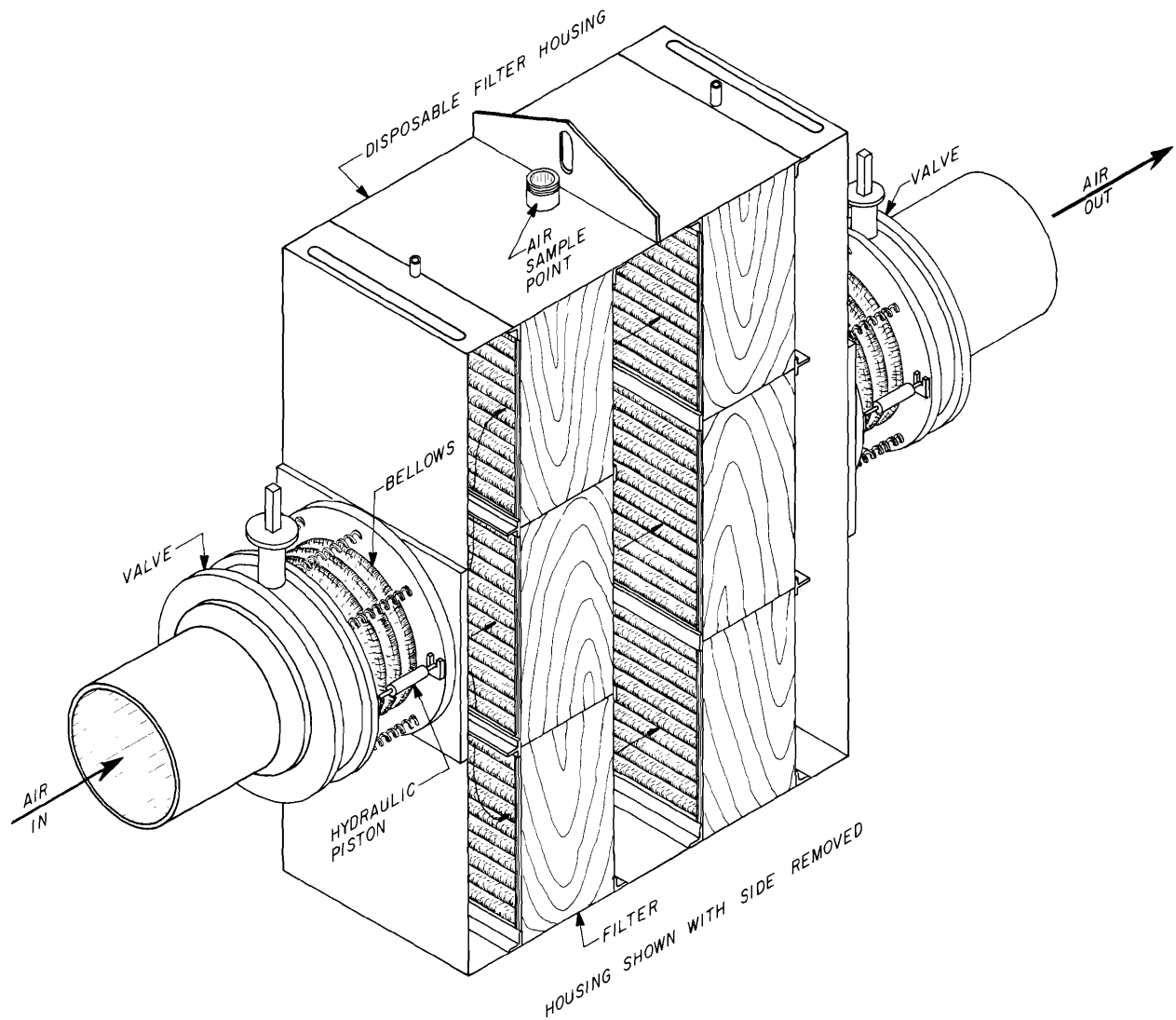


Fig. 6.6. TURF Ventilation and Off-Gas Filter Unit.

brought into the job to appraise the system as to its adequacy for an "improved-risk" classification and to test all components not already Factory Mutual approved. To date, they have approved the use of the system and all previously untested components except the pressure-reducing valves and the control panel, which have not yet been procured and turned over to them for test.

6.5 DEVELOPMENT OF EQUIPMENT FOR THE THORIUM-URANIUM RECYCLE FACILITY

Procedures and equipment are being developed to adapt the sol-gel process to a completely remote operation, as required for the Thorium-Uranium Recycle Facility (TURF).

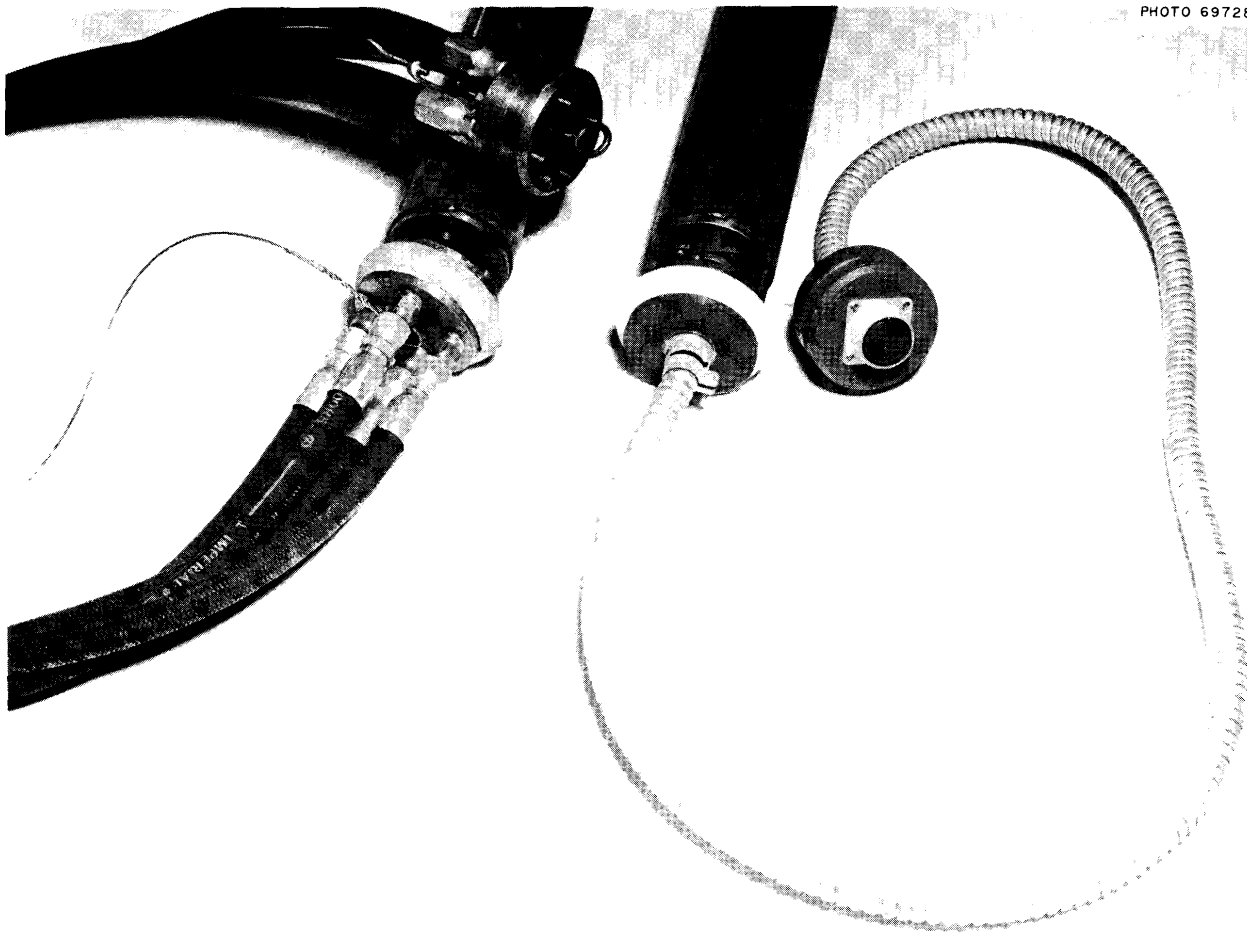


Fig. 6.7. TURF Service Sleeve Electrical Connector.

The portion of the process equipment for which the Chemical Technology Division has primary responsibility is that used to produce fired thoria-urania particles suitable for use in power-reactor fuel elements. This equipment will consist of liquid-handling equipment for storing, transferring, and metering the uranyl nitrate solution, and for preparing, transferring, and metering the thoria-urania sol; a sol dryer; a furnace for calcining the gel; and supporting equipment located both inside and outside the cell. Installation and testing of a 3-in.-ID vertical tube calcining furnace are in progress. Equipment to simulate the TURF cells has been installed, and experimental tests in this cell mockup were started.

Vertical Tube Furnace

The calciner for the sol-gel oxide in TURF will be a vertical ceramic tube furnace. A gel composed of $\text{ThO}_2\text{-UO}_3$ will be fed into the top of the tube and, in passing down the tube, will be fired to 1150°C . The UO_3 will be reduced to UO_2 by Ar-H_2 flowing up the tube. A test installation, including a prototype vertical tube furnace (VTF) (Fig. 6.9), a nonheated vertical tube, and the product-removal mechanism (Fig. 6.10), was built and operated. Results so far show that the VTF meets requirements of capacity, product quality, control ability, and operability; however, the product occasionally bridges in the tube just as it enters the highest

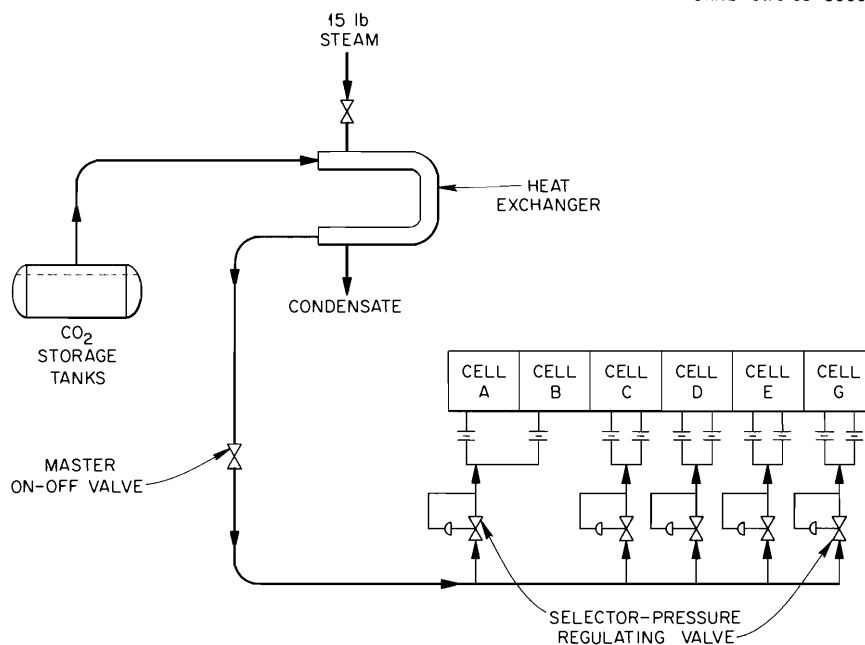


Fig. 6.8. TURF Cell Fire-Protection System - Gaseous CO₂.

temperature zone of the furnace. This poses a potentially serious question as to the reliability of the furnace operation. Since bridging also frequently results in breakage of the ceramic tube, lengthy repairs in the remote facility are a possibility. Present efforts are directed toward preventing bridging and finding methods of breaking bridges without breaking the tube. These recent efforts have been encouraging and are expected to furnish procedures permitting reliable operation of the furnace.

Mockup equipment to simulate the TURF cells has been installed, and experimental tests of the service equipment and maintenance procedures were started. Procedures for replacing the alpha windows and for using the stepped service plugs and the bent-tube service penetrations were developed or demonstrated. Tests of the lighting system and of the use of the closed-circuit television system and the rectilinear manipulator for maintenance operations are in progress.

Liquid-Handling Equipment

A preliminary design and layout has been made for the major items in this category. It is planned to mount the equipment for handling the uranyl nitrate solution on one frame and the thoria-urania sol handling equipment on a second frame. This arrangement will provide for relatively simple construction and installation and for replacement of vulnerable equipment, the principal items of which are the transfer pumps and the control valves. An isometric view of this equipment layout is shown in Fig. 6.11. The salient feature of the design of the bulk of this equipment is use of the maximum amount of already proved components. Items in this category include the uranyl nitrate pump, the sol blend tank and pump (similar to items used in the Kilrod Facility), the uranyl nitrate storage tank (similar to the shielded annular ²³³U transfer cask), and piping disconnects (Grayloc and TRU disconnects). The novel features of the design

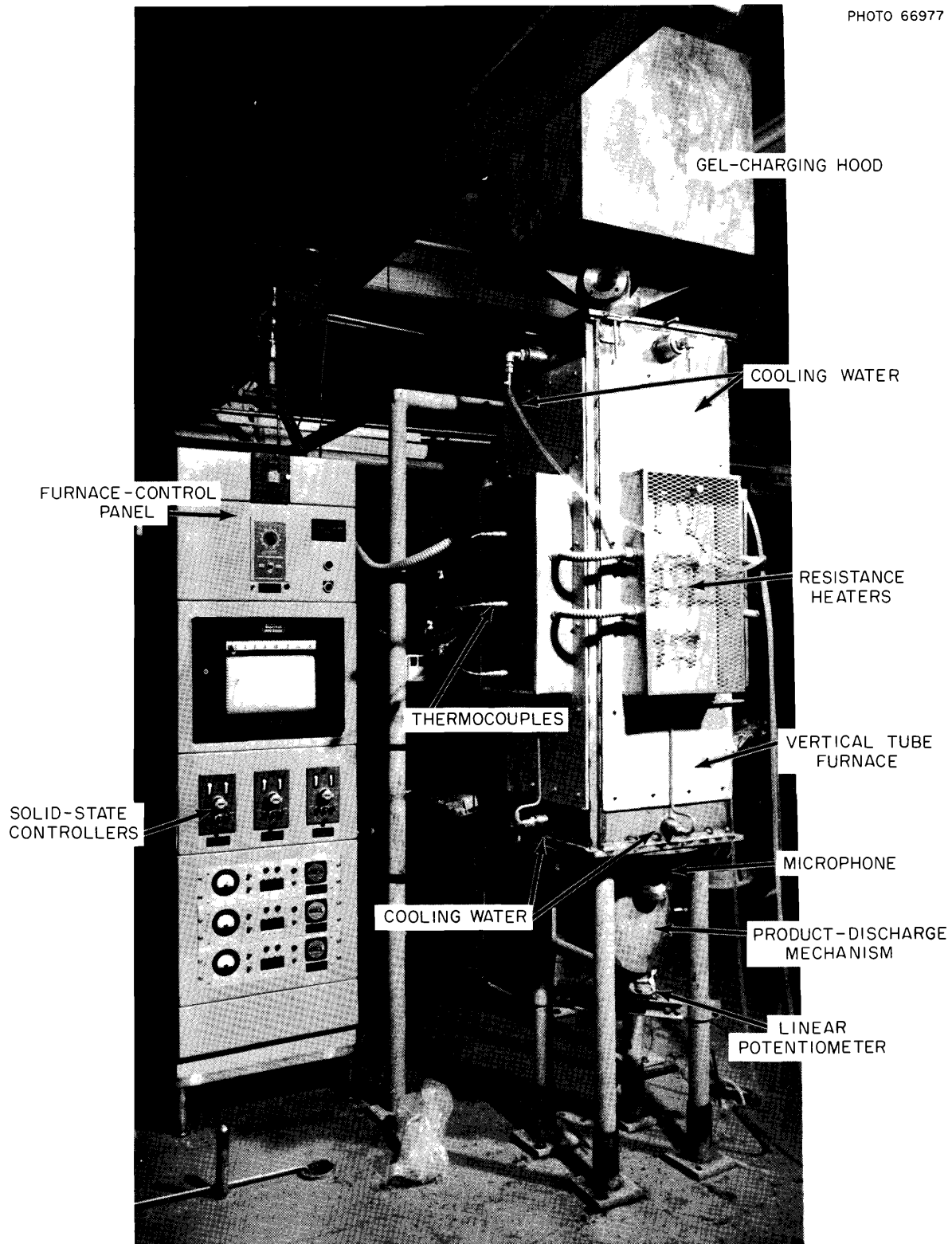


Fig. 6.9. Vertical Tube Calciner Test Apparatus.

PHOTO 66695

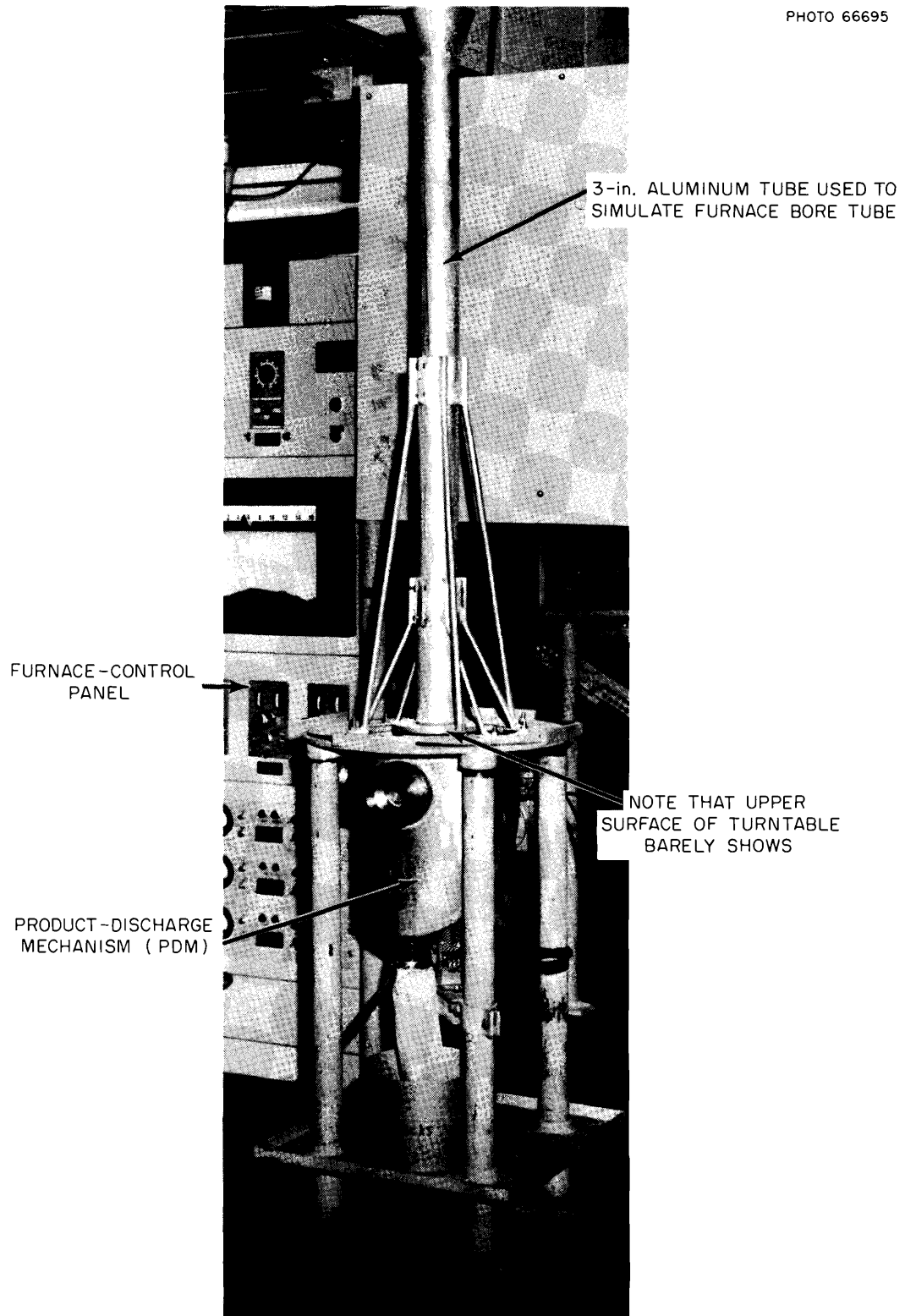


Fig. 6.10. Test Apparatus Used for Testing Feed-Control Device of Vertical Tube Furnace.

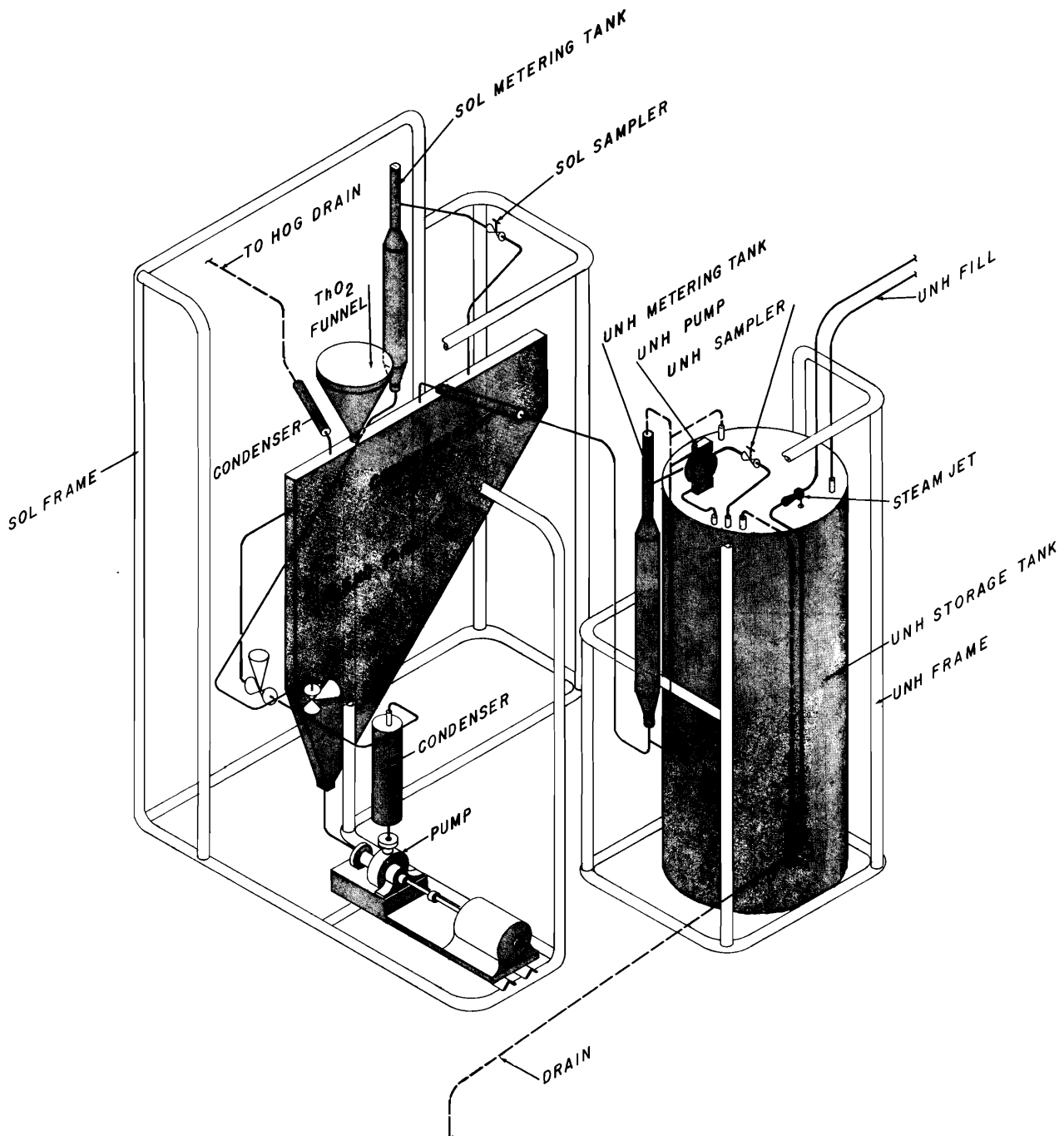


Fig. 6.11. TURF Liquid-Handling Equipment.

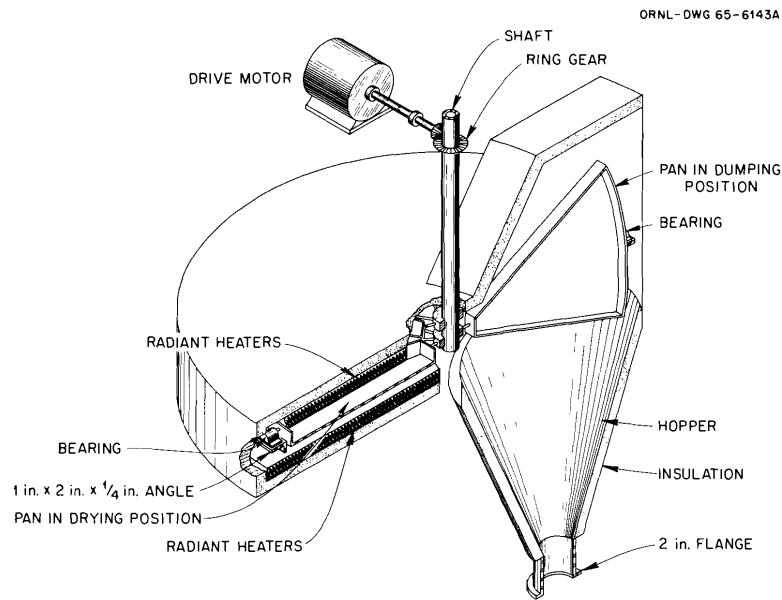


Fig. 6.12. TURF Tilting-Pan Dryer.

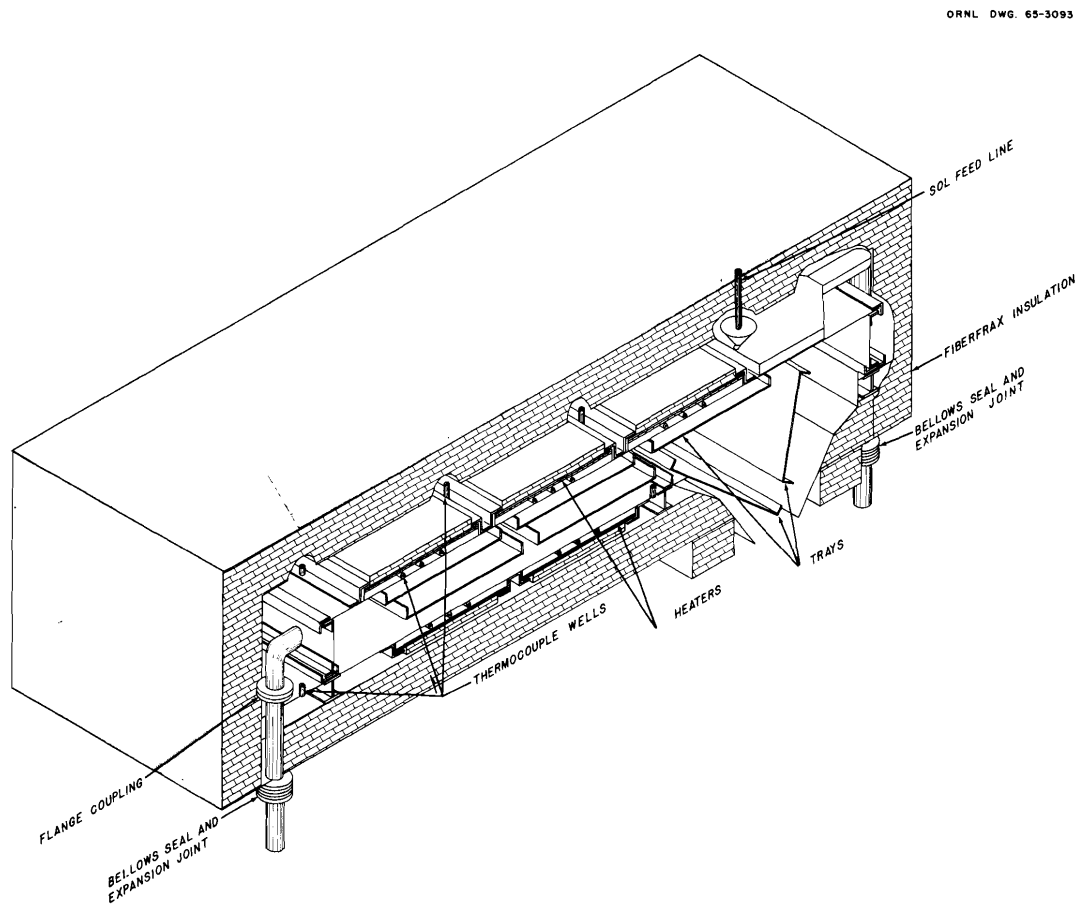


Fig. 6.13. TURF Continuous Tray Dryer.

deal with specific details to permit remote maintenance of the vulnerable items, sampling, and addition of thoria powder to the blend tank. Final detailing and construction will be accomplished during the coming year.

Sol Dryer

Two different versions of a tray-type dryer were designed. The first was a "carousel" type in which wedge-shaped trays would be moved from

station to station by rotating a central shaft from which the trays would be suspended (Fig. 6.12). The second design featured rectangular trays mounted on an endless chain, with provisions for keeping the trays horizontal at all times except during and immediately after the dumping operation (Fig. 6.13). Since it was realized that designers of industrial dryers were better equipped to accomplish certain phases of the design, a specification was prepared for the device and sent out to various commercial concerns for bid.

7. Separations Chemistry Research

7.1 EXTRACTION OF METAL CHLORIDES BY AMINES

In view of the potential for increased use of amine extractants, a systematic survey is being made of the extraction characteristics of many metals from hydrochloric acid and acidified lithium chloride solutions with representative amines.

Data are shown in Fig. 7.1 for the extraction of 20 different metal ions from LiCl-0.2 M HCl and HCl solutions over the range 0.5 to 10 M total chloride. Extractions of 29 other metal ions were reported previously.¹⁻³ In all tests the solvents were 0.1 M solutions of representative primary, secondary, tertiary, and quaternary amines in diethylbenzene. With few exceptions the extraction power of the amines for the various metals varied in the following order: Aliquat 336 (quaternary amine) > Alamine 336 (tertiary amine) > Amberlite LA-1 (secondary amine) > Primene JM (primary amine). Usually, extraction coefficients were slightly higher from the salt solutions than from hydrochloric acids, but the shapes of the extraction curves for the two systems are similar. Metals having maximum extraction coefficients in excess of 1000 include Sn(IV), Sb(V), Au(III), Hg(II), Tl(I), Po(IV), and U(VI). Metals having maximum extraction coefficients ranging from 10 to 1000 include In(III), Sb(III), Te(IV), Te(VI), Ta(V), W(VI), Re(VII), Os(IV), and Bi(III). Metals having maximum extraction coefficients in the range 0.1 to 10 include Rh(III), Hf(IV), Pb(II), and Th(IV). Extraction data are not included for 11 metals for

¹Chem. Technol. Div. Ann. Progr. Rept. June 30, 1962, ORNL-3314, p. 104.

²Chem. Technol. Div. Ann. Progr. Rept. May 31, 1963, ORNL-3452, pp. 170-71.

³Chem. Technol. Div. Ann. Progr. Rept. May 31, 1964, ORNL-3627, p. 179.

which maximum extraction coefficients were less than 0.1. This group includes Li, Na, K, Cs, Be, Mg, Ca, Ba, Al, La, and Eu.

7.2 EXTRACTION OF METAL NITRATES BY AMINES⁴

In survey extractions of metal nitrates by amines, Cu, Ag, Au, Sb, and Se were extracted from nitric acid solutions by 0.1 and 0.2 M trilaurylamine nitrate in toluene.⁵ Of these, only gold was strongly extracted (Fig. 7.2), with a broad maximum near 4 M HNO₃ and a slight decrease with increase of nitric acid concentration to 12 M. The extraction pattern of copper was very similar but lower by a factor of 10⁵, while silver, in between, showed a shallow minimum near 3 M HNO₃. The dependences of the extraction coefficients on amine concentration are close to first power for all, except above 3 M HNO₃ for silver (greater) and for mercury (less).

Continued studies of the behavior of nitrate complexes of nitrosylruthenium in amine extraction used computer analysis of the variation of the apparent extraction coefficient with phase ratio to determine the mole fractions of the extractable species.^{5,6} The results indicate that at least two extractable species exist in 12 M HNO₃, the less extractable probably being a hydrated trinitrato

⁴Work done by the Department of Nuclear Engineering, MIT, under subcontract.

⁵P. J. Lloyd and E. A. Mason, *Equilibrium Extraction Characteristics of Alkyl Amines and Nuclear Fuels Metals in Nitrate Systems* (subcontract No. 1327), MITNE-43 (Dec. 2, 1963); MITNE-50 (Aug. 3, 1964).

⁶P. J. Lloyd and E. A. Mason, *Equilibrium Extraction Characteristics of Alkyl Amines and Nuclear Fuels Metals in Nitrate Systems* (subcontract No. 1327), MITNE-54 (Oct. 24, 1964).

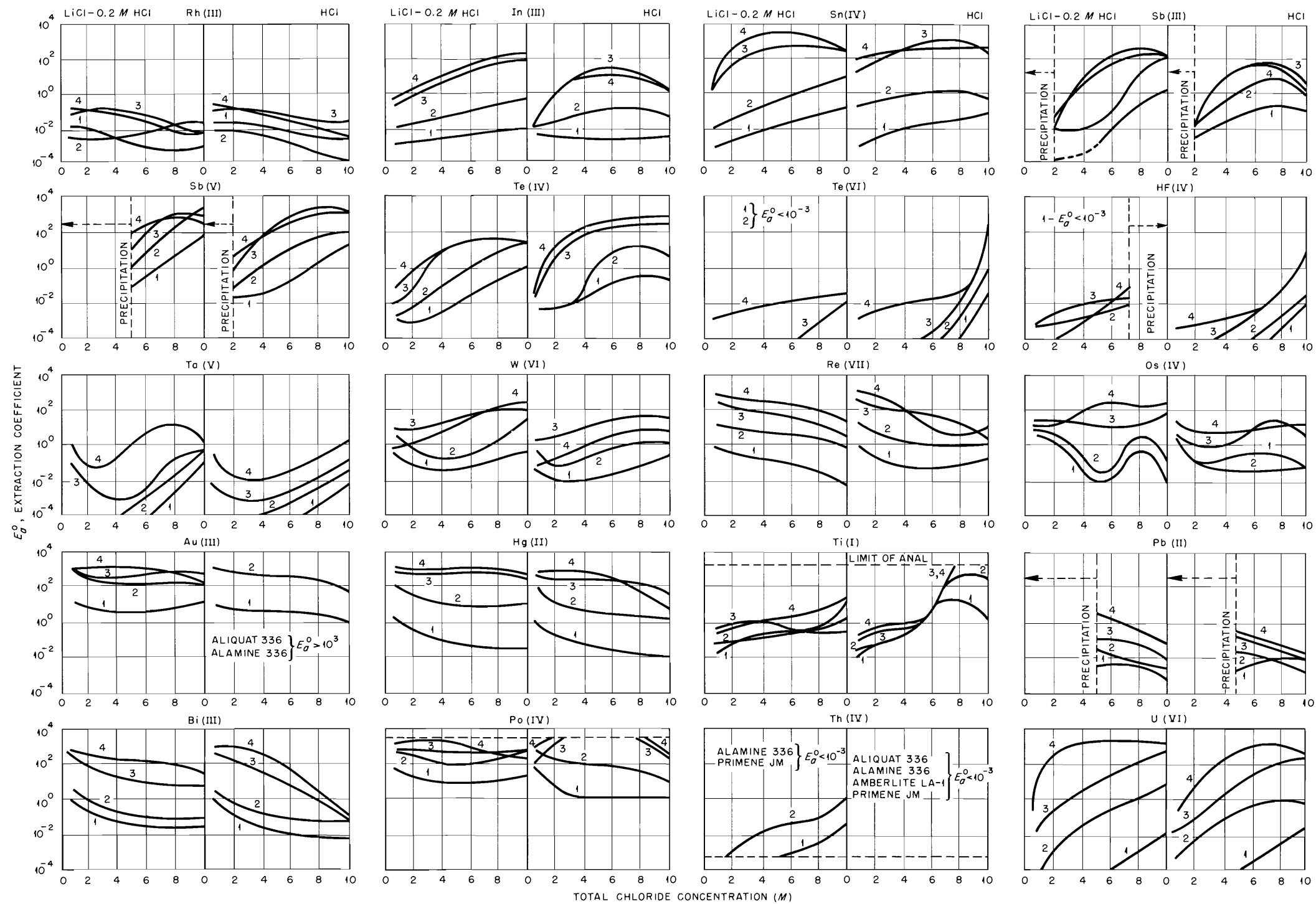


Fig. 7.1. Extraction of Metal Chlorides with Amines. Organic phase: 0.1 M solutions of (1) Primene JM ($RR'R''CNH_2$, 18 to 24 carbon atoms); Amberlite LA-1 ($RR'R''CNHC_{12}H_{23}$, 24 to 27 carbon atoms); (3) Alamine 336 (R_3N , $R = n$ -octyl, n -decyl mixture); and (4) Aliquat 336 [$R_3(CH_3)N^+$, $R = n$ -octyl, n -decyl mixture] mixture in diethylbenzene. With Aliquat 336, 3 vol % of tridecanol was added to the solvent phase to prevent the formation of a third phase. Amines were in the chloride form. Aqueous phase: 0.01 M metallic ion [except for Ta(V), Pu(IV), Tl(I), Os(IV), W(VI), and Re(VII), where tracer amounts were used] in HCl or LiCl-0.2 M HCl solutions (0.5 to 10 M in total chloride). Contact time: 10 min at a phase ratio of 1:1.

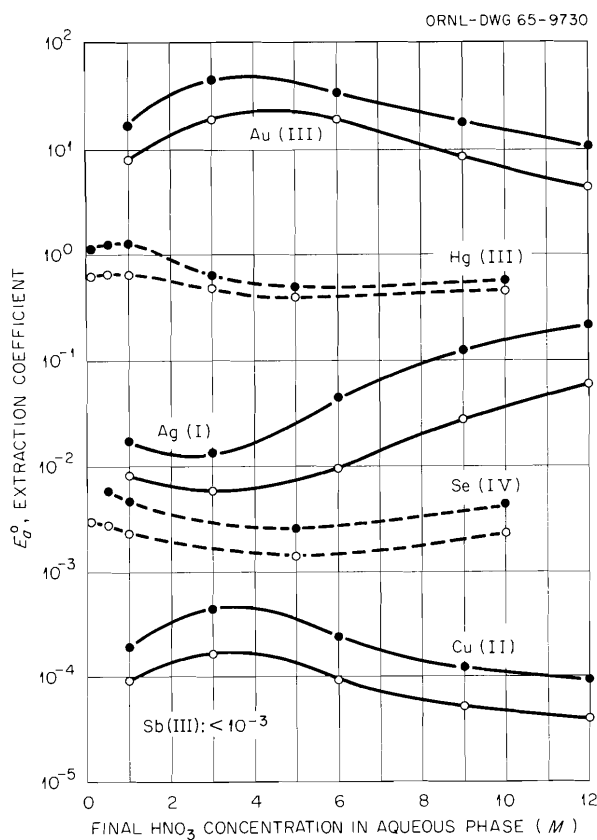
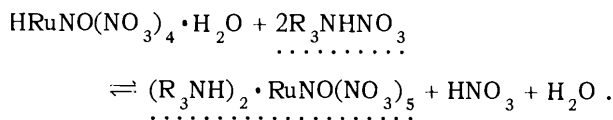
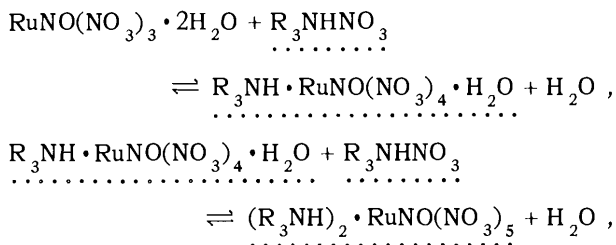


Fig. 7.2. Extraction of Metal Nitrates with Trilaurylamine Nitrate. O, TLA concentration 0.1 M in toluene. ●, TLA concentration 0.2 M in toluene.

complex, and the more extractable being a tetranitrato (possibly plus pentanitrato) complex. On dilution to 3 M HNO₃, these are hydrolyzed to a nonextracting species, approximately following first-order kinetics with rate constants of about 0.01 min⁻¹ and 0.10 to 0.15 min⁻¹ respectively. Once extracted, the less-extractable species is converted in the organic phase to the more-extractable species, with a rate constant of about 0.075 min⁻¹. On the basis of these results, the following extraction reactions are suggested (dotted underlines marking the organic phase):



7.3 REAGENTS FOR SEPARATING POLONIUM(IV) FROM BISMUTH

The isotope ²¹⁰Po, a useful heat source, is produced by irradiating metallic bismuth. A suitable method for recovering the polonium must have the capability of separating milligram quantities of ²¹⁰Po from kilogram quantities of bismuth. Several solvent extraction reagents for polonium have been examined previously,^{7,8} including alcohols, chelating agents, ethers, ketones, tributyl phosphate (TBP), and tertiary amines. Tributyl phosphate and tertiary amines showed promise for use in ²¹⁰Po recovery from hydrochloric acid solutions of the composition most likely to be produced by dissolving irradiated bismuth, that is, 6 to 10 M HCl nearly saturated with bismuth.⁹ Recently, tests have been made with additional solvent extractants, including (1) other neutral organophosphorus reagents [i.e., di-(*sec*-butyl) phenylphosphonate (DSBPP), diamyl amylphosphonate (DAAP), tri-*n*-octyl phosphine oxide (TOPO)] and (2) other amine types [i.e., branched primary (Primene JM), branched secondary (Amberlite LA-1), straight-chained tertiary (Alamine 336), and the quaternary compound corresponding to that tertiary amine (Aliquat 336)]. Tests have been made with TBP to provide a standard for comparison.

Coefficients and calculated separation factors for extraction of polonium and bismuth from separate 8 M HCl solutions with the different reagents, ordinarily dissolved in diethylbenzene (DEB), are shown in Table 7.1. Extractions were also made from solutions in which the HCl concentrations varied from 0.5 to 10.0 M, but only the 8 M HCl data are shown, since in most cases the polonium-bismuth separations and the polonium extractions were near maximum at this acid concentration. It is apparent from the data that several amines and

⁷I. M. Kolthoff, P. J. Elving, and E. B. Sandell, *Treatise on Analytical Chemistry*, part II, vol. 6, Interscience, New York, 1964.

⁸J. C. Sheppard and R. Warnock, *J. Inorg. Nucl. Chem.* **26**, 1421-27 (1964).

⁹H. V. Moyer, *Polonium*, TID-5221, p. 166 (July 1956).

Table 7.1. Extraction of Polonium and Bismuth from 8 M HCl

Aqueous phases:

Polonium – 8 M HCl with about 0.2 μC of $^{210}\text{Po(IV)}$ per milliliterBismuth – 8 M HCl with 0.005 to 0.01 M $^{209}\text{Bi(III)}$ + trace $^{210}\text{Bi(III)}$

Mixing – Organic phases scrubbed twice with equal volumes of 8 M HCl before extraction; extraction for 10 min at about 25°C; organic/aqueous-phase ratio = 1

Reagent	Molarity in DEB	Extraction Coefficient, E_a^o		Calculated Separation Factor
		Po	Bi	
TBP	0.3	5.3	0.03	175
DSBPP	0.3	4.5	0.04	110
DAAP	0.3	73	0.06	1200
TOPO	0.3	>4000	0.1	>4000
Primene JM ^a	0.1	1.2	0.02	60
Amberlite LA-1 ^a	0.1	40	0.054	740
Alamine 336 ^a	0.1	>3000	0.9	>3300
Aliquat 336 ^a	0.1 ^b	~ 3000	1.0	~ 3000

^aFor structure see Sect. 7.1.^bContains also 3 vol % tridecyl alcohol.

neutral organophosphorus compounds show potential utility in polonium-bismuth separations.

Two other variables of major practical significance, extractant concentration and choice of diluent, were examined briefly. Extraction coefficients for polonium from 6 to 8 M HCl varied with the third power of the free or uncomplexed TBP concentration (0.05 to 1.0 M in DEB), the 1.3 power of TOPO concentration (0.05 to 0.5 M), and the 1.0 power of Amberlite LA-1 concentration (0.01 to 0.1 M). The third-power dependency for TBP has been observed previously.¹⁰ As expected, a wide variation in polonium extractability was achieved by using a variety of diluents. From 8 M HCl, for example, the extraction coefficient with 0.3 M DAAP varied from $E_a^o = 160$ in aliphatic Amsco 125-82, to 75 in DEB, to 0.5 in chloroform.

Future studies will be made to evaluate and compare the several possible process flowsheets

suggested by the survey experiments described above. For example, one possible process could include extracting of the 6 to 10 M HCl feed with 0.2 to 0.3 M DAAP in DEB or *n*-dodecane, scrubbing bismuth from the pregnant organic phase with 8 M HCl, and recycling of the scrub to the feed solution. Preliminary tests have shown that polonium is easily stripped from the solvent by 0.5 N HNO₃.

Since the process studies will require the use of larger amounts of polonium, with an attendant increase in level of radioactivity, it would be desirable to use a nonradioactive, but similarly behaving, stand-in element. Cursory evaluations have been made of tellurium. It was found that tellurium extraction coefficients with TBP and Alamine 336 were 100 to 1000 times lower at 2 M HCl than were those for polonium, and were 2 to 3 times lower at 8 M HCl. Thus, tellurium will have only limited utility as a stand-in for polonium in solvent extraction systems.

¹⁰K. W. Bagnall and D. S. Robertson, *J. Chem. Soc.* 1957, 509–12.

7.4 NEW EXTRACTION REAGENTS

Substituted Phenols

Fourteen new substituted phenols were tested for their ability to extract cesium from dilute caustic solutions (Table 7.2). Many of the new compounds were synthesized (by Monsanto Research Corporation, under subcontract to ORNL) to test variations in structure from the previously established good extractants, 4-*sec*-butyl-2-(α -methylbenzyl)phenol (BAMBP), 4-chloro-2-benzylphenol (Santophen-1), and 4-chloro-2(α -methylbenzyl)phenol. Although some of the new phenols, under certain conditions, extract cesium more strongly than BAMBP, none appears to have the combined extraction characteristics (extraction power, diluent compatibility, selectivity, etc.) superior to those of BAMBP. Replacing the para-substituted *sec*-butyl group of BAMBP with a *tert*-butyl or phenyl group had little effect on cesium extraction, but replacement with a benzyl decreased extractions. Replacing the *sec*-butyl group with an *n*-butyl or α -methylbenzyl group reduced the compound's solubility in Amsco 125-82 (aliphatic diluent), although cesium extractions were still strong. Use of an aliphatic diluent is ordinarily preferred, since cesium extraction coefficients are much higher for most phenols in aliphatic than in aromatic diluents. For a series of compounds with a *sec*-butyl group in the para position, and comparing various ortho-substituted groups, results were best with an α -methyl or β -styryl group in the ortho position; however, poor results were obtained when the ortho group was benzyl, benzoyl, or *sec*-butyl. Of the compounds tested thus far, the highest cesium extraction ($E_a^0 = 210$) was obtained with 4-chloro-2-(4-*n*-butylbenzyl)phenol, but phase-separation properties of this compound, at least in Amsco 125-82 diluent, are poor.

7.5 PERFORMANCE OF DEGRADED REAGENTS AND DILUENTS

In radiochemical processing by solvent extraction, degradation of the solvent phase can cause unsatisfactory operation. The amount of degradation varies with the materials used and with the extent of their exposure to radiation and reactive chemicals during the processing of the aqueous feed. Studies of several aspects of extractant and

diluent degradation have been made at ORNL, and summaries of prior work have been published.^{11,12} This year, studies have been continued on the stabilities of alkylbenzenes, especially diethylbenzenes, and of the reagent di-(*sec*-butyl) phenylphosphonate.

Isolation and Identification of Diethylbenzene Degradation Products

Last year's report demonstrated that degradation of diethylbenzenes (DEB's) by nitric acid in the presence or absence of ^{60}Co gamma radiation gave similar products. A principal *p*-DEB degradation product, 4-ethylacetophenone, was identified. The products containing nitrogen were concentrated but not identified. Since that time, with techniques such as column chromatography (elution from alumina at room temperature with petroleum ether), infrared absorption analysis, nuclear magnetic resonance spectra, and elemental analysis, the major *p*-DEB nitration product has been identified as 1- α -nitroethyl-4-ethylbenzene. This compound accounts for more than 95% of the degradation products which contain nitrogen and is probably an intermediate in the formation of the ethylacetophenone. Some ethylbenzoic acid (less than 1% of the initial DEB) has been isolated from the reaction mixture, and the ketone and nitro compounds corresponding to this acid should also be present. Infrared absorption spectra indicate that ring nitration may have occurred, but in smaller amounts. Gas chromatograms showed that the types and distribution of products were similar for each of the pure *o*-, *m*-, and *p*-DEB isomers and for commercial isomeric mixtures.

Measurement of the Heat of Diluent Degradation by Differential Thermal Analysis

When a diluent is used in a solvent extraction process, it is imperative to know whether its degradation may involve hazardous chemical reactions or products which are explosively unstable under process conditions. In this regard, in cooperation with W. H. Baldwin of the Chemistry

¹¹C. A. Blake, W. Davis, Jr., and J. M. Schmitt, *Nucl. Sci. Eng.* 17, 626-37 (1963).

¹²*Chem. Technol. Div. Ann. Progr. Rept. May 31, 1964, ORNL-3627, p. 180.*

Table 7.2. Cesium Extraction by Substituted Phenols: Effects of Reagent Structure

Procedure: Phenol solution contacted for 5 min with an equal volume of 0.01 or 0.1 M NaOH 10^{-4} M in Cs, plus ^{134}Cs tracer

Phenol	Concentration (M)	Diluent ^a	0.01 M NaOH		0.1 M NaOH	
			Final pH	E_a°	Final pH	E_a°
4-sec-Butyl-2-(α -methylbenzyl) (BAMBP) ^b	1.0	DIPB	11.5	1.8	12.8	20
	1.0	Amsco	11.7	18	12.6	100, 120
	0.5	Amsco + 2% TDA	11.9	1.8	12.7	10
4-n-Butyl-2-(α -methylbenzyl)	1.0	DIPB	9.4	0.45	12.5	82
4-tert-Butyl-2-(α -methylbenzyl)	1.0	Amsco	10.5	2.5	12.3	92
4-Benzyl-2-(α -methylbenzyl)	1.0	Amsco	10.3	0.51	12.3	14
4-Phenyl-2-(α -methylbenzyl)	1.0	Amsco	9.6	1.4	12.6	78
2,4 bis(α -Methylbenzyl)	0.5	Amsco + 2% TDA	11.8	4.5	12.6	22
4-sec-Butyl-2-benzyl	0.5	DIPB + 2% TDA		0.32	12.6	ppt.
4-sec-Butyl-2-benzoyl	1.0	Amsco	10.3	<0.01	12.5	<0.01
4-sec-Butyl-2-(β -styryl)	1.0	Amsco	8.7	1.2	11.7	35
2,4 di-sec-Butyl	1.0	DIPB	11.7	0.02	12.7	0.02
4-Chloro-2-benzyl (Santophen-1) ^b	1.0	DIPB	10.2	0.6	11.7	15
4-Chloro-2-(4-n-butylbenzyl)	1.0	Amsco	10.5	3.5	12.6	210 ^c
4-Chloro-2-hexyl-5-methyl	1.0	DIPB	10.5	0.04	12.6	0.32
4-Chloro-2,6 bis(α -methylbenzyl)	1.0	DIPB	11.7	<0.01	12.9	0.05
4-m-2,6-Dibenzyl	1.0	DIPB	11.7	0.28	12.7	2.5
4-nonyl-2-Methyl	1.0	DIPB	10.9	<0.01	12.7	0.06

^aAmsco = Amsco 125-82 (refined aliphatic diluent). DIPB = diisopropylbenzene. TDA = tridecanol.

^bSame data as reported previously.

^cVery slow phase separation.

Division, a differential thermal analysis (DTA) method has been developed to measure heat evolved during diluent degradation. A necessary feature of this method is the heating of mixtures of either aliphatic or aromatic diluents, tributyl phosphate (TBP), nitric acid, and water in a single phase. Nitrobenzene, which does not react with any of these components under the conditions of the tests, is used as the solvent. The use of a single phase has the potential drawback of giving different results than would be obtained in a two-phase solvent extraction system. However, similar gas chromatograms were obtained for *p*-DEB after boiling with 2 *M* HNO₃ for 4 hr and after heating the single-phase DTA system (2.5 ml of 1.0 *M* TBP in *p*-DEB, 1 ml of 90% HNO₃, 9 ml of nitrobenzene) to 100°C. This is strong evidence that the decomposition reactions were similar, although the conditions for degradation were different. The quantity of DEB degrading during the DTA test was estimated from the chromatogram, and the heat evolved during its decomposition was estimated from the thermogram. From these it was estimated that the heat of degradation of *p*-DEB with dilute nitric acid is 50 to 70 kcal/mole. Parallel tests with diisopropylbenzene indicated a heat of degradation of about 40 kcal/mole. In comparison, the heat of nitration of benzene to nitrobenzene is known to be 27 kcal/mole, the heat of oxidation of hydrogen to water is 58 kcal/mole, and the heat of solution of hydrochloric acid is 17 kcal/mole. Exothermic degradation in tests with *n*-dodecyl benzene was observed on the thermograms, but the total amount of material degraded was too small to enable determination of the heat of reaction. In another application of DTA, some concentrated DEB degradation products (the still-pot residue from a vacuum distillation of DEB that had been degraded by nitric acid) were sorbed on alumina and heated. Exothermic reaction began at 160°C.

Effect of Degradation on Flash Point

The closed-cup flash points of nitric-acid-degraded 1 *M* TBP in DEB and fresh 1 *M* TBP in DEB were almost the same: fresh 1 *M* TBP/DEB, 138°F; and 1 *M* TBP/DEB boiled 4 hr with 2 *M* HNO₃, 140°F.

Extraction of Fission Products by Degraded DEB

The extraction of hafnium and fission product zirconium-niobium by TBP-diluent combinations ordinarily increases when the diluent is degraded, and this property is frequently used to measure the extent of diluent degradation. From the results of previous tests¹¹ of this type with nitric-acid-degraded DEB, it was concluded that the degradation of contaminants in the DEB, rather than degradation of DEB itself, was principally responsible for the observed increase in fission product extraction. Recently, additional tests supported the conclusion.

For example, in one test series a poor-quality isomeric DEB mixture was subjected to four degradation-purification cycles. In each cycle, the DEB was boiled with 2 *M* HNO₃ for 4 hr, and the degraded DEB resulting was purified by vacuum distillation for use in the succeeding cycle. After each degradation, a sample was made to 1 *M* with fresh TBP and tested for ¹⁸¹Hf extraction. The extraction coefficients decreased with each successive degradation: $E_a^o = 3.3, 1.1, 0.25, \text{ and } 0.13$. Since the ratio of isomers changed only slightly in this experiment (*m:p:o* was 1:0.83:0.24 initially and 1:0.69:0.24 finally), the rapid decrease in hafnium extraction is believed to reflect a selective depletion of impurity.

In other tests it was found that neither of the major DEB degradation products described above accounts for the high extraction power of degraded DEB. While the hafnium extraction coefficient of a 1 *M* TBP/DEB solution boiled with 2 *M* HNO₃ for 16 hr was 15, solutions of fresh 1 *M* TBP/DEB containing purified 4-ethylacetophenone or 1- α -nitroethyl-4-ethylbenzene in approximately the same concentrations (about 10%) as they occurred in the degraded DEB gave hafnium extraction coefficients of 0.001 and 0.31 respectively. The extraction by fresh 1 *M* TBP/DEB containing no additive was 0.001.

Stability of Alkylbenzenes Made from α -Olefins

Production of biodegradable detergents has made alkylbenzenes (alkylates) derived from straight-chained α -olefins available in quantity at prices competitive with *n*-dodecane or diethylbenzene.

Three commercial products, each prepared from α -olefins in the C_9 to C_{14} range, were examined with regard to their stability toward nitric acid degradation. As indicated by a high organic-phase nitrogen concentration and a contribution to high ^{181}Hf extraction, each of these products was found to degrade severely when boiled for 4 hr with 2 M HNO_3 . This behavior is in contrast to that of *n*-hexyl- and *n*-nonylbenzene, which have good stability under the same conditions.

Examination by gas chromatography of the alkylates used in these tests showed each to have at least 17 components. Other workers¹³ have shown that while α -olefins were used in the synthesis of the alkylates, most of the products were secondary alkylbenzenes and that a high percentage of these had phenyl substitution on the interior carbon atoms of the olefin. No *n*-alkylbenzenes were observed, and a significant amount (about 10%) of more highly branched isomers and other hydrocarbons were found. Such branching provides focal points for attack by nitric acid and explains the observed instability.

Stability of Di-(*sec*-butyl) Phenylphosphonate

Undiluted di-(*sec*-butyl) phenylphosphonate (DSBPP), a solvent extraction reagent with excellent ability to separate uranium from thorium,¹⁴ was irradiated (^{60}Co gamma-ray source) to 100 whr/liter while being stirred with 2 M HNO_3 . The fission product extraction power of the irradiated material was less than that of irradiated TBP in a comparable test. Each reagent was nitrated to the extent of about 0.05 mole of nitrogen per mole of reagent. It was interesting to find that about one-third of the nitrogen was removed from both reagents by scrubbing with strong alkalis (e.g., 1 M LiOH) and that, at the same time, the fission product extraction abilities were reduced to very low levels. The degree of reagent nitration noted in these tests was not predicted from previous tests^{14,15} in which the reagent had been irradiated with a limited amount of nitric acid dissolved in

the organic phase, and further tests are being made to explain these results.

Phenyl-substituted organophosphorus reagents have been reported¹⁶ to be susceptible to formation of phenol groups on the benzene ring ortho to the attached phosphorus atom. However, infrared absorption by the irradiated DSBPP in the 3200-wave-number region attributable to phenol groups of this type was negligible in a method where the lower limit of analysis is 1 part in 250.

7.6 BIOCHEMICAL SEPARATIONS

The transfer ribonucleic acids (t-RNA's) are critical components in the first steps of protein synthesis. Specific t-RNA's transport the 20 different amino acids to the ribosome, the site of protein synthesis, following formation of the amino acyl-RNA by a corresponding specific amino acyl synthetase enzyme. Many biochemical and physicochemical experiments that could help elucidate the details of the amino acid transfer steps have not been feasible due to the lack of sufficient quantities of highly purified specific t-RNA's. To meet this need, the biochemical separations program was undertaken, in conjunction with the Biology Division, to investigate methods for the preparation of purified specific t-RNA's from *E. coli*.

Last year, progress was reported¹⁷ on the development of a method for recovering mixed t-RNA's from *E. coli*. This method has received additional attention. In the current procedure the cells are broken with phenol to recover nucleic acids; then higher-molecular-weight RNA and DNA are removed by an isopropanol fractionation step, final purification of the mixed t-RNA's is achieved by a batch operation on a diethylaminoethyl-cellulose column. The process is being scaled up to provide larger amounts of mixed t-RNA's suitable for subsequent separation into purified specific t-RNA's.

As a result of recent studies, a new reverse-phase column (extraction) chromatography system

¹³W. J. Carnes, *Anal. Chem.* **36**, 1197-1200 (1965).

¹⁴C. A. Blake *et al.*, *Comparison of Dialkyl Phenylphosphonates with TBP in Nitrate Systems*, ORNL-3374 (Jan. 8, 1963).

¹⁵*Chem. Technol. Div. Chem. Dev. Sect. C Monthly Progr. Rept. November 1959*, ORNL-CF-59-11-132 (Jan. 12, 1960).

¹⁶E. S. Lane and A. Pilbeam, *The Radiation Decomposition of Some Phenyl Substituted Organo-Phosphorus(V) Extractant Systems*, AERE-M-1284 (January 1964).

¹⁷A. D. Kelmers and M. P. Stulberg, "The Separation of Transfer-RNA by Reverse Phase Chromatography," presented at the 49th Meeting of Federation of American Societies for Experimental Biology, Atlantic City, N.J., April 9-14, 1965.

based on anion exchange properties has been devised. It affords significant resolution of the mixed t-RNA's and permits the preparation of certain purified specific t-RNA's. Quaternary ammonium compounds were evaluated as extractants, since they maintain anion exchange ability at the neutral pH necessary to protect the t-RNA from hydrolysis reactions. A series of screening experiments were carried out to select a combination of quaternary ammonium extractant and organic diluent compatible with aqueous t-RNA solutions. Of the combinations studied, only dimethyldilaurylammonium chloride in isoamyl acetate consistently gave satisfactory phase disengagement. Hydrophobic diatomaceous earth was then chosen as the column packing to support this organic phase in the form of a thin film. It was selected since it is not wetted by the aqueous phase and has a high surface area with a minimum of porous structure. In the chromatography experiments the t-RNA mixture was dissolved in a dilute aqueous NaCl solution and loaded on the column. The specific t-RNA's were then eluted sequentially by an increasing concentration of NaCl in the eluting solution. The presence of 0.01 M Mg²⁺ in the eluting solution had a pronounced effect on the chromatographic resolution of the specific t-RNA's, sharpening some t-RNA peaks and broadening others. Magnesium ion is known to interact with t-RNA to change the secondary structure, and this apparently alters the interaction between t-RNA and the quaternary ammonium chloride. A magnesium concentration gradient was used in the eluting solution, in addition to the NaCl gradient, to obtain satisfactory chromatographic resolution of 16 specific t-RNA's, as shown in Fig. 7.3. A single peak each was obtained for alanyl-, histidyl-, isoleucyl-, lysyl-, methionyl-, phenylalanyl-, prolyl-, threonyl-, tyrosyl-, and valyl-t-RNA's. Asparagine and aspartic acid acceptance coincided in a single peak, suggesting that both were binding to the same t-RNA. Glutamine charging was obtained only with the first column-breakthrough fractions. If this is glutamyl-t-RNA it must be quite different from the others, since it was not retarded by the column. Two distinct arginyl-t-RNA and five leucyl-t-RNA peaks were obtained, showing in one column experiment a resolution obtained by other experimenters only after more than a thousand countercurrent solvent extraction stages.

As a result of these data, attention was directed toward the preparation of samples of purified

Table 7.3. Purification of Phenylalanyl-t-RNA

Chromatography Experiment	Recovery (%) ^a	Concentration Factor	
		Pooled Fractions	Peak Fraction
Initial	100	1	1
After first	91	13	23
Pooled for second	74		
After second	54	24	29

^aDetermined by assay for phenylalanine acceptance after each experiment, and expressed as percentage of the initial amount of phenylalanyl-t-RNA.

phenylalanyl-t-RNA. A sample of the mixed t-RNA's was chromatogrammed, and the resulting fractions were assayed for phenylalanine acceptance. The main portion of the phenylalanyl-t-RNA peak was pooled and rechromatogrammed. Following this, the phenylalanyl-t-RNA was recovered in a symmetrical ultraviolet-absorbing peak, indicating that it was substantially purified. The data (Table 7.3) show that 54% of the initial phenylalanyl-t-RNA was recovered at a concentration 24 times the initial concentration. The question of absolute purity, or the number of moles of phenylalanine accepted per mole of t-RNA, cannot be accurately established, since the molar extinction coefficient for phenylalanine-accepting t-RNA has not been determined. When a reasonable approximate value for the molar extinction coefficient was used, the material in the peak chromatography fraction was estimated to be at least 74% pure phenylalanyl-t-RNA.

Larger-scale experiments are under way to recover the phenylalanyl-t-RNA from 14 g of commercial, mixed t-RNA's. It will be made available for further biochemical and physicochemical experiments.

7.7 EXTRACTION PROPERTIES OF LANTHANIDE AND ACTINIDE COMPLEXES

In the development of the Talspeak process for separating trivalent actinides from lanthanides by extraction with di(2-ethylhexyl)phosphoric acid

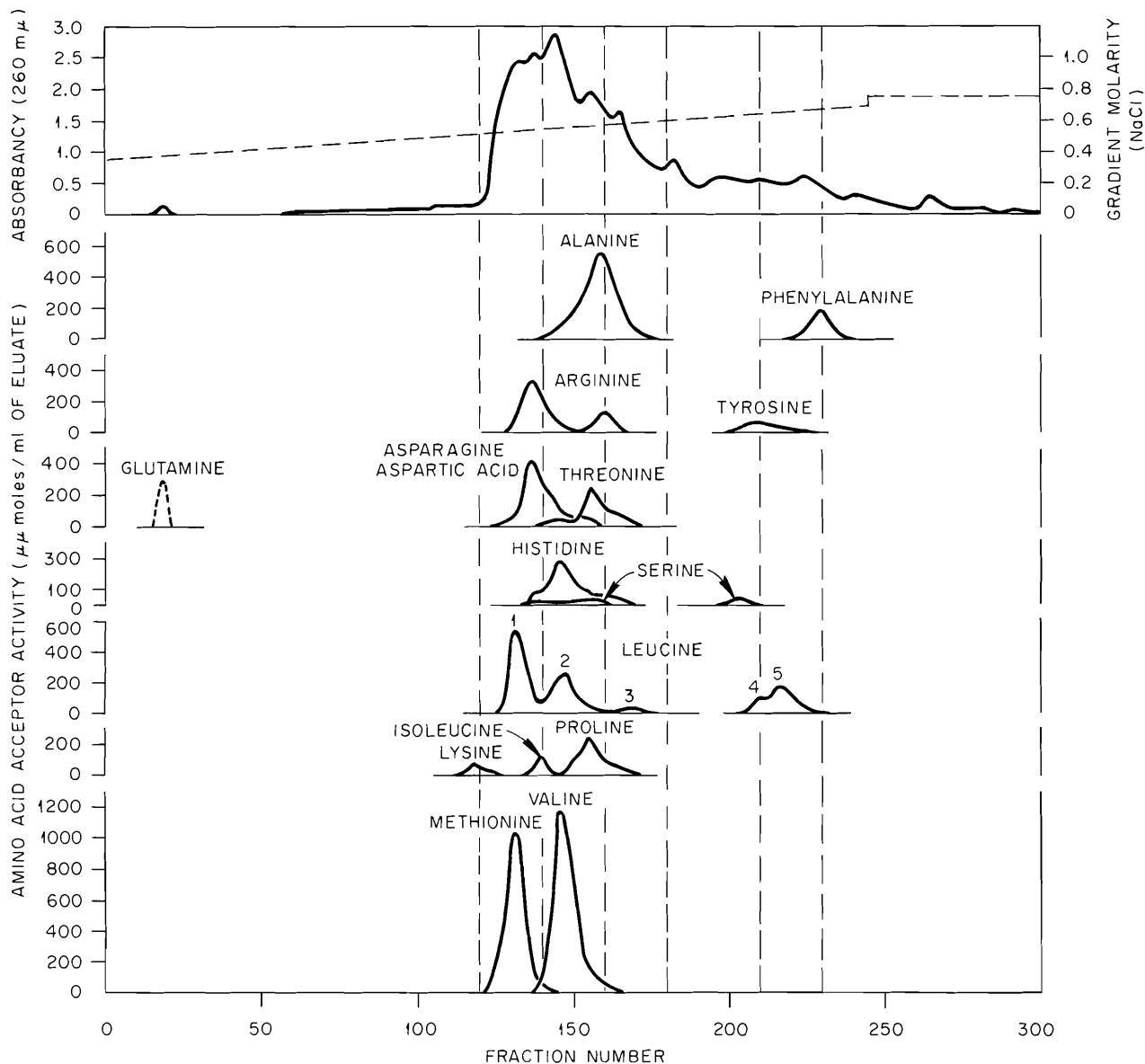


Fig. 7.3. Chromatograph of a 100-ml Sample of Commercial t-RNA on a Column 9 mm in Inner Diameter and 8 ft Long.

(HDEHP) from lactic acid solutions containing sodium diethylenetriaminepentaacetate (Na_5DTPA) (see Sect. 5.6), it was observed that HDEHP solutions extracted lanthanum up to a concentration of about 1.5 equivalents per mole of HDEHP, that is, to 50% higher loading than would be possible with formation of a simple lanthanum organophosphate salt. The extraction was then examined in

detail to explain the high loading and to determine what significance it might have in process use.

Measurable lactate was extracted in all tests (1 M HDEHP extracting from 1 M lactic acid, pH 3). When the concentration of extracted lanthanum was less than 0.01 M, the extracted lactate concentration was constant at about 0.015 M. When more lanthanum was present, the lactate extraction

increased, for example, to 0.05 M lactate at 0.1 M La, and to 0.5 M lactate at 0.45 M La. This latter corresponds rather closely to extraction of $\text{LaC}_3\text{H}_5\text{O}_3^{2+}$, consistent with the observed high loading.

Since the mole ratio of extracted lactate to extracted lanthanum varies with the absolute lanthanum concentration, this must contribute at least in part to the complicated extraction isotherms found in this system (Fig. 7.4). As the organic-phase lanthanum concentration increases from about 0.03 to about 0.1 M, its extraction coefficient increases abruptly. This is shown by the slopes in Fig. 7.4, and more clearly by a direct plot of the extraction coefficient in Fig. 7.5. (Similar plots at other concentrations of Na_5DTPA show that it decreases the extraction by complex formation but has only minor effects on the shape of the isotherm.) Corresponding extractions of americium from lanthanum solutions gave a curve (Fig. 7.5) qualitatively similar to that for lanthanum, with indicated separation factors ranging from greater than 300 at organic lanthanum concentrations below 2 g/liter to 90 at 20 g/liter.

7.8 RECOVERY OF RUBIDIUM FROM ORES

The phenol extraction (Phenex) process, originally developed for recovering fission product cesium from reactor-fuel reprocessing wastes (Sect. 8.1) and subsequently for the recovery of cesium from ores,^{18,19} has now been developed for recovering rubidium from alkaline-ore leach liquors. The process, which includes extraction with a substituted phenol and acid stripping, is very similar to the process developed for recovering cesium except that a higher pH is required for effective rubidium extraction. Extractions of alkali metals with the substituted phenols are in the order: $\text{Cs} > \text{Rb} > \text{K} > \text{Na} > \text{Li}$, with separation factors between adjacent members of the series being in the range 10 to 20.

¹⁸Chem. Technol. Div. Ann. Progr. Rept. May 31, 1963, ORNL-3452, p. 176.

¹⁹Chem. Technol. Div. Ann. Progr. Rept. May 31, 1964, ORNL-3627, p. 188.

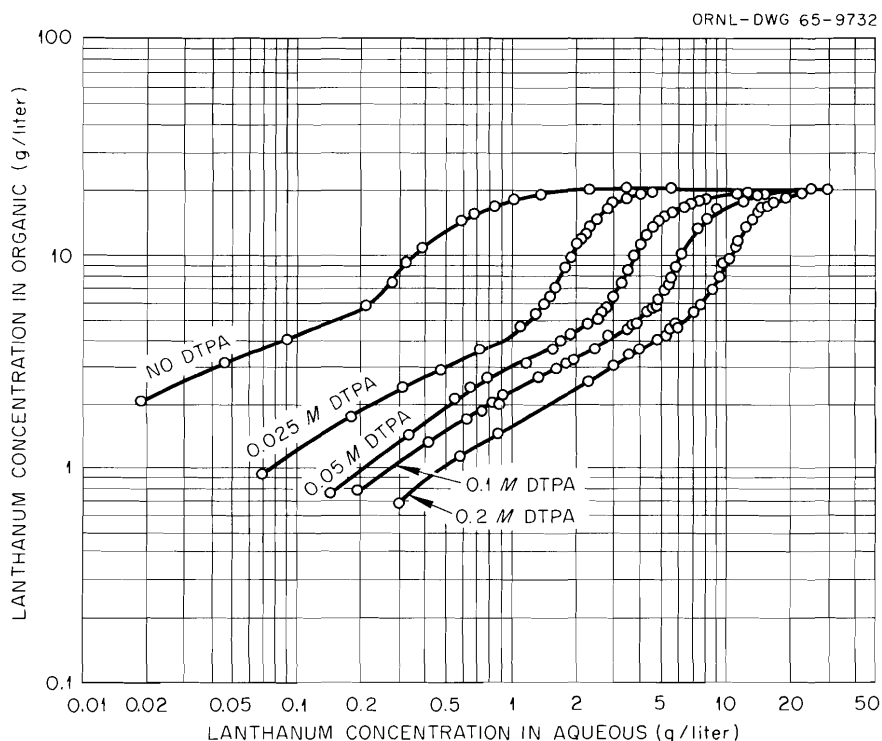


Fig. 7.4. Lanthanum Extraction Isotherms. Organic phase: 0.3 M HDEHP in DIPB. Aqueous phases: various DTPA concentrations, 1 M lactic acid plus lanthanum lactate.

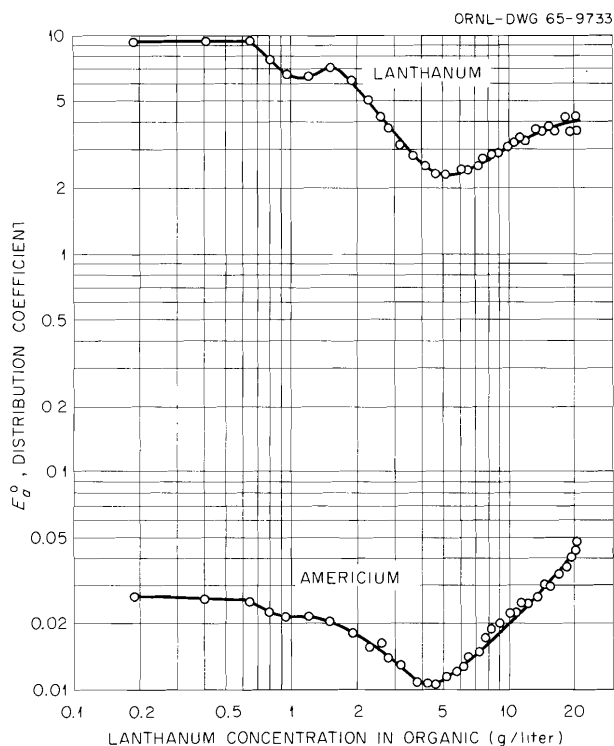


Fig. 7.5. Extraction of Lanthanum and Americium by HDEHP from Lactate-DTPA Solutions. Organic phase: 0.3 M HDEHP. Aqueous phase: 1 M lactate, 0.05 M DTPA, pH 3.3.

Recovery from Alkarb

Alkarb (an alkali-metal carbonate by-product of the lithium industry), which contains about 18% rubidium, 2% cesium, and 38% potassium, is a good source of rubidium and, to a lesser extent, cesium. Alkarb is soluble in water to more than 600 g/liter. Two process arrangements appear to be satisfactory for recovering rubidium and cesium from Alkarb: (1) extraction of cesium in a primary cycle followed by extraction of rubidium in a second cycle at a higher pH, and (2) coextraction of cesium and rubidium at high pH followed by selective stripping of rubidium from the extract to obtain separation from cesium.

In a batch-countercurrent test demonstrating the coextraction procedure, 97.5% of the rubidium and more than 99% of the cesium were recovered from Alkarb solution with 1 M 4-sec-butyl-2-(α -methylbenzyl)phenol (BAMBP) in Amsco 125-82. Three extraction and three water-scrub stages (Fig. 7.6) were used. The solvent/feed/scrub water flow

ratios were 9.0/1.0/1.65. Decontamination factors (feed to scrubbed extract) for rubidium were 47 from potassium and 250 from sodium. The scrubbed extract contained about 5% potassium, based on rubidium, but a much purer product could, of course, be obtained by using more scrub stages.

The feed solution for the above test was prepared by dissolving Alkarb in water to a concentration of 500 g/liter and adjusting this solution with caustic to a pH above 14. The amount of caustic added was equivalent to the rubidium plus cesium in the solution, plus about 0.8 M excess.

In selectively stripping rubidium from the extract with acid to obtain separation from cesium, the acid concentration and phase ratio in the stripping system are chosen so that the amount of acid supplied is less than the amount equivalent to the rubidium in the extract. This procedure was not demonstrated in a countercurrent system. However, data from batch tests in which the extract was cascaded against successive one-fifth volumes of 0.1 M HCl show the ease with which rubidium is stripped, compared with cesium:

Number of Contacts	Total Amount Stripped (%)	
	Cs	Rb
1	4	27
2	8	55
3	15	81
4	73	>99

Recovery from Pollucite Liquors

Raffinates from the recovery of cesium from pollucite¹⁹ contain small concentrations of rubidium that are recoverable by phenol extraction. In batch-extraction tests at a phase ratio of 1/1, coefficients for extraction of rubidium from a pollucite raffinate (0.35 g of rubidium per liter) with 1 M BAMBP in Amsco 125-82 were 1.3, 2.9, and 5, respectively, at pH's of 12.4, 12.7, and 12.9. Increasing the BAMBP concentration from 1 M to 1.5 M approximately doubled the extraction coefficient. An isotherm for extraction of rubidium with 1 M BAMBP in Amsco 125-82 from a raffinate adjusted to pH 13 showed a maximum solvent loading of about 1.3 g of rubidium per liter. At

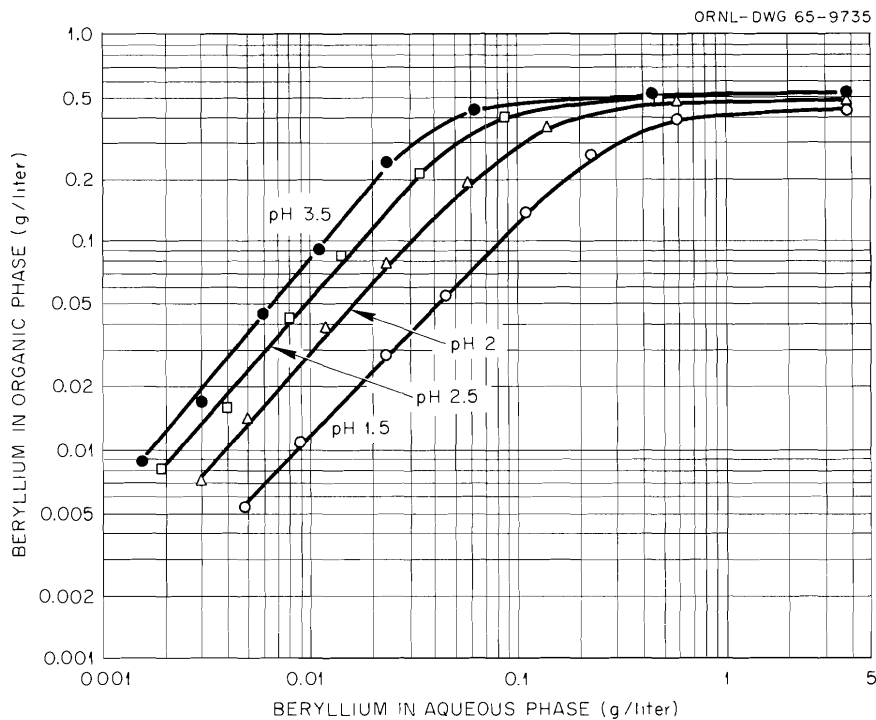


Fig. 7.7. Extraction of Beryllium with 0.3 M Amine 21F81 in Solvesso 100. Aqueous phase: 1 M SO_4^{2-} , concentration of beryllium varied in the range 0.01 to 4.5 g/liter. Contact time: 10 min at phase ratio of 1/1.

requirements therefore depend on the amount of beryllium rather than the amount of amine in the system. Stripping is most effective when about 1 equivalent of fluoride for each equivalent of beryllium in the extract is fed to the system. With larger amounts of fluoride, less beryllium is stripped, presumably due to formation of some extractable beryllium fluoride complexes. The total amount of beryllium stripped in batch tests (Fig. 7.8) increased from 75% with a fluoride-to-beryllium mole ratio of 1.1/1 to 96% with a ratio of 2.3/1, and then decreased to 80% with a ratio of 4.6/1. In these tests, 0.3 M amine 21F81 was stripped by contact first with an ammonium fluoride-ammonium sulfate solution and then with four successive volumes of 0.01 M H_2SO_4 . Each contact was at an organic/aqueous phase ratio of 6/1. Small amounts of fluoride, extracted in the initial contact, greatly enhance the efficiency in subsequent stripping with 0.01 M H_2SO_4 . According to the flowsheet being tested, the strip product solution is neutralized with ammonia to precipitate beryllium and is then filtered. Some of the filtrate

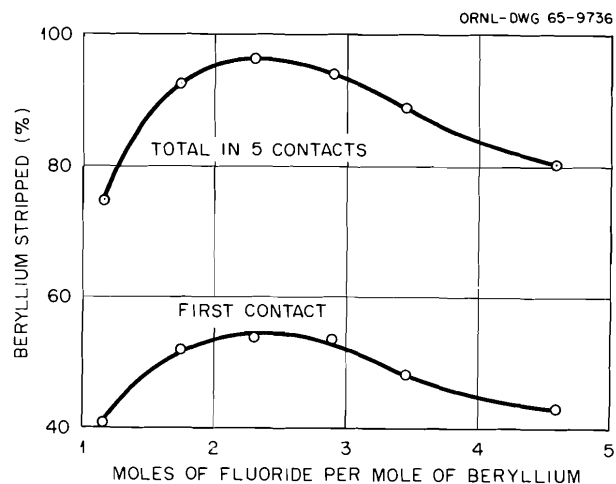


Fig. 7.8. Stripping Beryllium with Fluoride Solutions. Organic phase: 0.3 M Amine 21F81 in Solvesso 100 (loaded to the extent of 0.29 g of Be per liter). Procedure: organic phase contacted with 0.1 M $(\text{NH}_4)_2\text{SO}_4$ solutions that were 0.23 to 0.93 M in F^- , and then with four successive volumes of 0.01 M H_2SO_4 . All contacts at organic/aqueous phase ratio of 6/1.

(which contains fluoride) is returned to the first stripping stage to decrease requirements for makeup fluoride.

7.10 RECOVERY OF ACID BY AMINE EXTRACTION

A tentative process previously outlined²¹ for the recovery and purification of phosphoric acid by tertiary amine extraction was tested with a sample of wet-process phosphoric acid obtained from the TVA Pilot Plant in Muscle Shoals, Alabama. Isotherms for extraction of phosphoric acid from the TVA liquor with Alamine 336 show an increase in loading of the organic phase to about 70 g of H_3PO_4 per liter, with increasing aqueous phosphoric acid concentration, and then a rapid drop-off in loading (Fig. 7.9). In these tests the organic phase was cascaded against fresh volumes of liquor. The drop-off in loadings is caused by dis-

²¹Chem. Technol. Div. Ann. Progr. Rept. May 31, 1963, ORNL-3452, p. 177.

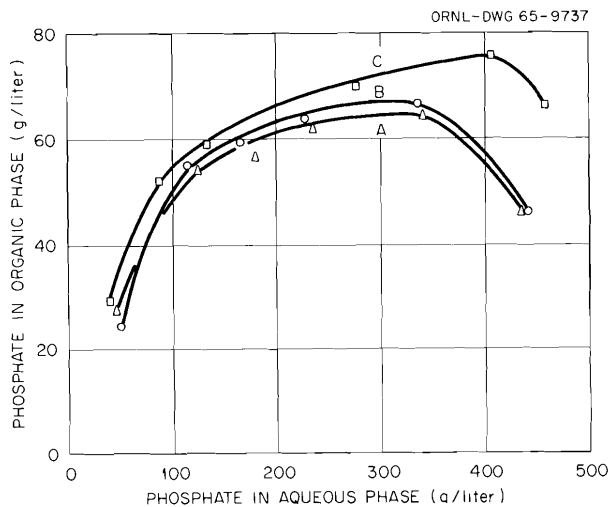


Fig. 7.9. Extraction of Phosphoric Acid with Alamine 336. Aqueous: wet-process phosphoric acid from TVA containing, in grams per liter, 490 PO_4 , 11.4 Fe, 3.3 Al, 0.4 Ca, 4.5 Si, and 15 SO_4 . Organic: 0.5 M Alamine 336 in (a) 90% Amsco 123-15-10% isodecanol or (b) Solvesso 100. In (c), most of the sulfate was removed from the liquor (by extraction with Alamine 336) prior to extraction with 0.5 M Alamine 336 in 80% Amsco 123-15-20% isodecanol.

placement of extracted phosphoric acid with sulfuric acid, present in the liquor at a concentration of about 0.25 M. Interference from sulfuric acid was decreased (curve c) by preferentially extracting it with an amine in a prior extraction step. Separation from sulfuric acid can also be obtained in the stripping cycle, since the phosphoric acid is preferentially stripped with water. The sulfuric acid (and some phosphoric acid) remaining in the solvent can then be stripped with ammonium hydroxide to give a mixed ammonium sulfate-ammonium phosphate product. Recoveries of phosphate from the liquor are limited to about 90%. The residual phosphate is present as metal phosphate salts and, as such, is not extractable.

In batch extraction-water stripping tests, the decontamination factors for phosphoric acid were more than 100 from silica, sulfate, and aluminum, and 5 from iron. The separation from iron was much poorer than expected on the basis of tests with synthetic liquors. Surprisingly, phase separation was much faster in both the extraction and stripping steps when mixing was with the aqueous phase continuous than with the organic phase continuous. However, even with aqueous-continuous mixing, separation of the phases was very slow.

These preliminary studies were not adequate to define the potential of the process. More information is needed about the acceptability of the products and process economics, compared with those for competitive recovery processes. Also, unless the rate of phase separation in the solvent extraction system can be improved, commercial utility is questionable for this reason alone.

7.11 RECOVERY OF THORIUM FROM GRANITIC ROCKS

As described previously,²²⁻²⁴ granitic rocks are being evaluated as a future source for large tonages of thorium (and uranium), which eventually

²²Chem. Technol. Div. Ann. Progr. Repts. May 31, 1961, ORNL-3153, p. 102; June 30, 1962, ORNL-3314, p. 182; May 31, 1963, ORNL-3452, p. 196; and May 31, 1964, ORNL-3627, p. 193.

²³K. B. Brown et al., "Thorium Reserves in Granitic Rock and Processing of Thorium Ores," in *Proceedings of the Thorium Fuel Cycle Symposium, Gatlinburg, Tenn., Dec. 5-7, 1962*, TID-7650, Book I.

²⁴H. Brown and L. T. Silver, *Proc. Intern. Conf. Peaceful Uses At. Energy, Geneva, 1955*, 8, 129 (1956).

will be needed for power-reactor systems. After tests of a large variety of granitic rocks from different locations, principal interest has centered on the Conway granite formations of New Hampshire. These have a relatively high thorium content and respond well to process treatment. Based on surface and drill-core data obtained by Rice University investigators under subcontract to ORNL, reserves of thorium and uranium in the outer 1000 ft of the main Conway formations are estimated at about 35 million and 10 million tons respectively. About two-thirds of these reserves are recoverable by ordinary methods.

At this time, the experimental program on evaluating granites is almost complete, and final reports covering the exploration program, process studies, and cost estimates are being prepared. During the past year, experimental studies included development of a different procedure for leaching granite and further studies on recovering thorium and uranium from the leach liquors by amine extraction.

Leaching Tests

Effective recovery of thorium and uranium from Conway granite was obtained by an acid-cure-percolation-wash procedure similar to those used in certain copper and uranium mills. The ore is agglomerated by mixing it with relatively concentrated sulfuric acid at high pulp density, and the

agglomerated ore is "cured" for several hours and then percolation washed in a fixed bed. Estimated capital and operating costs are considerably lower, and recoveries are about the same for this leaching method compared with the method proposed previously (6 hr leach with 2 *N* H₂SO₄ at room temperature, and 60% pulp density).

Preliminary small-scale tests of the acid-cure procedure indicated that about 85% pulp density is optimum and that, at this pulp density, the acid concentration should be 3 to 4 *N*. Extending the curing time beyond 5 hr increased acid consumption without significantly increasing recoveries. Curing the ore at about 45°C increased recoveries by about 10%, compared with recoveries at room temperature, but acid consumption also was higher.

Amine Extraction of Thorium and Uranium

Thorium and uranium were coextracted effectively from a Conway-granite leach liquor with a mixture of a primary amine (1-nonyldecylamine) and a secondary amine (N-benzylheptadecylamine). The primary amine serves mainly to extract thorium, and the secondary amine to extract uranium, although each extracts both metals to some extent. With each amine at 0.01 *M* concentration, extraction coefficients were more than 400 for thorium and more than 200 for uranium (Table 7.4).

Table 7.4. Extraction of Thorium and Uranium from Granite Leach Liquor with Amine Mixture

Organic: 0.01 *M* 1-nonyldecylamine + 0.01 *M* benzylheptadecylamine in 99% kerosene-1% tridecanol

Aqueous: Conway granite leach liquor (pH 0.9) containing, in g/liter, 0.035 Th, 0.007 U, 1.32 Fe(II), 0.13 Fe(III), 0.7 Al, 0.03 Ti, 0.13 Zr, 0.18 PO₄, and 0.65 F

Contact time: 10 min

Ratio (aq/org)	Analysis (g/liter)				Extraction Coefficient, E_a°	
	Organic		Aqueous		Th	U
	Th	U	Th	U		
1	0.038	0.006	<0.001	0.00003	>38	200
3	0.10	0.021	<0.001	0.00009	>100	230
7	0.25	0.044	<0.001	0.0002	>250	220
11	0.37	0.077	<0.001	0.0004	>370	190
15	0.44	0.089	<0.001	0.001	>440	90

Process Demonstration

A bench-scale demonstration was made of a complete leaching-solvent extraction flowsheet for recovering thorium and uranium from a composite of three Conway-granite drill cores crushed to -20 mesh. In treating 11 kg of granite containing 59 ppm thorium and 16 ppm uranium, the overall recoveries were 60% for thorium and 65% for uranium. The tests included mixing 1-kg batches of crushed ore with a solution about 4 *N* in H_2SO_4 at 85% pulp density for 10 min, curing in a 2-in.-diam column for 5 hr at room temperature, and washing in place in the column with raffinate from the solvent extraction operation (Fig. 7.10). The initial solution collected from the column was relatively concentrated in the metal values and was designated as pregnant liquor. A portion of this was fortified with concentrated sulfuric acid and used for agglomerating the next batch of ore, while the remainder was passed to the solvent extraction circuit. The last wash solution collected from the column was stored and used for washing the next batch of ore. Sulfuric acid consumption in leaching was 54 lb per ton of ore. More than 98% of the thorium and uranium were extracted from the pregnant liquor (0.052 g of thorium and 0.015 g of uranium per liter) in two mixer-settler stages with 0.01 *M* 1-nonyldecylamine-0.01 *M* *N*-benzylhepta-

decylamine in 99% kerosene-1% tridecanol at an aqueous/organic phase ratio of 6/1. The extract was stripped in two stages with 0.25 *M* Na_2CO_3 solution at an aqueous/organic ratio of 1/8. Acidifying the strip solution with sulfuric acid and neutralizing with ammonia gave a precipitate which, after calcination, contained about 70% thorium-plus-uranium oxides.

Physical operation of the percolation-wash column was highly satisfactory. The effluent was clear, and the ore showed no tendency to deagglomerate. The pressure drop in the column was low.

Recovery Costs

A new estimate of costs for recovering thorium and uranium from granites was prepared with the aid of A. H. Ross and Associates of Toronto, Canada. Because of simplifications made in the process flowsheet, which reduced capital and operating costs, the new estimated costs are more than 25% lower than the costs estimated previously.^{22,23} Costs for recovering thorium and uranium from granite of the composition of the Conway drill-core composite used in the demonstration run are estimated at about \$35 per pound of thorium-plus-uranium recovered.

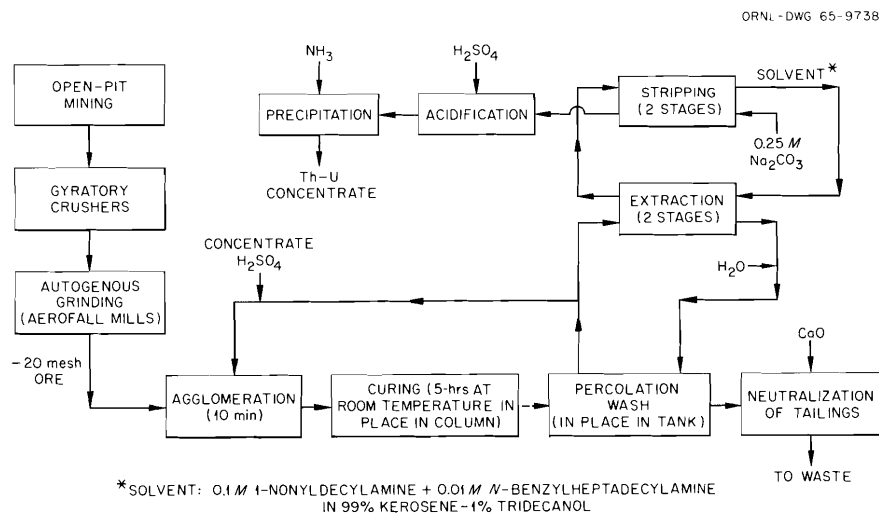


Fig. 7.10. Flowsheet for Recovering Thorium and Uranium from Granite.

7.12 SEPARATION OF BIOLOGICAL MACROMOLECULES

The recovery of biologically important substances, present in only small quantities in the initial cells, requires the treatment of large amounts of the source material to obtain significant quantities of the desired substance. For example, to obtain gram amounts of the phenylalanine transfer ribonucleic acid (t-RNA) from *E. coli* bacteria, a facility for treating 100-kg quantities of bacteria is necessary. Similarly, the preparation of other macromolecules, for example, enzymes, also requires the processing of large amounts of material.

In order to produce the amounts of specific macromolecules needed for biochemical and physicochemical studies, a large-scale facility was designed and is being built. It is expected to be in use early in fiscal year 1966. The procedures for recovering many biological macromolecules have a number of common unit operations, for example, processing at about 4°C to avoid degradative reactions, centrifuging (at about 4°C) to separate solids, and further purifying by various types of column chromatography. Consequently, it was possible to design a versatile facility for producing a wide variety of macromolecules. The room is 20 ft long and 12 ft wide, and the temperature is held at about 4°C. The apparatus consists of several sizes of refrigerated centrifuges and other equipment.

The initial operation will consist in the preparation of 100-g batches of mixed t-RNA's from *E. coli*, to support the Biochemical Separations Research activities (Sect. 7.6). As process details for the recovery of specific t-RNA's, for example, phenylalanine t-RNA, are defined, gram amounts of these materials will also be prepared. As these processes are mastered, attention will be directed toward other materials, such as aminoacyl synthetase and DNA polymerase enzymes.

7.13 EXTRACTION OF ALKALINE EARTHS BY DI(2-ETHYLHEXYL)PHOSPHORIC ACID

The study of strontium extraction by di(2-ethylhexyl)phosphoric acid (HA) in benzene²⁵ was

²⁵W. J. McDowell and C. F. Coleman. "Sodium and Strontium Extraction by Di(2-ethylhexyl)phosphate: Mechanisms and Equilibria," *J. Inorg. Nucl. Chem.* (in press).

extended to a comparison with all the other alkaline earths except radium. Extractions from 4.0 M (Fig. 7.11) and 0.5 M NaNO₃ aqueous solutions were measured as functions of the two variables aqueous-phase pH and organic-phase HA concentration. These data were analyzed by the methods developed in the previous study of strontium extraction to obtain a fairly definite indication of the principal organic-phase species involved in the extraction of each.

All the curves of log E_a^o vs pH are similar in shape, showing the linear portion at low pH followed by a maximum, a decrease, and a leveling off above pH 6 or 7. The slope of the initial linear portions is 2, consistent with cation exchange between M^{2+} and $2H^+$. The order of extractability of the ions is: Be >> Ca > Mg \geq Sr > Ba. Thus, except for magnesium, the extractability increases with increasing charge density on the ion. This is the same direction of order as was found in extraction of alkali ions by the same extractant,²⁶ while it is the reverse of the order usually found for sorption by sulfonic or carboxylic acid resins.

In general, the maximums in the E_a^o -vs-pH curves are relatively higher and sharper for the more-extractable ions. (The high beryllium curve in Fig. 7.11 is truncated by the analytical limit encountered.) As was previously shown,²⁵ the degree of neutralization of HA, expressed as the organic-phase composition $NaA/\Sigma A$, yielding the maximum extraction is related to the stoichiometry of the predominant extraction species of M^{2+} (present at tracer concentration). These compositions are near $NaA/\Sigma A = 0.33$ for barium, strontium, and calcium, consistent with complexes $MA_2 \cdot 4HA$ as already identified for strontium, but between 0.4 and 0.5 for magnesium, suggesting a shift toward $MgA_2 \cdot 2HA$.

The dependence of extraction coefficient on HA concentration varies somewhat over the range 0.015 to 0.5 M HA (Fig. 7.12). The log-log slopes indicate that in extraction from 4 M NaNO₃, calcium (at high HA concentrations), strontium, and barium form $MA_2 \cdot 4HA$, which was the conclusion reached from the positions of the extraction maximums. Calcium (at low HA concentrations) and beryllium probably form more $MA_2 \cdot 2HA$. In extraction from 0.5 M NaNO₃, not only calcium but also magnesium,

²⁶*Chem. Technol. Div. Ann. Progr. Rept. June 30, 1962, ORNL-3314, p. 112.*

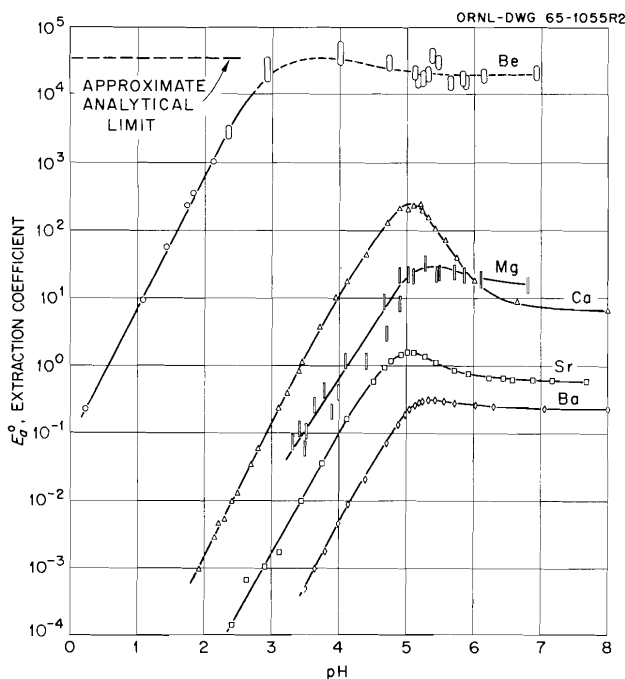
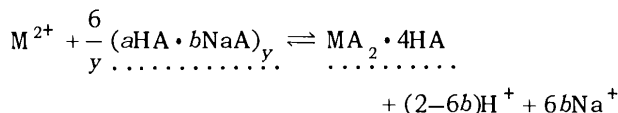


Fig. 7.11. Extraction of $10^{-4} M$ Be, Ca, Sr, and Ba, and $0.01 M$ Mg from $4 M$ NaNO_3 by $0.125 M$ Di(2-ethylhexyl)phosphate in Benzene.

strontium, and barium (beryllium not ascertained) shift from $\text{MA}_2 \cdot 4\text{HA}$ at high HA concentration to $\text{MA}_2 \cdot 2\text{HA}$ at low concentration.

Since the HA concentration-dependence data were obtained at low pH, where the extractant is almost entirely in the acid form and the power dependence on hydrogen ion concentration is -2 , the possibility of extraction of a metal mononitrate or hydroxide seems to be eliminated. The shift in the association ratio A/M from 6 to 4 could reflect a change in the coordination number of the metal or, more probably, replacement of a part of the HA by water. The suggested extraction reactions (dotted underlines indicate organic-phase species) are:



for barium and calcium as well as for strontium²⁵ at $\Sigma A \geq 0.125 M$ and for magnesium at $\Sigma A > 0.25 M$;

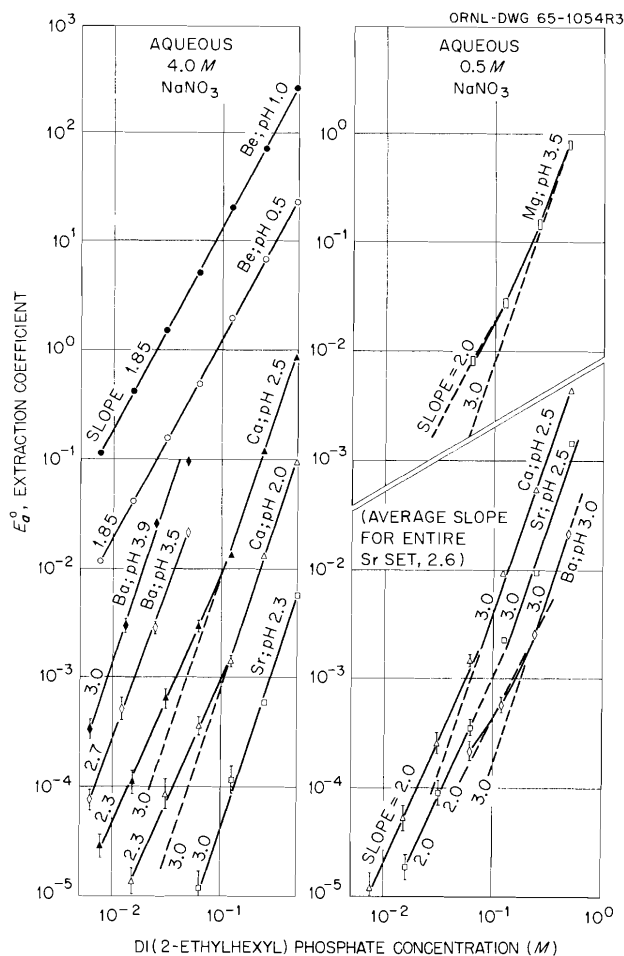
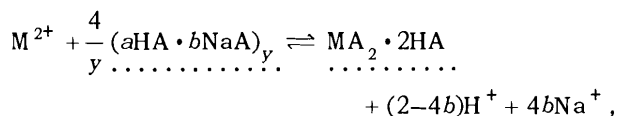


Fig. 7.12. Extraction of Alkali Metals from Aqueous NaNO_3 by Di(2-ethylhexyl)phosphate in Benzene: Reagent-Concentration Dependence.

with probably some water also extracted, at lower HA concentrations for calcium and magnesium, for strontium and barium from $0.5 M$ NaNO_3 only, and under all conditions tested for beryllium.

7.14 INTERMOLECULAR BONDING IN ORGANIC MIXTURES

In the testing and interpretation of distribution systems, qualitative or quantitative information is frequently required about intermolecular association between solute species or between solute and diluent. Several different physical properties are used to detect such association in the organic solutions studied in this laboratory, including infrared absorption, nuclear magnetic resonance

(nmr), diluent vapor pressure, light scattering, relative viscosity, and, recently,²⁷ dielectric constant.

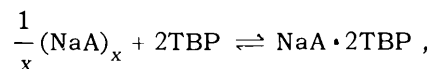
Sodium and Strontium Di(2-ethylhexyl)phosphates

In tests reported previously, the dielectric constants of mixtures indicated intermolecular bonding between tributyl phosphate (TBP) and the sodium complex $\text{NaA} \cdot 3\text{HA}$, but not between TBP and $(\text{HA})_2$ [di(2-ethylhexyl)phosphoric acid], at concentrations up to 0.2 *M*, in *n*-octane.²⁷ In extension of these tests to other important species in the HA-strontium-sodium extraction system, nonlinear variation of the dielectric constant of mixtures indicated interaction between TBP and the strontium complex $\text{SrA}_2 \cdot 4\text{HA}$ and much stronger interaction between TBP and the salt SrA_2 , again at concentrations up to 0.2 *M*. A relatively high dielectric constant for 0.2 *M* SrA_2 , 3.55 as compared with 2.13 for TBP and 2.04 for $\text{SrA}_2 \cdot 4\text{HA}$ and $(\text{HA})_2$, supports previous suggestions that the strontium salt is polymerized and hydrated. Polymerization of SrA_2 is also indicated by the relative viscosity of $(\text{HA})_2$ - SrA_2 mixtures, which remains constant as the equivalent ratio $\text{SrA}_2/\Sigma \text{A}$ increases from 0 to about 0.9 and then increases abruptly by a factor of at least 5 as $\text{SrA}_2/\Sigma \text{A}$ approaches 1. The dielectric constant also increased abruptly as $\text{SrA}_2/\Sigma \text{A}$ approached 1.

In connection with the dielectric measurements, dipole moments of several of the compounds were obtained over a range of concentrations in *n*-octane. The dipole moment of SrA_2 increased approximately linearly from 8.3 Debye units at 0.0015 *M* to 12.8 Debye units at 0.1 *M*, presumably reflecting increase of the polymerization and hydration mentioned above. The values for the others changed only slightly with concentration: $\text{SrA}_2 \cdot 4\text{HA}$, 4.0–4.9 at 0.002–0.03 *M*; $\text{NaA} \cdot 3\text{HA}$, 3.5–4.5 at 0.008–0.25 *M*; $(\text{HA})_2$, 2.5–3.1 at 0.015–1 *M*; TBP, 2.4–3.0 at 0.015–1 *M*.

Strong association of TBP with the salt NaA (or complete replacement of acid molecules in the complex $\text{NaA} \cdot 3\text{HA}$ by TBP), rather than formation of an NaA-HA-TBP mixed complex, was indicated by the average aggregation numbers of a series of mixtures in dry *n*-octane, measured by isopiestic

balancing against azobenzene. With the mole ratio $\text{NaA}/\Sigma \text{A}$ constant at $\frac{1}{2}$ and $\Sigma \text{A}/\text{TBP}$ varied from 0 to 4, the apparent average aggregation numbers varied from 1 to 3.3, rather closely consistent with complete association according to the reaction



with $x \geq 4$.

BAMBP

Combinations of BAMBP [4-*sec*-butyl-2-(α -methylbenzyl)phenol] with two synergizing organic acids and with three diluents of different hydrogen-bonding capabilities were examined in several ways for possible intermolecular association. In most of the tests the two components were mixed at a total concentration of 0.5 or 2 *M*, in carbon tetrachloride. Nonlinear variation of the dielectric constants of mixtures and downfield chemical shift of a single resonance for the combined acid and hydroxyl protons indicated hydrogen bonding of BAMBP with $(\text{HA})_2$. Infrared spectra confirmed the association by the appearance of a new absorption band at 3374 cm^{-1} . The absorbances plotted according to Job's method of continuous variation indicated formation of a 1:1 complex, BAMBP \cdot HA, but only in small amounts. The nmr spectra of BAMBP mixed with 4-phenylvaleric acid also indicated hydrogen bonding, but infrared spectra did not show a new absorption band.

The nmr spectra showed a small upfield shift of the phenolic proton resonance when BAMBP was dissolved (0.05 to 2 *M*) in chloroform, and large downfield shifts when acetophenone and octanol-1 were the solvents. Dielectric constants of these mixtures diluted to 0.5 *M* with carbon tetrachloride varied nonlinearly for acetophenone and octanol, indicating association, but linearly for chloroform. In agreement, infrared spectra of the same series of solutions showed new absorption bands (near 3650 cm^{-1}) with acetophenone and with octanol, but not with chloroform.

TBP \cdot H₂O

Tributyl phosphate dissolves water in approximately a 1:1 mole ratio, and there is controversy

²⁷ Chem. Technol. Div. Ann. Progr. Rept. May 31, 1964, ORNL-3627, p. 198.

as to whether or not this reflects existence of an association species $\text{TBP} \cdot \text{H}_2\text{O}$. In connection with measurement of activities in TBP-water mixtures (see below), the dielectric constants of the mixtures were examined for possible evidence of association. At 25°C the dielectric constant ϵ increases along a nearly linear curve (slightly convex upward) from 8.13 to 10.57 as the water content increases from zero to saturation at 6.8 vol % H_2O (0.51 mole fraction), as compared with 78.54 at 100% H_2O . These results did not show clearly whether or not there is a break at 0.5 mole fraction (1:1 mole ratio). The measurements were repeated at 2°C , where the water solubility is increased to 7.0 vol % (0.53 mole fraction) to obtain better definition above the 0.5 mole-fraction point. The entire system was placed in a cold room held at $2 \pm 0.5^\circ\text{C}$ to avoid difficulties from temperature gradients and condensing moisture. The results (Fig. 7.13) show a small but definite break at mole fraction 0.505 (1:0.98 mole ratio) and thus indicate that a real (although probably very weakly bound) association species $\text{TBP} \cdot \text{H}_2\text{O}$ does exist.

7.15 SYNERGISM IN THE EXTRACTION OF STRONTIUM BY DI(2-ETHYLHEXYL)PHOSPHORIC ACID

Previously reported examination of the synergistic extraction of strontium by di(2-ethylhexyl)phosphoric acid (HA) plus tributyl phosphate (TBP) showed up to a fourfold enhancement of the extraction coefficient $E_a^\circ(\text{Sr})$ in an aliphatic diluent, although only slight effects in an aromatic diluent.²⁸ The mechanism of the synergism is being studied through the effects of varying several different conditions in the system $\text{Sr}(\text{NO}_3)_2$, NaNO_3 , HNO_3 , or NaOH/HA , TBP, *n*-octane.

In the absence of TBP, $\text{NaA} \cdot 3\text{HA}$ and $\text{SrA}_2 \cdot 4\text{HA}$ have been identified as important species in the organic phase.²⁹ One obvious hypothesis to explain the synergism is that TBP might replace part

²⁸Chem. Technol. Div. Ann. Progr. Rept. May 31, 1963, ORNL-3452, p. 182.

²⁹W. J. McDowell and C. F. Coleman, "Sodium and Strontium Extraction by Di(2-ethylhexyl)phosphate: Mechanisms and Equilibria," *J. Inorg. Nucl. Chem.* (in press).

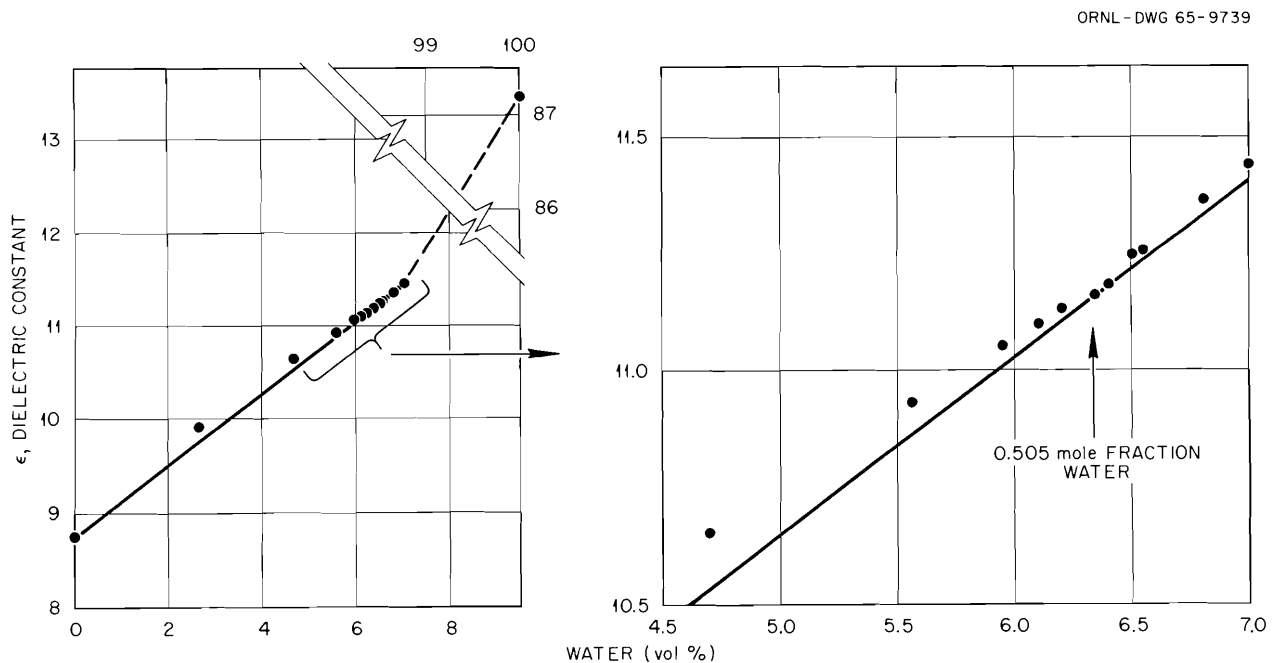


Fig. 7.13. Dielectric Constants of TBP-Water Mixtures at 2°C .

or all of the HA associated with the strontium to give a more favorable extracted complex. If so, the position of the maximum in the $E_a^{\circ}(\text{Sr})$ vs pH curve should shift to higher values of $\text{A}^-/\Sigma \text{A}$ and hence higher pH, and the maximum should decrease (relative to extraction at high pH) or disappear, since the complexing by TBP should not be affected directly by pH. These expectations are at least partly borne out by the curves for different TBP concentrations (Fig. 7.14a).

Detailed analyses of the effects of varying TBP and varying HA emphasized solutions with the combined concentrations of TBP and HA at 0.3 M or less, since auxiliary studies indicated that intermolecular association between TBP and HA is negligible up to at least that concentration. Some comparisons were also made at higher concentrations, including undiluted TBP. Two-phase-continuous titrations with radiotracer determination of the changing strontium distributions gave families of $\log E_a^{\circ}(\text{Sr})$ vs pH curves as functions of varying TBP and varying HA (Fig. 7.14). These data were analyzed in the manner previously developed for extractions by HA alone.²⁹ Values of the pH power dependence i (defined by the relation $\log E_a^{\circ}(\text{Sr}) \propto i \text{pH}$ or $E_a^{\circ}(\text{Sr}) \propto [\text{H}^+]^{-i}$) were obtained from the slopes in Fig. 7.14. These are compared in Fig. 7.15, as a function of the degree of neutralization of HA, with the values to be expected for each of several possible organic-phase strontium species. (These species might also contain TBP, which would not affect the value of i .) The experimental points curve across the lines for the different species in a manner consistent with the working hypothesis of replacement of HA by TBP.

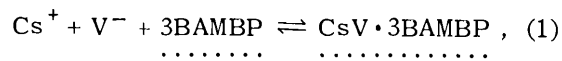
The pH dependence values i were combined with the extraction coefficients to examine the dependence of extraction on the concentrations of HA and of TBP, by means of plots of $\log E_a^{\circ}(\text{Sr})[\text{H}^+]^i$ vs $\log [\text{HA}]_{\text{TBP}}$ and vs $\log [\text{TBP}]_{\text{HA}}$. At low pH the power dependence on HA concentration is 2, indicating reaction of strontium with 4HA (two dimers) instead of with 6HA, as in the absence of TBP. If the coordination number of the strontium is unchanged, this suggests $\text{SrA}_2 \cdot 2\text{HA} \cdot 2\text{TBP}$. When more than about 10% of the HA is neutralized ($\text{NaA}/\Sigma \text{A} \geq 0.1$), the power dependence on HA concentration decreases; and at $\text{NaA}/\Sigma \text{A} \geq 0.4$ it becomes less than 1. However, the corresponding HA:Sr ratios cannot yet be calculated because the degree of aggregation of HA and NaA in the presence of TBP has not yet been determined.

The corresponding tests of power dependence on TBP concentration give curved plots, showing that there is some function not yet accounted for that varies with the TBP concentration. Within this uncertainty, the results suggest a negative power dependence on TBP concentration in the range of $\text{NaA}/\Sigma \text{A}$ between 0.05 and 0.6, rising toward +3 or +4 at high $\text{NaA}/\Sigma \text{A}$. The negative values suggest that through that region the ratio TBP:HA is greater in the average organic-phase sodium species than it is in the strontium species. The latter rising values (like the i values in Fig. 7.15) are consistent with progressive displacement of HA by TBP, such as to form $\text{SrA}_2 \cdot 2\text{HA} \cdot 2\text{TBP}$ and $\text{SrA}_2 \cdot 4\text{TBP}$.

7.16 SYNERGISM AND DILUENT EFFECTS IN THE EXTRACTION OF CESIUM BY 4-sec-BUTYL-2- α -METHYLBENZYLPHENOL (BAMBP)

The detailed study of the extraction of alkali ions (especially cesium) by substituted phenols³⁰ was continued with investigation of the synergistic extractions obtained by adding organic acids to BAMBP and of the effects of different types of diluents.

The organic acids examined were di(2-ethylhexyl)phosphoric acid (HA), monoheptadecyl tetrapropenylsuccinic acid (HS), and 4-phenylvaleric acid (HV). These two carboxylic acids differ considerably in that the alkali salts of HV distribute principally to the aqueous phase. The salts of HS and HA, and the acid forms of all three, remain in the organic phase. The coefficient $E_a^{\circ}(\text{Cs})$ for extraction of cesium by BAMBP-HV mixtures is nearly independent of pH through the range 7.5 to 10 and varies with the third power of the BAMBP concentration (0.2 to 2 M BAMBP in CCl_4). In this region the HV exists entirely as the salt, and the principal extraction reaction is probably



where the dotted underlines indicate the organic phase. Two other reactions may also be involved:

³⁰B. Z. Egan, R. A. Zingaro, and B. M. Benjamin, "Extraction of Alkali Metals by 4-sec-Butyl-2- α -methylbenzylphenol," *Inorg. Chem.* (in press).

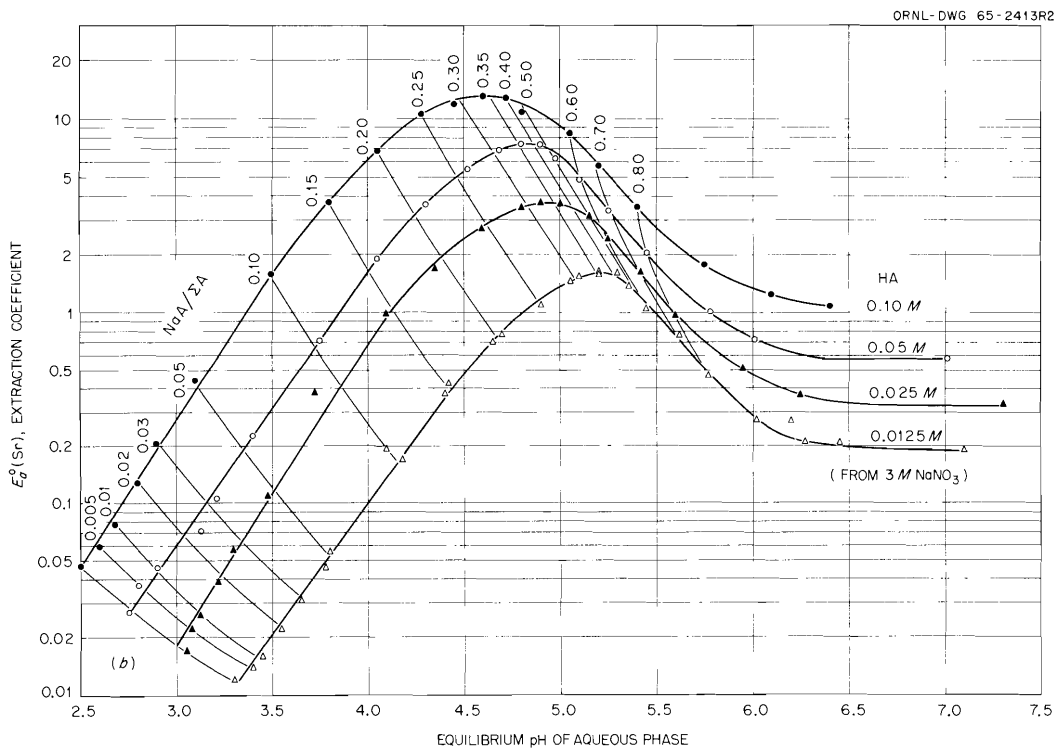
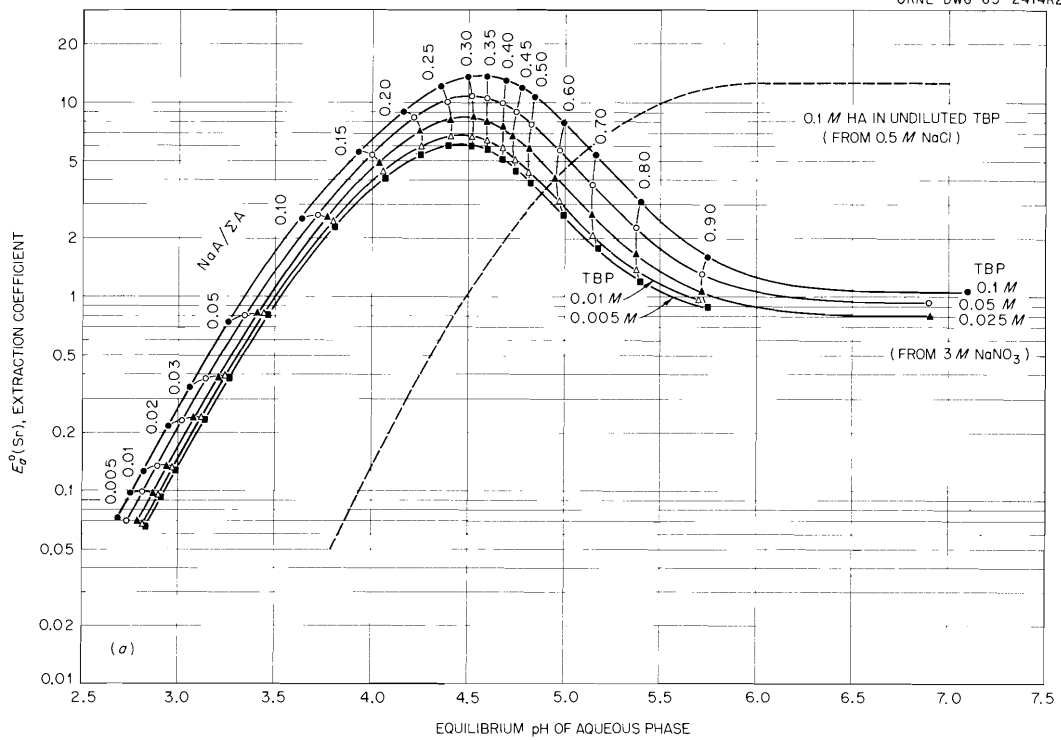


Fig. 7.14. Strontium Extraction from 3 M NaNO_3 and 0.5 M NaCl Solutions by Di(2-ethylhexyl)phosphoric Acid-Tributyl Phosphate Mixtures. (a) HA concentration constant at 0.1 M; (b) TBP concentration constant at 0.2 M, in *n*-octane.

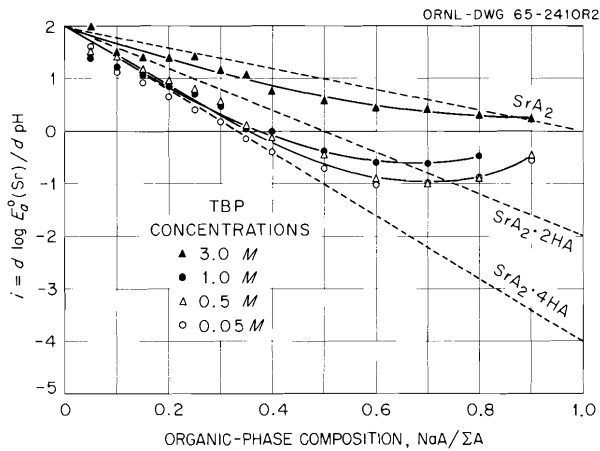


Fig. 7.15. Influence of TBP on pH Dependence of Strontium Extraction by Di(2-ethylhexyl)phosphoric Acid. Concentrations: 0.1 M HA + O 0.05 M, Δ 0.5 M, \bullet 1.0 M TBP in *n*-octane, extraction from 3 M NaNO₃; \blacktriangle 0.1 M HA in undiluted TBP, extraction from 0.5 M NaCl. The dashed lines show the dependences expected for formation of the strontium compounds, as shown or in additional association with TBP.

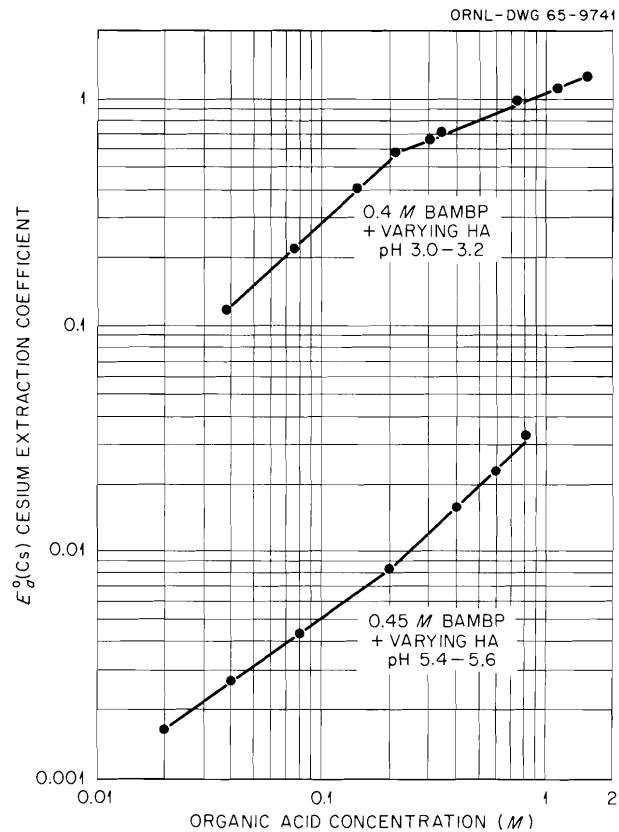
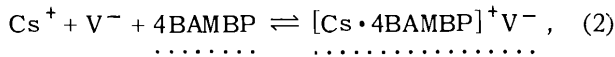
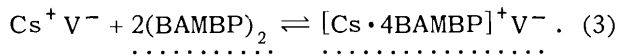


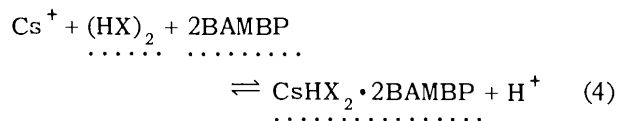
Fig. 7.16. Synergistic Cesium Extraction by BAMBP plus Organic Acids. Di(2-ethylhexyl)phosphoric acid (HA) and heptadecyl tetrapropenylsuccinic acid (HS) in CCl₄; 1.3×10^{-4} M Cs initial.



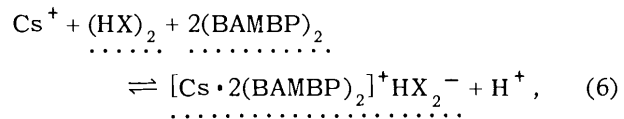
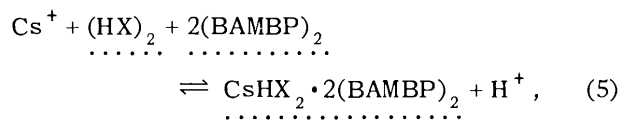
and, at high BAMBP concentrations where it is considerably dimerized,



At low pH, where the HV remains entirely in the organic phase, the reagent dependence changes to second power with respect to total BAMBP concentration and becomes first power with respect to the HV concentration. When HV is replaced by HA or HS, the dependence on BAMBP concentration remains second power, but the dependence on organic acid concentration is less than first power, and appears to shift slightly at about 0.2 M (Fig. 7.16). Both carboxylic and phosphoric acids are dimerized in carbon tetrachloride. The equilibrium reaction is probably



and perhaps also



where HX represents HV, HA, or HS. Equilibrium (5) implies a coordination number of 6 instead of 4; 6 is probably reasonable for the large cesium ion, especially at low organic-phase cesium concentrations. Infrared spectra and dielectric constants of mixtures indicate that a 1:1 HA-BAMBP adduct is formed in carbon tetrachloride solution, although to only a small extent (cf. Sect. 7.14). No interaction between HV and BAMBP was indicated. Nuclear magnetic resonance (nmr) spectra indicate

increased strength of hydrogen bonding on addition of the organic acids to BAMBP and show that the acid and phenolic protons are in rapid exchange.

The second part of the current cesium extraction studies, to help resolve the effects of BAMBP-BAMBP and BAMBP-diluent association on the BAMBP-cesium association, is a comparison of diluents of different hydrogen-bonding capabilities. Besides carbon tetrachloride (no hydrogen-bond formation), these are octanol-1, a hydrogen-bonded donor-type molecule; acetophenone, a non-hydrogen-bonded donor-type molecule; and chloroform, a non-hydrogen-bonded, acceptor-type molecule. The chemical shifts in nmr spectra confirmed the expectation of strong hydrogen bonding by association of the phenolic proton with the alcohol and ketone oxygens, and some hydrogen bonding by association of the phenolic oxygen with the hydrogen of chloroform. (Infrared spectra and dielectric constants of ternary mixtures in carbon tetrachloride indicated association of BAMBP with acetophenone and with octanol, but not with chloroform.) In agreement with this, cesium extraction coefficients by BAMBP in chloroform diluent are parallel to those in carbon tetrachloride and somewhat lower, while those at high BAMBP concentrations in octanol and acetophenone are considerably lower (Fig. 7.17), reflecting the competition for the BAMBP by its strong association with the donor diluents. Moreover, at lower BAMBP concentrations the dependence of $E_a^{\circ}(\text{Cs})$ on BAMBP concentration drops from third to first power. This is ascribed to substitution of donor diluent molecules for the donor BAMBP molecules in solvation of the cesium BAMBPate.

7.17 KINETICS OF EXTRACTION OF IRON BY DI(2-ETHYLHEXYL)PHOSPHORIC ACID

Kinetic measurements continued in the extraction by di-(2-ethylhexyl)phosphoric acid (HA) of iron(III), an important representative of several very slow extraction equilibria with this reagent. As in the tests previously reported,³¹ the extraction rate is first order with respect to aqueous iron concentration under all conditions tested. The rate constant, $k = -d \log [\text{Fe}]/dt$, increases with increasing HA concentration, but with different power de-

³¹Chem. Technol. Div. Ann. Progr. Rept. May 31, 1964, ORNL-3627, p. 204.

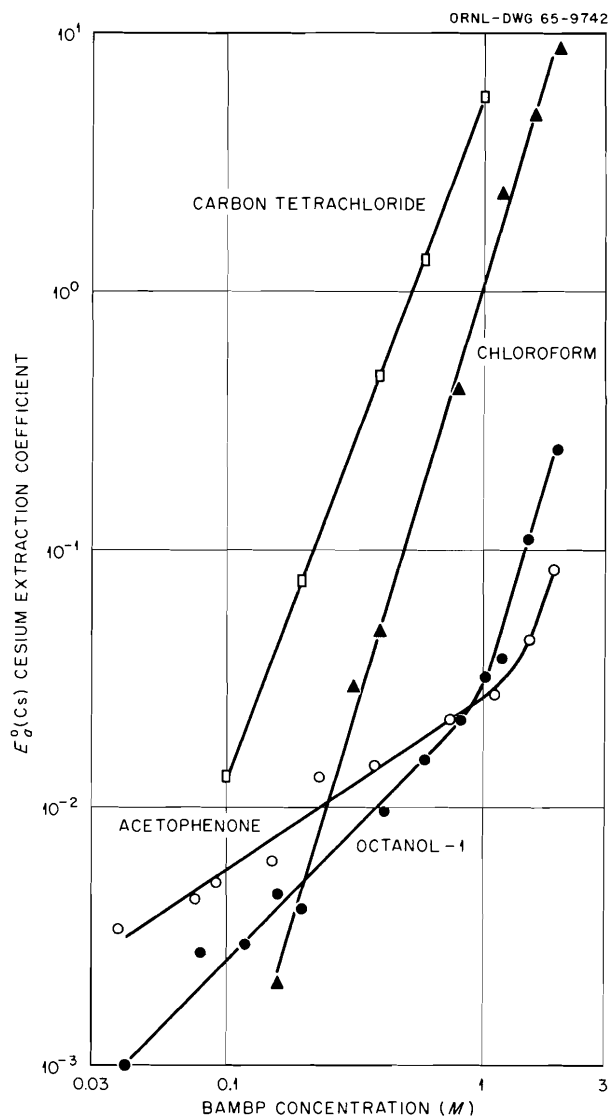


Fig. 7.17. Effect of Diluent Type on Cesium Extraction by BAMBP. Initial aqueous cesium concentration, 0.010 to 0.015 M. Extraction coefficients normalized to pH 12.1.

pendence at low and high concentrations (Fig. 7.18). The log-log slopes are about 0.3 below 0.2 M HA and nearly 1.5 above 0.5 M. The rate constant also increases with decreasing aqueous acid concentration. When the data of Fig. 7.18 are replotted (log-log) against the aqueous perchloric acid concentration, a nearly straight line is found at each HA concentration, with slopes changing from about -1 at $[\text{HA}] \leq 0.1$ to about -1.8 at $[\text{HA}] \geq 1.0$.

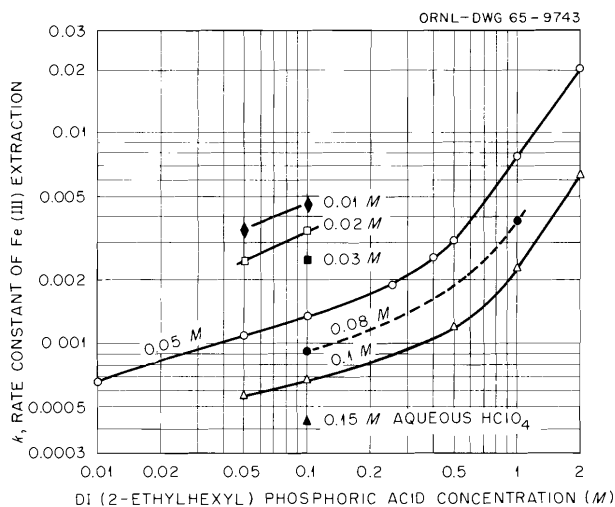


Fig. 7.18. Effects of Extractant Concentration and Acidity on Rate of Iron Extraction. Initial iron concentration, 0.002 M; ionic strength constant at 2 M ($\text{HClO}_4 + \text{NaClO}_4$); 25°C; diluent, *n*-octane.

The rate constant decreases with increasing aqueous perchlorate concentration, log-log slope -0.6 with 0.1 M HA and 0.05 M aqueous acid. If this should be attributed entirely to ferric perchlorate association (rather than to effects of ionic strength per se), it would fit an association quotient $Q = [\text{FeClO}_4^{2+}]/[\text{Fe}^{3+}][\text{ClO}_4^-] \approx 1$, in comparison with values of 0.6 to 6 from various sources.³²

Several aspects of the test results indicate that the extraction rate is controlled by a chemical reaction at the interface. The extraction rate varies directly with the interfacial area in otherwise identical tests [phases stirred on each side of a relatively quiescent interface,³³ $k = 0.0036(\text{cm}^2/\text{cm}^3)$ with 0.1 M HA and 0.02 M aqueous acid], but it is almost independent of the stirring rate. Moreover, the activation energy calculated from rates measured at 25, 40, and 60°C was 10 kcal/mole with 1 M HA and 15 kcal/mole with 0.1 M HA, consistent with rate control by a chemical reaction and rather higher than would be expected for rate control by diffusion. The difference in activation energy at high and low HA concentrations, together with the differences in

acid dependence and HA concentration dependence (Fig. 7.18), indicates a shift of rate control between steps or between paths at about 0.4 M HA.

7.18 ACTIVITY COEFFICIENTS OF THE SOLVENT PHASES

Diluent vapor-pressure lowering, determined by direct differential pressure measurement and by isopiestic balancing, has continued to be used for investigation of departures from ideality in the behavior of organic solutions of solvent extraction systems. These departures from ideality are calculated either as activity coefficients, or as apparent aggregation numbers of real or hypothetical polymeric species assumed to behave ideally.

Trioctylamine Sulfate

In continued testing of the possible effects of water content on aggregation of amine salts, the apparent average aggregation number \bar{n} of tri-*n*-octylamine normal sulfate (0.2 *m*, in benzene) was found to increase slightly with increasing water activity, but still remaining close to 1:

$a_{\text{H}_2\text{O}}$	0	0.33	0.50	0.75	0.902	1
\bar{n}_{TOAS}	0.85	0.85	0.99	1.09	1.10	
\bar{n}_{TOAHS}	3.60	3.67	3.69	3.59	3.50	
\bar{n}_{TOA}	1.15					1.02

The normal sulfate values, like those for the bisulfate³⁴ and the dry, free-base amine, are from isopiestic balancing. The value for water-saturated free-base amine is from direct vapor-pressure difference measurements.³⁵

Since the apparent average aggregation numbers of tri-*n*-octylamine and its sulfate salts have not yet resolved the anomalies in its mass action behavior, the variations of the actual activity coefficients of the organic-phase solutes are being determined. Activity coefficients were previously reported for the free-base trioctylamine in dry

³²R. H. Horne, *Nature* 181, 410 (1958).

³³J. B. Lewis, *Chem. Eng. Sci.* 3, 248 (1954).

³⁴*Chem. Technol. Div. Ann. Progr. Rept. May 31, 1964, ORNL-3627, p. 207.*

³⁵K. A. Allen and A. L. Myers, Abstr. No. 68, p. 27R, 139th ASC Meeting, March 1961; recalculated in ORNL-3785 (in press).

benzene,³⁶ and for water in benzene solutions of mixtures of TOA, TOAS, and TOAHS.³⁴ The activity coefficient of the normal sulfate TOAS has now been measured at concentrations up to 0.58 *m* in dry benzene by isopiestic balancing (Fig. 7.19). The apparent molal volumes were determined to be 89.4 ml per mole of benzene and 857 ml per mole of TOAS. Contrary to the original expectations, the sulfate salt shows rather less departure from ideality than does the free-base amine. Similar measurements are in progress with the bisulfate salt.

Activities in TBP-Water Mixtures

To resolve a discrepancy between published values, the activity of TBP when saturated with water at 25°C was determined by a series of isopiestic measurements of water solubility vs water activity, via the Gibbs-Duhem relation. The concentration of water at saturation in TBP (the solubility at $a_w = 1$) is 3.58 *M*, or mole fraction $X_w = 0.511$, and it decreases as the water activity decreases. Below $a_w = 0.75$ ($X_w \leq 0.36$) it conforms almost exactly to Henry's law:

$$a_w = (2.073 \pm 0.01) X_w . \quad (1)$$

³⁶Chem. Technol. Div. Ann. Progr. Rept. May 31, 1963, ORNL-3452, p. 187.

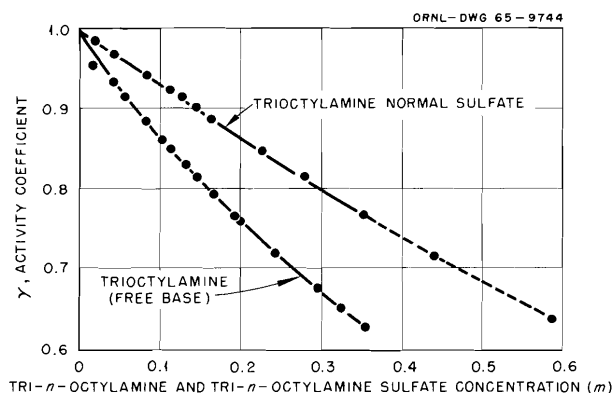


Fig. 7.19. Activity Coefficients of Tri-*n*-octylamine and Its Normal Sulfate in Dry Benzene, 25°C. Isopiestic vapor balancing: TOA vs triphenylmethane, TOAS vs azobenzene.

The activity of TBP was calculated, with pure TBP as the standard state, by rearrangement and integration of the Gibbs-Duhem equation for a two-component system:

$$\ln a_{\text{TBP}} = - \int_0^{a_w} \frac{X_w}{(1 - X_w)a_w} da_w . \quad (2)$$

The function $X_w/(1 - X_w)a_w$ is essentially linear vs a_w between 0 and 0.53 and concave upward from there to $a_w = 1$ (Fig. 7.20).

For integration of Eq. (2), the lower and upper portions of the curve were fitted by least squares to a linear and a cubic equation:

$$X_w/(1 - X_w)a_w = 0.4774 + 0.29550 a_w , \quad (3)$$

$$X_w/(1 - X_w)a_w = -0.17176 + 3.3821 a_w - 5.0377 a_w^2 + 2.879 a_w^3 . \quad (4)$$

The resulting values of a_{TBP} are nearly equal to their corresponding mole fractions, $a_{\text{TBP}} = X_{\text{TBP}} \pm 0.003$ for X_w between 0 and 0.4. At saturation with water, $X_{\text{TBP}} = 0.489$ and $a_{\text{TBP}} = 0.515$.

The activities and activity coefficients of water and TBP are summarized as their partial molal free

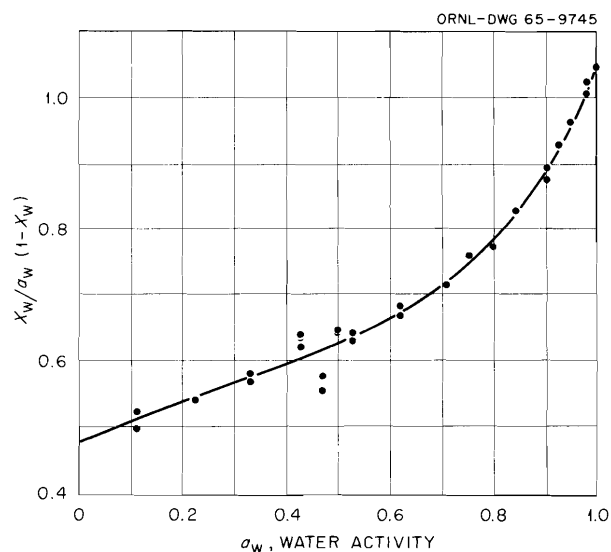


Fig. 7.20. Water Solubility in Tributyl Phosphate as a Function of Water Activity. For integration of the Gibbs-Duhem relation. X_w = mole fraction of water.

energies of solution and their excess partial molal free energies at 25°C (Fig. 7.21). The excess partial molal free energies are positive for both: 31 cal per mole of TBP and 397 cal per mole of water in the water-saturated TBP. Since positive deviations usually correspond to differences in molecular attractive forces and negative deviations to compound formation, these results support conclusions that bonding forces between water and TBP are very weak direct evidence of $\text{TBP} \cdot \text{H}_2\text{O}$ association at 2°C from dielectric measurements (cf. Sect. 7.14).

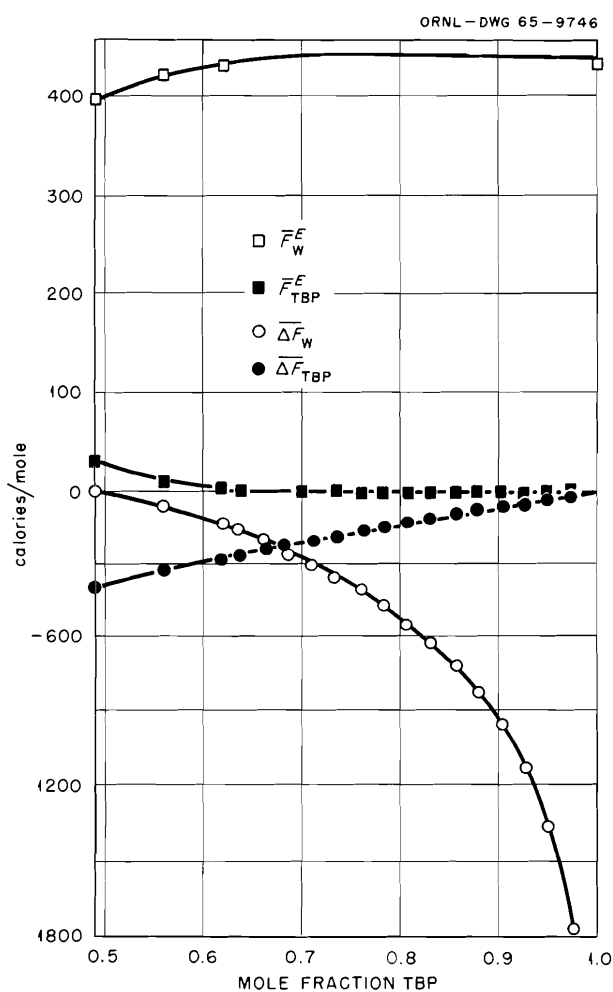


Fig. 7.21. Partial Molal Free Energies of Solution and Excess Partial Molal Free Energies in TBP-Water Mixtures.

Sensitive Differential Manometer

In continuing improvement of the equipment and techniques for precisely measuring small vapor-pressure differences,³⁷ the possibility of using an inverted cup floating in mercury for the sensing element was examined by derivation of its equation of motion³⁸ and by trial of a preliminary model. The equation giving the pressure difference Δ as a function of the observable change in height of the float Δh above a fixed reference is:

$$\Delta = \rho g \Delta h \left(\frac{r_0^2}{r_i^2} - 1 \right) \frac{1 - A_t/A_m}{1 - A_t A_0/A_m A_i}, \quad (5)$$

³⁷Chem. Technol. Div. Ann. Progr. Rept. May 31, 1964, ORNL-3627, p. 206.

³⁸W. J. McDowell, R. M. Fuoss, and C. F. Coleman, "A Precision Inverted, Floating-Cup Manometer for Differential Vapor Pressure Measurements," submitted for publication in *Chemical Engineering*.

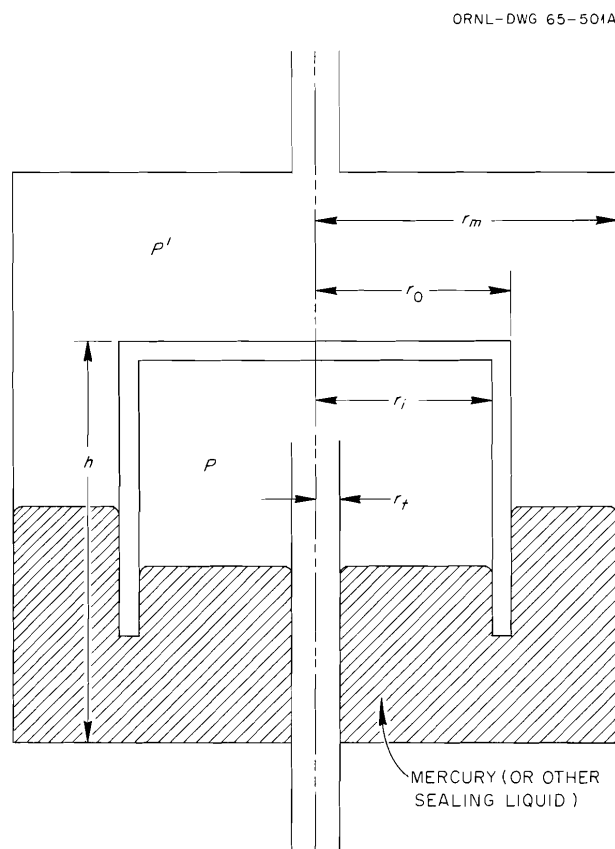


Fig. 7.22. Schematic Diagram of Floating-Cup Differential Manometer.

where the A 's are horizontal areas corresponding to the radii marked in Fig. 7.22, ρ is the density of mercury (or other sealing liquid), and g is the acceleration of gravity. When A_t is much smaller than A_m (the lower entry tube occupies negligible area), and A_i is nearly equal to A_0 (the cup wall is very thin), Eq. (5) simplifies to:

$$\Delta \approx \rho g \Delta h (r_0^2/r_i^2 - 1). \quad (6)$$

A preliminary mockup with a stainless steel cup of approximately 4 cm radius, floating in mercury,

showed a twentyfold increase in sensitivity over a simple mercury manometer. A model is being made with target dimensions of $r_m = 6$ cm, $r_t = 0.5$ cm, $r_i = 4$ cm, and wall thickness = 0.0508 cm. For these dimensions the term neglected in Eq. (6) should be only 1.00018, and the sensitivity (with mercury) should be about 40 times that of a simple mercury manometer. This model will be used to check for possible nonreproducible effects (e.g., variable interfacial tension and changing contact angles), and to test the suitability of readout devices.

8. Recovery of Fission Products by Solvent Extraction

The objective of the fission product recovery program is to develop processes applicable to large-scale recovery and purification of fission products from reactor-fuel-processing wastes. The program includes basic chemical research, development of recovery methods, and development of engineering procedures to carry out these operations. Large quantities of certain fission products are being requested for industrial, space, and other applications, and there is evidence that the demand will increase. Also, aside from their utility for recovering useful fission products, the recovery methods developed are of interest for fractionating wastes to ease certain waste-disposal problems.

Since its inception the principal emphasis in this program has been on the development of solvent extraction methods because they are particularly versatile and readily adaptable to large-scale operations. Thus far, a solvent extraction process using di(2-ethylhexyl)phosphoric acid (D2EHPA) has been successfully developed for recovering ^{90}Sr and mixed rare earths. A modification of this process has been developed and operated in plant scale at the Hanford Atomic Products Operation. New processes have also been developed in the laboratory for recovering cesium with substituted phenols and for recovering zirconium-niobium and possibly yttrium and ruthenium. The combination of these developments with previous studies on rare-earths separations and on the recovery of technetium, neptunium, and plutonium affords an integrated solvent extraction flowsheet for the recovery of nearly all valuable components from waste liquors. Current studies are aimed at consolidating, optimizing, and completing these developments and at devising new processes that might provide even greater advantages in operations and cost.

8.1 CESIUM

Results continued to be favorable in the development of the Phenex process¹⁻³ for recovering cesium from alkaline solutions by extracting with substituted phenols and stripping with dilute acid. Nearly all recent test work was with 4-sec-butyl-2-(α -methylbenzyl)phenol (BAMBP), which has more attractive extraction properties than other phenols examined. The studies included further examination of the selectivity of BAMBP for cesium over contaminants and evaluation of its chemical stability.

Extraction Selectivity

The high selectivity of BAMBP for alkali metals was further confirmed by measuring the extractability of some metals that had not been tested previously. Coefficients for extraction of Ca, Ba, Mo, and Tc with 1 *M* BAMBP in Amsco 125-82 were all less than 0.01 under conditions (sodium nitrate-sodium tartrate solution, pH 11.7) where the cesium coefficient was 3.

Stability of BAMBP

In previous studies³ with simulated feeds, BAMBP demonstrated good radiation and chemical stabilities under conditions expected for the cesium recovery flowsheet. In agreement with Hanford results, however, extensive degradation (with loss

¹*Chem. Technol. Div. Ann. Progr. Rept. June 30, 1962, ORNL-3314, p. 120.*

²*Ibid., May 31, 1963, ORNL-3452, p. 189.*

³*Ibid., May 31, 1964, ORNL-3627, p. 209.*

of cesium extraction power) occurred when BAMBP was contacted with acid nitrite solutions. Introduction of nitrite into the nitric acid stripping system is possible by entrainment of the aqueous liquor in the organic extract and by radiolytic decomposition of nitric acid in the stripping system. Further studies, therefore, are being made to better define conditions under which significant reaction with nitrite occurs and to forestall the reaction if possible. Indications are that degradation can be avoided.

Table 8.1 shows data for tests in which 1 M BAMBP in Amsco 125-82 was contacted for several days at room temperature with various solutions

and then subjected to a standard cesium extraction test. Treatment with 0.1 M HNO₃ for seven days had no apparent effect on the extraction properties of the solvent, but treatment with 0.1 M HNO₃ that was 0.01 M in NaNO₂ increased the extraction coefficient by a factor of 2 or 3. Spectrophotometric examination of the treated solvent showed an absorption peak at 371 mμ, which Hanford chemists have found to be indicative of nitrated BAMBP. Extensive degradation occurred on contact with 0.1 M HNO₃-0.1 M NaNO₂. After a few hours contact with this solution, the cesium extraction coefficient was 3 to 5 times higher than for untreated solvent, but extending the contact time to

Table 8.1. Chemical Stability of BAMBP

Solvent-treatment conditions: 1 M BAMBP in Amsco 125-82 contacted at 25°C with aqueous solutions of composition shown. At each sampling time, the aqueous phase was replaced with fresh aqueous phase. Samples of the treated solvent were scrubbed with 1 M NaNO₃ solutions (pH 12) and subjected to standard cesium extraction tests.

Contacting Conditions			Contact Time (days)	Cesium Extraction Coefficient, ^a E _a ^o
Aqueous Solution				
HNO ₃ (M)	NaNO ₂ (M)	NH ₂ SO ₃ H (M)		
No treatment				4.2, 4.8, 4.9
0.1			1	4.7
			3	4.7
			7	5.4
0.1	0.01		3	10.7
			5	10.3
			7 ^b	11.6
0.1	0.1		0.1	23
			0.8	16
			4 ^b	0.09
0.1	0.1	0.2	0.2	5.1
			1	5.6
			5	4.3
			9 ^c	4.6
Simulated Hanford tank-farm supernatant: 8 M Na ⁺ , 3 M NO ₃ ⁻ , 3 M NO ₂ ⁻ , 1 M CO ₃ ²⁻ , pH 10.4			0.1	4.7
			0.8	6.9
			4	8.3
			7 ^c	12.6

^aExtraction at a phase ratio of 1/1 from solution 3 M in NaNO₃ and containing 0.1 g of cesium per liter (and ¹³⁴Cs tracer) at pH 12.

^bSpectrophotometry showed a strong absorption peak at 371 mμ.

^cNo absorption peak at 371 mμ.

four days almost completely destroyed the extraction power. This effect was efficiently counteracted in another test, however, by adding sulfamic acid to the 0.1 M HNO₃-0.1 M HNO₂ solution to destroy the nitrite. With this procedure, extraction coefficients for solvent samples contacted for up to nine days were the same as for untreated solvent, and no indication of BAMBP nitration was found by spectrophotometry. Also, there was no apparent degradation when the solvent was contacted for seven days with simulated Hanford tank waste supernatant that was 3 M in nitrite at a pH of 10.4.

The above results emphasize that contact of BAMBP with acid solutions containing nitrite should be avoided. As a precaution against nitrite attack, it seems advisable to add a small amount of a nitrite-destroying agent, such as sulfamic acid, to the strip solution.

8.2 ISOLATION OF CERIUM AND PROMETHIUM

The most useful rare-earth isotopes are ¹⁴⁴Ce and ¹⁴⁷Pm. Studies of methods for separating them from the mixed-rare-earths product derived from the di(2-ethylhexyl)phosphoric acid recovery process were continued.

Cerium Oxidation and Extraction

In studies described previously³ on separating cerium from other rare earths by oxidizing it with silver-catalyzed persulfate and extracting with D2EHPA, good recoveries were obtained only when the oxidation was performed at elevated temperatures and with the solvent phase present. In these tests, the nitric acid concentration in the aqueous feed was 1.3 M. It has now been established that the oxidation rate is at a maximum when the aqueous phase is about 2 M in HNO₃. At this acidity, nearly complete oxidation can be obtained with the solvent phase absent, and this procedure is preferred to avoid extended contact of the solvent with the hot oxidizing solution. In tests with a mixed-rare-earth feed 0.055 M in cerium and 2 M in HNO₃, more than 98% of the cerium was oxidized (and subsequently extracted with D2EHPA) in 20 to 30 min at 60°C, using 1.8 moles of persulfate (0.1 M S₂O₈²⁻) per mole of cerium (Fig. 8.1). Under the same conditions but with the aqueous

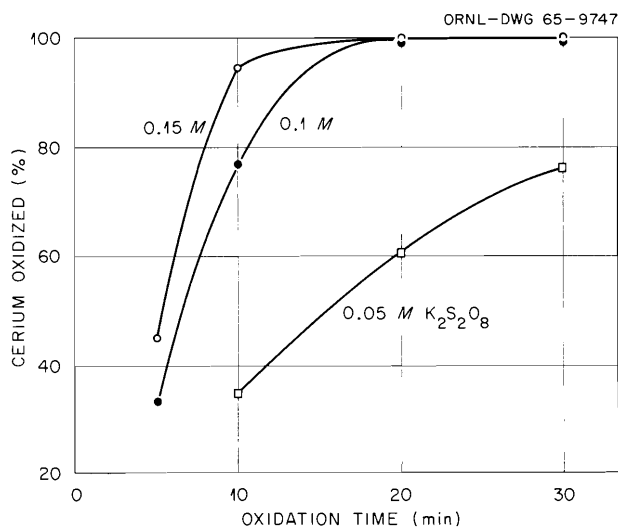


Fig. 8.1. Oxidation of Cerium with Silver-Catalyzed Persulfate at 60°C. Procedure: solid K₂S₂O₈ added to solution 2 M in HNO₃ and containing, in grams per liter, 8.0 Ce(III), 3.8 La, 2.8 Pr, 2.5 Nd, 1.2 Sm, 0.3 Eu, and 2 AgNO₃. Amount of cerium oxidized determined by extraction of cerium from sample of oxidized solution with 0.3 M D2EHPA in Amsco 125-82 at a phase ratio of 1/1.

phase 3 M in HNO₃, 60% of the cerium was oxidized in 10 min and 92% in 20 min.

Promethium Separation

The isolation of promethium from the other rare earths (after cerium removal) was studied with several types of solvent extraction reagents including tributyl phosphate (TBP), D2EHPA, 2-ethylhexylphenylphosphonic acid, and amines. Results were best in the first two systems.

Separations with TBP. — The ability of TBP to separate the individual rare earths in a concentrated nitric acid system is well known⁴ and is the basis of a process^{5,6} developed for isolating promethium from other fission product rare earths. Since this process was developed for

⁴D. F. Peppard et al., *J. Phys. Chem.* 57, 294-301 (1953).

⁵Boyd Weaver and F. A. Kappelmann, *Purification of Promethium by Liquid-Liquid-Extraction*, ORNL-2863 (Jan. 29, 1960).

⁶T. A. Butler, *Radioisotopes Phys. Sci. Ind., Proc. Conf. Use, Copenhagen, 1960*, vol. II, p. 413, IAEA, 1962.

small-scale promethium recovery, and since flowsheet conditions were chosen to permit operation in 20-stage mixer-settler equipment then available, the specified flowsheet is not necessarily optimum for large-scale promethium recovery. Preliminary tests indicate that, with a modest increase in the number of stages, the flows of TBP and scrub acid per unit of promethium can be greatly reduced to make the process more attractive for large-scale use.

In batch tests with a simulated mixed-rare-earths feed traced with ^{147}Nd and ^{148}Pm , the Pm/Nd separation factor increased from 1.7 to 2.1 with increase in aqueous nitric acid concentration from 10 to 14 M (Fig. 8.2). Other tests showed no significant change in the Pm/Nd separation factor as the TBP concentration was changed from 100 to 60 vol % by dilution with Amsco 125-82. Also, both the promethium extraction coefficient and the Pm/Nd separation factor were fairly insensitive to changes in loading of 100% TBP in the range of 5 to 25 g of rare earths per liter.

Separations with D2EHPA. — Peppard⁷ reported a separation factor of about 2.5 between adjacent

⁷D. F. Peppard *et al.*, *J. Inorg. Nucl. Chem.* **4**, 344–48 (1957); *ibid.* **5**, 141–46 (1957); *ibid.* **7**, 276–85 (1958).

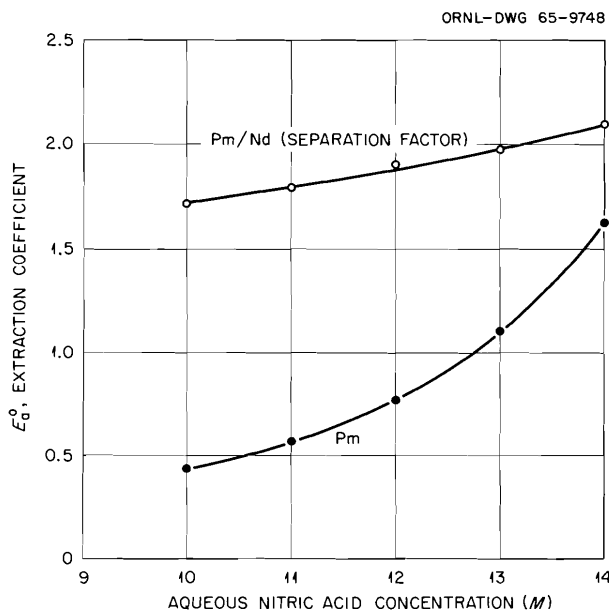


Fig. 8.2. Extractions of Rare Earths with 100% TBP. Aqueous phase: nitric acid solutions containing ^{148}Pm and ^{147}Nd tracers and, in grams per liter, 13 Nd, 3.6 Sm, and 0.25 Eu. Contact: 2 min at 1/1 phase ratio.

rare earths for extractions with D2EHPA in toluene. However, extractions of rare earths with D2EHPA in this diluent are very weak, and results of continuous-extraction tests⁸ in which D2EHPA in an aliphatic diluent (Amsco 125-82) was used for separating promethium from neodymium were not encouraging owing to the low separation factor (i.e., 1.6) obtained. Recently, this system was reexamined, and it now appears that a practicable process using D2EHPA can now be outlined. In this process, separation factors between adjacent rare earths of about 2.5 are realized by maintaining a relatively low acidity (0.2 to 0.4 M) in the extraction and scrubbing systems. The Amsco 125-82 diluent is modified with an aromatic diluent such as diisopropylbenzene to depress the rare-earth extraction coefficients. This improves process control by allowing use of more concentrated D2EHPA solutions than is otherwise possible (without obtaining excessively high extraction coefficients at these low acidities), thereby minimizing loading effects. The process appears to have appreciable advantage over the TBP–nitric acid process since separation factors are higher and the required aqueous-phase acidity is much lower (0.3 M vs 12 M HNO_3). Demonstration runs in mixer-settler equipment are planned to verify the feasibility of the process.

Separations with 2-Ethylhexylphenylphosphonic Acid. — In extractions from 0.75 M HNO_3 with 2-ethylhexylphenylphosphonic acid in diisopropylbenzene, separation factors between adjacent rare earths were about 2.5. Rare-earth extraction coefficients with this reagent are considerably higher than those obtained with D2EHPA under comparable conditions. However, precipitation of rare earths occurred in some tests, indicating a relatively low solubility of the rare-earths–extractant complex in the diluent, which may limit potential process usefulness of this extractant.

Separations with Amines. — In extractions of rare earths with a primary amine (Primene JM) from acid sulfate solutions and from acid sulfate solutions containing chelating agents, the separation factors were too low to be of process interest.

⁸B. L. Perez and R. E. McHenry, *Solvent Extraction Separation of Neodymium and Promethium Using Di(2-ethylhexyl)phosphoric Acid as Extractant*, ORNL-TM-184 (1962).

8.3 RUTHENIUM

A number of potential ruthenium extractants were tested with simulated Purex feeds, but none performed as well as the tertiary amines. Extraction of ruthenium with a tertiary amine and stripping with caustic apparently represents a practicable flowsheet, although expected recoveries are low, possibly not exceeding 25%. In preliminary tests of methods for separating ruthenium from technetium (which tends to follow ruthenium in this flowsheet), ruthenium was quantitatively precipitated as mixed oxides by adding a small amount of ethanol to a simulated strip solution and boiling. Nearly all the technetium remained in solution. Hot-cell tests with an actual waste solution are planned to determine if ruthenium will behave as in tests with the simulated wastes.

8.4 TREATMENT OF WASTE THAT CONTAINS DISSOLVED STAINLESS STEEL OR LARGE AMOUNTS OF ALUMINUM ION

The present fission product recovery processes were developed for treating wastes similar to the Purex wastes produced at the Hanford facility. Studies were recently begun to determine if the present processes can be adapted to other reactor fuel processing wastes or if other processes will be required.

Waste That Contains Dissolved Stainless Steel

Preliminary tests showed that strontium and rare earths can be recovered from "stainless steel" reactor-fuel reprocessing (Darex) wastes by the di(2-ethylhexyl)phosphoric acid (D2EHPA) extraction process provided that some changes are made in the feed-adjustment procedures. Adding two moles of tartrate per mole of iron, chromium, and nickel and diluting by a factor of 4 or 5 gave feeds stable up to a pH of about 12. Although smaller amounts of citrate gave more stable feeds than tartrate at lower pH's, heavy precipitation occurred on adjustment to pH 12. Strontium extraction from these feeds in the pH range of 2 to 5 was ineffective because of excessive extraction of chromium and nickel. However, interference from these elements was overcome by adding complexing agents such as ethylenediaminetetraacetic acid (EDTA)

or preferably sodium diethylenetriaminepentaacetate (Na_5DTPA). In a batch countercurrent test with adjusted simulated Darex waste, better than 99% of the strontium, cerium, and europium were extracted with 0.3 M D2EHPA–0.15 M TBP–Amsco 125-82 in five extraction and two scrub stages. The feed/solvent/scrub (0.2 M HNO_3) ratios were 5/5/1. The simulated waste solution (1.25 M in Fe(III), 0.38 M in Ni, 0.18 M in Cr, 0.75 M in HNO_3 , 0.0035 M in Sr, and about 0.01 M in Σ RE) was adjusted before extraction by adding 2 moles of tartrate and 0.5 mole of Na_5DTPA per mole of iron, chromium, and nickel and raising the pH to 4.0 while diluting by a factor of 5. Cesium was extracted effectively from the raffinate from the strontium–rare-earths recovery step with 1 M BAMBP in Amsco 125-82. In batch tests, cesium extraction coefficients were 1.8, 8.6, and 15, respectively, at pH's of 11.1, 12.1, and 12.4.

Waste That Contains Large Amounts of Aluminum Ion

With simulated waste that contains large amounts of aluminum (TBP-25 waste, 1.7 M in Al^{3+}), pH adjustment of the uncomplexed waste solution with caustic caused precipitation of aluminum above pH 0.0, although the solution was adjusted to pH 3 with NH_4OH without precipitation. Adding 2 moles of sodium tartrate per mole of aluminum and adjusting the pH with caustic gave stable solutions up to pH 10. Other complexants tried, including EDTA and fluoride, were not so effective. In batch extractions (2-min contact) of tartrate-complexed feed with 0.3 M D2EHPA–0.15 M TBP–Amsco 125-82, strontium extraction coefficients reached a maximum value of 2 at pH 4. Cerium coefficients, which ranged from 20 to 48 in the pH range of 2.3 to 3.9, were at maximum at about pH 3.

8.5 ENGINEERING STUDIES

The flow capacity and efficiency of a single-stage mixer-settler (mixer 6 in. in diameter and 6 in. high; settler 6 in. in diameter and 26 in. high) were determined using a substituted phenol (BAMBP) for recovering cesium from simulated Purex 1WW. This equipment is a satisfactory prototype for obtaining the data necessary for design and scaleup of mixer-settlers. The flow

capacity is limited by flooding, with the dispersion going out with either the aqueous or organic stream from the settler. The depth of the dispersion band increased exponentially with increased flow but was nearly independent of the speed of the agitator in the mixer. For extraction at the normal flow ratio (A/O) of 5:1 and with aqueous-phase-continuous mixing, the flow capacity (total flow) was 290 gal/hr per square foot of settler area. With recycle of solvent to obtain a 1:1 ratio in the mixer, the capacity with organic-phase-continuous mixing was 130 gal hr⁻¹ ft⁻². Entrainment in both streams was low (less than 0.5 vol %) with either mode of operation. For stripping at the normal flow ratio of 1/5 and with organic-phase-continuous mixing, the flow capacity was 730 gal hr⁻¹ ft⁻². Recycle of the aqueous phase to obtain a 1:1 ratio gave a lower flow capacity: 320 gal hr⁻¹ ft⁻² for aqueous-phase-continuous mix-

ing, and 420 for organic continuous. Entrainment was less than 0.5 vol % in both streams. Since recycle of the minor phase is not necessary to obtain low entrainment, the flowsheet can be run at the normal flow ratios set by the equilibria to obtain the maximum flow capacity of the settlers.

Stage efficiencies greater than 90% were easily attained for both extraction and stripping. The efficiency data for a range of throughput and mixing-power input in Table 8.2 show that, for extraction, 100% stage efficiency was obtained with 2.3 min residence time in the mixer at a power input of 2.2 hp per 1000 gal. Less than 1 min of residence time was required at 9 hp per 1000 gal. The stage efficiency for stripping was slightly less than for extraction at the same mixing conditions. The efficiency increased from 82 to 92% when the residence time was increased from 0.77 to 1.5 min at a power input of 6.6 hp per 1000 gal.

Table 8.2. Stage Efficiency of Mixer-Settlers for Recovery of Cesium by 1 M BAMBP in Amsco 125-82

Aqueous feed: Adjusted simulated Purex 1WW, pH 13; contained (moles/liter) 0.17 Fe³⁺, 0.033 Al³⁺, 0.003 Cr³⁺, 0.003 Ni²⁺, 3.0 Na, 1.5 NO₃⁻, 0.33 SO₄²⁻, and 0.33 tartrate

Strip solution: 0.2 M HNO₃

Flow Ratio, A/O	Residence Time in Mixer (min)	Power Input (hp per 1000 gal)	Efficiency (%)
Extraction, Aqueous Phase Continuous			
5/1	2.3	2.2	100
5/1	0.92	2.2	85
5/1	0.92	9.0	100
1/1	2.0	1.8	99
1/1	0.55	1.8	98
Stripping, Organic Phase Continuous			
1/5	1.5	6.6	92
1/5	0.77	6.6	82

9. Chemistry of Protactinium

The purpose of this program is to study the chemistry of protactinium, with emphasis on systems potentially applicable to separations processes. Protactinium has an extreme tendency to hydrolyze, and present knowledge does not permit handling it reliably above trace concentrations in most chemical systems. Studies of the behavior of protactinium in sulfuric acid solutions were continued, utilizing primarily the solvent extraction method. Studies in hydrochloric acid solutions are being initiated. Exploratory spectrophotometric measurements in both sulfuric and hydrochloric acids were initiated, and absorption peaks not previously reported were observed for certain protactinium solutions in $18 M H_2SO_4$.

The purification and recovery of the ^{231}Pa borrowed from England for use in preparing ^{232}U were completed, and all this material has been returned to England.

9.1 EXTRACTION FROM SULFURIC ACID SOLUTIONS

Studies of the extraction of protactinium from sulfuric acid solutions have continued, with emphasis on the increase in extraction with increasing protactinium concentration. Much more data have now been obtained for its distribution between $2.5 M H_2SO_4$ and $0.03 M$ triaurylamine in diethylbenzene, especially at relatively high concentrations (Fig. 9.1); all points in the graph represent equilibrium measurements. Most measurements were made with a carefully purified stock solution containing 3.6 mg of protactinium per ml ($0.016 M$) in $2.50 M H_2SO_4$. This solution was stable for at least four months. Equilibra-tions were carried out in glass.

Initial measurements showed that extraction from the stock solution increased very slowly for periods of at least several weeks.

Variation of the phase-volume ratio from 0.5 to 5 (organic phase/aqueous phase) (\blacktriangledown points, Fig. 9.1) showed that the fraction of the protactinium that extracted was nearly independent of the phase ratio. As the protactinium concentration in the aqueous phase was decreased by dilution at constant acidity, the concentration of the protactinium extracted into the organic phase remained relatively constant, and the concentration in the aqueous phase dropped sharply (Δ points, Fig. 9.1). These observations indicate that part of the protactinium in $2.5 M H_2SO_4$ is in a relatively inextractable form which is in slow equilibrium with species that are extractable.

The rate of extraction was investigated more carefully by mixing 2 ml of both the stock protactinium solution and the organic phase for specified times and then withdrawing samples of each phase (Fig. 9.2). After 1 min of mixing (and 1 min for centrifuging and sampling), the concentration of protactinium in the organic phase was only 0.08 mg/ml. After a second minute of mixing (total elapsed time, 7 min), the concentration increased to 0.12 mg/ml. The amount extracted continued to increase with time to 0.34 mg/ml after 3 hr, 0.8 mg/ml after 5 days, and finally to 1.1 mg/ml (vs 2.9 mg/ml in the aqueous phase) after 3 to 6 weeks (∇ point, Fig. 9.1). These results suggest that the concentration of protactinium in the readily extractable form in the stock solution is something less than 0.08 mg/ml, probably around 0.02 to 0.04 mg/ml; and that the inextractable species are slowly converted to extractable ones. The increase in extraction with time (Fig. 9.2) is a measure of the rate at which extractable species are formed.

After a number of extraction experiments, the organic and aqueous phases were separated and contacted with a new volume of the opposite phase. Results showed that each of the two

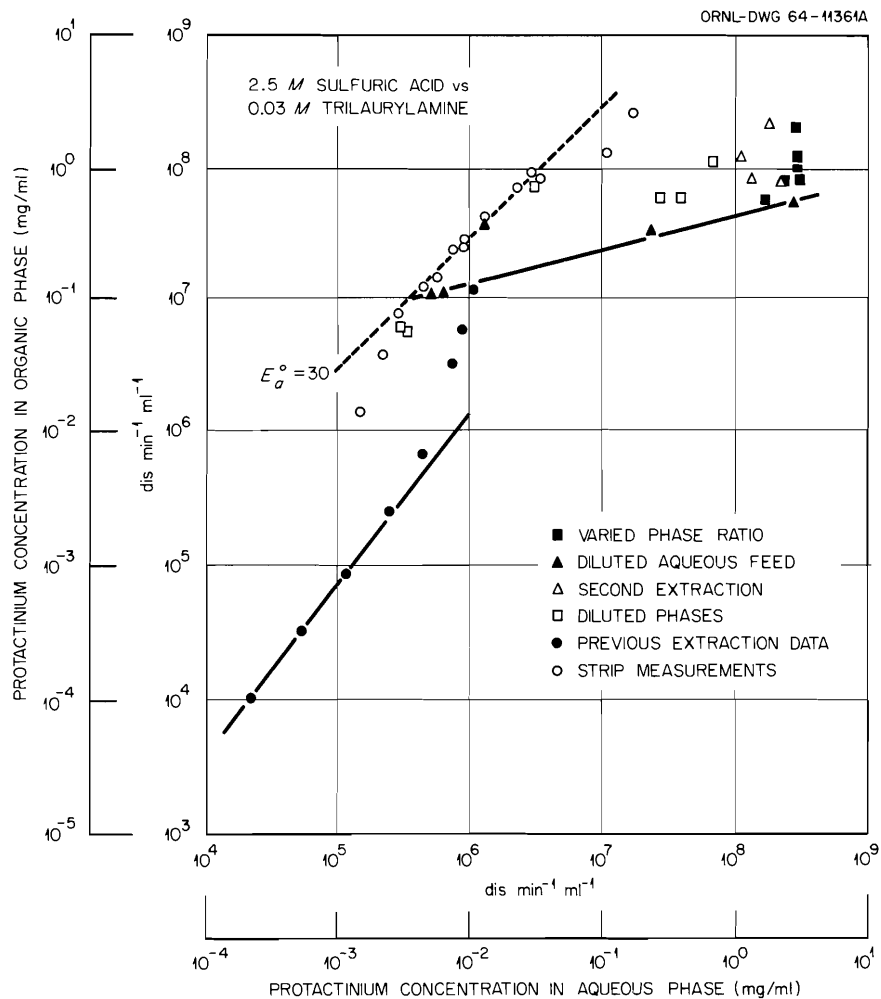


Fig. 9.1. Effect of Protactinium Concentration on Distribution.

phases contained a protactinium species that behaved in an entirely different manner from that in the other phase. The second extraction (x points, Fig. 9.1) was generally very similar to the first, with extraction increasing slowly for some days. Successive extraction experiments indicate that the amount of protactinium extracted from the aqueous phase is primarily dependent on the time of equilibration, and is little affected by dilution of the organic phase, so long as the protactinium concentration is greater than a few hundredths of an mg per ml in the aqueous phase.

Stripping experiments gave protactinium distribution results quite different from those of extraction experiments (● points, Fig. 9.1); equilibrium aqueous-phase concentrations were

as much as 100 times less in the strip solution than in the original extraction. Equilibrium was generally reached in a few hours at most. Dilution of the organic phase (constant amine concentration) resulted in re-extraction of part of the stripped protactinium. Most of the measurements gave an extraction coefficient (E_a^0) of about 30 (Fig. 9.1), at least for aqueous-phase protactinium concentrations from about 0.007 to 0.03 mg/ml. At higher and lower concentrations, where other, less extractable species are present in the aqueous phase, lower extraction coefficients were observed. This value of 30 probably represents the extraction coefficient of the protactinium species we have been calling the "extractable species," and it is the dominant species in the organic phase in equilibrium with

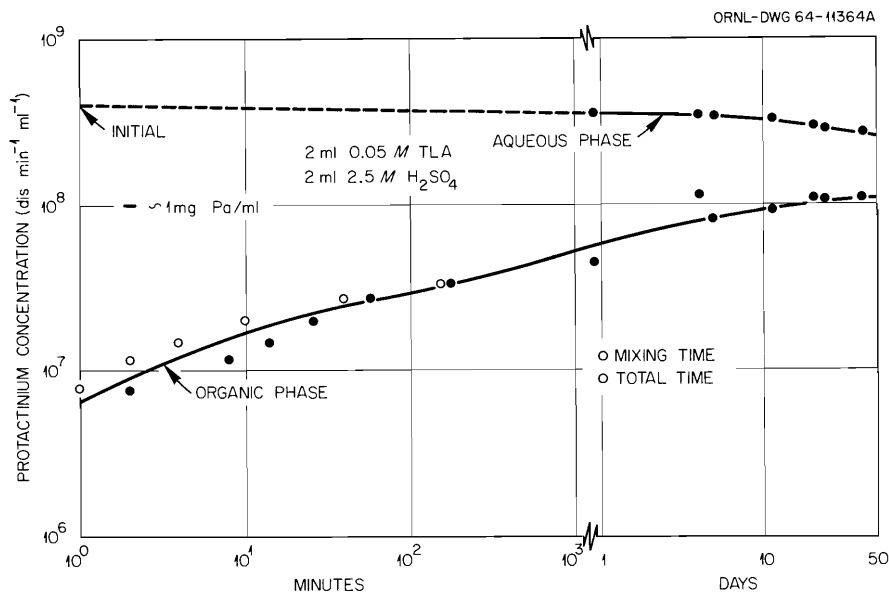


Fig. 9.2. Rate of Extraction of Protactinium.

aqueous solutions that contain more than 0.01 mg/ml of protactinium. Both this observation and the kinetic data indicate that the concentration of this extractable species in 2.5 M H_2SO_4 reaches a maximum value at about 0.03 mg/ml. If more protactinium is present, it exists in relatively inextractable forms in quite slow equilibrium with the extractable species.

These data, together with those reported last year (all summarized in Fig. 9.1), support the following interpretation: In 2.5 M H_2SO_4 containing protactinium at concentrations less than 0.004 mg/ml, extraction coefficients are very nearly constant; therefore, the complexity of the protactinium species is the same in both phases. At slightly higher protactinium concentrations, the extraction coefficient increases sharply, indicating that extracted species are polymeric, relative to the average protactinium species in the aqueous phase. At still higher protactinium concentrations, there is scatter in the data, but extraction coefficients decrease as the protactinium concentration increases, indicating increasing polymerization in the aqueous phase. Kinetic measurements support the proposal of extensive polymerization of protactinium at high concentrations in the aqueous phase and indicate that these larger polymers are in slow equilibrium with the smaller polymeric material which is relatively more extractable.

9.2 ABSORPTION SPECTRA IN SULFURIC ACID SOLUTIONS

The preceding interpretation of extraction data, based on postulating polymeric species of protactinium existing in sulfuric acid solutions, is supported by the published spectrophotometric data, which show that Beer's law is not obeyed in the concentration range 10^{-3} to 10^{-2} mg/ml in 2.2 M H_2SO_4 solution.¹ However, the range of parameters covered was rather limited. The reported spectra show a major absorption peak in the range 212 to 220 $m\mu$, depending on concentrations, but the measurements extended to only slightly below 210 $m\mu$. A more comprehensive study of the spectra of protactinium was initiated, utilizing a Cary model 14 spectrophotometer modified for safe handling of alpha-active materials. This instrument permits measurements to shorter wavelengths, possibly to 185 $m\mu$. Only preliminary results are available, but they indicate that the method of sample preparation has a marked influence on the spectrum of the solution.

The stock solution from the solvent extraction tests described above (3.6 mg/ml of protactinium in 2.50 M H_2SO_4) gave a single, rather

¹R. Guillaumont *et al.*, *Compt. Rend.* **248**, 3298 (1959).

broad peak at 203 $m\mu$, with a molar extinction coefficient of about 10^4 . The spectrum of a solution resulting from adding 150 μ l of this solution to 5 ml of concentrated sulfuric acid showed a peak at 225 $m\mu$, with a molar extinction coefficient of 2×10^4 . Almost the same spectrum was obtained when protactinium from the stock solution was precipitated with ammonium hydroxide and the hydroxide was dissolved in concentrated sulfuric acid, and also when the hydroxide was ignited to 600°C before dissolving it in concentrated sulfuric acid.

An entirely different spectrum was obtained from a concentrated sulfuric acid solution of some protactinium oxide of somewhat uncertain history (it had been carried through the usual anion exchange purification procedure, but it contained substantial amounts of impurities, probably derived from glass). This material gave a well-defined peak at 250 $m\mu$, a valley at 210 $m\mu$, and increasing absorption down to 190 $m\mu$, indicating a second peak at shorter wavelengths. The molar extinction coefficient for the 250- $m\mu$ peak was about 2×10^5 . Precipitating the protactinium from this solution (as the hydroxide) and redissolving it in concentrated sulfuric acid caused only small changes in the spectrum. Upon dilution with water the 250- $m\mu$ peak diminished rapidly and disappeared at an acid concentration of about 12 *M*. Subsequently, peaks grew in at 275 and 232 $m\mu$.

The spectra of both solutions, however, were changed substantially by heating to the fuming temperature of sulfuric acid. A much sharper peak at close to 200 $m\mu$ appeared, and the peaks at 225 or 250 $m\mu$ decreased greatly. Drastic heating was required to bring about this change — heating in a boiling water bath for 1.5 hr had no effect. The sharpest peaks were observed after fuming the sulfuric acid to dryness and redissolving the residue. However, there is some question about these spectra, especially with regard to any quantitative interpretation, because any small amounts of organic material are decomposed by fuming sulfuric acid, resulting in a somewhat brownish solution in some cases. Such solutions do absorb light in the ultraviolet region of the spectrum; but in numerous tests of blanks, no sharp peaks have been observed except at 320 $m\mu$, and, in particular, no peak similar to that at 200 $m\mu$ for the protactinium solutions has been observed.

We hope to learn why these two solutions give different spectra and why both give still a third spectrum after heating. Subsequently, the effect of both sulfuric acid and protactinium concentrations will be studied.

9.3 RECOVERY OF PROTACTINIUM

The recovery of the ^{231}Pa borrowed from England for use in preparing ^{232}U was completed. The recovery from process solutions was completed and reported last year, but the amount of protactinium in the final products was somewhat less than expected. A review of the records indicated that the most likely place where a significant amount of protactinium could have been lost was in the equipment used for the original ^{232}U recovery program about three years ago. The reason for this is that the ^{232}U activity was so high that it completely masked the protactinium activity. The equipment used for the ^{232}U program was exhumed from the burial ground, and the polyethylene dissolver vessel and two polyethylene resin columns were recovered. No other component gave a significant radiation reading.

The resin columns gave gamma readings of 1 to 2 r/hr, indicating that they contained little protactinium. However, the resin was removed and leached with HCl-HF solution, but almost no protactinium was found. The dissolver vessel gave radiation readings over 100 r/hr, much higher than expected. Some of the radioactive material appeared to be loose inside the vessel. The dissolver was cut in two in a hot cell and leached three times with 9 *N* HCl–4 *N* HF solution. A total of 1.65 g of ^{231}Pa was recovered, nearly all in the first leach and less than 1% in the last. There was also some ^{232}U and attendant ^{232}U daughter activity, resulting in very high gamma activity.

These solutions were processed through the usual anion exchange purification procedure, using HCl-HF solutions for ^{232}U removal. Finally, the protactinium was extracted with either di-isobutylcarbinol or Alamine 336 and stripped with HCl-HF solution. The protactinium was precipitated with ammonium hydroxide, filtered, and fired at 500°C for 3 hr. The product weighed 2.85 g, and alpha analysis showed that 1.65 g was ^{231}Pa . There were no other significant alpha activities. Impurities accounted for

about 1 g of this material, and emission spectra showed the major impurities to be Al, Ca, Na, and Si, with smaller amounts of B, Ba, Fe, Mg, Ti, and no detectable niobium. It is not understood how such large amounts of these materials

got into the product, and, in particular, how so much calcium, the major impurity, followed protactinium through the purification cycle. This product has been shipped to England, completing the recovery operation.

10. Irradiation Effects on Heterogeneous Systems

10.1 RADIOLYSIS OF WATER ADSORBED ON SILICA GEL

The study of irradiation effects on heterogeneous systems has been focused on the radiolysis of water adsorbed on silica gel. In some cases the radiolysis of a material in the adsorbed state proceeds with an apparent G value much higher than that for the pure material. This has been interpreted as an energy transfer from the adsorbent to the adsorbed phase. Several years ago we observed in our laboratory that the silica gel-water system showed such an effect. Accordingly, this system, whose surface characteristics have been studied by many investigators and are fairly well known, was selected for further investigation to find out if energy transfer really occurred, and if so, to attempt to determine the mechanism. Such an energy transfer, as well as being of fundamental interest, could have application to chemonuclear processes and to radiation processing in the presence of catalysts.

Experimental

The radiation source contains 80 curies of ^{90}Sr - ^{90}Y and delivers 700,000 rads/hr to the silica-gel sample.¹ The sample is held in a disk-shaped stainless steel container with a 2.5-mil-thick window which can be brought into opposition with the source-capsule window. A layer of silica-gel granules about 1.3 mm thick (approximately 0.5 g) is used.

The rate of water radiolysis was determined by periodic measurement of the amount of hydrogen accumulated in the chamber. Hydrogen appears to be the only detectable gaseous product. The rate

of hydrogen evolution was not constant but varied with the total irradiation time (Fig. 10.1) for three different types of adsorbents. From the maximum rate of hydrogen evolution, $G(\text{H}_2)$ values were computed, based on the energy absorbed by the entire sample and based on the energy absorbed by the water alone. The fraction of the energy absorbed in the water is assumed to be proportional to the weight percent of water present, since the electron densities of silica gel and water differ by less than 10%. During an experiment the water content remained constant to within a fraction of 1%.

Results

Measurements have been made on three silica gels and on porous glass. The properties of these materials are given in Table 10.1. Maximum hydrogen production rates were determined for each adsorbent at various water contents, and $G(\text{H}_2)$ values were computed, based on the maximum rates. The results in terms of surface coverage are shown in Figs. 10.2 and 10.3. More data for the porous glass are desirable, but the entire batch of material was used in making the measurements reported. (A fresh sample of adsorbent is used for each point to avoid problems connected with cumulative irradiation time.) A second batch prepared by the same recipe gave only half the hydrogen yield.

A coverage of 0.12 mg of H_2O per m^2 of gel represents a surface that is completely covered with silanol groups (Si-OH). Additional water is only physically adsorbed and easily removed. Producing a monolayer of physically adsorbed water would require between 0.12 and 0.24 mg of H_2O per m^2 of surface, depending on how many water molecules bridge two adsorption sites. For these calculations, it is assumed that there are eight hydroxyl groups per 100 A^2 of surface.

¹Chem. Technol. Div. Ann. Progr. Rept. May 31, 1964, ORNL-3627, pp. 220-23.

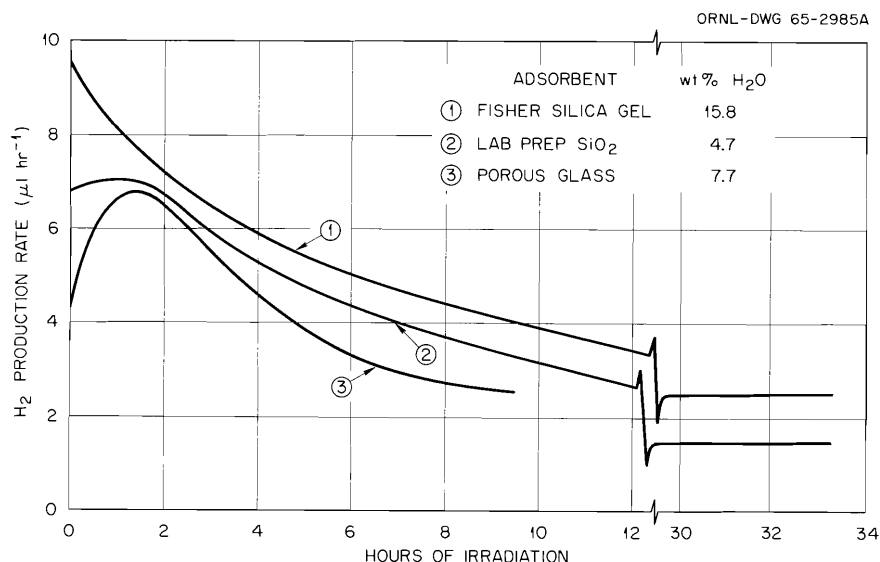


Fig. 10.1. Effect of Irradiation Time on the Hydrogen Yield from the Radiolysis of Adsorbed Water.

Table 10.1. Properties of Adsorbents

Adsorbent	Specific Surface Area (m ² /g)	Average Pore Radius (A)	Mean Pore Radius (A)
Fisher silica gel, untreated	682	10.1	6.9
Laboratory-prepared silica gel	227	50.7	50.1
Porous glass	155	23.8	23.1
Fisher silica gel, NH ₄ OH washed and fired	65	24.5	23.5

Water is not adsorbed monolayer by monolayer in a nice orderly fashion, but the calculations give values that can be used as rough guides.

Figure 10.2 shows that at low coverages the $G(H_2)$ values calculated, based on energy absorbed in the water alone, rise sharply with water content. As additional layers of water are added, the $G(H_2)$ values decrease. The decrease is very steep for material of high specific surface area, possibly because of the very small pore size. It is apparent that the additional water "deactivates"

any energy transfer process. (The total hydrogen production rate drops off, also showing that the deactivation is not merely a dilution of the energy transfer effect with additional water.)

Figure 10.3 shows the results calculated according to the amount of energy absorbed in the total sample. It is interesting that the sharpness of the maximum decreases with increasing specific surface area. (Perhaps the curve for the Fisher silica gel should be drawn with a rounded top instead of a point – this may be better for the curves in Fig. 10.1 also.) The interesting implication of these curves is that in the presence of a solid that has a large specific surface area, the $G(H_2)$ value is greater than that measured for pure water, even when it is calculated according to the amount of energy adsorbed by the entire silica-gel-water sample. The $G(H_2)$ value for water is about 0.45. The $G(H)$ value for the hydrogen-radical yield is 2.9, and the G value for the destruction of water² [$G(-H_2O)$] is 3.6. Thus, a $G(H_2)$ of 1.8 would imply complete utilization of all of the energy absorbed by both the silica gel and water to produce one half of a hydrogen molecule for every water molecule destroyed. Our maximum observed $G(H_2)$ of 1.72 is very close to this value.

²A. O. Allen, *The Radiation Chemistry of Water and Aqueous Solutions*, pp. 44–48, Van Nostrand, Princeton, New Jersey, 1961.

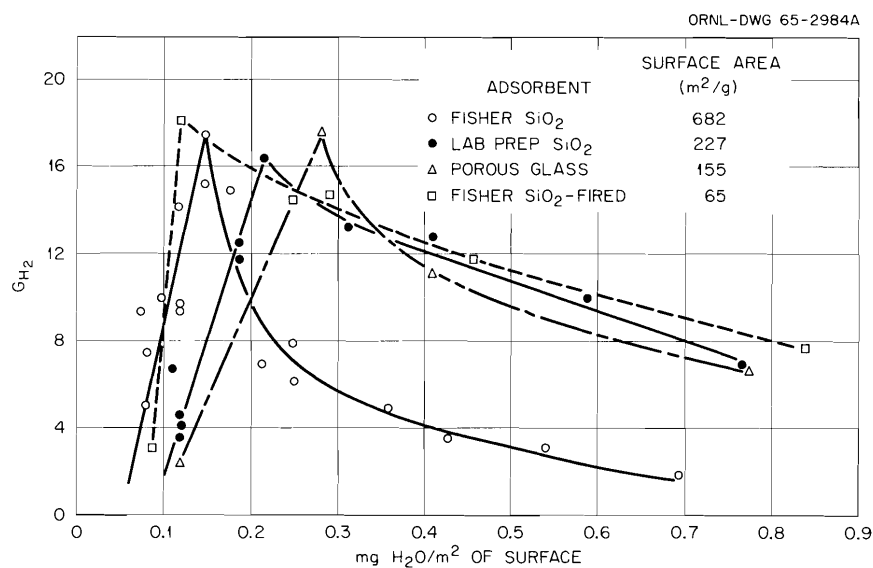


Fig. 10.2. $G(H_2)$ Values for the Radiolysis of Adsorbed Water – Calculated from the Energy Absorbed by the Water Only.

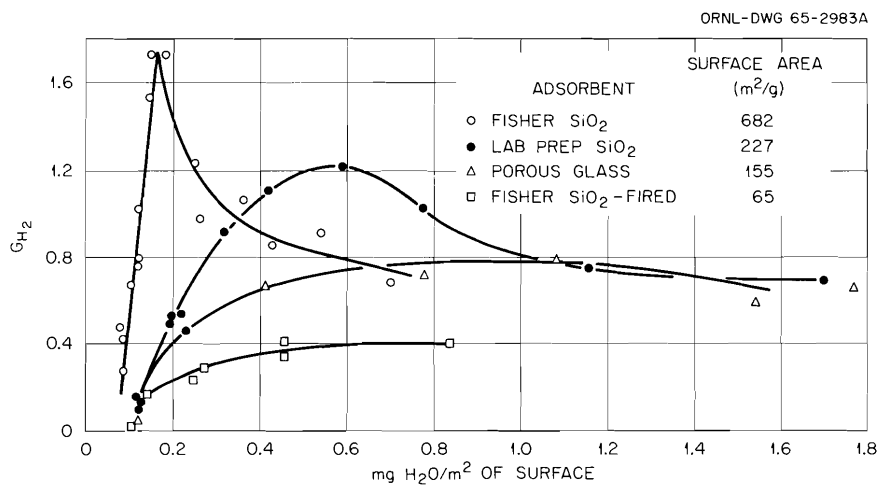


Fig. 10.3. $G(H_2)$ Values for the Radiolysis of Adsorbed Water – Calculated from the Energy Absorbed by the Entire System.

11. High-Temperature Chemistry

The purpose of this program¹ is to develop and exploit various spectrophotometric techniques for studying the properties of aqueous solutions, primarily those of uranium and the higher transuranium, rare-earth, and transition-group elements. A spectrophotometer, associated cells, and other systems have been specially designed for ORNL by the Applied Physics Corporation to aid in these studies. The system is being constructed by Applied Physics and ORNL; installation is scheduled for July–August 1965. The design is such that solutions containing high levels of alpha-active elements of interest in heavy-element chemistry can be ultimately studied. The system will permit the study of the solution chemistry behavior and equilibria, reaction kinetics, and spectral properties of elements and complex species in solution up to the vicinity of the critical point of water, 372°C. Subsequent divisions of this section present various areas of work relevant to this program, their current status, and the overall relationship of the various parts to the project as a whole.

11.1 FABRICATION STATUS OF THE HIGH-TEMPERATURE, HIGH-PRESSURE SPECTROPHOTOMETER SYSTEM

The program for the absorption spectrophotometric study of aqueous solutions at high temperatures and high pressures has been discussed previously.^{2–5} A high-temperature, high-pressure spectrophotometer, associated high-temperature, high-pressure absorption cells and other equipment, and related subsystems have been especially designed for ORNL under subcontract by the Applied Physics Corporation (APC), of Monrovia, California. The

design and development were completed this year. The prototype absorption cell, fabricated by APC, and other equipment were delivered to ORNL by the subcontractor. The program for the construction of the spectrophotometer system was started in September 1964.

The spectrophotometer system is being constructed by the Applied Physics Corporation, the Engineering and Maintenance Division at Oak Ridge Gaseous Diffusion Plant (ORGDP), and the Special Projects Shop at the Y-12 Plant and is scheduled for completion by July 1965. The main spectrophotometer is scheduled for delivery in August. It is anticipated that installation of the locally constructed subsystems can begin by July 1 so that most all such work can be completed prior to arrival and installation of the main spectrophotometer.

The test facility for experimentation with the absorption cell was operated during part of this past year. It can be used for the hydrostatic and gas-pressure testing of the cells or other equipment to at least 10,000 psi with the absorption cell at the maximum temperatures anticipated and up to the critical point of water. Adequate monitoring, recording, linear temperature programming, and other control equipment for the efficient operation of the test facility are available. Testing of the prototype cell was completed during the first part of this fiscal year. A number of changes were made to the APC design of the prototype cell. Each change or improvement made in the design is either the result of experimental work or

²*Chem. Technol. Div. Ann. Progr. Rept. May 31, 1964, ORNL-3627, pp. 224–30.*

³*Chem. Technol. Div. Ann. Progr. Rept. June 30, 1962, ORNL-3314, pp. 187–90.*

⁴*Chem. Technol. Div. Ann. Progr. Rept. May 31, 1963, ORNL-3452, pp. 211–15.*

⁵*Anal. Chem. Div. Ann. Progr. Rept. Nov. 15, 1963, ORNL-3537, pp. 39–45.*

¹Joint program with the Analytical Chemistry Division.

detailed theoretical calculations and stress analysis. Interrelated effects have also been considered.

A schematic layout of the absorption cell and the related pump loop and heating system for the spectrophotometer system and a photograph of the prototype cell and component parts have been presented previously. A schematic layout of the principal components and special features of the spectrophotometer system has also been presented previously.

11.2 SPECTRAL STUDIES OF IONIC SYSTEMS

Uranyl Ion in Perchlorate Media

Initially we chose to work with pure perchlorate systems because they are not only of intrinsic interest but also serve as reference data for spectral studies of the uranyl ion in systems containing complexing agents. Experiments were carried out for the uranyl ion in perchloric acid and in perchlorate systems in the acid-excess region (to 10 *M* acid), at the stoichiometric point, and in the acid-deficient region up to a hydroxyl number (average number of hydroxyls bound per uranyl ion) of 1.1 over the temperature range of 25 to 95°C at several ionic strengths and at several uranyl ion concentrations. Resolution (Sect. 11.4.1) of the absorption spectra of uranyl (0.01 *M*) perchlorate into the individual absorption bands has been completed at 2.9, 0.98, 0.5, 0.3, 0.014, 0.009, and 0.002 *M* excess H^+ , including about 16 temperatures at each acidity. Many experiments at higher acidities have also been carried out. Studies of the results and correlation of the results with the experimental parameters are under way for the various uranyl concentrations, acidities, temperatures, ionic strengths, etc. All the digitized data (about 700 spectra) have been preprocessed (smoothed) and prepared (CDC 1604 computer programs; see Sect. 11.4.4) for resolution with program MRØCØS on the IBM-7090 computer.

To serve as a reference and orientation for present and future discussions relevant to this subject, an example of some recently obtained absorption-spectrum results are presented here for uranyl ions in perchlorate solution. The results are for the uncomplexed and unhydrolyzed state. We will consider hydrolyzed species as a special case of complex ions. The spectrum is shown in Fig. 11.1, and pertinent resolved parameters for the uranyl

ion are given in a later section (Fig. 11.4). The error plot for this spectrum is shown in Fig. 11.2. The asterisks represent the experimental data points, which were obtained at 5-Å intervals from 3325 to 5000 Å. In Fig. 11.1, only every third data point is plotted, for clarity. Figure 11.1 is a CALCOMP plot and is part of the direct computer output of program MRØCØS (Sect. 11.4.1).

The complicated spectrum of the uranyl ion between 3300 and 5000 arises from several vibrationally perturbed electronic transitions; 14 distinct absorption bands are observed in this wavelength interval. Each band overlaps the adjacent bands and results in the rather ill-defined summed spectrum observed (see Sect. 11.4.3). This overlapping, coupled with the fact that the individual transitions react in different ways to changes in temperature or solution parameters, complicates the spectra and their interpretation even further. With this overlapping, it was formerly impossible to obtain the parameters (position, intensity, and width) of any given single absorption band or transition by ordinary computational procedures. However, computer techniques recently developed for the mathematical resolution of complex, overlapping spectra were successfully applied to a study of the fundamental parameters of the absorption spectra of the uranyl ion and related systems.

Even under conditions where complexation or hydrolysis effects are nonexistent or very minimal, changes are observed, for example, in all three parameters of each band with all experimental conditions invariant except temperature. The spectra obtained for the uranyl ion in different complexing systems (e.g., sulfate) represent the summed absorption (for each transition) of the possible species: uncomplexed UO_2^{2+} , UO_2SO_4 , $UO_2(SO_4)_2^{2-}$, $UO_2(SO_4)_3^{4-}$, and any hydrolyzed species present, if acid-deficient conditions exist in the particular solution. Changes in the individual band parameters are the result of the effects of complex-ion formation on the spectral bands which represent the electronic and vibrational parameters of the parent ion. These changes, as will be shown later, are very dramatic (see Sect. 11.2.3).

The positions of the bands all shift toward the red, linearly with increasing temperature. Plots of the temperature vs the wavelength of maximum absorption appear nearly parallel for the various bands and show temperature coefficients of about 0.12 to 0.25 Å/°C (0.69 to 1.3 $cm^{-1}/°C$). The band intensities are either nearly invariant or show

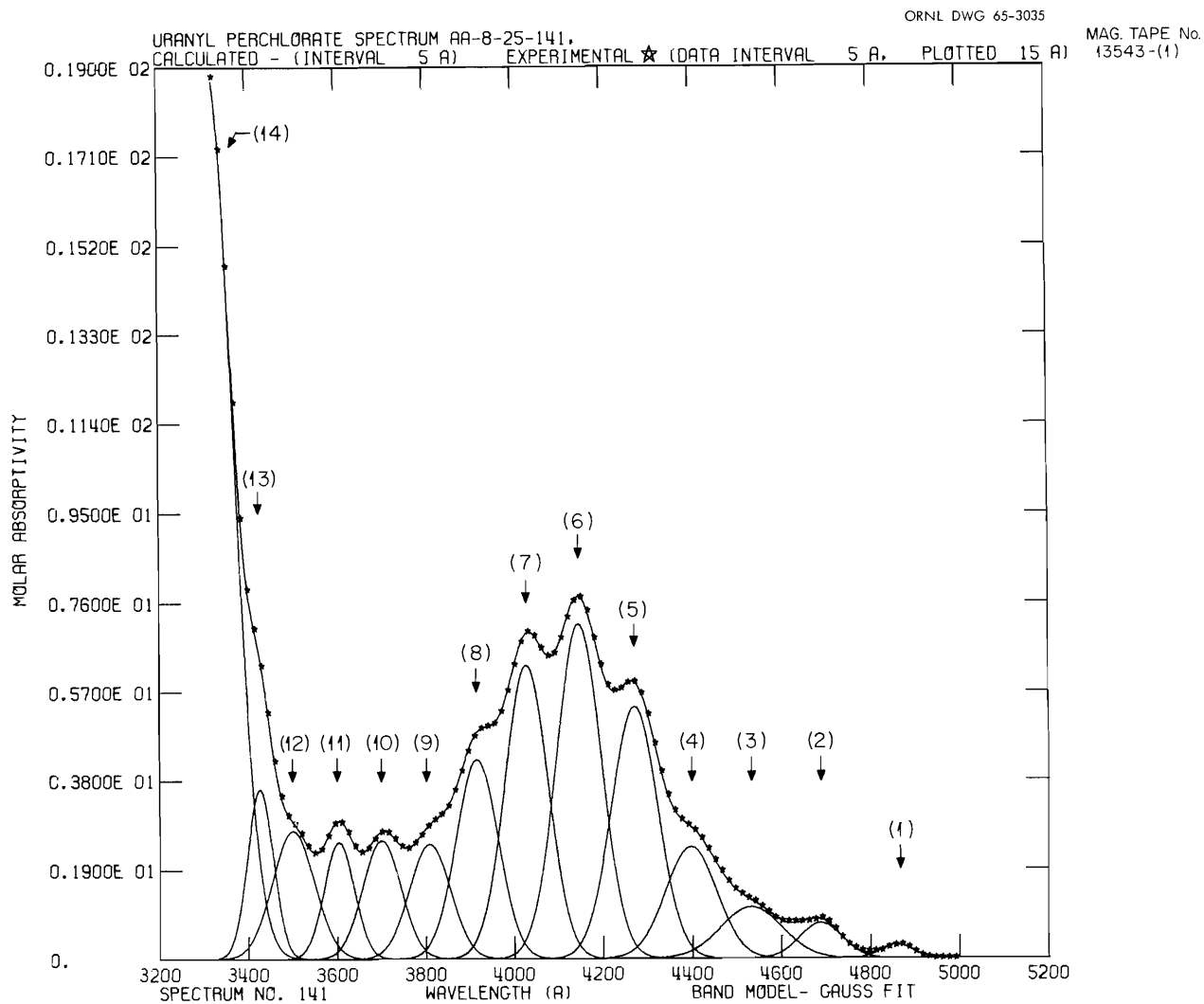


Fig. 11.1. Spectrum of $\text{UO}_2(\text{ClO}_4)_2$. Comparison of the experimental and the nonlinear least-squares calculated spectrum showing the resolved bands. Wavelength mode. UO_2^{2+} concentration = 0.00915 M; H^+ concentration = 0.014 M (HClO_4); temperature, 25.0°C; $\mu = 3.00$ (ionic strength).

a slight linear increase with increasing temperature. The half-band widths exhibit moderately large increases with temperature; they appear to be linear but have somewhat varying temperature coefficients. All the bands show an increase in the integrated absorption (area), to varying degrees, with an increase in temperature.

Theoretical Interpretations of the Spectra of Uranyl Ion Systems

In view of several fairly recent reports and the new information yielded by our recent results, a

few points concerning the interpretation of UO_2^{2+} spectra are in order. Many areas of conflict are reported in the literature. A theory of the uranyl ion explaining its spectroscopic behavior is only rudimentary. Much of the work is rather empirical, and very little published work exists on either the correlation of experimental facts with theory or the interpretation of the spectra of the uranyl ion and its actinyl analogs. The importance and inherent difficulty of the extension of such work to the higher actinide elements beyond uranium are obvious. As a result of the lack of properly developed analytical techniques for obtaining accurate

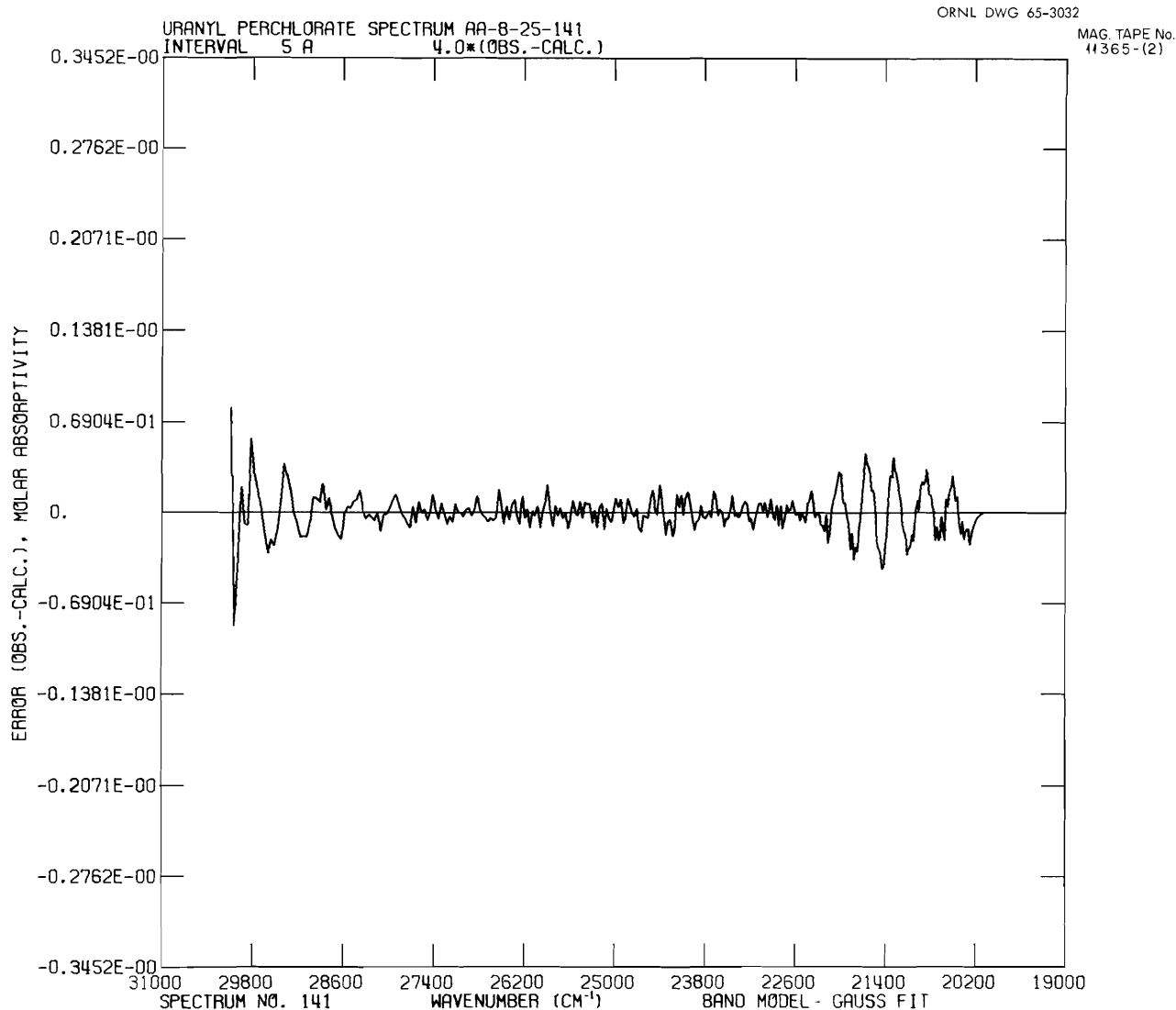


Fig. 11.2. Least-Squares Fitting Error for the Resolution of the $\text{UO}_2(\text{ClO}_4)_2$ Absorption Spectrum. Wavelength mode. UO_2^{2+} concentration = 0.00915 M; H^+ concentration = 0.014 M (HClO_4); temperature, 25.0°C; $\mu = 3.00$ (ionic strength).

values for parameters of the electronic and vibronically perturbed transitions which must be considered, much of the work to date has been carried out with inferred or empirically chosen values. The utilization of properly resolved and analyzed spectra will make a significant contribution in this regard and yield considerably greater accuracy.

We tested a theoretical model previously proposed from the theoretical works of McGlynn and Smith⁶ [using a $\text{UO}_2(\text{NO}_3)_2(\text{aq})$ spectrum] for assignment of the 3320- to 5000-Å spectrum to a first-excited-state triplet perturbed by two higher energy states.

The previously assumed areas for the underlying bands do not conform to the band definition observed in the experimental spectrum and could not

⁶S. P. McGlynn and J. K. Smith, "The Electronic Structure, Spectra, and Magnetic Properties of Actinyl Ions, Part I. The Uranyl Ion," presented at the Symposium on Molecular Electronic Spectroscopy, American Chemical Society Meeting, Cleveland, Ohio, Apr. 16, 1960; *J. Mol. Spectry.* **6**, 164-87 (1961); see also: "Part II. Neptunyl and the Ground States of Other Actinyls," *J. Mol. Spectry.* **6**, 188-98 (1961); S. P. McGlynn and W. C. Neely, "Electronic Structure, Spectra, and Magnetic Properties of Oxyocations. III. Ligation Effects on the Infrared Spectrum of the Uranyl Ion," *J. Chem. Phys.* **35**(1), 105-16 (1961).

sum up to the spectrum. We tested the previously proposed division of the visible absorption bands into a triplet state and found that the ratios of the lifetimes of the absorption transitions did not correspond to the calculated ratios for the perturbation of the triplet regions 1 and 3 by singlet region 4. Significantly, by the use of very accurate data, with the perchlorate system, we found an additional band, 13, in the near-ultraviolet region of the visible, which has been found to be part of the same transition as represented by the bands in the 3325- to 5000-Å region. A close examination of the profile and structure of the experimental and the resolved spectrum led us to propose a different assignment of bands into the various levels of a proposed triplet, consisting of bands 1-3, 4-8, and 9-13, as triplet regions 1, 2, and 3. We attempted to resolve by computer techniques the uranyl absorption spectrum according to the previously proposed model,⁶ but this model was converted by the nonlinear least-squares computer method to the same resolved absorption bands that we found.

The oscillator strengths and lifetimes of the three main regions were calculated and analyzed. In agreement with the type of model previously proposed, we calculated from perturbation theory the lifetime ratios of regions 1 and 3 of the triplet as perturbed by the band of lower energy of the two uv transitions, assumed previously and at the same present time to be singlet states. This yielded lifetime ratios for regions 1 and 3 of the triplet perturbed by region 4 that agree to within 15% of those ratios calculated, which is considered excellent agreement. The perturbation of triplet region 2 by the higher lying energy uv band, region 5, is probable, though less certain. We found a multiplet splitting of 3200 cm^{-1} for the triplet, which is in reasonable agreement with the theoretical value of 3050 cm^{-1} , and is somewhat closer than the value (2500 cm^{-1}) found for the previously proposed band-distribution model.⁶

Fluorescent spectra of UO_2^{2+} in perchlorate solutions were studied, and six bands were observed (Fig. 11.3). The first or highest energy band occurs at the center of our proposed triplet region 1, and the spacing between the first two higher energy fluorescence bands is almost exactly equal to the spacing between the first two lowest energy absorption bands, 1 and 2, and is in good agreement with the fact that the fluorescence spectrum arises from the lowest lying excited

state; other fluorescence transitions form higher levels decaying radiationlessly. This, in part, confirms the proposal of a triplet state for the uranyl ion. More detailed experimental work in the low-uv spectral region and with complexed systems is needed to aid in a further refinement of the model. This work is in progress.

The Effects of Nitrate Complexation and Hydrolysis on the Spectra of the Uranyl Ion

We studied the effect of nitrate complexation on the spectrum of UO_2^{2+} over the range 0 to 3.5 M (with NaNO_3) at 25°C and at 0.05 M UO_2^{2+} . The ionic strength μ was held at 3.00 with NaClO_4 up to 2.5 M NO_3^- , and at 4.00 at higher nitrate concentrations. The acidity was held at 0.100 M excess HClO_4 to prevent hydrolytic perturbations of the spectral bands (see below). A series of spectral studies were also made at 0.01 M UO_2^{2+} , with nitrate concentrations up to 1.85 M , at $\mu=3.00$, and 0.1 M HClO_4 . This yielded $\text{NO}_3^-/\text{UO}_2^{2+}$ ratios ranging from 0 to 185. Marked changes in the various band parameters from the resolution of the spectra were observed and appear to occur in some cases at different band positions than at 0.05 M UO_2^{2+} . The experimental facts clearly show that the effects of nitrate complexation are not reflected in "general" changes in the observed spectra, as might be inferred from a cursory examination of an unresolved, observed, or "summed" spectrum, and clearly preclude the use of intensity measurements on an observed or experimental spectrum as quantities to be used in calculations concerning the distribution of complex-ion species. Obviously, certain of the excited levels are more involved in the bonding making up the complex ion than are other levels.

A series of resolved spectra of the UO_2^{2+} system have also been obtained for progressively more hydrolyzed UO_2^{2+} solutions in pure perchlorate solutions at 0.2178 M UO_2^{2+} , $\mu=3.00$, temperature = 25°C. The acidity range in this series ranged from the acid-excess region (2.346 M HClO_4) stepwise to the stoichiometric point and then in very fine steps into the acid-deficient or hydrolytic region (to 0.035 M excess OH^- or a hydroxyl number of 0.161). A second series of experiments were conducted at a lower UO_2^{2+} concentration (and constant $\mu=3.00$) of 0.00915 M , at hydroxyl numbers up to 1. At each hydroxyl number, a

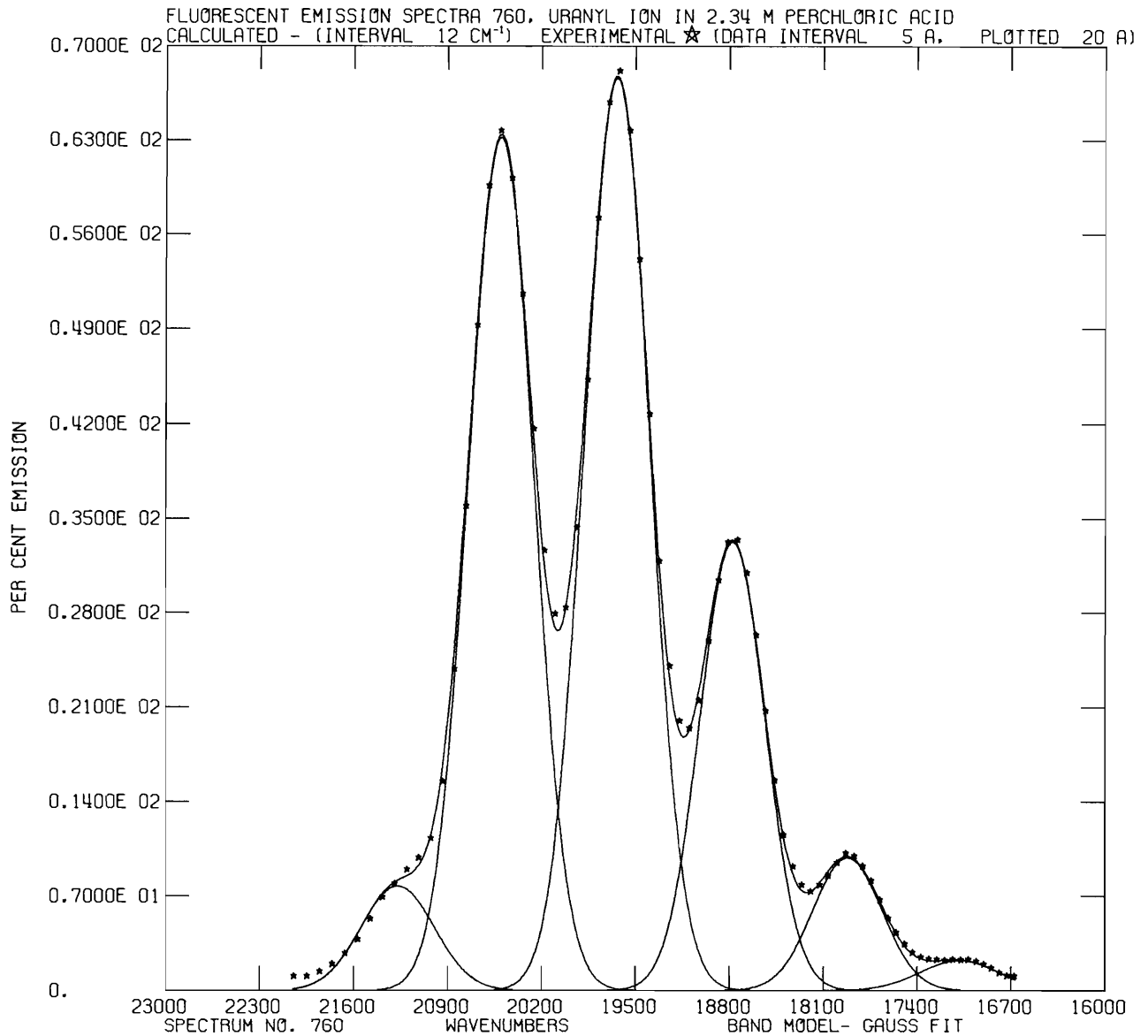


Fig. 11.3. Fluorescence Spectrum of the Uranyl Ion in Perchlorate Medium. Comparison of the experimental and the nonlinear least-squares calculated spectrum showing the resolved bands. Wavenumber mode. UO_2^{2+} concentration = 0.218 M; H^+ concentration = 2.346 M (HClO_4); temperature, 28°C; $\mu = 3.00$ (ionic strength).

series of spectra were obtained at about 11 temperatures from 25 to 95°C. Progressing into the hydrolyzed region, the effects on the spectral bands become more marked, and, considering the area of visible region in its entirety, there is an area increase with progressive hydrolysis. In marked contrast to the results of the nitrate experiments, there is generally an intensity and area increase for all the bands; no bands have been found to decrease in area. The effects of hydrolysis

begin at about 0.03 M excess acid, due apparently to self-hydrolysis of the UO_2^{2+} ion.

11.3 MEASUREMENT OF LIQUID DENSITIES AT HIGH TEMPERATURE AND HIGH PRESSURES

As an important adjunct to the program for the spectrophotometric study of solutions at high

temperature and high pressures, a method was devised⁷ for measuring the densities of aqueous solutions at temperatures up to about 300°C and at the requisite pressures. A knowledge of solution densities vs temperature is required to calculate the ionic concentration of solutions at temperatures up to the critical point of water (372°C) from the known or measured concentration values of the solutions prepared for study. From room temperature to the critical point, water increases nearly threefold in volume, and the increase is particularly marked at temperatures higher than about 250°C.

A special high-temperature, high-pressure autoclave (dilatometer) and related facilities have been designed and built⁸ to permit the accurate measurement of liquid densities at high temperature and high pressures. The design and mode of operation of the present system are such that densities of solutions can be determined at 370 to 371°C, within a maximum error of 0.6%. The autoclave can be operated up to 5000 psi at 400°C.

The liquid volume of a weighed solution of a known composition is determined in an autoclave constructed from titanium; the density is determined from the weight of the solution and the position of the vapor-liquid interface as measured via x-ray photography. General characteristics and a photograph of a disassembled view of the autoclave before welding have been presented previously.⁵

The densities of about 25 uranyl perchlorate solutions that had been studied spectrophotometrically were measured pycnometrically to 95°C. For comparison with the high-pressure dilatometer results, a solution of uranyl perchlorate was measured at temperatures from 25 to 400°C. At 95°C, the dilatometer results agreed with the pycnometric results to within 0.4%.

The density of water was measured at numerous temperatures up to the critical point. Agreement with steam-table values was obtained to within 0.5% up to about 275 to 300°C, using a conventional thermocouple temperature measuring and recording system. At higher temperatures, the error increased because the temperature was not

known accurately enough. From about 300°C to the critical point, the expansion (or specific volume) of water is extremely temperature sensitive and increases rapidly. Consequently, it is necessary to know the temperature to within 0.1°C or better in order that accurate corrections can be made for the amount of water transferred to the vapor phase. Some equipment installed recently permits the measurement of the temperature to within about 0.05°C, and we will be able to maintain good accuracy all the way to the critical point. Work with the much more accurate temperature-monitoring system is in process.

11.4 COMPUTER PROGRAMS FOR SPECTROPHOTOMETER STUDIES

Mathematical Resolution of Complex Overlapping Spectra and Spectral Fine Structure

A generalized nonlinear least-squares computer program (MRØCØS) for the mathematical resolution of complex overlapping spectra has been completed.⁹ All our original goals for this major computer program have been met. The program, a significant extension and modification of our earlier programs of this type, will resolve complex, overlapping spectral bands and fine structure and is now available for the IBM-7090 computer and automatic off-line plotting equipment. Some of the many different types of output and calculated quantities that may be obtained are shown in Fig. 11.4 for the resolution of the spectrum of UO_2^{2+} .

For a particular mathematical function as the spectral band model, three parameters, position, height, and width, define the band in its entirety. A set of trial parameters for the initial iteration of the nonlinear least-squares spectral resolution program is arrived at as follows: Estimates are made of the three parameters for each band in the spectrum by successive approximations, starting at the long-wavelength end of the spectrum. Trial runs on the computer are made. If the trial parameters are not too far off, the program will converge with successive iteration; otherwise it will diverge. These approximations are repeated until an approximate set of parameters is obtained which will

⁷N. A. Krohn and R. G. Wymer, "X-Ray Method for Determining Liquid Densities at High Temperatures and Pressures," *Anal. Chem.* **34**, 121 (1962).

⁸In collaboration with T. G. Rogers, Chemical Technology Division summer student, 1962, 1963, and 1964.

⁹In collaboration with E. C. Long and O. W. Russ of the Central Data Processing Center, Scientific Programming Section, Oak Ridge Gaseous Diffusion Plant.

A) COMPUTING MODE: WAVELENGTH (Angstroms)

URANYL PERCHLORATE SPECTRUM AA-B-25-141. 0.00915 M URANYL, 0.01N HClO₄. SPECTRUM SERIES CODE NUMBER
 UNITS ARE MOLAR ABSORPTIVITY AND ANGSTROMS. -- AA-B-25-141

CONVERGED BAND PARAMETERS

CONVERGENCE IN 7 CYCLES

BAND POSITIONS AND ENERGIES					BAND INTENSITIES			HALF-BAND WIDTHS		
BAND NO.	WAVELENGTHS	ERROR	WAVENUMBERS	ELECTRON VOLTS	KCAL/MOLE	MOLAR ABSORPTIVITY	ERROR	ANGSTROMS	ERROR	WAVENUMBERS
1	4.8507E 03	8.4055E-01	21050E 04	2.5513E 00	5.8022E 01	2.8367E-01	5.8299E-03	8.1344E 01	2.1032E 00	3.4440E 02
2	4.8637E 03	1.8071E 00	21183E 04	2.6448E 00	6.0965E 01	7.4831E-01	2.6152E-02	1.1034E 02	2.5072E 00	5.0213E 02
3	4.8727E 03	7.4145E 00	21202E 04	2.7348E 00	6.3055E 01	1.0876E 00	5.6289E-02	1.6070E 02	1.5355E 01	7.8240E 02
4	4.8970E 03	1.6581E 00	21278E 04	2.8188E 00	6.4890E 01	2.3748E 00	1.3001E-01	1.3405E 02	7.4735E 00	6.7333E 02
5	4.9270E 03	5.7409E-01	21314E 04	2.9028E 00	6.6917E 01	5.3711E 00	9.2745E-02	1.2122E 02	2.6724E 00	6.6466E 02
6	4.9462E 03	4.2692E-01	2.4118E 04	2.9872E 00	6.8930E 01	7.1377E 00	7.9949E-02	1.1787E 02	2.1249E 00	6.8576E 02
7	4.9275E 03	5.8961E-01	2.4829E 04	3.0778E 00	7.0962E 01	6.2676E 00	1.0940E-01	1.1335E 02	2.7692E 00	6.9800E 02
8	4.9188E 03	9.2671E-01	2.5583E 04	3.1658E 00	7.2989E 01	4.2449E 00	1.3677E-01	1.1074E 02	4.7761E 00	7.2292E 02
9	4.9091E 03	1.4837E 00	2.6365E 04	3.2543E 00	7.5031E 01	2.4448E 00	1.1804E-01	1.0803E 02	7.3700E 00	7.4472E 02
10	4.9000E 03	1.1827E 00	2.7121E 04	3.3494E 00	7.7227E 01	2.5202E 00	1.2810E-02	1.0093E 02	4.4800E 00	7.3710E 02
11	4.9052E 03	6.8228E-01	2.7738E 04	3.4386E 00	7.9275E 01	2.4849E 00	8.9863E-02	7.8971E 01	2.1050E 00	6.0747E 02
12	4.9012E 03	1.3920E 00	2.8487E 04	3.5399E 00	8.1615E 01	2.7242E 00	2.8869E-02	1.1042E 02	6.6513E 00	9.0234E 02
13	4.9270E 03	4.0278E-01	2.9173E 04	3.6163E 00	8.3378E 01	3.6183E 00	1.8589E-01	6.7519E 01	1.2707E 00	5.7470E 02
14	4.9171E 03	3.9140E-01	3.0147E 04	3.7370E 00	8.6159E 01	1.8925E 01	2.9978E-02	1.2278E 02	1.0954E 00	1.1162E 03

SUM OF SQUARES OF DEVIATIONS = 8.0575E-02
 STANDARD DEVIATION = 1.4565E-02

BAND NUMBER	BAND AREA	BAND AREA ERROR	BAND SPACING			
			BAND NUMBER	ANGSTROMS	WAVENUMBER	ELECTRON VOLTS
1	2.4563E 01	8.1127E-01				
2	8.7988E 01	3.9837E 00				
3	1.9664E 02	2.0824E 01	1-2	1.7077E 02	7.4695E 02	8.2939E-02
4	3.910E 02	2.6547E 01	2-3	1.5825E 02	7.3063E 02	8.0249E-02
5	6.954E 02	1.9408E 01	3-4	1.3557E 02	6.7761E 02	8.3997E-02
6	8.953E 02	1.9808E 01	4-5	1.2847E 02	6.7445E 02	8.3488E-02
7	7.5610E 02	2.2719E 01	5-6	1.2672E 02	7.0432E 02	8.7308E-02
8	5.8038E 02	2.8328E 01	6-7	1.1870E 02	7.1881E 02	8.8112E-02
9	2.814E 02	2.3419E 01	7-8	1.1499E 02	7.4952E 02	8.7958E-02
10	2.7078E 02	1.3615E 01	8-9	1.0855E 02	7.4437E 02	8.8558E-02
11	2.0889E 02	9.4899E 00	9-10	1.0829E 02	7.4622E 02	8.5229E-02
12	3.2077E 02	1.9585E 01	10-11	9.3883E 01	7.1855E 02	8.8828E-02
13	2.4058E 02	1.4828E 01	11-12	1.0838E 02	8.3838E 02	1.0150E-01
14	2.3719E 02	2.2913E 01	12-13	7.4044E 01	6.1888E 02	7.6648E-02
15			13-14	1.1044E 02	9.7324E 02	1.2064E-01

*(UO₂) = 0.00915 M; H⁺ = 0.014 M; μ = 3.00 (ionic strength); temperature = 25.0°C; cell optical path length = 10,000 cm.

**Liter/A/mole-cm.

B) COMPUTING MODE: WAVENUMBERS (cm⁻¹)

URANYL PERCHLORATE SPECTRUM AA-B-25-141. 0.00915 M URANYL, 0.01N HClO₄. SPECTRUM SERIES CODE NUMBER
 UNITS ARE MOLAR ABSORPTIVITY AND WAVENUMBERS. -- AA-B-25-141

CONVERGED BAND PARAMETERS

CONVERGENCE IN 7 CYCLES

BAND POSITIONS AND ENERGIES					BAND INTENSITIES			HALF-BAND WIDTHS		
BAND NO.	WAVENUMBERS	ERROR	ANGSTROMS	ELECTRON VOLTS	KCAL/MOLE	MOLAR ABSORPTIVITY	ERROR	WAVENUMBERS	ERROR	ANGSTROMS
1	2.0502E 04	3.8258E 00	41869E 03	2.5513E 00	5.8022E 01	2.8367E-01	5.8020E-03	3.4091E 02	8.7992E 00	8.0485E 01
2	2.2327E 04	7.2537E 00	41685E 03	2.6438E 00	6.0957E 01	7.3063E-01	2.4635E-02	4.9520E 02	1.0775E 01	1.0807E 02
3	2.2047E 04	3.3689E 01	41539E 03	2.7330E 00	6.3011E 01	1.0632E 00	5.4161E-02	7.7482E 02	7.0204E 01	1.5945E 02
4	2.2722E 04	7.8296E 00	41400E 03	2.8188E 00	6.4894E 01	2.3534E 00	1.1420E-01	6.7896E 02	3.5382E 01	1.3142E 02
5	2.3501E 04	2.4401E 00	41273E 03	2.9008E 00	6.6801E 01	5.3406E 00	8.3588E-02	6.5812E 02	1.9325E 01	1.2020E 02
6	2.4107E 04	2.8752E 00	41162E 03	2.9863E 00	6.8897E 01	7.1362E 00	8.0270E-02	6.2762E 02	1.8152E 01	1.1815E 02
7	2.4615E 04	4.0116E 00	41069E 03	3.0766E 00	7.0921E 01	6.2604E 00	1.2706E-01	6.9681E 02	1.7763E 01	1.1318E 02
8	2.5228E 04	4.4157E 00	40981E 03	3.1638E 00	7.2934E 01	4.3104E 00	1.4886E-01	7.3385E 02	3.4864E 01	1.1268E 02
9	2.6239E 04	1.3027E 01	40893E 03	3.2528E 00	7.4988E 01	2.4640E 00	1.2923E-01	7.4220E 02	5.4077E 01	1.0783E 02
10	2.7018E 04	8.8936E 00	40824E 03	3.3481E 00	7.7194E 01	2.5837E 00	8.0159E-02	7.3744E 02	3.5005E 01	1.0113E 02
11	2.8791E 04	5.0703E 00	40808E 03	3.4375E 00	7.9254E 01	2.7046E 00	9.4502E-02	6.0743E 02	1.7294E 01	7.9000E 01
12	2.9588E 04	1.0808E 01	40808E 03	3.5380E 00	8.1572E 01	2.4918E 00	2.4448E-02	8.9690E 02	5.4021E 01	1.1013E 02
13	3.0146E 04	3.4279E 00	40808E 03	3.6458E 00	8.3359E 01	3.4993E 00	1.7717E-01	5.6832E 02	1.0707E 01	6.8812E 01
14	3.0188E 04	3.4798E 00	40808E 03	3.7368E 00	8.6159E 01	1.8922E 01	2.9651E-02	1.1047E 03	9.4559E 00	1.2161E 02

SUM OF SQUARES OF DEVIATIONS = 8.1458E-02
 STANDARD DEVIATION = 1.4645E-02

BAND NUMBER	BAND AREA	BAND AREA ERROR	OSCILLATOR STRENGTH	BAND SPACING			
				BAND NUMBER	ANGSTROMS	WAVENUMBER	ELECTRON VOLTS
1	1.0602E 02	3.4897E 00	1.4406E-07				
2	3.8613E 02	1.4885E 01	1.8876E-06				
3	8.7688E 02	9.1358E 01	3.7949E-06	1-2	1.7016E 02	7.4698E 02	9.2894E-02
4	1.8218E 03	1.2117E 02	7.3978E-06	2-3	1.5828E 02	7.1881E 02	9.9208E-02
5	3.7813E 03	9.7543E 01	6.4200E-05	3-4	1.3557E 02	6.7861E 02	8.3858E-02
6	5.2158E 03	1.1444E 02	2.2581E-05	4-5	1.2847E 02	6.7288E 02	8.4017E-02
7	4.4435E 03	1.5344E 02	2.0186E-05	5-6	1.2672E 02	7.0557E 02	8.7462E-02
8	3.5811E 03	1.9277E 02	1.8380E-05	6-7	1.1870E 02	7.0808E 02	8.7773E-02
9	1.8888E 03	1.7474E 02	8.4281E-06	7-8	1.1499E 02	7.0741E 02	8.7716E-02
10	1.8988E 03	1.0597E 02	8.4553E-06	8-9	1.0838E 02	7.2511E 02	8.8683E-02
11	1.6018E 03	7.6242E 01	8.9358E-06	9-10	1.0829E 02	7.4748E 02	9.5493E-02
12	2.5899E 03	1.8884E 02	1.1128E-05	10-11	9.3883E 01	7.2088E 02	8.9338E-02
13	2.1319E 03	1.1436E 02	9.1464E-06	11-12	1.0838E 02	8.4817E 02	1.0098E-01
14	2.2218E 03	1.9362E 02	9.4347E-05	12-13	7.4044E 01	6.2831E 02	7.7518E-02
15				13-14	1.1044E 02	9.7768E 02	1.2182E-01

*(UO₂) = 0.00915 M; H⁺ = 0.014 M; μ = 3.00 (ionic strength); temperature = 25.0°C; cell optical path length = 10,000 cm.

***Liter/mole-(cm)².

Fig. 11.4. Parameters for the Nonlinear Least-Squares Computer Resolution of the Absorption Spectrum of UO₂²⁺ in Perchlorate Media.

begin to converge. Then, successive iterations will result in more nearly correct parameters, until the preset least-squares convergence criteria are met. The resolved bands then permit one to study various parameters of individual transitions without interference from overlapping bands.

A recently written spectral synthesis code, SPECSYN (part of program MRØCØS), also facilitates the deduction of the initial input band parameters. This program *synthesizes* a spectrum, over any given range, from one's *estimates* of the individual band parameters of an experimental (or theoretical) spectrum and a spectral band model chosen (Sect. 11.4.2). It tabulates the data and then plots the individual bands and resulting synthesized spectrum on the CALCOMP plotter; then, if desired, it plots the observed spectrum for comparison on the same graph. The program uses the same input parameter and observation-tape format used by the nonlinear least-squares spectral resolution program. Any plotting interval (either on a cm^{-1} or angstrom basis) can be used. This SPECSYN mode of operation helps one to arrive more quickly at acceptable input-parameter estimates for the least-squares matrix program than do trial and error procedures.

A small part of the tabulated output for the particular case of UO_2^{2+} under consideration from program MRØCØS is shown in Fig. 11.4. This gives the resolved band positions (represented in various energy units), intensities, and half-band widths for all 14 bands at this temperature, with the associated statistical errors for each parameter calculated from the nonlinear least-squares analysis of the spectrum. The table is shown in two parts, with positions and half-band widths on a wavelength and wavenumber basis and with the intensity parameter (height) on a molar absorptivity basis for both cases. The complete format of data output from MRØCØS can be obtained with more data than that shown here, including detailed data for the iterative nonlinear least-squares fitting and other relevant calculations. A discussion of the operational procedures involved in MRØCØS is beyond the scope of a progress report.

Spectral Band Model and Profile Studies

Functions Useful for Representing Spectral Bands. – The literature shows that some substances

in some spectral regions (e.g., the ultraviolet-visible) conform more nearly to Gaussian character, while other substances in other regions (e.g., the infrared) are more nearly of a Lorentz-function shape; however, most bands do not fit either type precisely. Consideration has been given to the most appropriate function for representing the shape of a single spectral band and to what factors contribute to the broadening of the "line" into a band in the condensed systems that liquid represents.

Computer Programs. – Work with the Voigt function led us to combine the two functions (G and L) in a manner such that the fraction of Gaussian and Lorentzian character of a band can vary from 0 to 1. This fraction is an independently variable parameter in the nonlinear least-squares procedures, in addition to the height, width, and position of the individual bands that comprise the observed summation curve. To illustrate the difference in the character of an absorption spectral band using a Gaussian, a Lorentzian, and the 50-50 G-L combination function that we have derived, Fig. 11.5 shows a band of identical parameters of width, height, and position, but with a change of model. The pronounced broadening of the "wings" may be noted as one adds Lorentzian character, as opposed to the rapid decrease of the Gaussian. The combined function has been programmed and incorporated into MRØCØS. This function, the Gauss-Lorentz combination function, is in its effect very similar to the Voigt function. However, it is in a form such that it does not require one to choose a fixed G/L ratio for a band fitting but will permit the complete variance of the G/L ratio as an independently variable parameter in the nonlinear least-squares calculations.

In some studies of UO_2^{2+} spectra complexed by nitrate, where one would perhaps expect to observe Lorentz-type broadening as a result of solution and complexation interactions, the combination G-L function used for the resolution has given a slightly smaller sum of squares (with the G-L fraction parameter freely varying for all bands) in the resolution than the pure Gaussian model. Lorentz-type broadening character was added predominantly to certain of the bands. It appears that this function will be very useful for studying complexation and many different types of broadened spectral bands.

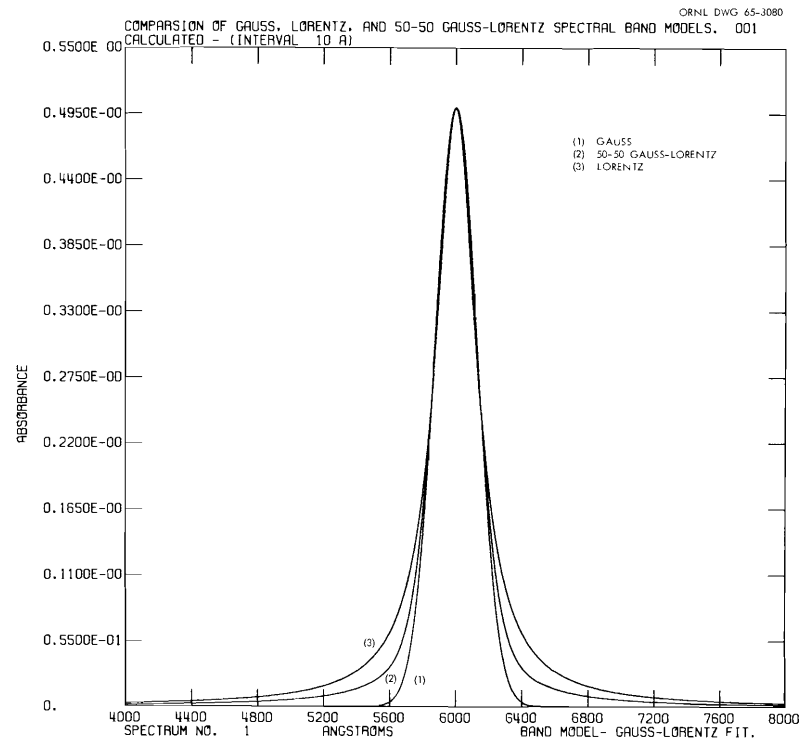
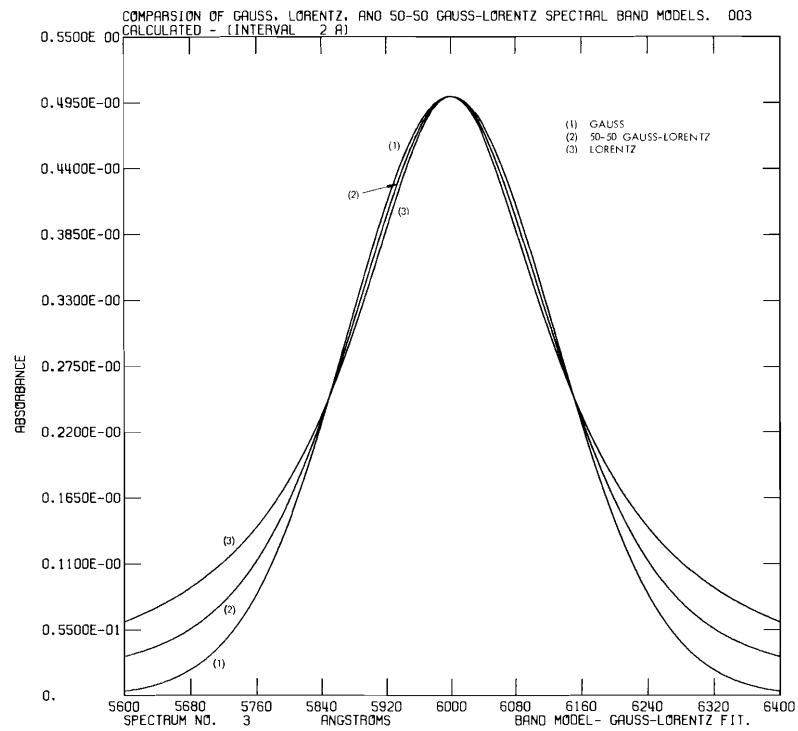


Fig. 11.5. Spectral Bands Illustrating the Difference in Band Contours when Generated with a Gaussian, a Lorentzian, or a Gaussian-Lorentzian (50-50%) Combination Function. Identical band parameters of position, intensity, and width generated with computer program MRØCØS in the SPECSYN mode. The broadening and very gradual intensity decrease in the "wings" and the somewhat more narrow top caused by the addition of Lorentzian character may be noted.

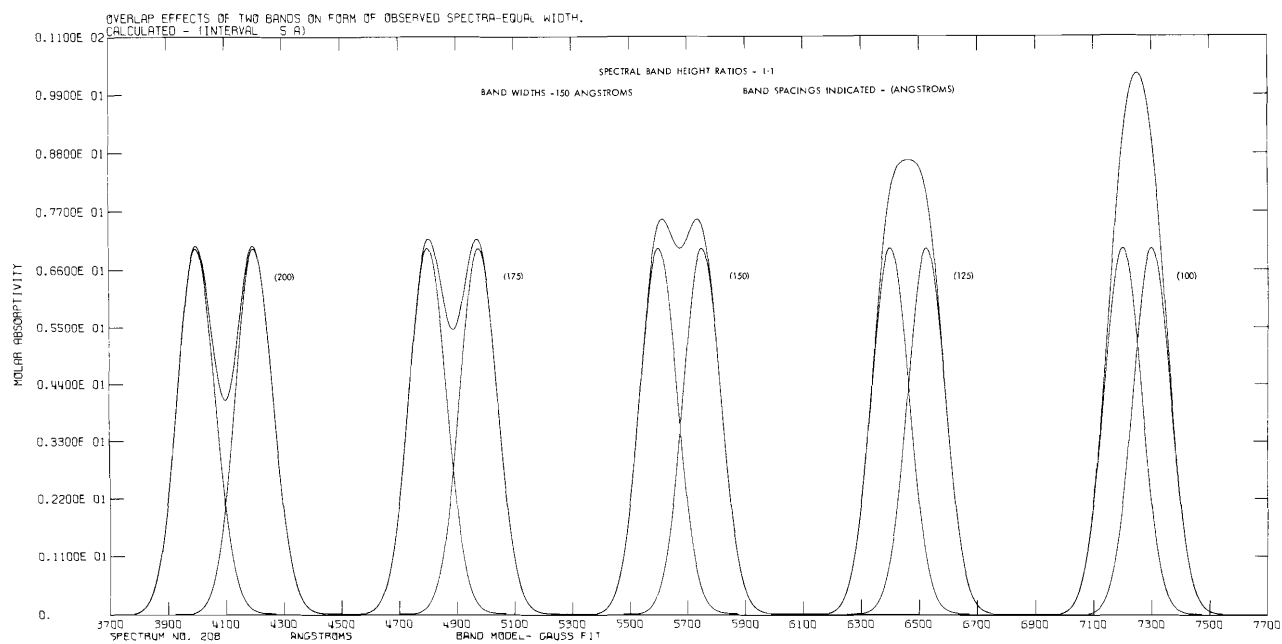
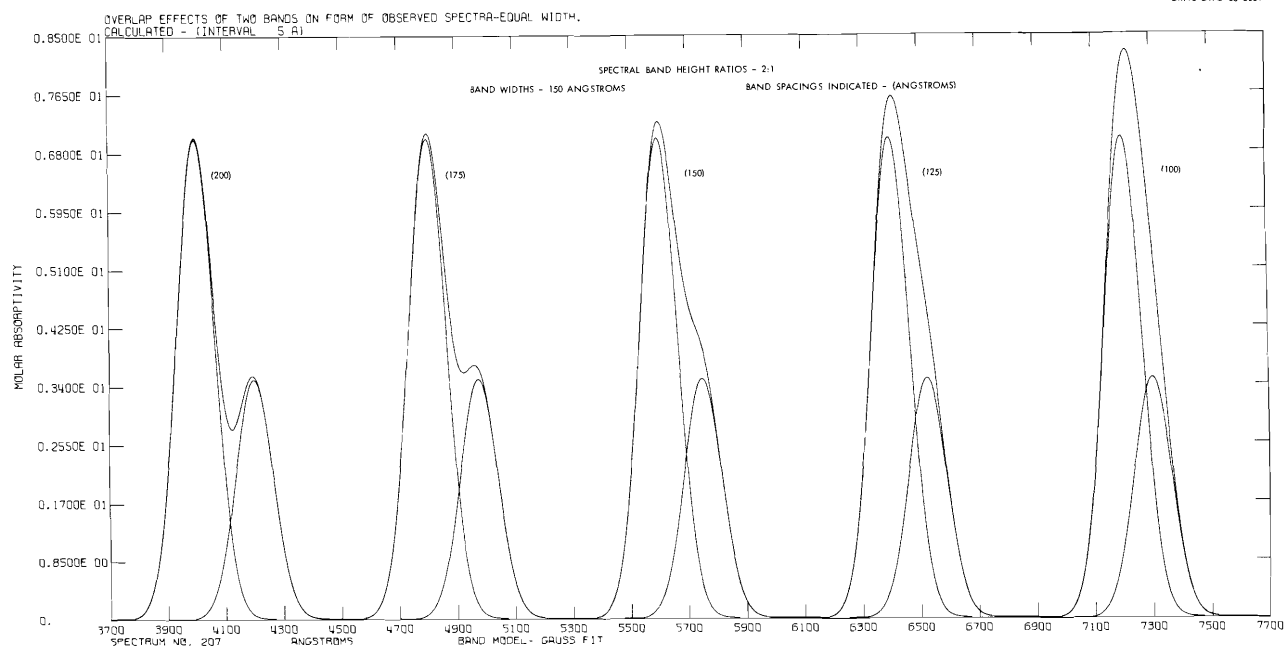


Fig. 11.6. Spectral Bands Illustrating the Effects Caused by Band Overlap. Upper set - two bands of equal width and an intensity ratio of 2:1; lower set - equal width and height. The summed spectrum and the band contours observed are caused by progressively closer spacings and were generated with computer program MRØØS in the SPECSYN mode. The progressively more undefined character and incorrect position indications of one or both of the bands with decreasing spacing may be noted.

Spectral Band Overlap Studies

In work involving measurements on absorption spectra, it is frequently difficult to detect the presence and/or position of a band or bands of relatively low intensity, overlapped by bands of higher intensity or larger width, and of equal-intensity bands at close spacings. For spectral bands located well apart in a spectrum, the positions along the energy axis can usually be located with reasonable precision. The more severe the overlapping, the more the shape characteristics of one or more of the bands become obscured.

It is particularly difficult to assign a precise position to a band of relatively low intensity overlapped by a larger band because it appears in the obscured spectrum as a shoulder or inflection or even as an asymmetry of the larger band. Almost invariably, the overlapping produces "apparent" changes in the wavelengths of maximum absorption that are observed. In tabular presentations of spectral data from nonresolved spectra this is one of the major sources of error.

To aid in developing facility for deducing approximate values for the parameters of the underlying band structure in complex overlapped spectra, we are using program MRØCØS (operating in the SPECSYN mode; see Sect. 11.4.1) to generate overlapped spectra of two or more bands of various height, width, and degree of separation. A library of such plots which can be uniformly correlated is being developed and will be made available for general use.

Figure 11.6 shows part of the results of two such calculations of overlap effects for two bands of equal width moved progressively closer together – in one case of equal intensity and then for a 2:1 intensity ratio. Marked variations in the shape of the summed curves (which would correspond to a portion of an observed or experimental spectrum) may be seen, together with displacement of the maxima of the "point of inflection" of the composite curve from the maxima of the component curves. Many such forms of the summed curves can be obtained – forms that would not have been expected a priori.

Convolute Smoothing of Digitized Spectral Data

The output of digitized spectral data from a spectrophotometer system gives absorption or intensity data as a function of wavelength. At intermediate to high absorbances, and at low light levels, the "noise" associated with the output from the spectrophotometer may be significant, particularly when a multiplier phototube or detector is used. With a strip-chart recording, the noise is usually manually averaged out before the data is hand reduced. However, for a digital system, any given absorbance point punched out on a card or tape may contain a contribution from a noise pulse. This noise contribution must be removed before the data can be further analyzed by various types of mathematical techniques or other procedures utilizing digital computation.

A set of computer programs and subroutines have been written^{10,11} for the CDC 1604-A computer to smooth spectral data. A least-squares convolution smoothing technique is employed. This technique and the gross general features of the program were briefly described previously.^{2,5} The programs are very versatile in that all probable combinations of experimental spectral data, optical cell-balance data, and conical-screen attenuator data can be handled and smoothed. Several different programs have been written to handle various combinations of spectral data, cell-balance data, and attenuator-suppression data.

The data output may be obtained in various forms under program options. This includes: tabulated data on the off-line printer, CALCOMP curve plotting of the rough and/or smoothed spectral data, output as a smoothed card deck, and the preparation of a binary-coded-decimal (BCD) magnetic tape. The smoothed output data are compatible with the input format requirements of the nonlinear least-squares program MRØCØS.

¹⁰In collaboration with T. G. Kabele, co-op student from Northwestern University, January–March 1963; part-time, summer, 1963.

¹¹In collaboration with R. P. Rannie of the Mathematics Division of ORNL.

12. Mechanisms of Separations Processes

The thermodynamics of solvent extraction by tributyl phosphate (TBP)–hydrocarbon-diluent solutions are being studied by means of vapor pressure measurements and analytical partition data. The multicomponent systems under study include the three-component system containing uranyl nitrate, nitric acid, and water, and the three- and four-component systems containing TBP, hydrocarbon diluent, water, and uranyl nitrate or nitric acid.

12.1 ACTIVITIES OF THE THREE COMPONENTS IN THE SYSTEM: WATER–NITRIC ACID–URANYL NITRATE HEXAHYDRATE AT 25°C

Partial pressures of water and nitric acid over solutions containing water, nitric acid, and uranyl nitrate hexahydrate (UNH) were measured at 25°C by use of the vapor transpiration technique for solutions 0 to 2.3 *m* in UNH and 1 to 14 *m* in HNO₃. These data were analyzed in terms of activities in the two-component systems water–nitric acid and water–uranyl nitrate hexahydrate by using an integral form of the Gibbs-Duhem equation. A four-parameter functional representation describing the variation of water and nitric acid activities with acid and UNH concentrations was obtained. The same parameters are contained in an equation (obtained by use of cross-differentiation) that describes the variation of the UNH activity coefficient with acid and UNH concentrations.

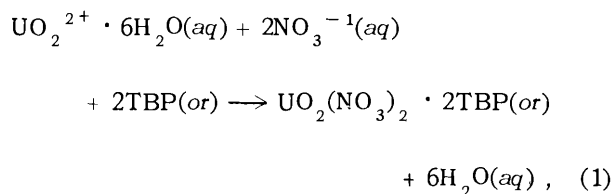
Standard deviations of calculated water and nitric acid activities were about ±10%. In spite of these uncertainties, this work should be of considerable use in analyzing solvent extraction data and may be useful in future studies of the interactions between the two solutes of a ternary system.

12.2 ACTIVITIES OF TRIBUTYL PHOSPHATE IN MIXTURES CONTAINING TRIBUTYL PHOSPHATE, URANYL NITRATE, AND WATER

The distribution of uranyl nitrate (UN) and water between 100% TBP and an aqueous phase containing uranyl nitrate hexahydrate (UNH) was determined by chemical analyses of both phases after equilibration at room temperature (25 ± 2°C). These data were used as a basis for calculating the activities of TBP in this three-component two-phase system. The calculations are based on the Gibbs-Duhem equation, on the activities of H₂O and UNH in the two-component aqueous solutions, and on the fact that TBP is only very slightly soluble in aqueous UN solutions (less than 0.0016 mole/liter).

Rational activities of TBP were calculated from data obtained by graphical integration of the Gibbs-Duhem equation for aqueous UN concentrations (equilibrium) ranging from 0.04 to 1.75 moles/liter. These activities are listed in Table 12.1.

The equilibrium involved in the reaction between TBP and UNH is described by the reaction



with a thermodynamic equilibrium constant (molar scale) as shown in Eq. (2):

$$K_{2/y_{\text{U2T}}}^c = \frac{{}^{\text{or}}C_{\text{U2T}} [\text{H}_2\text{O}]^6}{[\text{UNH}] [\text{TBP}]^2}. \quad (2)$$

Square brackets indicate activities; ${}^{\text{or}}C_{\text{U2T}}$ is the molar concentration of the complex $\text{UO}_2(\text{NO}_3)_2$.

Table 12.1. Rational Activities of TBP in TBP- $\text{UO}_2(\text{NO}_3)_2\text{-H}_2\text{O}$
Solutions at $25 \pm 2^\circ\text{C}$

Aqueous $\text{UO}_2(\text{NO}_3)_2$ Concentration (<i>m</i>)	TBP Activity	Aqueous $\text{UO}_2(\text{NO}_3)_2$ Concentration (<i>m</i>)	TBP Activity
0	0.515		
0.05	0.504	1.05	0.0402
0.10	0.467	1.10	0.0362
0.15	0.413	1.15	0.0326
0.20	0.357	1.20	0.0294
0.25	0.306	1.25	0.0266
0.30	0.262	1.30	0.0241
0.35	0.226	1.35	0.0218
0.40	0.195	1.40	0.0198
0.45	0.170	1.45	0.0180
0.50	0.148	1.50	0.0164
0.55	0.130	1.55	0.0149
0.60	0.114	1.60	0.0136
0.65	0.101	1.65	0.0124
0.70	0.0890	1.70	0.0114
0.75	0.0790	1.75	0.0104
0.80	0.0702	1.80	0.00959
0.85	0.0626	1.85	0.00881
0.90	0.0559	1.90	0.00812
0.95	0.0500	1.95	0.00748
1.00	0.0448	2.00	0.00691

2TBP in the organic phase; and $y_{\text{U}_2\text{T}}$ is its molar activity coefficient. Activities of UNH and H_2O were calculated from equational representations of the activity coefficients of UNH and the activities of water published by Davis and others.¹ Activities of TBP were interpolated from the data of Table 12.1, and the concentration of the complex ${}^{\text{or}}\text{C}_{\text{U}_2\text{T}}$ was assumed to be equal to the concentration of UN in the organic phase. It was observed that the right side of Eq. (2) was an exponential function of the con-

centration ratio ${}^{\text{or}}\text{C}_{\text{UN}}/{}^{\text{or}}\text{C}_{\text{TBP}}$ (Fig. 12.1), or

$$\ln (K_2^c/y_{\text{U}_2\text{T}}) = A + B \frac{{}^{\text{or}}\text{C}_{\text{UN}}}{{}^{\text{or}}\text{C}_{\text{TBP}}}, \quad (3)$$

where

$$\exp A = K_2^c/y_{\text{U}_2\text{T}}^w \quad (4)$$

and

$$\exp \left(B \frac{{}^{\text{or}}\text{C}_{\text{UN}}}{{}^{\text{or}}\text{C}_{\text{TBP}}} \right) = y_{\text{U}_2\text{T}}^w/y_{\text{U}_2\text{T}} \cdot \quad (5)$$

¹W. Davis, Jr. *et al.*, *J. Phys. Chem.* **69** (July 1965).

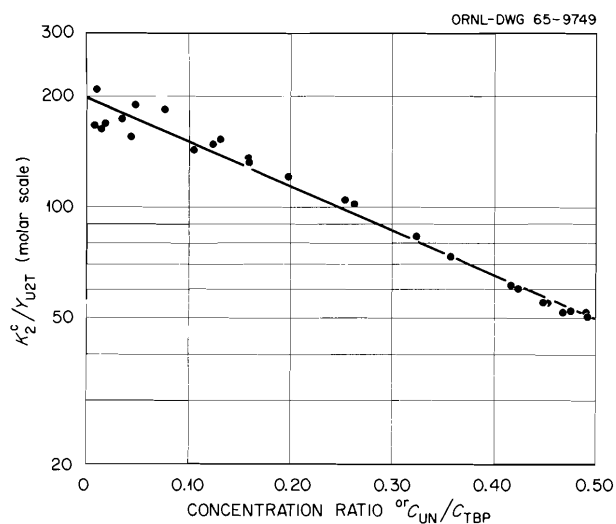


Fig. 12.1. The Quotient K_2^c/y_{U2T} as a Function of Organic-Phase Loading.

The superscript w indicates the activity coefficient of the complex $UN \cdot 2TBP$ at infinite dilution in water-saturated TBP. Values of K_2^c/y_{U2T}^w and B , found by least-squares analyses, are 198.7 and -2.771 , with standard deviations of 4.7 (2.4%) and 0.083 (3.0%) respectively.

Partial molar volumes of H_2O , UN , and TBP were determined from organic-phase density and concentration data. The partial molar volumes, in milliliters per mole, were calculated as 17.3, 92.6, and 273.9, with estimated standard deviations of 0.2, 0.4, and 0.5 respectively. The data indicate that these partial molar quantities are independent of concentration changes for organic (equilibrium) uranyl nitrate concentrations ranging from 0.038 to 1.53 moles/liter. The partial molar volume of the complex $UO_2(NO_3)_2 \cdot 2TBP$, calculated from the above data, is 640.6 ml/mole. The free energy change for the partition reaction [Eq. (1)] is estimated to be -7.47 kcal/mole.

An empirical equation representing the densities of organic phases (equilibrium) containing uranyl nitrate, water, and TBP was obtained by fitting measured density data to an equation with molar concentrations of UN and H_2O as independent variables [Eq. (6)]:

$${}^or\rho_i = \left[0.9724(1000 - 17.34 {}^orC_{H_2O} - 92.51 {}^orC_{UN}) + 18 {}^orC_{H_2O} + 394 {}^orC_{UN} \right] / 1000. \quad (6)$$

This equation reproduced measured organic-phase densities, with a standard deviation of 1.7 mg/ml, over the UN concentration range 0 to 1.53 M (0 to 1.9 m).

12.3 COMPUTER RESOLUTION OF SPECTROPHOTOMETRIC DATA ON URANYL NITRATE-NITRIC ACID-WATER SYSTEMS

A generalized nonlinear least-squares computer program for the resolution of spectrophotometric data has been written and tested. The mathematical basis of the program is the Gauss-Newton method, modified to control parameter changes by minimizing the sums of squares of the residuals as a function of the fractional change allowed in the correction vector. This program was able to resolve spectrophotometric data obtained for uranyl nitrate-nitric acid solutions 0.1 to 1.4 M in uranium and 0.01 to 2 M in HNO_3 into the contributions of 13 Gaussian bands in the wavelength region 3400 to 5000 \AA .

At higher acid concentrations (up to 8 M) the bands in certain regions of the spectrum become indistinct, and the modified Gauss-Newton program is no longer able to converge to the minimum variance in absorbance. A SHARE program for least-squares estimation of nonlinear parameters was obtained and modified for use on the CDC 1604-A computer. This program performs an optimum interpolation between the Gauss-Newton method and the gradient method (steepest descent), the interpolation being based upon the maximum neighborhood in which the truncated Taylor series gives an adequate representation of the nonlinear model.² With this program, spectral data for 0.1 M uranium and 0.01 to 8 M nitric acid have been resolved. It is anticipated that the remainder of the spectral data (0.25 to 1.4 M uranium and 2 to 8 M nitric acid) will also be resolved with the aid of this computer program.

Figure 12.2 gives some preliminary information on the variation in band area as a function of nitric acid concentration at constant uranium concentration (0.1 M). It is anticipated that this type of data will yield information on complexation of the uranyl ion by nitrate in aqueous nitric acid.

²D. W. Marquardt, *J. Soc. Ind. Appl. Math.* 11, 431 (1963).

ORNL-DWG 65-9750

BAND NO.	WAVELENGTH OF MAX. ABSORB. (0.1 M U; 0.006 M HNO ₃) ANGSTROMS
2	4692
3	4539
4	4394
5	4269
6	4146
7	4026
8	3917
9	3810
10	3701
11	3602

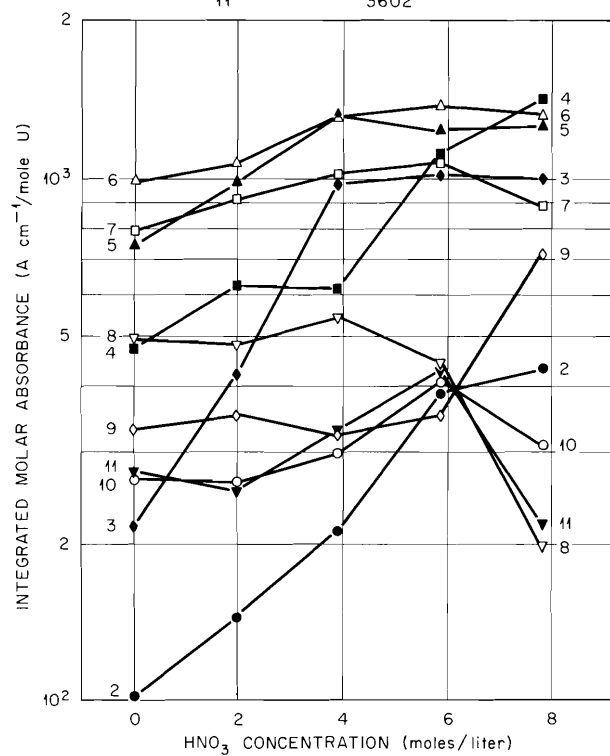


Fig. 12.2. Variation in Resolved Spectral Band Areas of 0.1 M Uranyl Nitrate as a Function of Nitric Acid Concentration.

13. Chemical Engineering Research

Chemical engineering research is an aggregate of studies which, while generally pertinent to the Division's applied programs, are fundamental in nature or pursue attractive new ideas. The fundamental studies usually arise from interesting effects noted during work on programs with more specific commitments. On the other hand, work begun on new ideas frequently becomes part of applied programs as the work matures.

The work reported this year includes: the operation of the stacked-clone contactor with a variety of solvent systems (including 100% TBP and hexone) to show a wide range of applicability; further experimental work with the effect of radiation on the coalescence of liquid droplets, which clarifies the significance of the most important variables and provides a basis for an explanation; the adoption of a laser light source for the detection of aerosol particles in a gas stream by light scattering and a technique for manipulating the pulse from the light detector to give a more meaningful signal; and a comprehensive treatment of all the available data on flooding of solvent extraction pulsed columns to test over 200 proposed correlating equations.

13.1 THE STACKED-CLONE CONTACTOR

The stacked-clone contactor, a high-speed solvent extraction device, was developed for application to radiochemical processing and features high flow capacities, high extraction efficiencies, low contact time per stage, and low solution holdup. It consists of a cascade of axially aligned liquid cyclones, each of which acts as a single countercurrent extraction stage. Counterflow in each stage is created by the induced underflow effect. The development of the functioning components with an identification of an optimum configuration was reported in the

last annual progress report.¹ The development has proceeded to the use of a seven-stage stainless steel experimental model to explore the usable range of system properties and operating conditions.

Operability of the device at flow ratios (A/O) as high as 50 was demonstrated by extracting uranyl nitrate from 3 M NaNO₃ with 18% TBP in Amsco, with performance equivalent to that at a flow ratio of 3. The entrainment of organic in the aqueous raffinate was considered low in that it comprised less than 0.5% of this stream when four polishing clones were used. However, at a flow ratio of 15, this entrainment amounted to 5% of the organic solvent fed. Operation at extreme flow ratios also presented a problem in interface control because the rate of response in one direction was so different from the rate of response in the other. At high A/O ratios, interface control was nicely effected by using the clone adjacent to the disengaging chamber exclusively for interface control, introducing the aqueous feed into the second clone rather than into the disengaging chamber. A special, smaller clone worked well in this service.

Tests of several minor equipment variations were tried, but they served only to strengthen confidence in the Mark X design (Fig. 13.1). Tests proved that the performance of the newer stainless steel model is equivalent to that of the previous plastic experimental contactor.

Studies made at progressively higher TBP concentrations (1 M NaNO₃ salting) from 5 through 40% showed similar throughputs of about 4 liters/min (A/O = 3) at stage efficiencies of about 65%. For pure TBP, the throughput dropped to 1.6 liters/min, and extraction of uranium was complete.

¹Chem. Technol. Div. Ann. Progr. Rept. May 31, 1964, ORNL-3627, pp. 235-39.

ORNL-DWG 64-8277

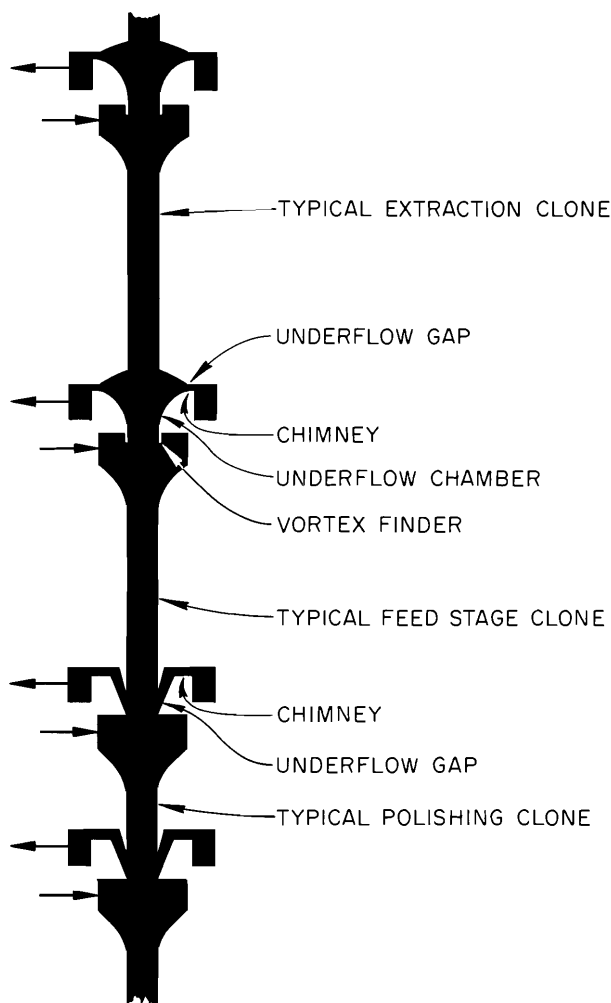


Fig. 13.1. Clone Shapes, Underflow Chambers, and Other Functioning Components of the Stacked-Clone Contactor.

A deviation from the practice of operating at an extraction factor near unity to facilitate stage-efficiency calculations for both extraction and stripping operation was made for the purpose of demonstrating the complete solute-recovery capabilities of the contactor. With 30 and 60% TBP and appropriate flow ratios to give extraction factors higher than 5, uranium removal from a feed containing 18 to 20 g of uranium per liter was greater than 99.9%.

The Purex flowsheet was successfully demonstrated in the unit, although the throughput was

somewhat low, being 1.6 liters/min for extraction ($A/O = 0.45$) and 2.2 liters/min for stripping ($A/O = 1.88$). These flows represent uranium capacities of 140 and 95 kg/day respectively.

The most important physical properties of the solutions affecting flow capacity appear to be interfacial tension, viscosity of the aqueous phase, and the density difference between phases. Data in Table 13.1 reflect the importance of these properties for several extraction systems. Tests with aqueous phases consisting of 1 M NaNO_3 , 0.8 M $\text{Al}(\text{NO}_3)_3$ -0.5 M HNO_3 , or 1.25 M Na_2CO_3 , with a 38% TBP-Amsco organic phase, exhibit significant trends. The flow capacity of a hexone-acetic acid system was unusually high, considering the physical properties involved, being 7 liters/min ($A/O = 3$). This system has exhibited high flow capacities in other solvent extraction contactors and may point out the existence of some other intrinsic property necessary to describe flooding behavior.

In spite of the striking behavior of the hexone system, a first attempt to correlate flow capacities with physical properties is shown in Fig. 13.2. A dimensionless correlating parameter based on previous solvent extraction work was employed.² As additional systems are tested, it is hoped that a better correlation will evolve, preferably one based on fundamental physical laws upon which the stacked-clone contactor operates.

13.2 EFFECT OF IONIZING RADIATION ON COALESCENCE IN LIQUID-LIQUID SYSTEMS

Work on the effect of ionizing radiation on the coalescence of drops on a plane interface was completed, and a mechanism which explains the data was postulated.

The data are presented in Table 13.2. In the absence of radiation, average drop lifetimes on a plane interface of the same phase show the expected variations with temperature, liquid properties, and drop diameter. The lifetimes are controlled by film drainage and are somewhat longer in these experiments than those reported in the literature.

²J. D. Thornton, "Liquid-liquid Extraction Part XIII: The Effect of Pulse Wave-Form and Plate Geometry on the Performance and Throughput of a Pulsed Column," *Trans. Inst. Chem. Engrs.* 35, 316 (1957).

Table 13.1. Effect of Solution Physical Properties on the Flow Capacity of the Stacked-Clone Contactor at 40°C

Aqueous Phase	Organic Phase	$\Delta\rho$, Density Difference (g/cm)	μ_c , Aqueous-Phase Viscosity (centipoises)	γ , Interfacial Tension (dynes/cm)	Flow Capacity (liters/min)	
					A/O = 3	A/O = 10
1 M NaNO ₃	5% TBP-Amsco	0.285	0.73	18.5	3.95	4.97
2 M NaNO ₃	5% TBP-Amsco	0.329	0.80	18.6	4.27	4.84
1 M NaNO ₃	18% TBP-Amsco	0.255	0.73	13.5	3.08	4.42
2 M NaNO ₃	18% TBP-Amsco	0.299	0.80	13.5	3.43	5.33
3 M NaNO ₃	18% TBP-Amsco	0.361	0.92	13.6	4.00	5.50
1 M NaNO ₃	30% TBP-Amsco	0.228	0.73	11.1	3.64	5.03
1 M NaNO ₃	40% TBP-Amsco	0.207	0.73	10.0	3.52	4.92
3.0 M NaNO ₃	53% TBP-Amsco	0.315	0.99	10.8	3.64	5.03
3.6 M NaNO ₃	61% TBP-Amsco	0.298	0.99	10.5	3.27	4.33
2 M NaNO ₃	100% TBP-Amsco	0.132	0.80	8.6	1.71	2.38
3.6 M NaNO ₃	100% TBP-Amsco	0.225	0.99	9.6	1.84	2.55
0.8 M Al(NO ₃) ₃ , 0.5 M HNO ₃	38% TBP-Amsco	0.305	1.24	8.9	1.86	
1.25 M Na ₂ CO ₃	38% TBP-Amsco	0.262	1.31	6.7	1.43	
2 M HNO ₃	30% TBP-Amsco	0.249	0.76	8.6	2.53	3.19
0.01 M HNO ₃	30% TBP-Amsco	0.181	0.68	9.2	2.23	2.75
0.005 M CH ₃ COOH	Hexone	0.205	0.66	7.4	6.96	a

^aAt 25°C.

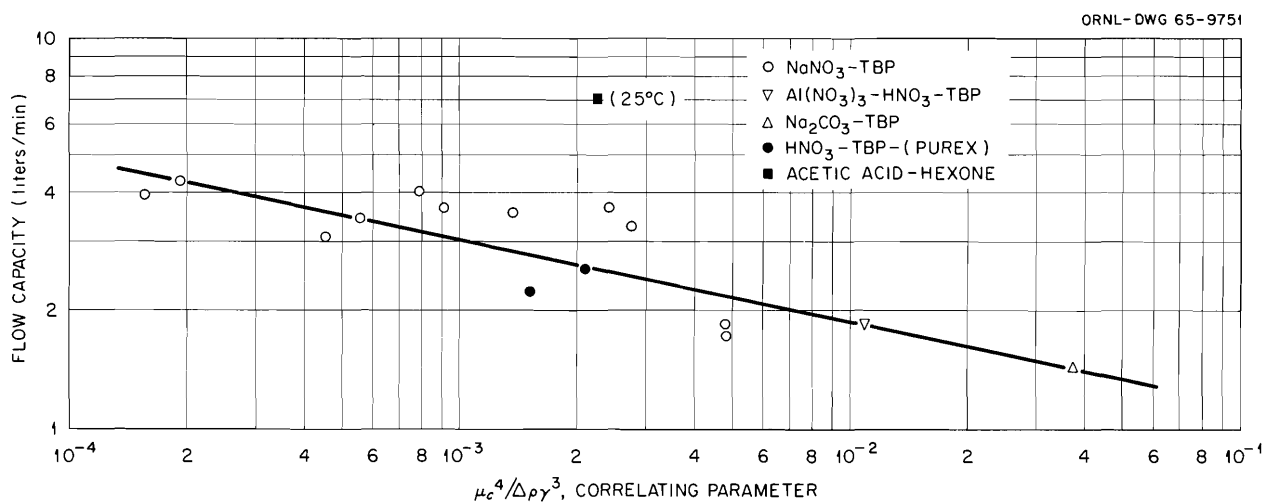


Fig. 13.2. Initial Flow-Capacity Correlation. Temperature, 40°C; Mark X contactor.

Table 13.2. Summary of Coalescence Runs

Series	System	Temperature (°C)	Pressure	D, Diameter (cm)	Average Lifetime of Drop (sec)	ϕ, Flux		Probability
						ϕ, Flux	ϕD ² σC	
						×10 ⁶	×10 ⁻²⁴	
1	Water/benzene	25	1 atm	0.487	14.7			
				0.512	16.5			
				0.552	24			
				0.643	33	200 ^a	900 ^b	0.0
2	0.3 M UNH/heptane	25	1 atm	0.416	4.5	2.0	6.02	1.0
						1.0	3.01	0.66
						0.3	0.905	0.13
3	0.2 M LiCl/heptane	25	1 atm	0.388	3.8	2.0	5.70	0.2
						0.8	2.30	0.16
						0.4	1.148	0
4	0.3 M UNH/hexane	25	1 atm	0.490	5.2	1.30	5.43	1.00
			6-in. vacuum		4.7	1.22	5.09	0.92
			11-in. vacuum		5.4	1.15	4.80	0.78
			15-in. vacuum		4.9	1.11	4.63	0.78
5	0.3 M UNH/hexane	10	1 atm	0.499	6.4	0.90	3.90	0.83
		25			5.2	1.30	5.43	1.00
		40			3.7	0.86	3.49	0.70
		50			3.4	0.81	3.26	0.59
6	0.3 M UNH/hexane	25	1 atm	0.595	10.4	0.74	4.56	0.74
				0.532	6.65	0.69	3.40	0.69
				0.490	5.2	1.30	5.43	1.30
				0.454	4.0	0.59	2.12	0.59
7	0.5 M LiNO ₃ /hexane	25	1 atm	0.490	18	1.08	11.68	0.0
			11-in. vacuum		20	1.04	11.23	0.0
7A	0.5 M LiNO ₃ (high fired)/hexane	25	1 atm	0.522	7.35	1.01	12.39	0.22
			12-in. vacuum		7.75	0.88	10.8	0.17
8	0.3 M UNH/hexane	25	1 atm	0.490	5.2	1.30	5.43	1.00
	0.3 M UNH/heptane			0.416	4.5	2.0	6.02	1.00
	0.3 M UNH decane			0.499	6.6	0.87	0.378	0.66
9	0.3 M UNH-Na Lauryl Sulfate/hexane	25	1 atm	~0.15	45	1.58	0.619	0.0
	0.3 M UNH/hexane-ethomeen T			~0.21	27	1.43	1.21	0.0

^aFast neutrons.

^bRecoil protons.

Of particular interest in these experiments are the results of irradiating the apparatus with neutrons during an experiment with the aqueous phase either 0.3 M in ^{235}U or 0.2 to 0.5 M in ^6Li . As had been reported last year,³ coalescence on impact occurs with some probability during irradiation. Additional experiments show this probability to increase linearly with the product of neutron flux, macroscopic cross section of the target nuclide, and square of the diameter of the drop (Fig. 13.3). This product, with concentration in moles per liter and cross section in barns, turns out to be very nearly equal numerically to the number of particle tracks originating within $10\ \mu$ of the front hemisphere of the drop, every second.

³Chem. Technol. Div. Ann. Progr. Rept. May 31, 1964, ORNL-3627, pp.239-41.

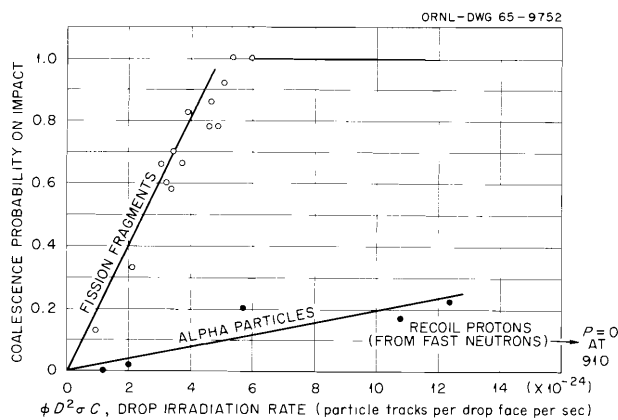


Fig. 13.3. Coalescence Probability on Impact vs Drop Irradiation Rate.

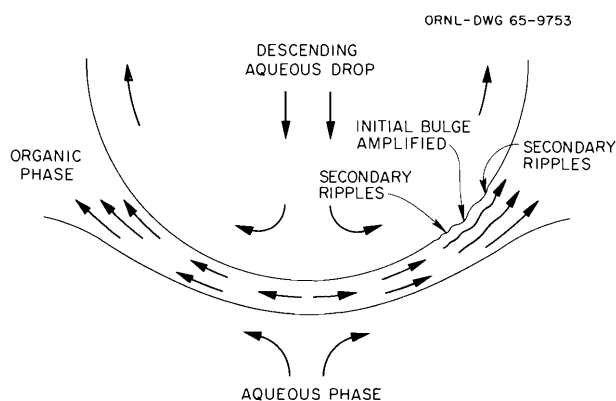


Fig. 13.4. Schematic Representation of Radiation-Destabilized Drop During Impact with Plane Interface.

It appears that about 5 fission tracks/sec or about 50 alpha tracks/sec will ensure coalescence on impact. As was also reported last year and subsequently verified, raising the temperature, going to more (or less) volatile solvents, and pulling a vacuum on the system all have no detectable effect on the probability of coalescence. These negative results have been taken as evidence that nucleation of a vapor bubble at the interface is not the process that destabilizes the drop and initiates coalescence.

The proposed mechanism is as follows: (1) a fission fragment (or alpha particle) is generated so its track approaches or crosses the interface at a small angle, this interface being the one upon which the drop rests. (2) Many of the free radicals left in the wake of the fission fragment (or alpha particle) diffuse to or across the interface before recombining. (3) In crossing the interface, about half will leave a hydroxyl group attached to a hydrocarbon molecule in the other phase. (4) This molecule is surface active, will move into the interface, and will cause a marked decrease in interfacial tension over a small area. This area will expand and diffuse away after a few seconds, but, while in existence, acts as a local "weak spot" in the interface. (5) On the surface of a drop, to maintain pressure equilibrium, the local radius of curvature must decrease proportionally to the decreased local interfacial tension, producing a bulge. (6) If this bulge is properly situated on the leading face of a drop, the flow of the continuous phase over it at impact will amplify the bulge by Bernoulli lift. (7) Ripples propagate from the bulge in the classical mechanism of Helmholtz interfacial instability, as shown schematically in Fig. 13.4. (8) This disturbance grows and provides several points at which the film can rupture and start the coalescence.

13.3 IN-LINE DETECTION OF PARTICLES IN GAS STREAMS BY SCATTERED LIGHT

The particle-size distribution and concentration of an aerosol can be determined by measuring the frequency and intensity of light reflected by individual particles in a gas stream which pass through an optically sensitive volume if the particle concentration is low enough to prevent coincidence of particles in the sensitive volume.

An aerosol spectrometer based on this principle of aerosol characterization will have application in the Gas-Cooled Reactor program, where it is desirable to be able to determine aerosol concentration and size distribution in the flowing gas coolant, and in other processes where aerosols are important.

The experimental program is directed toward the development of a detection cell usable as an in-line instrument and the development of suitable electronic components for analysis of the detection-cell signal.

Detection Cell

The main emphasis in the development of the detection cell has been on the production of a well-defined, small, intense primary light source. Two types of light sources have recently been

used in a detection cell previously described.⁴ First, a conventional 100-w tungsten-filament lamp was focused and stopped down by slits to about 0.5 mm square. This produced a beam about 0.5 mm square at the detection point. The second type of primary light used was a focused, continuous neon-helium laser operating with a hemispherical configuration in a TEM_{00} mode at about 1 mw (Fig. 13.5).

Monodispersed latex aerosols in the diametral size range 0.37 to 1.37 μ were formed by atomizing latex hydrosols and introduced into the detection cell. Measurements of the electrical signal were made from photographs of an oscilloscope attached

⁴Chem. Technol. Div. Ann. Progr. Rept. May 31, 1964, ORNL-3627, p. 242.

ORNL-DWG 65-9754

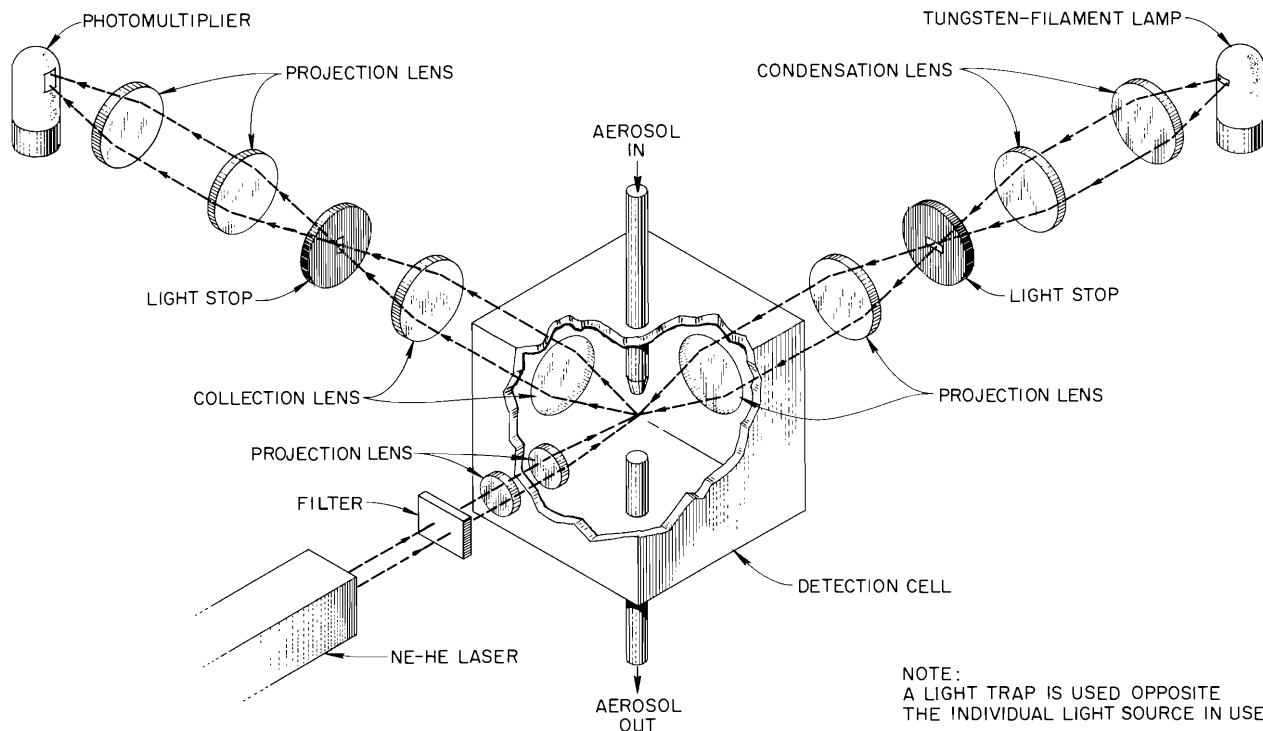


Fig. 13.5. Detection Cell Used in Experimental Program. Arranged for either a tungsten-filament lamp or a neon-helium laser.

to the preamplifier of the photomultiplier signal. The average pulse heights for the aerosols had almost a linear dependence on particle diameter, and the signal-to-noise ratio varied from 1.5 to 7.0 with the tungsten light and from 3.2 to 24.4 with the laser light (Table 13.3). The significantly higher signal-to-noise ratio for the laser was achieved by both an increase in light intensity at the detection volume and a decrease in background noise due to the characteristics of coherent light. Thus, the laser appears to be the best light source.

Analysis of Photomultiplier Signal

The electronic analyzing system will have the capability of measuring the magnitude and number of signals produced by the detection cell. The best system to date is composed of a preamplifier to give signal strength, an amplifier with both integration and differentiation to shape the signal for triggering the analyzer, a triggering device that allows the multichannel pulse-height analyzer to interrogate the signal at the proper time, and a 400-channel pulse-height analyzer for determining signal strength and distribution (Fig. 13.6).

Table 13.3. Maximum Signal Voltage from the Photomultiplier Preamplifier Measuring Scattered Light from Latex Aerosols

Average Particle Diameter (μ)	Average Maximum Signal Voltage (v)		Standard Deviation of Maximum Signal Voltage (v)		Signal-to-Noise Ratio of Average Maximum Signal Voltage	
	Laser ^a	Tungsten-Filament Lamp ^b	Laser ^a	Tungsten-Filament Lamp ^b	Laser	Tungsten-Filament Lamp
Filtered air (noise)	0.009	0.010			1.0	1.0
0.37	0.029	0.015	0.010	0.005	3.2	1.5
0.57	0.056	0.027	0.015	0.022	6.2	2.7
0.87	0.11	0.042	0.035	0.014	12.2	4.2
1.37	0.22	0.070	0.15	0.019	24.4	7.0

^a50 signals sampled for each particle size.

^b12 to 25 signals sampled for each particle size.

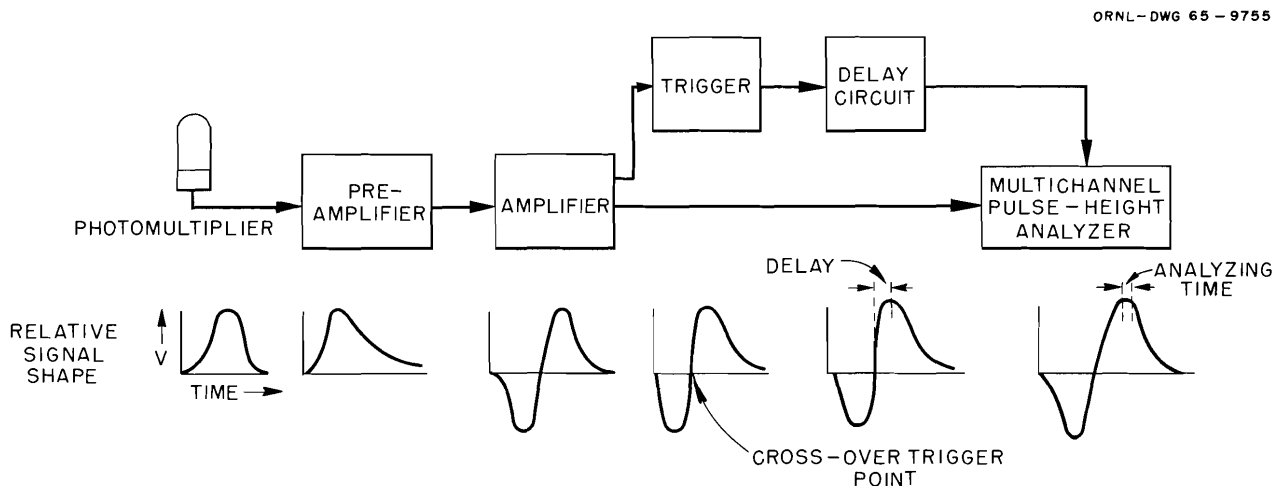


Fig. 13.6. Electronic System for Analyzing the Detector Signal.

13.4 SOLVENT EXTRACTION ENGINEERING STUDIES: CORRELATION OF PULSED-COLUMN FLOODING DATA

Although pulsed columns are widely used in radiochemical solvent extraction processes, correlations of performance with system variables have been inconsistent, diverse in form, and generally unreliable. A study has been undertaken to accumulate all the available data in the literature (2300 data points representing 23 different chemical systems) and to use these to test the various correlating equations by employing a multiple-regression analysis. More than 250 equations have been tested. The experimental data include: aqueous and organic continuous operation, with and without mass transfer occurring, in columns containing sieve-plate cartridges and nozzle-plate cartridges fabricated from either metals or plastics. The data also include runs made with "zebra"-type cartridges, where operation is aqueous continuous in portions of the column and organic continuous in other portions, and where both metal and plastic pulse plates may be in the same column. Only data involving non-sinusoidal wave pulses were omitted.

In the operating region where flooding is caused by insufficient pulsation, flow capacities can be accurately predicted from only the flow ratio and the pulsing conditions.⁵ Flooding in the emulsion region, however, is more complex. Indeed, the data are less accurate because pulsed columns may run for considerable time at capacities exceeding flooding before the phenomenon becomes obvious. Many reported flooding data are, therefore, in error on the high side. Further, the manner in which flooding occurs may vary from one chemical system to another and from one pulsed column to another. Consequently, the correlations start from attempts to explain the behavior of individual droplets and extend into the empirical technique of curve fitting.

In the development of the correlating equations, up to 13 variables were used, including the column diameter, pulse-plate spacing, hole size and free area, the pulse amplitude and frequency, solution densities and viscosities, and interfacial tension. It is possible that the inclusion of additional

properties such as interfacial viscosity would improve the correlations. The definition and measurement of such variables should be one aim of future research.

The correlating equations generally put the variables together in the form of dimensionless groups, following the previous works of Pike^{6,7} and Thornton.⁸ Provision was made to divide the data into subsets for special purposes, such as testing the statistical significance of a new group as a correlating parameter. For this, data

⁶F. P. Pike *et al.*, *The Application of Statistical Procedures to a Study of the Flooding Capacity of a Pulse Column. I. The Behavior of the System Trichloroethylene-Water. II. Statistical Design and Analysis* (by G. E. P. Box and J. S. Hunter), ORO-140 (1955).

⁷F. P. Pike, *The Flooding Capacity of a Pulse Column on the Benzene-Water System*, ORO-141 (1954).

⁸J. D. Thornton, "Liquid-Liquid Extraction Part XIII: The Effect of Pulse Wave-Form and Plate Geometry on the Performance and Throughput of a Pulsed Column," *Trans. Inst. Chem. Engrs.* **35**, 316 (1957).

Table 13.4. Range of Variables Tested

Representative of 1111 flooding points obtained with an aqueous-continuous system containing metal sieve plates and no mass transfer

Variable	Units	Range
Continuous phase		
Flow	ft/hr	0.840-414.0
Density	g/cm ³	0.994-1.403
Viscosity	centipoises	0.791-22.2
Dispersed phase		
Flow	ft/hr	1.38-352.0
Density	g/cm ³	0.684-1.454
Viscosity	centipoises	0.411-5.69
Interfacial tension	dynes/cm	3.70-42.0
Pulse amplitude	in.	0.095-3.15
Pulse frequency	cycles/min	6.80-420.0
Hole diameter	in.	0.02-0.188
Column diameter	in.	1.00-12.0
Pulse-plate free area	%	8.10-62.1
Pulse-plate spacing	in.	0.50-4.0

⁵*Chem. Technol. Div. Ann. Progr. Rept. May 31, 1964, ORNL-3627, pp. 244-46.*

from a single pulsed column and chemical system having replicated data points were used. The coefficients for each correlating equation were evaluated by using only the experimental data involving no mass transfer, continuous aqueous phase, and metal sieve plates (1111 data points). For these data points, the range of each of the 13 basic variables is shown in Table 13.4. The coefficients obtained with these data were then used in testing the fit of the other data sets. The analysis was performed with the CDC-1604

digital computer, using a general-purpose multiple-regression program.

Several of the correlations predicted flooding within the error of the data. New coefficients were generated for the previous correlation of Thornton (emulsion flooding region only) that allow greater confidence in the use of this equation. Finally, new equations modeled after Pike's but with additional terms, which predict flooding in both regions, have been developed; these offer greater accuracy.

14. Reactor Evaluation Studies

This program is supported jointly by the Reactor Division and the Chemical Technology Division and includes studies on various proposed advanced-reactor and fuel-cycle systems to determine feasibility and costs. The work in this Division during the past year included calculation of the costs of fuel shipping and processing and of preparing sol-gel oxide in connection with the advanced converter evaluation,¹ with the ²³³U value study,² and other reactor evaluation programs. Also included were the development of computer codes for calculating shipping and processing costs and overall cost of nuclear power, and for calculating individual and gross concentrations and radioactivities of thorium, uranium, transuranium elements, and fission products produced during reactor operation at constant flux or constant power. A manual of the design of casks for shipping spent fuel was published. Criticality problems and neutron-gamma shielding problems in fuel-cycle plants were also studied.

14.1 STUDIES OF THE COST OF SHIPPING REACTOR FUELS

Last year's annual report described the development of a computer program, NORA, for calculating the cost of shipping and processing spent fuel. This year, NORA was extended to cover the shipping of gamma-active fresh fuels and fuel chemicals. This was done to make the code more useful in the study of thorium-²³³U fuel cycles, in which the processed fuels are gamma-radioactive. This activity results from the formation

¹M. W. Rosenthal *et al.*, *A Comparative Evaluation of Advanced Converters*, ORNL-3686 (January 1965).

²M. W. Rosenthal *et al.*, *The Fuel Value of U-233 in High-Temperature Gas-Cooled and Spectral-Shift Reactors* (ORNL report in preparation).

of ²³²U and ²²⁸Th in the reactor; these nuclides remain in the uranium and thorium product streams from the processing plant and subsequently decay to form gamma-emitting daughters. The code is designed to calculate the radioactivity of these daughters based on given concentrations of ²³²U and ²²⁸Th at the time of reactor shutdown and on the time intervals from shutdown to reprocessing and shipping. After calculating the radioactivity, the code designs a cask with the required shielding.

These features of the code were used in the study undertaken by the Reactor Division to determine the effect of ²³²U content on the value of ²³³U. Shipping costs were calculated for all parts of the fuel cycle. This included the cost of shipping fresh fuel elements, spent fuel elements, and fuel chemicals, such as uranyl nitrate solution and thorium nitrate crystals. Several cases were considered, involving (1) no recycle of uranium or thorium, (2) recycle of uranium only, and (3) recycle of both uranium and thorium. Various total nuclear-electric capacities also were considered, since costs tend to lessen markedly as shipping capacity increases. Two types of fuel element were studied, the SSCR and the HTGR. The designs were identical with those used in the advanced converter evaluation.¹ The major assumptions used in calculating the shipping cost are listed in Table 14.1.

Some of the results of this study are shown in Table 14.2 (fresh fuel elements) and in Figs. 14.1 and 14.2 (fuel chemicals). The concentrations of ²³²U and ²²⁸Th are given in parts per million of total uranium plus thorium at the time of reactor shutdown, except where otherwise noted. It was assumed that casks would be shared among 15 identical reactors of 1000 Mw (electrical) each.

Figure 14.1 shows shipping costs calculated for uranyl nitrate solution contaminated with ²³²U and its decay products. Casks were assumed to

Table 14.1. Assumptions Used in Shipping Cost Calculations

1. Casks are shared; maximum cask utilization is 80% (20% idle time)
2. Casks are purchased; cask cost is \$1.00 per pound of cask weight
3. Fixed charge rate on casks is 22%/year
4. Property insurance per trip is 0.0004 times the value of cask and contents
5. Maximum allowable loaded weight is 220,000 lb
6. Casks are empty on the return trip
7. Shipment is by rail. Shipping distances are 1000 miles each way for fresh fuel and 500 miles each way for fuel chemicals. Freight rates are:
500 miles: Empty \$0.0121/lb
Full \$0.0129/lb
1000 miles: Empty \$0.0181/lb
Full \$0.0193/lb
8. Round trip time is 12 days for 500 miles and 16 days for 1000 miles
9. Handling cost is \$500 per round trip

Table 14.2. Shipping Costs for Fresh SSCR and HTGR Fuel Elements

Distance = 1000 miles each way

Element Type	Shipping Capacity (metric tons of U + Th shipped per year)	Shipping Cost (dollars per kilogram of U + Th)				
		No Recycle	Recycle Uranium Only		Recycle Uranium and Thorium	
			20 ppm ²³² U + Th	100 ppm ²³² U + Th	20 ppm ²³² U, 0.1 ppm ²²⁸ Th	20 ppm ²³² U, 1.0 ppm ²²⁸ Th
SSCR	15	1.00	1.30	1.51	1.53	1.82
	60	0.75	0.94	1.09	1.10	1.31
	240	0.50	0.67	0.78	0.79	0.94
	960	0.49	0.65	0.76	0.77	0.92
HTGR	15	2.50	5.85	7.19	8.17	9.44
	60	2.30	5.10	6.26	7.12	8.22
	240	2.15	4.97	6.12	6.94	8.02
	960	2.10	4.95	6.10	6.92	8.00

have an inside diameter of 2 ft and an inside length of 12 ft. Each cask carries 800 liters of solution containing 200 g of uranium per liter. Criticality control is achieved by dividing the inner container with parallel plates spaced $\frac{1}{2}$ in. apart. The plates are of stainless steel, $\frac{1}{8}$ in. thick, containing 1%

boron. The thickness of the lead shielding varied from 2.5 to 7.5 in., depending on ²³²U concentration. In Fig. 14.1 it should be noted that the ²³²U concentration has been expressed in parts per million of uranium, rather than of uranium plus thorium.

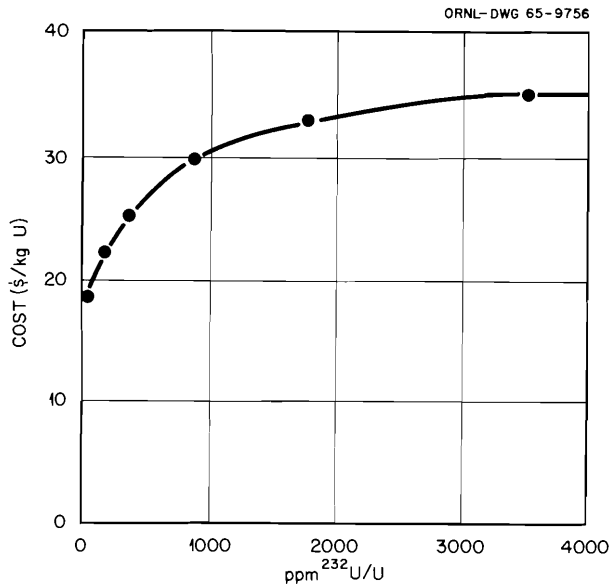


Fig. 14.1. Effect of ^{232}U Content on Cost of Shipping Uranyl Nitrate Solution.

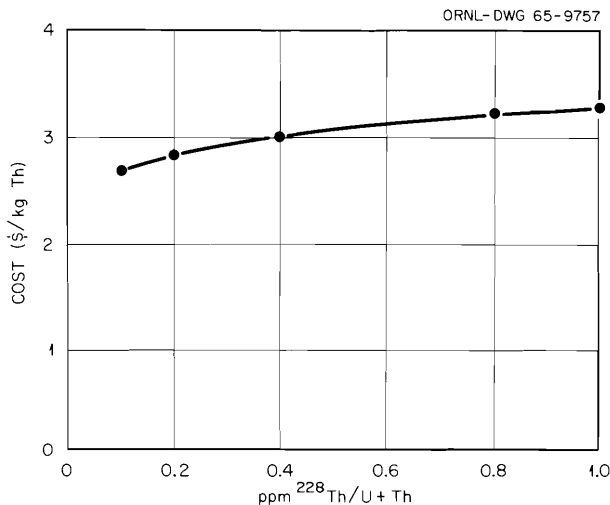


Fig. 14.2. Effect of ^{228}Th Content on Cost of Shipping Thorium Nitrate Crystals.

Figure 14.2 shows shipping costs for thorium nitrate tetrahydrate crystals. Inside diameter and inside length of cask were assumed to be 3 ft and 15 ft. Each cask carries 2520 kg of thorium in four stainless steel drums. The thickness of the lead shielding ranges from 5 to 7 in., depending on ^{228}Th content.

14.2 STUDIES OF THE COST OF PROCESSING FUEL

Advanced Converter Fuels

In support of the advanced converter evaluation program,¹ fuel processing cost estimates were made for six types of advanced converter reactors: (1) uranium-fueled pressurized-water (PWR), assumed to include also boiling-water; (2) thorium-fueled spectral-shift-controlled (SSCR); (3) uranium-fueled, pressure-tube, heavy-water-cooled and -moderated (HWR-U); (4) thorium-fueled, heavy-water (HWR-Th); (5) thorium-fueled high-temperature gas-cooled (HTGR), of the "TARGET" type; and (6) uranium-fueled sodium-graphite (SGR).

The cost estimates are summarized in Figs. 14.3 to 14.5. These estimates represent an updating of the preliminary numbers presented in last year's annual report. Figures 14.4 and 14.5 are based on a 15% annual fixed-charge rate (FCR) on total capital investment; this rate is about equal to that applicable to the first privately financed commercial reactor-fuel processing plant, Nuclear Fuel Services (NFS).³ At an FCR of 22%, which would be more typical for most privately owned chemical companies, the unit costs would be about 25% higher.

These cost estimates for the evaluation were made for hypothetical future nuclear power economies of 15,000 Mw (electrical) of a given reactor type, with all the fuel from that reactor type being processed in a single-purpose plant designed to exactly match its load. Thus, the differences in annual throughput rate and nominal daily capacity shown in Figs. 14.3 and 14.4 are caused by differences in burnup, thermal efficiency, and discharge batch size for the various reactor types. Table 14.3 shows the estimated processing contribution to nuclear power cost as a function of the size of the industry, from 5000 to 20,000 Mw (electrical). In this table, the burnup values are held constant at approximately the economic optimum indicated by consideration of overall fuel cycle costs at 15,000 Mw (electrical), though the optimum burnup would be higher for an industry of smaller size, and vice versa. All other things

³"Chemical Processing Plant," hearing before the Joint Committee on Atomic Energy, 85th Congress, May 14, 1963, U.S. Govt. Printing Office, 1964.

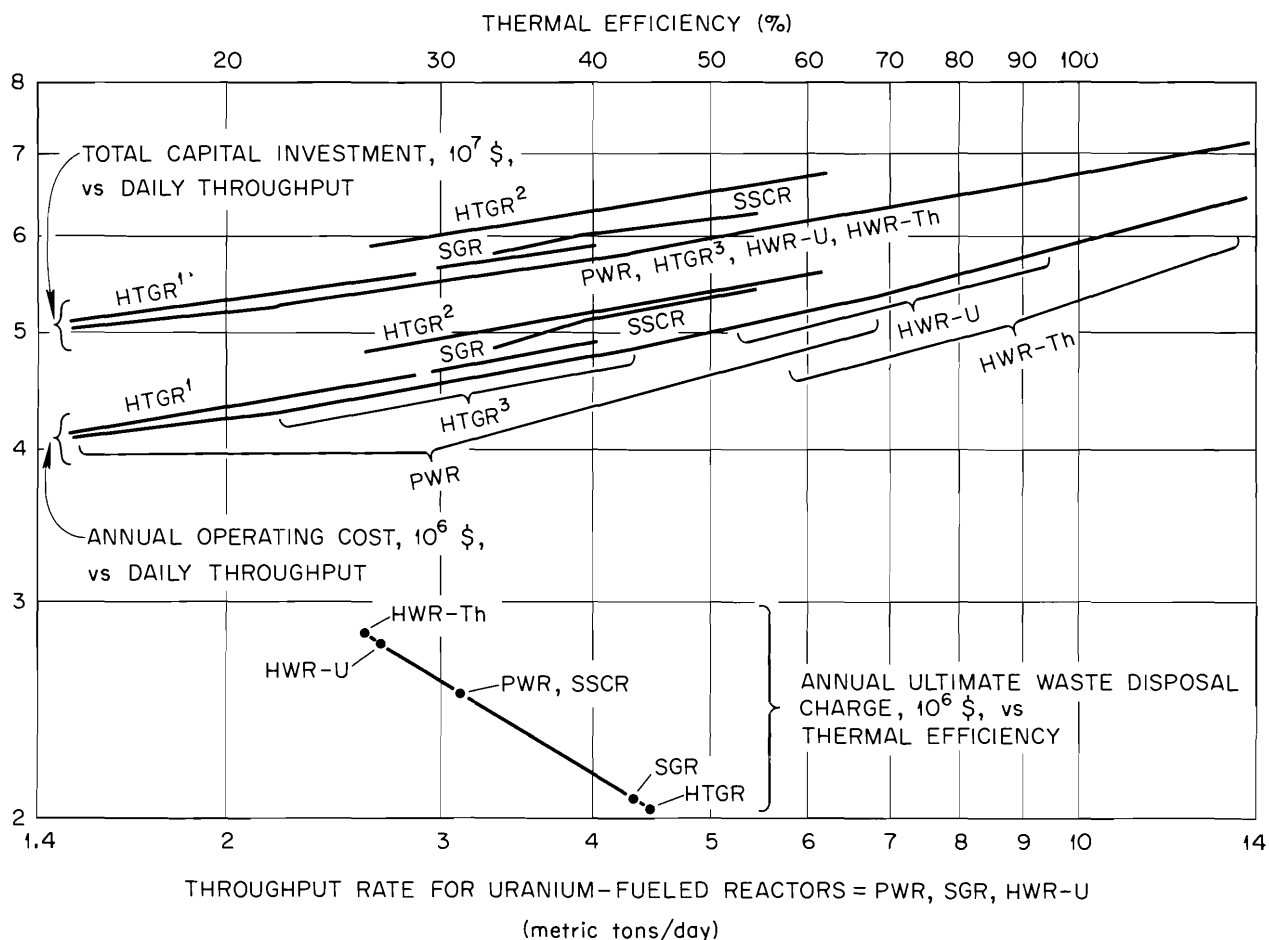


Fig. 14.3. Capital, Operating, and Ultimate Waste-Disposal Costs for Single-Purpose Processing Plants Serving a 15,000-Mw(electrical) Nuclear-Power Industry. Superscripts on HTGR labels refer to alternative processing schemes (see text).

being equal, the power cost of processing decreases with increasing burnup, thermal efficiency, and batch size, is lower for uranium fuels than for thorium, and is lower for metal-clad oxides than for carbon-carbide-graphite or sodium-bonded fuels. The combined interplay of all these considerations in this study was to minimize differences in cost per kwhr (electrical), although the costs in dollars per kilogram of fuel varied widely.

For all fuels except HTGR, all the uranium and plutonium, or thorium and uranium, in one processing batch (assumed to be the same as one reactor-discharge batch) were dissolved together and then partitioned and decontaminated by solvent extraction. For HTGR fuels, three alternative schemes proposed under the TARGET concept were con-

sidered: (1) mixed thorium-uranium fuel, as with the other reactors; (2) thorium and uranium in separate particles before irradiation, with the thorium-plus-bred-uranium particles processed separately from the high-burnup-uranium particles; and (3) separate particles as in (2) but with the high-burnup-uranium particles discarded directly to waste disposal instead of being processed, on the basis that their high ^{236}U content makes recycle of this uranium to HTGR reactors undesirable from the overall economics and physics points of view. Scheme (2) costs more than scheme (3) and would have to be justified on the basis of a market value (for reactors other than HTGR) in excess of the additional cost of \$1 to \$2 per fissile gram recovered.

Table 14.3. Fuel Processing Costs as a Function of Number and Type of Reactors

The superscripts 1, 2, 3 refer to three alternative HTGR processing schemes (see text).

	PWR-U	HWR-U	SGR-U	SSCR-Th	HWR-Th	HTGR-Th
Burnup, Mwd/metric ton	21,000	11,100	22,000	28,800	27,800	58,000
Thermal efficiency, %	31.1	26.8	43.6	31.2	26.1	44.4
Batch size, metric tons	33.9	19.5	12.2	66.3	13.5	7.89
Processing cost, mills/kwhr (electrical), 15% FCR						
5 reactors ^a	0.332	0.396	0.321	0.357	0.381	0.306 ¹
10 reactors	0.201	0.237	0.195	0.212	0.232	0.184 ¹
15 reactors	0.154	0.177	0.144	0.159	0.173	0.138 ¹ 1.149 ² 0.135 ³
20 reactors	0.125	0.136	0.104	0.116	0.125	0.099 ¹

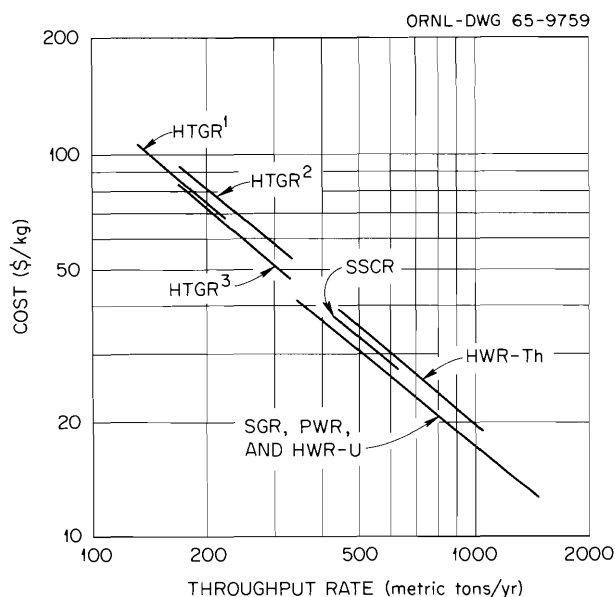
^aNumber of 1000-Mw (electrical) reactors.

Fig. 14.4. Fuel Processing Cost as a Function of Throughput Rate in Single-Purpose Plants Serving a 15,000-Mw(electrical) Economy. Based on a 15% fixed-charge rate on capital. Superscripts on HTGR labels refer to alternative processing schemes (see text).

These cost estimates were based on modifications of previous estimates of processing-plant costs, by Du Pont,⁴ and of ultimate waste-disposal costs, by ORNL.⁵ They are conservatively high

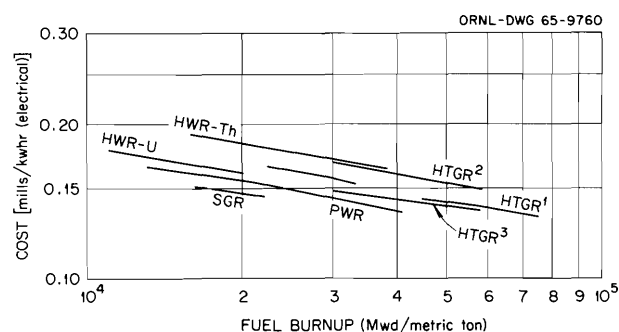


Fig. 14.5. Power Cost of Fuel Processing in a 15,000-Mw(electrical) Advanced-Converter Nuclear Economy. Based on a 15% fixed-charge rate on capital. Superscripts on HTGR labels refer to alternative processing schemes (see text).

in that they would predict higher costs than the actual NFS pricing formula for a plant of comparable fuel-processing capability, and also in penalizing thorium fuels for their known processing disadvantages vis-a-vis uranium while not granting

⁴W. H. Farrow, Jr., *Radiochemical Separations Plant Study. Part II. Design and Cost Estimates*, DP-566 (March 1961).

⁵J. O. Blomeke et al., *Estimated Costs for Management of High-Activity Power Reactor Processing Wastes*, ORNL-TM-559 (May 13, 1963).

any cost credit for potential advantages such as the possibility that only one solvent extraction cycle will be sufficient since the thorium-uranium recycle scheme may require remote fabrication anyway. On the other hand, they may not be quite so conservative in assigning only a moderate head-end cost penalty to SGR and HTGR fuels on the assumption that present development programs will be successful. These estimates for the advanced converter evaluation agree with those made earlier for large desalination reactors,⁶ except that the earlier estimates made less allowance for turnaround time between batches and for ultimate waste disposal and used a 7.7% fixed-charge rate (for municipal or similar financing).

Costs in an Expanding Economy

The cost studies described above assumed an "equilibrium" economy with the spent fuel equivalent to 5000, 10,000, 15,000, or 20,000 Mw (electrical) of a given reactor type being processed in a plant designed to match its load and operating at constant full load. A dynamic economy starting small and growing large over a number of years cannot automatically expect to experience processing costs as low as those equivalent to a static economy of the same size at any given time. A processing plant must be built at a particular time and with a particular design capacity. It may be able to increase its actual capacity somewhat over a period of time as a result of technological improvements and inherent overcapacity in its basic design, but it cannot be built initially to match a small reactor economy and then be expanded incrementally each year at marginal additional cost to keep up with the load as the reactor economy grows. Thus, in general a processing plant will be oversized initially, enough so that it can eventually achieve unit costs low enough to give it an economic life long enough to permit it to recover its capital investment plus an acceptable rate of return on investment and still meet actual or potential competition from other plants. Since such a plant must start up on less than a full load, its average load over its life will be less than its equilibrium capacity,

and hence its average unit costs over its life will be higher than the calculated equilibrium costs. This "startup penalty" can be appreciable for plants, such as spent-fuel processing plants, which have a high ratio of capital cost to operating cost. In the case of the NFS plant, the USAEC is providing a "base load" during the first five years of operation, permitting a pricing policy based on a full load for an assumed 15-year plant life. The USAEC has indicated a willingness to provide a base load also for a second private processing plant, but this type of support cannot be assumed for all future plants in a private competitive economy.

A study of optimum processing plant size, timing, and location in a growth economy has been started. A computer code will be developed to calculate the minimum cost strategy as a function of input assumptions regarding growth curve, cost-scaling factors, financing conditions, regulatory and competitive conditions, etc. As a first step in this study, an economic evaluation of HTGR head-end processing costs was made for the design and cost estimate presented in Sect. 1.8.2 of this report.⁷ This head-end facility could handle the fuel from up to 10,000 Mw (electrical) of HTGR reactors, but a reasonable estimate is that it might be ten years after the first commercial-size HTGR begins to discharge fuel before the HTGR industry reaches 10,000 Mw (electrical). A present-worth economic analysis, similar to that of Rosenthal *et al.*,¹ indicated head-end capital and operating unit charges varying from less than \$30/kg for a plant with a full load for 15 years to more than \$130/kg for the same plant with a growing load for only 7 years. It was indicated that the plant size was not optimum for the growth curve assumed, but the optimum size has not yet been calculated.

14.3 STUDIES OF THE COST OF PREPARING FUEL BY THE SOL-GEL PROCESS

The value of ^{233}U as fuel in reactors, compared with the alternative use of ^{235}U at a known price, depends not only on the physics characteristics of ^{233}U itself, compared with those for ^{235}U , and of the reactor in which it is used but also on any

⁶Chem. Tech. Div. Ann. Progr. Rept. May 31, 1963, ORNL-3452, p. 24.

⁷E. L. Nicholson, L. M. Ferris, and J. T. Roberts, *Burn-Leach Processes for Graphite-Base Reactor Fuels Containing Carbon-Coated Carbide or Oxide Particles*, ORNL-TM-1096 (Apr. 2, 1965).

cost differences in the fuel cycles of ^{233}U and ^{235}U outside the reactor. Since it is believed that the sol-gel process will play an important part in thorium fuel cycles, a detailed cost study of preparing fuel by this process was made for the ^{233}U value study.²

Three flowsheets, representing different recycle conditions, at four different scales of operation were considered separately for the SSCR and HTGR reactor types. Flowsheet 1 was for no recycle; that is to say, fuel was prepared from ^{235}U and unused thorium. Flowsheet 2 was for fuel preparation from unused thorium and for recycle of the ^{233}U . Flowsheet 3 was for recycle of both thorium and ^{233}U . Two subcases of flowsheet 2 were considered, one for ^{233}U containing relatively low concentrations of ^{232}U , typical of early stages of recycle, and the other for relatively high concentrations of ^{232}U , typical

of equilibrium recycle conditions. The four scales of operation considered were 15, 60, 240, and 960 metric tons of thorium plus uranium per year. The sol-gel product was assumed to be urania-thoria fragments for the SSCR and urania-thoria-carbon spheroids for the HTGR.

Tables 14.4 and 14.5 present a summary of all the estimated capital and operating costs. These costs are based on:

1. selection of process equipment based on pilot-plant-proved technology except for a few steps such as spheroidization, where bench data were used;
2. on-stream efficiency of 85%, or 310 days/year for production plus facility cleanout between different fuel compositions;
3. loss of heavy metal and in-process recycle as shown on flowsheets.

Table 14.4. Sol-Gel Cost Summary: SSCR Reactor

Throughput (metric tons/year)	Flowsheet Figure ^a	Capital Cost (thousands of dollars)	Operating Cost (dollars per kilogram of U + Th)	Total Cost (dollars per kilogram of U + Th)	
				22% Capital Charges	15% Capital Charges
15	1	900.6	25.83	39.04	34.84
	2	985.5	25.84	40.29	35.69
	2 high	1696	25.84	50.71	42.80
	3	1456	25.79	47.14	40.35
60	1	1250	7.14	11.72	10.27
	2	1375	7.15	12.19	10.59
	2 high	2589	7.15	16.64	13.62
	3	2231	7.10	15.28	12.68
240	1	2228	2.61	4.65	4
	2	4049	2.63	6.34	5.16
	2 high	4644	2.63	6.89	5.53
	3	4045	2.58	6.29	5.11
960	1	4765	1.17	2.16	1.91
	2	7694	1.18	2.94	2.38
	2 high	8864	1.18	3.21	2.56
	3	7510	1.13	2.85	2.30

^a1: no recycle

2: recycle uranium only, low ^{232}U concentration

2 high: recycle uranium only, high ^{232}U concentration

3: recycle uranium and thorium

Table 14.5. Sol-Gel Cost Summary: HTGR Reactor

Throughput (metric tons/year)	Flowsheet Figure ^a	Capital Cost (thousands of dollars)	Operating Cost (dollars per kilogram of U + Th)	Total Cost (dollars per kilogram of U + Th)	
				22%	15%
				Capital Charges	Capital Charges
15	1	909.8	25.83	39.18	34.93
	2	990	25.84	40.36	35.74
	2 high	1109	25.84	42.11	36.93
	3	1458	25.79	47.18	40.37
60	1	1338	7.14	12.05	10.49
	2	1449	7.15	12.46	10.77
	2 high	1660	7.15	13.24	11.30
	3	2349	7.10	15.61	12.97
240	1	2377	2.61	4.79	4.10
	2	2750	2.63	5.15	4.35
	2 high	3228	2.63	5.59	4.69
	3	4260	2.58	6.48	5.24
960	1	5091	1.17	2.35	1.97
	2	6385	1.18	2.64	2.18
	2 high	7720	1.18	2.95	2.39
	3	8854	1.13	3.16	2.51

^a1: no recycle

2: recycle uranium only, low ²³²U concentration

2 high: recycle uranium only, high ²³²U concentration

3: recycle uranium and thorium

Additional information, including detailed flowsheets and itemized breakdowns of estimated costs, is given in refs. 2 and 8.

It can be seen that substantial unit cost reduction is achieved by going to the higher scales of production. The cost penalty for recycling ²³³U and thorium, compared with the alternative of using ²³⁵U and unused thorium, is about 30%.

14.4 COMPUTER CODE FOR STUDIES OF OVERALL POWER COSTS

A study was begun for developing a computer code that would calculate power cost by using subroutines for calculating fabrication costs, shipping costs, chemical processing costs, etc.

⁸F. E. Harrington and J. M. Chandler, *A Study of Sol-Gel Fuel Preparation Costs for SSCR and HTGR Reactors*, ORNL-TM-1109 (Apr. 6, 1965).

Some progress has already been made in developing such subroutines. The purpose of the overall code will be to facilitate the optimization of the fuel cycle and the evaluation of competing reactors by comparison of power costs. By power cost here is meant a constant cost in mills per kilowatt-hour applicable over the entire life of the reactor project. This cost represents the income that must be received in order to pay off the investment in the specified number of years, while earning the specified rates of return on stocks and bonds and providing for all operating expenses.

As a first step in this study, a code was written (POWERCO) that calculates power cost from given annual component costs (fabrication, shipping, etc.). The calculation is based on the fundamental requirement of investment payout. The code makes provision for straight-line or sum of the years' digits depreciation and for four optional modes of bond repayment.

The payout of investment is given by a tabulation that shows the gradual decline of the outstanding capital investment to zero over the life of the project. Each year the amount of outstanding investment is diminished by an amount equal to the cash income minus the sum of cash expenses and earnings. Once a complete schedule of cash expenditures has been established, the power cost can be easily calculated, using the criterion that the investment must become zero at the end of the project. This procedure is fundamentally equivalent to the present-worth method of accounting for expenses and incomes, which derives its validity from the payout calculation described. By calculating power cost in this way, it is not necessary to depend on the fixed-charge-rate concept. However, the true fixed-charge rates on depreciable and nondepreciable capital can be derived from the results of the calculation. The true magnitude of the average fuel working capital can also be derived. The code calculates and displays these figures. Because these are rigorously compatible with the true power cost, they can be used as a check against more conventional methods of determining fixed-charge rates and fuel working capital.

One of the results observed thus far is that the fixed-charge rates and fuel working capital for a given project will depend on the mode of bond repayment specified. Also, the fixed-charge rate on nondepreciable capital may exceed that on depreciable capital, as already indicated by the Oyster Creek analysis⁹ and by Rosenthal *et al.*¹

The next phase of the study will be to develop and incorporate the codes for generating the component costs. This will include a time-cycle code for calculating the time points at which the various cash expenses are paid. Both the magnitude of the expenditures and the timing of their occurrence will be considered during the optimization procedure.

14.5 THE TRUFIZ COMPUTER CODE

A computer code (TRUFIZ) is being developed to calculate individual and gross concentrations and activities of the transuranium and fission product isotopes produced in nuclear reactors.

⁹Jersey Central Power and Light Company, *Report on Economic Analysis for Oyster Creek Nuclear Electric Generating Station* (Feb. 17, 1964).

The basic mathematical equations for transuranium and fission-product isotope production at constant flux and at constant reactor power have been developed. Fissile materials considered were ^{233}U , ^{235}U , ^{239}Pu , and ^{241}Pu . The fertile materials considered are ^{232}Th and ^{238}U , with the buildup of the other even-numbered uranium and plutonium isotopes also taken into account.

The TRUFIZ program will be coded in FORTRAN-63 for the CDC 1604A computer at ORNL. A variety of problems of interest will be run.

14.6 MANUAL OF SHIPPING-CASK DESIGN

A report covering the design of shipping casks for the transport of radioactive materials has been issued as ORNL-TM-681. The topics covered include criticality and nuclear safety, heat transfer, structural integrity, shielding, contamination regulations, and accidents as applied to shipping casks for radioactive materials.

The document is being reviewed, after which it will be released to the public.

14.7 CRITICALITY CONTROL IN FUEL CYCLE PLANTS

Criticality calculations were made with the DTK neutron transport code to determine allowable sizes of dissolver baskets for various UO_2 and $\text{UO}_2\text{-ThO}_2$ fuels, allowable sizes of unpoisoned regions in tanks packed with borosilicate-glass Raschig rings, safe dimensions of furnaces for coating fuels with pyrolytic carbon, and the reactivity of arrays of fuel elements in casks designed by the MYRA and NORA codes. Briefly, the results are as follows:

1. Boron poison may be incorporated in the walls of the dissolver basket to largely negate the effect of reflection by a dilute fissile solution.
2. The reactivity of tanks containing fissile solution and borosilicate-glass Raschig rings is not appreciably increased by including 2-in.-ID unpoisoned pipes, at an edge-to-edge spacing of 12 in., within the tank.
3. An 18-in.-diam fluidized-bed furnace for coating 100- to 300- μ -diam microspheres of 10% $^{235}\text{U}_2$ -90% ThC_2 with a 120- μ layer of pyrolytic carbon was calculated to be subcritical under normal

and abnormal process conditions, including flooding with water.

4. Large numbers of 4- to 6-in.-diam canisters containing ^{235}U -carbon- H_2O may be arrayed compactly if there is 2 to 3 in. of boron-foam glass between canisters.
5. Arrays of CETR, Yankee Atomic, and SSCR fuel elements in casks designed by the NORA code are subcritical. The elements are enclosed in a boron-poisoned network that serves the dual purpose of absorbing neutrons and conducting heat to the surface of the cask.

15. Chemical Applications of Nuclear Explosions

The purpose of this program is to provide research and development in selected areas of the Plowshare Program, especially those areas requiring knowledge of chemistry or metallurgical engineering to determine feasibility. Areas in which research was performed last year included (1) completion of flowsheet development for the recovery of transplutonium elements produced by a nuclear detonation in salt (Project Coach); (2) electrochromatographic methods for separating individual transplutonic elements; (3) hypervelocity-jet sampling as a means of removing a specimen after irradiation in the neutron flux of a detonation but ahead of the detonation shock wave; and (4) a feasibility study of synthesizing chemicals by a nuclear detonation. Other areas of the Plowshare Program in which laboratory studies were initiated are: the measurement of the rate of exchange of tritium with natural gas, which is one of the phenomena expected in the stimulation of gas production from wells (Project Gasbuggy), and studies of the distribution of fission products in ore deposits, including their effect on chemical processing methods used for final recovery. In ore recovery applications, emphasis is being placed on recovery of magnesium oxide or magnesium from olivine ores in the Appalachian region, and copper from copper ores of the Rocky Mountain region.

15.1 PROJECT COACH

In Project Coach it was proposed that a 5- to 10-kiloton nuclear device designed for producing maximum neutron fluxes be detonated underground in a bedded-salt formation near Carlsbad, New Mexico, for producing milligram or larger quantities of transcurium elements. The Coach detonation was originally planned for 1963, but it was postponed because of technical difficulties re-

lated to the development of a suitable neutron-producing device. Laboratory development of processes for recovering transplutonium elements from the salt debris was completed, and further work was deferred until a suitable device is developed.

The isotopes to have been produced by the shot would have been dispersed into 10,000 to 35,000 tons of debris, which would have been mined about a year after the detonation to allow time for fission product decay. Because shipping costs for large tonnages of the radioactive debris are high, an on-site chemical plant for concentrating the actinides to a primary concentrate would have been required. The primary concentrate would then have been shipped to an existing AEC site for final processing.

Laboratory development of a process for recovering transplutonium elements that were to have been produced by Project Coach was completed. The tentative process flowsheet was tested on kilogram samples of the Project Gnome shot debris, which is of high silicate content and is presumed to be similar to the debris expected from the proposed Coach shot. The recovery, according to the flowsheet, consists in (1) leaching the salt with water to isolate the water-insoluble residue, which contained 99% of the transplutonium elements; (2) leaching the residue with boiling hydrochloric or nitric acid to dissolve the transplutonium elements; and (3) concentrating the transplutonium elements by "carrying" on a calcium oxalate precipitate that can subsequently be converted to the oxides. Results of two demonstrations with kilogram samples of Gnome debris indicated that the process could recover 80 to 95% of the transplutonium elements. Difficulties encountered in centrifuging the colloidal silica and washing the centrifuge cake were resolved by adding gelatin to aid in the dehydration of the silica. Thus, dense and

reasonably washable centrifuge cakes were obtained. The transplutonium elements were concentrated by a factor of 500 to 1000 in the oxalate precipitate, based on their concentrations in the original salt debris.

15.2 FOCUSING ELECTROPHORESIS FOR SEPARATION OF HEAVY ELEMENTS

Focusing electrophoresis did not appear promising as a method for separating heavy elements in milligram amounts. The literature¹ had indicated that focusing electrophoresis was applicable to the final isolation of elements such as einsteinium and fermium. In focusing electrophoresis, ions are focused to their isoelectric points on strips of filter paper. The position of the isoelectric point is a function of the pH gradient and complexing-agent concentration along the strip. The concentration profiles are adjusted by suitable choice of acid concentration in the anode compartment and complexing-agent concentration in the cathode compartment.

In the present study, HCl was always used in the anode compartment, and the complexing agents ethylenediaminetetraacetic acid (EDTA), nitriloacetic acid (NTA), diethylenetriaminepentaacetic acid (DTPA), and 1,2-cyclohexyldiaminetetracetic acid (DCTA) were tested in the cathode compartment. Applied voltages used were 200 to 400 vdc, and currents were 5 to 20 ma. Lanthanide pairs – Y-Ce, La-Sm, Ce-Gd, Pm-Dy, Ce-Pr, and Ce-La – were used as standards for transplutonium elements. In all cases, focusing was observed, but separation bands were always overlapped, indicating poor separation. Variation in the length of the time the voltage was applied beyond about 30 min, and changing of reagent concentrations in the electrode compartments, did not significantly improve separations. Equilibration of filter paper strips with anode and cathode solution for 17 hr before use did not improve separations either.

15.3 HYPERVELOCITY JET-SAMPLER DEVELOPMENT

Tests to demonstrate a jet-sampler method for recovering a target irradiated about a meter from

¹E. J. Schumacher, *Chem. Div. Ann. Rept. for 1963*, UCRL-10624, pp. 208–14.

a detonating nuclear device were conducted at the Vincentown, New Jersey, test area under a purchase order issued by ORNL to Frankford Arsenal. Copper or iron targets (25 mm in diameter) were focused into jets, using explosive charges, and were directed along the axis of a flight chamber 18 in. in diameter and 55 ft long. Focusing was accomplished, and the target material traversed the length of the chamber at rates comparable to or faster than those at which the shockfront develops and moves out in a nuclear detonation. Measurements made at the point where the jets emerged from the flight chamber indicated that a coherent long-range jet was obtained and that more than 50% of the target material was present in the jet at that point.

Recently, 13 larger cones (90 mm in diameter) containing gold targets (2 g) were prepared for jetting because the gold simulates a transplutonium target better. It is planned to irradiate the gold targets at ORNL to incorporate ¹⁹⁸Au tracer. Also, a target retriever was constructed at the exit of the flight chamber. In it, each jet will be slowed by passing through several feet of gel and then through several feet of water. That portion of the gel that contains jet particles (the jet track) will be separated and mixed with the water and then passed through a Millipore filter to collect the jetted particles. The filter will be analyzed at ORNL to determine the fraction of the gold target recovered. The ¹⁹⁸Au tracer provides a sensitive means of locating the jetted gold anywhere in the system but decays soon enough not to interfere with subsequent activation analysis of the filters at ORNL.

It is believed that this test will demonstrate that a target can be accelerated and moved faster than the shockwave from a nuclear explosion to a receiver at least 100 m away, and that over 50% of the target can be recovered at the receiver.

15.4 FEASIBILITY OF PRODUCING CHEMICALS WITH NUCLEAR EXPLOSIVES

A very brief cost analysis showed that the application of nuclear explosions to the production of chemicals is uneconomic. The chief disadvantage is the very high unit cost of the power produced, unless very large devices are used (Table 15.1). Assuming industrial power

Table 15.1. Estimate of Unit Power Costs Using Underground Nuclear Explosives

1 kiloton = 10^{12} cal = 1.16×10^6 kwhr

Yields (kilotons)	Cost of Device (\$)	Estimated		Estimated Drilling Cost ^a (\$)	Estimated Operations Cost ^a (\$)	Total Cost (\$)	Unit Power Cost (mills/kwhr)		
		AEC Service Charge (\$)	Drill Depth (ft)				Device 100% Heating Efficiency	Device ^b 30% Heating Efficiency	Total Power Cost at 100% Efficiency
1	350,000	150,000	450	100,000	500,000	1,100,000	301	1000	950
10	350,000	150,000	970	150,000	750,000	1,250,000	30.1	100	108
100	460,000	290,000	2100	300,000	1,000,000	2,050,000	3.96	13.2	17.7
1000	570,000	430,000	4500	600,000	2,000,000	3,600,000	0.49	1.63	3.1

^aEstimated cost according to G. W. Johnson, *Excavation with Nuclear Explosives*, UCRL-5917 (Nov. 1, 1960).

^bA nuclear device has about 30% heat efficiency for reactions that require a temperature of 1000°C.

to cost 4 to 6 mils/kwhr at the bus bar of conventional steam plants, economically competitive production of chemicals with nuclear explosives would have to result (1) from the fact that reaction products could be mined from the bomb debris more cheaply than the reactants; (2) from the use of the earth as a "furnace," thus eliminating costly process equipment; or (3) from the extreme pressures and temperatures produced by the device but not available through conventional technology. There is a possibility that reaction products such as water-soluble salts or gases might be mined more cheaply than reactants that require conventional mining methods, and that the use of the earth as a "furnace" could eliminate some production equipment. Nevertheless, when costs of decontaminating the product from fission products are considered, these possible advantages appear to be more than offset. An extensive literature survey of high-temperature and/or high-pressure chemical reactions did not uncover any likely economic applications.

15.5 STIMULATION OF NATURAL GAS WELLS BY NUCLEAR DEVICES: PROJECT GASBUGGY

In feasibility studies of the stimulation of gas production from wells by nuclear devices (Project Gasbuggy), it is important to consider the relative distributions of tritium gas (produced by the device) to the groundwater and to the natural gas

(e.g., methane) initially present in the cavity. Because of the extreme temperatures and pressures at the instant of detonation and shortly thereafter, this can be measured realistically only in an actual nuclear test. However, laboratory tests, recently begun, may provide an indication of the tritium distribution to be expected. Variables to be studied include temperature, pressure, concentration of gases, and possible catalytic effects of the minerals surrounding the test cavity. Another important consideration is whether the eventual exchange of tritium between groundwater and the methane after well production is started is a significant factor in determining the quality of the gas.

15.6 MAGNESIUM ORES

A survey has been started to determine whether the Plowshare Program can benefit the mineral industry, and therefore the economy, of the Appalachia region. Based on discussions with representatives from the TVA and the U.S. Geological Survey. It was concluded that one possibility might be the recovery of magnesium products (and perhaps by-product nickel and chromium) from olivine deposits in this area. These deposits contain hundreds of millions of tons of essentially unaltered olivine (about 48% MgO), and the deposits are sufficiently large to consider use of nuclear explosives. As a basis for evaluating current process possibilities based on

up-to-date technology, prior work done by TVA is being reviewed. If it is concluded that a potentially profitable area of investigation exists, olivine samples will be obtained, and process development studies will be started.

15.7 COPPER ORES

Fracturing of copper ore deposits with nuclear explosives, followed by in situ leaching to recover

the ore, is being studied for the AEC by the U.S. Bureau of Mines and Lawrence Radiation Laboratory. Oak Ridge National Laboratory will cooperate by studying problems that might arise from the introduction of radioactive contaminants into the processing cycle. Until copper ore that has been broken by nuclear explosives is available, simulated broken ore, leach solutions, etc., will be prepared in the laboratory. A standin sample of domestic ore from the Sierra Copper Flats, New Mexico has been obtained from the Bureau of Mines.

16. Preparation and Properties of Actinide-Element Oxides

The immediate purpose of this program is to determine the microstructural, surface-chemical, and colloid-chemical properties of thoria that control its behavior in relation to sol-gel processes. Techniques which have been developed for studying thoria are to be extended to urania and plutonia as well as to other actinide-element oxides.

16.1 FUNDAMENTAL STUDIES OF THORIA SOLS AND GELS

Progress and Status

The adsorption of aqueous nitric acid on colloidal crystalline thoria has been determined and expressed in terms of thermodynamic quantities. These data are consistent with the assumption that the thoria has a surface-adsorption capacity of one nitrate ion per two surface sites on cubo-octahedral particles, which manifest these two types of faces about equally. Hydrous amorphous precipitated thoria has been found to undergo spontaneous crystallization at room temperature in water when aged over a period of months. Simple desiccation in dry air at room temperature or warming to 90°C shortens the time scale of this aging effect from months down to hours. The solids fraction at which the sol sets to a gel, the sol viscometric behavior, and the surface capacity for peptizing adsorbents are profoundly altered by this transformation.

Application of various particle-size and particle-shape-determining measurements to colloidal crystalline sol-gel process thoria leads to apparent discrepancies whose resolution then leads to the postulation that nearly centrosymmetric single crystallites of thoria agglomerate weakly, and to some extent reversibly, into stringy agglomerates.

Currently, further viscometric work to define better the agglomeration forces and the shapes of

the agglomerates is in progress. Studies of the adsorptive capacity of the thoria surface for uranyl ion in nitric acid and the extension to urania of the colloid characterization methods developed for thoria have begun.

Experimental Work

Adsorption of Nitric Acid on Colloidal Thoria. — Figure 16.1 shows values of an apparent equilibrium “constant” K at 26°C vs the mole fraction of surface adsorption sites that reacted with nitric acid. Data from three sets of experiments are shown as being representative of a larger body of data. The constant K is defined by

$$K = \frac{(H^+) (0.5 - \theta)}{\theta},$$

where (H^+) is the hydrogen ion concentration in the interparticle fluid outside the electrical double layer and θ is the mole fraction of surface sites that have adsorbed nitric acid. The moles of surface sites were calculated from the surface area (determined by the BET method) of a gel made from the sols on which the adsorption measurements were made, and the consistency of this area was checked to within normal experimental error, roughly $\pm 5\%$, against the area predicted for particle sizes as forecast by x-ray line broadening. The density of surface sites per unit area is more compatible with the assumption of equal exposure of (100) and (111) faces than with the assumption that only one kind of face is exposed. A site density of 11.4 micromoles/m² was assumed, based on averaging the calculated surface density of metal ions in the cubic and octahedral faces of a thoria crystal. This value compares with 10.6

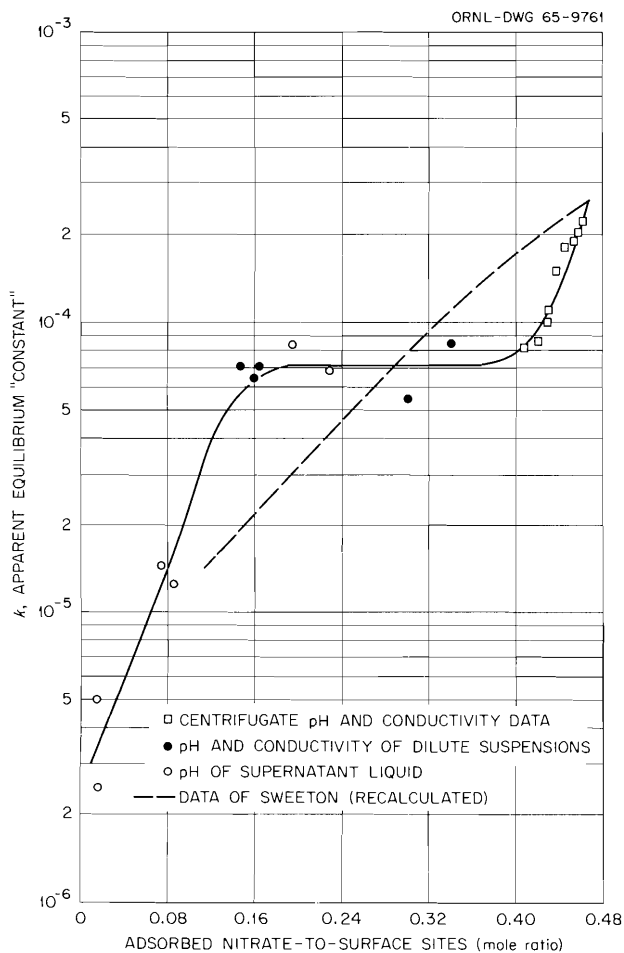


Fig. 16.1. Change in Apparent Surface Equilibrium "Constant" as a Function of Surface Coverage at 26°C.

derived by Spaepen *et al.*¹ and with a value of about 1.4 by Sowden *et al.*² if an equivalence of two surface sites per adsorbed nitrate is assumed. Data at surface coverages greater than $\theta = 0.3$ were taken by analyzing the centrifugates of successive ultracentrifugations of a stable thoria sol. At lower coverages the sols are not stable, and analyses of the supernatant liquid over settled thoria particles were employed. The differences between these data and those of Sweeton³ are

¹G. J. Spaepen, R. T. Wember, and M. E. Wadsworth, *Adsorption of Silicic Acid on Thoria - Determined by Infrared Spectroscopy*, Tech. Rept. V, Contr. 1075 (June 30, 1959).

²R. G. Sowden, B. R. Harder, and K. E. Francis, *Electrophoretic Studies of Thoria and Plutonia Suspensions*, Pt. 2, AERE-R 3269, Harwell, Fig. 3 (March 1960).

³Reactor Chem. Div. Ann. Progr. Rept. Jan. 31, 1963, ORNL-3417, pp. 122-23.

within experimental error over most of the range; such departures as might be genuine differences appear to have arisen in correcting for the changes in available area of the sample as the flocculation state or available area of the colloid changes with surface coverage. In addition, these thorias, prepared in different ways, may possess real differences in surface heterogeneity.

Data scatter has been such that numerous replications have been required to distinguish the proposed "flat" in the coverages between about 0.16 and 0.36 from a simple uniform decrease across the range. This flat corresponds to a free energy change of -5.7 kcal/mole for adsorption. By applying the Clausius-Clapeyron equation to adsorption data over the temperature range 0 to 90°C, the corresponding enthalpy was estimated to be -7.6 kcal/mole and the entropy of adsorption about -7 eu. The rather small entropy of adsorption implies little loss of freedom of the nitrate upon adsorption. In comparison, the entropy for hydration of thoria gel is -22 eu,⁴ implying strong ordering and loss of freedom.

Aging of Colloidal Thoria. - Although thoria is one of the least soluble and most refractory oxides, hydrous amorphous thoria is able spontaneously to undergo profound morphological changes upon extended aging at room temperature either in acid media of low ionic strength or in alkaline media of high ionic strength.

Figure 16.2 is an electron micrograph of the predominantly fibrillar particles of freshly precipitated thoria. The particles in the upper left are clumped agglomerates of the fibrillar particles, which are seen more distinctly in the main field of the photograph. According to Dobry, Mathieu-Sicaud, and Guinand,⁵ the occasional spheroidal particles are "rolled-up" fibrillar particles. Figures 16.3 and 16.4 are photomicrographs of this same thoria after two years of aging at room temperature, the former at about pH 3 in dilute nitric acid and the latter at about pH 8 in 1 M NH_4NO_3 . The fibrillar particles have disappeared, and compact crystalline particles have appeared. The freshly precipitated thoria exhibited an amorphous x-ray diffraction pattern, whereas the aged samples

⁴B. D. Chun, M. E. Wadsworth, and F. A. Olson, *Dehydration Kinetics and Equilibrium Water Vapor Adsorption by Thoria Gel*, Tech. Rept. XX, Contr. 2176 (July 31, 1963).

⁵A. Dobry, S. Guinand, and A. Mathieu-Sicaud, *J. Chim. Phys.* **50**, 501-6 (1953).

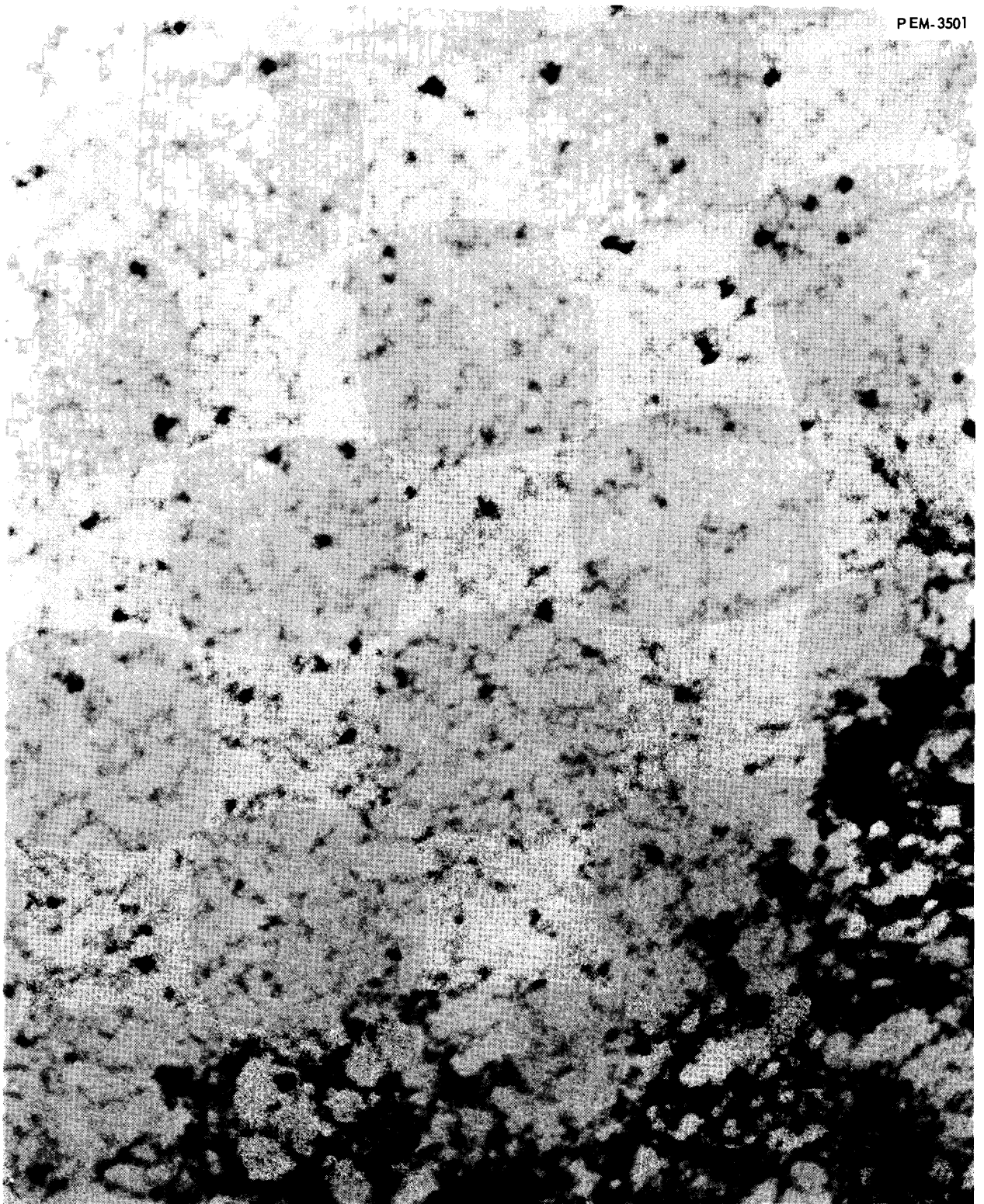


Fig. 16.2. Fresh Hydrous Amorphous Precipitated Colloidal Thoria Particles.

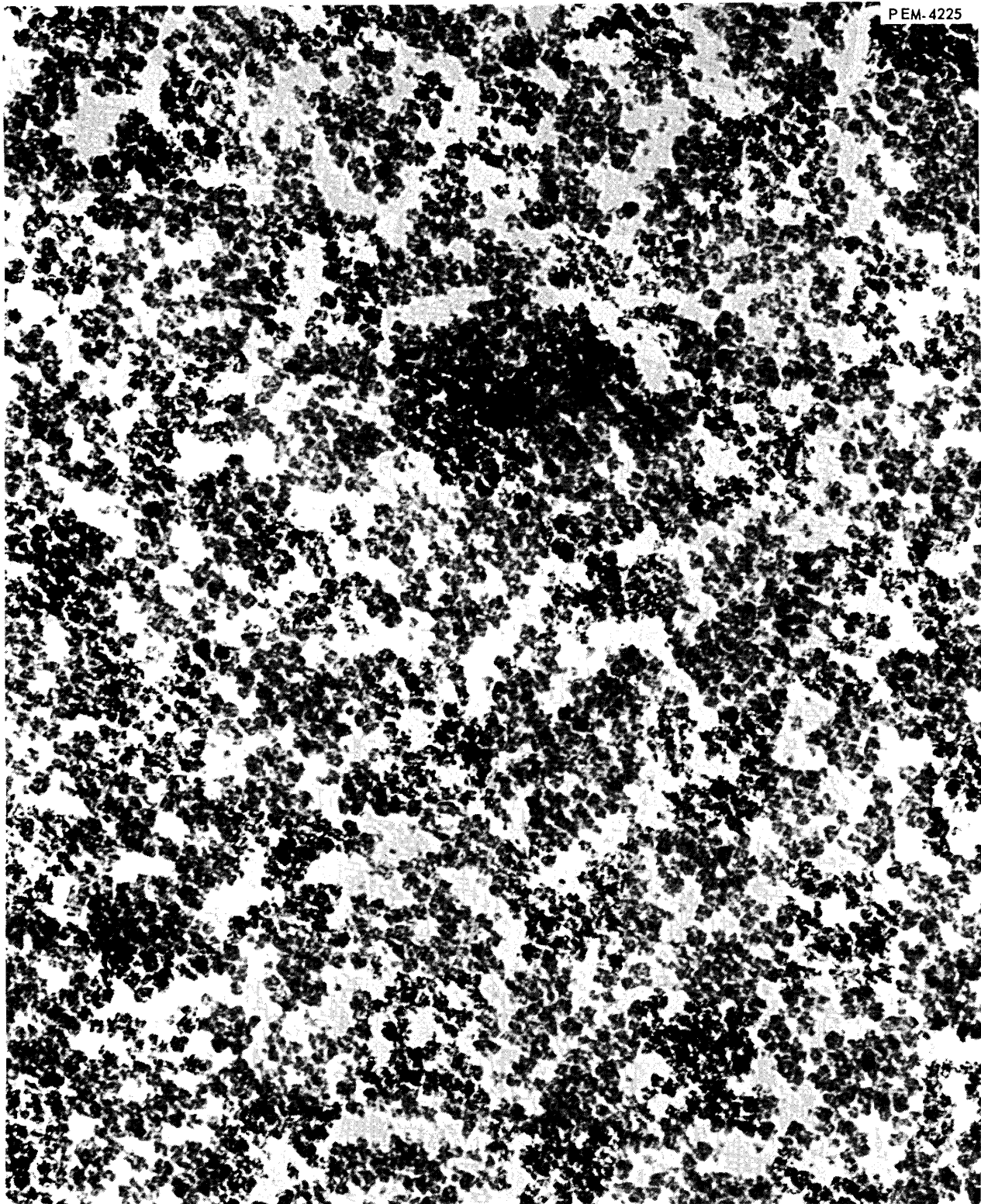


Fig. 16.3. Thoria Spontaneously Crystallized from Amorphous Thoria in Acid Media.

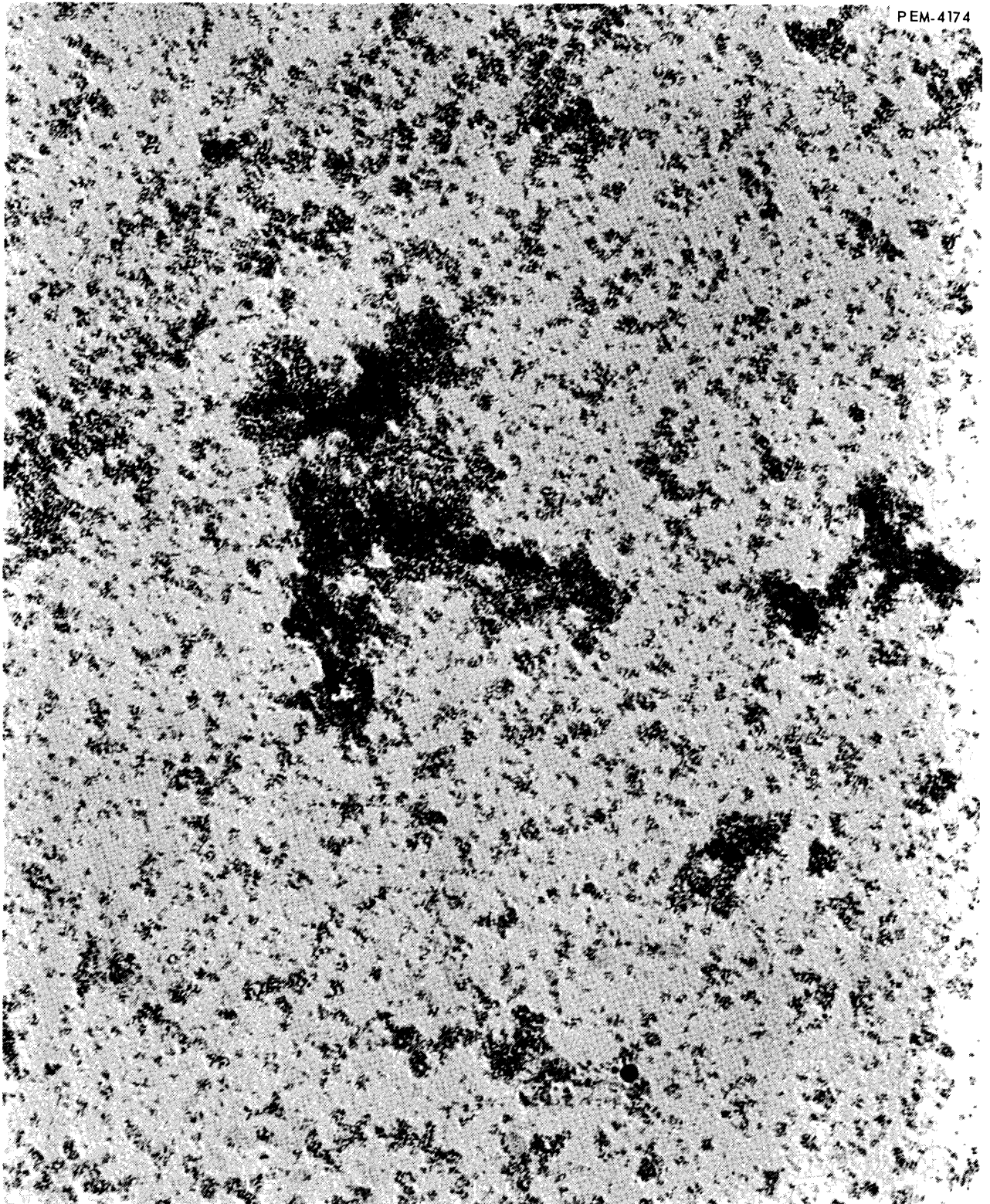


Fig. 16.4. Thoria Spontaneously Crystallized from Amorphous Thoria in Alkaline Media.

show crystal diffraction lines whose widths correspond to crystal diameters of 43 and 36 Å respectively. Despite the larger crystal size, however, recrystallization was less complete in the acid sample than in the alkaline sample.

Viscosity of Dilute Thoria Sols. — The viscosities of thoria sols (116-A crystallites) in the concentration range of 0.08 volume fraction solids and lower were investigated at pH 2.0 and 3.6. The former pH corresponds to near surface saturation with nitrate, with θ approximately 0.49, and the latter to θ approximately 0.30, which is at the lower limit of sol stability. The values of reduced viscosity $[(\eta/\eta_0)-1]/\phi$ are tabulated (Table 16.1) for various solids volume fractions ϕ and for various temperatures, along with the corresponding nominal prolate spheroidal axial ratios for the particles as calculated by the method of Simha.⁶ The viscosity at the highest solids volume fraction probably reflects particle-particle interaction rather than particle shape.

Reduced viscosities in the pH 3.6 medium were even higher at comparable solids volume fraction

than at pH 2, ranging from 35 to 57, and corresponded to prolate spheroidal axial ratios of about 20 to 1. They were not, however, reproducible in time nor when the temperature of the sample was cycled between 20 and 30°C. The sols at pH 3.6 (interparticle fluid) appeared to be undergoing very slow, partially irreversible flocculation leading to flocs of greater and greater axial ratio in time. These flocs could be reverted toward smaller axial ratios by holding the sol at 30°C, but the reversion was not sufficient to reproduce the initial values prior to room-temperature aging of several weeks.

Characterization of Thoria Sols by Electrometric Apparent-pH Measurements. — The apparent pH of the sol is commonly used to define the state of thoria sols for empirical process control in the sol-gel process. This apparent pH can and usually does differ more than tenfold from the true pH of the interparticle fluid outside the electrical double layer in a sol. The relation between the apparent electrometric pH and the real pH of the equilibrium interparticle fluid can be roughly estimated by use of the ideal Donnan equilibrium

$$\text{pH}_a = 2 \text{pH}_b - \log_{10} (\text{NO}_3^-) ,$$

⁶R. Simha, "Effect of Shape and Interaction on the Viscosity of Dilute Solutions of Large Molecules," *Proc. Intern. Rheol. Congr., 1st Congr., 1948*, pp. II-68, II-76, North-Holland, 1949.

Table 16.1. Reduced Viscosities of Dilute 116-A-Crystallite Thoria Sols at pH 2

Solids Volume Fraction, ϕ	Temperature (°C)	Reduced Viscosity	Nominal Prolate Spheroidal Axial Ratio
3.9×10^{-4}	19.88	9.6	7.7
	25.25	8.0	6.7
	33.18	6.5	5.5
3.9×10^{-3}	19.87	9.0	7.4
	25.24	8.7	7.3
	33.20	8.7	7.3
8.8×10^{-3}	19.87	10.1	8.1
	25.24	9.9	7.9
	33.40	9.9	7.9
1.9×10^{-1}	21.19	12.9	9.6
	25.30	12.8	9.5
	25.35	12.8	9.5
	33.23	12.6	9.4
7.5×10^{-1}	19.87	31	~17

where pH_a is the apparent sol electrometric pH, pH_b is the pH of the equilibrium interparticle fluid, and (NO_3^-) is the nitrate molarity of the sol.

Data from Figs. 3.14 and 3.15 of ORNL-3385⁷ were recalculated in terms of surface coverage and are compared in Figs. 16.5 and 16.6 with the apparent pH values predicted by nitrate analyses and the independently derived surface equilibrium data (Fig. 16.1), using the Donnan equilibrium. Considering that a single value of K was used as a basis for calculation and the likelihood of interferences which were not evaluated, such as preemption of some surface adsorption by carbon dioxide adsorbed from the air, the agreement is good.

⁷D. E. Ferguson, *Status and Progr. Rept. for Thorium Fuel Cycle Development*, Dec. 31, 1962, pp. 39-40.

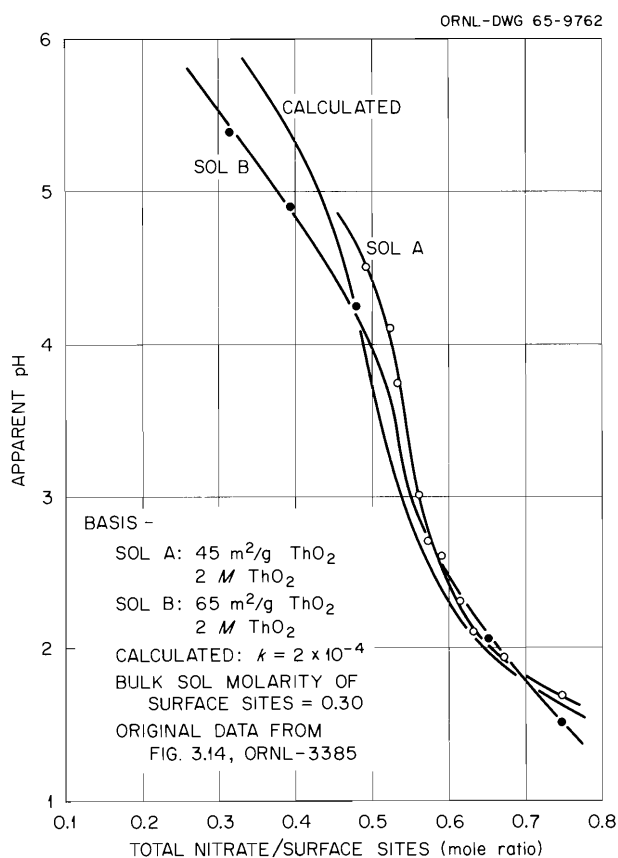


Fig. 16.5. Comparison of Thoria Sol Apparent-pH Titration Data with Predicted Apparent pH from the Ideal Donnan Equilibrium.

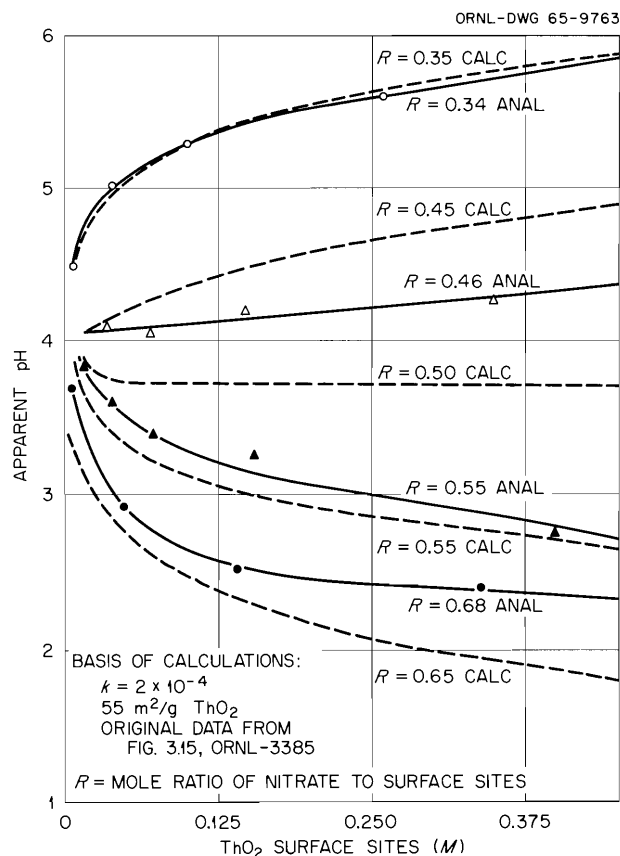


Fig. 16.6. Comparison of Thoria Sol Apparent-pH Dilution Data with Predicted Apparent pH from the Ideal Donnan Equilibrium.

16.2 SURFACE AND SINTERING PROPERTIES OF SOL-GEL THORIA

The work reported here was done under sub-contract with the University of Utah, M. H. Wadsworth in charge.

Progress and Status

Weight-loss data for the low-temperature (below 600°C) dehydration of thoria gel has been fitted to equations derived from absolute-reaction-rate theory in terms of energies of activation. The free energy, enthalpy, and entropy of activation of dehydration are 27 kcal/mole, 10 kcal/mole, and -45 eu respectively. The enthalpy and entropy of dehydration were found to be 9.1 kcal/mole and +22.2 eu respectively. Equipment for making

dilatometric measurements that will permit converting these weight losses into volume changes is being assembled and tested.

The kinetics of shrinkage during the calcination of crushed, compacted (–400 mesh) thoria gel at temperatures between 600 and 1100°C could not be correlated either with previous shrinkage data for large gel fragments or with any of the rational sintering models, probably because of superposition of intra- and interparticle sintering. Sintering of crushed, compacted thoria gel after the ultrafine fraction had been removed gave results consistent with a grain-boundary-diffusion model.

Initial grain-growth studies in thoria gels being calcined at temperatures between 1000 and 1120°C show erratic growth and breakdown of large grains before the onset of normal grain growth. The activation energy for normal grain growth is 35.6 kcal/mole.

Infrared spectroscopy of thoria gels that have been predried at 225°C in vacuum suggests that all water except surface hydroxyls is removed by this treatment and that possibly about 20% of the surface hydroxyls are removed. Three O–H stretching frequencies are found for the thoria gel in this condition, one corresponding to free, individual O–H groups and the others to hydroxyls in some form of association. Further work to characterize the surface hydroxyls and adsorbed water is under way; deuterium oxide, alcohols, and ammonia adsorbents are being used.

Experimental Work

The shrinkage of crystalline sol-gel-type thoria gels at temperatures below 600°C has been shown to be a dehydration process whose weight loss was fitted to the equation

$$\ln \left(\frac{w_0}{w_0 - \Delta w} \right) = \frac{kT}{h} (e^{-\Delta F^\ddagger / RT}) t ,$$

where ΔF^\ddagger is the activation free energy of dehydration, 27 kcal/mole,

k = Boltzmann's constant,

h = Planck's constant,

R = the gas constant,

t = time,

T = absolute temperature,

w_0 = original sample weight, and

Δw = change in sample weight at time t .

The enthalpy and entropy of activation were found to be 10 kcal/mole and –45 eu respectively. The enthalpy and entropy of dehydration, derived from equilibrium water vapor pressure over the gel, were +9.1 kcal/mole and +22.2 eu respectively. This weight-loss data will be converted to volume change when the dilatometric studies are made.

Sintering of Thoria Gels at Temperatures Between 600 and 1100°C. – Attempts to reproduce the sintering behavior of single thoria-gel particles using compacts of crushed gel yielded data that did not correlate with any known single-mechanism sintering model. The very high percentage of particles less than 1 μ in size in the –400-mesh gel powder of the crushed gel compacts leads to the belief that intra- and interparticle sintering were being superimposed in the gel-shrinkage data for the compacts. By using a –100 +400-mesh particle size cut for making compacts, it was possible to confirm that the earlier anomalous results were due to the presence of ultrafine particles, which promoted significant interparticle sintering. With the larger-particle-size cut, the isothermal shrinkage rate became consistent with a grain-boundary-diffusion sintering model.

Initial Grain-Growth Studies of Thoria Gel. – Thoria gel calcined in nitrogen at temperatures from 860 to 1000°C shows the normal grain-growth pattern characteristic of small grains that increase steadily in size. Between 1000 and 1120°C, however, an erratic growth of large grains which subsequently break down into smaller grains was observed. Figure 16.7 shows electron micrographs of replicas of gel fracture surfaces which show this anomalous pattern of grain growth. Pre-calcination temperature, precalcination time, and calcination atmosphere were found to influence this type of grain growth and breakdown. Under reducing conditions, more than one cycle of growth and breakdown could sometimes be observed in a single sample. Following this initial erratic growth pattern, normal grain growth ensued, with an activation energy of 35.6 kcal/mole for sintering at 1000 to 1100°C. It is thought that nitrate, which was detectable by infrared spectroscopy for samples calcined for as long as 30 min at 1000°C, may be related to the foregoing erratic behavior, or

PHOTO 69018A

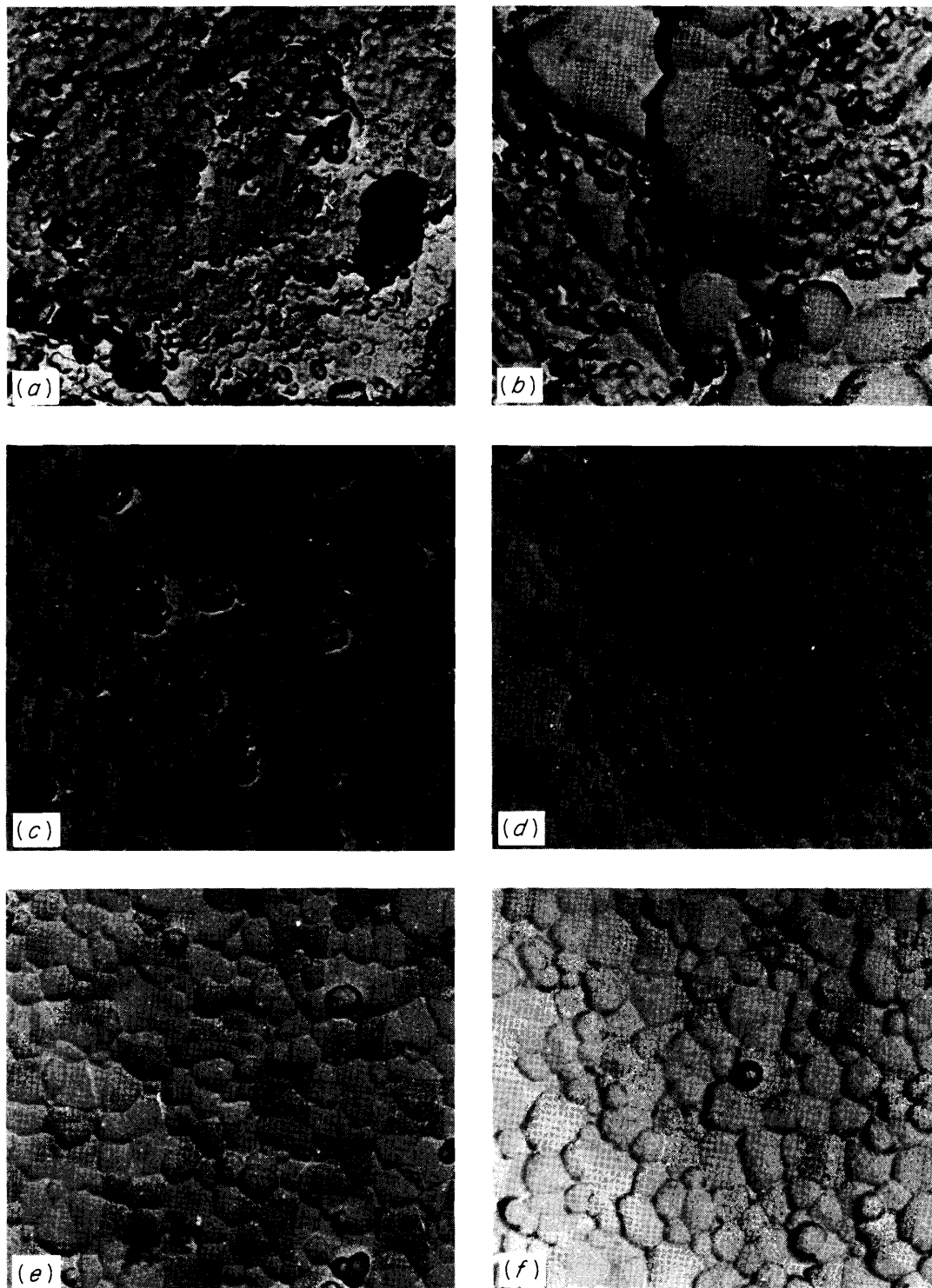


Fig. 16.7. Electron Micrographs of Thoria Fired in Nitrogen Atmosphere at 1122°C for (a) 5 min, (b) 15 min, (c) 30 min, (d) 60 min, (e) 90 min, and (f) 210 min. 28,000 \times .

perhaps large transient shrinkage stresses are involved.

Infrared Spectroscopy of Thoria Surfaces. — The primary goal of this work is to describe the chemical and physical state of the water and nitrate adsorbed on thoria gels. Other adsorbates being studied are deuterium oxide, methanol, and ammonia. Thoroughly wetted thoria gels show a broad adsorption band for O—H stretching, extending from 3800 to 2400 cm^{-1} . This band is resolved into three bands at 3735, 2650, and 3515 cm^{-1} upon heating the gel for 20 hr at 225°C. Use of the extinction coefficient of hydroxyls on silica gel ($10^5 \text{ cm}^2/\text{mole}$) to estimate the amount of hydroxyl on the thoria yielded 10 hydroxyls per 100 Å^2 , which is reasonably close to, but somewhat below, the value of 12.7 hydroxyls estimated for dihydroxy thorium surface sites in the (100)

crystal face. Additional reversibly sorbable water could be removed by heating to 450°C in vacuum, but complete dehydration was not achieved. Shifts in band intensities with degree of hydration and of band frequencies upon exchange of the surface hydroxyl with deuterium oxide suggest that some surface hydroxyls are comparatively isolated from neighboring hydroxyls and that some are associated in clusters. Adsorption of ammonia on a partially denitrated thoria surface led to absorption bands at 2910, 2820, 2790, and 1110 cm^{-1} . The bands correspond neither to ammonia nor to ammonium ion, and heating the sample to 245°C does not remove all the ammonia. These data suggest that the ammonia may have undergone relatively strong chemisorption on the thoria, perhaps forming a coordination compound with the thorium ions on the surface.

17. Assistance Programs

The Chemical Technology Division provided assistance to others on several projects. The Eurochemic Assistance Program was continued. Under this program, the Laboratory is coordinating the exchange of information between Eurochemic and the various AEC sites and is currently supplying the U.S. Technical Advisor to Eurochemic during the construction and startup periods. The Division continued to supply technical liaison between the Laboratory, the AEC, and the construction and cost-plus-fixed-fee contractors for the High Radiation Level Analytical Laboratory. Consultation on construction of the two plant-waste-improvement projects was continued. Assistance on alpha-laboratory design included the preparation of two design studies for a 32-laboratory Alpha Laboratory Facility. Engineering assistance was provided the Health Physics Division on two large experiments: disposal of intermediate-level radioactive waste by hydrofracturing and disposal of high-level radioactive waste in salt. To provide additional ^{233}U storage space in Building 3019, the design and installation of a facility for storing 400 kg of ^{233}U as uranyl nitrate solution were completed. A facility for testing combinations of absolute filters and charcoal beds in the Nuclear Safety Pilot Plant was designed and is being installed. Advanced shielding codes were used to calculate the gamma and neutron radiation dose rates from fission sources through shields of concrete, water, CH_2 , and mixtures of H_2O or CH_2 with lead, iron, and boron up to 150 cm thick. Irradiation-contamination-decontamination evaluations were made on selected protective coatings and plastics.

17.1 EUROCHEMIC ASSISTANCE PROGRAM

The Laboratory continued to coordinate the Eurochemic Assistance Program for the exchange

of information between Eurochemic and the several AEC sites included in the program. In addition, the Laboratory is supplying the services of the U.S. Technical Advisor, E. M. Shank, who will remain at Mol, Belgium, during the construction and startup phases of the Eurochemic plant.

During the past year, 493 USAEC-originated documents and 89 drawings and miscellaneous items of information were sent to Eurochemic. Ten Eurochemic documents written in English were received, reproduced, and distributed. In addition, one Eurochemic report and eight Saint Gobain design reports written in French were translated, retyped, reproduced, and distributed.

R. Rometsch, formerly Research Director and Acting General Manager, was appointed General Manager of Eurochemic. It appears from present construction progress that cold testing of the last process units (solvent extraction) can begin by January 1966 and that the Eurochemic plant may start hot operation near the end of 1966.

17.2 PROJECTS FOR IMPROVING ORNL WASTE SYSTEMS

The Chemical Technology Division continued to provide consultation to the General Engineering and Construction and the Operations Divisions on several projects for improving ORNL waste systems. The recently completed low-level waste (LLW) and intermediate-level waste (ILW) collection and transfer systems in Melton Valley were put into service in November 1964, when about 5000 gal of ILW from the Nuclear Safety Pilot Plant was received into the central ILW collection tanks in Melton Valley. The LLW system was tested by transferring water from the High Flux Isotope Reactor waste ponds to the emergency impoundment basin and to the LLW treatment plant. The Molten Salt Reactor Experiment

facility and the Transuranium Processing Plant are scheduled to be connected to the Melton Valley waste systems during 1965.

Installation of piping and equipment for the ILW evaporator, Building 2531, was 70% complete when this work was stopped January 1, 1965, because of a delay in delivery of the two stainless steel, water-cooled, 50,000-gal high-level-waste storage tanks to be housed in the evaporator facility. Because the sampling room for the entire facility will be situated above the storage-tank vault, the evaporator cannot be operated until the vault has been sealed. The tanks were received and installed in the vault in March, and work on the project was resumed on April 5. The project is scheduled for completion by December 31, 1965. A request for \$1,825,000 (a \$125,000 increase) has been submitted for the evaporator and storage tanks and for the Melton Valley waste systems. The original request was for \$1,700,000.

Criteria were prepared by the Chemical Technology Division, and a design study and cost estimate were made by the General Engineering and Construction Division, for equipping the six 20-year-old central concrete waste tanks (W-5 through W-10) of the ILW system with an off-gas manifold and filter to the ORNL cell-ventilation system. This study resulted in detailed plans and specifications for providing a 500-cfm sweep of air at 0.30 in. (water gage) negative pressure through each tank and thence through filters to the central stack. The estimated cost is \$49,600; this might be reduced to less than \$40,000 by simpler plans. A recommendation that this project be completed was made to the Director of Radiation Safety and Control. Because these tanks now vent directly to the atmosphere in the center of the main ORNL area, fumes of organic solvents in aqueous waste tend to accumulate in tank W-5, and the radioactivity level of the other five tanks will increase tenfold when they become receivers of concentrate from the new ILW evaporator.

17.3 A DEMONSTRATION OF THE DISPOSAL OF SOLID, HIGH-LEVEL RADIOACTIVE WASTE IN SALT

Project Salt Vault, a Health Physics Division field demonstration of the disposal of high-level solid radioactive waste in a salt mine at Lyons,

Kansas, is scheduled to begin operation in September 1965. The engineering design and equipment development was coordinated in the Chemical Technology Division. Although all major items of equipment were designed and fabrication started last fiscal year, system improvements and ancillary devices were designed this year to ensure greater reliability and safety of the operations. The demonstration is unique in that radioactive materials are transferred from the shipping cask on the surface to the mine-floor storage area, 1000 ft below, without the use of hot-cell facilities. About 2,000,000 curies of activity will be transferred at six-month intervals over a two-year period.

A shielded waste transporter (Fig. 17.1), consisting of a standard two-wheel construction tractor coupled with a special trailer and radiation shield, was built, tested, disassembled, transferred into the mine, and reassembled. The shield will handle waste cylinders up to 12 in. in diameter and 9 ft long. The shield thickness is about 9 in. lead equivalent and weighs about 25 tons. The machine can be maneuvered with ease within the narrow confines of the mine and will allow precise placement of the solidified waste in the storage holes. In the current experiments, solid waste is simulated by two 90-day-cooled Engineering Test Reactor fuel elements hermetically sealed in a canister.

The fuel-element canister incorporates a mechanical- and a weld-seal design, either of which will pass the most rigid helium leak detection tests. Four thermocouples measuring the central plate temperatures of the fuel elements are provided by a special ribbon-type thermocouple assembly.

A shipping cask was modified and provided with water cooling to dissipate the 7 kw of heat from fourteen 60-day-cooled elements. Engineering tests were run to prove the design; electric heaters were used to simulate decay heat. Tests showed that the cask was capable of easily handling a 100% thermal overload. Two 24-hr tests were conducted without circulation of coolant and indicated that no damage to the cask or release of radioactive material should occur under these conditions. The hazards analysis was accepted and approved by the AEC and the Bureau of Explosives. A cold test of loading of the fuel at Idaho showed that no major difficulty would be involved in remote welding of the canister closure.

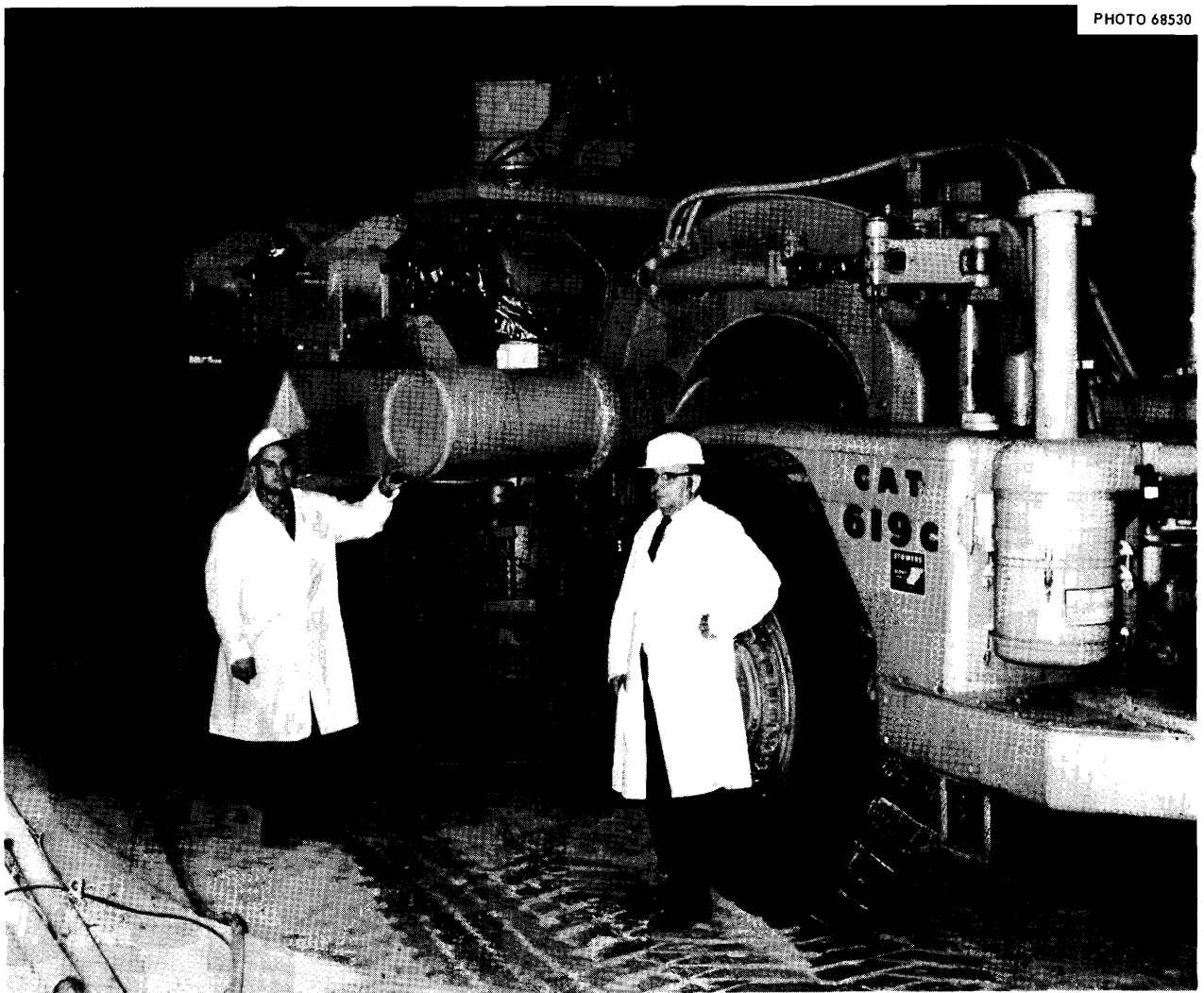


PHOTO 68530

Fig. 17.1. Shielded Waste Transporter for Carrying Solid Radioactive Waste Containers in Project Salt Vault.

Several design changes in the cask and canister were made to simplify hot-cell loading operations.

17.4 DISPOSAL OF RADIOACTIVE WASTE BY HYDROFRACTURING

The Chemical Technology Division continued to supply engineering consultation and liaison to the Health Physics Division in the design, construction, and operation of a prototype hydrofracturing facility for disposing of aqueous intermediate-level waste in lower Melton Valley. The shale-fracturing experiment is designed to test a new

method for permanent disposal of intermediate-radioactivity-level waste solutions. This method consists of the mixing of the waste solution with cement and other additives and the injection of the resulting grout into a shale formation at a depth of 700 to 1000 ft below the surface. The injected grout forms a thin horizontal sheet several hundred feet across and irregular in shape. The grout then solidifies to fix the radioactive wastes in the formation. An injection facility was built, and a series of five injections was made in the spring of 1964 to test the operation of the equipment, the performance of the mix, and the underground behavior of the grout sheet.

Four inspection wells in the vicinity of the first series of waste injections were cored to a depth of 1000 ft. Samples of the several grout sheets recovered from the cores were analyzed to evaluate the mixes used in the various test injections. In addition, cores from these wells helped establish the geological features of the injection zone and supplied limited information on the underground dispersion of the grout sheets.

Unexpectedly, the grout sheets that formed during the injections were mostly south of the injection well; no grout sheets were found in the wells 100 ft north (N 100) and 125 ft northwest (NW 125) of the injection well, and the grout sheets from only two injections were found in the NE 125 well. Grout sheets from all five injections were found in the S 100 well. The grout sheets of all injections were essentially horizontal and parallel. Evidence of the formation of multiple grout sheets during a single injection was found only for injection 5 in well NE 125; in this well the grout sheet of injection 5 was found in four main layers within a vertical distance of about 2 ft.

An analysis of samples of the grout sheets indicated that the grout is denser and stronger than laboratory samples with an equivalent composition, that considerable underground mixing occurs between the grout injected early and the grout injected late, and that the amount of cement in a mix can be reduced (thereby reducing the cost) without adversely affecting the mix. Almost no escape of radioactive constituents occurred during the coring of the grout sheets of injections 5 and 4; no flow of water was observed from these grout sheets. A backflow of several thousand gallons of water containing a trace of ^{137}Cs was noted when the grout sheet of injection 3 was cored; this resulted from improper control of mixing during the injection, and subsequent separation of water from the grout. Even here, however, nearly all the injected radionuclides were retained.

The injection facility was modified to incorporate changes in the mix-proportioning equipment so that mixes with lower ratios of cement to waste could be handled. A mass flowmeter, a device that continuously weighs the flow of solids, was installed on the solids feed stream, and a liquid flowmeter was installed on the waste stream. Signals from these instruments are

integrated to give a direct reading of the ratio of solids to liquid.

Several types of explosive charges were satisfactorily tested in an abandoned well to evaluate the feasibility of using these charges to slot the casing of the injection well before each injection.

An injection of 100,000 gal of waste solution was made to evaluate the behavior of a mix containing relatively little cement (a cheap mix), to evaluate the plant modifications for controlling the proportioning of mix and waste solution, and to further evaluate the use of explosive charges to slot the casing of the injection well. Cores will be obtained from the grout sheet of injection 6 to aid in evaluation of the mix. Following this, the facility will be modified for use in the regular disposal of Laboratory waste.

17.5 CONSTRUCTION AND STARTUP OF THE HIGH RADIATION LEVEL ANALYTICAL LABORATORY

The High Radiation Level Analytical Laboratory (HRLAL) has been in continuous operation since December 1964. Consultation and liaison to the Analytical Chemistry Division by the Chemical Technology Division were continued during the startup period. All H. K. Ferguson Company construction and all ORNL installation and modification work were completed in February 1965. The Ferguson construction during the past year consisted primarily of the installation of radioactive and process waste drains, a new road around the building, a stack-area fence, and winterizing improvements to the cooling towers. The ORNL installation and modification work consisted of the installation of cell manipulators, stack and liquid-waste monitors, health physics instrumentation, absolute filters, etc.; topsoiling and seeding of the construction site; and performing numerous miscellaneous modifications to operating equipment and instrument systems. All the Ferguson and most of the ORNL work was performed under the HRLAL construction directive (CL-256). Other significant accomplishments for the year included: (1) setting up of a programmed maintenance schedule for all building and process equipment, (2) training of operating personnel, (3) preparation of numerous operating procedures and emergency procedures, (4) procurement of

replacement equipment and spare parts for critical process equipment, and (5) the preparation of data sheets for routine operation and inspection.

17.6 HIGH-LEVEL ALPHA LABORATORY

Preliminary design and cost evaluation studies for a high-level alpha laboratory were continued and have culminated in the preparation of a budget submission. The laboratory, which will be administered by the Analytical Chemistry Division, is estimated to cost about \$5,000,000. It will be located in Melton Valley and will occupy an area of about 45,000 ft². In addition to office, service, and cold-laboratory support facilities, the building will contain twenty-eight 16- by 32-ft alpha laboratories and a 32- by 64-ft high-bay area, providing analytical, chemical, metallurgical, and chemical engineering facilities with capabilities for handling up to 100 curies of ²³⁹Pu equivalent and a lesser amount of alpha-gamma- or alpha-neutron-emitting materials.

At the request of management, alternative designs were evaluated; these include subdividing the integrated facility into two parts and attaching each as additions to the High Radiation Level Analytical Laboratory (Building 2026) and the Thorium-Uranium Fuel Cycle Development Facility (Building 7930). It was concluded that this alternative would result in too much duplication of facilities and that the overall cost would be considerably higher than for an integrated facility.

17.7 STORAGE FACILITY FOR ²³³U, BUILDING 3019

Since ORNL now serves as a national storage and dispensing agency for reactor-produced ²³³U nuclear fuel, expanded and improved storage, purification, and handling facilities were added in Building 3019 to better discharge this responsibility. Five conventional cylindrical storage tanks with a nominal capacity of 250 gal each (3 ft in diameter and 5 ft long) have been installed in the pipe tunnel to store ²³³U as nitrate solutions.

The separate tanks permit the storage of ²³³U solution according to the level of ²³²U contaminant present, thereby allowing the more desirable low-²³²U-content material to be kept separate. Four hundred kilograms of ²³³U may be stored at

a critically safe concentration of 180 g of ²³³U per liter with 70% full tanks; presently, however, the concentration is being kept at a more convenient 100 g/liter.

The tanks are made of type 304L stainless steel and depend on the use of fixed nuclear poison, present in the form of borosilicate-glass Raschig rings, which fill each tank and the emergency catch pan underneath the tanks. The boron content and isotopic ratio of the glass are carefully specified; the B₂O₃ content must be between 11.8 and 12.8%, with the ¹⁰B-to-¹¹B ratio equal to 0.25. Thirty-one percent of the volume of the tank is occupied by randomly packed glass rings.

The storage tanks (Fig. 17.2) are unit-shielded by 4 in. of lead and are located in the 50-ft length of pipe tunnel opposite cells 3 and 4. They are separated from the rest of the pipe tunnel by concrete walls 3½ ft thick. Enough space remains for three and possibly four more tanks identical to those presently installed.

A 1-kg/day, single-cycle, two-column solvent extraction miniature facility was installed in an alpha-contained laboratory located in the Building 3019 gallery. This system augments the existing Thorex solvent extraction system, which can process 6 kg of ²³³U per day. The small-scale columns are of type 304L stainless steel, with a glass end, filled with 16-gage perforated pulse plates on ¼-in. spacing. Micro-bellows pumps supply controlled flows within the system up to 30 ml/min, and a rising-film evaporator capable of concentrating the final product to 200 g/liter is included. The first-cycle aqueous feed and raffinate tanks are unit-shielded with 4 in. of lead; it may also be necessary to lightly shield the extraction column.

Dry-solid storage-space capacity for ²³³U was increased to about 100 kg of ²³³U as an oxide encapsulated in welded aluminum cans. Eight additional storage wells, 5 in. in outer diameter and 12 ft deep, lined with 4-in. (iron pipe size) pipe, were drilled from the penthouse in Building 3019 into the dividing wall between cells 4 and 5. A similar set of nine holes 8 ft 3 in. long were put into the dividing wall between cells 3 and 4 the previous year.

During the past year, about 20 kg of stored ²³³U was separated from the radioactive daughters of ²³²U for designated AEC uses. The ²³³U inventory has been increased by the addition of

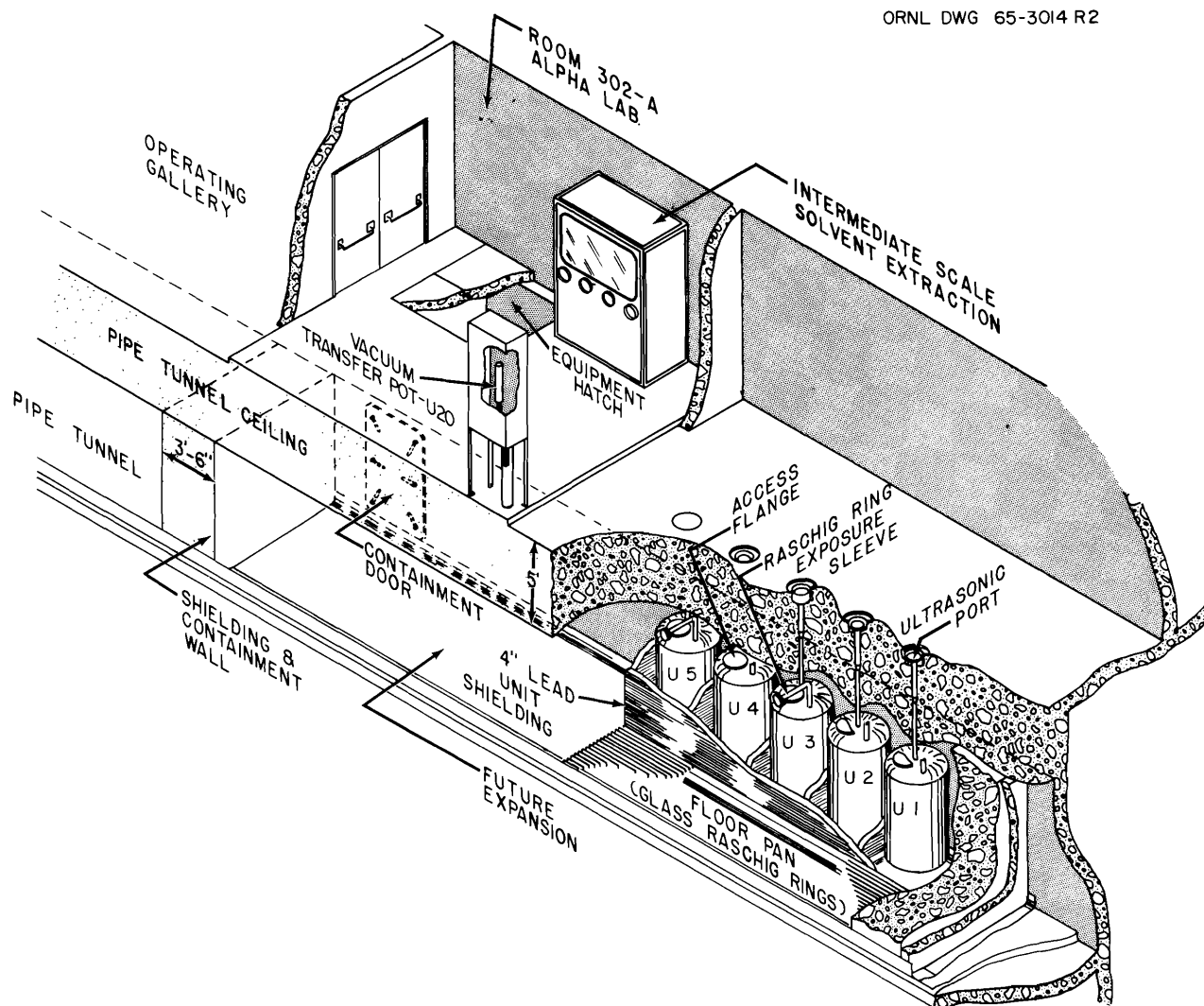


Fig. 17.2. Layout of ^{233}U Storage Facility, Building 3019.

40 kg containing 45 ppm of ^{232}U and 80 kg containing 200 ppm of ^{232}U . Prior to the new acquisitions, nearly 50 kg of ^{233}U with a ^{232}U content of 38 ppm was on hand.

17.8 FILTER TESTS IN THE NUCLEAR SAFETY PILOT PLANT

A system was designed and installed by the Chemical Technology Division for testing absolute-filter-charcoal-bed combinations in the Nuclear Safety Pilot Plant (NSPP) operated by the Reactor Division. Major components of the system include a Demister, absolute filter, and

a charcoal bed incorporated in a remotely removable canister (Fig. 17.3), a sealed compressor for gas circulation, and three May-pack samplers. The Demister is designed to remove entrained moisture from steam-air mixtures generated during reactor accident conditions. Calculations¹ indicate that its efficiency for removing 1- to 5- μ -diam droplets is greater than 99%. The absolute filter will remove radioactive particles larger than 0.3 μ in diameter, and the charcoal bed will remove elemental iodine and iodine compounds

¹A. H. Peters, *Application of Moisture Separators and Particulate Filters in Reactor Containment*, DP-812 (December 1962).

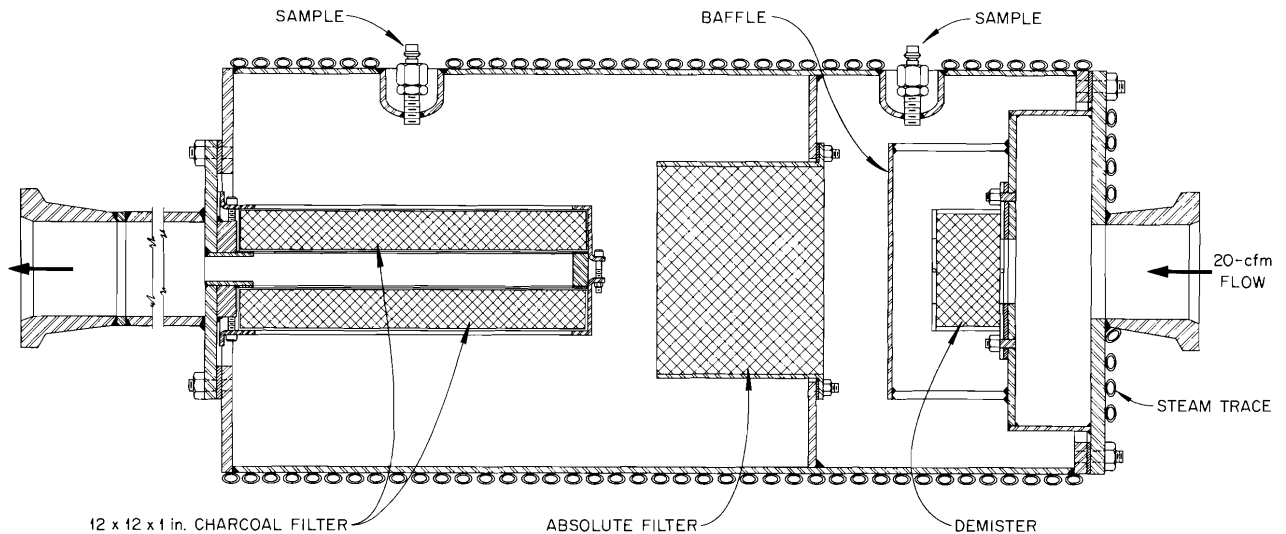


Fig. 17.3. Filter Canister for Filter Tests (Nuclear Safety Pilot Plant).

such as methyl iodide. Radioactive gases and particles for the NSPP tests will be generated by melting irradiated fuel elements with a plasma torch in a steam-air atmosphere. The system is designed for a flow of 20 cfm of steam and gas at 300°F and 50 psig pressure.

The Demister design is based on the work of Peters.¹ It contains a 2-in.-thick style 321 SR York Demister² mat of Teflon³ fibers (0.8 mil in diameter) woven together with stainless steel wires (6 mils in diameter). Velocities through the Demister will be up to 8 fps, and the pressure drop will be less than 1.0 in. H₂O. The absolute filter will be a circular Flanders style 7061R-q filter with aluminum separators and glass-fiber filter medium containing a binder to provide high wet strength. The pressure drop across a clean filter will be about 1.8 in. H₂O. Two Flanders 11-in.² charcoal beds packed with coconut-shell activated carbon (Pittsburgh, type PCB, -12 +30 mesh) will be used for the final cleanup stage in the canister. A standard chloropicrin test will be specified for the charcoal beds before delivery by the vendor.

²Registered trademark, O. H. York Co., Inc.

³Registered trademark, E. I. du Pont de Nemours and Co., Inc.

The compressor will be one designed and built by the Reactor Division for in-pile service. Impeller speeds up to 12,000 rpm will be obtained by varying the input power frequency externally with a variable-speed motor-generator set. This will eliminate the need for a bypass valve to control the flow through the system. The compressor will be positioned downstream of the canister, as shown in Fig. 17.4. Three May-pack samplers will be used for sampling the gases passing through the canister. Samples will be taken from the containment vessel to determine the system inlet conditions. Other sample points will include, downstream of the Demister, the absolute filter and the charcoal bed. Block valves will be provided for isolating the samplers from the canister and also for isolating the system from the containment vessel during periods when the filter-test equipment is not in operation.

17.9 STUDIES OF RADIATION SHIELDS FOR FISSION SOURCES

Calculations were made of the spatial radiation dose rates from point isotropic fission sources in various shield materials commonly used in cell walls, cell windows, and shipping casks. This

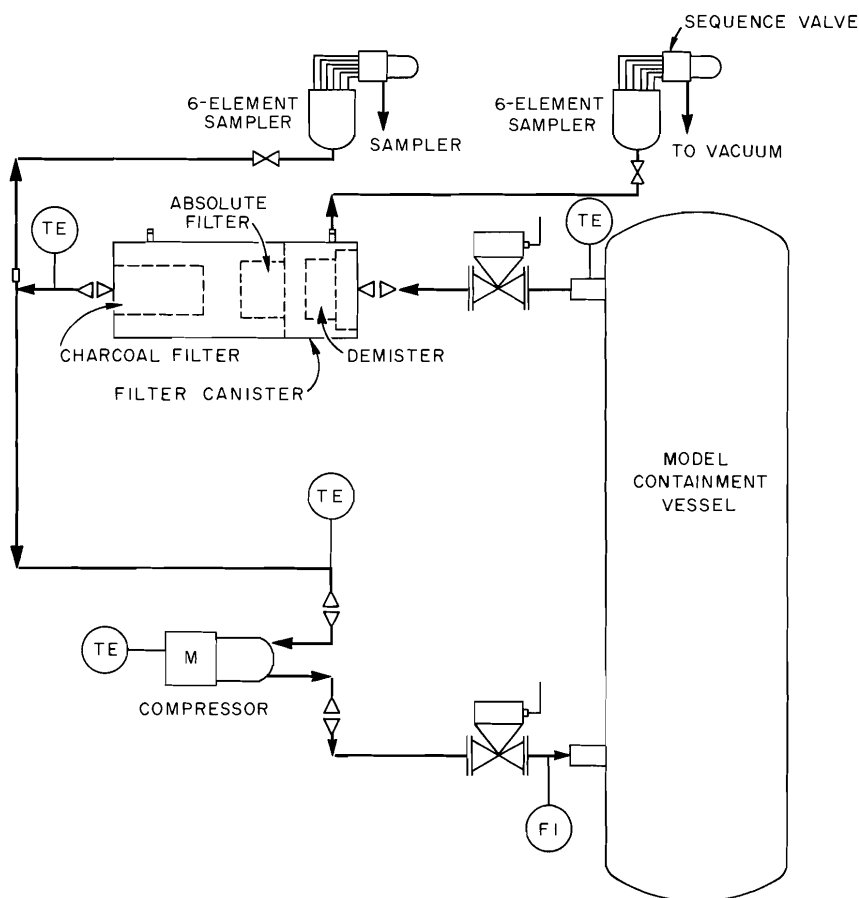


Fig. 17.4. Schematic Flow Diagram for Filter Tests (Nuclear Safety Pilot Plant).

work is an outgrowth of the study of advanced shield calculational techniques that was begun in support of the shield design of the Transuranium Processing Plant and radioisotope power sources for space applications. These data and the calculational techniques are directly applicable in our continuing design of shields for sources that emit neutrons from spontaneous fission.

The basic tools used in the shield analysis were an IBM-7090 computer and four codes for calculating the spatial distribution, energy spectrum, and dose from neutrons and photons: RENUPAK⁴ for fast neutrons, DTK⁵ for neutrons of low energy, SDC⁶ for primary gammas, and

SAGE⁷ for capture gammas. The effect of fission spectrum was explored, and dose rates were calculated for shields of water, CH₂ (paraffin, polyethylene, oil, etc.), mixtures of H₂O and CH₂ with other elements, and several concretes.

⁴J. Certainé, E. de Dufour, and G. Rabinowitz, *Nucl. Sci. Eng.* 12, 446 (1962).

⁵B. G. Carlson *et al.*, *DTF Users Manual*, UNC Phys/Math-3321 (1963).

⁶E. D. Arnold and B. F. Maskewitz, *SDC-A Shielding Design Code for Fuel Handling Facilities*, ORNL-3041 (in preparation).

⁷M. R. Fleishman, *A SANE-SAGE Users Guide*, UNUCOR-634 (1963).

Codes

RENUPAK solves the neutron transport equation in an infinite homogeneous medium using a moments method. In these calculations, point fission sources and spherical geometry were chosen, and the spatial moments were fitted exponentially to obtain the spatial energy-differential flux of neutrons having energies from 1 kev to 18 Mev in lethargy steps of 0.1. The elemental cross sections were obtained from the United Nuclear Corporation.

DTK is a one-dimensional multigroup program for solving the neutron transport equation by the S_n method. These calculations were made by using the S_4 approximation, spherical geometry, and 18-group cross sections. The spatial thermal-neutron flux and neutron capture rates were calculated by using a finemesh and initial flux guesses estimated from RENUPAK results.

SDC uses tabulated attenuation coefficients and buildup factors to evaluate the semianalytic shielding formulas for homogeneous shields. Nine energy groups were used to approximate the gamma source from fission, including prompt gammas and those from fission products at saturation.

SAGE is a Monte Carlo code for solution of the gamma transport problem in spherically symmetrical multilayer geometry. Splitting and "Russian roulette" are used for importance sampling. The spatial distribution of neutron captures from DTK results and published capture-gamma spectra⁸ were used as source input.

Effect of Fission Spectrum

Most of the basic calculations of neutron penetration in the shield materials were made by using the ^{235}U thermal-fission spectrum. These data were then used as a point of departure for other similar spectra. A comparison of the effect of the fission neutron spectrum on the fast-neutron dose rate in water and hydrous iron ore concrete is shown in Fig. 17.5. These dose rates from a unit point isotropic fission source were calculated with the RENUPAK code by using the Cranberg

⁸E. P. Blizard and L. S. Abbott, *Reactor Handbook, III B, Shielding*, p. 98, Interscience, 1962.

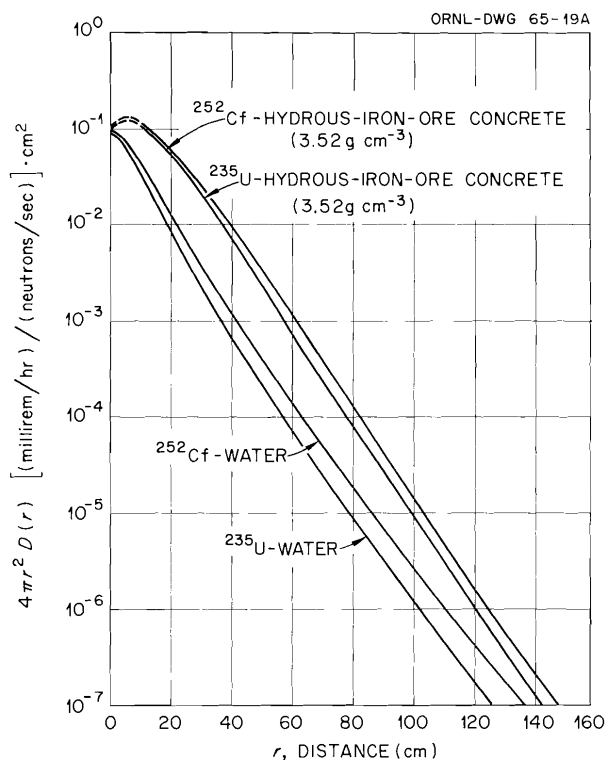


Fig. 17.5. Fast-Neutron Dose Rate in Water and Hydrous-Iron-Ore Concrete as a Function of the Distance from a Unit Point Isotropic Fission Source of ^{235}U and ^{252}Cf .

spectrum for ^{235}U and a similar fit of the ^{252}Cf spectrum. The spectra are:

$$\text{for } ^{235}\text{U}, N(E) = 0.453e^{-E/0.965} \sinh(2.29E)^{1/2},$$

$$\text{for } ^{252}\text{Cf}, N(E) = 0.373e^{-0.88E} \sinh(2.0E)^{1/2},$$

where $N(E)$ is the fraction of neutrons per unit energy range emitted in fission, and E is the neutron energy in Mev.

The fast-neutron dose rate at a distance of 125 cm in water is 2.5 times higher from the ^{252}Cf spectrum than from ^{235}U . At the same distance in the hydrous iron ore concrete, the dose rate from the ^{252}Cf spectrum is only 1.65 higher than from the ^{235}U spectrum. It is to be expected that the dose rate from the ^{252}Cf spectrum will tend to approach the dose rate from the ^{235}U spectrum in shields having appreciable quantities

of moderate to high atomic number elements, which have large inelastic scattering cross sections in the Mev region.

Water, CH₂, and Mixtures

The fast-neutron, primary-gamma, and capture-gamma dose rates and thermal-neutron flux in water and CH₂-5 wt % boron as calculated by the RENUPAK, DTK, and SDC codes are shown in Figs. 17.6 and 17.7. A ²³⁵U fission spectrum is assumed. In water, the capture-gamma rays are 2.23-Mev photons from capture in hydrogen. In the borated paraffin, the predominant gamma rays are the 0.478-Mev gamma from capture in ¹⁰B and the 2.23-Mev gamma from hydrogen. The calculated dose rates are sufficiently accurate for the shield calculations of interest based on the comparison (Fig. 17.6) of the calculated thermal-

neutron flux in water with the transformed experimental results reported by Trubey.⁹

Fast-neutron dose rates in CH₂ and mixtures of H₂O and CH₂ with other shield materials, as calculated with RENUPAK, are shown in Fig. 17.8. The hydrogenous shields with 50 vol % iron or lead are appreciably more effective than water in attenuating fission neutrons.

Concretes

The calculated spatial dose rate from fast neutrons and primary and capture gammas and the thermal-neutron flux in normal concrete (type H, Table 17.1) are shown in Fig. 17.9. Because of the relatively low density of normal

⁹D. K. Trubey, *Calculation of Fission-Source Thermal-Neutron Distribution in Water by the Transformation Method*, ORNL-3487 (1964).

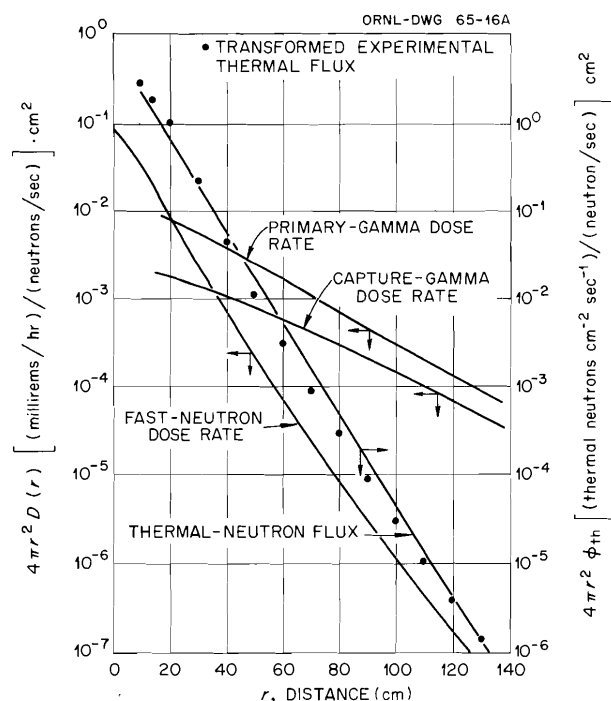


Fig. 17.6. Fast-Neutron, Primary-Gamma, and Capture-Gamma Dose Rate, and Thermal-Neutron Flux in Water as a Function of the Distance from a Unit Point Isotropic Fission Source of ²³⁵U.

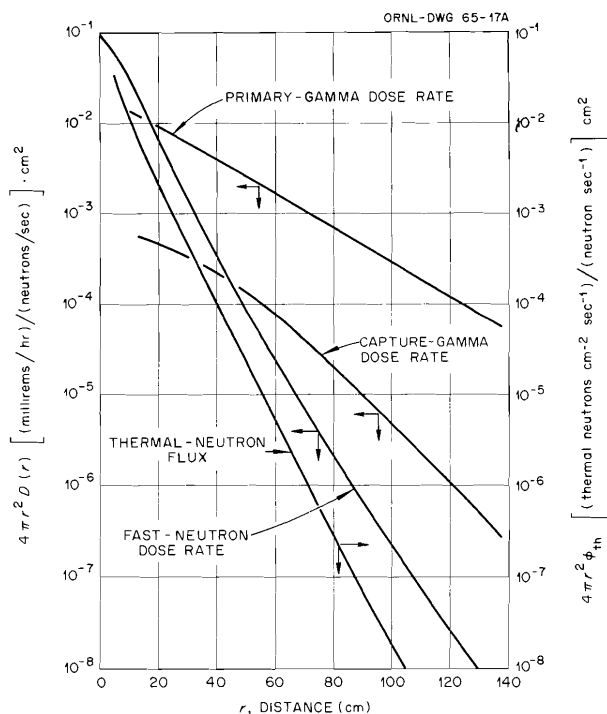


Fig. 17.7. Fast-Neutron, Primary-Gamma, and Capture-Gamma Dose Rate, and Thermal-Neutron Flux in CH₂-5 wt % Boron (Density 1.00 g/ml) as a Function of the Distance from a Unit Point Isotropic Fission Source of ²³⁵U.

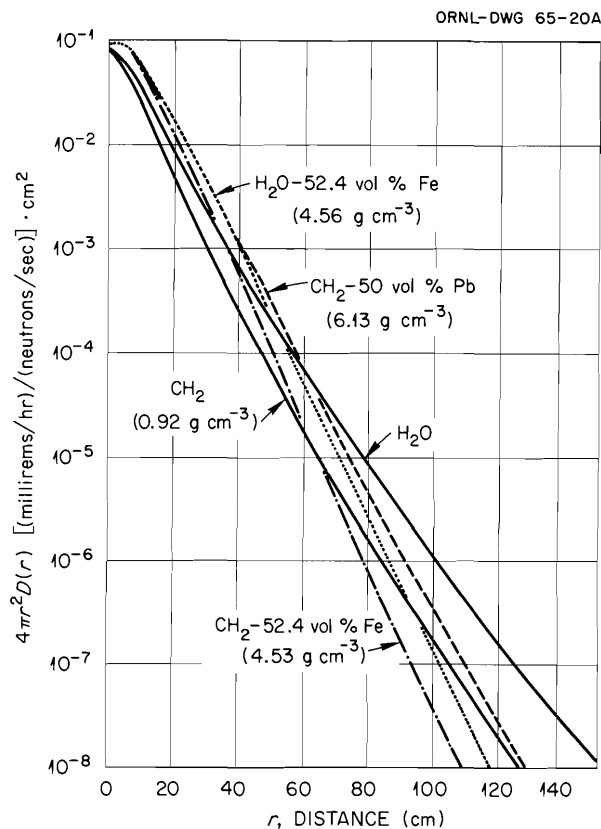


Fig. 17.8. Fast-Neutron Dose Rate in Various Hydrogenous Materials as a Function of the Distance from a Unit Point Isotropic Fission Source of ²³⁵U.

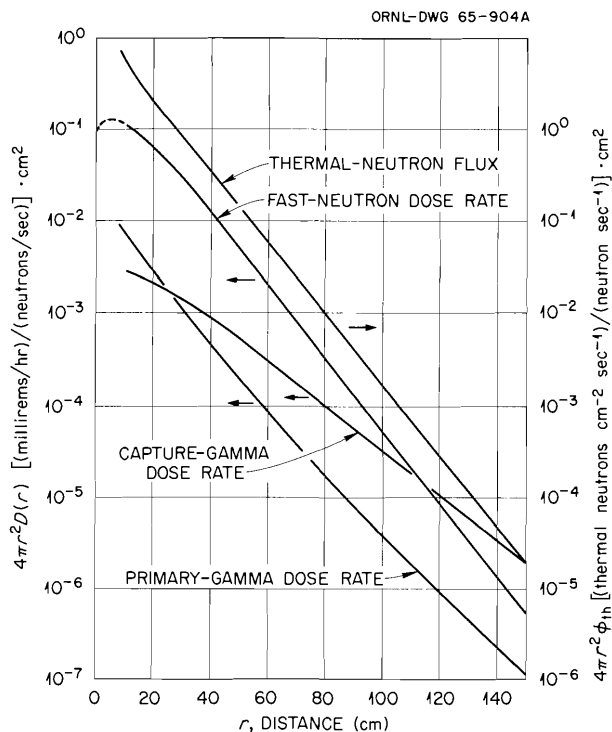


Fig. 17.9. Fast-Neutron, Primary-Gamma, and Capture-Gamma Dose Rate, and Thermal-Neutron Flux in Normal Concrete as a Function of the Distance from a Unit Point Isotropic Fission Source of ²³⁵U.

Table 17.1. Composition of Concretes Assumed for Shield Analysis

	Type of Concrete							
	A	B	C	D	E	F	G	H
	Hydrous Iron Ore	Hydrous Iron Ore	Hydrous Iron Ore	Hydrous Iron Ore	Limonite	Ferrophos-Serpentine	Magnetite-Serpentine	Normal
Elemental Density, g/cm ³								
<u>H</u> ^a	0.0215	0.0160	0.0108	0.00538	0.0370	0.0208	0.0122	0.0200
<u>O</u>	1.304	1.261	1.218	1.176	1.113	0.7805	1.180	1.116
<u>Fe</u> , Cr, Mn, V	1.960	1.960	1.960	1.960	1.189	1.355	1.181	
<u>Si</u> , Al, Mg, S, P	0.108	0.108	0.108	0.108	0.165	1.044	0.457	0.491
<u>Ca</u> , Ti	0.128	0.128	0.128	0.128	0.227	0.196	0.458	0.612
<u>C</u>								0.118
Total	3.522	3.473	3.425	3.377	2.731	3.396	3.288	2.357

^aCross sections for the underlined element were used in calculating the fast-neutron dose.

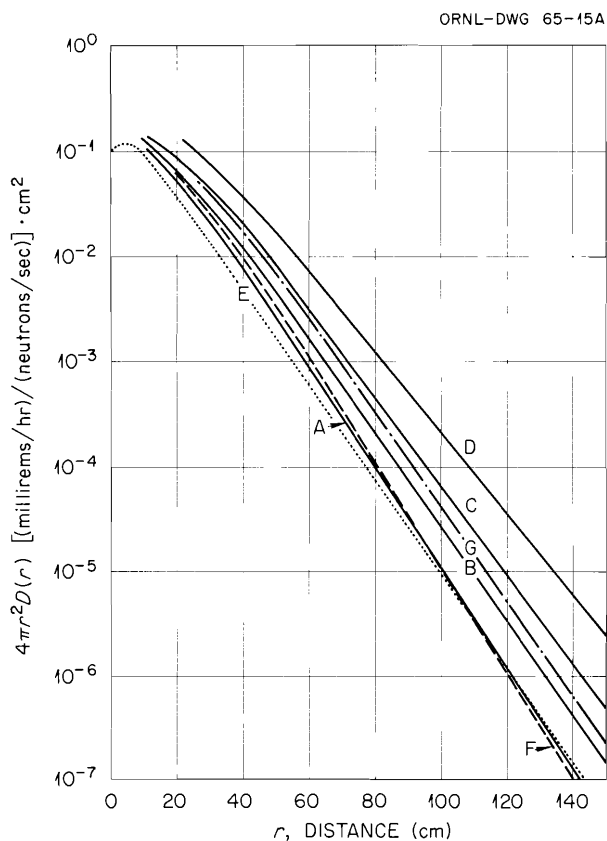


Fig. 17.10. Fast-Neutron Dose Rate in Various Concretes as a Function of the Distance from a Unit Point Isotropic Fission Source of ^{235}U .

concrete, capture gammas are the primary contributor to the total dose when the concrete thickness exceeds 110 to 120 cm.

The calculated fast-neutron dose rates in other concretes, of assumed composition given in Table 17.1, are shown in Fig. 17.10. The calculated fast-neutron dose rates are very dependent on the hydrogen content of the concretes, and, to a lesser extent, on the total density.

17.10 IRRADIATION AND DECONTAMINATION EVALUATION TESTS ON SELECTED PROTECTIVE COATINGS¹⁰

Protective coatings and other plastic materials were evaluated for radiation damage and decontaminability. A ^{60}Co gamma source supplied the radiation, and 3 M HNO_3 was used to clean

irradiated samples contaminated with a mixture of radioactive nuclides. The investigation was made primarily to evaluate various protective coatings for use in hot laboratories and fuel-processing facilities at ORNL, where they are used in hot cells, transfer areas, laboratories, and general service areas. The most severe exposure will be incurred by coatings on the concrete surfaces of hot cells, where they will be subjected to high radiation (alpha, beta, gamma, and neutrons) and periodic submergence in deionized water. The anticipated level of gamma radiation is from 10^4 to 10^5 r/hr and of neutron exposure from 4.2×10^4 to 2.1×10^5 neutrons $\text{cm}^{-2} \text{sec}^{-1}$. Some of the coatings must also withstand abrasion from heavy wheeled carts, etc., and the attack of cleaning reagents. Performance data on only some of the better coatings are reported here. Plastics (not coatings) were also tested for service in hot-cell areas where experimental chemical-process-development studies are conducted; data on these materials are reported elsewhere.¹⁰

Epoxy, modified phenolic, polyester, vinyl, and inorganic coatings were evaluated both in air and in deionized water to obtain comparative ratings after an exposure to ionizing radiation in a ^{60}Co gamma source at intensities from 0.9 to 2.08×10^6 r/hr. The results indicate that the epoxy, modified phenolic, and inorganic zinc protective coatings are more resistant to gamma radiation than the other generic types tested.

The vinyl coatings, although not as resistant to radiation as the epoxies, were more resistant than anticipated and should be useful in many applications, particularly since they display good decontaminability. A summary of the top-rated coatings for resistance to radiation is given in Tables 17.2 and 17.3. Table 17.2 gives data for use when the coatings are submerged in deionized water and Table 17.3 for exposure in air. The irradiation values given in the last column are the radiation levels at which the coatings were judged to have failed to provide a seal for the coated concrete or metal surface they were designed to protect.

The polyamid-cured epoxy coatings were more resistant to radiation than the other organic

¹⁰G. A. West and C. D. Watson, *Gamma Radiation Damage and Decontamination Evaluation of Protective Coatings and Other Materials for Hot Laboratory and Fuel Processing Facilities*, ORNL-3589 (February 1965).

Table 17.2. Gamma Irradiation Levels at Which 12 Epoxy, Modified Phenolic, and Vinyl Protective Coatings Failed when Immersed in Deionized Water

Trade Name	Manufacturer	Type	Irradiation
Tygoweld No. 54060	U.S. Stoneware Co.	Epoxy	4.81×10^9 r
No. 74-66 System ^a	Amercoat Corp.	Epoxy	4.78×10^9 r
Plasite 7155	Wisconsin Protective Coating Co.	Modified phenolic	4.5×10^9 r
No. 66-66 System ^a	Amercoat Corp.	Epoxy	$1.0-3.6 \times 10^9$ r
Coroline 505.2 ^a	Ceilcote Co.	Epoxy	$1.34-3.0 \times 10^9$ r
UC 9647 ^a	Pittsburgh Plate Glass Co.	Epoxy	2.33×10^9 r
UC 12168 ^a	Pittsburgh Plate Glass Co.	Epoxy	$1.83-2.33 \times 10^9$ r
Phenoline 368-300 System ^a	Carboline Co.	Modified phenolic	$1.02-1.14 \times 10^9$ r
Phenoline 300-302-300 System ^a	Carboline Co.	Modified phenolic	$1.02-1.14 \times 10^9$ r
Series A	David E. Long Corp.	Vinyl	8.79×10^8 r
86-99-99 System	Amercoat Corp.	Vinyl	6.9×10^8 r
86-33HB System	Amercoat Corp.	Vinyl	6.6×10^8 r

^aFiberglas-impregnated for structural strength.

Table 17.3. Gamma Irradiation Levels at Which 9 Epoxy, Modified Phenolic, Inorganic, and Vinyl Protective Coatings Failed when Irradiated in Air

Trade Name	Manufacturer	Type	Irradiation
No. 74-66 System ^a	Amercoat Corp.	Epoxy	$>1 \times 10^{10}$ r
No. 66-66 System ^a	Amercoat Corp.	Epoxy	$>1 \times 10^{10}$ r
Phenoline 368 System	Carboline Co.	Modified phenolic	$>1 \times 10^{10}$ r
Colma Protective Coating	Sika Chemical Co.	Epoxy	$>1 \times 10^{10}$ r
No. 1680 over Dimetcote No. 3	Amercoat Corp.	Inorganic	$>1 \times 10^{10}$ r
No. 86-99 System	Amercoat Corp.	Vinyl	6.6×10^9 r
Rustbond Primer No. 6C, Polyclad 933-1, Polyclad 1200-20 System	Carboline Co.	Vinyl	4.9×10^9 r
No. 38-88 System	Amercoat Corp.	Vinyl	4.38×10^9 r
Series A	David E. Long Corp.	Vinyl	4.28×10^9 r

^aImpregnated with Fiberglas.

coatings when immersed in deionized water. However, this ultimate resistance depends on the type and amount of fillers, additives, and anti-oxidants used, and the curing conditions. In general, all coatings tested were less affected

by radiation when exposed in air than when immersed in deionized water.

If a coating is reinforced with Fiberglas fabric, it is generally more resistant to radiation in water exposure and retains its resistance to im-

Table 17.4. Decontamination Factors Obtained from Irradiation-Contamination-Decontamination Tests with Four Protective Coatings

Trade Name	Manufacturer	Type	Total Decontamination Factor ($\times 10^3$)
RO-221 Primer, TP-216 Seal with a silicone release agent	U.S. Stoneware Co.	Vinyl	9.3
No. 66-66 System ^a	Amercoat Corp.	Epoxy	6.3
Nukemite 40	Amercoat Corp.	Vinyl	4.5
Rustbond 6C Primer, Polyclad 933-1, Polyclad 1200-20	Carboline Co.	Vinyl	3.6

^aImpregnated with Fiberglas.

compact better than an unreinforced coating. However, Fiberglas fabric does not appear to extend the useful life of a coating irradiated in air. On the other hand, dispersion of Fiberglas filler did not seem to improve a coating's resistance to gamma radiation in either water or air exposures. The color of the coating does not appear to affect its resistance to radiation. Light colors are useful for light reflection up to about 5×10^8 r of gamma radiation. Most of the vinyl coatings were more resistant to radiation in air than in previously reported tests.

To evaluate the decontaminability of the protective coatings, a solution of mixed fission products having a total activity of 0.86 to 3.0 r/hr was dried on the surface of each irradiated material

tested, and decontamination was done by flushing the contaminated spot with water, scrubbing it with 3 M HNO₃, and counting the residual radioactivity. The coatings were also evaluated by visual observation, physical comparison, and measurement by coating-evaluation instruments before and after the radiation-decontamination tests. The decontamination factors achieved in these tests for the four most decontaminable coatings are shown in Table 17.4. In general, the vinyl and glossy epoxy coatings were the easiest to decontaminate. Decontamination is accomplished best on (1) a hard, smooth, nonporous, and acid-resistant coating or (2) hard, nonporous undercoats with a seal coat that is easily removed by reagents.

removal of fission product poisons from the core. These are mandatory operations for a successful thermal breeder. Since fluoride salts have been selected as the most suitable fuel solvent, we have available to us, in attacking these problems, the maturing technology of fluorine chemistry and particularly our experience with the Molten-Salt Volatility Process.

A paper study and a preliminary cost estimate were made of a chemical processing plant for a 1000-Mw (electrical) Molten-Salt Breeder Reactor, which is to be a two-region system utilizing an LiF-ThF₄ (71-29 mole %) blanket and an LiF-BeF₂-UF₄ (about 68.5-31.2-0.3 mole %) fuel stream.¹ The study employed a new approach to chemical processing plant design by integrating the processing and reactor plants into the same physical structure to avoid duplication of services and facilities and to reduce operating costs. Processing of both streams will be carried on continuously to minimize the holdup of fissile and fertile materials. The entire plant for processing both fuel and fertile streams can be installed in two cells located adjacent to the reactor cell, having a combined area no greater than 1100 ft² and headroom of about 40 ft.

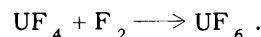
The most attractive process for the fuel salt consists of fluorination of the salt to remove the uranium, which is subsequently purified by sorption on NaF. The residual salt is processed by vacuum distillation to recover the LiF and BeF₂, concentrating fission products in the still bottoms. The fuel salt is reconstituted by continuously sorbing the UF₆ directly in the distillate. The blanket processing consists only in the removal of product uranium by fluorination, since the fission products will accumulate at a rate small enough to permit their economical removal by a purge stream. A schematic diagram of the major process steps is shown in Fig. 18.1.

An MSBR power station operating at 1000 Mw (electrical) would require a fuel stream processing rate of about 15 ft³/day and a fertile stream rate of 105 ft³/day. It is estimated that the fixed capital cost would be \$5,500,000 and that the direct operating cost could be \$604,000 per year.

¹C. D. Scott and W. L. Carter, *Molten Salt Breeder Reactor Fuel and Fertile Stream Processing*, ORNL-3791 (1965).

18.1 CONTINUOUS FLUORINATION OF MOLTEN SALT

Fluorination converts the uranium tetrafluoride in the salt to volatile hexafluoride according to the reaction:



Since some fission and corrosion products (Mo, Ru, Nb, Cr, Te, and Tc) also form volatile fluorides, the gases are passed through traps of MgF₂ and NaF pellets at 400°C. These sorbers retain the contaminants while passing UF₆, which is subsequently collected in a cold trap at -70°C for recycle to the reactor fuel stream.

Previous experience with batch fluorination of UF₄ in molten salt showed that nearly complete volatilization of UF₆ can be obtained at reasonable rates by sparging the salt with fluorine. The major problem associated with making this step continuous is corrosion, which appears preventable by use of a frozen layer of salt on the vessel wall or by use of gas-phase-continuous fluorination in which the salt is sprayed as droplets into fluorine gas.

Previous technology includes tests on a batch frozen-wall fluorinator in support of the molten-salt fluoride volatility process. Internal heat generation was provided by resistance heating, using nickel electrodes and 60-cycle ac power. This system was operable with gas flowing through an unheated line that entered the fluorinator at a point below the surface of the molten salt.

It should be noted that electrodes will not be necessary for a fluorinator operating on the fuel stream from an MSBR since adequate internal heat generation will be provided by decay of fission products in the salt.

For the reference 1000-Mw (electrical) reactor it was necessary to cool the fuel stream for 1.5 days to reduce the specific heat generation rate to 3×10^4 Btu hr⁻¹ ft⁻³ to facilitate temperature control.¹

To get adequate uranium recovery with reasonable fluorine utilization, countercurrent contact of the salt with the fluorine seems necessary, which logically suggests the use of a tower. The behavior of such a system is being explored in a 1-in.-diam nickel fluorinator having a salt depth of 48 in. and a salt feed tank with sufficient volume to maintain a salt flow of 20 ml/min for

an 8-hr period. Although this experimental unit corrodes rapidly, it will yield mass transfer data.

18.2 DISTILLATION OF MOLTEN SALT

The expensive ${}^7\text{LiF}$ and BeF_2 can be recovered from the fluorinated fuel salt semicontinuously by distillation. This approach was originally suggested by M. J. Kelly of the Reactor Chemistry Division, who demonstrated the feasibility of distillation.² The uranium-free salt may be fed continuously to a still pot that accumulates the less volatile fission products while the BeF_2 and ${}^7\text{LiF}$ are boiled off. Because the vapor pressure of BeF_2 is 100 times that of LiF , the still pot will contain little BeF_2 . At 1000°C , the still will operate at a pressure of about 1 mm Hg. The still bottoms will be discharged with a cycle time probably determined by the heat generation of the accumulated fission products.

Fission products ZrF_4 , SnF_2 , RbF , CsF , and CdF_2 are more volatile than LiF and will not be separated from the carrier salt by distillation; but the others, including the high-cross-section rare earths, are less volatile and can be separated.

The current experimental work has been directed toward the determination of the relative volatilities of the rare-earth fission products with respect to LiF . The relative volatility α_{AB} is defined as:

$$\alpha_{AB} = \frac{y_A/x_A}{y_B/x_B},$$

where A and B refer to two components, and y and x are the vapor phase and liquid phase mole fractions respectively. When component A is present in small quantities, the ratio of the mole fractions of B in vapor and the liquid approaches unity and

$$\alpha_{AB} = y_A/x_A,$$

and the relative volatility becomes a form of Henry's law constant. The lower the relative volatilities of the fission products with respect to LiF , the more effective will be the separation.

The experimental apparatus included a cold finger to condense the vapor phase in a small

vessel containing salt brought to the desired temperature and pressure (Fig. 18.2). This method had the virtue of being rapid and relatively simple and was capable of producing results accurate within a factor of 2. The success of the method was largely attributed to the fact that condensation was rapid enough to prevent any selection, while sufficient liquid phase was used so that its composition did not change appreciably. The fact that the major constituent was the more volatile worked to minimize the experimental error, which is thought to be in the same order as the analytical error.

The fission product contaminants of main concern are the rare earths. Of these, the ones that will be present in the largest amount or that will present the largest neutron loss are Nd, Sm, Pm, Pr, Eu, La, and Ce. Initial experimental tests have been made on all of these rare-earth fluorides except Pm. The results show that the average relative volatilities of the trivalent rare earths in LiF varied from 0.01 to 0.05 (Table 18.1). There appears to be a trend toward decreasing

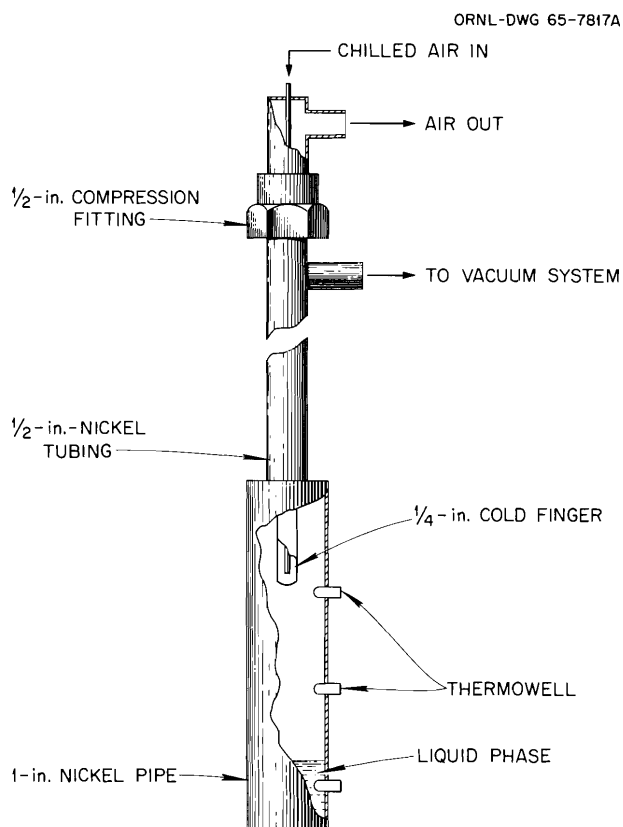


Fig. 18.2. Equilibrium Still with Cold Finger.

²W. R. Grimes, *Reactor Chem. Div. Ann. Progr. Rept.*, Jan. 31, 1965, ORNL-3789.

Table 18.1. Relative Volatilities of Rare-Earth Fluorides in Lithium Fluoride

Test No.	Rare-Earth Fluoride	Liquid Mole Fraction	Average Relative Volatility			
			900°C	950°C	1000°C	1050°C
1	CeF ₄	0.0067	0.133	0.167		0.208
2	SmF ₃	0.01	0.033			0.009
3	NdF ₃	0.01	0.025			0.016
4	PrF ₃	0.001		0.038	0.020	0.014
5	EuF ₃	0.001	0.041	0.037	0.028	0.012
6	CeF ₃	0.01	0.043	0.033		0.018
7	LaF ₃	0.001	0.035	0.024		
8	LaF ₃	0.01	0.051	0.027	0.011	0.008

relative volatility with increasing temperature. Cerium tetrafluoride showed a relative volatility of about 0.15. Scouting tests with CsF showed it to have a relative volatility somewhere between 6 and 16.

These results compare favorably with some of M. J. Kelly's data³ taken from a batch distillation test in which an MSRE-type salt was used, from which average relative volatilities of 0.05 and 0.02 for LaF₃ and SmF₃, respectively, were calculated.

These relative volatility values are high enough to warrant serious consideration of a rectification system.

18.3 RECONSTITUTION OF FUEL FOR A MOLTEN-SALT BREEDER REACTOR

Since the carrier salt and UF₆ are purified separately, they must be recombined for return to the reactor. Previous technology includes dry reduction in a tall column where the UF₆ and hydrogen are introduced into an H₂-F₂ flame to produce a dry UF₄ powder. Such a process would not be desirable here because of the difficulties in handling solids. An alternative that has been demonstrated by preliminary experiments to be feasible uses the simultaneous absorption and

reduction of UF₆ into a molten-salt phase containing UF₄. This could be carried out continuously in a column in which the barren salt and UF₆ are introduced at the bottom, along with some salt containing UF₄, which is recycled from the top. As the salt and UF₆ progress up the column, the UF₆ will be absorbed in the salt and be reduced to an intermediate fluoride, which is further reduced to UF₄ as it passes into a hydrogen reduction section. The introduction of hydrogen also provides the HF-H₂ sparging usually given to makeup salt and thus prepares it for return to the reactor after filtration.

Initial tests indicate that the sorption step is very rapid. It may be desirable, however, to keep the fluoride content of the intermediate fluoride below that equivalent to UF₅ to minimize corrosion.

Tests were made in a 4-in.-diam reaction vessel, the off-gas of which was conducted to two NaF traps: One trap was used only during UF₆ addition to the salt, and the other for collecting all other HF or UF₆. Three runs were made in which UF₆ was bubbled into 5320 g of ZrF₄, 863 g of LiF, and about 61.8 g of UF₄. At the operating temperature of 600°C, the molten salt depth in the vessel was 12 in.

After sparging the salt with nitrogen, UF₆ was introduced at a rate of 1.5 g/min for about 30 min. Material balances were obtained from samples of the molten salt and the traps. For the second and third runs, analyses of the sodium fluoride trap gave the amount of UF₆ that escaped absorption. It was concluded that complete absorption of the UF₆ had occurred, to the limit of detection.

Data on the oxidation state of the uranium after absorption are not conclusive, showing complete reduction to UF₄ during the first and second tests and the equivalent of 60% reduction of the UF₆ to UF₄ during the third. It is likely that reaction with the metal container was significant.

18.4 CHROMIUM FLUORIDE TRAPPING

Among the problems associated with the terminal recovery of the uranium from the fuel salt of the Molten-Salt Reactor Experiment (MSRE) is the separation of chromium fluoride from UF₆. The chromium, which will be present as a result of corrosion during fuel-salt treatment, will be volatilized as CrF₄ or CrF₅ when the salt is fluorinated with fluorine to produce UF₆. Packed beds

³M. J. Kelly, ORNL, unpublished data, May 21, 1965.

of pelleted NaF at 400°C have been found to effectively trap the chromium.

In each of eight tests, the chromium-containing gas stream was generated by bubbling fluorine through a 3-kg charge of nominal 38 mole % ZrF_4 -62 mole % NaF at 650°C to which had been added about 60 g of CrF_3 . The tests used gas rates of 0.4 to 0.9 std liter/min for 2 to 5 hr, during which time 11 to 20 g of chromium fluoride was volatilized. Three NaF beds having a diameter of $1\frac{1}{2}$ in. were used in series, giving a total bed length of 6 ft. Two types of NaF pellets were used: $\frac{1}{8}$ -in. cylindrical pellets obtained from the Harshaw Chemical Company, which had a surface area of $1\text{ m}^2/\text{g}$ and a void fraction of 0.45, and $\frac{3}{16}$ -in.-diam pellets produced at the Paducah Gaseous Diffusion Plant, which had a surface area of $0.074\text{ m}^2/\text{g}$ and a void fraction of 0.277. A maximum loading of 0.04 g of chromium per gram of NaF was observed for the Harshaw material, and a maximum loading of 0.136 g of chromium per gram of sodium fluoride was observed for the Paducah material. The chromium was concentrated near the external surface of the Harshaw pellets, but much deeper penetration was

found for the Paducah material. The loadings observed for the Paducah material are considered adequate for application in processing the MSRE fuel; however, the possibility of interaction of UF_6 with the CrF_5 -NaF complex should be explored. Typical profiles for the distribution of chromium on the sodium fluoride beds are shown for the two types of pellets in Fig. 18.3.

18.5 ALTERNATIVE PROCESSING METHODS FOR A MOLTEN-SALT BREEDER REACTOR

While the fluorination-distillation route to processing the fuel salt is attractive, it is recognized that there may be other schemes which are more direct and more economical.

The obvious alternative would be to remove the high-cross-section contaminants from the salt rather than vice versa. The suggested methods for effecting this can be grouped as follows: (1) exchange of the detrimental elements in the salt for innocuous ones in a fixed solid phase such as a refractory oxide or carbide; (2) controlled reduction either by an electrode or by a metallic reductant, with assimilation of the poisons into either the electrode or a separate molten metal phase; or (3) the use of reduction or the addition of a reagent to precipitate the poisons for removal by filtration. The potential simplicity of contacting a molten metal with the molten salt has led to serious exploratory work on the second method; however, insolubility of rare-earth-beryllium intermetallics has led to work in the third method, which couples attractive chemistry with the formidable engineering problem of collecting finely divided particles from the molten salt.

Referral to the standard free energies of formation at 1000°K of the fluorides of interest shows LiF to be the most stable with the lowest free energy. The alkaline-earth fluorides are next stable, and the rare-earth fluorides lie between the alkaline-earth fluorides and BeF_2 . Thorium and uranium fluorides come next, then zirconium, chromium, zinc, iron, and the metals of increasing nobility. From simple electrochemistry one would expect that to reduce the rare earths the uranium and beryllium must first be reduced. This picture can be altered by the formation of complexes or intermetallic compounds. It appears, however, that circumventing the reduction of uranium is so unlikely that removal by fluorination prior

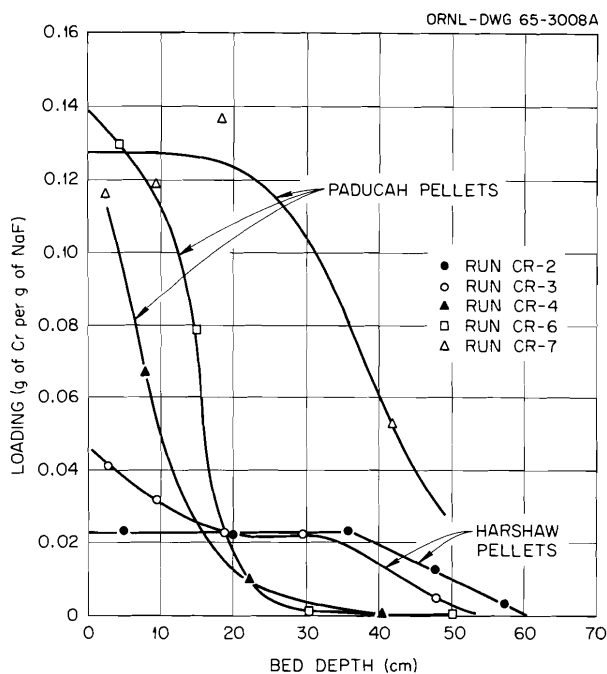


Fig. 18.3. Relation Between Chromium Loading and Distance for Sodium Fluoride Pellets Supplied by Harshaw Co. and Paducah Gaseous Diffusion Plant.

to subsequent treatment of the carrier salt is necessary.

Experimental extractions were made by melting about 6 g (3 ml) of 67-33 mole % LiF-BeF₂ containing "cold spikes" of La (0.7%), Gd (0.5%), and Sr (0.2%), together with an equal volume of the metal extractant in a mild steel or graphite crucible 0.6 in. in diameter and 3 in. long. A protective atmosphere of pure argon at 5 psig was provided in a containment vessel of nickel tubing 1 in. in diameter and 8 in. long, supported vertically and heated by a conventional split-tube electrical resistance furnace. The nickel vessel was shaken gently for a contact time of 12 to 90 min, then given about 30 to 60 min for settling, after which the two phases were allowed to freeze. The crucible was then sacrificed, and the salt and metal phases were broken apart, when possible, at the interface. In all cases, some cleanup of the blackened surfaces of each phase by filing and wire brushing was necessary prior to sampling.

The results from 11 such extractions (Table 18.2 show that only very strong reductants such as the Al-Mg-Sn metal or high-lithium-content alloys appeared successful. Closer scrutiny,

however, shows that, in each case, either an undesirable ion had been introduced into the salt or substantial reduction of beryllium had occurred. It was further observed that significant amounts of black particles accumulated at the interface for the most successful runs. This material was isolated in one case and identified as Be₁₃La. Subsequent study showed that all the rare earths and many other metals form intermetallic compounds of the form Be₁₃M, which are highly insoluble in either the salt phase or any metal phase tested.

A series of experiments exploring the utility of these compounds was made by contacting salts similar to those used in the metal extraction runs with powdered beryllium. From 60 to 90% of the trivalent rare earths were removed when the metal was present at 13 times the stoichiometric requirement (temperature: 550 to 600°C). Rare earths with a stable divalent state, such as europium, and the alkaline earths were not affected. Preliminary tests using lithium metal as a reductant indicate that this is a superior route to the formation of Be₁₃M precipitates. The solids formed are granular and are easily separated by either filtration or sedimentation.

Table 18.2. Liquid Metal Extractants for the Decontamination of Barren MSR Core Salt

Conditions: graphite crucibles, except where noted; argon atmosphere (1 ppm O₂) at 5 psig
Initial salt composition: Li₂BeF₄ containing 0.7 wt % La, 0.8% Gd, 0.2% Sr as fluorides

Run No.	Initial Alloy Composition (at. %)	Equilibrium Conditions		Loss of Beryllium Inventory to Metal Phase (%)	Distribution Ratio, $K_D = C_{\text{metal}}/C_{\text{salt}}$			Remarks
		Temperature (°C)	Time (min)		La	Gd	Sr	
1	81 Al-19 Li	700	35	0.22	1.7	1.1	0.008	Poor phase separation; alloy heterogeneous; $\rho_{\text{alloy}} \approx \rho_{\text{salt}}$
2	65 Al-35 Mg	650	12	0.05	3.3	1.7	0.11	Samples heterogeneous; $\rho_{\text{alloy}} \approx \rho_{\text{salt}}$
3	20 Al-20 Mg-60 Sn	580	50	0.60	10.0	5.0	5.0	Al, Mg, and Sn found in salt, 5% each; two alloy phases, Mg ₂ Sn found in each, K_D 's all same in each

Table 18.2.(continued)

Run No.	Initial Alloy Composition (at. %)	Equilibrium Conditions		Loss of Beryllium Inventory to Metal Phase (%)	Distribution Ratio, $K_D = C_{\text{metal}}/C_{\text{salt}}$			Remarks
		Temperature (°C)	Time (min)		La	Gd	Sr	
4	0.38 Ce-1.1 Li-98.5 Sn	560	80	2.0	6.6	5.9	0.056	$\rho_{\text{alloy}} > \rho_{\text{salt}}$; Be loss largely in interface crud; recoveries: 69% Ce, 88% La, 92% Gd, 52% Sr
5	3.5 Ce-10.5 Li-86 Sn	560	20	0.15	1.07	0.4	3.0	<500 ppm Sn in salt; recoveries: 6% La, 6% Gd, 88% Sr, 110% Ce
6	100 Sn	570	90	0.004	0.0007	0.0001	0.0004	Recoveries: 86% La, 99.8% Gd, 94% Sr
8	20 Li-80 Sn	510	64	0.004	0.05	0.01	0.01	<500 ppm Sn in salt
9	22 Li-78 Sn	660	65	0.040	1.6	0.5	0.2	Alloy filtered into salt; CeF_4 also in salt here, $K_D(\text{Ce}) = 0.5$; alloy heterogeneous; recoveries: 126% La, 72% Gd, 67% Sr, 142% Ce
10	50 Li-50 Sn	550	250	0.002	1.0	0.02	0.17	0.1% Sn in salt
11	50 Li-50 Sn	822	60	0.002	0.012	0.0016	0.53	2% Sn in salt; phase separation good; olive-colored surface deposit on alloy
12	50 Li-50 Sn	520	30	0.009	2.2	0.55	2.0	<500 ppm Sn in salt; alloy heterogeneous
13	70 Li-30 Sn	800	30	0.020	0.01	0.005	0.14	Mild steel crucible; recoveries: 82% La, 91% Gd, 70% Sr; some alloy dispersed in salt
14	99 Li-1 Sn	560	60	3.8	3.0	2.6	1.1	Mild steel crucible; $\rho_{\text{alloy}} < \rho_{\text{salt}}$
15	100 Li	550	20	~5	0.33-0.8	1-20	1.2	Mild steel crucible; low K_D results are for bulk metal, high ones for black interfacial crud; Be loss probably higher than in run 14 since Be_{13}La identified in dark salt by x-ray analysis

19. Water Research Program

Work by the Chemical Technology Division on the Water Research Program is reported directly to the Office of Saline Water, and only an abstract appears in this report (see the Summary).

Publications, Speeches, and Seminars

ASSISTANCE PROGRAMS

- Goeller, H. E., E. M. Shank, and W. M. Sproule, *List of Information Sent to and Received from the Eurochemic Co., January 1, 1964, Through June 30, 1964 (Categorized)*, ORNL-TM-685, Suppl. 2 (August 1964).
- Goeller, H. E., E. M. Shank, and W. M. Sproule, *List of Information Sent to and Received from the Eurochemic Co., July 1, 1964, Through December 31, 1964 (Categorized)*, ORNL-TM-685 (Feb. 26, 1965).
- Salmon, Royes, *A Computer Code (CDC 1604A or IBM 7090) for Calculating the Cost of Shipping Spent Reactor Fuels as a Function of Burnup, Specific Power, Cooling Time, Fuel Composition, and Other Variables*, ORNL-3648 (August 1964).
- Salmon, Royes, "Economics of Irradiated Fuel Shipments," *Chem. Eng. Progr. Symp. Ser.* **61**(56) (1965); presented at the American Institute of Chemical Engineers Meeting, Boston, Mass., Dec. 10, 1964.

WATER RESEARCH PROGRAM

- Coleman, C. F., "Properties of Organic-Water Mixtures. II. Solubilities and Activity Coefficients of Sodium Chloride and Potassium Chloride in N,N-Dialkylamides Containing Water," *J. Phys. Chem.* **69**, 1377 (1965).
- Thomas, D. G., "Forced Convection Mass Transfer. Part II. Effect of Wires Located Near the Edge of the Laminar Underlayer on the Rate of Forced Convection from a Flat Plate," to be published in *American Institute of Chemical Engineers Journal*.

RADIATION EFFECTS ON CATALYSTS

- Krohn, N. A., "The Design and Calibration of an 80 Curie ^{90}Sr Beta Irradiator," to be published in *Nucleonics*.
- Krohn, N. A., "The Effects of Radiation on Heterogeneous Catalysts," presented at Texas Women's University, Denton, Tex., Jan. 15, 1965.

CHEMICAL ENGINEERING RESEARCH

- Haas, P. A., and H. F. Johnson, "A Model and Experimental Results for Drainage of Solution Between Foam Bubbles," presented at the American Chemical Society National Meeting in Chicago, Aug. 30-Sept. 4, 1964.
- Ryon, A. D., and R. S. Lowrie, *Efficiency and Flow Capacity of Pulsed Columns Used for the Separation of Uranium from Thorium by Solvent Extraction with Di-sec-butylphenylphosphonate*, ORNL-3732 (January 1965).

Scott, C. D., "Analysis of the Combustion of Graphite-Uranium Fuels in a Fixed Bed or Moving Bed," presented at the American Chemical Society Meeting, Chicago, Aug. 31-Sept. 4, 1964.

Scott, C. D., and J. M. Holmes, *Emergency Environmental Control System for the Tunnel Grid Shelter*, ORNL-TM-1067 (Jan. 18, 1965).

CHEMICAL APPLICATIONS OF NUCLEAR EXPLOSIVES (CANE)

Bond, W. D., "Chemistry of the Recovery of Transplutonium Elements from Underground Nuclear Explosions in Rock Salt," presented at Tennessee Academy of Science, Memphis, Tenn., Nov. 27-28, 1964; to be published in *Journal of the Tennessee Academy of Science*.

Bond, W. D., *Production of Tritium by Contained Nuclear Explosions in Salt. II. Laboratory Studies of the Reduction of Alkaline Earth Sulfates by Hydrogen*, ORNL-3334, Part II (August 1964).

SEPARATIONS CHEMISTRY RESEARCH

Egan, B. Z., R. A. Zingaro, and B. M. Benjamin, "Extraction of Alkali Metals by Substituted Phenols," presented at 20th Southwest Regional Meeting of the American Chemical Society, Shreveport, La., Dec. 3-5, 1964.

Egan, B. Z., and R. A. Zingaro, "Extraction of Alkali Metals by Substituted Phenols," Research and Technology Concentrates of *Chem. Eng. News* 42(50), 39 (1964); presented, under the ORNL Traveling Lecture Program, at the University of South Florida, Tampa, Feb. 23, 1965, at Florida Atlantic University, Boca-Raton, Feb. 25, 1965; to be published in *Inorganic Chemistry*.

Egan, B. Z., R. A. Zingaro, and B. M. Benjamin, "Extraction of Alkali Metals by 4-sec-Butyl-2-(α -methylbenzyl)phenol (BAMBP)," to be published in *Inorganic Chemistry*.

CLASSIFIED

Culler, F. L., Jr., *Rover Annual Report*, ORNL-3627, Suppl. 1 (CONFIDENTIAL).

Culler, F. L., Jr., *Rover Report for May-June 1964*, ORNL-TM-934 (August 1964) (CONFIDENTIAL).

Culler, F. L., Jr., *Rover Report for July-August 1964*, ORNL-TM-975 (October 1964) (CONFIDENTIAL).

Culler, F. L., Jr., *Rover Report for September 1964*, ORNL-TM-986 (Oct. 30, 1964) (CONFIDENTIAL - UNDOCUMENTED).

Culler, F. L., *Rover Report for October-November 1964*, ORNL-TM-1046 (Jan. 21, 1965) (CONFIDENTIAL).

SOLVENT EXTRACTION TECHNOLOGY

Arnold, W. D., and D. J. Crouse, "Radium Removal from Uranium Mill Effluents with Inorganic Ion Exchangers," to be published in *Industrial and Engineering Chemistry*.

Arnold, W. D., D. J. Crouse, and K. B. Brown, "Solvent Extraction of Cesium (and Rubidium) from Ore Liquors with Substituted Phenols," to be published in *Industrial and Engineering Chemistry*.

Blake, C. A., "New Developments in Chemical Separations by Solvent Extraction," presented at Traveling Lecture No. 7, Savannah State College, Savannah, Ga., Nov. 10, 1964.

Blake, C. A., "Solvent Extraction Research at the Chemical Technology Division of the Oak Ridge National Laboratory," presented at the Chemical Engineering Division Seminar, Argonne National Laboratory, Argonne, Ill., Jan. 8, 1965.

- Coleman, C. F., "Amine Extraction in Reprocessing," International Atomic Energy Agency, *At. Energy Rev.* **2**(2), 3-54 (1964).
- Coleman, C. F., "Properties of Organic-Water Mixtures. II. Solubilities and Activity Coefficients of Sodium Chloride and Potassium Chloride in N,N-Dialkylamides Containing Water," to be published in *Journal of Physical Chemistry*.
- Horner, D. E., D. J. Crouse, K. B. Brown, and B. Weaver, "Recovery of Fission Products from Aqueous Solutions by Solvent Extraction," *Metallurgical Society Conference Series. Metallurgical Society of AIME, Unit Processes in Hydrometallurgy (Aqueous Purification), Dallas, Texas, February 25-28, 1963*, ed. by M. E. Wadsworth and F. T. Davis, Gordon and Breach Science Publishers, 150 Fifth Avenue, New York.
- McDowell, W. J., and C. F. Coleman, "Investigation of Possible Intermolecular Bonding in Some Mixtures of Phosphate Extractants by Use of Dielectric Measurements," presented at the Tennessee Academy of Science Meeting, Memphis, Tenn., Nov. 27-28, 1964.
- McDowell, W. J., and C. F. Coleman, "Sodium and Strontium Extraction by Di(2-ethylhexyl) phosphate: Mechanisms and Equilibria," presented at the 148th National American Chemical Society Meeting, Aug. 30-Sept. 4, 1964, Chicago, to be published in the *Journal of Inorganic and Nuclear Chemistry*.
- Myers, A. L., W. J. McDowell, and C. F. Coleman, "Degree of Polymerization of Di(2-ethylhexyl)phosphoric Acid and Sodium Di(2-ethylhexyl)phosphate in Wet Benzene by Differential Vapor Pressure Measurements," *J. Inorg. Nucl. Chem.* **26**, 2005-11 (1964).
- Roddy, J. W., and C. F. Coleman, "Activity Coefficients of Reference Solutes for Isopiestic Measurements in Organic Solutions," presented at Tennessee Academy of Science Meeting, Memphis, Tenn., Nov. 27-28, 1964.
- Weaver, B., and F. A. Kappelmann, *Talspeak: A New Method of Separating Americium and Curium from the Lanthanides by Extraction from an Aqueous Solution of an Aminopolyacetic Acid Complex with a Monoacidic Organophosphate or Phosphonate*, ORNL-3559 (August 1964).

PROGRESS REPORTS

- Bond, W. D., and J. W. Landry, *Chemical Applications of Nuclear Explosions (CANE) - Progress Report for July 1 to September 30, 1964*, ORNL-TM-963 (Oct. 5, 1964).
- Bond, W. D., and J. W. Landry, *Chemical Applications of Nuclear Explosions (CANE): Progress Report for October 1 to December 31, 1964*, ORNL-TM-1040 (Jan. 26, 1965).
- Brown, K. B., *Chemical Technology Division, Chemical Development Section C, Status and Progress Report on Separations Research and Development*, ORNL-3785 (April 1965).
- Burch, W. D., *Transuranium Quarterly Progress Report for Period Ending August 31, 1964*, ORNL-3739 (May 1965).
- Whatley, M. E., *Unit Operations Section Monthly Progress Report, June 1964, Chemical Technology Division*, ORNL-TM-936 (Sept. 23, 1964).
- Whatley, M. E., *Unit Operations Section Monthly Progress Report, August-September 1964, Chemical Technology Division*, ORNL-TM-1027 (March 1965).
- Whatley, M. E., *Unit Operations Section Monthly Progress Report, October 1964, Chemical Technology Division*, ORNL-TM-1069 (May 1965).
- Whatley, M. E., *Unit Operations Section Monthly Progress Report, February 1965, Chemical Technology Division*, ORNL-TM-1094 (May 1965).

POWER REACTOR FUEL PROCESSING

- Blanco, R. E., "Aqueous Reprocessing Chemistry for Irradiated Fuels. Proceedings of a Symposium, April 23-26, 1963," to be published in *Nuclear Science and Engineering*.
- Bradley, M. J., and L. M. Ferris, "The Effect of Phase Distribution on the Hydrolysis of Uranium Monocarbide-Dicarbide Mixtures," to be published in the *Journal of Inorganic and Nuclear Chemistry*.
- Bradley, M. J., and L. M. Ferris, "The Effect of Tungsten on the Hydrolysis of Uranium Dicarbide," *Inorg. Chem.* **4**, 597 (April 1965).
- Bradley, M. J., and L. M. Ferris, "Hydrolysis of Thorium Carbides Between 25 and 99°C," *J. Inorg. Nucl. Chem.* **27**, 1021 (May 1965).
- Bradley, M. J., J. H. Goode, L. M. Ferris, J. R. Flanary, and J. W. Ullmann, "Reactions of Reactor-Irradiated Uranium Monocarbide with Water and Aqueous Solutions of NaOH, HCl, and H₂SO₄," *Nucl. Sci. Eng.* **21**, 159 (1965).
- Bradley, M. J., and T. M. Kegley, Jr., "Correlation of Composition with the Microstructures of Arc-Cast Thorium Carbides," to be published in *Journal of the Electrochemical Society*.
- Bradley, M. J., Merle D. Pattengill, and L. M. Ferris, "Reactions of Thorium Carbides with Aqueous Sodium Hydroxide Solutions," to be published as a note in *Inorganic Chemistry*.
- Culler, F. L., Jr., et al., "Advances in Aqueous Processing of Power Reactor Fuels," presented at the Third International Conference on the Peaceful Uses of Atomic Energy, Geneva, Switzerland, Aug. 31-Sept. 9, 1964; to be published in the Proceedings.
- Ferris, L. M., *A Burn-Leach Process for Recovery of Uranium from Rover Fuel: Terminal Report of Laboratory Development*, ORNL-3763 (March 1965) (CONFIDENTIAL).
- Ferris, L. M., and M. J. Bradley, "Reactions of the Uranium Carbides with Nitric Acid," presented at the 149th National Meeting, American Chemical Society, Detroit, April 4-9, 1965; *J. Am. Chem. Soc.* **87**, 1710 (April 1965).
- Flanary, J. R., J. H. Goode, M. J. Bradley, J. W. Ullmann, L. M. Ferris, and G. C. Wall, *Hot-Cell Studies of Aqueous Dissolution Processes for Irradiated Carbide Reactor Fuels*, ORNL-3660 (September 1964).
- Flanary, J. R., J. H. Goode, M. J. Bradley, L. M. Ferris, J. W. Ullmann, and G. C. Wall, "Head-End Dissolution Processes for UC and UC-PuC Reactor Fuels," *Nucl. Appl.* **1**, 219 (1965).
- Flanary, J. R., J. H. Goode, A. H. Kibbey, J. T. Roberts, and R. G. Wymer, *Chemical Development of the 25-TBP Process*, ORNL-1993, Rev. 2 (October 1964).
- Gens, T. A., *Thermodynamic Calculations Relating to Chloride Volatility Processing of Nuclear Fuels. II. The Capacity of Chlorine for Transporting Plutonium Tetrachloride Vapor During Reaction of U₃O₈-PuO₂ with Carbon Tetrachloride*, ORNL-3693 (October 1964).
- Gens, T. A., and G. J. Atta, *Thermodynamic Calculations Relating to Chloride Volatility Processing of Nuclear Fuels. The Gas-Phase Reduction of Uranium Tetrachloride to the Trichloride with Carbon Monoxide*, ORNL-TM-829 (Apr. 22, 1964).
- Goode, J. H., *Changes in Uranium Isotopic Composition of Irradiated ThO₂-UO₂ Fuel Samples*, ORNL-TM-1024 (Jan. 4, 1965).
- Goode, J. H., and J. R. Flanary, *Dissolution of Irradiated, Stainless-Steel-Clad ThO₂-UO₂ in Fluoride-Catalyzed Nitric Acid Solutions: Hot-Cell Studies on Pelletized, Arc-Fused, and Sol-Gel-Derived Oxide*, ORNL-3725 (January 1965).
- Moore, J. G., J. H. Goode, J. W. Ullmann, R. H. Rainey, and J. R. Flanary, *Adsorption of Protactinium on Unfired Vycor: Initial Hot-Cell Experiments*, ORNL-3773 (April 1965).
- Nicholson, E. L., L. M. Ferris, and J. T. Roberts, *Burn-Leach Processes for Graphite-Base Reactor Fuels Containing Carbon-Coated Carbide or Oxide Particles*, ORNL-TM-1096 (Apr. 2, 1965).

- Nicholson, E. L., L. M. Ferris, and J. T. Roberts, "Burn-Leach Processes for Graphite-Gas Reactor Fuels Containing Carbon-Coated Carbide or Oxide Particles, presented at the EURATOM symposium on "Fuel Cycles of High-Temperature Gas-Cooled Reactors," Brussels, Belgium, June 10-11, 1965.
- Roberts, J. T., L. M. Ferris, E. L. Nicholson, R. H. Rainey, and C. D. Watson, "Reprocessing Methods and Costs for Selected Thorium-Bearing Reactor Fuel Types," ORNL-TM-1139 (May 14, 1965); presented at the International Atomic Energy panel on "The Utilization of Thorium in Power Reactors" at Vienna, Austria, June 14-18, 1965.

FLUORIDE VOLATILITY PROCESSING

- Bennet, M. R., G. I. Cathers, R. P. Milford, W. W. Pitt, Jr., and J. W. Ullmann, "A Fused-Salt Fluoride-Volatility Process for Recovering Uranium from Spent Aluminum-Based Fuel Elements," presented at the 148th American Chemical Society Meeting, Chicago, Sept. 3, 1964; to be published in *Industrial and Engineering Chemistry, Process Design and Development*.
- Carr, W. H., R. E. Brooksbank, S. Mann, and R. P. Milford, "Recovery of Uranium from Spent Zirconium-Based Reactor Fuels in the Oak Ridge Volatility Pilot Plant," presented at American Chemical Society Meeting, Chicago, Aug. 31-Sept. 4, 1964.
- Carter, W. L., and J. B. Ruch, *A Cost Estimate for Bulk Disposal of Radioactive Waste Salt from Processing Zirconium-Uranium Fuel by the ORNL Fluoride Volatility Process*, ORNL-TM-948 (Sept. 25, 1964) (CONFIDENTIAL).
- Katz, Sidney, "A Laboratory Evaluation of the Chemical and Physical Phenomena Associated with Cyclic Sorption-Desorption of Uranium Hexafluoride on Sodium Fluoride," presented at the American Chemical Society Meeting, Chicago, Aug. 31-Sept. 4, 1964.
- Katz, Sidney, "Use of High-Surface-Area Sodium Fluoride to Prepare $MF_6 \cdot 2NaF$ Complexes with Uranium, Tungsten, and Molybdenum Hexafluorides," *Inorg. Chem.* **3**, 1598 (1964).
- Mailen, J. C., "Volatilization of Uranium as the Hexafluoride from Drops of Molten Fluoride Salt," presented at the American Chemical Society Meeting, Chicago, Sept. 2, 1964.
- McNeese, L. E., and S. H. Jury, "Removal of Uranium Hexafluoride from Gas Streams by Sodium Fluoride Pellets," presented at the American Chemical Society National Meeting, Chicago, Aug. 31-Sept. 4, 1964.
- McNeese, L. E., and C. D. Scott, *Reconstitution of MSR Fuel by Reducing UF_6 Gas to UF_4 in a Molten Salt*, ORNL-TM-1051 (Mar. 11, 1965).
- Milford, R. P., *Proposed Design of a Fluidized-Bed Fluoride-Volatility Pilot Plant for Installation at Oak Ridge National Laboratory*, ORNL-TM-972 (Oct. 26, 1964).
- Youngblood, E. L., R. P. Milford, R. G. Nicol, and J. B. Ruch, *Corrosion of the Volatility Pilot Plant INOR-3 Hydrofluorinator During Forty Fuel-Processing Runs with Zirconium-Uranium Alloy*, ORNL-3623 (March 1965).

TRANSURANIUM ELEMENT PROCESSING

- Baybarz, R. D., "Alpha Radiation Effects on Concentrated LiCl-HCl Solutions and the Use of Methanol as an Inhibitor of Acid Loss," to be published in *Journal of Inorganic and Nuclear Chemistry*.

- Baybarz, R. D., "Dissociation Constants of the Transplutonium Element Chelates of Diethylenetriamine-pentaacetic Acid (DTPA) and the Application of DTPA Chelates to Solvent Extraction Separations of Transplutonium Elements from the Lanthanide Elements," to be published in *Journal of Inorganic and Nuclear Chemistry*.
- Baybarz, R. D., "Anion Exchange Separation of the Transplutonium Elements with Ethylenediamine-tetraacetic Acid (EDTA)," presented at the Symposium on the Chemistry of the Heavy and Other Artificial Elements, Detroit, Apr. 5-9, 1965.
- Burch, W. D., "The ORNL Transuranium Program," presented at Argonne National Laboratory, Argonne, Ill., Feb. 12, 1965.
- Mackey, T. S., *Development of an Air-Operated Metal-Diaphragm Pump for the Transuranium Processing Facility*, ORNL-TM-995 (Oct. 16, 1964).
- Yarbro, O. O., *TRU Disconnect Ferrule and Clamp Details*, ORNL-TM-1097 (May 1965).

WASTE TREATMENT AND DISPOSAL

- Blomeke, J. O., and J. T. Roberts, "Waste Management," to be published in *Annual Review of Nuclear Science*.
- Clark, W. E., L. Rice, and D. N. Hess, *Evaluation of Hastelloy F and Other Corrosion-Resistant Structural Materials for a Continuous Centrifuge in a Multipurpose Fuel-Recovery Plant*, ORNL-3787, (April 1965).
- Davis, W., Jr., P. S. Lawson, and H. J. deBruin, "Activities of the Three Components in the System Water-Nitric Acid-Uranyl Nitrate Hexahydrate at 25°C," presented at the 149th National Meeting of the American Chemical Society in Detroit, Apr. 4-9, 1965; *J. Phys. Chem.* **69** (July 1965).
- Davis, W., Jr., A. H. Kibbey, and E. Schonfeld, "Laboratory Demonstration of the Two-Step Process for Decontaminating Low-Radioactivity-Level Process Waste Water by Scavenging-Precipitation and Foam Separation," ORNL-3811 (in press).
- Davis, W., Jr., and H. J. deBruin, "New Activity Coefficients of 0-100 Percent Aqueous Nitric Acid," *J. Inorg. Nucl. Chem.* **26**, 1069-83 (1964).
- Holmes, J. M., *Survey of Nuclear Fuel Services, Inc., Waste Compositions*, ORNL-TM-1013 (Dec. 7, 1964).
- Milford, R. P., E. F. Stephan, L. K. Matson, P. D. Miller, and W. K. Boyd., "Cathodic Protection in Fused Fluoride Salts at 1200°F," presented at the NACE Conference, St. Louis, Mo., Mar. 15-19, 1965; to be published in *Corrosion*.
- Rainey, R. H., and A. Facchini, *The Separation of Long-Lived Fission Product Elements by Using Ethylenediaminetetraacetate in an Electrodialysis Cell*, ORNL-TM-1035 (Feb. 17, 1965).
- Schonfeld, E., "Effect of Impurities on Precipitation of Calcium," *J. Am. Water Works Assoc.* **56**(6) (June 1964).
- Schonfeld, E., and W. Davis, Jr., "Softening and Decontaminating Waste Water by Caustic-Carbonate Precipitants and Filtration in a Slowly-Stirred Sludge-Blanket Clarifier: Laboratory Development and Semi-Pilot-Plant Testing," submitted for publication in the *Journal of the Water Pollution Control Federation*.
- Schonfeld, E., *Equilibrium Constants and Concentrations in the Reactions of Nitrogen and Oxygen at 400° to 5000°K*, ORNL-TM-968 (Oct. 5, 1964).
- Schonfeld, E., A. H. Kibbey, and W. Davis, Jr., *Determination of Nuclide Concentrations in Solutions Containing Low Levels of Radio-Activity by Least-Squares Resolution of the Gamma-Ray Spectra*, ORNL-3744 (January 1965), presented at the Eighth Conference on Analytical Chemistry in Nuclear Technology, Gatlinburg, Tenn., Oct. 6-8, 1964.

- Schonfeld, E., A. H. Kibbey, and W. Davis, Jr., "The Determination of Nuclide Concentrations in Solutions Containing Low Levels of Radioactivity by Least-Squares Resolution of the Gamma-Ray Spectra," to be published in *Analytical Chemistry*.
- Schonfeld, E., "Improved Accuracy in Determination of Radionuclide Concentrations Containing Fast-Decaying Isotopes by Least-Squares Resolution of the Gamma-Ray Spectra," presented at the 1965 International Conference on Modern Trends in Activation Analysis, College Station, Tex., Apr. 19-22, 1965.
- Whatley, M. E., C. W. Hancher, and J. C. Suddath, "Engineering Development of Nuclear Waste Pot Calcination," *Chem. Eng. Progr., Symp. Ser.* **60**(53) (1964).
- Yee, W. C., and W. Davis, Jr., "Effects of Gamma Radiation on Cation Exchange Resin Under Simulated Processing Conditions," presented at the American Nuclear Society Winter Meeting, San Francisco, Nov. 30-Dec. 3, 1964; *Trans. Am. Nucl. Soc.* **7**(2), 446 (1964).

THORIUM FUEL-CYCLE DEVELOPMENT

- Chandler, J. M., and F. E. Harrington, *A Study of Sol-Gel Fuel Preparation Costs for SSCR and HTGR Reactors*, ORNL-TM-1109 (Apr. 8, 1965).
- Clinton, S. D., "Sol-Gel Process Studies," presented at the Chemical Engineering Division Seminar, Argonne National Laboratory, Chicago, Dec. 18, 1964, and at the Naval Research Reserve Company 6-3 at ORINS Science Teacher Training Building, Feb. 10, 1965.
- Clinton, S. D., "Engineering Design Problems for Irradiation of Nuclear Fuel Specimens," presented at the University of Cincinnati Graduate School Seminar, Cincinnati, Ohio, Mar. 11, 1965.
- Ferguson, D. E., O. C. Dean, and D. A. Douglas, "The Sol-Gel Process for the Remote Preparation and Fabrication of Recycle Fuels," presented at the Third International Conference on the Peaceful Uses of Atomic Energy, Geneva, Switzerland, Aug. 31-Sept. 9, 1964; to be published in the Proceedings.
- Helton, D. M., *A Survey of the Literature on Hydrated Actinide Oxide Sols and U(IV) and U(VI) Hydrolysis Reactions*, ORNL-TM-1052 (Feb. 5, 1965).
- Kelly, J. L., A. T. Kleinstaub, S. D. Clinton, and O. C. Dean, "Sol-Gel Process for Preparing Spheroidal Particles of the Dicarbides of Thorium and Thorium-Uranium Mixtures," to be published in *Industrial and Engineering Chemistry, Process Design and Development*.
- Nichols, J. P., R. E. Brooksbank, and D. E. Ferguson, "Radiation Exposures in Fabricating ²³³U-Thorium Fuels" (Revised), to be published in *Nuclear Applications*.
- Wymer, R. G., *Preliminary Studies of the Preparation of UO₂ Microspheres by a Sol-Gel Technique*, ORNL-TM-1110 (Apr. 19, 1965).

PROTACTINIUM CHEMISTRY

- Campbell, D. O., "Studies of the Behavior of Protactinium in Sulfuric Acid," presented at the Colloquium on the Physical Chemistry of Protactinium, Institute of Radium, Paris, France, July 1965.

MISCELLANEOUS

- Arnold, E. D., *Handbook of Shielding Requirements and Radiation Characteristics of Isotopic Power Sources for Terrestrial, Marine, and Space Applications*, ORNL-3576 (April 1964).

- Arnold, E. D., "Shielding Requirements and Radiation Characteristics of Isotopic Power Sources for Terrestrial, Marine, and Space Applications," presented at the 1964 Annual Meeting of the American Nuclear Society, San Francisco, Nov. 30, 1964.
- Blanco, R. E., H. W. Godbee, and J. M. Holmes, *Trip Report: TVA Fertilizer Plant at Muscle Shoals, Wilson Dam, Alabama*, ORNL-TM-1016 (Dec. 9, 1964).
- Blanco, R. E., *Production of Hydrogen, Fertilizer, and Other Industrial Chemicals in a Multipurpose Atomic Reactor Complex for Distillation of Sea Water*, Technology Seminar, ORNL-TM-1076 (Apr. 23, 1965).
- Davis, L. P., "Deposition of Submicron-Size Particles in Ventilation Ducts," presented at the International Symposium on Surface Contamination, Gatlinburg, Tenn., June 8-12, 1964.
- Guthrie, C. E., and J. P. Nichols, "Possibilities and Consequences of Major Accidents in Radiochemical Plants," presented at the American Nuclear Society Meeting, Philadelphia, June 14-19, 1964.
- Haws, C. C., "A New Process for Preparing Nuclear Reactor Fuel Elements," presented at the University of Cincinnati Graduate School Seminar, Cincinnati, Ohio, Mar. 11, 1965.
- Landry, J. W., "This Atomic World and Peaceful Nuclear Explosives," presented to the Traveling Exhibit Managers of the American Museum of Atomic Energy, Oak Ridge, Tenn., Aug. 17, 1964.
- Landry, J. W., "Project Plowshare," presented at U.S. Army Nuclear Science Seminar, Oak Ridge Institute of Nuclear Studies, Oak Ridge, Tenn., Aug. 18, 1964.
- Landry, J. W., "Project Plowshare and Its Mining Applications," presented at joint meeting of the Mining Engineers' Society, Minerals and Metallurgy Society, and American Nuclear Society at the University of Wisconsin, Madison, Sept. 30, 1964 (sponsored by the ORNL Traveling Lecture Program).
- Landry, J. W., "Project Plowshare, or How I Learned to Love the H-Bomb," principal address, presented at Eighth Conference on Analytical Chemistry in Nuclear Technology, Gatlinburg, Tenn., Oct. 6-8, 1964.
- Landry, J. W., "Scientific and Industrial Applications of Nuclear Explosives," presented at Thermo-nuclear Division Seminar, ORNL, Oct. 22, 1964.
- Landry, J. W., "Project Plowshare," presented at the Fifteenth Annual U.S. Navy Nuclear Sciences Seminar, Oak Ridge Institute of Nuclear Studies, Oak Ridge, Tenn., Nov. 30-Dec. 12, 1964.
- Landry, J. W., "Project Plowshare," presented to Oak Ridge Section of Institute of Electrical and Electronic Engineers, Oak Ridge, Tenn., Dec. 10, 1964.
- Landry, J. W., "The Peaceful Atom and Project Plowshare," presented to the Fountain City Methodist Men's Club, Knoxville, Tenn., Dec. 14, 1964.
- Landry, J. W., "Industrial and Scientific Uses of Nuclear Explosives," presented at the annual dinner meeting of the East Tennessee Chapter, Health Physics Society, Oak Ridge, Tenn., Jan. 16, 1965.
- Landry, J. W., "Practical Uses of Nuclear Explosives," presented to the Eaton Crossroads Ruritan Club, Eaton Crossroads, Tenn., Jan. 19, 1965.
- Landry, J. W., "Some Possible Industrial Applications of Nuclear Explosives," presented at the Chemical Technology Division Section-C Seminar, ORNL, Feb. 4, 1965.
- Landry, J. W., "Project Plowshare - The Research and Development Program on Peaceful Nuclear Explosives," presented at the Instrumentation and Controls Division Seminar, ORNL, Feb. 11, 1965.
- Landry, J. W., "Industrial Applications of Nuclear Explosives," presented at the Tennessee Valley Authority Experimental Gas-Cooled Reactor Seminar, Oak Ridge, Tenn., Feb. 23, 1965.
- Landry, J. W., "Industrial Applications of Nuclear Explosions and Waterway Developments," presented to the U.S. Naval Reserve, Knoxville, Tenn., Mar. 3, 1965.

- Landry, J. W., "Big Blasts for Big Business," presented to the Knoxville Chapter, Society for Advancement of Management, Knoxville, Tenn., Mar. 9, 1965.
- Landry, J. W., "Practical Uses of Nuclear Dynamite," presented to Lenoir City Rotary Club, Lenoir City, Tenn., Mar. 11, 1965.
- Landry, J. W., "Constructive Nuclear Explosives," an interview on *Areascope*, WBIR-TV, Knoxville, Tenn., Mar. 14, 1965.
- Landry, J. W., "Constructive Nuclear Explosives," presented to Knoxville Sertoma Club, Knoxville, Tenn., Mar. 24, 1965.
- Landry, J. W., "Into Plowshares and Spades," presented to Kingston Rotary Club, Kingston, Tenn., Mar. 30, 1965.
- Landry, J. W., Counseling and Plowshare literature was given to the Girl Scouts of America, Oak Ridge, Tenn., for a Plowshare science project, Jan. 26, Feb. 14, Mar. 7, and Apr. 10, 1965.
- Landry, J. W., "Peaceful Nuclear Explosives," presented to noon luncheon of Tennessee Association of Student Councils Convention, Oak Ridge, Tenn., Apr. 23, 1965.
- Landry, J. W., "Industrial and Civilian Applications of Nuclear Explosives," presented at Union Carbide Corporation Paducah Gaseous Diffusion Plant, Paducah, Ky., May 18, 1965.
- Landry, J. W., "Project Plowshare: The Peaceful Uses of Nuclear Explosives," presented under the auspices of the Oak Ridge National Laboratory Traveling Lecture Program at a joint seminar, Roanoke College and U.S. Naval Research Reserve, Roanoke, Va., May 20, 1965.
- Long, J. T., *Engineering for Nuclear Fuel Reprocessing*, Chapter 11, "Auxiliary Equipment," book sponsored by AEC and written by J. T. Long.
- McCorkle, K. H., "Sols and Gels: The Colloidal State of Matter," *Intern. Sci. Technol.* **39** (March 1965).
- Meservey, A. B., "ORNL Decontamination Research," presented at Vallecitos Meeting of Dec. 3 and 4, 1964; presented at the winter meeting of AEC-sponsored Reactor Decontamination Information Exchange Group, Vallecitos, Calif., Dec. 3 and 4, 1964.
- Meservey, A. B. "Decontamination and Film Removal," Chap. 6 in *Decontamination of Nuclear Reactors and Equipment*, ed. by J. A. Ayres (HAPO), to be published by AEC.
- Nichols, J. P., "Calculations of Concrete Shields for Fission Sources," presented at the Eleventh Annual Meeting of the American Nuclear Society, Gatlinburg, Tenn., June 21-24, 1965.
- Shappert, L. B., *Results of Impact Tests Performed on 55-gal Drum-Type Birdcages*, ORNL-3735 (December 1964).
- Shappert, L. B., *Preliminary Experimental Gas-Cooled Reactor Spent Fuel Shipping Cask Design*, ORNL-TM-1001 (January 1965).
- Shappert, L. B., "Results of a Testing Program for Unirradiated Fissile Material Containers," presented at the International Symposium on Packaging and Transportation of Radioactive Materials, Sandia Corporation, Albuquerque, N. M., Jan. 12-15, 1965.
- Shappert, L. B., *Manual for AIChE Nuclear Engineering Division Symposium Chairman* (March 1965).
- Shappert, L. B., "Results of a Testing Program for Unirradiated Fissile Material Containers," in *Proceedings of the International Symposium on Packaging and Transportation of Radioactive Materials*, SC-RR-65-98 (April 1965).
- Shappert, L. B., *A Guide to the Design of Shipping Casks for the Transportation of Radioactive Material*, ORNL-TM-681 (April 1965).
- Shappert, L. B., and K. W. Haff, "The International Symposium for Packaging and Transportation of Radioactive Materials," *Nucl. Safety* **6**(4) (1965).

Shappert, L. B., and J. W. Langhaar (coeditors), "Nuclear Engineering," part XIV, *Chem. Eng. Progr. Symp. Ser.* **61**(56) (1965).

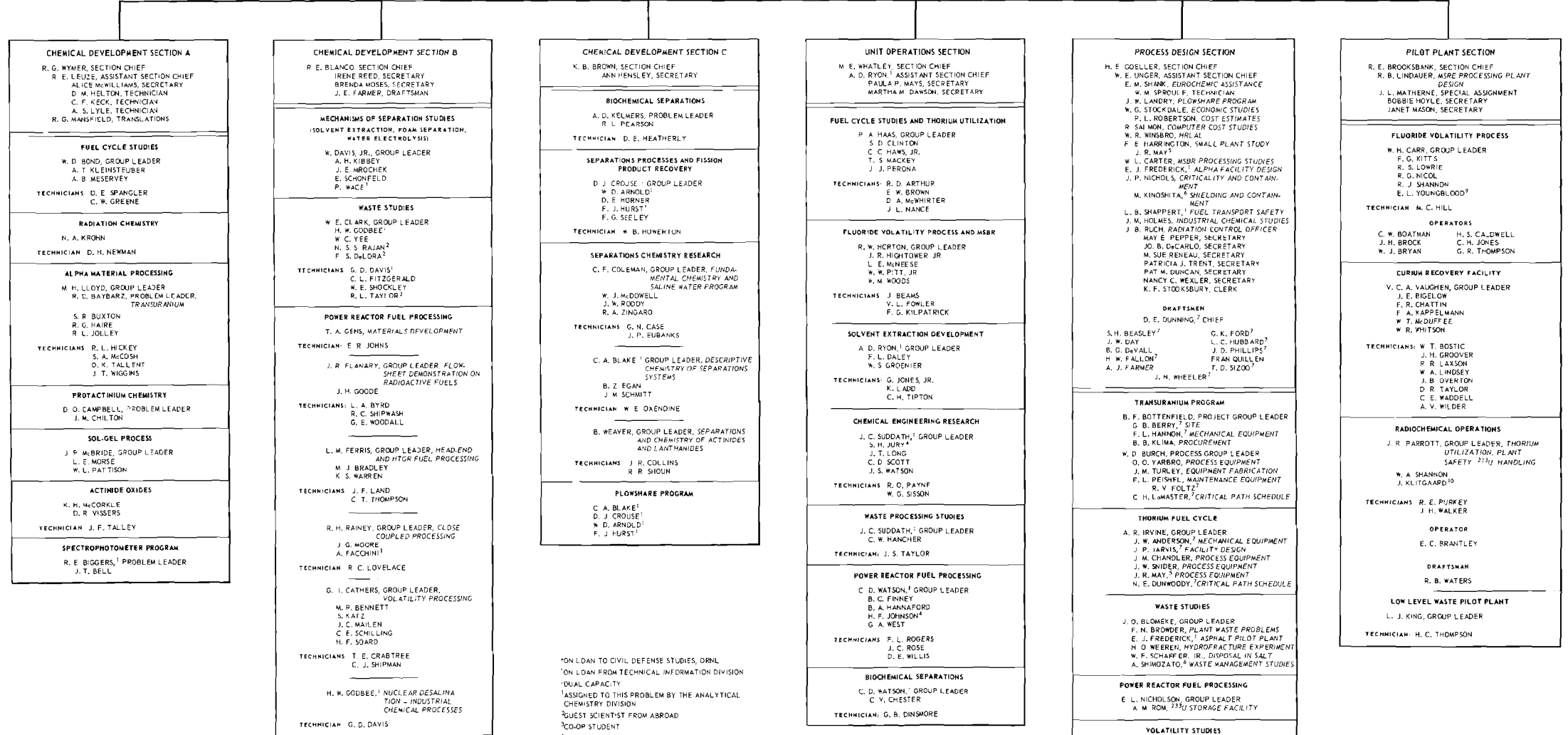
Watson, C. D., "Radioactivity Decontamination Procedures Used in the United States," Summary for Eurochemic Hot Laboratory Program Planning Committee, Oct. 8, 1964.

CHEMICAL TECHNOLOGY DIVISION

D. E. FERGUSON, DIRECTOR
 NANCY ELLISON, SECRETARY
 GAYLE SHARP, SECRETARY
 J. C. BRESSE, ASSISTANT DIRECTOR
 BETH CHRISTIAN, SECRETARY
 H. B. WHESELE, REPORTS EDITOR

H. B. GRAHAM, ADMINISTRATIVE ASSISTANT
 RUTH WILLIAMS, SECRETARY
 W. O. GREEVER, PROCUREMENT
 LUCILLE KUYKENDALL, SECRETARY

LONG RANGE PLANNING COMMITTEE
 A. T. GRESKY
 E. D. ARNOLD
 C. E. GUTHRIE, RADIATION OFFICER
 J. T. ROBERTS
 J. W. ULLMANN
 P. B. CAMARGO
 ELAINE HICKMAN, SECRETARY
 TECHNICIAN: P. F. HAYDON



¹ON LOAN TO CIVIL DEFENSE STUDIES, DRNL
²ON LOAN FROM TECHNICAL INFORMATION DIVISION
³DUAL CAPACITY
⁴ASSIGNED TO THIS PROBLEM BY THE ANALYTICAL CHEMISTRY DIVISION
⁵GUEST SCIENTIST FROM ABROAD
⁶COOP STUDENT
⁷CONSULTANT, UNIVERSITY OF TENNESSEE
⁸GUEST SCIENTIST FROM AUSTRALIA
⁹GUEST SCIENTIST FROM JAPAN
¹⁰ON LOAN FROM GENERAL ENGINEERING AND CONSTRUCTION DIVISION
¹¹ON LOAN FROM PLANT AND EQUIPMENT DIVISION
¹²ON LOAN TO ARGONNE NATIONAL LABORATORY
¹³GUEST SCIENTIST FROM DENMARK

..C

..

O

..

..)

ORNL-3830
UC-10 – Chemical Separations Processes
for Plutonium and Uranium
TID-4500 (45th ed.)

INTERNAL DISTRIBUTION

1. Biology Library
- 2-4. Central Research Library
5. Laboratory Shift Supervisor
6. Reactor Division Library
- 7-8. ORNL – Y-12 Technical Library
Document Reference Section
- 9-28. Laboratory Records Department
29. Laboratory Records, ORNL R.C.
- 30-31. E. L. Anderson
32. S. E. Beall
33. Arnold Berman
34. D. S. Billington
35. C. A. Blake
36. R. E. Blanco
37. E. P. Blizard
38. J. O. Blomeke
39. C. J. Borkowski
40. R. E. Brooksbank
41. G. E. Boyd
42. J. C. Bresee
43. R. B. Briggs
44. K. B. Brown
45. F. R. Bruce
46. W. D. Burch
47. W. H. Carr
48. G. I. Cathers
49. J. M. Chandler
50. W. E. Clark
51. C. F. Coleman
52. J. A. Cox
53. D. J. Crouse
54. F. L. Culler
55. W. Davis, Jr.
56. D. A. Douglas
- 57-186. D. E. Ferguson
187. L. M. Ferris
188. J. R. Flanary
189. J. L. Fowler
190. J. H. Frye, Jr.
191. J. H. Gillette
192. H. E. Goeller
193. A. T. Gresky
194. W. R. Grimes
195. P. A. Haas
196. Richard Hamburger
197. J. P. Hammond
198. C. S. Harrill
199. A. Hollaender
200. R. W. Horton
201. A. R. Irvine
202. W. H. Jordan
203. M. T. Kelley
204. J. A. Lane
205. C. E. Larson
206. R. E. Leuze
207. M. H. Lloyd
208. R. S. Livingston
209. H. G. MacPherson
210. R. A. McNees
211. R. P. Milford
212. D. R. Miller
213. E. C. Miller
214. K. Z. Morgan
215. L. Nelson
216. E. L. Nicholson
- 217-218. R. B. Parker
219. R. E. Pahler
220. R. H. Rainey
221. J. T. Roberts
222. A. D. Ryon
223. A. F. Rupp
224. H. E. Seagren
225. M. J. Skinner
226. A. H. Snell
227. J. C. Suddath
228. E. H. Taylor
229. V. C. A. Vaughen
230. W. E. Unger
231. B. J. Young
232. C. D. Watson
233. B. S. Weaver
234. A. M. Weinberg
235. M. E. Whatley
236. G. C. Williams
237. R. G. Wymer
238. J. J. Katz (consultant)
239. C. W. J. Wende (consultant)
240. P. H. Emmett (consultant)
241. C. E. Winters (consultant)

EXTERNAL DISTRIBUTION

242. R. W. McNamee, Union Carbide Corporation, New York
243. Sylvania Electric Products, Inc.
244. Research and Development Division, AEC, ORO
245. Dr. Barendregt, Eurochemic, Mol, Belgium
246. Giacomo Calleri, CNEN, c/o Vitro via Bacdisseras, Milano, Italy
247. D. J. Carswell, Radiochemical Laboratory, The New South Wales University of Technology, P.O. Box 1, Kensington, Sydney, N.S.W., Australia
248. E. Cerrai, Laboratori CISE, Casella Postale N. 3986, Milano, Italy
249. David Dyrssen, The Royal Institute of Technology, Department of Inorganic Chemistry, Kemisträgen 37, Stockholm 70, Sweden
250. Syed Fareeduddin, Indian Rare Earths Ltd., Army and Navy Building, 148 Mahatma Gandhi Road, Bombay 1, India
251. J. M. Fletcher, United Kingdom Atomic Energy Authority, Atomic Energy Research Establishment, Harwell, Berks, England
252. W. A. Graf, Manager, Plant Design, Atomic Products Division, General Electric Company, Box 450, Palo Alto, Calif.
253. H. Irving, Department of Inorganic Chemistry, University of Leeds, Leeds, England
254. T. Ishihara, Chemical Engineering Laboratory, Japan Atomic Energy Research Institute, Tokyo, Japan
255. A. S. Kertes, Hebrew University, Jerusalem
256. Jorgen Klitgaard, Eurochemic, Mol, Belgium
257. Y. Marcus, Israel Atomic Energy Commission, Tel Aviv, Israel
258. E. Glueckauf, Atomic Energy Research Establishment, Harwell, Berks, England
259. P. Regnaut, C.E.N. Fontenay-aux-Roses, Boite Postale No. 6, Fontenay-aux-Roses, Seine, France
260. R. Rometsch, Eurochemic, Mol, Belgium
261. A. J. A. Roux, Director of Atomic Energy Research, South African Council for Scientific and Industrial Research, Box 395, Pretoria, South Africa
262. Jan Rydberg, Department of Nuclear Chemistry, Chalmers Tekniska Hogskola, Gibraltargatan 5 H, Goteborg, Sweden
263. M. Shaw, AEC, Washington
264. Erik Svenke, Director, Department of Chemistry, Atomic Energy Company, Stockholm 9, Sweden
265. D. G. Tuck, University of Nottingham, Nottingham, England
266. B. F. Warner, United Kingdom Atomic Energy Authority, Production Group, Windscale and Calder Works, Sellafield, Seascale, Cumberland, England
267. R. A. Wells, Dept. of Scientific and Industrial Research, National Chemical Laboratory, Teddington, Middlesex, England
268. M. Zifferero, Comitato Nazionale per l'Energia, Nucleare, Laboratorio Trattamento Elementi Combustibili, c/o Istituto di Chimica Farmaceutica e Tossicologica dell'Universita, Piazzale delle Scienze, 5, Rome, Italy
269. M. Claude Jean Jouannaud, Department Head, Plutonium Extraction Plant, Marcoule (Gard), France
270. Prof. Louis Gutierrez-Jadra, Director de Planta Pilotos e Industriales, Junta de Energia Nuclear, Ciudad Universitaria, Madrid (3), Spain
271. W. G. Belter, AEC, Washington
272. J. A. Lieberman, AEC, Washington
273. W. H. Regan, AEC, Washington
274. H. Bernard, AEC, Washington
275. P. Schmid, Federal Institute for Reactor Research, Wurenlingen, AG, Switzerland
- 276-514. Given distribution as shown in TID-4500 (45th ed.) under Chemical Separations Processes for Plutonium and Uranium Category (75 copies - CFSTI)

11

1
2
3
4
5
6
7
8
9
10
11
12
13
14
15
16
17
18
19
20
21
22
23
24
25
26
27
28
29
30
31
32
33
34
35
36
37
38
39
40
41
42
43
44
45
46
47
48
49
50
51
52
53
54
55
56
57
58
59
60
61
62
63
64
65
66
67
68
69
70
71
72
73
74
75
76
77
78
79
80
81
82
83
84
85
86
87
88
89
90
91
92
93
94
95
96
97
98
99
100

